2016

Proboscidea as palaeoenvironmental indicators in Southeast Asia

Mika Rizki Puspaningrum
University of Wollongong

PROBOSCIDEA AS PALAEOENVIRONMENTAL INDICATORS IN SOUTHEAST ASIA

By:
Mika Rizki Puspaningrum
University of Wollongong
Australia

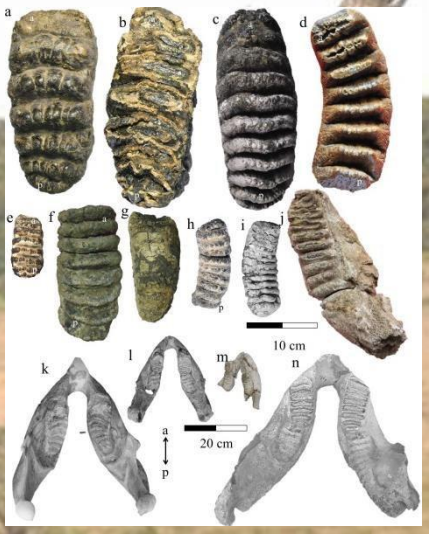

PROBOSCIDEA AS PALAEOENVIRONMENTAL INDICATORS IN SOUTHEAST ASIA

A thesis submitted in fulfilment of the requirements
for the award of the degree

Doctor of Philosophy

from

University of Wollongong

by

Mika Rizki Puspaningrum

Bachelor of Science, Biology, Institut Teknologi Bandung
Master of Science, Geology, Institut Teknologi Bandung

Centre for Archaeological Science

School of Earth & Environmental Sciences

2016

Certification

I, Mika R. Puspaningrum, declare that this thesis, submitted in partial fulfilment of the requirements for the award of degree Doctor of Philosophy, in the School of Earth and Environmental Sciences, Faculty of Science, Medicine and Health, University of Wollongong, is wholly my own work unless otherwise referenced or acknowledged. The document has not been submitted for qualifications at any other academic institution.

Mika R. Puspaningrum

October 11th, 2016

ABSTRACT

The carbon ($\delta^{13}C$) and oxygen ($\delta^{18}O$) isotope compositions of living and fossilized animal skeletal tissues have been widely used as a proxy of faunal palaeodiet and terrestrial palaeoenvironment. Despite having a remarkable record of the Late Neogene to Quaternary and as evolutionary hotspot of fossil fauna diversity, stable isotope approach has rarely been applied to the fossil assemblages in Southeast Asia. This area is important for a comprehensive biogeographic setting, due to the availability of mainland, continental islands and oceanic islands in one region. In this study, stable carbon and oxygen isotope composition analysis was applied on proboscidean tooth enamel samples from various fossil-bearing sites in the mainland and islands in Southeast Asia, also Siwalik and Linxia Basin, ranging in age from the Middle Miocene to present. The aim of this research was to reconstruct the interactions between past environmental changes and the evolution of the fossilized and living proboscidean taxa in mainland and island Southeast Asia.

Stable carbon and oxygen isotope composition analyses were conducted on tooth enamel samples from localities in mainland Asia (Linxia Basin, Siwalik, Irrawaddy, Tha Chang and Laos), continental islands (Java and Sumatra) and oceanic islands (Sulawesi, Sangihe, Luzon, Flores, Timor and Sumba). The $\delta^{13}C$ of carbonate from fossil enamel reflects the $\delta^{13}C$ of the dominant type of food consumed when the enamel was formed, and is thought not to change after its formation (e.g. Bocherens et al., 1996, Cerling et al., 1997a, Kohn et al., 1998) . The $\delta^{13}C$ on tooth enamel is thus commonly used to assess whether herbivores had a diet dominated by grass (C_4 plants, including most tropical grasses: grazers) or dominated by leafy browse (C_3 plant: browsers), or a mixed diet of both types of plants (mixed feeders). Meanwhile, the $\delta^{18}O$ value reflects the meteoric and geographical condition affecting animal's drinking water (e.g. Dansgaard, 1964). Initial exploration of strontium isotope ($^{87}Sr/^{86}Sr$) analysis to predict the migration of fauna was applied on Proboscidea, reptilian and small mammal species from Java and Flores.

The Order Proboscidae, superfamily Elephantoidea, is used in this study due to their wide dispersal over a large range of habitats and climatic zones, including remote oceanic islands, which are located beyond the dispersal ability of most other megaherbivores. Moreover, their occurrences in the fossil records are continuous, both in mainland and on islands. The analytical sample includes fossils of the Family Gomphoteriidae (genus Platybelodon and Sinomastodon), the Family Stegodontidae (genus Stegolophodon and Stegodon) and the Family Elephantidae (genus Archidiskodon, Stegoloxodon, Palaeoloxodon and Elephas), as well as living Elephas maximus. For supplementary, tooth samples of other taxa: the Early-Middle Pleistocene Celebochoerus heekereni (Suidae) from Sulawesi, murine rodents and crocodile from Flores, were analysed.

The carbon and oxygen isotopic result in this study suggest a distinctive diet of three different age groups: the Middle Miocene - Pliocene taxa and the latest Middle Pleistocene – modern taxa are dominantly browsing, while the Pliocene – Middle Pleistocene taxa are dominantly grazer. The distinction of diet between age groups suggests that two major vegetal changes occurred between the Middle Miocene and present. The first floral turnover was a shift from a C_3 dominated to a C_4-dominated vegetation that occurred around the latest Miocene - Pliocene in mainland Asia. In the island Southeast Asia that only became habitable for land mammals after the latest Pliocene - Early Pleistocene, this shift is observed at around the late Early Pleistocene. The second turnover from a C_4- dominated to C_3 dominated vegetation occurred almost simultaneously in both mainland and islands at the latest Middle Pleistocene. When co-occurring, there is no indication of niche separation among Proboscidean taxa, between Proboscidea and ungulates, Proboscidea and hominins, as well as between Proboscidea and murine rodents. Partial distinction of niches is only observed between Proboscidea and Suidae.

Following vegetation changes that resulted in either adaptation or extinction of proboscidean lineages between the Middle Miocene and present, the dietary related evolution of proboscidean lineages is suggested. Combining this result with dental morphology data and isotopic result, the first observed dietary evolution of Proboscidea is many low crowned Proboscidea that were specialized in C_3 browsing went extinct following the change from C_3-dominated to C_4-dominated vegetation. This transition has been observed in the latest Miocene in mainland Asia, but in insular Southeast Asia, this dietary change occurred in the earliest Pleistocene. The low-crowned browser taxa were then replaced by grazer taxa, which later developed higher hypsodonty and extra plates per molar that better-fitted a grass-dominated diet. The extinction of most grazer taxa coincided with the second vegetation turnover in the late Middle Pleistocene, while the surviving taxa switched to a browsing diet, despite their high hypsodonty. An exception occurred in pygmy insular taxa, which survived the floral turnover C_3 to C_4-dominated vegetation in the Early Pleistocene due to their flexible diet, yet went extinct after the arrival of successive taxa that generally had larger body size. Meanwhile, the extinction of well-adapted taxa during the Late Pleistocene could be linked to human (Homo sapiens) predation.

The preliminary $^{87}Sr/^{86}Sr$ analysis provides a hint at different migratory behaviour and roaming areas among individuals. The results also give an insight that co-occurring taxa with a similar dietary signal might not share the same habitat, as one taxon from Java (Stegodon trigonocephalus) was rather a local dweller while another taxon from the same time period (Elephas hysudrindicus) had migrated further away from the taphonocoenosis during its lifetime. The similarity of their diet suggests that particular type of vegetation was indeed widely distributed in the palaeohabitat, regardless of the difference in geography and lithology.

ACKNOWLEDGEMENTS

Eating an elephant is indeed a big task, so does reconstructing what they ate and how their surrounding environment was when they lived. Reconstructing the palaeoenvironment of these elephants over the past four years has been a long-running learning time for me, and I would like to thank all the people that have helped me through this journey.

First of all, I would like thank my supervisor, Gert van den Bergh for giving me such a great opportunity to study and such a fascinating part of palaeontology that I have been interested since I was a kid. I have learnt so many things under your supervision, for helped me in developing critical thinking, and for being there every time I had a question or I needed comments. I greatly appreciated your support, advises, encouragement and understanding through this long process. Very special thanks to my co-supervisor, Allan R. Chivas, for allowing me to do analysis in the Geochemistry Laboratory, for your prompt reading of many drafts and many advices with stable isotope analysis. I am also great indebted to Yahdi Zaim for introducing me to vertebrate palaeontology, recommended me to do this study and for the support despite my inconsistency. I would also like to express my gratitude to the late Mike J. Morwood, Iwan Kurniawan, Adam Brumm and the late Rokhus A. Duwe, for being a great help and inspiration in various fields. I thank Wahyu Saptomo and Suyono for the great help with the administrations.

I would like to thank the University of Wollongong for providing an International Postgraduate Research Scholarship (IPRS) and an International Postgraduate Tuition Award (IPTA) that have allowed me to study at the university. This research has been funded by an Australian Research Council Grant to Gert van den Bergh (FT100100384).

This research would have not been possible without the help from all institution and people that collaborated in the field and provided me with samples for this study. For that I thank:

1. The former and present directors of Geological Agency of Indonesia and staff: Ruly Setiawan and Dida Yurnaldi.
2. The former and present directors of Museum Geologi Bandung and staff: Fachroel Aziz, Erick Setyabudi, Makmur, Unggul Prasetyo, Halmi Insani, Hani Oktariani and Ifan Y.P. Suharyogi
3. Director of Pusat Penelitian Arkeologi Nasional and staffs: Sujatmiko, Thomas Sutikna, and Sri Wasisto.
4. Director of Balai Penelitian Situs Manusia Purba Sangiran and staff: M. Hidayat, B. Sancoyo, Widiyono, U. S.Yuwana, Sukamto, Marlia and Pipit Poedji.
5. Curators of the Dubois Collection of Naturalis Biodiversity Center, Leiden Reinier van Zelst and John de Vos.

6. Director of NRIPM, Nakhon Ratchasima Rajabhat University, Thailand and its staff: Wickanet Songtham, Jaroon Duangkrayom and D. Chokchaloemwong.
7. National Museum of the Phillipines
8. Director of Balai Arkeologi Yogyakarta and staff: Sofwan Noerwidi.
9. Chavalit Vidthayanon, Pak Dakri and Tanti.

I am also greatly indebted to David Wheeler and Florian Dux, for assisting me during the analysis process in the Geochemistry Laboratory, UOW. Hubert Vonhof, Renée Janssen, Jeroen J.L. van der Lubbe, Josephine C.A. Joordens, Suzan Verdegaal and Remy van Baal for the assistance during the analysis process at the Stable Isotope Laboratory of the Earth Sciences Department, Free University Amsterdam. I would also like to express my gratitude to the late A.T. Rahardjo, Yan Rizal and Aswan Abdurahman, for the support, discussion and advice in geology and stratigraphy. Indra Sutisna, for excellent assistance in selecting, recording and organising fossil samples, and as a friend who patiently listened to my palaeontological complains and frustrations. Christine Hertler, for providing her time for in depth discussion and inspiration of how to present my data. Personel involved in the fieldworks: T. Suryana, S. Sonjaya, A. M. Saiful, B. Burhan, L. Siagian, D. Susanti, S. Lauti, M. Moore, S. Hayes, Y. Perston, H. J. M. Meijer, E. E. Laksmana, A. Rahmadi, Y. Sofyan and local workers who helped me during fieldwork.

Thank to my fellow (and former) PhD students: Venera Espanon, Deirdre Ryan, Amy Blakemore, Anna Habeck, Nathan Jankowski, Omar Mohammad, Stephanie Kermode, Lili Yu, Rafael Carvalho, Tom Doyle, Chris Owers, Brent Koppel, Tsun You Pan, Qing Zhang, Ammar Manna, Shawna Yang, Yujie Guo, Farrah Adnan, Maria Schaarschmidt, Ryan Manton, Wanchese Saktura, Jessica Walsh and S. E. Sukandar, for the talks, lunches, cakes, coffees and jocularity. Special thanks to Daniela Müller, Rudi Hendra and again, Florian Dux, for always listening to my frustration and share my joyful days. To everyone in the School of Earth and Environmental Sciences at the University of Wollongong, thanks for always share a greeting or a smile.

Finally thank to my family for the unwavering love and support, my parents, Uminingsih and the late Kabti Bowo Leksono, Bram, Melia and the late Soewarno D.S., I can never thank you enough. My Indonesian family in Wollongong: Nelmy P., Lita L., Iftitah R.D., Aisyah P.M., Luki C., S. Aryani, Dhimas W.M., Randu M. and Retno A.H., for all the good foods and always makes me feel at home. Novian M. K., Kristyarin D.A., Wahyu Dwijo, Sukiato K., Gathot D. H., Daya L. D., Almando Geraldi, and Sra H.P., for always be a great help and support, despite being far away.

I might need to write another thesis in order to thank all the people who helped me writing this thesis, therefore I also need to thank everybody I can not mention one by one here, and if I have forgotten someone please excuse me; as Venera told me: some neurons were consumed to write a thesis.

Table of Contents

List of Figures

Chapter 6

Chapter 7

List of Tables

List of common abbreviations and symbols

$\delta^{13}C$	: ratio of stable isotopes ^{13}C /^{12}C $\delta^{18}O$
	: ratio of stable isotopes ^{18}O /^{16}O
ARKENAS	: Pusat Penelitian Arkeologi Nasional
BCF	: Bulu Cepo Fault
BPSMPS	: Balai Penelitian Situs Manusia Purba Sangiran
cf.	: conferre (comparable to)
CMB	: Central Myanmar Basin
CO_2	: carbon dioxyde
CV	: Chavalit Vidthayanon's collection
dex	: dextral (right)
DKR	: Dakri's collection
ENSO	: El Niño–Southern Oscillation
ESB	: East Sengkang Basin
EWF	: East Walanae Fault
Fm.	: Formation
frg.	: fragment
H.K.	: Haupt-Knochenschicht (bed of bones)
ka	: kilo annum (thousand years)
LBB	: Leang Bulu Bettue
LFI	: Lower fossil interval (So'a Basin)
LGM	: Last Glacial Maximum
LLU	: Lower Lahar Unit
LSI	: Lesser Sunda Islands
LT	: Lakibong Triangle
Ma	: Mega annum (million years)
masl	: modern average sea level
MFI	: Middle Fossil Interval (So'a Basin)
MGB	: Museum Geologi Bandung
MIS	: Marine Isotope Stage
NBC	: Naturalis Biodiversity Center
NMP	: National Museum of Phillipines
NRIPM	: Northeastern Research Institute of Petrified Wood & Mineral Resources
sin	: sinistral (left)
sp.	: species (for unspecified species)
Sr	: strontium
SST	: sea surface temperature
UFI	: Upper Fossil Interval (So'a Basin)
VPDB	: Vienna Pee Dee Belemnite
WFZ	: Walanae Fault Zone
WSB	: West Sengkang Basin
WWF	: West Walanae Fault

Chapter 1. Introduction

1.1 Scope of the thesis

In recent decades, the multi-isotope approach has increasingly been applied as a powerful proxy for analysing palaeoclimate, palaeoenvironmental conditions, dietary preferences and habitat use of modern and fossil animals and humans. The molar teeth enamel of mammals is especially favoured since it contains high-resolution multi-annual stable isotope records of environmental parameters (Bocherens et al., 1996, Cerling and Sharp, 1996, Cerling et al., 1997a, Lee-Thorp and Sponheimer, 2003, Passey and Cerling, 2006, Zazzo et al., 2010, Zin-Maung-Maung-Thein et al., 2011, Metcalfe and Longstaffe, 2012). However, the application of this analysis is still limited in Southeast Asia, especially in the island environment. In this thesis, multi-isotope (carbon, oxygen and strontium) analysis was used to reconstruct the palaeoenvironment of the mainland and island Southeast Asia, within the time interval between Miocene and present. Proboscidea taxa, especially Elephantoidea, were used in this study due to their wide dispersal and continuous occurrence, both on the mainland and the many islands of Southeast Asia, including isolated oceanic islands, which lie beyond the dispersal abilities of most other land mammals (Sondaar, 1977, Palombo, 2007). Geology, stratigraphy, chronology, palaeontology and palaeoclimate data will be incorporated in the discussion to provide a better reconstruction of changing environments and faunal adaptation.

1.2 Proboscidea as palaeoenvironmental indicators in Southeast Asia

The only extant species of Proboscidea, Elephas maximus, in Southeast (SE) Asia forms a small remnant of a more widespread Proboscidean diversity during the Neogene and Quaternary (Shoshani, 1998). Although extant elephants can no longer be found in many areas at present, several taxa succeeded in colonising mainland and island SE Asia during the Miocene to Holocene, and elephant species are comparatively abundant elements in many fossil records. Moreover the Proboscidea are one of a few Asian-origin mammalian taxa that succeeded in crossing the Wallace line despite ocean

barriers, and therefore their distribution covered a large area and a wide range of habitats, including the remote islands of SE Asia (van den Bergh, 1999, van den Bergh et al., 2001) and their occurrence is commonly continuous in fossil records.

Although the majority of natural habitats in modern mainland and island SE Asia are dominated by C_3 vegetation (plants using C_3 photosynthetic pathway, usually broad-leaves trees, shrubs and herbs), in the past this area underwent several environmental changes. The initial collision of the Indian Subcontinent with Asia created a mosaic of lowlands and highlands, extensive freshwater lakes and the formation of drier more open vegetation in regions experiencing rain-shadow effects. Stable isotope studies of a variety of proxies, including pedogenic carbonate, grass phytoliths and mammalian tooth enamel record global expansion of C_4 plants and simultaneous spread of grassland since the Late Miocene (Cerling et al., 1997a), including in mainland Southeast Asia (Quade et al., 1992, Nelson, 2007, Zin-Maung-Maung-Thein et al., 2011, Suraprasit et al., 2014). The timing of C_4 expansion varied considerably among regions. The earliest expansion is documented in East Africa, beginning around 10 Ma and accelerating after 4 Ma (Cerling et al., 2011, Levin et al., 2011). Invasion of C_4 vegetation (plants using C_4 photosynthetic pathway, usually grasses in open environments) recorded from sediments of the Himalayan foreland and Arabian Peninsula was slightly delayed, until after ~8 Ma and accelerating at 4 Ma (Quade and Cerling, 1995, Behrensmeyer et al., 2007, Huang et al., 2007), while expansion north of the Tibetan Plateau only started at ~7.5 Ma (Zhang et al., 2009). However, most of island SE Asia was still submerged prior to the Pliocene (Hall, 2013, Meijaard, 2003), thus the timing of C_4 expansion would be different from that of mainland Asian, and is yet to be confirmed.

Animals in different trophic levels record the stable isotope ratios (C, O and Sr) of their ingested food into their mineralised skeletal and dental tissue, such as bone, dentine and tooth enamel (DeNiro and Epstein, 1978, Hoppe et al., 1999, Tütken and Vennemann, 2009, Maurer et al., 2012, Ecker et al., 2013). For herbivores, their dietary isotopic compositions directly represent the type of plant food and drinking water with a degree of fractionation for both small and large bodied animals. The concept is quite simple: for herbivores, when they ingest plants, the carbon isotope ratios contained in the plants and the oxygen isotope ratios contained in the drinking water are absorbed during metabolism, and are preserved in minerals of body tissues. While for carnivores, their

isotopic compositions represent the diet of their herbivore prey, also with a degree of fractionation. The isotopic ratios preserved in fossil hard tissues can be measured and analysed, thus providing information about the diet when these tissues were formed during the life history of the organism. Dental enamel proved to be an ideal tissue for this study as it is less susceptible to diagenetic alteration than bone or dentine (Ayliffe et al., 1994, Koch et al., 1997, Lee-Thorp and Sponheimer, 2003, Tütken et al., 2006, Tütken and Vennemann, 2009, Bocherens et al., 2011, Domingo et al., 2013); enamel better preserves a high-resolution in vivo stable-isotope record of environmental parameters (Tütken et al., 2007). In this study, all carbon-isotope ($\delta^{13}C_{sample\text{-}VPDB}$ in ‰ = ($[^{13}C/^{12}C]_{sample}$ / $[^{13}C/^{12}C]_{VPDB}$−1) x 1000) and oxygen-isotope values ($\delta^{18}O_{sample\text{-}VPDB}$ in ‰ = ($[^{18}O/^{16}O]_{sample}/[^{18}O/^{16}O]_{VPDB}$−1) x 1000) of specimens are reported relative to the Vienna Pee Dee Belemnite (VPDB) standard.

As the largest herbivores in their environment, and, as generalist feeders, Proboscidean dietary adaptations are closely linked to the availability of certain types of vegetation, to climate change-induced variability of vegetation and to the ability to adapt to these changes (Cerling et al., 1999, Sukumar, 1993). In elephants, unlike other mammals, molars are formed during a large portion of their lifespan (Driak, 1937, Dirks et al., 2012). Thus, isotopic ratios in molars that are formed during the juvenile and adult stages can reveal dietary differences between distinct age groups. Since the mineralisation of tooth enamel is a progressive process, seasonal variations in climatic conditions can be recorded along the growth axis of the enamel. High crowned teeth especially, which may form during a period of over a year (Kohn et al., 1998, Sharp and Cerling, 1998, Feranec and MacFadden, 2000) can give information on seasonal variations (MacFadden and Higgins, 2004, Nelson, 2005, Zin-Maung-Maung-Thein et al., 2011, Tütken et al., 2013, Aiglstorfer et al., 2014).

The reconstruction of palaeoenvironment and mammalian palaeoecology in mainland and insular SE Asia is critical for understanding adaptation and succession of species in response to environmental change. Rather than using an entire faunal assemblage to gain information on palaeohabitat and environment, the approach here focuses on Proboscidean taxa, especially Elephantoidea, as suitable media for investigating palaeoenvironments as:

1. Their occurrence is comparatively abundant and continuous in the fossil record,

2. They have great diversity of genera widely dispersed and adapted to different habitats. Unlike other large Asiatic mammals, they succeeded in crossing the Wallace line despite the difficulties of crossing ocean barriers.
3. Their molar teeth enamel contains a stable isotope record of multi-annual environmental parameters.
4. Their occurrences are commonly associated with hominin species, and where such hominin remains are sparse and unavailable for destructive analysis, the Proboscidea may provide palaeoenvironmental information relevant to the hominin.

By incorporating biostratigraphy and geochronology with the stable-isotope results obtained in this study, the timing of changes in palaeoenvironment that covers large spatial and temporal ranges can be produced. Furthermore, in the case of co-occurrence of different Proboscidea species, a temporal and/or spatial pattern of inter-specific competition can be reconstructed.

1.3 Selection of the sites

The spatial biogeographic setting addressed in this study is divided into three categories: mainland or continent, continental island, and oceanic island. The mainland or continent is defined as the large continuous landmass not fully surrounded by ocean, which remains as land as sea-level rises. Especially in biogeography, the mainland is defined as the area of "genetic source" that became the origin of dispersal or migration of species (MacArthur and Wilson, 1967). The mainland sites in this study include the Miocene mammalian fossil beds in the Linxia Basin, Tibetan Plateau, Western China and three Neogene to Quaternary mammalian fossil localities: the Siwalik beds near Haripur, North India, the Irrawaddy beds in the Central Basin of Myanmar and the Tha Chang sandpit, Khorat Plateau, north-eastern Thailand (Figure 1.1). These localities were selected due to their rich fossil records from the Neogene and Quaternary. Elephantoidea taxa from these localities are considered as ancestral taxa that migrated to the islands and underwent differentiation and speciation during the isolation of islands.

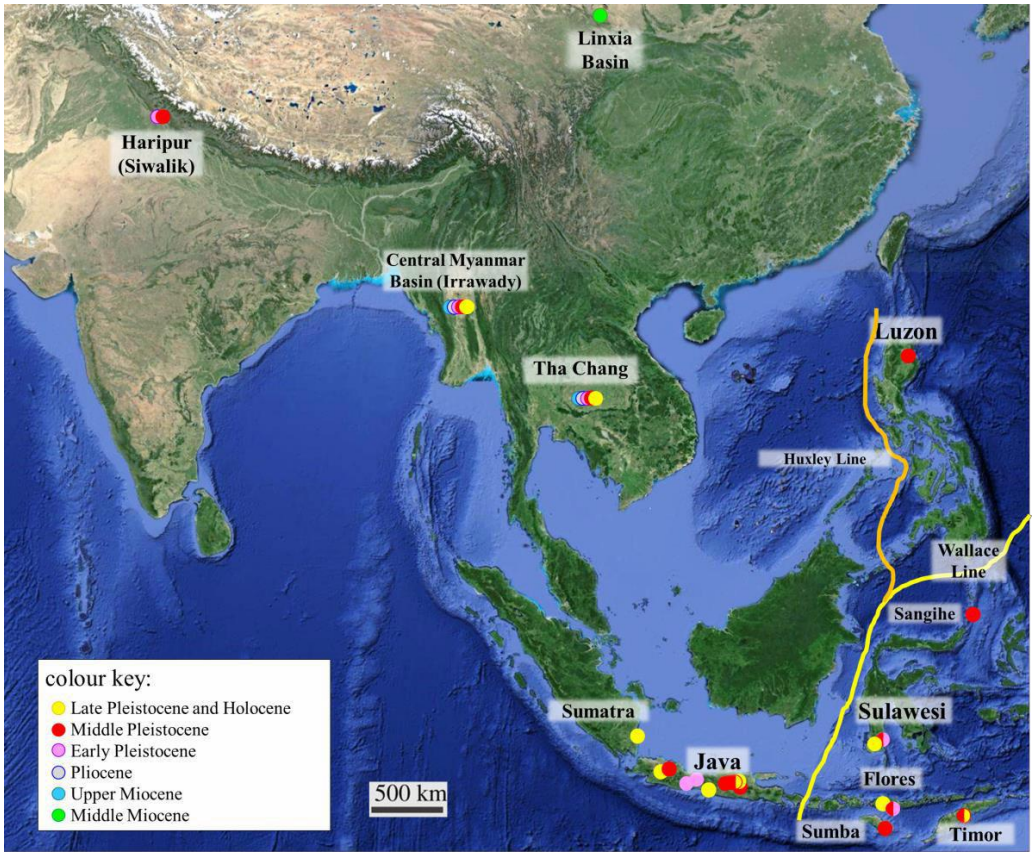

Figure 1.1 Fossil localities in Southeast Asia, with indicated age, which have yielded Proboscidean taxa that were analysed in this study. The landmass to the west of Wallace (Huxley) Line, known as Sundaland, is periodically connected to mainland Southeast Asia during lower sea levels. The transitional region between the Asian and Australian zoogeographic provinces east of Wallace (Huxley) Line, known as Wallacea, remained physically separated from the mainland by deep ocean barriers.

As the opposite of mainland, island is defined as any area smaller than a continent or mainland and entirely surrounded by water, which may occur in oceans, seas, lakes or rivers. The continental islands and oceanic islands are distinguished by their connectivity to the mainland. The continental/mainland islands are located on the continental shelf, which became isolated from the mainland during high sea-level and were connected to the mainland during low sea-level (Darlington, 1957, Alcover et al., 1998). These islands are separated from the mainland by relatively shallow water. In SE Asia, this area is well-known as Sundaland, and consists of Sumatra, Java, Borneo and other small islands on the Sunda Shelf. Only Java and Sumatra (Fig 1.1) are included in this study, due to the lack of Elephantoidea fossils on other islands.

By contrast, oceanic islands are those located on oceanic plates and are surrounded by water even at the lowest sea levels (Darlington, 1957, Alcover et al., 1998). Many of

these islands are volcanic in origin. Since these islands are never connected to the mainland, the only way for terrestrial faunal migration is by crossing ocean barrier(s). The islands in this category included in this study are: Sulawesi, Luzon and Sangihe, as well as the chain of smaller islands in the southeast, known as the Lesser Sunda Islands (included in this study: Flores, Sumba and Timor).

1.4 Aims of the study

The aim of the study is to use fossilized and living Proboscidean, especially Elephantoidea, to reconstruct the interactions between past environmental changes and the evolution of the Proboscidea in mainland and island Southeast Asia, by analysing feeding ecology, dietary preferences and habitat preferences. The study deals with Proboscidea that lived in both mainland and island settings between the Middle Miocene and present. The main focus of this study is high-resolution stable-isotope records ($\delta^{13}C$, $\delta^{18}O$) from fossil and living Proboscidean tooth enamel, and integration of these results with dental morphology, stratigraphy, as well as available geochronology and palaeoclimate data of mainland and island Southeast Asia. These aspects include reconstruction of spatial and temporal dietary adaptation of successive Proboscidean taxa induced either by global or local factors, implications of monsoonal palaeoclimate that forced vegetation coverage shifts from C_3 to C_4 dominated vegetation due to the C_4 biomass expansion and vice versa in both mainland and island SE Asia.

To achieve these aims, the following questions are addressed:

1. Are there noticeable temporal diet shifts, from C_3-dominated diets to increasingly C_4-dominated diets and vice versa, in Proboscidea lineages of successive faunal assemblage? If so, when did these marked shifts take place?
2. Is there a correspondence between temporal dietary shifts and global vegetation and climatic change?
3. Is there inter-specific competition for food resources and/or niche preferences among Proboscidea taxa, especially between Elephas and Stegodon where both taxa co-occur in both mainland and island settings?

4. Were extinctions of Proboscidea taxa in the mainland and insular Southeast Asia caused by environmental change, or other factors such as inter-specific competition, anthropogenic effects, or a combination of these factors?
5. Is there a noticeable adaptive response between dental morphology and feeding behaviour (diet) of successive species on the mainland and islands?

1.5 Originality and significance of the study

This research represents an original contribution to knowledge in the application of established multi-isotope techniques to a region not yet well examined. Stable carbon and oxygen isotope analysis of fossils and living mammalian taxa are widely used to reconstruct dietary and habitat preference for Africa, Europe and America (i.e. Cerling et al., 1997, Feranec and McFadden, 2000, Palombo et al., 2005). However, stable isotope analysis of mammalian fauna has scarcely been applied in the SE Asian region. So far, a few dietary stable isotope studies have been applied for Neogene and Quaternary faunal assemblage in mainland SE Asia (i.e. Morgan et al., 1994, Merceron et al., 2004, Nelson et al., 2007, Pushkina et al., 2010, Zin Maung Maung et al., 2010), yet similar data are still largely lacking from the islands of Southeast Asia. The use of stable isotopes of mammalian fauna to analyse Quaternary palaeoenvironments in insular Southeast Asia is limited to the Middle Pleistocene-Holocene of Java and Sumatra (Janssen et al., 2016) and the Late Pleistocene of Borneo (Krigbaum, 2005). Hence, the immediate implication of this research is in providing a stable isotope record of Neogene and Quaternary faunal assemblages, especially from a variety of Proboscidean taxa, and which is lacking in Asia. This study also provides a better understanding of dietary preference of Elephantoidea as megaherbivores within an ecosystem and how these taxa adapted or failed to adapt, in response to environmental change.

Additionally, strontium isotopes have not been applied to palaeoenvironmental reconstruction in any Southeast Asian fossil locality before. The preliminary strontium isotope data reported here should be considered as an initial exploration of their potential future use in tropical environments.

In this study, differences between mainland and island Proboscidean taxa in terms of timing and adaptations during vegetation and environmental change is reconstructed and compared. These include: extinction or adaptation in response to environmental change and niche partitioning between co-occurring taxa. Moreover, the correlation between environmental and climatic change versus anthropogenic impacts on megaherbivore extinction patterns, in both mainland and island settings is suggested for particular taxa.

1.6 Thesis outline

The thesis is organized into 7 further chapters, as summarised below:

- Chapter 2 contains an explanation of the palaeontological background required for this study and the principles of multi-element isotopes as applied to palaeoenvironmental reconstruction.
- Chapter 3 outlines the chosen materials and methodology.
- Chapters 4 to 6 present results and interpretation of each locality: the Mainland Southeast Asia and Sundaland, including Java and Sumatra (Chapter 4), the islands of Sulawesi, Sangihe and Luzon (Chapter 5) and the Lesser Sunda Island (including Flores, Timor and Sumba in Chapter 6). Each chapter begins with an introduction to the geology and palaeogeography related to the colonisation of fauna, as well as an overview of established faunal assemblages and successions. The introduction is followed by brief explanation of analysed materials, stable isotope results, palaeoenvironment interpretation and conclusion.
- Chapter 7 explores the preliminary results and interpretation of $^{87}Sr/^{86}Sr$ analysis applied to the faunal assemblages of Java and Flores.
- Chapter 8 discusses the correlation of the data for the palaeoenvironmental interpretations of mainland and island Southeast Asia, as well as conclusions and recommendations for future research directions.

Chapter 2. Palaeontological and stable isotope background to the thesis

2.1 Proboscidea in Southeast Asia

2.1.1 Origin, diversity and distribution

In this study, two taxanomical groups are commonly mentioned: Elephantoidea and Proboscidea. Proboscidea is group of proboscis-bearing mammals that share these distinct characteristics (Shoshani and Tassy, 1996a): experienced an early development of the upper incisors into enlarged second incisors forming tusks, loss of the first premolar tooth, tooth enamel with a keyhole prism cross section (von Koenigswald et al., 1993) and the radius positioned or fixed in a pronation position. Following Tassy's (1996b) and Shoshani and Tassy's (2005) phylogenetic reconstruction of Proboscidea (Table 2.1), two genera analysed in this study belong to the Superfamily Gomphotherioidea and other taxa belong to superfamily Elephantoidea. The two superfamilies have the character "horizontal tooth displacement" as distinct characteristic, but this character is more pronounced in Elephantoidea. The superfamily Gomphotherioidea (including a single family Gomphotheriidae), or the true gomphoteres, is characterised by the possession of bunodont teeth, posttrite conules on molars and trilophodont intermediate molars (dp4 and M1, Tassy, 1996b). The Gomphotheriidae taxa included in this study are genera Platybelodon and Sinomastodon.

The Superfamily Elephantoidea is characterised by minimum tetralophodont molars (Kalb et al., 1996b, Tassy, 1996b), highly developed horizontal molar succession (Tassy, 1988), especially in more apomorphic (advanced) families. Included in this study are families Stegodontidae (including genera Stegolophodon and Stegodon) and Elephantidae (including genera Archidiskodon, Stegoloxodon, Palaeoloxodon and Elephas).

Table 2.1 A simplified non-ranked, classification of the Proboscidea, at the family level. The classification of taxa analysed in this study are displayed to the genus level (written in bold; modified after Shoshani and Tassy, 2005, Wang et al., 2012, Meyer et al., 2017)

Mammalia Linnaeus, 1758
Theria Parker and Haswell, 1897
Placentalia Owen, 1837 (=Eutheria Huxley, 1880)
Epitheria McKenna, 1975
Ungulata Linnaeus, 1766
Uranotheria McKenna, Bell et al., 1997 (=Paenungulata Simpson, 1945, in part)
Tethytheria McKenna, 1975
Tethytheria incertae sedis Genus Anthracobune Pilgrim, 1906†
Proboscidea Illiger, 1811
Proboscidea incertae sedis Family Moeritheriidae Andrews, 1906†
Plesielephantiformes Shoshani et al., 2001
Family Numidotheriidae Shoshani and Tassy, 1992†
Family Barytheriidae Andrews, 1906†
Elephantiformes Tassy, 1988
Elephantiformes incertae sedis Genus Hemimastodon Pilgrim, 1912†,c
Family Palaeomastodontidae Andrews, 1906†
Family Phiomiidae Kalandadze and Rautian, 1992†
Elephantimorpha Tassy and Shoshani, 1997 in Shoshani et al., 1998
Mammutida Tassy and Shoshani, 1997 in Shoshani et al., 1998†
Superfamily Mammutoidea Hay, 1922†
Family Mammutidae Hay, 1922†
Elephantida Tassy and Shoshani, 1997 in Shoshani et al., 1998
Superfamily Gomphotherioidea Hay, 1922†
Family Gomphotheriidae Hay, 1922 (trilophodont gomphotheres)†
Subfamily Amebelodontinae Barbour, 1927†
Genus **Platybelodon** Borissiak, 1928†
Subfamily Sinomastodontinae Wang et al., 2012†
Genus **Sinomastodon** Tobien et al., 1986†
Superfamily Elephantoidea Gray, 1821
Family incertae sedis Genus Tetralophodon Falconer, 1857 (tetralophodont gomphothere)†
Family incertae sedis Genus Morrillia Osborn, 1924 (tetralophodont gomphothere)†
Family incertae sedis Genus Anancus Aymard, 1855 (tetralophodont gomphothere)†
Family incertae sedis Genus Paratetralophodon Tassy, 1983 (tetralophodont gomphothere)†
Family Stegodontidae Osborn, 1918†
Genus **Stegolophodon** Schlesinger, 1917†
Genus **Stegodon** Falconer, 1857†
Family Elephantidae Gray, 1821
Subfamily Stegotetrabelodontinae Aguirre, 1969†
Subfamily Elephantinae Gray, 1821
Genus **Archidiskodon** Pohlig 1888†
Genus **Stegoloxodon** Kretzoi, 1950†
Genus Loxodonta Anonymous, 1827*
Genus **Palaeoloxodon** Matsumoto, 1924†*
Genus **Elephas** Linnaeus, 1758
Genus Mammuthus Brookes, 1828†

† = extinct taxa

* = Palaeoloxodon was thought to be closely related to Elephas and thus included ini the Tribe Elephantini along with Mammuthus. However in a light of recent ancient DNA analysis (Meyer et al., 2017) indicating that Palaeoloxodon antiiqus and Loxodonta cyclotis are sister taxa, thus invalidating the Tribe Elephantini.

So far, 19 genera and 65 species of the Proboscidea are recorded from the mainland and islands of Southeast Asia (Hooijer, 1955, Nanda, 1977, Vasishat et al., 1978, Johnson et al., 1982, Tassy, 1983, Tobien et al., 1986, Kalb et al., 1996a, Saegusa, 1996, van den Bergh, 1999, Nanda, 2002, Kunimatsu et al., 2005, Pillans et al., 2005, Saegusa et al., 2005, Suganuma et al., 2006, Thasod, 2007, Wang et al., 2007b, van den Bergh et al., 2008, Thasod et al., 2012, Wang et al., 2012a, Jin et al., 2009, Patnaik, 2013). Members of Gomphotheriidae were dominant between the Early to Late Miocene and the post-Miocene lineage of this family is rarely found. The distribution of this group is restricted to the mainland, except for one species of the Gomphoteriidae family, Sinomastodon bumiajuensis, is recorded from the Early Pleistocene in Java.

According to Shoshani (1998) the common ancestor of Elephantoidea was presumably from Africa and which migrated into Eurasia during the earliest Miocene, or perhaps even the latest Oligocene, from which followed futher migrations and radiations of Elephantoidea taxa. Kalb et al. (1996) considered that Eurasia was the origin and the centre of radiation of the family tetralophodont Gomphotheriidae. The tetralophodont gomphoteres are considered ancestral to both the Stegodontidae and Elephantidae (Tassy, 1996, Shoshani and Tassy, 2005).

The successor clade, Stegodontidae, includes only two members: genera Stegolophodon and Stegodon. However, this clade successfully radiated and became dominant in many localities in Southeast and East Asia between the Pliocene and Late Pleistocene. Saegusa et al. (2005) suggest that the lineage of Stegodontidae has an Asian origin, considering that most of the primitive forms of Stegodontidae were found in Asia and there has been a recent finding of an older transitional form between Stegolophodon and Stegodon from South East Asia (Saegusa et al., 2005).

In contrast to the Stegodontidae, the Elephantidae family is considered to have an African origin (Osborn, 1936, Maglio, 1973, Todd and Roth, 1996). The member of this clade (Archidiskodon / Palaeoloxodon / Stegoloxodon) only began to enter mainland Asia since the Pliocene and led towards the lineage of the modern Elephas genus that was adapted to the warmer climates of Southern Asia.

Besides having high diversity, Elephantoidea also had a wide distribution in Southeast Asia. Members of Elephantoidea once colonized a variety of landscapes in Southeast Asia. As a result of the Indoaustralia-Eurasia tectonic collision that coincided with lowered sea levels since the Pliocene, the island areas of Southeast Asia were vastly enlarged. Due to their ability to swim, many Elephantoidea underwent sea-crossings to reach these newly emerged islands. Either on the mainland or on islands, several Elephantoidea taxa commonly overlapped in time and space.

The Stegodontidae and Elephantidae even reached islands east of Wallace Line. As for Stegodontidae, only genus Stegodon successfully reached and colonised the islands of Southeast Asia, while their older relative, Stegolophodon, has not been found on the islands. Stegodon is considered the most successful sea-farer among Elephantoidea, since its fossils are found as far as the Lesser Sunda Islands (LSI). A primitive (Stegoloxodon) and a derived (Palaeoloxodon and Elephas) form of Elephantidae also succeed in sea-crossing. However, these genera only reached as far as Java, the Philippines and Sulawesi, but not to Lesser Sunda Islands.

2.1.2 Morphology and evolution of Proboscidea dental elements

The dental formula of Proboscidea is similar to that of other herbivores, with a total of 26 teeth which develop during their lifetime. Their dental formula is: incisor 1/0(1), canine 0/0, deciduous premolar 3/3, and molar 3/3. Most mammals, including older Proboscidea clades, replace their teeth in vertical manner, which is, a new tooth develops and replaces the old one from above or below. Instead of replacing their teeth in a vertical manner, members of the Elephantoids have an extremely derived character of replacing their teeth in a horizontal progression, which is referred to as horizontal displacement (Fig. 2.1). Horizontal tooth displacement is an extremely complex process involving bone modifications that began to evolve towards the end of the Oligocene epoch (Shoshani, 1996). All Elephantoidea members exhibit this unique character, but it is far more visible in Stegodontidae and Elephantidae.

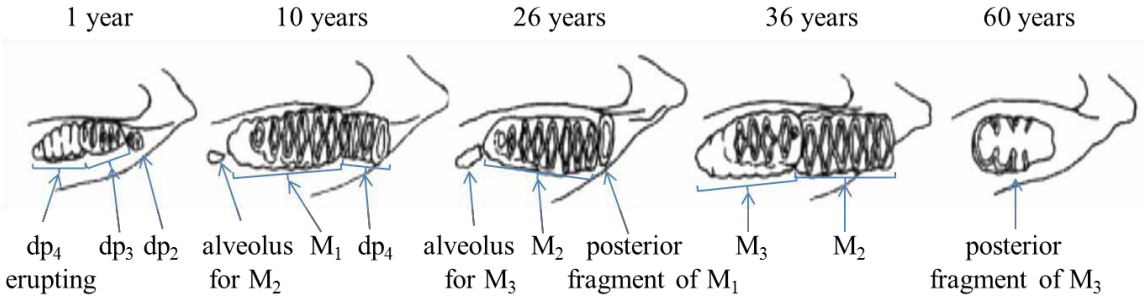

Figure 2.1 A portrayal of five relative stages of tooth displacement and movement in the mandibles of African elephants (Loxodonta africana). Through time, younger teeth are displaced by the older ones from behind. Successive cheek teeth become larger and contain more plates. By the time an elephant is aaround 60s years old, the last molar is worn out. There will be no new tooth to displace it, and the animal is not able to chew its food, thus the individual will then die from starvation if not killed by a predator (modified after Shoshani, 1996).

Over the course of their lifetime Proboscidea have six cheek teeth in each jaw quadrant. These teeth are dp2, dp3, dp4, M1, M2 and M3, where dp (deciduous) teeth are premolars, and M teeth are molars. In this study, teeth located in the upper jaw indicate by superscript number and lower jaw teeth in subscript number. For example: dp^4 means upper 4^{th} deciduous premolar and M_3 means lower 3^{rd} molar. In more advanced Gomphotheriidae and Elephantoidea, each tooth is successively longer, wider, and heavier. A newborn advanced Gomphotheriidae and Elephantoidea has two or three cheek teeth in one jaw quadrant and, as it becomes older, new teeth develop from behind in the back of the jaws and slowly move forward. Simultaneously, the previous teeth are worn away, and move forward, until small remnants of the molars remain, which either fall out of their mouth, or are swallowed and excreted in the animal's faeces (Shoshani, 1996). Newer and bigger teeth displace the older ones five times (Fig. 2.1). Each tooth has different characteristics. Dp2s have an oval shape with only 2-3 ridges/lamelae, dp3s and dp4s are widening in the posterior direction, each with consecutive molar being larger and containing more ridges than its predecessor. The M1 and M2 are often difficult to distinguish due to the similarity in shape; both may have similar width at the anterior and posterior ends, while the widest part is located in the middle part of the molars. The M2s are distinguished from the M1s by having more ridges/lamellae and a larger size. The M3s are distinguishable by having the highest number of ridges/lamellae of all molars and the width of the lamellae taper in posterior direction, whereas M1s and M2s have a more rectangular outline shape. Each tooth was

formed during different ontogenic stages. According to the ontogenic age, the development of dI^2s, dp2s and dp3s were formed during the pre-natal stage, the dp4-M1 formed around the weaning to post-weaning period, and M2-M3 represent pre-adult to adult dental development (Shoshani, 1996, Kozawa et al., 2001, Dirks et al., 2012).

An advantage of the horizontal displacement and dental wear degrees for palaeontological and archaeological studies is that the relative age of individuals upon death and death assemblages of a population in particular localities can be estimated. Although for extinct taxa with unknown life history, the deviation of relative ages may be larger.

Each proboscidean premolar and molar consists of several transverse plates or lophs (Shoshani, 1996). These plates are called lamella in family Elephantidae and loph(id)s or ridges in older families. The plates are actually extensions of multiple infolding that come in from either side, to meet in the middle (Hillson, 2005). Each ridge consists of several cusps, which are raised points on the crowns of teeth (Nelson, 2015). This type of premolar and molar is called bunolophodont (Tassy, 1996a). The main evolutionary trend of Elephantoidea teeth is toward the augmentation of both loph and cusp in the loph (Tassy, 1996a). Primitive taxa such as Platybelodon, Sinomastodon, Tetralophodon, and Anancus only have a maximum of 6 lophs and 4 cusps in a loph. Later taxa such as Stegodon, Stegoloxodon, Elephas and Palaeoloxodon reach more than 10 lophs, and even 20 in Elephas and Palaeoloxodon, while the cusps can reach up to 10 in a loph (Shoshani and Tassy, 1996b). Dental nomenclature used in this study is presented in Figure 2.2.

As in other mammals, the Elephantoid's cheek teeth are composed of two main elements: crown and roots. The crown is coated by layer of hard and shiny enamel and a layer of a bone-like tissue called cement. Underlying these surface layers and forming the main structure of the tooth is a very tough and resilient tissue called dentine. Dentine is also found in the root. The infolding pattern of the enamel will be exposed on the occlusal surface as it gradually worn away (Hilson, 2001). This worn stepwise morphology has been called stufenbildung by Janensch (1911). Each taxon has its unique stufenbildung, so that the stufenbildung may be used to identify to the level of species (Saegusa et al., 2005).

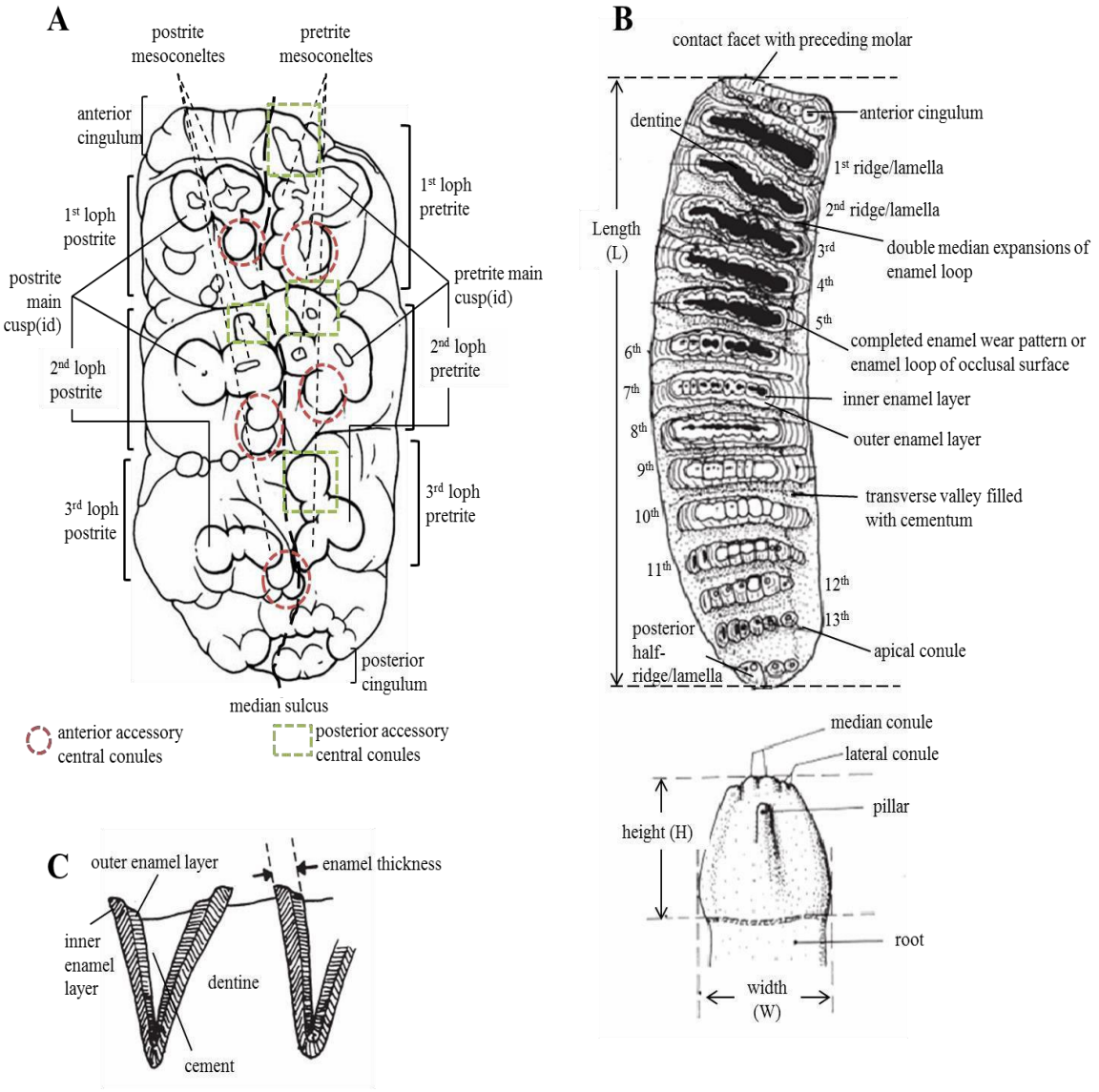

Figure 2.2 A. Gomphotheriidae dental nomenclature (dextral M^2) modified from Tassy (1996). **B**. Advanced Stegodontidae and Elephantidae dental nomenclature (dextral M_3) modified from van den Bergh (1999); the terminology "ridge" is used for Stegodontidae, while "lamella" is used for Elephantidae, both are comparable to loph(id). **C**. Stepwise wear or stufenbildung developed at the occlusal surface of the enamel in Stegodon molars, due to the differential resistance to wear of the inner and outer enamel layers.

There is a general tendency for an increase in complexity of the crown pattern and increase in the length of the teeth in successive proboscidean lineages (Cerling et al., 1999). The change in dental morphology of Proboscidea over time appears to be a response to aid processing the available food source (Cerling et al., 1997b). The earliest proboscidean genera possess low-crowned molars comprising a few series of lophids with rounded cusps. This morphology accommodates less abrasive plant food, which

mainly comprises C_3 plants. The increase in the crown-height (hypsodonty), multiplication of lophid numbers and thinning in the enamel layer that occurred in later Elephantoidea genera represent adaptation to an abrasive grazing diet (Cerling et al., 1997b, Lister, 2013, 2014). This general tendency has been suggested based on study of mainland Asian localities. However, this adaptive trend in island environments remains yet to be studied.

2.1.3 Ecological importance of Proboscidea as megafauna

Regardless of different criteria for body weight threshold (Martin, 1984, 1990, Owen-Smith, 1992) and ecological impact (Wroe et al., 2004, Louys et al., 2007, Hansen and Galetti, 2009), even the smallest Proboscidea are included as megafauna. With their large body mass, Proboscidea probably always became the largest herbivore in any given ecosystem. Moreover, on isolated islands with impoverished faunal assemblages, Proboscidea commonly became the only megaherbivore in the ecosystem.

An individual Elephas maximus consumes 135 to 300 kg of plant food and 100 – 225 litres of drinking water in a day (Sukumar, 1993). By enumerating the proportion of plant species eaten by modern elephants (Elephas maximus and both Loxodonta species) in different seasons, numerous studies (Wing and Buss, 1970, Field and Ross, 1976, Sukumar, 1990, Cerling et al., 1999) conclude that recent elephants are generalist feeders and predominantly browsers in almost all environments. The proportions of grass consumption vary according to seasonal availability and habitat types. In habitats where both types of plants are available, grasses are generally preferred during the early rainy season, when newly grown soft grasses are available. Tall grasses are a less preferred food option, unless browse plants are limited as in predominantly grassland habitat (Sukumar, 1990). Furthermore, the above mentioned authors agree that the proportion of browse/grass in the elephant diet and the variability of consumed plant species more or less represent the seasonal availability of the habitat.

Conversely, the feeding behaviour of elephants may also play an important role in the modification of landscape and vegetation types. Sukumar (1993) and Cumming et al. (1997) observed a habit of uprooting small and undergrowth trees as well as disrupting canopy coverage of larger trees, possessed by both Asian and African elephants. This

habit in wider scale allows sunlight to reach the ground and thereby stimulate the growth of vegetation in the understorey layer of forest or woodland (Laws, 1970). The cropping of plant materials by elephants also limit vegetation density in open land and thus keeps the open land clear of canopied vegetation. By assuming that extinct species of Elephantoids might have similar behaviour as their extant relatives, extinct Elephantoids definitely played a more significant role in palaeoenvironment modification on a much larger scale with their wider distribution and variety of species (Schüle, 1992).

2.2 Principles of stable isotopes as palaeoecological indicators

2.2.1 Carbon isotopes

2.2.1.1 Carbon fixation of plants and incorporation of ^{13}C in animal tissue

The carbon isotope ratio (expressed as $\delta^{13}C$) incorporated in the body tissue of extant and extinct herbivores reflect the diet and ecology of the animal. The different assimilation rates of ^{13}C and ^{12}C (contained in atmospheric CO_2) between different groups of plants are transferred into herbivore body tissue (DeNiro and Epstein, 1978, Lee-Thorp and van der Merwe, 1987, Cerling et al., 1997a, Tütken and Vennemann, 2009, Ecker et al., 2013). These body tissues preserve dietary information as to the plant groups consumed. The largest factor affecting variation of carbon isotope compositions in plants is due to the different photosynthetic pathways utilized to fix the CO_2 from the atmosphere. There are three different photosynthetic pathway used by terrestrial plants: the C_3 (the Calvin Cycle); the C_4 (Hatch–Slack cycle) and the CAM (Crassulacean Acid Metabolism) pathways (Ehleringer et al., 1997). C_3 plants utilize the RuBisCO (ribulose bisphosphate carboxylase) enzyme to form three-carbon sugars in their photosynthetic metabolism process. C_3 plants include most species of trees, shrubs and high-altitude or high-latitude grasses. Plants that survive solely on C_3 fixation (C_3 plants) tend to thrive in areas with moderate sunlight intensity, moderate temperatures, moderate carbon dioxide concentrations, and plentiful groundwater (Raven and Edwards, 2001).

C_4 plants, which include low latitude or tropical grasses and sedges, have an additional preliminary step that uses PEP (phosphoenolpyruvate) carboxylase in mesophyll cells to fix CO_2 resulting in a four-carbon acid, which is then transferred to bundle sheath cells, decarboxylated, and the CO_2 is then fixed in a second step using RuBisCO (Farquhar et al., 1989, Ehleringer and Cerling, 2002). In contrast to C_3 plants, C_4 plants are limited to environments with a mild or cold growing season, very sunny environments, or, in some cases, in dry climates (Ehleringer et al., 1997). Thus the physiological adaptation of C_4 plants increase the CO_2 assimilation efficiency, and as a by-product, the water use efficiency of C_4 plants is greater than that of C_3 plants (Hatch, 2002, Tipple and Pagani, 2007). The third photosynthetic pathway, CAM, performs CO_2 fixation at night time via the C_4 pathway; the fixed CO_2 is stored as four-carbon acids to be released during the day and fixed via the C_3 pathway when the plant's stomata can be closed to conserve water (O'Leary, 1988). This group includes xeric-adapted desert succulents, tropical epiphytes, and aquatic plants and often corresponding with environments under climatically stressful conditions, such as increased aridity (Keeley and Rundel, 2003). CAM plants usually comprise only a marginal biomass in ecosystems and do not represent the expected food for the large mammalian herbivore taxa sampled for this study.

The carbon isotope composition difference among three different pathways is caused by the ^{13}C isotope discrimination by PEP carboxylase or RuBisCo. In the preliminary step of the C_4 photosynthesis pathway, ^{13}C is enriched during the diffusion of CO_2, interconvension of CO_2 and HCO_3^-, and also during the incorporation of CO_2 (O'Leary, 1988). Thus, the $\delta^{13}C$ of C_4 plants shows more positive values than in C_3 plants. In modern plant tissues, $\delta^{13}C$ values of most C_3 plants range between -35‰ and -22‰, whereas most C_4 plant $\delta^{13}C$ values fall between -17‰ and -9‰ (Bender, 1971, Vogel, 1980, van der Merwe and Medina, 1989). On the other hand, CAM plants yield $\delta^{13}C$ values between -10‰ and -20‰, partially overlapping with the range of C_4 plants (O'Leary, 1988). However, CAM plants are disregarded in this study since such desert-adapted plants were unlikely to have grown on mainland or island Southeast Asia during the Miocene to Recent.

Consumption of aquatic plants also needs consideration in affecting mammal $\delta^{13}C$ values, since a few herbivores are reported to consume substantial amount of aquatic

plants. The $\delta^{13}C$ values of various aquatic plants are commonly more positive than those of C_3 plants and often close to C_4 plant values, although their photosynthetic pathway resembles that of C_3 plants. However, due to slow diffusion of CO_2 in water, isotope fractionation occurs as the CO_2 supply is limited (O'Leary, 1981).

Besides the interspecific variations of photosynthetic pathways, O'Leary (1981) suggests minor factors affecting variation in $\delta^{13}C$ values of plants such as intraspecific variations (varies up to 3‰), different isotopic enrichment in plant organs, and effect of temperatures (values becomes more negative by up to 2‰ with an increase of temperature). Within the several plant organs, leaves, stems and roots possess the most negative $\delta^{13}C$ values. In comparison to leaves, tubers are about 2‰ more positive while seed and fruit are up to 10‰ more positive. However, since the proportion of seed, fruit and tuber consumption is minor especially for a large elephant (Sukumar, 1993), such ingestion would only give a slight increase in their bioapatite $\delta^{13}C$ values.

The ingested plant carbon is incorporated in herbivore skeletal and dental tissues as mineralized bioapatite. This crystal bioapatite contains a small amount of structural carbonate (CO_3^{2-}). The carbon isotope composition of the carbonate ($\delta^{13}C_{CO3}$) in bioapatite reflects the $\delta^{13}C$ value of the bulk diet (DeNiro and Epstein, 1978). However, during transfer to the body tissues, the carbon isotope ratio changes from the original ratio of the plant, and will be stored in the tissue with a different ratio compared to the original food consumed. ^{13}C isotope enrichment in the enamel bioapatite varies among herbivores, carnivores and omnivores relative to the ratio of ingested food. The average $\Delta^{13}C$ enamel-diet enrichment factor in herbivores is 14.1± 0.5‰ (see Figure 2.3), with a total range between 12.6‰ and 14.7‰ (Lee-Thorp et al., 1989, Cerling et al., 1997b, Cerling et al., 1999, Passey et al., 2005). Meanwhile in carnivores and omnivores such as pigs, primates and rodents, the enrichment is 9‰ for bone and enamel apatite relative to their diet (Lee-Thorp et al., 1989, Koch, 1998, Cerling et al., 1999, Bocherens et al., 2000, Kohn and Cerling, 2002, Bocherens and Drucker, 2007). The $\delta^{13}C$ values of enamel between -21‰ and -10‰ reflect a purely C_3 diet (browsers predominantly consuming leaves of C_3 plants), whereas values between -2‰ and 4‰ indicate a predominantly C_4 diet (grass eaters or grazers), with intermediate values reflecting a mixed diet (Cerling et al., 1997a, MacFadden et al., 1999, Cerling and Harris, 1999, Feranec, 2007, Pushkina et al., 2010). However, in large herbivores, including

Proboscidea, an $\delta^{13}C$ enamel value as high as −8‰ can be still explained by a pure C_3 diet and is the recommended conservative threshold for large-bodied herbivores, corresponding to a dietary intake with a $\delta^{13}C$ value of −22‰, which is within the range of observed values for pure C_3 ecosystems (Cerling et al., 1997a, Cerling et al., 1999, MacFadden et al., 1999, Pushkina et al., 2010).

The change in carbon isotopic composition of atmospheric CO_2 must be taken into account when comparing isotope compositions of fossil and modern faunas. Since the beginning of the industrial revolution in 1850, the modern atmospheric CO_2 ($\delta^{13}C$ CO_2=−8 ‰) has become depleted in ^{13}C compared with pre-industrial atmospheric CO_2 ($\delta^{13}C$= −6.5‰), due to the fossil-fuel burning of ^{12}C-rich hydrocarbons and deforestation (Friedli et al., 1986, Marino and McElroy, 1991), and this trend is continuing. Therefore for modern fauna samples, a correction factor of 1.5‰ is included for each measured $\delta^{13}C$ value.

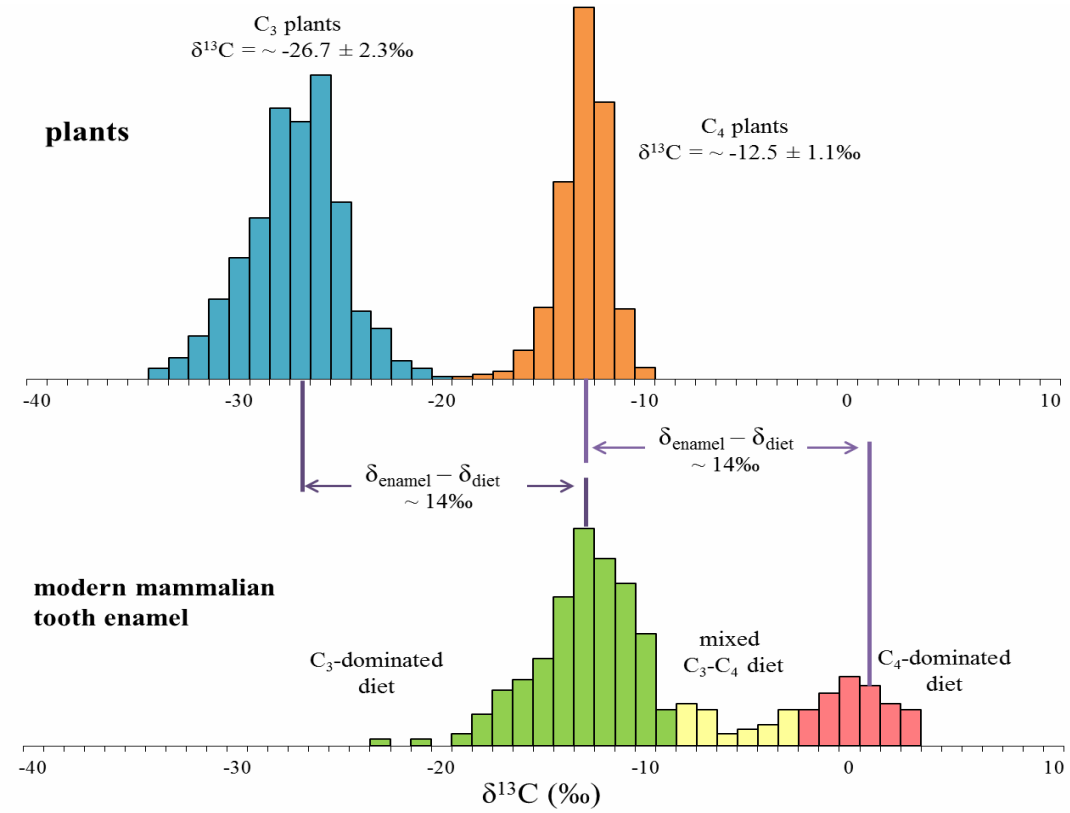

Figure 2.3 Histogram of $\delta^{13}C$ for modern plants and modern tooth enamel (modified from Cerling et al., 1997b), showing a shift of ~ 14‰ between $\delta^{13}C_{enamel}$ and $\delta^{13}C_{diet}$.

2.2.1.2 Classification of vegetation and application to the fossil isotopic record

Before proceeding with the reconstruction of palaeovegetation in the subsequent chapters, it is important to define formal terminology of vegetation structural categories. Various schemes have been used to classify the tropical and subtropical vegetation of mainland and island Southeast Asia (de Rosayro, 1974, Whitmore, 1984, Blasco et al., 1996, Stibig et al., 2007). In this study, vegetation terminology is adopted from (de Rosayro (1974), Blasco et al. (1996)) and Cerling et al. (2011) that are based on canopy density. The principal vegetation types mainly include forest, woodland, thicket and grassland formations. Forest is defined as an area with continuous stand of trees of at least 10-m tall with interlocked canopy, with a coverage density of >80%). In Blasco et al. (1996), the forest category is further differentiated into rain forest formations (including: tropical lowland evergreen and semi-evergreen rain forests, upper and lower tropical montane rain forest, peat swamp and fresh-water swamp forests), mangroves and monsoon/deciduous forest formations (including dry evergreen forest, tropical dry and moist deciduous forests).

There are four different vegetation types that have a canopy coverage varying between 40 and 80% and a field layer dominated by grasses: woodland, bushland, thicket and shrubland. These vegetation types are defined by the height of woody plants. Woodland is an open stand of trees at least 8 m tall. Bushland is an open stand of bushes usually between 3 and 8 m tall. Thicket is a closed stand of bushes and climbers usually between 3 and 8 m tall, while shrubland is an open or closed stand of shrubs up to 2 m tall. The general terminology "woodland" is used to categorize these four functionally distinct vegetation types, since the isotopic method cannot clearly distinguish between woodland, bushland, thicket and shrubland (Cerling et al., 2011).

The vegetation types that have the least canopy cover are wooded grassland and grassland. Wooded grassland is defined as a land covered with grasses and other herbs, with canopy cover between 10% and 40%, while grassland is land covered with grasses and other herbs, with woody cover <10%. The terminology savannah, which is defined as 'mixed tree-grass systems characterized by a discontinuous tree canopy in a conspicuous grass layer' (Ratnam et al., 2011), is also used in this study. This term commonly includes the structural categories of wooded grassland and grassland (Cerling et al., 2011, 2015).

At the landscape scale, mixed vegetation commonly occurs. Included in the mixed vegetation category are: mosaics of forest and woodland, and mosaics of woodland and grassland (Blasco et al., 1996).

Knowing the $\delta^{13}C$ of mammals' bioapatite enables dietary reconstructions of fossils and to distinguish grazers from browsers (Cerling et al., 1997a, MacFadden et al., 1999). This allows inferring the type of habitat and vegetation cover where the mammals lived, since C_3 and C_4 plants usually grow in distinct habitats, dictated by environmental and climatic factors such as aridity, sunlight availability, and vegetation density (Heaton, 1999; Diefendorf et al., 2010; Kohn, 2010).

By using the standard error of enrichment factor of $\delta^{13}C_{enamel}$ values from the modern vegetation biomes and correction for latitudinal differences, Cerling and Harris (1999) suggest $\delta^{13}C_{enamel}$ values of -20 to -12.1 ‰ represent a feeding habitat in closed canopy forest (rainforest and monsoon forest), -12.1 to -7.7‰ as open canopy biomes (such as dry and wet woodland-savannah, dry scrubland, dry monsoonal forest or dry C_3 grassland). Values between -7.7 and -2.1 ‰ are expected for mixed to open habitat where C_3 and C_4 vegetation are available (woodland, wooded grassland and grassland), the more negative values indicate a larger proportion of C_3 plants, which decreases gradually to more positive $\delta^{13}C$ values (Passey et al., 2002). The proportion between C_3 and C_4 plants in the mixed habitat may also vary due to seasonal influence. Meanwhile, $\delta^{13}C_{enamel}$ values more positive than -2.1‰ are expected for open and dry grassland with pure C_4 plants.

2.2.2 Oxygen isotopes

While $\delta^{13}C$ values are commonly used to determine an animal's diet, the $\delta^{18}O$ values provide information the relative condition of an animal's ingested body water as a complex function of climate (precipitation and temperature), diet, physiology and geographical condition (Dansgaard, 1964, Longinelli, 1984, Ayliffe and Chivas, 1990, Bocherens et al., 1996, Kohn, 1996, Kohn et al., 1996).

2.2.2.1 Incorporation of ^{18}O in animal tissue

The $\delta^{18}O$ value is incorporated in the mineral phase of skeletal and dental tissues mostly bound as phosphate (PO_4^{3-}) and carbonate (CO_3^{2-}), with the greater amount being incorporated in the phosphate. Carbonate comprises only 2–4 % of the skeletal or dental mineral phase (Tütken and Vennemann, 2009). The PO_4 component is less susceptible to inorganic diagenetic alteration than the CO_3 component. However, the CO_3 component suffers less from isotopic exchange due to microbial-mediated alteration (Domingo et al., 2013). Therefore, both are usable for the reconstruction of the in vivo signal of animals, as the $\delta^{18}O$ values of the phosphate and carbonate components are correlated (Iacumin et al., 1996). Thus, $\delta^{18}O$ values preserved in fossil enamel help to reconstruct climatic conditions as well as infer information concerning animal ecology. In this study, only the $\delta^{18}O$ incorporated in the carbonate phase has been measured. In vertebrates the skeletal and dental bioapatite oxygen isotope values are controlled by a number of factors, such as direct intake of meteoric drinking water and by water from food intake, body temperature and inhaled oxygen. Meanwhile, $\delta^{18}O$ values of drinking water are strongly influenced by climate as well as local geography.

2.2.2.2 Animal physiology *and drinking behaviour in controlling* $\delta^{18}O_{enamel}$ values

For endothermic terrestrial mammals like Proboscidea, the body temperature and the oxygen isotope equilibrium fractionation between the body water and bioapatite is constant. Thus the bioapatite $\delta^{18}O$ values of vertebrate skeletal and dental tissues are mainly controlled by the composition of ingested meteoric water ($\delta^{18}O_{H2O}$) (Longinelli, 1984, Luz et al., 1984, Luz and Kolodny, 1985, Kohn et al., 1996, Bocherens et al., 1996, Levin et al., 2006, Tütken, 2014), thus their $\delta^{18}O_{enamel}$ should be best suited for tracking local meteoric water values. For certain ectothermic vertebrates such as the crocodile, that only mineralise bioapatite of their bones and teeth in a narrow temperature window, $\delta^{18}O$ values are also mainly controlled by the composition of ingested meteoric water (Barrick et al., 1999, Amiot et al., 2007). However, since the body temperature of ectothermic animal is determined by the ambient water

temperature, they directly reflect the $\delta^{18}O$ of their habitat and thus ectothermic animals have generally lower $\delta^{18}O$ values (Bocherens et al., 1996, Clementz et al., 2008).

Drinking behaviour of the animal must be considered as a secondary factor affecting the $\delta^{18}O$ value in the bioapatite. The $\delta^{18}O$ values of terrestrial dominant and obligate drinkers, which obtain most of their body water from drinking water, mainly depend on the values of meteoric water. As modern elephant species are considered as obligate to predominant drinkers (Sukumar, 1990, Morris et al., 2006), their $\delta^{18}O_{enamel}$ strongly reflects the ingested meteoric water (Levin et al., 2006). Considering morphological and anatomical similarity to modern elephants, older Proboscidea taxa are assumed to possess similar drinking behaviour as modern dominant to obligate drinkers. Meanwhile more drought-tolerant species (i.e. Suidae and smaller mammals), usually exhibit less negative values as they gain proportionally more water from leaves, fruits, and seeds, which are more enriched in ^{18}O (Kohn, 1996, Kohn et al., 1996). Plant roots and stems usually display depleted $\delta^{18}O$ compared to other parts of the plants and have rather similar values as meteoric water (Tütken and Vennemann, 2009). The photosynthetic pathway of plant food could also influence $\delta^{18}O_{enamel}$, especially for drought-tolerant species. There is a tendency for the leaf water in C_4 plants to be more ^{18}O-enriched than water in C_3 plants, with the difference diminishing from an average of ~5‰ in arid environments to ~1‰ in humid environments (Helliker and Ehleringer, 2002). Furthermore, ^{18}O is enriched during metabolic processes and incorporation in to the body tissues, thus the $\delta^{18}O_{enamel}$ values would be higher compared to the $\delta^{18}O_{H2O}$ values (Luz et al., 1984, 1990, Ayliffe and Chivas, 1990, 1994).

2.2.2.3 Climate control on the $\delta^{18}O$ values of meteoric drinking water

The stable oxygen isotope composition of meteoric water ($\delta^{18}O_{H2O}$) exhibits spatial variation across the Earth's surface, and is closely related to regional climate regimes. The main factors are mean air temperature and the amount of precipitation-evaporation (Dansgaard, 1964, Rozanski et al., 1992, Gat, 1996). In tropical areas, where the difference between coldest and warmest temperature is not extreme and the temperature is higher than 20° C for most of time, temperature has a rather weak influence on stable isotopes in precipitation (Gat, 1996, Araguás-Araguás et al., 1998). Instead, the amount

of precipitation, the degree of air mass rainout during moisture transport and potential evapo-transpiration predominantly control the ratio of oxygen isotopes in regional meteoric water, which directly influence the $\delta^{18}O$ values in available surface drinking water (Hoffmann and Heimann, 1997, Araguás-Araguás et al., 1998, Aggarwal et al., 2004). In such contexts, the ^{18}O values decrease when the amount of precipitation increases or when the evaporation decreases and vice versa (Dansgaard, 1964). The isotopic values of meteoric water for different regions is determined by moisture source of the region (see explanation in Section 2.3.3)

In tropical SE Asia, seasonal variability and monsoon strength are the dominant controls on $\delta^{18}O$ values in meteoric water. The extent of the seasonal $\delta^{18}O$ range within the studied area is recorded by several proxies, as presented in Table 2.1. With an assumption that such variability also occurred in the past, the difference in the measured $\delta^{18}O$ values of tooth enamel, can be considered as the seasonal difference. In addition, extreme climate conditions such as El-Niño Southern Oscillation (ENSO) events, would also significantly affect the seasonal variability of meteoric $\delta^{18}O_{H2O}$ values (Charles et al., 1997, Beaufort et al., 2001, Stott et al., 2002).

Table 2.2 The amplitude of inter-annual $\delta^{18}O$ from several proxies.

proxy	**reference**	**difference between annual minimum and maximum $\delta^{18}O$ values**
tropical tree rings (Thailand, Java, Laos, Vietnam)	Poussart et al., 2004, Xu et al., 2011, Sano et al., 2012	4‰ to 12‰
rainwater (weather stations in SE Asia main cities)	WMO IAEA and WMO WMO, 2006	4‰ to 10‰
cave dripwater (Borneo)	Cobb et al., 2007	4.4‰ to 6‰
terrestrial bivalve mollusc	Stephens and Rose, 2005, Marwick and Gagan, 2011	3‰ to 6‰

2.2.2.4 Local geographic control on the $\delta^{18}O$ values of meteoric drinking water

Besides climatic conditions, the local $\delta^{18}O_{H2O}$ values of meteoric water are also influenced by local geographic conditions, such as latitude, altitude or distance from the moisture source area and morphology of the water body (Dansgaard, 1964, Rozanski et al., 1993, Higgins and MacFadden, 2004, Levin et al., 2006), as summarised in Fig. 2.4. The "continental effect", also referred to as the distance-from-coast effect, defined as a progressive ^{18}O depletion in precipitation with increasing distance from the moisture source area (in this case, the ocean), varies considerably from area to area and from season to season, even over a low-relief profile (Dansgaard, 1964). The higher the latitude as well as altitude, the $\delta^{18}O$ values are lower (Rozanski et al., 1993). It is also strongly correlated with the temperature gradient and depends both on the topography and the climate regime.

Local parameters, such as evaporation in ponds or streams originating at high altitude must also be taken into consideration for the interpretation of the bioapatite oxygen isotopic composition, since it may provide drinking water to terrestrial vertebrates with $\delta^{18}O$ values different from those of local precipitation (Dansgaard, 1964, Bocherens and Drucker, 2007).

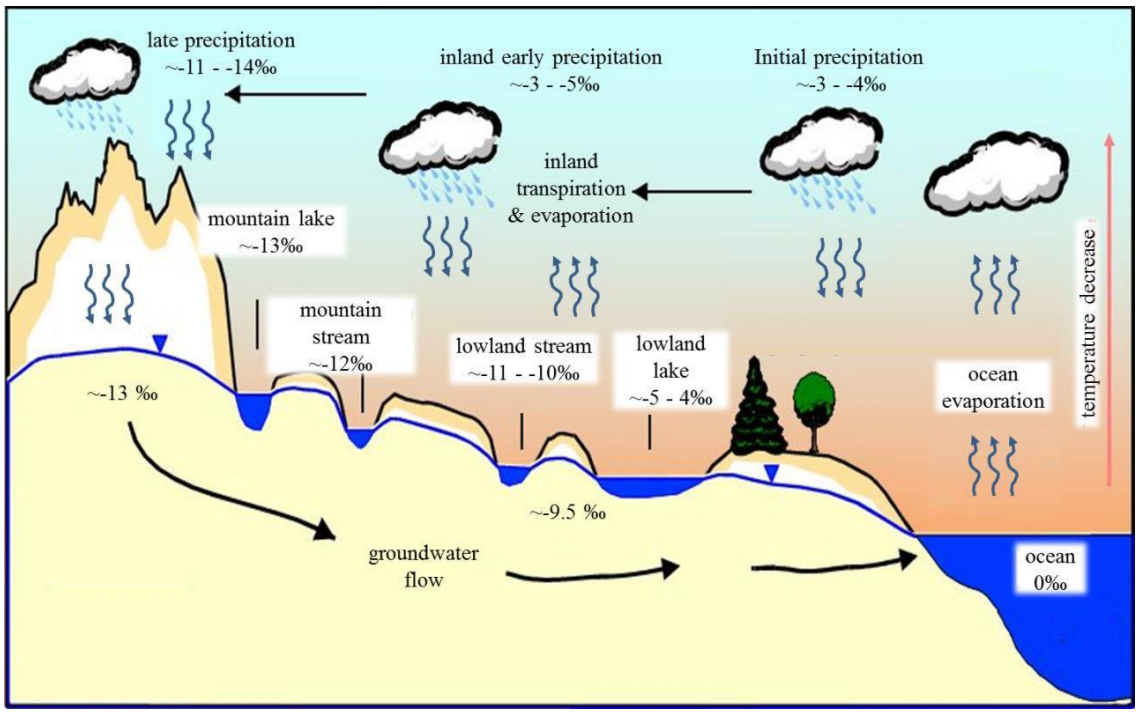

Figure 2.4 Geography (altitude and hydrological body type) and continental effect of $\delta^{18}O$ contents in hydrological cycle (hydrological cycle picture redrawn from Hydroisotop Gmbh,

2011), with $\delta^{18}O$ values taken from Eichlinger et al., 1983, Coplen et al., 2000, Watzel and Heidinger, 2006).

2.3.3 Strontium isotopes ($^{87}Sr/^{86}Sr$) in bioapatite: a potential indicator of animal migration

In addition to carbon and oxygen isotopes, strontium isotopes are widely applied as an isotopic fingerprint of the bedrock substrate in palaeontology and archaeology (Blum et al., 2000, Bentley, 2006, Tütken et al., 2006, Tütken, 2014, Aiglstorfer et al., 2014). Some of the ^{87}Sr isotope is a product of the decay of ^{87}Rb with a half-life of 49.3 Ga. Thus depending on the $^{87}Rb/^{87}Sr$ ratio and age of the rock, $^{87}Sr/^{86}Sr$ ratios differ in rocks of different lithology and geologic age. For igneous rocks, old crustal rocks have a high $^{87}Sr/^{86}Sr$ of 0.711 and young mantle-derived volcanic rocks have ratios around 0.703. Marine carbonates have intermediate values of 0.707 to 0.709 depending on geological age (McArthur et al., 2001).

Strontium is released by weathering processes from the rocks/minerals to the environment and enters as bioavailable strontium via plant uptake and then into the food chain. Strontium is mostly ingested with the food and subordinate amounts with the drinking water. Unlike the light element stable isotopes such as ^{12}C and ^{18}O, $^{87}Sr/^{86}Sr$ is not significantly fractionated during metabolism, tissue formation and biomineralisation. Thus bioavailable Sr isotope signatures are incorporated from the environment directly and unchanged into bioapatite of skeletal and dental materials (Price et al., 2002, Maurer et al., 2012). Therefore the $^{87}Sr/^{86}Sr$ ratio can be used to distinguish local from non-local individuals and migration patterns of the individuals (Beard and Johnson, 2000, Feranec et al., 2007, Arppe et al., 2009, Copeland et al., 2011), provided that regional lithological $^{87}Sr/^{86}Sr$ differences are significantly distinct.

2.3 Significance of interdisciplinary studies in the Southeast Asian palaeontological record

2.3.1 Geological significance

Southeast Asia is an area of complex geological history and unstable landscape (Audley-Charles, 1981, Simandjuntak and Barber, 1996, Hall, 1998, 2001, 2012b). Present-day Southeast Asia is the result of tectonic activity spanning more than 300 Ma (Audley-Charles et al., 1988, Metcalfe, 1988, 2011, van Oosterzee, 2000). However, the most important tectonic activity in SE Asia is the current collision between the Eurasian Plate, the northward moving Indian and Australian Plates and the westward moving Pacific Plate. These collisions brought together continental fragments (Hall, 2011), drove the formation of volcanic arcs and deep ocean trenches (Hall and Smyth, 2008, Simandjuntak and Barber, 1996), forced orogeny and uplift of ocean floor (Hall, 2011), and thereby caused the emergence and submergence of islands (Hall, 1996, 2001, 2012b).

Within SE Asia, these tectonic processes have provided the variability of geomorphology and rapidly changing palaeogeography (Hall, 2001), and thus provide wide ranges of habitats for terrestrial fauna. Geological factors have also directly influenced large-scale climatic and environmental evolution. The uplift of the Himalaya-Tibetan Plateau has been thought to influence enhanced aridity in the Asian interior and the onset of the Indian and east Asian monsoons, intensification of the east Asian monsoons, and increased variability of the Indian and east Asian monsoons (An et al., 2001, Dettman et al., 2003). Meanwhile formation of new islands in the Wallacean and southwest Pacific caused displacement of oceanic circulation within the Indo-Pacific warm pool (IPWP), causing variability of monsoon intensity throughout time (De Deckker et al., 2003).

Furthermore, tectonic uplift and volcanism have variably influenced sedimentation history and landscape evolution. Due to the large variability of local geological factors, a more detailed geological history and sedimentology related to the establishment of palaeoenvironmental reconstructions are explained in separate chapters (Chapters 4-7).

2.3.2 Biogeographical significance

Throughout the Neogene to recent, mainland SE Asia has been a land area (Hall, 2001, 2009) and migration of terrestrial fauna within the continent was not hindered by ocean barriers. Some geographic barriers such as mountain ranges or deserts might have hindered or prevented further dispersal of land mammals. Continental taxa are generally distributed over wider areas than their island relatives. Continental regions are characterised by balanced faunas, since faunal exchange is more likely to have occurred continuously.

Faunal succession in mainland SE Asia and continental islands (Sundaland) reflects a unique relationship (van den Bergh et al., 2001), as the Pleistocene faunas of Sundaland (mainly Java) show great affinity with closely related taxa from the Siwaliks/Irrawaddy, which acted as the major source for new migrations to the SE edge of the continental landmass during the course of the Quaternary (de Vos et al., 1994, Mishra et al., 2010). Migration of terrestrial fauna and its turnover in Sundaland are controlled by a series of periodic sea-level fluctuations down to 120 m below present sea level (Chappell and Shackleton, 1986). During periods of lowered sea levels, which were generally combined with decreasing rainfall, a wide savannah corridor was formed through exposed lands, encouraged migration of fauna between mainland Asia and the then connected continental islands (Bird et al., 2005). De Vos et al. (1994) refer to the migration route from the Asian mainland to Sundaland as the Siva-Malayan route. Meanwhile during periods of high sea-level, overland expansion of fauna to these continental islands was restricted and the population of terrestrial fauna could become isolated. The reconstruction of physiographic change of island Southeast Asia affected by sea-level fluctuations down to 120 m below modern sea-level (Figure 2.5) is demonstrated by a series of palaeogeographic maps presented by Voris (2000). However his reconstructed maps should be used with some caution, as the reconstruction of ancient shorelines based on present-day depth contours, neglecting the influence of tectonics and volcanism.

The continental island fauna commonly comprises mainland elements and reached a balanced faunal assemblage at times when islands were connected to the mainland. But during disconnection and isolation, continental taxa became confined to islands and may have undergone vicariance, the effect of being geographically separated. This

commonly resulted in differentiation into new varieties or even species. On longer isolation of continental islands, most Elephantoidea taxa experienced this vicariance process that commonly led to endemism. It made them different from their relatives in the mainland. A detailed explanation of these turnovers within Java is presented in Chapter 4.

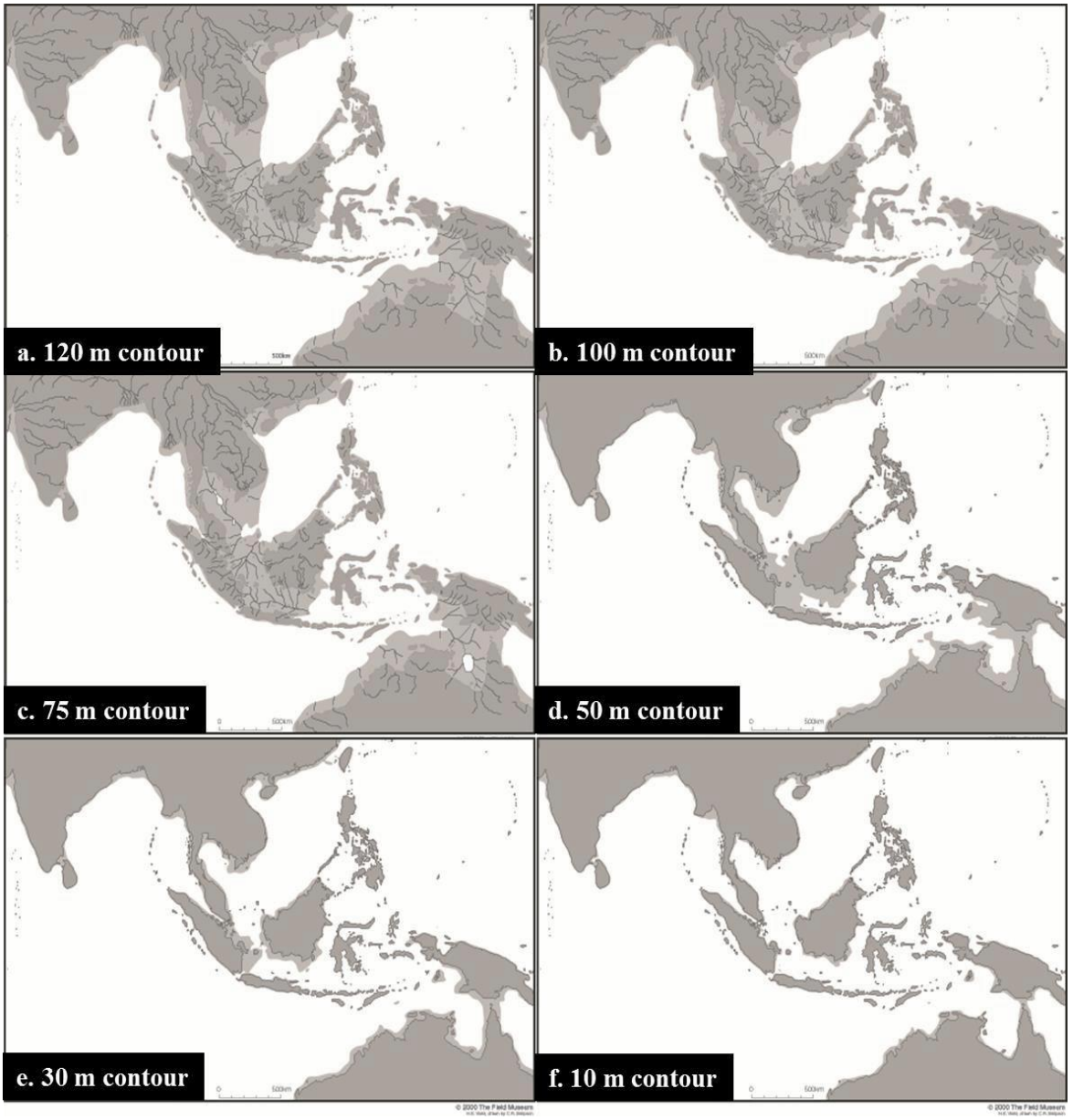

Figure 2.5. Maps of tropical Southeast Asia and Austral-Asia illustrating depth contours of 120 m (a), 100 m (b), 75 m (c), 50 m (d), 30 m (e) and 10 m (f) below present level, as modelled by Voris (2000). Reproduction of maps is courtesy of the Field Museum of Natural History.

Oceanic islands included in this study are located in a transitional zone between Asia and Australia known as Wallacea. This region is renowned for its complex geology and biogeography (Wallace, 1876, Hall, 2012b). The region consists of several microcontinental fragments, oceanic plateaus, together with ophiolites from various areas of origin transferred to this area over millions of years (Hamilton, 1979, Abbott and Chamalaun, 1981, Audley-Charles, 1981, Hall, 1996, 1998). Wallacea is of considerable evolutionary interest, as this area records the sharpest zoogeographical division of the world (Whitmore, 1981, Keast, 2001). The fauna and flora of this area represent the transition between these two continental landmasses: Sunda and Sahul. However, due to the deep ocean barriers, the islands of Wallacea remains physically isolated from both continental landmasses, thus causing the faunal association of Wallacea to exhibit a high degree of endemism. The isolation of islands not only affected endemism of species, but also caused various degrees of dwarfism of large-sized animals (Sondaar, 1977, Heaney, 1986, Mayr, 2000, Raia and Meiri, 2006, Lomolino et al., 2012, van der Geer et al., 2016). Thus, fossils of dwarfed Elephantoidea species have been found in Java (van den Bergh, 1999, van den Bergh et al., 2001) as well as in several Wallacean islands (Hooijer, 1969b, Sartono, 1969, 1979, van den Bergh et al., 2008). Despite consisting of oceanic islands that are considered to have been isolated since their emergence, apparently some islands of the Wallacean islands were inhabited from the Early to Late Pleistocene by various Elephantoidea taxa and other Asiatic terrestrial faunal elements. Since the islands in the southern part of Wallacea, known as the Lesser Sunda Islands (LSI) have emerged relatively recently during the Pleistocene as the result of tectonic and volcanic process, the first terrestrial fauna colonisation of the LSI probably occurred later than in Sulawesi (van den Bergh et al., 2001). Mammalian dispersal routes into and within the Wallacean islands is dealt with in Chapter 5.

Biogeographically, continental and island Southeast Asia represents an important region of Proboscidea distribution and evolution. Mainland Southeast Asia was once a centre of maximum Proboscidea diversity during the Miocene, while during the Quaternary, there was more biodiversity on the islands of Southeast Asia, owing to allopatric

speciation events on emerging islands. Wallacea (Timor) records the furthest SE Eurasian distribution of Proboscidea, but they never reached Australia. Despite having a relatively good record of Proboscidean fossils, detailed palaeoenvironmental analysis is still lacking in this area (Maloney, 1995, Gagan et al., 2000, Dam et al., 2001).

Furthermore, whether the isolation of insular populations from the mainland not only affected the morphology of Proboscidea, but also affected their feeding behaviour, has yet to be studied. Lister (2013) has shown that changes in environment, diet and morphology of African Proboscidea fossils did not temporarily coincide across a record spanning the last 20 Ma. Mainland and island SE Asia offers an excellent opportunity to test if the change of environment and dietary behaviour came before morphological adaptation.

2.3.3 Climatic and environmental significance

2.3.3.1 Neogene and Quaternary palaeoenvironmental/palaeoclimatic events

Global and regional palaeoenvironment and palaeoclimate throughout the Neogene and Quaternary has been reconstructed by using various proxies. A widely used framework, the global oxygen-isotope record for benthic foraminifers from Miocene to Present is combined with regional climatic, tectonic and biotic events as shown in Figure 2.5.

Continuous marine and terrestrial deposits and micropalaeontological data record a period of globally warmer and wet climate that occurred during the Early and Middle Miocene, resulting in a higher average temperature and higher sea-level stands (Miller et al., 1987, 2005, Bartek et al., 1991, Wright et al., 1992, Zachos et al., 1992, 1997, Cramer et al., 2011). At the height of the Miocene Climatic Optimum (MCO, ~17-15 Ma), temperature trended slightly higher as much as 6°C warmer than the present average temperature (Miller et al., 2005, You et al., 2009, Cramer et al., 2011, Foster et al., 2012, Hauptvogel and Passchier, 2012), which is thought to be associated with a significant retreat of the Antarctic ice sheet (de Boer et al., 2010). A major permanent cooling step, known as the Middle Miocene Climate Transition (MMCT), occurred since ~14.8 Ma, associated with increased production of cold Antarctic deep waters and

a major growth of the East Antarctic ice sheet. The MMCT was followed by a gradual cooling by 10 Ma (Wright et al., 1992, Flower and Kennett, 1993, 1994).

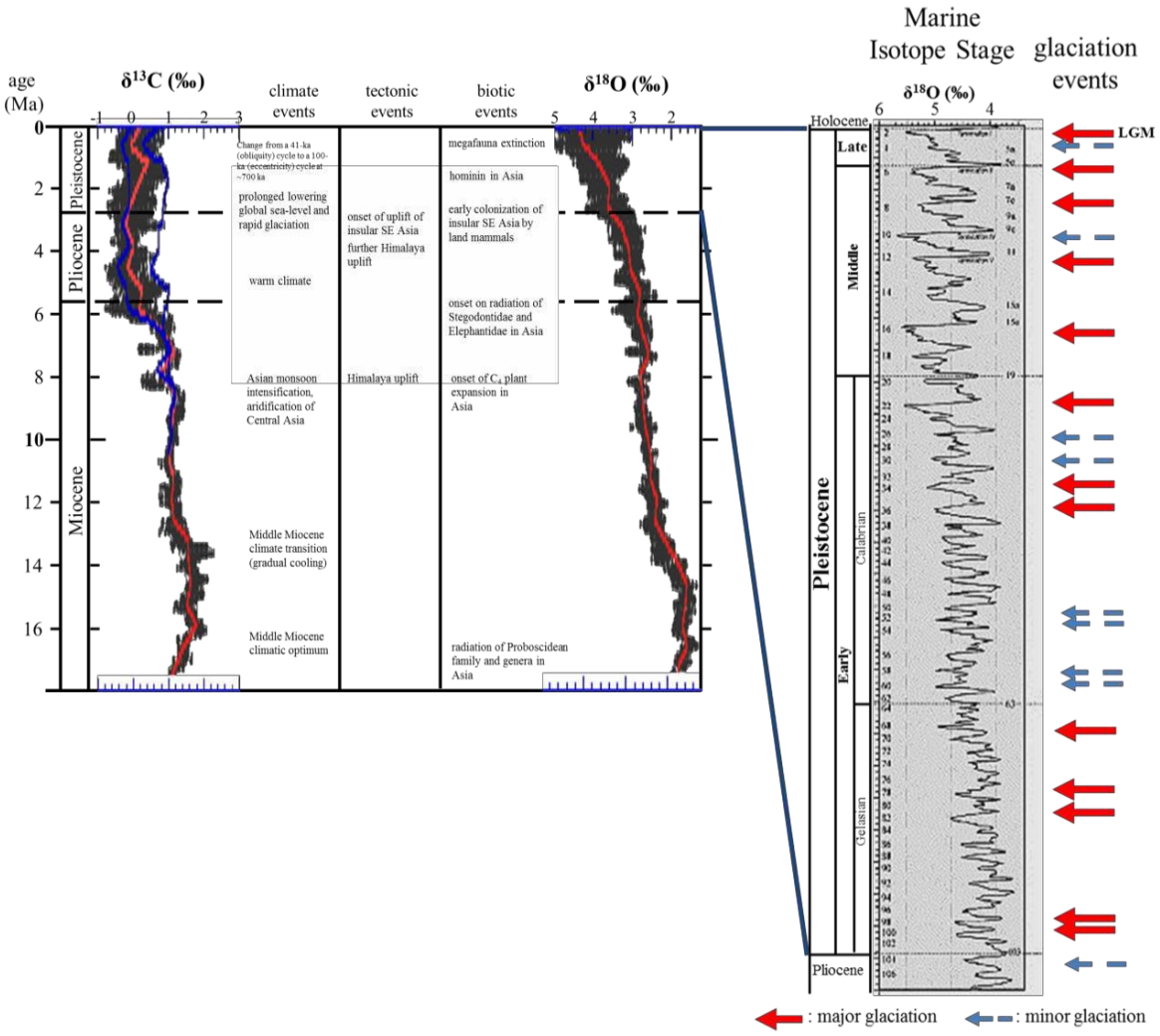

Figure 2.6 Compiled global deep-sea carbon and oxygen isotope records from Middle Miocene to present (modified after Zachos, 2001), with major regional climate, tectonic and biotic events (compiled from references mentioned in the text), as well as major and minor glaciation events during the Pleistocene (modified after Ehlers and Gibbard, 2007)**.**

The Asian monsoons are an important climatic component in the studied area. The onset of the Asian monsoons occurred between 9 and 8 Ma, recorded from continuous aeolian deposits found in China and in marine cores from the Indian and North Pacific oceans (An et al., 2001, Zheng et al., 2004). The onset of the Asian monsoon at about 9-8 Ma coincided with an increase in aridity or a change in the precipitation source, detected in the change in oxygen-isotope values ($\delta^{18}O$) of soil carbonates in Pakistan

(Quade et al., 1989). The increase of $\delta^{18}O$ accompanies changes in vegetation ($\delta^{13}C$) from C_3 (broad-leaf forests) to C_4 (grasses) in Pakistan beginning about 8 Ma (Cerling et al., 1997b). Microflora and pollen records also suggest a change from mixed needle-leaf and/or broad-leaf forests (C_3 plants) to grassland (C_4 plants) vegetation along the Tibetan plateau (Ma et al., 1998, Sanyal et al., 2004), China (Jiang and Ding, 2009) and Thailand (Sepulchre et al., 2010) at about 8 Ma. All of these events imply increasing seasonality due to the Asian Monsoon intensification by about 8 Ma, which is thought to be a result of coeval uplift episodes in the Himalayan-Tibetan region and to the Northern Hemisphere glaciation (An et al., 2001, Zheng et al., 2004). However, an increase in aridity and grassland expansion had up to then influenced the interior part of Asia alone. Whereas along the coastal area of emerged Sundaland (including present day peninsular Malaya, as well as some parts of Borneo and Sumatra) vegetation was still dominated by coastal and low-land rainforests during the Miocene to Early Pleistocene (Sémah, 1997, Sémah et al., 2010, Morley and Morley, 2013). Additional cooling continued through the Late Miocene until the early Pliocene (~6 Ma), indicated by moderate rising of mean marine $\delta^{18}O$ values (Flower and Kennett, 1993, 1994, Wright et al., 1992).

The Early Pliocene (between 6 Ma and 3.6 Ma) is marked by a subtle warming trend, a considerable increase in variability monsoonal strength and overall weakening seasonality (Poore and Sloan, 1996, An et al., 2001, Zheng et al., 2004). During the mid-Pliocene (3.6-3 Ma), the sea surface temperature in the tropical and mid-latitude Pacific were possibly warmer by as much as 3-4° C than at the present (Dowsett et al., 1996, Dowsett and Robinson, 2009), which is associated with initial restriction of circulation between the Pacific and Atlantic (Haug et al., 2001). Global eustatic sea-level during the Early Pliocene is estimated to have been ~25 m higher than present (Miller et al., 2005, Dwyer and Chandler, 2009, de Boer et al., 2010).

A progressive cooling and increasing seasonality occurred after 3 Ma as indicated by a sharp increase in sediment supply in the Indian Ocean, enhanced aeolian fluxes in the Tibetan Plateau and interior of Asia, as well as an increasing trend in $\delta^{18}O$ values trend of benthic foraminifers from the South China Sea (An et al., 2001, Tian et al., 2004, Vandenberghe et al., 2004, Zheng et al., 2004, Klotz et al., 2006). This may correspond with the onset of the major phase of Northern Hemisphere glaciation (Tiedemann et al.,

1994) and another uplift phase of the Himalayan-Tibetan plateau (An et al., 2001, Zheng et al., 2004).

The Pleistocene is marked by continuation of the late Pliocene cool and dry period, as well as repeated glacial-interglacial cycles. Raymo et al. (1998) suggests that through the Pliocene and early Pleistocene global climate variations were governed largely by changes in the Earth's orbital obliquity signal (41 ka cycles). Following the middle Pleistocene shift, the climate variation over the last ~900-800 ka is dominated by 100 ka orbital eccentricity cycles (Clemens and Tiedemann, 1997, Mudelsee and Stattegger, 1997, Medina-Elizalde and Lea, 2005). Glacial periods are marked by colder and often drier climates, a weaker Asian monsoon and seasonality, as well as lower eustatic sea-levels with maximum amplitude of -120 m (Tudhope et al., 2001, Lambeck et al., 2002, An et al., 2011). Ehlers and Gibbard (2007) identified thirteen major glacial events, as well as many minor glacial events (Fig 2.5). The latest glacial stage (LGM) occurred during MIS 2 (22-11.7 ka). Tropical sea surface temperature (SST) changes during the LGM are reported to have varied according to several proxies for palaeotemperature change. This difference ranged from of 2-3° C (Ruddiman et al., 1984, Gagan et al., 2000, Stott et al., 2002, De Deckker et al., 2003) to 4-6° C (Bush and Philander, 1998, van der Kaars, 1998, Visser et al., 2003) lower than present day tropical SST.

In contrast, interglacial cycles are commonly associated with relatively warmer and more humid conditions between the glacial cycles with more extreme seasonal change and intensification of monsoonal strength, as it is at present (Tudhope et al., 2001, de Garidel-Thoron et al., 2005, An et al., 2011). In the Early Pleistocene, prolonged interglacial cycles occurred during MIS 97-83 and 49-37, while the preceding interglacial optimum occurred during the Late Pleistocene Eemian Stage (MIS 5, 131–114 ka). A strong glacial-interglacial shift and the occurrence of arid conditions probably further affected the availability of C_3 and C_4 vegetation coverage in SE Asian habitats. Cooler and drier climates during the Pleistocene glacial periods hampered expansion of rainforest cover and allowed an increase of open woodland and grassland biotopes (Dam et al., 2001).

At the present interglacial period (Holocene), the modern habitats encountered in the studied areas are characterized by a large range of climatic and ecological conditions due to the wide range in different geographical stratifications (Blasco et al., 1996, Peel

et al., 2007), ranging from a semi-arid continental alpine climate to tropical wet climate. The Linxia Basin and the Siwaliks are areas with semi-arid continental climates with an average annual precipitation of 500 to 1000 mm, mainly from summer monsoon precipitation (Jones and Harris, 2013). Tropical dry/monsoonal climates with an average annual precipitation between 1000 and 1500 mm occur in central Myanmar, northeast Thailand and most parts of the LSI islands. This type of climate shows most distinctive differences between wet and dry seasons. Meanwhile, the climate in Sumatra, Sulawesi and Luzon is predominantly tropical humid, with the rainfall more evenly distributed throughout the year and annual variations of temperatures lower than on the continent. The average annual precipitation of these areas commonly reach more than 2000 mm (Jones and Harris, 2013). A gradual change of climatic zones occurs in Java and Flores, with tropical humid ecoregions predominant in the western part of the islands merging to gradually change into tropical dry/monsoonal conditions toward the eastern part of these islands (Peel et al., 2007).

2.3.3.2 Regional circulation and isotope distributions

The consistently warm temperature of the western Pacific warm pool (WPWP) and Indo-Pacific warm pool (IPWP) acts as the major source of latent heat that circulated globally through the Hadley and Walker circulations (Tapper, 2002). These circulations dictate the distribution of the heat pool, the strength of the monsoon, including precipitation and moisture transport (evapotranspiration) and control air mass movements in the Inter Tropical Convergence Zone (ITCZ).

Precipitation in Southeast Asia is mainly distributed in three low-level cyclonic circulation systems originating from the South Pacific and Indian Oceans, each with different oxygen-isotope values (Fig. 2.6): the oceanic monsoon trough (OMT) with low $\delta^{18}O_{VSMOW}$ values (-5.2 to -6.7‰), the continental monsoon trough (CMT) with higher $\delta^{18}O_{VSMOW}$ values (-3.7 to -1.5‰) and the trade wind trough (TWT) with high $\delta^{18}O_{VSMOW}$ values (-2.7 to -2.1‰) (Aggarwal et al., 2004). Thus, variability and fluctuation of $\delta^{18}O_{VSMOW}$ values in each region depends on which circulation contributes the most to that region.

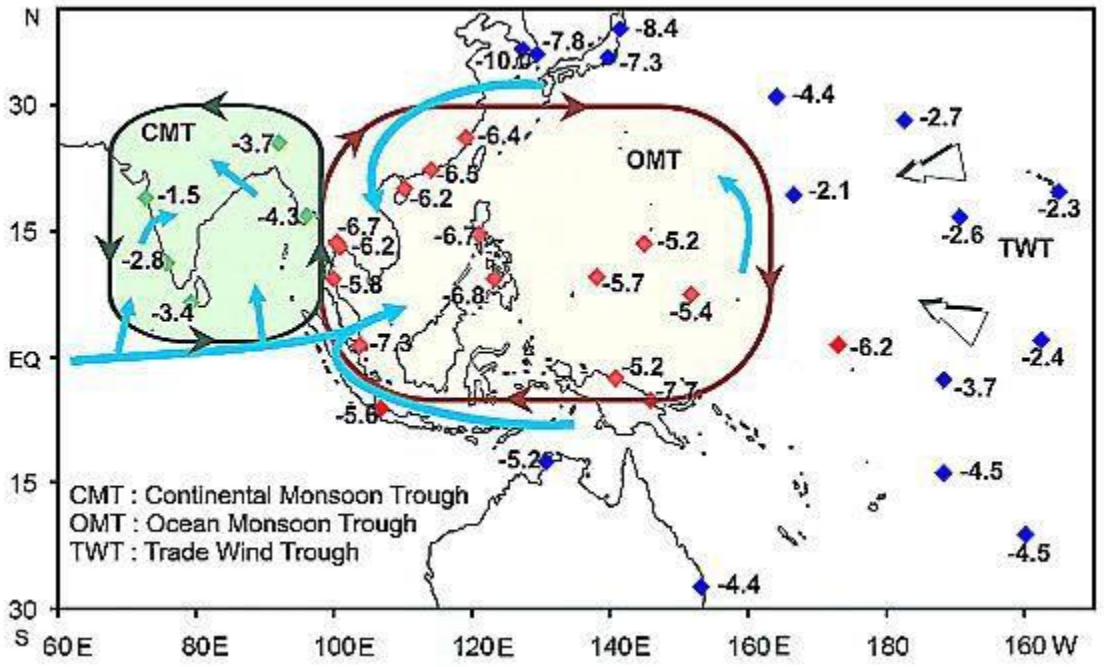

Figure 2.7 Correlation between regional isotope distributions and air circulation and moisture transport patterns in Southeast Asia. Lines with green and red arrows indicate air circulation in the CMT and OMT, respectively. Blue arrows in the CMT and OMT and black arrows in the TWT indicate moisture transport patterns (Aggarwal et al., 2004).

The moisture source of the CMT area is primarily derived from the Indian Ocean, which contains higher $\delta^{18}O$ values. Meanwhile, significant development of cyclonic circulation caused mixing air circulations (CMT, OMT and TWT) and seasonal isotope signatures due to spatial and temporal variability of moisture sources within the OMT (Lim et al., 2002). Based on analysis of meteorological and National Centers for Environmental Prediction (NCEP) re-analysis data, Lim et al. (2002) suggest that Indian Ocean moisture dominates during the initial stage of monsoon in the OMT, whereas that from eastern China and more northern latitudes may dominate during the later stages. Aggarwal et al. (2004) show that palaeoprecipitation in the CMT had also higher $\delta^{18}O$ values than that in the OMT, which is similar to the differences observed in present precipitation.

During the LGM, the oxygen isotope system was modified by: 1) a decrease in Hadley circulation that resulted in a decreased convection, convergence and monsoon strength (Rind and Perlwitz, 2004), which would reduce the seasonal range of $\delta^{18}O$ values; 2) a

depletion of global seawater isotopic composition with an average of 0.8‰ compared to present composition (De Deckker et al., 2003); 3) a depletion of $\delta^{18}O$ values of rainwater, especially in the continent and continental islands' interior, due to the rain out of moisture over the extension of land exposure (De Deckker et al., 2003, Aggarwal et al., 2004). However, for oceanic islands, this effect is probably less prominent due to limited land exposure; 4) reorganisation of ocean circulation (De Deckker et al. 2002), a breakdown of Walker circulation (Stott et al., 2002) and northward movement of the ITCZ, which caused a reduction of the cross equatorial trade winds (Turney et al., 2004) and a reduction in rainfall in the Australasian region (Nanson et al., 1992, Johnson et al., 1999) as well as in lowland Southeast Asia (Kershaw et al., 2001). However, in spite of a significantly weaker monsoon during the LGM, changes in the isotopic composition of the oceans, as measured in the isotopic composition of glacial period groundwater, reveal that the basic structure of air circulation and moisture transport patterns remained stable since the LGM (Aggarwal et al., 2004). Interpolated from the isotopic cycle during the LGM, the isotopic systems during previous glacial periods are presumed to have resembled the LGM. In contrast, enhanced circulation occurred during warmer interglacial periods, which caused the opposite effects as compared to glacial times (Thunell et al., 1994, Ravelo and Andreasen, 2000, Lambeck et al., 2002).

2.3.3.3 Present climate and vegetation of the study area

The present-day climate and type of vegetation cover of the study area varies greatly, depending on the geographical position. The Köppen-Geiger climate classification (Köppen and Geiger, 1930) based on Peel et al. (2007) is used here to classify the present day climate of the sub-areas of the study region, while the classification of vegetation refers to the FAO ecological zones classification (FAO, 2001). The annual mean precipitation data were obtained from OpenStreetMap licensed under the Open Data Commons Open Database License (ODbL). The classification of climate, vegetation and annual precipitation for each study area are presented in Table 2.3 as follows.

Table 2.3 Classification of climate, vegetation and annual precipitation of study area

Region	Köppen-Geiger climate classification	Vegetation classification	Annual Precipitation
Linxia Basin, Tibetan Plateau	BSk (Cold semi-arid)	Subtropical steppe	492 mm
Siwalik	BSh (Hot semi-arid)	Tropical shrubland	679 mm
Irrawaddy	Aw (Tropical monsoon or savanna climate)	Tropical dry forest	673-1624 mm
Khorat	Aw (Tropical monsoon or savanna climate)	Tropical moist deciduous forest	1093 mm
South Sumatra	Af (Tropical rainforest)	Tropical rain forest	1934-3455 mm
West Java	Af (Tropical rainforest) and Am (Tropical monsoon)	Tropical rain forest	1663-3442 mm
East Java	Am (Tropical monsoon) and Aw (Tropical monsoon or savanna climate)	Tropical moist deciduous forest, Tropical dry forest	1453-2428 mm
South Sulawesi	Af (Tropical rainforest) and Am (Tropical monsoon)	Tropical rain forest, Tropical moist deciduous forest	1854-1956 mm
Luzon	Af (Tropical rainforest)	Tropical rain forest	2140 mm
Flores	Am (Tropical monsoon) and Aw (Tropical monsoon or savanna climate)	Tropical moist deciduous forest to tropical savannah	1016-1857 mm
Timor	Aw (Tropical monsoon or savanna climate)	tropical savannah	847 mm
Sumba	Aw (Tropical monsoon or savanna climate)	tropical savannah	931 mm

2.3.4 Neogene-Quaternary biostratigraphic significance

Palaeontological study of mainland Southeast Asia started as early as the 1830s, mainly from the Siwalik deposits of the Indian subcontinent (Pilgrim, 1913) and Irrawaddy (Falconer, 1868, Colbert et al., 1938). Meanwhile in island Southeast Asia, especially in Java, most mammalian fossil fauna were discovered during the Dutch occupation since the 1850s (Theunissen et al., 1990). A wealth of information about the palaeontological

record and faunal succession has become available for Java over the past decades due to a large number of research projects and substantial discoveries of hominin fossils. In the last three decades, the fossil record of the other parts of mainland and islands SE Asia is rapidly catching up with the work that has been done in the Siwaliks and on Java, especially in localities where early hominins and their stone artefacts were found, such as Flores and Sulawesi, or at places where the Neogene-Quaternary section is most complete and accessible (i.e. Tibet Plateau). The palaeontological record from other regions (Khorat Plateau, Philippines, Sumba and Timor) is still poorly understood due to a lack of palaeontological and stratigraphic research.

Most of the early discovered fossils were obtained second or third-hand from surface collections by local villagers, which were then followed up by palaeontological expeditions. Early expeditions generally only focused on collecting large amounts of specimens, and apparently did not record detailed locality documentation, which left uncertainties regarding the exact stratigraphic position, (i.e. Sven Hedin Expeditions in Tibetan Plateau, Bohlin and Hedin, 1937, Bohlin, 1942, 1945, 1946, 1953) and fossil collection Java before 1888 (Martin, 1883, 1884, 1887, 1888, 1890). Better documentation of fossil records and stratigraphic context was obtained when systematic large-scale and well-planned excavations were conducted (i.e. Dubois excavations between 1888 and 1890 and the Selenka expedition between 1906 and 1908, both at Trinil, Java; Tibetan Plateau since the 1990s to present, excavations in Flores and Sulawesi from the 1990s to present). This enabled the establishment of a biostratigraphic scheme and faunal succession of the SE Asia regions. Reliability and resolution of faunal turnover in biostratigraphic frameworks are varied from one locality to another depending on the availability of interdisciplinary approaches (i.e. geochronology, lithostratigraphy and palaeoenvironmental studies) that have been used to establish the biostratigraphic framework of each region. In regions where fossil records, stratigraphy and geochronological data are lacking, interpretation of palaeoenvironment remains limited, as presented in Table 2.4.

Table 2.4 Summary of faunal successions of studied areas

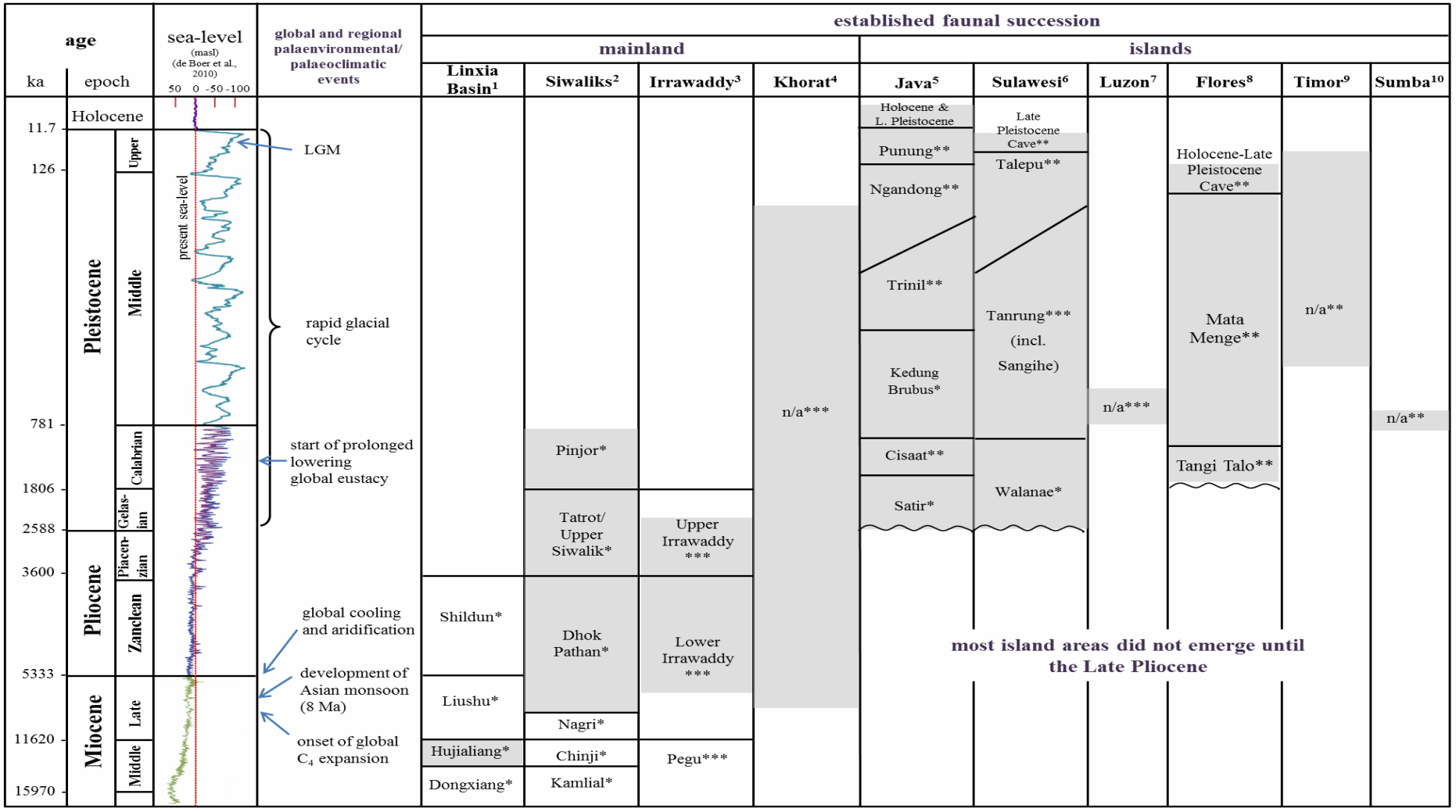

Sea-level scales are arranged differently to accommodate faunal succession in different areas. Grey shade indicates age interval analysed in this study. Numbers 1-10 indicate references for faunal assemblages as follows:

1. Li et al., 1995, Deng, 2004, Deng et al., 2004
2. Pilgrim, 1913, Cheema et al., 1977, Barry et al., 1982, Hussain et al., 1992
3. Takai et al., 2006
4. Hanta et al., 2005, Chaimanee et al., 2006, Thasod, 2007, Hanta et al., 2008, Thasod et al., 2012, Deng et al., 2013
5. de Vos et al., 1982, Sondaar, 1984, van den Bergh, 1999, van den Bergh et al., 2001, Joordens et al., 2015
6. van den Bergh, 1999, van den Bergh et al., 2001
7. Adams, 1910, Beyer, 1949, von Koenigswald, 1956, Lopez, 1972, Bautista, 1991, 1995, Croft et al., 2006, Heaney et al., 2011
8. van den Bergh, 1999, van den Bergh et al., 2001, Brumm et al., 2010
9. Hooijer, 1969, 1971, 1972c, Sartono, 1969
10. Sartono, 1979, van den Bergh, 2011

Asterisks (*) indicate the methods that were used to determine the age of faunal assemblages: *palaeomagnetic, **radiometric dating, ***interpolation from other faunal assemblages

Chapter 3. Materials and Methods

3.1 Materials

Identification and measurement of fossil and extant animal specimens were carried out for 28 different Proboscidean taxa, Celebochoerus heekereni, crocodiles and murine rodents from Southeast Asia mainland and island localities. Stratigraphic origins and grouping of samples from all analysed regions are explained in separate chapters (Chapters 4-6), while detailed information for each sample is presented in Appendix II.

Bulk enamel samples were also obtained from fossil and extant specimens. A series of enamel samples of individual molars from Elephas hysudrindicus from Sunggu locality, Java was also taken to study the seasonal change and the molar growth period for each individual. The specimens belong to MGB (Museum Geologi Bandung, Indonesia), ARKENAS (Pusat Penelitian Arkeologi Nasional, Jakarta, Indonesia), BPSMPS (Balai Penelitian Situs Manusia Purba Sangiran, Sragen, Indonesia), NBC (Naturalis Biodiversity Center, Leiden, Netherlands), NRIPM (Northeastern Research Institute of Petrified Wood & Mineral Resources, Nakhon Ratchasima Rajabhat University, Thailand), NMP (National Museum of Philippines) and private collections of Dr. Chavalit Vidthayanon (Thailand) and Mr. Dakri (Semedo, Central Java, Indonesia). The carbonate components of all samples were analysed for carbon and oxygen isotopic composition and 20 samples from Java and Flores were selected for $^{87}Sr/^{86}Sr$ analysis. Comparative data from previous studies are taken from Quade et al. (1992), Nelson (2007), Pushkina et al. (2010), Zin Maung Maung et al. (2011) and Janssen et al. (2016).

Enamel samples were taken from adult molars (M1/M2/M3), if available. These molars have been chosen for analysis because of their abundance in most fossil collections and to allow comparisons between individuals of similar ontogenic stages (adults). This strategy was used to avoid side effects such as sudden shifts in isotopic ratios caused by postnatal stress and weaning in juveniles (Dirks et al., 2012). In case of unavailability or of very small number of adult molars in a fossil assemblage (i.e. Liang Bua), pre-adult molars were also sampled with additional notes. The isotopic values of these pre-adult

individuals are tagged differently from samples from adult individuals and grouped differently in the statistical analysis. If isotopic values of juvenile individuals differed greatly from adult individuals, the isotopic values of pre-adult individuals would not be included in statistical analysis.

Ideally, enamel samples were taken from whole or slightly fragmented teeth, since it is easier to identify the species and rank of each molar. However in many cases only fragmentary molars were available for sampling, so that the exact molar ranks could not always be ascertained. The identification of these fragmented materials is based on distinct morphological characters (if observed), biometrical measurement and the locality/biostratigraphy where these fragment were found. To minimize any mistake in identification of fragmented specimens (e.g. the fragment of deciduous molar of larger taxon could be mistaken for and adult molar of a pygmy taxon) the fragmented samples had to meet the following criteria:

1. Fragmented specimens still have at least one distinct morphological character (i.e. Sinomastodon and Stegoloxodon), which can be identified and/or measured by biometric parameters and compared with range values of specimens from the same assemblage (e.g. transverse width of single ridges).
2. Fragmented specimens represent in situ finds, originating from a site where only a single taxon is known to occur. If there is evidence for more than one species in the locality, the species must be easily distinguishable from each other (i.e. Stegodon and Elephas)
3. If there was no other specimen available other than a surface collected fragment, the locality of where this specimen was collected should have clear lithostratigraphy/biostratigraphic context, and preferably contains only a single taxon.

All samples are listed in Appendix II, together with information on their taxonomic classification, molar rank, locality and information on whether they represent in situ versus surface-collected specimens.

3.2 Methods

3.2.1 Identification and measurement of fossil materials

The description and biometric measurement focus on molar structure since molar materials were exclusively used in this study. These methods are especially applied for new fossil findings that are considered as important to complete the incomplete description of existing species and also for specimens without proper identification in the collections. Morphological identification of each dental specimen is important to confirm the age of each individual and to ensure that each enamel samples are from different individuals, so that multiple isotopic measurements for a single individual can be avoided.

Description and biometric measurement of occlusal structure of Gomphotheriidae and primitive Stegodontidae molar materials follows Tassy (1996a) with slight revision as described in Figure 1.2A, while description and biometric measurement of advance Stegodontidae and Elephantidae molar materials follows Maglio (1973) as described in Figure 1.2B. Biometrical parameters used in this study are:

P: Number of lophids/ridges/lamellae present in one molar. Number indicates the number of observed main lophids/ridges/lamellae, ‘x’ indicates cingulum/half lophids occurs in the anterior and/or posterior, and ‘-‘ indicates incompleteness of the molar.

L: Maximum length of the molar (Fig. 1.2).

W: Maximum width of the molar, measured on the widest ridge of the molar.

w: Width of individual molar ridges.

H: Maximum height of a molar, measured vertically on the lateral side of the highest ridge, between the crown base and the apices of the digitations.

h: Height of individual molar ridges.

ET: Enamel thickness. ET is measured perpendicular to the anterior or posterior enamel surface of molar ridges (Fig. 1.2C).

h/w: Hypsodonty index, in which the maximum unworn height of individual ridges divided by maximum crown width, including cement (if any).

L/W: Ratio between the maximum length (L) and the maximum width (W).

LF: Laminar frequency, representing the number of ridges that occur in 10 cm along the longitudinal plane of the molar at the level of the transverse valley bottoms.

Morphological description and related information of all analysed Proboscidean taxa is presented in Appendix I.

3.2.2 Stable isotope analysis

3.2.2.1 Pre-treatment

Enamel samples were exclusively used in this study. Prior to the enamel sampling, the outer surface of the teeth was cleaned and abraded with a rotary handheld device to minimize the effect of contamination. Enamel samples were mechanically separated from dentine and then powdered by hand drilling with a diamond coated tip burr on a Dremel hand drill, or by crushing the sample with an agate mortar and pestle. Parts of the tooth with stronger coloration and visible cracks were avoided to minimize the effects of contamination and alteration. Approximately, 100 mg of powdered enamel was sampled from each tooth. Enamel was sampled across the tooth, from top to bottom. This strategy was used to obtain an average dietary signal obtained along the entire height of a lamella/ridge. From one specimen (Elephas hysudrindicus from Sunggu), a single tooth lamella was serial sampled at 2.5 mm intervals to analyse the seasonal fluctuations in feeding behaviour during the formation of the molar (see chapter 4.4.3.2.3). For a few tooth specimens, only a small broken fragment of enamel was used in order to reduce damage to rare museum specimens to a minimum. Such samples represent shorter time spans of life history than the averaged samples taken along the entire height of a crown. This information is also listed in Appendix II.

All samples were chemically pre-treated with 2% NaOCl (Natrium hypochlorite, for 24 hours) to oxidise organic residues and 0.1 M CH_3COOH (acetic acid, for 24 hours) to remove exogenous carbonates (Koch et al., 1997). Samples were rinsed with deionised water and dried after each chemical treatment. Pre-treated powders were used for C and O isotopic analysis.

3.2.2.2 Carbon and oxygen isotope measurement of the hydroxyapatite carbonate components

The isotopic analyses were performed in two laboratories. Most analyses were performed in the Geochemical Laboratory, School of Earth and Environmental Science, University of Wollongong, where ~5 mg of powder for each sample was reacted with 105% H_3PO_4 in the MultiPrep at 90° C to produce the CO_2. The liberated CO_2 was then measured for C and O isotopic ratio using Micromass PRISM III mass spectrometer. The measured C and O isotopic composition was calibrated using the standards NBS18 ($\delta^{18}O$ = −23.01‰, $\delta^{13}C$ = −5.04‰$_{VPDB}$) and the NBS19 ($\delta^{18}O$ = −2.20‰, $\delta^{13}C$=1.95‰$_{VPDB}$), NBS20 ($\delta^{18}O$ = −4.14‰, $\delta^{13}C$ = −1.06‰$_{VPDB}$), $CaCO_3$AR ($\delta^{18}O$ = −16.05‰, $\delta^{13}C$ = −28.31‰$_{VPDB}$), TTB-1 ($\delta^{18}O$ = −8.45‰, $\delta^{13}C$ = 0.58‰$_{VPDB}$), 811($\delta^{18}O$ = −10.71‰, $\delta^{13}C$ = −3.32‰$_{VPDB}$) and Chihuahua ($\delta^{18}O$ = −11.68‰, $\delta^{13}C$ = −7.91‰$_{VPDB}$).

In addition, analyses were performed in the Stable Isotope Laboratory of the Earth Sciences Department, Free University Amsterdam. 200-300 µg of sample powders were placed in exetainer vials and flushed with pure (99.99%) helium gas then reacted with H_3PO_4 at 45°C and were left to dissolve for 24 hours. Subsequently, the liberated CO_2 gas was analysed using a Thermo Finnigan GasBench II preparation device interfaced with a Thermo Finnigan Delta Plus mass spectrometer. The measured C and O isotopic composition was then calibrated using the standard IAEA-CO1 ($\delta^{18}O$ = −2.38‰, $\delta^{13}C$ = 2.41‰$_{VPDB}$). Standard reproducibility of routinely run lab standards for this technique typically is better than 0.10‰ for $\delta^{13}C$ and 0.15‰ for $\delta^{18}O$ (1σ). Some samples were analysed in both labs to compare the results for consistency.

3.2.2.3 $^{87}Sr/^{86}Sr$ of hydroxyapatite carbonate

A total of 20 representative samples from Java and Flores, also used for C and O analysis, were selected for $^{87}Sr/^{86}Sr$ analysis. Analyzed taxa include Stegoloxodon indonesicus, Sinomastodon bumiajuensis, Stegodon trigonocephalus, Elephas hysudrindicus, Stegodon sondaari, Stegodon florensis, crocodile, Muridae, and an additional sample of soil carbonate from Mata Menge that had been chemically pre-treated using 2% NaOCl. For $^{87}Sr/^{86}Sr$ analysis, 1–2 mg of pre-treated enamel and soil

carbonate powder were prepared in a clean laboratory. Sample material was weighed into rocket beakers, dissolved with HCl for the separation of Sr by conventional ion exchange chromatography using quartz glass columns filled with resin slurry. Subsequent purification of Sr was achieved in micro columns filled with Elchrom Sr-specified resin using the HNO_3–H_2O technique. Separated Sr samples were eluted loaded on Re single filaments and isotope ratio measurements were performed in a triple jump routine and applying exponential fractionation correction on the Finnigan MAT 262 TIMS mass spectrometers located at the department of Earth Sciences of the Free University Amsterdam. All $^{87}Sr/^{86}Sr$ data are reported relative to a value of 0.710243 for the routinely analysed NBS 987 standard. Sr in blanks was <0.01% of the total Sr in the samples.

3.2.3 Statistical analysis

A population that has three samples or more is eligible for statistical analysis. A population in this study is defined as a group of individuals within a species, within a subspecies or within a species that lived at different fossil-bearing layers/localities/geological times, based on the context of discussion. The statistical analysis has been performed using the PAST® software version 3.0 (Hammer, 2001).

A statistical summary of each $\delta^{13}C$ and $\delta^{18}O$ distribution was calculated for each population. Included in the summary statistic for each population are: the number of samples (N), mean value (Mean), median, standard error of the estimate of the mean (Std. error), population standard deviation (square root of variance), and range between minimum and maximum measured isotopic ratio.

Univariate analysis is used in this study to determine any significant differences between groups for one specific variable. Variables specific in this study, $\delta^{13}C$ and $\delta^{18}O$, are calculated separately to detect any significant difference for each isotopic variable. Kruskal-Wallis tests (see Davis and Sampson, 1986, Brown and Rothery, 1993 for details) are used to determine the difference between populations. The non-parametric Kruskal-Wallis univariate test is used for this study since analysed groups in general have unequal sample sizes and unequal variances (Kruskal and Wallis, 1952). The 95%

confidence interval is used to determine the difference between groups in both multivariate and univariate tests.

To determine the difference between each pair of groups, a pairwise comparison test is calculated and paired with the Kruskal-Wallis test. If the p value of both tests shows significant inequality of the medians ($p < 0.05$), the table of simple non-parametric “post-hoc" pairwise comparisons based on Bonferroni-corrected pairwise Mann-Whitney test (Mann and Whitney, 1947) is paired with the Kruskall-Wallis test. Both pairwise comparisons are also applying a 95% confidence interval. Both tests are applied for faunal assemblages in order to analyse any difference of diet preference and to detect niche separation between co-occurring taxa. Statistical analysis is also carried out to for each taxon that occurs in more than one faunal assemblage to explore temporal changes in feeding palaeoecology for each taxon as their response to environmental changes.

Chapter 4. Continental Southeast Asia and Sundaland

4.1 Geological context

4.1.1 Geology of mainland Southeast Asia and Sundaland

In mainland Asia, terrestrial mammalian fossil-bearing sediments occur in the basins that formed during the Palaeogene to Neogene. These basins developed as a consequence of the collision between the Indian subcontinent and Eurasia, collision between Australia and Sundaland, as well as local tectonic events that occurred since the Lower Eocene (Hall, 2001, Hall, 2013).

The Neogene and Quaternary fossil-bearing sediments are widely exposed adjacent to and south of the Himalayan Range. The basins that contain these sediments are the foreland basins that developed in response to the weight of crustal thickening when the Indian sub-continent collided and subducted under the Eurasian plate (DeCelles, 2011, Singh, 2013). These foreland basins (Figure 4.1) include the basins in the Siwalik area and other depressions south of the Himalayan Ranges. Due to the same collision, to the North of the Himalayan Range, a compressive force towards the continental crust of Asia caused the formation of back-arc basins. The compression-triggered contraction along with the associated rise, shortening and lateral extrusion were responsible for the formation and uplift of intramontane basins north of the Himalaya Mountains, including the Linxia Basin (Meyer et al., 1998, Tapponnier et al., 2001, Yin et al., 2002).

The Central Myanmar Basin (CMB), in which the Irrawaddy sedimentary sequences were deposited, is a fore-arc basin due to the northeastward subduction of the Bengal oceanic crust beneath the Asian continental plate located in Myanmar. This basin was formed as a result of transtension induced by India-Asia collision that commenced in the Eocene (Swe, 1981). This subduction resulted in volcanism during the Late Oligocene to Early Miocene, the mount Popa Volcano in the central part of the CMB (Bertrand and Rangin, 2003). Northward compression of the Indian subcontinent, combined with southeastward displacement of the Indochina block and northward

compression by the Australia-Asia plate collision produced the N-S trending pull-apart basins from Myanmar to Sumatra, including the CMB (Tapponnier et al., 1986, Maung, 1987, Replumaz and Tapponnier, 2003). The Neogene-Quaternary basin of the Khorat Plateau originated as a pull-apart basin induced by the southeast displacement of Indochina due to the India-Asia collision (Tapponnier et al., 1982, Tapponnier et al., 1986, Polachan et al., 1991, Leloup et al., 2001, Replumaz and Tapponnier, 2003).

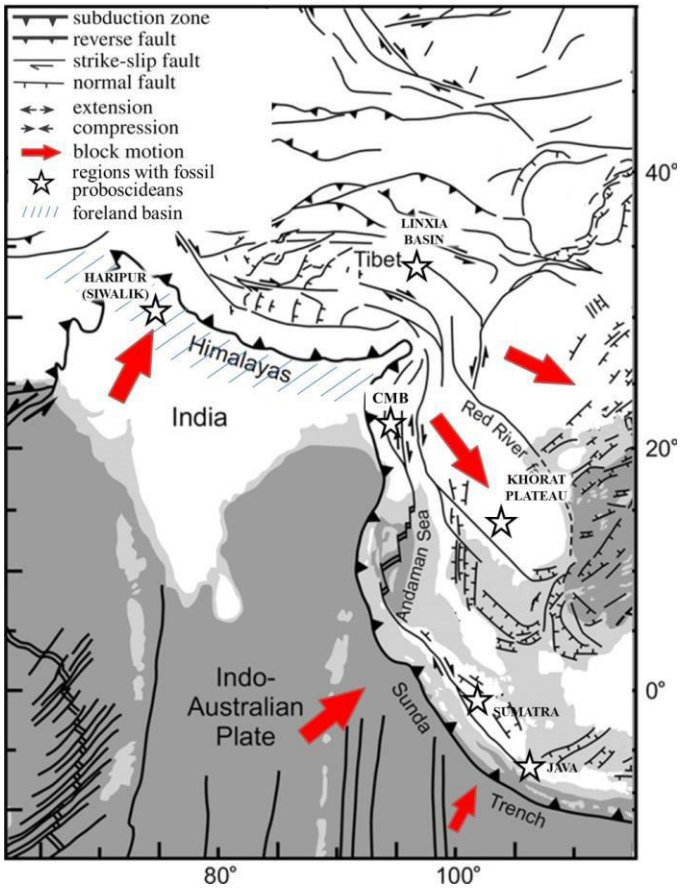

Figure 4.1 Tectonic map of Southeast Asia illustrating Cenozoic structures in the region and the displacement direction of major continental blocks and regions with fossil Proboscidea analysed in this chapter (modified after Tapponnier et al., 1982).

The early geology of the Sundaland is recorded in complexly deformed Late Paleozoic-Palaeogene sediments and associated volcanic and igneous rocks that form the basement rock of Sundaland (Katili, 1975, Hamilton, 1979, Simandjuntak, 2004, Hall and Smyth, 2008, Hall, 2012a, 2012b). After the Oligocene, the tectonic history of Sundaland is mainly controlled by the collision between the Asian and Indo-Australia plate, which induced the formation of basins and volcanic activity in the area. The early activity of

Asian-Indoaustralian subduction during the Oligocene resulted in the formation of the Java Sea Basin and Oligocene-earliest Miocene arc volcanics, which are exposed in the southern part of Java (known as Older Andesites) and the western part of Sumatra (van Bemmelen, 1949, Smyth et al., 2008).

Since the early Miocene, tectonic activity in Sundaland was dominated by regional contraction and uplift, which intensified during the Late Pliocene to Early Pleistocene and led to the full emergence of islands within the Sundaland. The subduction also caused intense volcanic activity all along the Sunda Arc region and generated the alignment of recent volcanoes on Java and Sumatra (Hall, 1998, 2009, 2012b, Hall and Smyth, 2008). The Palaeogene to Miocene sediments of Java and Sumatra are dominated by marine sediments, while the Pliocene and Early Pleistocene sediments mostly consist of deposits that are transitional from marine to terrestrial. These transitional sediments comprise coralline limestones, shallow marine clastics and volcaniclastics. Throughout the Early to Middle Pleistocene, the onset of glacioeustatic sea-level fluctuation effects enhanced the regressional phase and the sedimentation mostly occurred in terrestrial environments. These contain fossils of terrestrial vertebrates and clues for hominin migration and occupation. The geological process and glacioeustatic sea-level fluctuations that took place during the Early to Middle Pleistocene played an important role in controlling the connectivity or isolation of the Sunda islands (Hutchison, 1989, Voris, 2000) and strongly influenced the faunal turnover of Java (Sondaar, 1984, van den Bergh et al., 2001). Sequentially, during the late Pleistocene, tectonic activity is dominated by compressive uplift, leading to the formation of river terraces that are found in many localities in Java (Sartono, 1976). Meanwhile, Quaternary fossil-bearing sediments in Sumatra were only recorded in Late Pleistocene cave sediments (de Vos, 1983).

4.1.2 Stratigraphy and age of vertebrate fossil localities

4.1.2.1 Linxia Basin, Gansu, China

The origin of Platybelodon fossils analysed in this study is unknown. However, based on the description of morphological characters, size range (see Appendix I.1.1) and preservation, these fossils bear closest resemblance to fossils derived from the

Hujialiang Formation of the Linxia Basin. The Linxia Basin, ~200 km long and 75 km wide, is located in the northeastern part of the Tibetan Plateau, Gansu Province, western China. Most of the Platybelodon fossils were found in the Hujialiang Formation, while others originate from the Donxiang Formation (Deng et al., 2004, Wang et al., 2012a). The basin lies at elevations of 2000 -2600 m a.s.l., at the junction of the northeastern margin of the Tibetan Plateau and the western margin of the Loess Plateau (Figure 4.2). The Neogene and Quaternary sedimentary units in this basin overlie Palaeozoic meta-sedimentary terrestrial and marine sequences, as well as Palaeozoic to early Mesozoic plutonic rocks (Garzione et al., 2005). The Cenozoic sediments are well developed, consisting of 400 to 1600 m-thick Neogene and Quaternary lacustrine and fluvial sequences, which are rich in fossil faunas. Deposition of the Cenozoic deposits in the Linxia Basin began at 29 Ma and continued nearly without interruption until 1.7 Ma (Li et al., 1995, Fang et al., 2003). This Cenozoic red sediment is overlain by Late Quaternary loess and recent alluvium (Garzione et al., 2005).

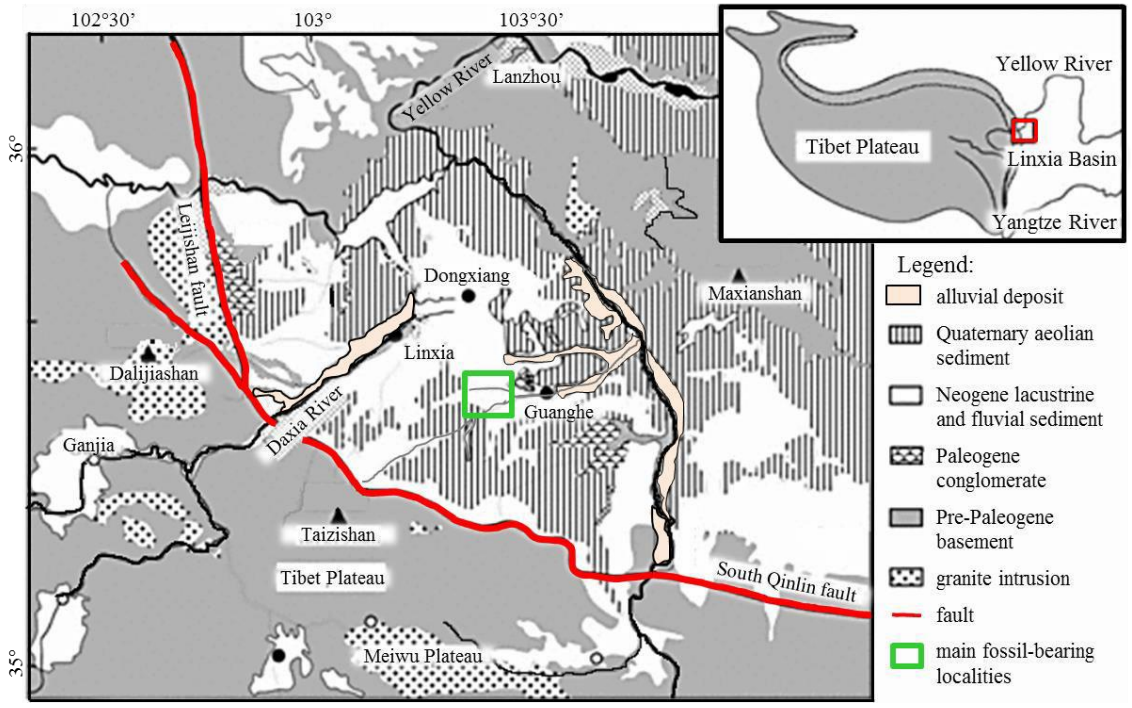

Figure 4.2 Simplified geological map of the Linxia Basin, main Middle Miocene mammalian fossil-bearing localities indicated by the green rectangle (redrawn after Li et al., 1995)

The Hujialiang Formation consists of 20-30 m thick greyish-green sandstone and conglomerate beds, which were deposited in a fluvial environment (Deng et al., 2004). Based on magnetostatigraphic correlation, Deng et al. (2012) suggest its age as late

Middle Miocene (~12.6 Ma). The Hujialiang Formation overlies the lower Middle Miocene Donxiang Formation and is overlain by the Late Miocene Liushu Formation. The Dongxiang Formation consists of brownish-red mudstones and siltstones, deposited in a lacustrine environment (Deng et al., 2004).

4.2.2.2 Tha Chang Sandpit, Khorat Basin, Northeast Thailand

The Tha Chang sandpits are located in the Chaloen Phra Kiat and Non Sung District of Nakhon Ratchasima Province. This area is part of the Khorat Plateau geological province. A geological map of the sand pits is presented in Figure 4.3 The basement lithology of this province is dominated by non-marine terrestrial Mesozoic red bed sequences, comprising the succession of the Huai Hin Lat, Nam Phong, Phu Kradung, Phra Wihan, Sao Khua, Phu Phan, and Khok Kruat Formations (Meesook et al., 2002). These lithological formations are overlain by evaporites of the Maha Sarakham Formation and the Phu Tok Formation (Satarugsa et al., 2005). Pre-Mesozoic plutonic, volcanic rocks, chert and Permian to Triassic marine sediment and Palaeogene basalt sparsely occurs in the lower part of the sequence. The latest Mesozoic formations are unconformably overlain by the Neogene and Quaternary fluvial and paludrine deposits of gravel, sand, silt and clay deposited by the ancient Mun River.

Vertebrate and flora fossils are abundant in these fluvial sediments (Suteethorn et al., 1997, Nakaya et al., 2002, Howard et al., 2003., Hanta et al., 2008, Deng et al., 2013a). Haines et al. (2004) subdivided the sequence into two units: a lower Fe-reduced unit, referred to as Unit A and an upper oxidised unit, referred to as Unit B. More recently, Duangkrayom et al. (2014) divided the sediment into 6 units (Unit 1-6, Fig. 4.3) based on lithofacies characteristics. Units 1-5 (Duangkrayom et al., 2014) are a more detailed subdivision of the Unit A of Haines et al. (2004), while Unit 6 is equivalent to their unit B. There is no radiometric date or palaeomagnetic data available for this region. Based on fossil content, Unit 1-5 are thought to be the latest Miocene to Pliocene in age, whereas Unit 6 is Pleistocene (Duangkrayom et al., 2014).

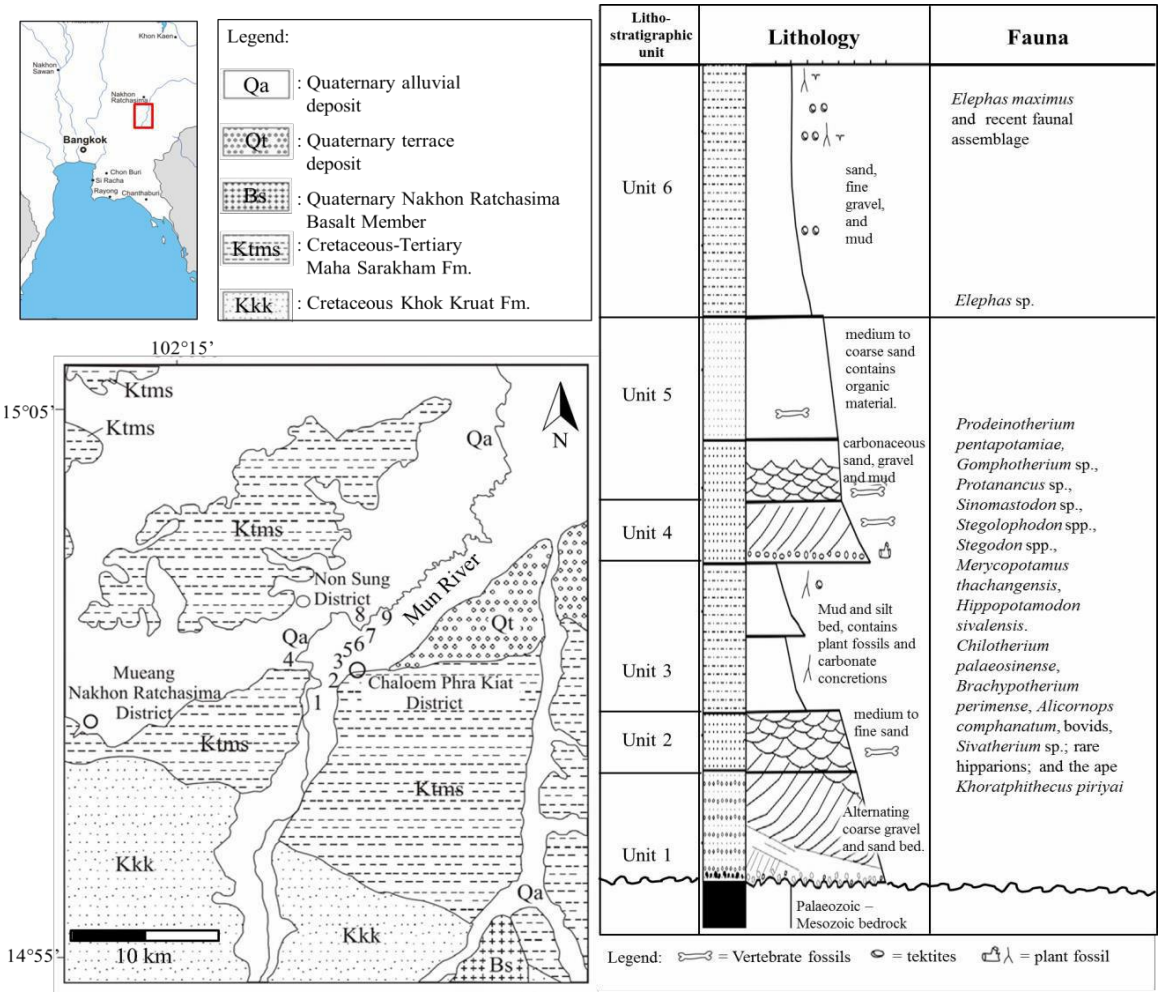

Figure 4.3 Left: Geological map of Tha Chang locality, showing location of sand pits (numbers 1-9) studied by the Thailand-Japan Expedition Team (modified from Hintong et al., 1984; Yuyen and Sirinavin, 1985, Thasod, 2007). Right: Sedimentary log of one of the sections (Section 4) analysed by Duangkrayom et al. (2014), showing lithostratigraphic units of fossil-bearing sequence in the Tha Chang locality (modified after Duangkrayom et al., 2014).

4.2.2.3 Upper Siwalik deposits around Haripur, Northern India

Deposits of the Siwalik Group are exposed continuously along the southern Himalayan foothills from the Potwar Plateau in western Pakistan to northern India (Figure 4.4a). This group consists of fluvial sediments dated between Miocene and Pleistocene. Based on the faunal content, Medlicott (1879) followed by Pilgrim (1913) classified the Siwalik Group as Lower, Middle and Upper Siwalik, further divided as (from older to younger): the Kamlial, Chinji, Nagri, Dhok Pathan, Tatrot, Pinjor and Boulder Conglomerate formations. All samples analysed in this study originate from the Upper Siwalik deposits around Haripur, Northern India (Figure 4.4b). The lithology of this group consists of the Tatrot, Pinjor and Boulder Conglomerate Formations.

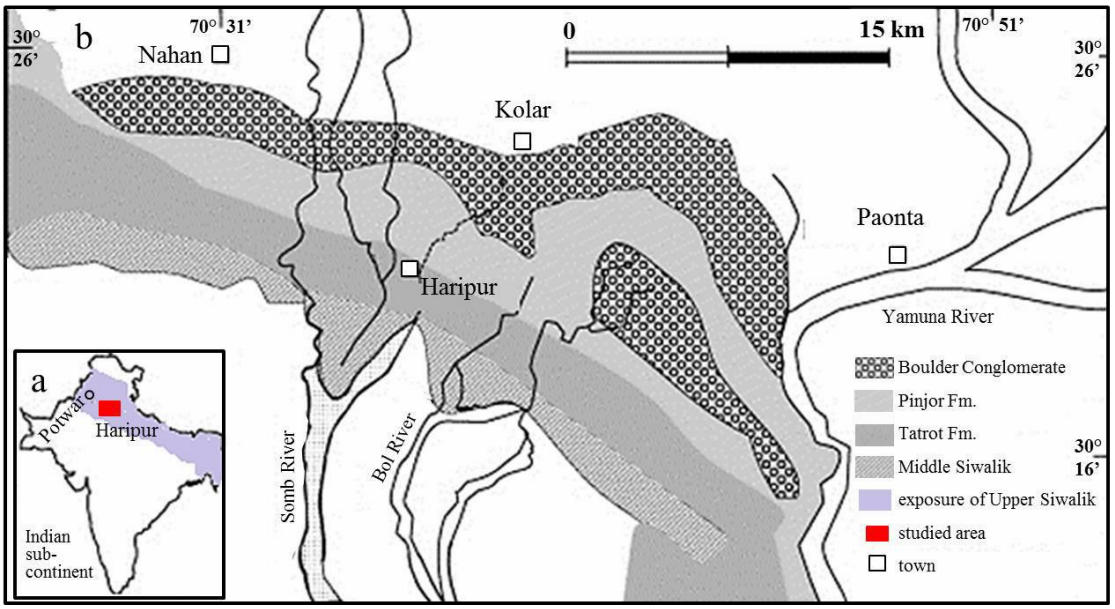

Figure 4.4 a: Map of the Indian sub-continent showing the distribution of the Siwalik Group sediments. **b:** Geological map showing lithostratigraphy of the Haripur and surrounding area in Himachal Pradesh, northern India, the locality of the fossil specimens analysed in this study (modified after Ghosh et al., 2004).

The Tatrot Formation is characterized by layers of thin grey sandstones, variegated mudstones and siltstones. The lithology of the Tatrot Formation gradually changes upward into brownish sandstones and mudstone characterizing the Pinjor Formation, while the Boulder Conglomerate Formation comprises gravels, sandstone and mud layers. The boundary between The Tatrot and Pinjor Formation is close to the Gauss-Matuyama magnetic reversal (Rangga Rao et al., 1995, Cande and Kent, 1995), suggesting an age estimation of 2.58 Ma. Meanwhile the boundary between the Pinjor Formation and Boulder Conglomerate has been found to be time transgressive, between 1.77 and 0.63 Ma (Rangga Rao et al., 1988, Rangga Rao et al., 1995, Nanda, 2002, Kumaravel et al., 2005).

4.2.2.4 Irrawaddy Bed, Myanmar

The Cenozoic and Quaternary mammalian fossil localities of the Irrawaddy beds are widely exposed along the Irrawaddy and Chindwin Rivers, which traverse the Central Myanmar Basin (CMB). Fossil localities of the CMB include: Chaungtha, Chaingazuk,

Gangaw, Gwebin, Mogok, Sulegone, Thanbinkan and Yenangyaung (Figure 4.5). The lithology of the Central Basin is divided into several units ranging from Eocene to Pleistocene. The Eocene to Middle Pleistocene basement of the basin (the Pegu Group) comprises predominantly marine sediments (Khin and Win, 1969, Stamp, 1922). The fossil-bearing beds that overlie this basement are mainly composed of fluviatile sediments derived from the Indo-Burman Ranges, Eastern Himalayas and Sino-Burman Ranges (Bender, 1983, Wandrey, 2006), known as the Irrawaddy Group (Bender, 1983). The thickness of the beds is estimated between 2000 and 3000 m.

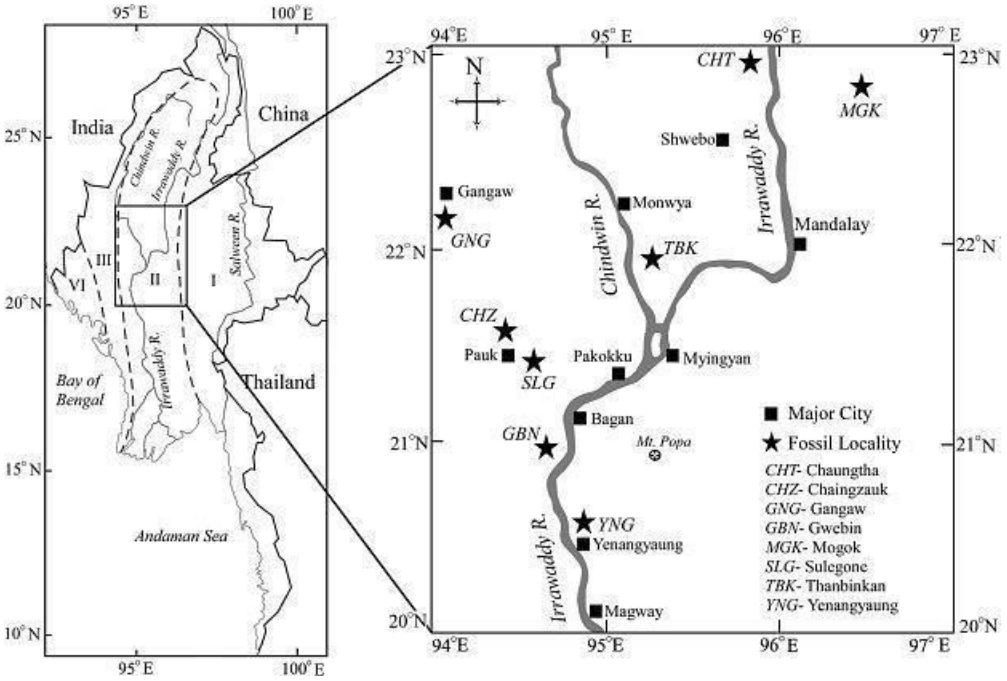

Figure 4.5 Map of Myanmar, showing four major geological regions and the localities of mammalian fossils in central Myanmar (Zin-Maung-Maung-Thein et al., 2010).

The Irrawaddy Group comprises Eocene-Miocene marine deposits and the Late Miocene-Early Pleistocene terrestrial deposits (Trevena et al., 1991, Zin-Maung-Maung-Thein et al., 2011), which cropping out in the east and west part of the basin. The Late Miocene to Early Pleistocene deposits consist of massive lithic sandstones and gravels that alternate with transgressive shallow marine shales, exposed in the central part of the CMB. Based on sedimentary facies and palaeocurrents, Trevena et al. (1991) suggested that north and south prograding tidal deltas and associated Proto-Irrawaddy River deposited sediments in this syncline. Subsequently, the Irrawaddy Group is in turn overlain by alluvium and Holocene deposits. Palaeomagnetic and radiometric

dating data are not available for this sequence, thus the age of the sediments were estimated based on the faunal content (Takai et al., 2006).

4.2.2.5 Sundaland: Java, Indonesia

The Quaternary mammalian fossil-bearing sediments of Java are exposed along the mountainous region in the middle part of the island (Figure 4.6). In western Java, the Quaternary basins containing mammalian fossils are mostly exposed in the Bogor Zone and North Serayu Hills, whereas in the eastern part, fossil localities are mostly exposed along the Kendeng Hills (Zaim, 2010). Because of a large number of Quaternary terrestrial basins in Java, lithological formations are different for each basin. However, based on the estimated age and lithological characters, these formations can be categorized into four groups: 1) the Late Pliocene-Early Pleistocene marine-terrestrial transitional sediments, 2) the Early Pleistocene terrestrial sediments, 3) the Middle Pleistocene fluviatile sediments and 4) the Middle-Late Pleistocene fluvial terrace, Holocene-recent alluvial sediments and cave deposits. Lithostratigraphic correlation of studied localities is presented in Figure 4.7. The lithostratigraphy of fossil-bearing sediments in Sumatra is not covered in this study, since all of the dental samples analysed originate from modern specimens.

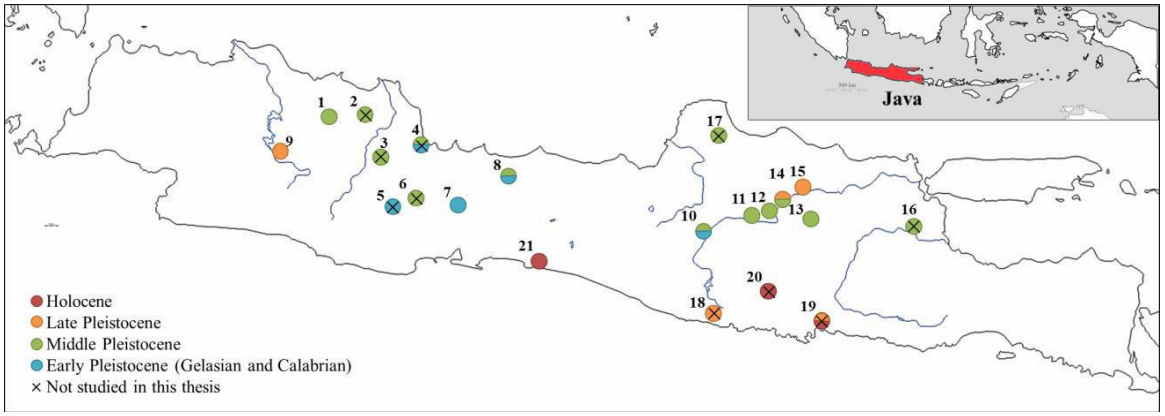

Figure 4.6 Schematic map of Java, including fossil localities mentioned in the text: 1 = Subang, 2 = Sumedang, 3 = Majalengka, 4 = Cirebon, 5 = Cijulang, 6 = Rancah, 7 = Bumiayu, 8 = Semedo, 9 = Cipeundeuy, 10 = Sangiran, 11 = Sambungmacan, 12 = Trinil, 13 = Kedung Brubus, 14 = Ngandong, 15 = Sunggu, 16 = Mojokerto, 17 = Pati Ayam, 18 = Punung Cave, 19 = Wajak Cave, 20 = Sampung Cave, 21 = Karang Bolong.

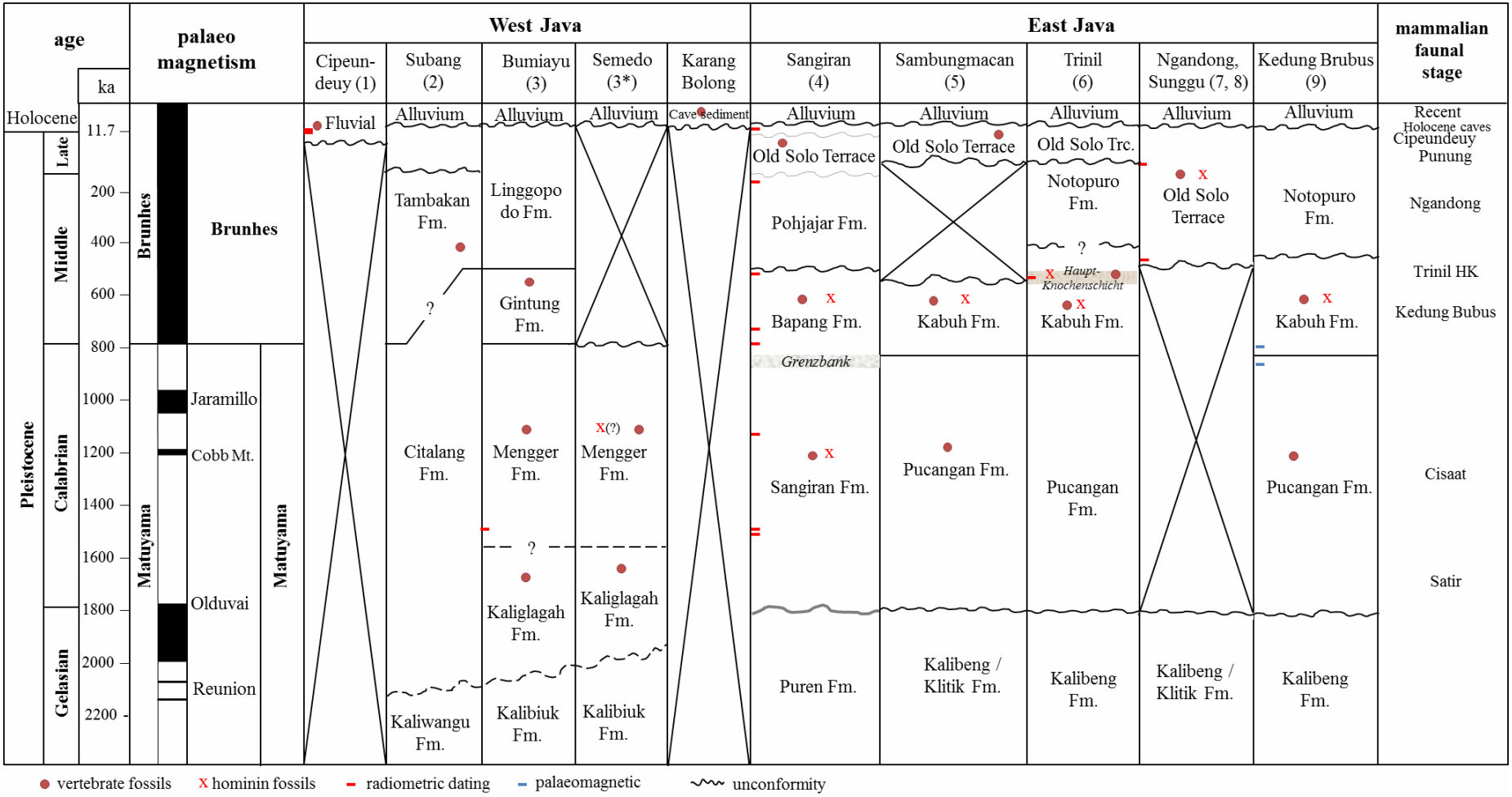

Figure 4.7 Lithostratigraphic correlations of the study areas in Java 1) Dam, 1994 and van den Bergh, 1999; 2) Djuhaeni and Martodjojo, 1989 and Zaim, 2010; 3) Zaim, 2010 4) Watanabe and Kadar, 1985, Bettis et al., 2004, and Hyodo et al., 2011; 5) Duyfes, 1936, Sibasaki et al., 1985 and Hertler and Rizal, 2005; 6) Duyfes, 1936, Watanabe and Kadar, 1985, and Joordens et al., 2015; 7) Duyfes, 1936, Watanabe and Kadar, 1985, and Indriati et al., 2011 8) van den Bergh and Kurniawan, 2010; 9) Duyfes, 1936, Watanabe andKadar, 1985, Mubroto et al., 1995.

4.2.2.5.1 Late Pliocene-Early Pleistocene marine-terrestrial transition sediments

The sediments from the Late Pliocene-Early Pleistocene constitute the base of Quaternary terrestrial deposits of Java. It is represented by sequences of sediments deposited in a shallow marine to tidal environments, including the Kaliwangu and Kalibiuk Formations in the western part of Java, and the Puren, Kalibeng and Klitik Formations in the east. The Kaliwangu, Kalibiuk, Puren and Kalibeng Formations are characterised by bluish marine clays and marls containing marine molluscs and ostracods. Sandy intercalations locally occur in the upper part of the sequences. At Trinil, the Kalibeng Formation is exposed in the bottom of the river bank as a white to yellowish-grey marine clay rich in foraminifers, conformably overlying siltstones, limestones, and bluish-grey clays from the same formation. Platy limestones from the older Klitik Formation are locally found in a few areas. These Late Pliocene-Early Pleistocene formations have eroded upper surfaces and are unconformably overlaid by younger sediments.

In Sangiran (Figure 4.8), thin sandy and tuff layers are exposed in the lower part of the Puren Formation, while at the top of the sequence a limestone layer composed almost entirely of Balanus, indicates an intertidal zone deposit. At the very top of the limestone beds, the occurrence of Corbicula indicates a regression and facies transition from a marine to terrestrial environment. Yoshikawa and Suminto (1985) recognized six tuff layers in the formation, labelled as Lower Tuff 1-4, Middle Tuff, and Upper Tuff. Fission track date of the lowest tuff layer (Lower Tuff 1), gave an age of 2.99±0.47 Ma (Suzuki et al., 1985). Shimizu et al. (1985) interpreted normal polarised strata as the Olduvai and Gauss in the sediment interval above Lower Tuff 1 and 2. Therefore the age of these sequences can be concluded as being Pliocene to Early Pleistocene.

Sémah (1997) reported palaeomagnetic sequence from the Kali Glagah Series in Bumiayu, along the Cisaat River. The palaeomagnetic record covers 100 m of sequence between the upper Kalibiuk and the Kaliglagah Formations (van der Maarel, 1932), including the Satir excavation (Figure 4.9). The sequence shows a reversed polarity correlated with the Early Matuyama Chron, with two intervals within the series are showing two different normal events. The normal interval near the boundary between the Kalibiuk and Kaliglagah Formation corresponds to the Réunion event (~2.14 Ma)

and a normal interval at the base of the Kaliglagah Formation is correlated with the Olduvai subchron (1.78-1.925 Ma).

4.2.2.5.2 Early Pleistocene terrestrial sediments

The Early Pleistocene terrestrial sediments of Java include the Citalang, Kaliglagah and Mengger Formations in the west, and also the Sangiran and Pucangan Formations in the east. The Citalang, Kaliglagah, Sangiran and Pucangan Formations unconformably overlie the Kaliwangu and Kalibiuk, Puren, and Kalibeng/Klitik Formations, respectively. Subsequently, the Mengger Formation conformably overlies the Kaliglagah Formation (Fig. 4.7).

The lower part of the Citalang, Kaliglagah, Sangiran and Kalibiuk Formations mainly consists of black clay layers, deposited in lacustrine/palustrine environments. The clays commonly contain lignite, freshwater molluscs (Sulcospira and Unio are identified from the Kaliglagah Fm.), as well as a few remains of earliest terrestrial vertebrate fauna. The fossil content suggests that the depositional environment was near-coastal fluvio-deltaic at the base of the sequence, and becoming increasingly terrestrial upwards (van den Bergh et al, 2005, Zaim, 2010). The upper parts of the sequences consist of medium to coarse andesitic sandstones. The sandstones commonly show cross bedding and coarsening upward with the inclusion of conglomerate layers towards the top. Coarser sediments in the upper part of the sequences suggest a change of depositional environment from lacustrine to fluviatile environments.

In Sangiran (Figure 4.8), the base of the Sangiran Formation consists of a lahar deposit, known as the Lower Lahar Unit (LLU, Watanabe and Kadar, 1985), which is characterized by a matrix-supported lahar deposit (Bettis et al., 2004, Zaim et al., 1999). Bettis et al. (2004) suggested 1.90 ± 0.02 Ma as the age of the LLU, which was obtained from $^{40}Ar/^{39}Ar$ dating on hornblende separates from six pumice lenses. Based on palaeomagnetic data, Hyodo et al. (1993, 2011) suggested that the age of the LLU is no older than 1.67 Ma, since the Olduvai normal event were recognized in the strata below the LLU. The LLU is overlain by thick black lacustrine clays intercalated with several thin layers of tuff, labelled as T0 to T11 (Yoshikawa and Suminto, 1985).

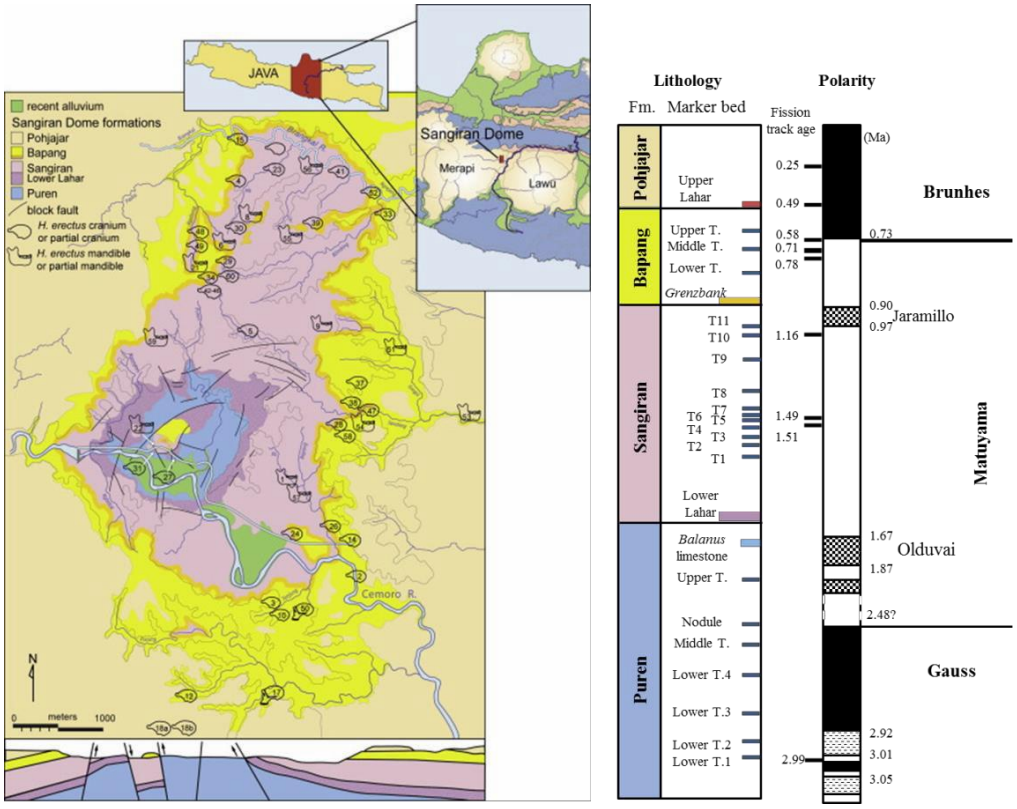

Figure 4.8 Schematic geological map of the Sangiran area (modified after Bettis et al., 2004), along with lithostratigraphy, fission track ages (Suzuki et al., 1985) and magnetic polarity (Hyodo et al., 1993, 2011).

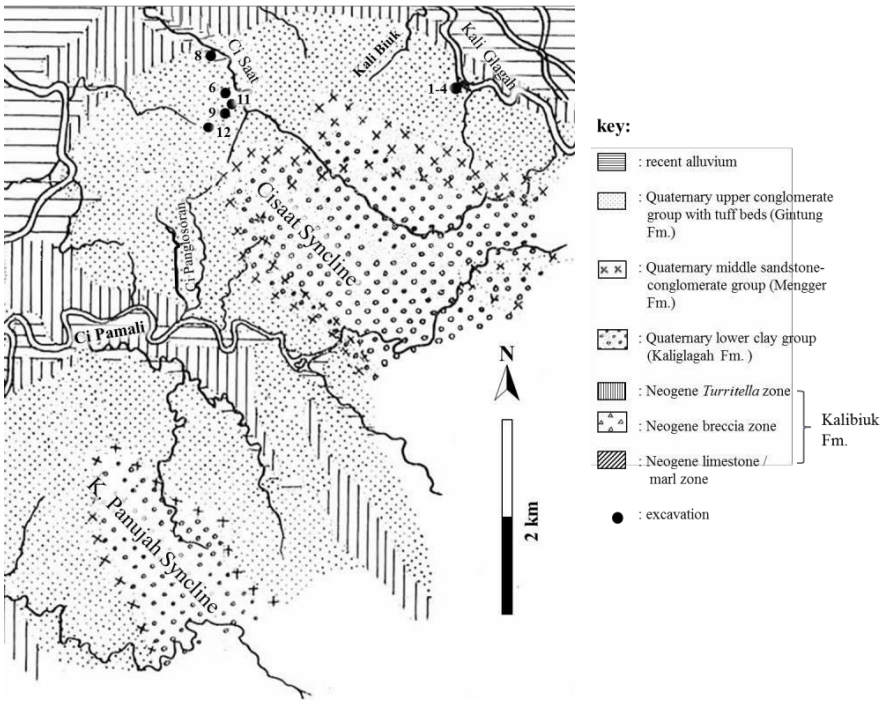

Figure 4.9 Geological map of the Bumiayu area (van der Maarel, 1932), showing the excavation trenches near Satir village (1-4). Vertebrate fossils were found in the Gintung Fm., Mengger Fm. and Kaliglagah Fm. The oldest fossil assemblages originate from excavations 1-4 and 8 just above the marine transition at the base of the Kaliglagah Fm.

The sandstone layers of the Sangiran Fm. containing various marine molluscs and are deposited on the black clays. This sandy interruption represents a sudden marine ingression that inundated the area during a period of sea level rise. Diatomite layers interrupted the deposition of the black clays, indicating that the basin remained brackish for a while (Hertler and Rizal, 2005). Fission track ages obtained from the black clays by Suzuki et al. (1985) are 1.51 ± 0.25 Ma (T5), 1.49 ± 0.32 Ma (T6), and 1.16 ± 0.24 Ma (T10). Shimizu et al. (1985) recognised reversed polarity associated with Matuyama chron from this interval. Thus, the overall age of the base of the Sangiran sequence can be considered as Early Pleistocene.

In Bumiayu, the Mengger Formation unconformably overlies the Kaliglagah Formation. The Mengger Formation consists of a series of pale grey tuffaceous sandstones and conglomerates, which were deposited as mudflows and debris flows, with some reworking by fluvial currents. The tuffaceous layers commonly contain pumice. The Mengger Formation was deposited on a distal volcanic apron during a period of syn-eruptive activity. Recently, Storey (personal communication to van den Bergh) has obtained a $^{40}Ar/^{39}Ar$ date of 1.53 ± 0.08 Ma for hornblende from pumices from the base of the Mengger Formation along the Cisaat River (unpublished data).

4.2.2.5.3 Middle Pleistocene fluvial sediments

The Middle Pleistocene fluvial sediments of Java include the Tambakan and Gintung Formations in the west, and the Bapang and Kabuh Formations in the east. The lithology of these formations comprises alternating clays, medium to very coarse conglomeratic sandstones commonly with planar cross-bedding structures and silty claystones. Lenses of clay occur in the conglomerate layers. This type of lithology indicates meanders and point-bar channel deposits, which most likely formed after the uplift of the Bogor Zone, Serayu Hills, Southern Mountain and Kendeng Hills (Hertler and Rizal, 2005). These formations are rich in vertebrate fossils.

In Sangiran, Sambungmacan and Kedung Brubus, a layer of calcareous breccia, known as the Grenzbank, forms a boundary between the Sangiran/Pucangan and Bapang/Kabuh Formations. Meanwhile in Trinil, a bed of volcanic ash is called Haupt-

Knochenschicht. Both the Grenzbank and Haupt-Knochenschicht (H.K.) layers are very rich in vertebrate fossils.

Within the Bapang Formation (Figure 4.8), Yoshikawa and Suminto (1985) recognised three tuff layers: The Lower Tuff, Middle Tuff, and Upper Tuff. Hyodo et al. (1993, 2011) suggested that the age of the Grenzbank is younger than 0.9 Ma, as the Jaramillo event lies just below the Grenzbank zone. The Upper Tuff layer marks the Brunhes-Matuyama reversal (Shimizu et al., 1985, Hyodo et al., 1993, 2011). The fission track ages obtained from tuff layers within the Middle Tuff are 0.78 Ma and 0.71 Ma, respectively, while the Upper Tuff layer is fission track dated at 0.58 Ma (Suzuki et al., 2008). A palaeomagnetic approach has been carried out in a section at the lowermost part of the Kabuh Formation at Kedung Brubus, which suggested that the age of this section corresponds with the Brunhes-Matuyama boundary (Mubroto et al., 1995). More recently, Joordens et al. (2015) dated sediment contained in the engraved shells originated from the main fossil layer of Trinil H.K., with $^{40}Ar/^{39}Ar$ and luminescence dating methods. These dating attempts are the first direct ages for sediments from the Trinil H.K., and suggested that the sediment is apparently younger than has been previously estimated. The maximum age obtained from the method is 0.54 ± 0.10 Ma ($^{40}Ar/^{39}Ar$), while the minimum age is 0.43 ± 0.05 Ma (luminescence).

The fluviatile Gintung, Bapang and Kabuh Formations are unconformably overlain by the Linggopodo, Pohjajar (also known as the Upper Lahar Unit) and Notopuro Formations, in respective order. The Linggopodo Formation consists of volcanic breccias and andesite lavas derived from volcanic activity during the end of the Late Pleistocene to Early Holocene (Zaim, 2010). The Pohjajar and Notopuro Formations comprise large boulders of andesite within a tuffaceous matrix, which were deposited during the Late Middle Pleistocene (Watanabe and Kadar, 1985). The various volcanic components in these formations indicate an increase in volcanic activity. However, these formations have not yielded a distinct vertebrate fauna.

4.2.2.5.4 Late Middle Pleistocene-Recent fluvial, terrace and alluvium

In the western part of Java, a Late Pleistocene fluvial sediment containing mammalian fossils is developed at Cipeundeuy, near Padalarang. The units consist of massive scoria

breccia, sandstone and conglomerate fluvial channel fills, multiple ash beds, and clayey fluvial sequences with sand insertions (van den Bergh, 1999). Radiocarbon ages for this sediment are 35,500 +4,600/-2,900 and 29,600 +450/-420, derived from layers above and below a fossil layer (Dam, 1994).

In the eastern part of Java, late Middle-Late Pleistocene strata are represented by Old Solo River terraces, which are exposed near Sangiran, Sambungmacan, Trinil, Ngandong and Sunggu. The deposits of the terraces mainly consist of point bar sequences, composed of loose and poorly sorted conglomerates, as well as cross bedded unconsolidated fluvial sandstones. These terraces are the remnants of the antecedent Old Solo River that existed prior to the uplift of the Kendeng Hills to their present altitude. The terrace fills are rich in vertebrate fossils, especially at Ngandong.

The Old Solo terraces are massively exposed in Ngandong and its surrounding village, such as at Pitu and Watualang. Along the Solo River, Sartono (1976) recognised six different terraces between Ngawi and Jipangulu. In descending order of relative height from the water level of the Solo River, the terraces are: Rambut (97 m), Kedungdowo (82 m), Getas (57 m), Ngandong (20 m), Jipangulu (7 m), and Menden (2 m). Rizal (1998) has distinguished only five terraces: the upper highest terrace (80-84 m amsl), lower highest terrace (75-78 m amsl), high terrace (56-62 m amsl), middle terrace (50-54 m amsl) and lower terrace (45-50 m amsl). Hominin and other vertebrate fossils occur mainly in the Ngandong/high terrace, which comprises muddy coarse grained sand with gravel in the lower part and coarse grained sand with pebbles in the upper part. The main fossil layer is located at about 56 m above sea-level or 20 m above the water level of the Solo River.

The dating results of the Ngandong terraces show conflicting ages. Bartstra et al. (1988) gave a preliminary U-series age of 50-100 ka from fossil bone and Swisher et al. (1996) ESR and U-series ages from bovids teeth are consistently younger than 100 ka. The samples were collected from an excavation in terrace remnants at Ngandong, and the ages were considered as a minimum age. However, the very young ages produced by Swisher et al. (1996) raised scepticism, since the U-series results are older than the ESR age, which is attributed to Uranium leaching. Hence, Indriati et al. (2011) made a more detailed study at the Ngandong and Jigar localities, including the locations of Oppenoorth's (1930s), Indonesia-Japan team (1970s) and Jacob's (1970s) excavations.

The dating results showed a maximum age of 546 ka from $^{40}Ar/^{39}Ar$ analysis of pumice samples and a minimum age of 143 ka from combined U-series and ESR analyses on enamel from in-situ collected mammal fossil teeth.

Additionally, a partial Elephas hysudrindicus skeleton was found at Sunggu, at 8.5 km northeast of Ngandong. The skeleton was excavated from a fluvial terrace of the Solo River, called the Menden Terrace. A maximum age obtained from Red TL dating of silty sandy layers directly below and above the Elephas skeleton have considerable error ranges of 166 ± 25 ka for the underlying, and 163 ± 19ka for the overlying layer (van den Bergh and Kurniawan, 2010).

4.2 Palaeogeography and faunal succession

4.2.1 Palaeogeography and influence of eustatic sea-level changes

The Khorat Basin and the Linxia Basin have been terrestrial environments since the Cretaceous. The uplift of the Tibetan Plateau only began around the Early Eocene and further significant uplift pulses are thought to have occurred about 10-8 Ma, further increasing the elevation of the Linxia Basin (Molnar et al., 1993, Fang et al., 2003). Uplift of the Khorat Basin to its recent altitude occurred only since the Miocene due to localised tectonic differentiation (Bunopas and Vella, 1992). Prior to the Eocene, the foreland basins south of the Himalayan Range were still under marine. This area was uplifted in the Early Eocene due to the India-Asia collision and remained as a terrestrial basin ever since then (Pilbeam et al., 1977, Parkash et al., 1980). Since its initial uplift in the Eocene, the CMB experienced palaeogeographic changes since the Neogene. During the Oligocene and Early Miocene, marine conditions prevailed in most of the Central Myanmar area and the depositional environments were transitional between marine and terrestrial. Throughout the Miocene to Pliocene, the folding phase of the Indo-Burman Ranges led to rapid infill of the basin as an area of terrestrial sedimentation, and the shoreline receded southward (Rodolfo, 1975).

In contrast to the mainland, full emergence of Java as an island and its habitability for terrestrial animals occurred only after the Pliocene. An interpretation of land and sea area distribution of Sundaland between the Palaeogene and Late Neogene is presented

in Hall (2009). At the time of a major fall of global sea level during the Mesozoic and Middle-Late Oligocene, a small part of West Java had been emerged (Haq et al., 1987). However, no mammalian fossils have ever been found in these sediments. Subsequently, Java was submerged during the most of the Palaeogene and Neogene (Hall, 2009).

During the Late Miocene (approximately 10 Ma), when the position of Sundaland was recognisable in its present form, part of Java re-emerged, in the form of a string of smaller islands. These islands were isolated from mainland Asia until the Late Pliocene/Early Pleistocene, when extensive uplift started due to a combination of intensive tectonic and volcanic processes (Hall, 1998, 2009, 2012a, 2013). The uplift of Java happened in a stepwise process, from the area called Proto-Java (including west and central Java, up to Sangiran), while the uplift of the eastern part was slightly delayed (van Bemmelen, 1949, de Vos et al., 2007). The uplift process of Java between the late Pliocene and Early Pleistocene eventually allowed terrestrial faunal inhabitation of the island from the Early Pleistocene. Between the end of the Early Pleistocene and the present, glacioeustatic sea level fluctuations generated by glacial-interglacial cycles replaced the importance of tectonic and volcanic activity as the main factor in determining exposed landmass area (Vrba et al., 1989). The sea-level fluctuations also influenced the Java-mainland connectivity and influenced the migration of the island mammals (van den Bergh, 1999). In the meantime, tectonics and volcanism still influenced the general Earth-shaping processes and the formation of river terraces.

Prior to 0.9 Ma, the amplitude of sea level fluctuation was lower. Any terrestrial fauna that reached Java at the time must have migrated by means of island hopping, since some areas of Sundaland were still a chain of smaller islands. The sea level fluctuations started to become more pronounced in affecting the distribution of land area since around 0.9-0.8 Ma (Bintanja et al., 2005). Sea level fluctuations with maximum lowering amplitudes down to 120 m below the present sea level were affecting the size of the land extension and connectivity among islands within Sundaland significantly, as demonstrated by Voris (2000). The low sea-level stand during glacial periods created recurring land corridors and extension of land area between mainland SE Asia and Java and enabling repeated overland faunal migrations from mainland Asia to Java (Bird et al., 2005). Subsequently, during high sea-level stands, Java was intermittently isolated,

thus restricting faunal migration and leading to isolation and allopatric speciation. Turnover between high and low sea-levels is reflected by the difference of faunal assemblages along the stratigraphic levels. These low sea-level stands lasted for prolonged periods of time, whereas the periods of isolations were relatively short-lived. Therefore the fauna from isolated periods are relatively rare. A detailed review of migration and inhabitation of fauna in Java is presented in van den Bergh (1999).

4.2.2 Faunal succession and age of the faunas

4.2.2.1 Mainland Southeast Asia

4.2.2.1.1 Huijialiang Fauna

The fossil fauna of the Huijialiang Formation, known as the Platybelodon Fauna, contains: Alloptox sp., Pliopithecus sp., Hemicyon teilhardi, Amphicyon tairumensis, Percrocuta tungurensis, Gomphotherium sp., Platybelodon grangeri, Zygolophodon sp., Anchitherium gobiensis, Alicornops sp., Hispanotherium matritense, Kubanochoerus gigas, Listriodon mongoliensis, Palaeotragus tungurensis, and Turcocerus sp. (Deng, 2004). This faunal assemblage corresponds with the Tunggurian Fauna from Nei Mongol Basin and Dingjeaergou Fauna from the Shaanxi Ningxia Basin (Deng, 2004, 2006). Since the radiometric dating was not available for this assemblage, the best age estimation of this fauna was obtained based on palaeomagnetic data, as suggested by Deng et al. (2013b). An extensive set of palaeomagnetic analysis within and between the various Linxia sections is given by Li et al. (1995) and Fang et al. (2003). Based on reinterpretation and correlation of the fossil bearing layer with the section made by Li et al. (1995) and Fang et al. (2003), Deng et al. (2013b) concluded that the normal palaeomagnetic polarity of Huijialiang Formation, from which the Platybelodon Fauna was obtained, best matches chron C5Ar, with an age of 12.6 Ma.

4.2.2.1.2 Tha Chang Fauna

So far, nine proboscidean genera, Gomphotherium, Prodeinotherium, Tetralophodon, Protanancus, Sinomastodon, Stegolophodon, Stegodon, Elephas (Thasod, 2007, Thasod

et al., 2012) and Anacus?, as well as rhinoceros, giraffes, antilopes, Hipparion sp., and Merycopotamus sp. (Hanta et al., 2005, Hanta et al., 2008) were found in the excavated sand pits near the Mun River. In addition, a hominoid species, Khoratpithecus piriyai (Chaimanee et al., 2006) and a large tortoise shell were also recovered from the sand pits. However, the establishment of a mammalian biostratigraphy of this area is complicated, since most of the fossils were probably reworked from different ages and deposited at nearly the same time because the fossils occur in the same channel sequence (Duangkrayom et al., 2014). Moreover, the relationship between fossils and the provenance lithology is commonly not clear as fossils were mostly recovered during the extraction of sand from the walls of the pits with a high-pressure water jet, and were then collected by local villagers working in the sand pits. Due to poor information of faunal association in stratigraphic units, the succession of probscidean taxa has been made primarily based on their evolutionary stage (Saegusa et al., 2005).

The Middle Miocene mammalian fauna includes gomphotheres and Prodeinotherium. The Late Miocene to Early Pliocene fauna comprises Sinomastodon, Stegolophodon, which co-occurred with a hominoid species, Khoratpithecus piriyai (Chaimanee et al., 2004, 2006). The late Pleistocene to Early Pleistocene fauna includes primitive Stegodon, while the Middle to Late Pleistocene fauna contains advanced Stegodon and Elephas (Nakaya et al., 2002).

4.2.2.1.3 Upper Siwalik Fauna

The Upper Siwalik Fauna found near Haripur and adjacent areas includes Proboscidea: Anancus sp., Stegodon insignis, Stegodon sp., Stegolophodon sp., Elephas planifrons, Elephas hysudricus; Perisodactyla: Hipparion sp., Cormohipparion sp., Equus sivalensis, Equus sp., Rhinoceros palaeindicus, Rhinoceros sivalensis, Coelodonta sp.; Artiodactyla: Hemibos spp., Bovidae indet., Antilope spp., Gazella sp., Hippohyus spp., Propotamochoerus spp., Hexaprotodon sivalensis, Sivatherium giganteum, Cervus spp., Camelus sp., Oryx sivalensis, Bos sp.; Rodentia, Insectivora, Lagomorpha, Carnivora and Primata (Flynn and Jacobs, 1982). So far, there is no detailed division and classification of Upper Siwalik fossil fauna from the Haripur area. However, interpolating from the first and last occurrence of the Upper Siwalik Fauna in the

Jammu region and the Potwar Plateau in Pakistan, the faunal assemblage of the Upper Siwalik in Haripur can be further divided as the Archidiskodon planifrons Interval (3.2 – 2.6 Ma, Barry et al., 1985, Basu, 2004, Patnaik and Nanda, 2010) and Elephas hysudricus Interval (2.6 – 1.7 Ma, Basu, 2004).

4.2.2.1.4 Lower and Upper Irrawaddy Faunas

A list of mammalian fauna of the Lower and Upper Irrawaddy is presented in Takai et al. (2006). Proboscidean taxa originating from the Lower Irrawaddy beds are: Stegolophodon latidens, Stegolophodon stegodontoides, Stegodon sp. indeterminate (primitive form), Stegodon elephantoides (primitive form) and Sinomastodon sp., while proboscidean taxa from the the Upper Irrawaddy Series are: Stegodon insignis birmanicus, Stegodon sp. indeterminate (derived form) and Elephas hysudricus (Takai et al., 2006). Based on fossil contents, the Lower Irrawaddy fauna bears a close resemblance with the fauna corresponding with the Dhok Pathan Formation of the Siwalik Group, suggesting a late Miocene to early Pliocene age. Meanwhile, the Upper Irrawaddy fauna can be correlated to the Tatrot and Pinjor Faunas of the Indian subcontinent, estimated to range from the Middle Pliocene to the Early Pleistocene (Takai et al., 2006).

4.2.2.1.5 Estimated chronological range of mainland Proboscidae

The analysed specimens include 12 proboscidean taxa described above. Numerical age estimation of chronological occurrence for each taxon is listed in Table 4.1. Median value of estimated ages of each taxon will be referred to in the chronologic stable isotope record in Section 4.4. However, it is important to note that the age of species occurrence here, especially for the chronological ordering of pre-Pleistocene, is a rough assumption based on available palaeomagnetic data or extrapolation from the occurrence of certain species in other localities, since radiometric dating data are unavailable for all localities or faunal assemblages. Therefore the positioning of each species in the timeline is not precise and should be used with caution.

Table 4.1 List of estimated ages for analysed Proboscidea taxa from mainland Asia.

taxa	localities	age range	references
Platybelodon cf. grangeri	Linxia Basin	15-11.1 Ma	Deng, 2004
Sinomastodon sp.	Tha Chang and Chaingazuk (Irrawaddy)	6-4 Ma	Zin Maung-Maung-thein et al., 2011
Stegolophodon cf. stegodontoides	Tha Chang	8.3-6 Ma (in Siwalik)	Tassy, 1983
Stegolophodon int. form	Tha Chang	Late Miocene (estimated between 8.3-6 Ma)	Saegusa et al., 2005
Stegodon cf. zdanskyi	Tha Chang	Late Miocene (estimated between 8.3-6 Ma)	Saegusa et al., 2005
Stegodon cf. elephantoides	Tha Chang	Early Pliocene (more primitive than the Irrawaddy form)	Saegusa et al., 2005, Thasod, et al., 2012
Stegodon insignis	Siwalik & Irrawaddy	3.6-1.7 Ma	Saegusa, 1996
Stegodon cf. orientalis	Tha Chang & Laos	1-0.13 Ma	Saegusa, 1996, Schepartz et al., 2005
Archidiskodon (Elephas) planifrons	Siwalik	3.2-2.6 Ma	Barry et al., 1985, Hussain et al., 1992, Basu, 2004, Patnaik and Nanda, 2010
Elephas hysudricus	Siwalik	2.7-0.8 Ma	Hussain et al., 1992, Dennell et al., 2006
cf. Palaeoloxodon namadicus	Tha Chang	Middle Pleistocene	Described as Elephas sp. in Thasod, et al., 2012
Elephas maximus	Tha Chang	Late Middle Pleistocene-Holocene	Vidya et al., 2009

4.2.2.2 Java

Earlier researchers proposed several biostratigraphic schemes for the faunal succession of Java. The first biozonation of terrestrial fauna was made by von Koenigswald (1933, 1934, 1935a, 1935b). This classical biozonation was later modified (Braches and Shutler, 1984, de Vos et al., 1982, Sondaar, 1984, Theunissen et al., 1990). The von Koenigswald's faunal succession contains various inconsistencies in determining succession (Braches and Shutler, 1984). Therefore the faunal assemblage based on de Vos et al. (1982) and Sondaar (1984) are more widely accepted and used. This faunal succession is based on the faunal contents from single localities or composite faunas from localities that are closely superposed in thick stratigraphic sequences. The mammalian biostratigraphic scheme of Java from old to young are: Satir Fauna, Cisaat Fauna, Trinil H.K. (Haupt-Knochenschicht = bed of bones) Fauna, Kedung Brubus

Fauna, Ngandong Fauna, Punung Fauna, Wajak Fauna. Van den Bergh (1999) added the Cipeundeuy fauna and regrouped the Wajak fauna along with those from other Holocene caves as the Holocene Cave Composite. Later Storm et al. (2013) showed that the Wajak fossil assemblage represents a wider age range, extending into the late Pleistocene. The faunal succession and the age of successive faunas used here have the most recent dating results of the sediments containing various faunal assemblages, incorporated.

4.2.2.2.1 Early Pleistocene: Satir and Cisaat Fauna

The oldest Satir Fauna is characterized by a few taxa from the Early Pleistocene. The Satir Fauna name originated from the excavation sites near Satir village at the base of the Kali Glagah Series near Bumiayu (Figure 4.9). The base of the Kali Glagah Formation is called the "lower sandstone conglomerate series group" on the geological map (ter Haar, 1934). Van der Maarel (1932) described the fossils from these excavations. The assemblage consists only of four species: Sinomastodon bumiajuensis, pygmy hippopotamus Hexaprotodon simplex, an unidentified deer and giant tortoise Geochelone. The faunal assemblage is also known as the Sinomastodon-Geochelone assemblage, and is thought to represents rather swampy or mangrove type environments (Hertler and Rizal, 2005). A similar assemblage can also be found in the lower stratigraphic levels of the "black clays" in Sangiran (Leinders et al., 1985, Matsu'ura, 1985).

In addition, a single molar of Stegoloxodon indonesicus (Kretzoi, 1950), a dwarfed species from Ci Panglosoran (a river) in the Bumiayu area is addressed as probably older than the Satir Fauna (van den Bergh et al., 1992). The specimen was found on the surface. Even so, the exposed lithology in the Ci Panglosoran represents the Lower Kaliglagah Formation (see Figure 4.9). If the specimen were transported, then it likely came from the surrounding lithology or even older, thus indicating that Stegoloxodon indonesicus is one of the first known Proboscidean taxa to have inhabited the island. A rare pygmy Stegodon species is also found in Sambungmacan (Aziz et al., 1995, van den Bergh et al., 1992) and Cirebon (van den Bergh, 1999). However, due to the uncertainty of the stratigraphic position of these fossils, the age can only be roughly estimated as Early Pleistocene.

In this study, the Satir fauna is represented by proboscidean individuals excavated in the base of the Kaliglagah Formation in Bumiayu and Semedo. The minimum age of 1.5 Ma for the Satir fauna is based on the age of the base of the Mengger Formation. The fission track dating of volcanic ash layers (T5 and T6, Figure 4.8) in the Sangiran Fm. (Suzuki et al., 1985, Leinders et al., 1985) at 1.5 Ma, are in agreement with the age of the Mengger Fm. The maximum age of this fauna is derived from the palaeomagnetic data from the boundary between the Kalibiuk and Kaliglagah formations at ~2.14 Ma (Sémah, 1997).

The Cisaat Fauna is insufficiently known and was originally proposed on hypothetical grounds (Sondaar, 1994). The assemblage is distinguished from the Satir Fauna by the replacement of Sinomastodon bumiajuensis and Hexaprotodon simplex by Stegodon trigonocephalus and Hexaprotodon sivalensis, also by the first occurrence of a large felid and the endemic Sus stremmi.

Since there is no actual type locality for the Cisaat fauna, this faunal stage will be represented by a group of fossil taxa found in the Sangiran Formation above tuff layers T5/T6 (see Table 4.2 for the list of taxa). Proboscidean taxa represented by the samples analysed are a single Sinomastodon bumiajuensis molar fragment and several Stegodon trigonocephalus remains found in situ and on the surface of the "black clay" of the Sangiran Formation. In situ fossil collection of this formation was carried out near the Bukuran site by Indonesian-Japanese team between 1977 and 1979. The excavation trenches are stratigraphically placed just above tuff layer T9 and approximately 10 m below tuff layer T10 (~1.16 Ma, Kadar et al., 1985). However, since many fossils were also surface collected from other locations where older layers are exposed, the maximum age of this group is estimated at 1.5 Ma (fission track age of T5 and T6 layer), while the minimum age is derived from the estimated age of the Grenzbank at 0.9 Ma (Hyodo et al., 1993, 2011). The presence of an in situ giant tortoise below T10 layer (~1.2 Ma) is considered as an indirect indication that Homo erectus had not yet migrated to Java at that time (van den Bergh, 1999), as the giant tortoises are an easy prey for hunter-gatherers and rapidly became extinct on islands where humans settled (Sondaar, 1981).

4.2.2.2.2 Middle Pleistocene: Trinil, Kedung Brubus and Ngandong Fauna

A major faunal turnover seems to have occurred at the beginning of the Middle Pleistocene, where there are major changes in the composition of taxa that post-date the Satir and Cisaat faunas. The subsequent younger Javanese faunas are characterized by an increasing exchange of faunal elements with the Southeast Asian mainland, which also indicates a better connectivity to the mainland.

For the Kedung Brubus Fauna, I follow the definition of de Vos et al. (1994) who defined this stage based on Dubois' fossil finds in the Kedung Brubus area. Compared to the Early Pleistocene faunas, The Kedung Brubus Fauna contains more variation of species, indicating a balanced fauna (Table 4.2 for the list of species). This fauna assemblage itself resembles quite closely the Trinil H.K. Fauna with a few exceptions. The Kedung Brubus fauna is thought to be established from the aggregate of two mammalian fossil-bearing horizons (von Koenigswald, 1940). In the meantime, no efforts were made to confirm or reject the existence of two vertebrate fossil horizons of different age. Considering the palaeomagnetic results (Mubroto et al., 1995), van den Bergh (1999) previously suggested that the age of this fauna is approximately 0.7-0.8 Ma. Additionally, fossil taxa found in situ and on the surface of the Bapang Formation (from Grenzbank to the Upper Tuff Layer, Figure 4.9) bear very close resemblance to the fossil taxa included in the Kedung Brubus fauna. Based on the similarity of fossil content, here I redefine the Kedung Brubus Fauna as the composite of the assemblage originating from the Kabuh Fm of the Kedung Brubus and the Bapang Fm. at Sangiran (Kedung Brubus + Bapang Fauna). Hence, the maximum and minimum age of this fauna is derived from the age of the Grenzbank and the Upper Tuff layer, with ages estimated between 0.9 and 0.58 Ma, respectively (Suzuki et al, 1985, Hyodo et al., 2011).

The successive Trinil H.K. Fauna originates from the type locality at Trinil, East Java, which is well-known due to the extensive excavations made by Dubois and Selenka. The assemblage includes Stegodon trigonocephalus with relatively smaller molar size (van den Bergh, 1999), a large proportion of Artiodactyla (especially cervids and bovids), Carnivora (including two endemic species: Panthera tigris trinilensis and Mececyon trinilensis), primates, as well as rare records of rodents (Table 4.2). Elephas hysudrindicus is absent in this assemblage. Leinders et al. (1985) reported a faunal assemblage from the Grenzbank layer in the Sangiran area that lacks E. hysudrindicus.

Table 4.2 List of mammalian species reported in the successive faunal stages of Java (after Aimi and Aziz, 1985, de Vos et al., 1994, van den Bergh et al., 2001, de Vos and Vu, 2001).

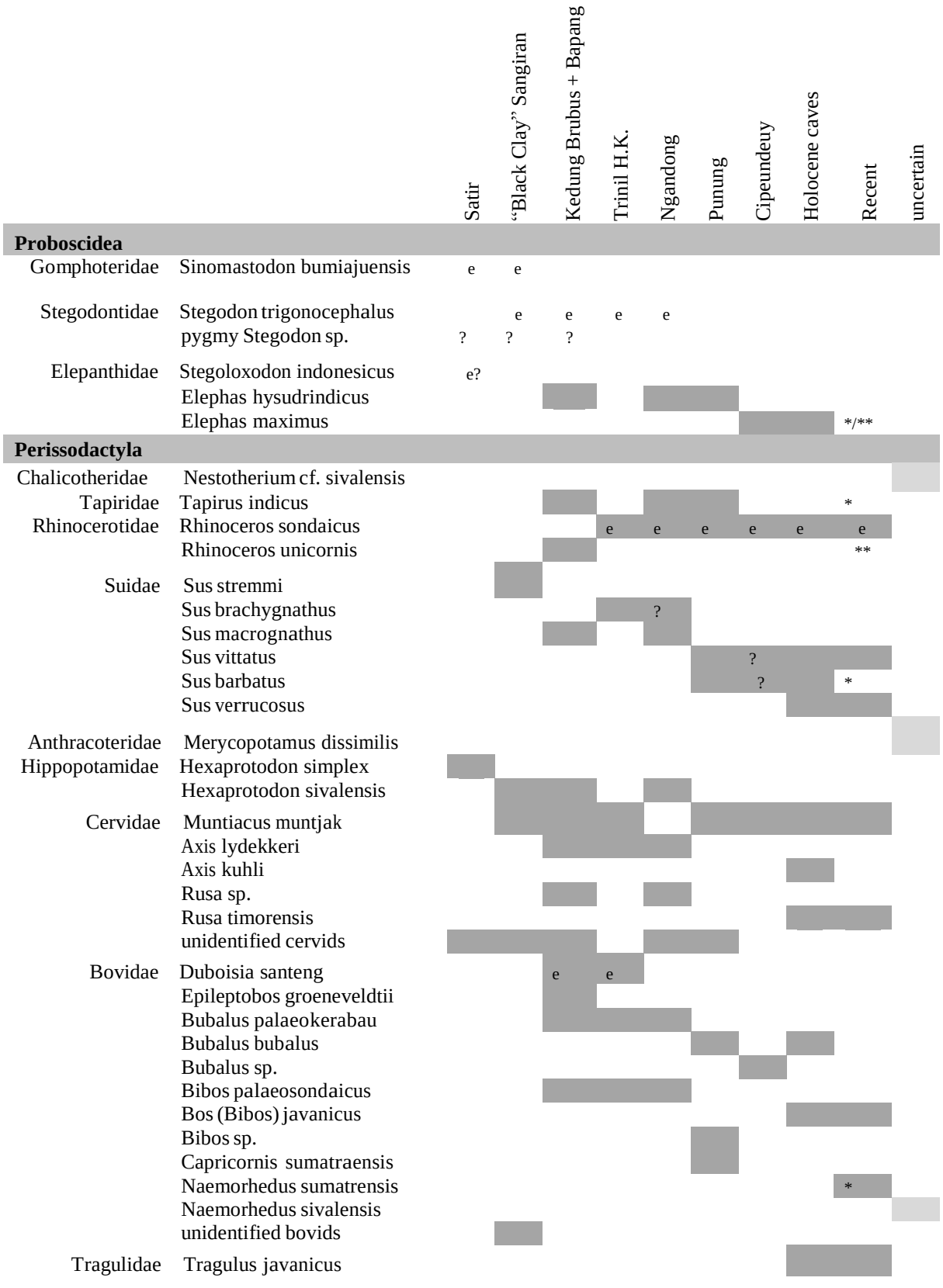

Carnivora		
Canidae	Mececyon trinilensis	
	Mececyon merriami	
	Cuon sp.	
Ursidae	Ursus malayanus	*
Mustelidae	Mustela lutreolina	
	Lutrogale palaeoleptonyx	
	Lutrogale robusta	
	Lutra lutra	
	Lutra sumatrana	
	Melogale personata	
	Martes flavigula	
	Amblonyx cinerea	
Viverridae	Viverrida indica	
	Arctictis binturong	
	Paradoxurus hermaphroditus	
	Arctogalidia sp.	
Mephitidae	Mydaus javanensis	
Prionodontidae	Prionodon linsang	
Herpestidae	Herpestes javanicus	
Felidae	Panthera tigris ssp.	? *
	Panthera pardus	e
	Panthera sp.	?
	Megaenteron sp.	
	Hemimachairodus zwierzycki	
	Homotherium ultimum	
	Neofelis nebulosa	
	Prionailurus bengalensis	
	Felis viverrina	
Hyaenidae	Hyaena brevirostris	
	Crocuta crocuta	
Primates		
Colobidae	Presbytis cristatus	*
	Presbytis comata	e
Cercopithecidae	Macaca nemestrina	
	Macaca fascicularis	
Lorisidae	Nycticebus coucang	
Hylobatidae	Hylobates syndactus	*
	Hylobates moloch	
Pongidae	Pongo pygmaeus	*
Hominidae	Homo erectus	
	Homo sapiens	
Pholidata		
Manidae	Manis palaeojavanica	e
	Manis javanica	e e
Lagomorpha		
Leporidae	Caprolagus lapis	
Insectivora		
Soricidae	Echinosorex sp.	*
Rodentia		
Hystricidae	Hystrix brachyura	
	Hystrix gigantea	
	Hystrix javanica	
Muridae	Rattus trinilensis	

*= extant in Sumatra and/or Borneo; **= extant in mainland Asia; e=endemic species; ?=uncertain stratigraphic occurrence.

Due to the similarity of Trinil H.K. and the taxa contained in the Grenzbank, the palaeomagnetic results from a fossil-bearing conglomerate near Kedung Cumpleng (15 km north of the Sangiran Dome, along the Kaliuter sections and just below the Grenzbank) had been used to determine the age of the Trinil H.K. Fauna. The Kedung Cumpleng layers shows a normal polarity, which was correlated with the Jaramillo Event (Shimizu et al., 1985). Under these circumstances, the age of the Trinil H.K. Fauna had previously been suggested to be as old as 0.9-1.0 Ma (van den Bergh, 1999, van den Bergh et al., 2001), and older than the Kedung Brubus Fauna stage.

However, recent dating result of the Haupt-Knochenschicht layer by Joordens et al. (2015) indicate that Trinil H.K. is younger than previous estimations by Leinders et al. (1985) and van den Bergh (1999). This younger date is certainly more reliable, since it is tested with direct chronological methods using in situ sediment from the actual fossil layer. Additionally, Aimi and Aziz (1985) reported that during the fossil collection, collected in situ and on the surface in the Grenzbank a few molar fragments were recognised as belonging to E. hysudrindicus, which were previously reported in as Elephas sp. indeterminate. Therefore the apparent absence of Elephas from the Trinil H.K. may be due to environmental factors.

Following the new dating results (Joordens et al., 2015), the Trinil fauna stage is now considered younger than the Kedung Brubus + Bapang Fauna. This new scheme would invert the faunal assemblage scheme by de Vos (1982) and Sondaar (1984). According to this interpretation, the continuation of several taxa from the Kedung Brubus to the following faunas would be interrupted in the Trinil Fauna. A group of taxa (i.e. Elephas hysudrindicus, Tapirus indicus, Sus macrognathus and Hexaprotodon sivalensis), which were all thought to occur in the Kedung Brubus Fauna, would then have disappeared during the Trinil stage and re-appeared during the Ngandong stage. Meanwhile, endemic taxa (Panthera tigris trinilensis and Mececyon trinilensis) appear in Trinil and no longer exist in younger faunas. An explanation could be that E. hysudrindicus, T. indicus, S. macrognathus and H. sivalensis only occurred during the period when Java was better connected to mainland SE Asia. During the Trinil faunal stage, Java was probably isolated from the mainland, and thus those temporary taxa could not cross, while other taxa became endemic due to allopatric speciation. In addition, reduction of land area might also have reduced the size of the surviving species. That condition

could explain why the molar and mandible size of Stegodon in the Trinil Fauna is relatively smaller than in the other "mainland" faunal assemblages (Kedung Brubus and Ngandong).

The Ngandong Fauna is known from material excavated from the Solo River terrace at Ngandong and surrounding localities by Oppenoorth during the 1930s (van den Bergh, 1999). The fossil-bearing terrace occurs 20 m above the present day Solo River. The vertebrate assemblage from this terrace deposit is presented in Table 4.2. The faunal composition of the Ngandong fauna is distinguished from the Kedung Brubus Fauna on a subspecies level for several taxa, including Homo erectus, showing more advanced characters (de Vos et al., 1994). However, due to the striking differences in preservation between specimens from Ngandong and the wide range of contradicting dating results, doubts have been raised whether the Ngandong Fauna actually represents a uniform fossil association (Westaway, 2002). The Solo River connects the Middle Pleistocene localities at Trinil and further upstream with the younger Pleistocene terraces at Ngandong. This factor cannot be excluded from the possibility that at least part of the fossils from older strata could have been redeposited in the Ngandong terraces. However, the fauna must have been younger than or including reworked materials from the Trinil Fauna and is certainly older than the Late Pleistocene Punung Fauna.

4.2.2.2.3 Punung, Cipeundeuy and Holocene Fauna

The next major turnover can be observed as the replacement of the Stegodon-Homo erectus faunas (Kedung Brubus- Trinil-Ngandong Faunas) by the Elephas-Homo sapiens fauna of the localities Punung and Wajak. Whereas the Ngandong fauna contains various archaic species, the subsequent Punung Fauna comprises a largely modern fauna lacking extinct mammals (Storm and de Vos, 2006, de Vos and Elias, 2007). The type locality of the Punung Fauna is contained in a breccia deposit of a cave in the Gunung Sewu limestones. The fauna documents the first known appearance on Java of several extant Southeast Asian species, including Elephas maximus, Helarctos malayanus and Hylobates syndactylus (Badoux, 1959). A human tooth attributed to Homo sapiens has also been claimed to belong to the Punung Fauna, which suggests the replacement of H. erectus by H. sapiens (Storm et al., 2005, Storm and de Vos, 2006).

Van den Bergh considered the age of fauna as 60-125 ka, based on the fauna similarity with dated Lida Ajer Cave, Djambu Cave and Sibrambang Caves in West Sumatra. More recently, Westaway et al. (2007), by using luminescence and uranium-series dating, provided an age of between 128 and 118 ka for cave sediment in Gunung Dawung, which corresponded with interglacial MIS 5 period.

Van den Bergh (in van den Bergh, 1999 and van den Bergh et al., 2001) proposed the Cipeundeuy Fauna, Holocene caves composites, and Recent fauna as an addition to the de Vos et al. (1982) and Sondaar (1984) faunal succession scheme. The faunal assemblage of Cipeundeuy originates from a sand quary near Padalarang, west of Bandung, West Java. The assemblage consists of Elephas maximus, Rhinoceros sondaicus, Muntiacus sp., bovids, cervids and Hystrix sp. The Cipeundeuy fauna differs from the Punung fauna by the absence of the genus Pongo, its limited number of species and from its distinct taphonomy (fluvial deposit). The radiocarbon date provides the age of this fossil assemblage at between 35.5 and 29.6 ka (Dam, 1994).

Based on the available dating evidence, van den Bergh et al. (2001) included the Wajak Fauna in the Holocene cave composite fauna along with the Sampung, Hoekgrot and Jimbe Caves. This assemblage consists entirely of modern Java fauna, which lacks Pongo, Tapirus and Elephas as important remarks. Radiocarbon analysis of some mammalian and human remains from Wajak provides an age between 6 ka and 10 ka for the Wajak Fauna (Storm, 1995; Shutler et al., 1996). However, recent U-series dating results on human bone fragments from Wajak indicate a minimum age of between 37.4 and 28.5 ka (Storm et al., 2013), corresponding with MIS 3. This date is significantly older than the radiocarbon dates. Given such discoveries, it is very likely that the assemblage from Wajak is a mix between Late Pleistocene and Holocene fossils. Incorporating the data discussed above, the age of the successive faunal stages and the occurrence of proboscidean species in Java is presented in Figure 4.10.

The extinction of Elephas maximus in Java is estimated to have occurred during historical times, although this species is still extant in Sumatra and in a small area in northeast of Borneo (Hedges et al., 2005, Sukumar, 2006, Cranbrook et al., 2008). Based on DNA analysis, Fernando et al. (2003) suggested that the small elephant population in Borneo maybe derived from a stock that originated from Java (Sunda

islands). However, to confirm this hypothesis, ancient DNA of subfossil E. maximus remains from Java should be analysed.

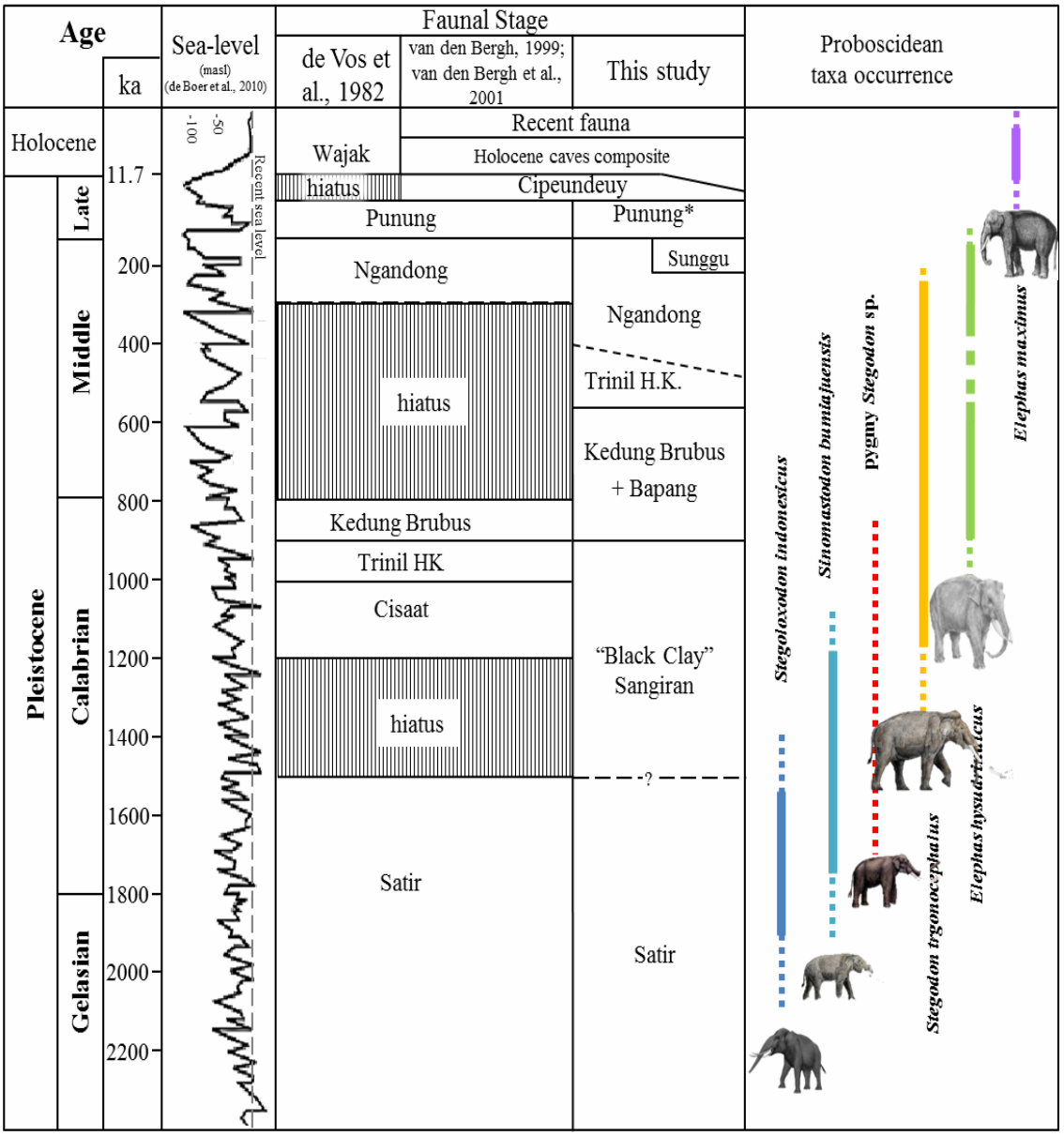

Figure 4.10 Scheme of the vertebrate faunal succession of Java based on recent dating results and the range of occurrence of Proboscidean taxa. The solid line shows the occurrence of fossils in sediments, while the dashed line shows hypothetical occurrences. The Punung Fauna is not analysed in this study.

4.3 Analysed materials

A total of 160 enamel samples of 17 proboscidean taxa from fossil-bearing sites in mainland Asia, Java and Sumatra were taken for stable isotope analysis. Morphological description of these taxa is given in Appendix I.

4.3.1 Gomphotheriidae

From mainland Asia, two taxa of the Gomphotheriidae were analysed. The Platybelodon cf. grangeri specimens (n = 6) analysed in this study are housed in the Piriya section in the NIRPM. Detailed information on the exact origin of the analysed specimens is unavailable, since all of the specimens were surface collected by local villagers. However, the fossilisation of analysed specimens is similar to those from the Linxia Basin rather than to fossils from other localities. According to Deng (2006), the age of these specimens can be considered as Middle Miocene. Three fragmentary Sinomastodon specimens analysed in this study originated from the Tha Chang (n = 1) and Irrawaddy (n = 2). Since all of the specimens are surface collected, the actual stratigraphic ages are unknown. However, interpolating from the occurrence of the genera in the lower biostratigraphical range of the Chaingzauk fauna of the Irrawaddy sediment, the age of Sinomastodon is estimated at between 6 and 4 Ma, or younger (Zin-Maung-Maung-Thein et al., 2011).

Meanwhile, Sinomastodon bumiajuensis is the only Gomphotheriidae recorded in Java. Eight S. bumiajuensis specimens originating from the Early Pleistocene (> 1.53 to 1.16 Ma) sediments in Bumiayu (n = 3), Semedo (n = 4) and Sangiran (n = 1) were sampled for stable isotope analysis. This species is included in the Satir Fauna (see 4.10 for age determination of species occurrence in Java).

4.3.2 Stegodontidae

4.3.2.1 Genus Stegolophodon

All Stegolophodon specimens analysed originate from mainland Asia. Twelve Stegolophodon stegodontoides samples originate from Ta Chang (n = 6) and Irrawaddy (n = 6). The exact stratigraphic position of the St. stegodontoides specimens is

unknown, however, the occurrence of this species can be estimated between the Late Miocene to the Early Pliocene (Zin-Maung-Maung-Thein et al., 2011). The St. stegodontoides samples from Tha Chang presumably are older than those from Irrawaddy, since more primitive traits (lower hypsodonty index and less lophid numbers in average) were observed from the St. stegodontoides specimens from Tha Chang (see Appendix I). Seven analysed Stegolophodon intermediate form samples also have unknown stratigraphic positions from Tha Chang. Since Stegolophodon has not yet been recorded from Pleistocene deposits, the occurrence is estimated to be between the Late Miocene and Early Pliocene as well.

4.3.2.2 Genus Stegodon

Four Stegodon species analysed originate from mainland Asia (Stegodon cf. zdansky, Stegodon cf. elephantoides, Stegodon insignis/ganesa and Stegodon orientalis), while two species (pygmy Stegodon sp. and Stegodon trigonocephalus) originate from Java. From the mainland, all Stegodon cf. zdansky (n = 5) and Stegodon cf. elephantoides (n = 11) samples originate from Tha Chang from unknown stratigraphic positions. The age of Stegodon cf. elephantoides is extrapolated to the occurrence in the Lower Irrawaddy Series (Early Pliocene). However, the occurrence of this primitive form in Tha Chang is probably slightly older than the Irrawaddy population. Meanwhile, since the morphology of S. cf. zdansky seems to be more primitive than Stegodon elephantoides and S. insignis from the Lower Pliocene of the Lower Irrawaddy sequence, the age of this species is estimated as older than Pliocene, presumably of Late Miocene age, which is the time that primitive Stegodon species first arose from Stegolophodon (Saegusa et al., 2005).

Stegodon insignis/ganesa molars analysed originate from Irrawaddy (n = 3) and the Siwalik Group in the vicinity of Haripur (n = 3). The age of this species is estimated at Late Pliocene-Early Pleistocene (Opdyke et al., 1979). In addition, Stegodon cf. orientalis molars were surface collected from the upper part of the Tha Chang Sandpits (n = 3) and from an unknown locality in Laos (n =1). The occurrence of this species is extrapolated from the age of the Ailuropoda-Stegodon Fauna from southern China, Panxian Dong, dated to between 130-300 ka (Schepartz et al., 2005).

Fifty four Stegodon trigonocephalus specimens analysed in this study originate from the Early to late Middle Pleistocene (1.16 Ma to 143 ka, see Appendix I for first and last occurrences of this species) sediments in Sangiran (both Bapang and Sangiran formations), Kedung Brubus, Trinil, Ngandong and West Java (Bumiayu and Subang from unknown age, most likely from the Middle Pleistocene). This species is included in the Cisaat (+ Sangiran), Kedung Brubus (+ Bapang), Trinil, Ngandong, and Middle Pleistocene West Java Faunas. Meanwhile, the pygmy Stegodon sp. (n = 2) were collected from the Early Pleistocene sediments in Sambungmacan and Cirebon. In this study, pygmy Stegodon sp. is thought to correspond with the Cisaat (Sangiran) Fauna.

4.3.3 Elephantidae

Members of family Elephantidae analysed in this study include: Archidiskodon planifrons, Elephas hysudricus, cf. Palaeoloxodon namadicus and Elephas maximus from mainland Asia, as well as Stegoloxodon indonesicus, Elephas hysudrindicus and Elephas maximus from Java. Additionally, modern Elephas maximus samples from Sumatra were also included.

Archidiskodon planifrons specimens (n = 2) were collected from the late Pliocene-Early Pleistocene (3.3 -2.6 Ma) Siwalik sediments located near Haripur. Specimens of Elephas hysudricus (n = 2) were also derived from the Upper Siwalik sediment located near Haripur, with ages estimated between 2.7 and 0.8 Ma (Hussain et al., 1992, Dennel et al., 2006). The exact stratigraphy of cf. Palaeoloxodon namadicus specimens from Tha Chang (n = 4) is unknown. However, this form was mostly surface collected from the locality where the upper part of Tha Chang fluvial sediment is exposed. Extrapolated from the occurrence of this species from other sites in SE Asia (Dennell et al., 2006, Nanda, 2008), the age of P. namadicus is estimated between the late Early and Middle Pleistocene. Additionally, four Elephas maximus samples originate from the uppermost part of Tha Chang sandpits were taken for this analysis. The age is estimated between the late Middle Pleistocene and the Late Pleistocene.

From Java, Stegoloxodon indonesicus specimens (n = 5) were collected from the Early Pleistocene sediments near Semedo (>1.5 Ma, see Appendix I for the species occurrence estimation). This species is thought to correspond with the Satir Fauna stage

or earlier. Twelve Elephas hysudrindicus specimens were recovered from the Middle Pleistocene sediments in Sangiran (Bapang Fm.), Kedung Brubus, Ngandong, Sunggu, Brebes and Bumiayu. In the faunal assemblage grouping, this species is included in the Kedung Brubus (+ Bapang), Ngandong, Sunggu and Middle Pleistocene West Java Faunas. The Elephas maximus specimens analyzed in this study were obtained from the Cipeundeuy faunal assemblage (n = 3, age estimated at 35 ka), Holocene (?) cave in Karangbolong (n = 1), and from extant populations from Sumatra (n = 5). The recent E. maximus originates from the wild (n = 4) and from captivity Way Kambas National Park (n = 1).

For statistical analyses, all samples from mainland Asia and Sundaland are grouped by their taxonomic classification (species and family) as well as chronological and spatial occurrence, since all samples span a large spatial range from and temporal range, from the Middle Miocene to present. A grouping of samples based on faunal succession is undertaken only for Java, since the dating and fauna succession of Java are better established. In addition, a serial sample analysis on an E. hysudrindicus molar was carried out to test if seasonal changes could be detected during the molar development.

Comparative stable isotope data from other studies include: Proboscidean taxa from the lower Dhok Pathan Formation in the Siwaliks (Nelson, 2007), Proboscidean taxa from Chaingazuk Fauna in Irrawaddy (Zin-Maung-Maung-Thein et al., 2011) and other fossil taxa, including cervids, bovids, suids, felids and hominin, from Sangiran and Trinil obtained from Janssen et al. (2016; Appendix III).

Isotopic analysis of Proboscidea from the Late Miocene sediments from Dhok Pathan, Siwalik Group, analysed by Nelson (2007) is included in this chapter in order to provide additional information on palaeoenvironment between 9 and 8 Ma. The proboscidean taxa from two different ages analysed by Nelson (2007) included Gompotheres (n = 4, from 9.3-9.2 Ma; n = 5, from 8.1-8.0 Ma), and Dinotherium (n=1, from 8.1-8.0 Ma). Proboscidean taxa analysed in Zin-Maung-Maung-Thein et al. (2011) included Stegodon (n = 11) and Sinomastodon (n = 1).

4.4 Isotopic analysis results

4.4.1 General results

A summary of measured $\delta^{13}C$ and $\delta^{18}O$ values ranges for each species is presented in Table 4.3. The $\delta^{13}C$ values of modern samples have been adjusted with a 1.5‰ correction factor. Individual and mean $\delta^{13}C$ (‰, $_{VPDB}$) and $\delta^{18}O$ (‰, $_{VPDB}$) values of all analysed species are presented in Figure 4.11. The MANOVA and Kruskal-Wallis test, paired with pairwise Mann-Whitney analysis were applied on the seventeen species and indicates that significant differences between species (MANOVA p values < 0.001, Kruskal Wallis post hoc p value for $\delta^{13}C$ variances = 1.16E-17 and p value for $\delta^{18}O$ variances p = 3.54E-6). Matrices of pairwise probability Benferroni corrected p values post hoc tests to determine significant differences between taxa are presented in Table 4.4.

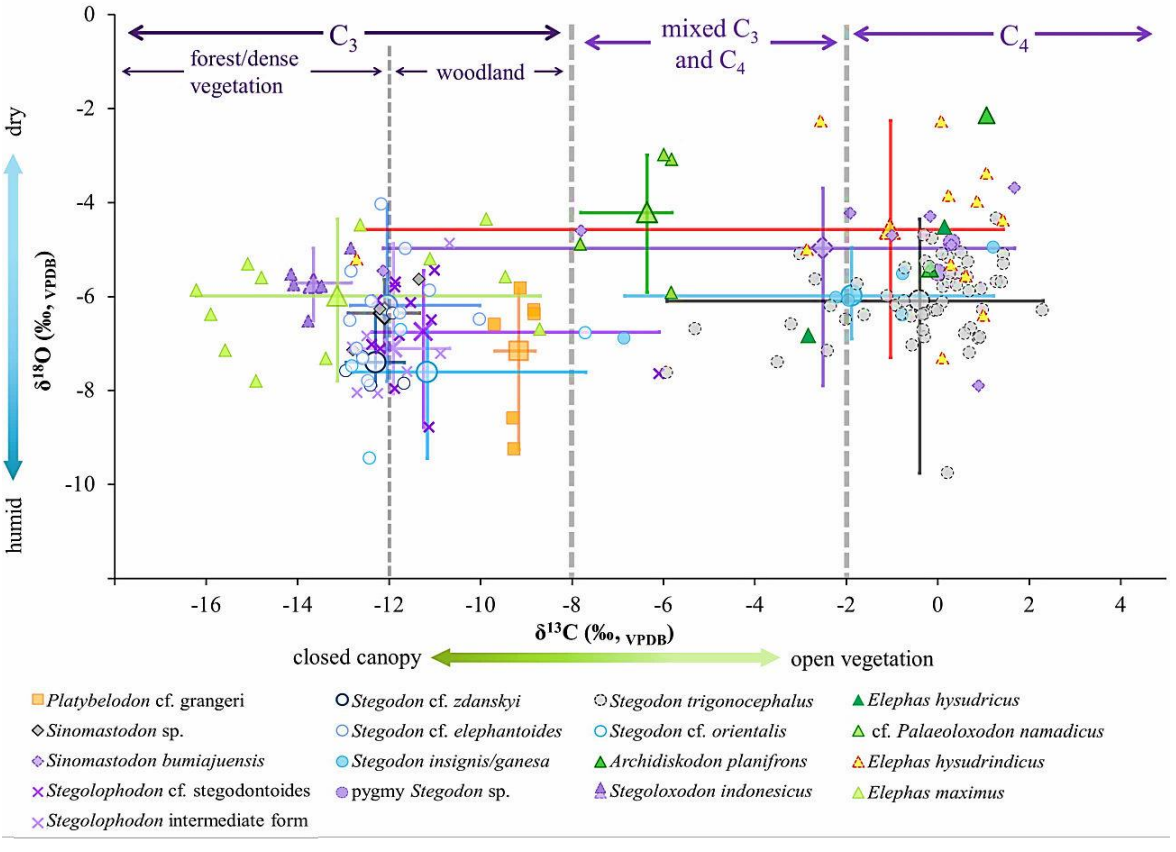

Figure 4.11 Mean $\delta^{13}C$ and $\delta^{18}O$ values and ranges of all analysed proboscidean samples analysed in this study from mainland Asia, Java and Sumatra. Dashed lines represent boundaries between vegetation and diet types (Cerling et al., 1997a, 1999, MacFadden et al., 1999, Passey et al., 2002, Feranec et al., 2007). Means are designated by the crossing of the range bars.

The $\delta^{13}C$ values of all analysed samples from mainland Asia and Sundaland range between -17.2 and 2.3‰ (enamel, $_{VPDB}$) and cover all types of diet. The $\delta^{13}C$ values of Platybelodon cf. grangeri, Sinomastodon sp., Stegoloxodon species, Stegodon cf. zdanskyi, Stegodon cf. stegodontoides, Stegodon cf. orientalis, Stegoloxodon indonesicus and Elephas maximus suggest that these taxa are predominantly C_3 feeders in both dense forest and woodland vegetation. Particularly, all Stegoloxodon indonesicus samples ($\delta^{13}C$ values between -14.1 and -12.8‰) are consistent with the range of dense forest dwellers, while the $\delta^{13}C$ values all Platybelodon samples (between -9.7 and -8.7‰) suggest that this species was foraging in a more open woodland vegetation. The $\delta^{13}C$ values of cf. Palaeoloxodon namadicus plot in the range of a mixed C_3-C_4 diet, Archidiskodon planifrons and pygmy Stegodon sp. in a predominantly C_4 diet, while Stegodon insignis, Elephas hysudricus and Stegodon trigonocephalus are in both mixed C_3-C_4 and dominant C_4 diet ranges. Sinomastodon bumiajuensis and Elephas hysudrindicus appear to represent more flexible feeders, as their $\delta^{13}C$ values are within the range of all diet types, although most of the samples plot in the predominantly C_4 diet range.

Of the family based-groupings, the Gomphoteriidae, Stegodontidae and Elephantidae are statistically undistinguishable (Kruskal-Wallis p = 0.0673). Meanwhile, the statistical results clearly depict significant differences in pairing between species with predominant C_3 and C_4 dietary preferences, as well as between the mixed feeder cf. Palaeoloxodon namadicus with most of the exclusively C_3 or C_4 feeders (Kruskall-Wallis test p value = 1.159E-17, see Table 4.4b for Benferroni corrected p values for each species pairing).

The $\delta^{18}O$ (enamel, $_{VPDB}$) values of all samples from mainland Asia and Sundaland cover a range between -9.7 and -2.2‰. On the family scale, the median $\delta^{18}O$ values of Elephantidae taxa are significantly higher than members of Gomphoteriidae and Stegodontidae (Kruskal Wallis p = 0.0205, Benferroni corrected p for Gomphotheriidae-Elephantidae pairing = 0.0217 and for Stegodontidae-Elephantidae pairing = 0.0003). At the species level, significantly higher $\delta^{18}O$ median values occur between the pairing of Sinomastodon bumiajuensis, Archidiskon planifrons, cf. Palaeoloxodon namadicus, Elephas hysudrindicus and most other species (see Table 4.4c for Benferroni corrected p values for each species pairing).

Table 4.3 Descriptive statistic for $\delta^{13}C$ and $\delta^{18}O$ values of proboscidean taxa from mainland Asia and Sundaland

taxa	n	$\delta^{13}C$ (‰, VPDB)					$\delta^{18}O$ (‰, VPDB)				
		mean	median	std. dev	std. error	range	mean	median	std. dev	std. error	range
Gomphotheriidae											
Platybelodon cf. grangeri	6	-9.2	-9.2	0.3	0.1	-9.7 to -8.8	-7.2	-6.5	1.4	0.6	-9.3 to -5.8
Sinomastodon sp.	3	-12.1	-12.2	0.7	0.4	-12.8 to -11.3	-6.4	-6.3	0.8	0.5	-7.2 to -5.6
Sinomastodon bumiajuensis	8	-2.5	-0.6	4.9	1.7	-12.1 to 1.7	-5.0	-4.7	1.3	0.5	-7.9 to -3.7
Stegodontidae											
Stegolophodon cf. stegodontoides	12	-11.3	-11.8	1.7	0.5	-12.4 to -6.1	-6.7	-6.7	1.0	0.3	-8.8 to -5.5
a. Tha Chang	6	-11.6	-11.7	0.5	0.2	-12.2 to -11.0	-6.1	-6.0	0.6	0.3	-7.1 to -5.5
b. Irrawaddy	6	-10.9	-11.8	2.4	1.0	-12.4 to -6.1	-7.4	-7.3	0.9	0.4	-8.8 to -6.1
Stegolophodon intermediate form	7	-11.9	-12.2	0.9	0.3	-12.8 to -10.7	-7.1	-7.2	1.1	0.4	-8.1 to -4.9
Stegodon cf. zdansky	5	-12.3	-12.4	0.5	0.2	-12.9 to -11.7	-7.4	-7.6	0.6	0.3	-7.9 to -6.4
Stegodon cf. elephantoides	11	-12.0	-12.4	0.9	0.3	-12.8 to -10.0	-6.1	-6.4	1.1	0.3	-7.8 to -4.0
Stegodon insignis/ganesa	6	-1.9	-1.4	2.7	1.1	-6.9 to 1.2	-6.0	-6.1	0.7	0.3	-6.9 to -5.0
a. Irrawaddy	3	-3.2	-1.9	3.2	1.9	--6.9 to -0.7	-6.2	-6.1	0.7	0.4	-6.9 to -5.5
b.Siwaliks	3	-0.6	-0.8	1.7	1.0	-2.2 to 1.2	-5.8	-6.0	0.8	0.4	-6.4 to -5.0
pygmy Stegodon sp.	2	0.2	0.2	0.2	0.2	0.0 and 0.3	-5.2	-5.2	0.5	0.3	-5.5 and -4.9
Stegodon trigonocephalus	54	-0.4	0.0	1.6	0.2	-5.9 to 2.3	-6.1	-6.1	0.9	0.1	-9.7 to -4.4
a. Ngandong	10	-1.8	-1.8	2.7	0.9	-5.9 to 2.3	-6.8	-6.7	0.5	0.2	-7.6 to -6.3
b. Trinil H.K.	10	-0.4	-0.1	1.4	0.5	-2.7 to 1.4	-6.1	-6.2	0.4	0.1	-6.7 to -5.5
c. Kedung Brubus + Bapang	21	0.2	0.2	0.7	0.2	-1.1 to 1.4	-5.9	-5.7	1.1	0.2	-9.7 to -4.4
d. Satir + Sangiran Fauna	6	-0.1	-0.2	0.8	0.3	-0.8 to 1.4	-6.2	-6.4	0.8	0.3	-7.1 to -5.1
e. West Java	7	-0.7	-0.3	1.5	0.6	-3.0 to 1.3	-5.7	-5.7	0.8	0.3	-7.2 to -4.7

taxa	n	$\delta^{13}C$ (‰, VPDB)					$\delta^{18}O$ (‰, VPDB)				
		mean	median	std. dev	std. error	range	mean	median	std. dev	std. error	range
Stegodon cf. orientalis	4	-11.2	-12.1	2.4	1.2	-12.8 to -7.7	-7.6	-7.1	1.3	0.6	-9.5 to -6.7
a. Tha Chang	3	-10.8	-11.7	2.7	1.6	-12.8 to -7.7	-7.0	-6.8	0.4	0.3	-7.9 to -6.7
b. Laos	1	-	-12.4	-	-	-12.4	-	-9.5	-	-	-9.5
Elephantidae											
Archidiskodon planifrons	2	0.5	0.5	0.9	0.6	-0.2 and 1.1	-3.8	-3.8	2.3	1.6	-5.4 and -2.2
Stegoloxodon indonesicus	5	-13.7	-13.8	0.5	0.2	-14.1 to -12.8	-5.7	-5.8	0.6	0.3	-6.5 to -5.0
cf. Palaeoloxodon namadicus	4	-6.4	-5.9	1.0	0.5	-7.8 to -5.8	-4.2	-4.0	1.4	0.7	-5.9 to -3.0
Elephas hysudricus	2	-1.4	-1.4	2.1	1.5	-2.8 to 0.1	-5.7	-5.7	1.6	1.2	-6.8 to -4.5
Elephas hysudrindicus	12	-1.0	0.3	3.9	1.1	-12.7 to 1.4	-4.6	-4.7	1.5	0.4	-7.3 to -2.3
a. Sunggu	1	-	-12.7	-	-	-12.7	-	-5.2	-	-	-5.2
b. Ngandong	1	-	-2.9	-	-	-2.9	-	-5.0	-	-	-5.0
c. Kedung Brubus + Bapang	8	0.3	0.5	1.2	0.4	-2.6 to 1.4	-3.9	-3.9	1.2	0.4	-5.6 to -2.3
d. West Java	2	-	-	-	-	0.1 and 1	-	-	-	-	-7.3 and -6.4
Elephas maximus	13	-13.1	-13.4	2.6	0.7	-16.21 to -8.70	-6.0	-5.9	1.1	0.3	-7.8 to -4.4
a. Tha Chang	4	-11.3	-11.3	1.9	0.9	-13.1 to -9.5	-5.1	-5.0	0.9	0.4	-6.1 to -4.4
b. Sumatra (after correction factor of 1.5‰)	5	-14.7	-15.6	2.1	0.9	-16.2 to -11.1	-6.0	-5.9	0.8	0.3	-7.2 to -5.2
c. Holocene cave deposit	1	-	-15.1	-	-	-15.1	-	-5.3	-	-	-5.3
d. Cipeundeuy	3	-12.3	-13.4	3.2	1.9	-14.9 to -8.7	-7.3	-7.3	0.6	0.3	-7.8 to -6.7

Table 4.4 Matrices of pairwise probabilities

a. of variance difference in $\delta^{13}C_{enamel}$ and $\delta^{18}O_{enamel}$ values among taxa. Values shown in red indicate significant p values ($\alpha \leq 0.05$) using MANOVA test.

	Pg	Sm	Sb	Sts	Sti	Sz	Se	Si	pS	St	So	Ap	Sli	Ehs	Pn	Ehd
Sm	23.9120															
Sb	0.0485	0.1423														
Sts	19.6420	93.2020	0.0001													
Sti	20.0300	85.3650	0.0017	96.9170												
Sz	20.8710	70.0040	0.0078	62.0750	120.4800											
Se	2.3984	132.3300	0.0001	37.9760	32.2060	22.1400										
Si	0.1952	0.3861	29.6450	0.0004	0.0084	0.0390	0.0003									
pS	1.7520	10.3790	51.6070	0.0247	0.3004	1.2877	0.0246	69.9500								
St	9.56E-10	3.69E-09	0.0876	9.00E-20	1.53E-15	3.38E-13	1.28E-20	38.1480	66.8390							
So	60.0040	52.1080	0.0460	56.5460	88.2670	99.9980	12.1510	0.2060	4.1323	5.86E-10						
Ap	0.9931	9.3635	31.8280	0.0121	0.1939	0.9400	0.0163	19.1200	99.9210	2.2067	3.0703					
Sli	1.3734	67.4770	0.0042	4.8434	9.3652	11.0930	38.8140	0.0142	0.9343	1.33E-15	7.0338	0.8591				
Ehs	3.6991	13.1600	77.3880	0.0850	0.6154	2.0946	0.0687	126.4000	119.4900	94.0820	6.1996	82.4640	1.3662			
Pn	1.7119	7.9288	5.0642	0.1281	0.4079	0.8887	0.2155	1.7471	14.0970	9.18E-06	2.1272	16.2970	1.3707	18.5480		
Ehd	0.0006	0.0041	46.0620	1.44E-07	9.84E-06	0.0001	1.67E-07	8.4653	78.8170	0.0084	0.0008	72.7160	4.10E-05	61.0380	0.5300	
Em	0.0800	61.4810	1.67E-06	0.9819	3.5618	4.5429	24.1510	8.09E-06	0.0025	8.00E-26	1.5756	0.0018	121.0900	0.0072	0.0227	1.71E-09

b. of mean difference in $\delta^{13}C_{enamel}$ values among taxa. Values shown in red indicate significant p values ($\alpha \leq 0.05$) using Mann-Whitney test.

	Pg	Sm	Sb	Sts	Sti	Sz	Se	Si	pS	St	So	Ap	Sli	Ehs	Pn	Ehd
Sm	0.8481															
Sb	0.000755	3.26E-05														
Sts	0.993	1	3.29E-05													
Sti	0.9083	1	3.26E-05	1												
Sz	0.7724	1	3.26E-05	1	1											
Se	0.869	1	3.26E-05	1	1	1										
Si	0.000119	3.26E-05	1	3.26E-05	3.26E-05	3.26E-05	3.26E-05									
pS	3.26E-05	3.26E-05	0.9264	3.26E-05	3.26E-05	3.26E-05	3.26E-05	0.9943								
St	3.28E-05	3.26E-05	0.992	3.26E-05	3.26E-05	3.26E-05	3.26E-05	0.9999	1							
So	0.9955	1	3.30E-05	1	1	1	1	3.26E-05	3.26E-05	3.26E-05						
Ap	3.26E-05	3.26E-05	0.8396	3.26E-05	3.26E-05	3.26E-05	3.26E-05	0.9773	1	1	3.26E-05					
Sli	0.1585	0.9998	3.26E-05	0.9695	0.9991	1	0.9997	3.26E-05	3.26E-05	3.26E-05	0.959	3.26E-05				
Ehs	4.41E-05	3.26E-05	1	3.26E-05	3.26E-05	3.26E-05	3.26E-05	1	0.9999	1	3.26E-05	0.9987	3.26E-05			
Pn	0.8913	0.01003	0.4133	0.07485	0.01656	0.006032	0.01177	0.1646	0.001144	0.005791	0.08798	0.000466	0.000113	0.05762		
Ehd	3.59E-05	3.26E-05	0.9999	3.26E-05	3.26E-05	3.26E-05	3.26E-05	1	1	1	3.26E-05	0.9999	3.26E-05	1	0.02879	
Em	0.1455	0.9997	3.26E-05	0.9634	0.9987	0.9999	0.9995	3.26E-05	3.26E-05	3.26E-05	0.9514	3.26E-05	1	3.26E-05	1.00E-04	3.26E-05

c. of mean difference in $\delta^{18}O_{enamel}$ values among taxa. Values shown in red indicate significant p values ($\alpha \leq 0.05$) using Mann-Whitney test.

	Pg	Sm	Sb	Sts	Sti	Sz	Se	Si	pS	St	So	Ap	Sli	Ehs	Pn	Ehd
Sm	0.9994															
Sb	0.1336	0.8615														
Sts	1	1	0.465													
Sti	1	0.9998	0.1646	1												
Sz	1	0.9881	0.0485	1	1											
Se	0.9943	1	0.9504	1	0.9971	0.9504										
Si	0.963	1	0.9913	0.9996	0.9765	0.8386	1									
pS	0.2652	0.9596	1	0.6799	0.3138	0.1131	0.991	0.9993								
St	0.9848	1	0.9766	0.9999	0.9912	0.9072	1	1	0.997							
So	1	0.9353	0.0175	0.9988	1	1	0.8329	0.6419	0.04621	0.7486						
Ap	0.0002	0.0245	0.9593	0.0026	0.0003	6.10E-05	0.05491	0.1274	0.861	0.08361	3.78E-05					
Sli	0.8094	1	0.9998	0.9878	0.8533	0.5669	1	1	1	1	0.3473	0.3237				
Ehs	0.7878	0.9999	0.9999	0.9845	0.8344	0.5393	1	1	1	1	0.3237	0.3473	1			
Pn	0.0030	0.1581	0.9997	0.0280	0.0042	0.0007	0.2794	0.4767	0.9953	0.3683	0.0002	1	0.7689	0.7914		
Ehd	0.0223	0.465	1	0.1353	0.0295	0.0061	0.6502	0.8389	1	0.7484	0.0018	0.9995	0.9724	0.9776	1	
Em	0.9635	1	0.9911	0.9997	0.9769	0.84	1	1	0.9993	1	0.6438	0.1265	1	1	0.4748	0.8375

Key: Pg = Platybelodon cf. grangeri, Sm = Sinomastodon sp., Sb = Sinomastodon bumiajuensis, Sts = Stegolophodon cf. stegodontoides, Sti = Stegolophodon intermediate form, Sz = Stegodon cf. zdanskyi, Se = Stegodon cf. elephantoides, Si = Stegodon insignis/ganesa, pS = pygmy Stegodon sp., St = Stegodon trigonocephalus, So = Stegodon cf. orientalis, Ap = Archidiskodon planifrons, Sli = Stegoloxodon indonesicus, Ehs = Elephas hysudricus, Pn = cf. Palaeoloxodon namadicus, Ehd = Elephas hysudrindicus, Em = Elephas maximus.

4.4.2 Temporal and spatial variation in feeding ecology

A summary of individual $\delta^{13}C$ and $\delta^{18}O$ values of all taxa from mainland Asia and Sundaland, arranged in chronological order, is presented in Figure 4.12.

4.4.2.1 Middle Miocene to Early Pliocene

The period between the Middle Miocene and Early Pliocene is represented by Platybelodon cf. grangeri, Stegolophodon cf. stegodontoides, Stegolophodon intermediate form, Stegodon cf. zdansky, Sinomastodon sp., and Stegodon cf. elephantoides. The $\delta^{13}C$ values of all samples from the Middle Miocene to Early Pliocene (-12.9‰ to -6.1‰) plot in the range of predominantly C_3 browsers, except for one Stegolophodon cf. stegodontoides individual from the Irrawaddy sequence that shows a mixed C_3-C_4 diet. The $\delta^{13}C$ range of Platybelodon cf. grangeri that represents the Middle Miocene suggests a feeding habitat in a more open woodland biome, while other taxa were foraging in both dense forest and woodland vegetation. The $\delta^{18}O$ value of earlier proboscidean taxa between the Middle Miocene and Early Pliocene are low (-9.3‰ to -4.0‰), suggesting humid conditions prevailed during this stage.

Despite originating from different localities and probably different ages, the $\delta^{13}C$ values of Stegolophodon cf. stegodontoides individuals from Tha Chang and Irrawaddy are statistically indistinguishable ($p = 0.5745$, Kruskal-Wallis test), while the $\delta^{18}O$ values of individuals from Tha Chang are significantly higher than those from Irrawaddy groups ($p = 0.0245$, Kruskal-Wallis test). This result suggests that the feeding habitats of both groups were similar in both regions while conditions of meteoric drinking water were distinct for each area, the Tha Chang region perhaps experienced drier conditions.

The $\delta^{13}C$ values of the Late Miocene-Early Pliocene Proboscidea from the Tha Chang sandpit (-12.9‰ to -10.0‰, mean = -12.0‰) are lower than unspecified Elephantoidea taxa from the Late Miocene-Early Pliocene Chaingazuk Fauna from the Irrawaddy Group (range between -12.6‰ and -5.4‰, mean = -10.3‰; this study and Zin-Maung-Maung-Thein et al., 2011), yet showing close resemblance to the Late Miocene Dhok Pathan Fauna from the Siwaliks Group (between -12.2‰ and -9.6‰, mean = -11.4‰, Nelson, 2007). There is no significant difference in $\delta^{13}C$ values ($p = 0.1732$, Kruskal-

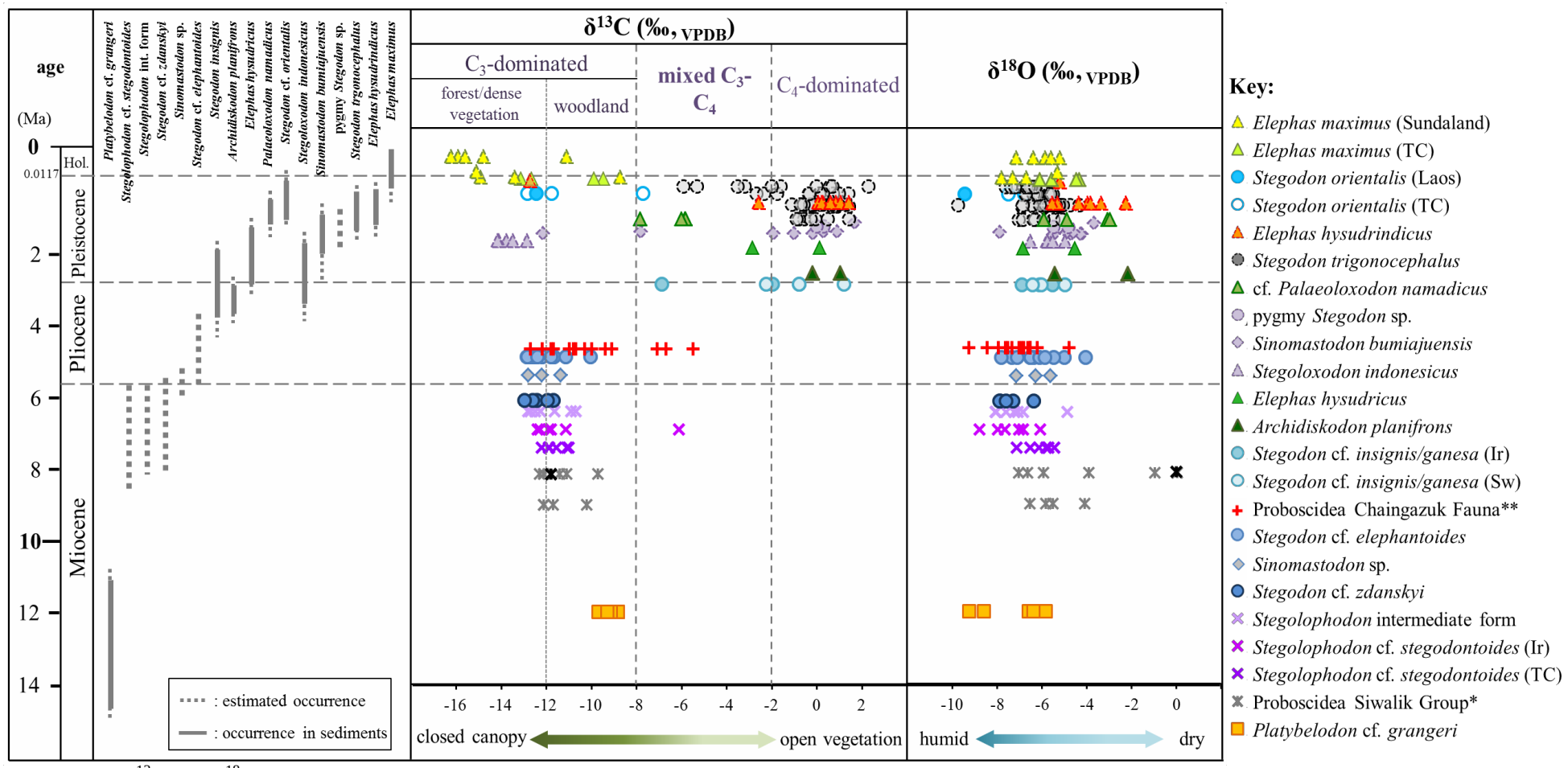

Figure 4.12 $\delta^{13}C$ and $\delta^{18}O$ values of analysed taxa from mainland Asia and Sundaland arranged in estimated chronological sequence. Points with solid outline indicate mainland samples, while points with dashed outline indicate Sundaland samples. Vertical dashed lines represent boundaries between vegetation and diet types (Cerling et al., 1997a, 1999, MacFadden et al., 1999, Passey et al., 2002, Feranec, 2007).
* : after Nelson, 2007, the darker shade indicates Deinotherium and lighter shade indicates Gomphothere (spp.); ** : after Zin-Maung-Maung-Thein et al., 2011; TC : Tha Chang; Sw : Siwaliks; Ir : Irrawaddy.

Wallis test) between three Late Miocene-Early Pliocene faunas (Late Miocene-Early Pliocene Proboscidea from the Tha Chang sandpit, Chaingazuk Fauna and Dhok Pathan Fauna). The number of individuals with higher $\delta^{13}C$ values indicating mixed feeding increases during the Early Pliocene (6-4 Ma), as shown in the Chaingazuk Fauna.

In comparison, $\delta^{18}O$ values of the Tha Chang Elephantoidea (-8.1‰ to -4.0‰, mean =6.6‰) are showing similarity to those from the Chaingazuk Fauna (-9.2‰ to -4.8‰, mean = -7.1‰; data from Zhin-Maung-Maung-Thein et al., 2011). Apart from Dinotherium and a Gompothere individuals from a younger age group that show significantly higher $\delta^{18}O$ values, the overall $\delta^{18}O$ values of Proboscidea from Tha Chang and Chaingazuk Faunas do not seems to show any significant difference from those of the Siwaliks Group (between −7.0 and 0.0‰, mean = -4.6‰; data from Nelson, 2007). However, the two significant differences also occur between the Siwaliks Group and Chaingazuk, as well as between the Siwaliks Group and the Late Miocene-Early Pliocene Elephantoidea from Tha Chang (Kruskal-Wallis p = 0.0022; Mann-Whitney pairwise's Benferroni corrected p between Siwaliks and Tha Chang = 0.0299 and between Siwaliks and Irrawaddy = 0.0024).

4.4.2.2 Late Pliocene to Middle Pleistocene

The period between the Late Pliocene to Early Pleistocene is represented by Stegodon insignis, Archidiskodon planifrons, Elephas hysudricus and Stegodon orientalis from mainland Asia, as well as Stegoloxodon indonesicus, Sinomastodon bumiajuensis, pygmy Stegodon sp., Stegodon trigonocephalus and Elephas hysudrindicus from Java. From the Late Pliocene, $\delta^{13}C$ values of the taxa originate from mainland Asia (-7.8‰ to 1.2‰) slightly shift toward more positive values than in the Miocene. Mixed C_3 and C_4 feeder and specialised C_4 grazers became dominant during the Pliocene. However, pure C_4 grazer individuals are not recorded among the specimens from Tha Chang. Correspondingly, the $\delta^{18}O$ values are also slightly increased in the Pliocene-Middle Pleistocene taxa (-6.9‰ to -2.2‰, mean = -5.1‰), suggesting increasing aridity. Comparative stable isotope data of mammalian fauna from surrounding areas are unavailable at this age.

In Java, the $\delta^{13}C$ values of the early inhabitants, Stegoloxodon indonesicus and a Sinomastodon bumiajuensis individual (-14.1‰ to -12.1‰) are consistent with herbivores that browsed C_3 plants in a dense forest vegetation. The $\delta^{13}C$ values of other, probably younger samples plot in a mixed C_3-C_4 or predominantly C_4 diet, which suggests more open grassy feeding habitats. Representing the latest Middle Pleistocene in Java, the $\delta^{13}C$ and $\delta^{18}O$ values of an Elephas hysudrindicus from Sunggu (-12.7‰ and -5.2‰, respectively) suggest that this individual consumed predominantly C_3 plants in a humid and densely forested environment. The isotopic values and palaeoenvironmental indication of this single E. hysudrindicus differs significantly from samples originate from the earlier stage of Middle Pleistocene. A more detailed result of taxa from Java will be discussed in Section 4.4.3.

The isotopic values of Stegodon insignis individuals from the Late Pliocene deposits of the Irrawaddy ($\delta^{13}C$ = -6.9‰ to -0.8‰; $\delta^{18}O$ = -6.9‰ to -5.5‰) are lower than individuals from the Siwaliks ($\delta^{13}C$ = -2.2‰ to -1.2‰; $\delta^{18}O$ = -6.0‰ to -5.0‰). However, there are no statistically significant differences between the values of the Irrawaddy and the Siwaliks groups. The $\delta^{13}C$ value of a single Stegodon cf. orientalis individual from Middle Pleistocene sediments from Laos (-12.4‰) falls within the range of Tha Chang individuals (-12.8‰ to -7.7‰) and its $\delta^{18}O$ values (-9.5‰) are significantly lower than those from the Tha Chang sandpits (-7.5‰ to 6.7‰).

Unlike the Archidiskodon planifrons individuals from the Siwaliks that shows a strong grazing signal, their insular close relative, Stegoloxodon indonesicus, had a significantly distinct dietary preference as a pure browser (p value = 3.2 E-5, Mann-Whitney test). Even so, the $\delta^{18}O$ values of the two species do not show any significant differences.

4.4.2.3 Late Pleistocene to Present

The period between the Late Pleistocene and Present is represented by Elephas maximus from both mainland Asia and Sundaland. The dietary preferences of all analysed samples from this interval shift back towards C_3-dominated diets since the Late Pleistocene, as the $\delta^{13}C$ values of analysed individuals shift into a more negative range (-16.2‰ to -7.7‰). The decrease in $\delta^{13}C$ values correspond with slightly lowering $\delta^{18}O$ values (between -9.5‰ and -4.4‰) from this interval compared to the foregoing

interval, which suggests an increase in humidity. Despite originating from different localities and ages, there is no significant difference noticeable among Elephas maximus populations from Tha Chang, Java and Sumatra, in both $\delta^{13}C$ and $\delta^{18}O$ values (Kruskall-Wallis test p value for $\delta^{13}C$ = 0.09933 and for $\delta^{18}O$ = 0.1118).

4.4.3 Successive faunal assemblages of Java

All analysed samples from Java cover a wide range of $\delta^{13}C$ (enamel, $_{VPDB}$) values between -17.2 and 2.3‰, while their $\delta^{18}O$ (enamel, $_{VPDB}$) values range between -9.7 and -2.3‰. The $\delta^{13}C$ values of the analysed samples span the range of all diets and feeding habitats (C_3, mixed C_3-C_4 and C_4). Plots of individual of $\delta^{13}C$ (‰, $_{VPDB}$) and $\delta^{18}O$ (‰, $_{VPDB}$) values and ranges of all analysed samples, which grouped by faunal assemblages, are presented in Figure 4.13A, followed by individual isotopic values and ranges for the Early Pleistocene assemblages (Fig 4.13B), the Middle Pleistocene assemblages (Fig. 4.13C) and the Late Pleistocene-recent assemblages (4.13D). In Figure 4.14, individual $\delta^{13}C$ and $\delta^{18}O$ values of all taxa from Java and Sumatra are arranged in chronological order, based on the estimated ages of the faunal assemblages. Matrices of pairwise probability Benferroni corrected p of Mann-Whitney post hoc test, to determine significant differences among faunal assemblages and all species from successive stages, is provided in Table 4.5.

Among all faunal assemblages, the $\delta^{13}C$ values of the Late Pleistocene-Recent Elephantoids are significantly lower than for all other faunas, with the exception of Elephantoids from the Satir Fauna (see Table 4.5.1A for Mann-Whitney test Benferroni corrected p of each pairing). The $\delta^{13}C$ values of the Satir Fauna Elephantoids are only significantly lower than for the Kedung Brubus + Bapang Fauna Elephantoids (Kruskal Wallis p = 3.416 E-6, Mann-Whitney test Benferroni corrected p = 0.0254), while pairings of samples from other faunal units are statistically indistinguishable. Correspondingly, significant differences in $\delta^{18}O$ values only occurs between the Elephantoids from the Kedung Brubus + Bapang and Ngandong faunal assemblages, where the $\delta^{18}O$ values of the Ngandong fauna are significantly lower than for the Kedung Brubus + Bapang (Kruskal Wallis p = 0.0005, Mann-Whitney test Benferroni corrected p = 0.0269).

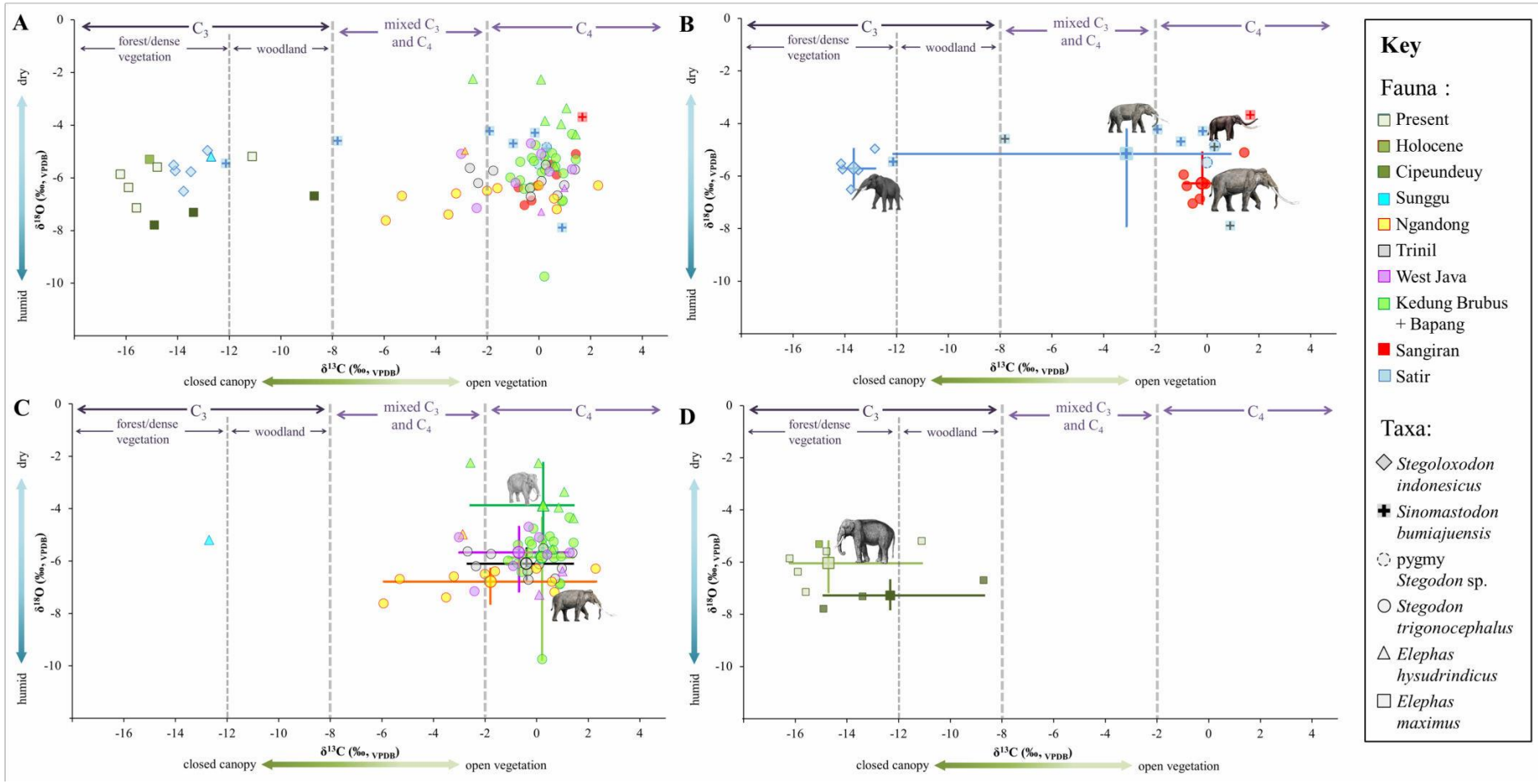

Figure 4.13 Mean $\delta^{13}C$ and $\delta^{18}O$ values and ranges of: analysed enamel samples from Java **A)** grouped by faunal assemblages, **B)** of Early Pleistocene assemblages (Satir and Sangiran assemblages), **C** of Middle Pleistocene assemblages (Kedung Brubus + Bapang, Trinil, Ngandong, West Java and Sunggu) and **D)** of Late Pleistocene, Holocene (samples of both ages are from Java) and Recent (the only specimens from Sumatra) ages. Different colours represent faunal assemblages, while different shapes indicate taxa. Dashed lines represent boundaries between vegetation and diet types (Cerling et al., 1997, 1999, MacFadden et al., 1999, Passey et al., 2002, Feranec et al., 2007). Means are designated by the crossing of the range bars.

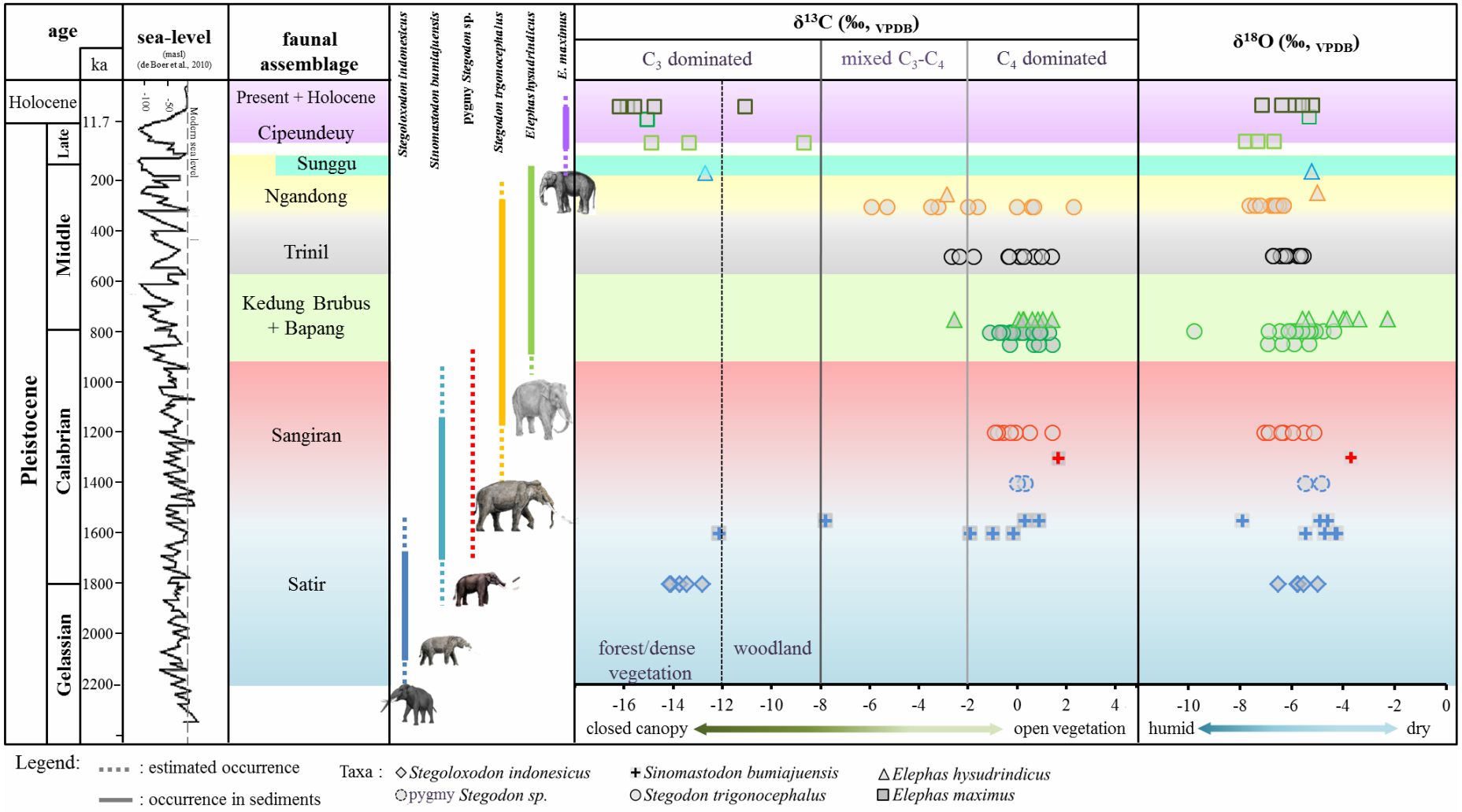

Figure 4.14 $\delta^{13}C$ and $\delta^{18}O$ values of analysed Elephantoidea taxa of Java and Sumatra in chronological sequence.

Table 4.5 Matrices of pairwise probabilities of mean difference in $\delta^{13}C_{enamel}$ and $\delta^{18}O_{enamel}$ values among **(A)** faunal assemblages and **(B)** species from Java. Values shown in red indicate significant p values ($\alpha \leq 0.05$) using Mann-Whitney test.

A	Fauna	1 $\delta^{13}C$, $\delta^{18}O$	2 $\delta^{13}C$, $\delta^{18}O$	3 $\delta^{13}C$, $\delta^{18}O$	4 $\delta^{13}C$, $\delta^{18}O$	5 $\delta^{13}C$, $\delta^{18}O$	6 $\delta^{13}C$, $\delta^{18}O$
1	Satir	-					
2	Sangiran	0.938, 1.000					
3	Kd. Brubus + Bapang	0.025, 1.000	1.000, 1.000				
4	Trinil	1.000, 0.359	1.000, 1.000	1.000, 0.444			
5	Ngandong	1.000, 0.066	1.000, 1.000	0.396, 0.027	1.000, 0.810		
6	West Java	1.000, 1.000	1.000, 1.000	1.000, 1.000	1.000, 1.000	1.000, 1.000	
7	Late Pleistocene to Present	0.095, 0.602	0.029, 1.000	0.001, 0.686	0.008, 1.000	0.006, 1.000	0.012, 1.000

B	Species	1 $\delta^{13}C$, $\delta^{18}O$	2 $\delta^{13}C$, $\delta^{18}O$	3 $\delta^{13}C$, $\delta^{18}O$	4 $\delta^{13}C$, $\delta^{18}O$	5 $\delta^{13}C$, $\delta^{18}O$
1	Stegoloxodon indonesicus	-				
2	Sinomastodon bumiajuensis	0.065, 0.722				
3	pygmy Stegodon	1.000, 1.000	1.000, 1.000			
4	Stegodon trigonocephalus	0.004, 1.000	1.000, 0.036	1.000, 1.000		
5	Elephas hysudrindicus	0.028, 1.000	1.000, 1.000	1.000, 1.000	1.000, 0.015	
6	Elephas maximus	1.000, 1.000	0.019, 0.276	0.677, 1.000	2.8E-5, 1.000	0.004, 0.128

Table 4.6 Matrices of pairwise probabilities of mean difference in $\delta^{13}C_{enamel}$ and $\delta^{18}O_{enamel}$ values among species co-occurring within faunal assemblages. Values shown in red indicate significant p values ($\alpha \leq 0.05$) using Mann-Whitney test.

A	Early Pleistocene faunas	1 $\delta^{13}C$, $\delta^{18}O$	2 $\delta^{13}C$, $\delta^{18}O$	3 $\delta^{13}C$, $\delta^{18}O$
1	Stegoloxodon indonesicus	-	-	
2	Sinomastodon bumiajuensis	0.0259, 0.0481		
3	Pygmy Stegodon	0.4882, 0.1752	1.0000, 0.3608	
4	Stegodon trigonocephalus	0.0487, 0.4113	1.0000, 0.0332	1.0000, 0.1336

B	Sangiran and Bapang Fm.	1 $\delta^{13}C$, $\delta^{18}O$	2 $\delta^{13}C$, $\delta^{18}O$	3 $\delta^{13}C$, $\delta^{18}O$	4 $\delta^{13}C$, $\delta^{18}O$	5 $\delta^{13}C$, $\delta^{18}O$
1	Stegodon trigonocephalus					
2	Elephas hysudrindicus	1.000, 0.008				
3	bovids*	0.752, 1.000	1.000, 0.265			
4	cervids*	1.000, 0.417	1.000, 0.785	0.695, 1.000		
5	suids*	0.003, 1.000	0.077, 0.018	0.146, 0.538	0.332, 0.186	
6	hominin*	0.002, 1.000	0.036, 0.036	0.402, 0.575	0.273, 0.207	1.000, 1.000

C	Trinil Fauna	1 $\delta^{13}C$, $\delta^{18}O$	2 $\delta^{13}C$, $\delta^{18}O$	3 $\delta^{13}C$, $\delta^{18}O$
1	Stegodon trigonocephalus	-	-	
2	bovids*	0.6178, 0.0151		
3	cervids*	0.3791, 0.0288	0.4882, 1.0000	
4	suids*	0.0275, 1.0000	0.0097, 0.7236	0.0369, 0.5533

* data from Janssen et al. (2016)

Both $\delta^{13}C$ and $\delta^{18}O$ values of all analysed taxa from Java show significant differences (Kruskal-Wallis test p for $\delta^{13}C$ = 1.23 E-6 and for $\delta^{18}O$ = 0.0002). Overall, the $\delta^{13}C$ values of Stegoloxodon indonesicus and Elephas maximus are significantly lower than all other species, especially Stegodon trigonocephalus and Elephas hysudrindicus (see Table 4.5.1B for Mann-Whitney test Benferroni corrected p of each pairing). Only the $\delta^{18}O$ values of S. trigonocephalus are significantly lower than for S. bumiajuensis (Benferroni corrected p = 0.0361) and E. hysudrindicus (Benferroni corrected p = 0.0148), while pairings among other species are statistically indistinguishable.

4.4.3.1 The Early Pleistocene assemblages

The Early Pleistocene fauna of Java includes Stegoloxodon indonesicus (n = 5) from Semedo, Sinomastodon bumiajuensis (n = 8) from Satir and "black clay" Sangiran faunas, pygmy Stegodon sp. (n = 2) from probably Early Pleistocene age, and Stegodon trigonocephalus (n = 6) from Sangiran. All taxa from the Satir fauna have $\delta^{13}C$ values (-14.1‰ to 0.9‰) consistent with expected range for herbivore foraging in closed canopy forests to open grasslands, while $\delta^{13}C$ values for all individuals from the Sangiran Fm. (-0.9 to 1.7‰) are indicative for grazing animals in savannah type vegetation. The low $\delta^{13}C$ values of Stegoloxodon indonesicus from the Satir Fauna (range between -14.1 and -12.8‰) suggest that this species was a specialized browser in a closed canopy forest environment. The $\delta^{13}C$ values are also significantly lower than for other Early Pleistocene species (Kruskal Wallis p = 0.0090, see Table 4.6A for Benferroni corrected p values of taxa pairings). The $\delta^{13}C$ values of Sinomastodon bumiajuensis from the Satir and Sangiran assemblages (between -12.1 and 1.7‰) are consistent with all diet ranges. Interestingly, the $\delta^{13}C$ values of analysed Sinomastodon bumiajuensis individuals can be seen as two different clusters: the C_3-mixed diets and C_4 diets. The C_3 and mixed diets are represented by an individual each; both were from West Java (Bumiayu and Semedo). The rest of individuals (from Semedo, Bumiayu and Sangiran) indicate a C_4 diet, where the only individual from Sangiran Formation has the highest $\delta^{13}C$ value. On the other hand, both Stegodon species have a more specific C_4 dietary preference ($\delta^{13}C$ values of pygmy Stegodon are 0‰ and 0.31‰, S.trigonocephalus between -0.8 and 1.4‰).

The $\delta^{18}O$ values of Stegoloxodon indonesicus (between -6.5 and -5.0‰) and Stegodon trigonocephalus (between -7.1 and -5.1‰) are significantly lower than for Sinomastodon bumiajuensis (between -7.9 and -3.7‰; Kruskal Wallis p value = 0.0396, see Table 4.6A for Benferroni corrected p values for the pairings). Although not statistically indistinguishable, the $\delta^{18}O$ values of pygmy Stegodon sp. (-5.5‰ and -4.9‰) are still higher than the average values of Sl. indonesicus and S. trigonocephalus.

4.4.3.2 The Middle Pleistocene assemblages

The Middle Pleistocene assemblages consist of two Proboscidean species: Stegodon trigonocephalus and Elephas hysudrindicus, distributed in the Kedung Brubus + Bapang, Trinil, Ngandong faunas, and from the Middle Pleistocene formations in West Java (Figure 4.13C). Comparative data of other non-Elephantoidea taxa from Sangiran and Trinil from Janssen et al., 2016 (Figure 4.15) were included to detect possible niche separation between co-occurring taxa from these localities.

The $\delta^{13}C$ values of all Stegodon trigonocephalus and Elephas hysudrindicus samples from the Kedung Brubus + Bapang assemblage (between -2.6 and 1.4‰) are concentrated within the range of herbivore grazing C_4 plants in a savannah vegetation, except for one E. hysudrindcus individual that falls in the range for a mixed diet. The $\delta^{13}C$ values of S. trigonocephalus from younger assemblages such as the Trinil fauna (range between -2.7 and 1.4‰), West Java composite assemblage (range between -3.0 and 1.3‰) and Ngandong (between -5.9 and 2.3‰), are consistent with a range for mixed C_3-C_4 and predominant C_4 diet in a relatively open vegetation. The grazer individuals are dominant in the Trinil and West Java faunas, while the proportion of mixed feeder individuals increases in the Ngandong fauna. Meanwhile, samples of E. hysudrindicus are rarely encountered in the West Java assemblage (originating from the Gintung and Tambakan Formations) and Ngandong Fauna, and are even totally absent from the Trinil fauna. The $\delta^{13}C$ values of two individuals from West Java (0.1‰ and 1.0‰) suggest a predominant C_4 diet in an open grassland habitat, while the only analysed individual from Ngandong ($\delta^{13}C$ = -2.9‰) was a mixed C_3-C_4 feeder. The $\delta^{13}C$ values of S. trigonocephalus and E. hysudrindicus from different Middle Pleistocene faunal assemblages are statistically indistinguishable (p value = 0.1448,

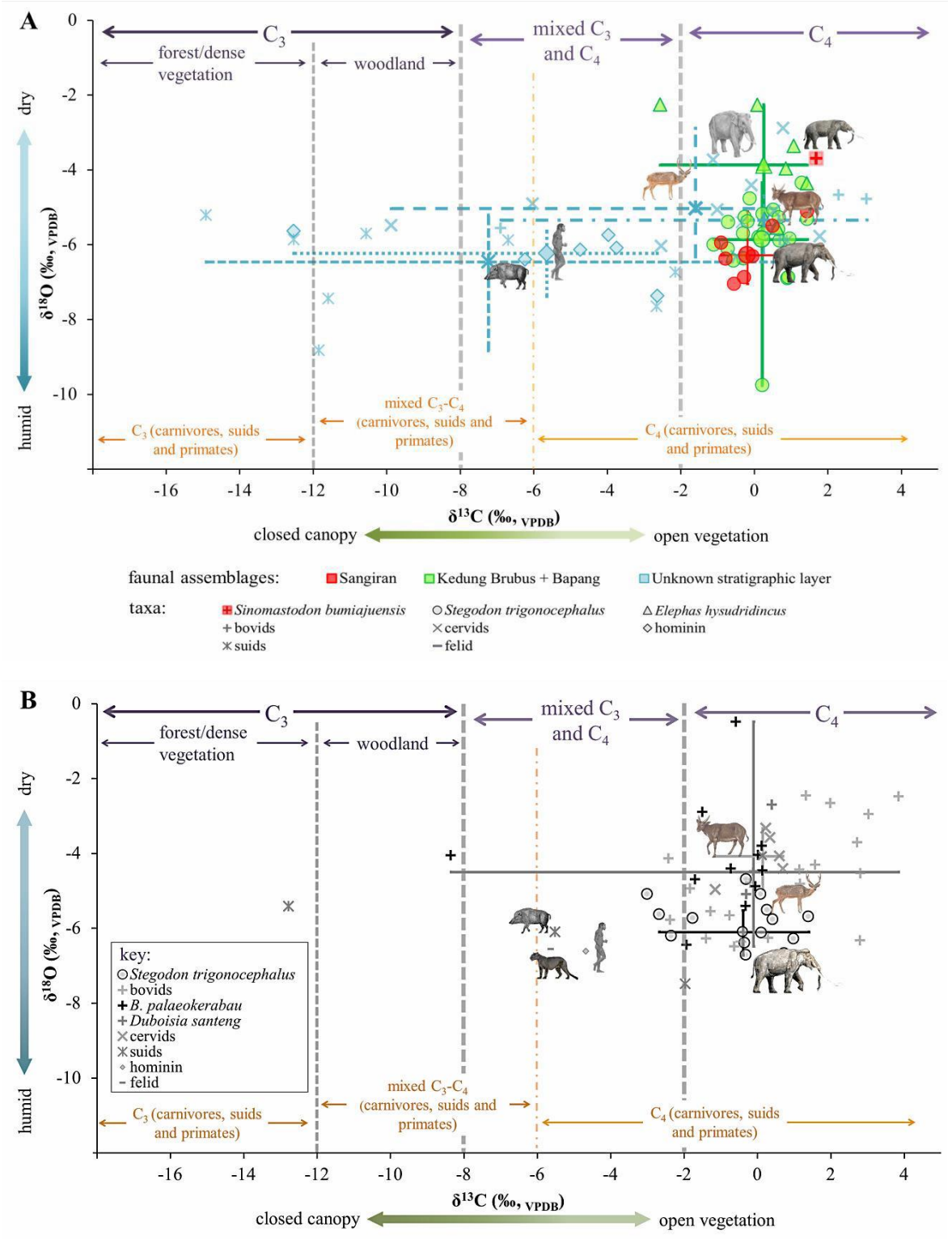

Figure 4.15 Mean $\delta^{13}C$ and $\delta^{18}O$ values and ranges of: **A.** all analysed samples from the Sangiran locality, including the Sangiran and Kedung Brubus + Bapang faunas and **B.** all analysed samples from the Trinil H.K. locality. Faunal assemblages are indicated by different colours, while taxa are indicated by different shapes. Comparative data of cervids, bovids, suids, hominins and felids are taken from Janssen et al. (2016). Indicate in caption why orange dashed line is different for the carnivores, primate and suids.

Kruskal-Wallis test). Nevertheless, there is a trend that the $\delta^{13}C$ values of the Middle Pleistocene faunas gradually become more negative in younger assemblages.

While all analysed S. trigonocephalus and E. hysudrindicus individuals from the Middle Pleistocene faunal assemblages represent open C_4-dominated vegetation to mixed C_3-C_4 grassland, the $\delta^{13}C$ value of the Elephas hysudrindicus individual from Sunggu (-12.7‰) fits in the expected range for predominant C_3 diet. The $\delta^{13}C$ value of the Sunggu individual, presumably represents the youngest occurrence of this species, is significantly more negative than all other analysed individuals from the Kedung Brubus + Bapang, Trinil, Ngandong and West Java assemblages.

Correspondingly, the $\delta^{18}O$ values of all analysed samples are high to moderate (-7.6‰ to 2.3‰, with an exception of a S. trigonocephalus individual from the Bapang Formation (9.7‰), which is strikingly lower in comparison to all other individuals. In those assemblages where the two species co-occurred, the $\delta^{18}O$ values of E. hysudrindicus are mostly higher than for S. trigonocephalus. However, statistical analysis of the two co-occurring species can only be applied to individuals from the Kedung Brubus + Bapang Fauna (Kruskal-Wallis test $p = 0.0008$, Mann-Whitney test Benferroni corrected $p = 9.44$ E-4), since the sample sizes of E. hysudrindicus in other assemblages are insufficient for statistical analysis. Within different assemblages, the $\delta^{18}O$ values of S. trigonocephalus from the Ngandong fauna are considered lower than for other groups, but only significantly lower compared to the individuals from the Kedung Brubus + Bapang Fauna (Kruskal-Wallis test $p = 0.0051$, Mann-Whitney test Benferroni corrected $p = 0.0142$).

4.4.3.2.1 Sangiran

Apart from Proboscidean species, the exact stratigraphic provenances of other taxa analysed by Janssen et al. (2016) are uncertain, as the specimens may either have been derive from the Sangiran Formation, the Bapang Formations, or of mixed origin. Taxa analysed by Janssen et al. (2016) include: cervids (n = 11), bovids (n = 7), suids (n = 10), and hominins (n = 6). A plot of individual values and the ranges of the $\delta^{13}C$ and $\delta^{18}O$ values of all samples from Sangiran area is presented in Figure 4.15A.

The $\delta^{13}C$ values of all herbivores from Sangiran (between -2.7 and 1.7‰ for elephantoids, between -6.9 and 3.1‰ for bovids, and between -9.9 and 1.8‰ for cervids) are indicative for predominantly C_4 grazers, while only four individuals are mixed feeders. Additionally, an outlier cervid individual has a $\delta^{13}C$ value (-9.9‰) that fits a C_3 browser in a more open vegetation preference. The $\delta^{13}C$ values of omnivores are more broadly distributed in all dietary types (range between -12.5 and -5.7‰ for hominins, and between -14.3 and -7.2‰ for suids). Although for hominins, the majority of samples except for one fit in the expected range for a C_4-dominated diet. Statistically, the $\delta^{13}C$ values of Elephantoidea in general are significantly higher than compared to both omnivore taxa (Kruskal-Wallis test p = 5.65 E-5, see Table 4.6B for Benferroni corrected p values of taxa pairings), while other pairings are statistically indistinguishable. The $\delta^{18}O$ values of E. hysudrindicus, bovids and cervids are generally higher than for S. trigonocephalus, suids and hominins. However, only the $\delta^{18}O$ values of E. hysudrindicus show statistical significant difference compared to S. trigonocephalus, suids and hominins (Kruskal-Wallis test p = 0.0001, see Table 4.6B for Benferroni corrected p values of taxa pairings).

4.4.3.2.2 Trinil

The analysed specimens from Trinil all originate from the Haupt Knochenschicht layer. Taxa analysed by Janssen et al. (2016) include: bovids (n = 25), cervids (n = 4), suids (n = 3), hominin (n = 1) and felid (n = 1). Individual data and range plots for Trinil are presented in Fig. 4.15B. Analysed herbivore individuals from the Trinil H.K. (including bovids, cervids and S. trigonocephalus) yielded individual $\delta^{13}C$ values that range between -2.7 and 3.9‰, indicating that they consumed predominantly C_4 vegetation. Most of these individuals plot in the expected range of predominant grazers, and only four individuals of S. trigonocephalus and bovids fit in the range of mixed feeders. Nevertheless, $\delta^{13}C$ values of these mixed feeder individuals are closer to the pure C_4 boundary, suggesting that their diet relied more on C_4 grasses. A single individual of B. palaeokerabau represents an outlier ($\delta^{13}C$ value of -8.4‰) indicates a C_3 feeding preference in open woodland vegetation. The $\delta^{13}C$ values of the carnivore and omnivores (between -5.6 and -2.0‰), are consistent with the range expected for predominant C_4 plant consumption and/or predating on grazer herbivores, except for the

$\delta^{13}C$ value of a single suid individual (-12.8‰) that indicates a C_3-dominated diet in an open canopy environment. Statistically, only the $\delta^{13}C$ values of suids are significantly different from all other taxa (Kruskal-Wallis test p = 0.0281, see Table 4.6C for Benferroni corrected p values of taxa pairings), while the $\delta^{13}C$ values of S. trigonocephalus, bovids and cervids are statistically indistinguishable.

The $\delta^{18}O$ values of all analysed taxa are moderate to high (between -7.5 and -0.5‰). The bovids and cervids have significant higher $\delta^{18}O$ values than S. trigonocephalus (Kruskal-Wallis test p = 0.0002, Benferroni corrected p for bovids-S. trigonocephalus = 0.0151 and for cervids-S. trigonocephalus = 0.0288) and suids (see Table 4.6C for Benferroni corrected p values of taxa pairings). As for felids and the single hominin, the sample numbers for these taxa are insufficient for statistical analysis. However, their individual $\delta^{18}O$ values are notably lower than for S. trigonocephalus, bovids and cervids.

4.4.3.2.3 Serial analysis of an Elephas hysudrindicus molar from Sunggu

A total of 29 serial samples were taken along the enamel of a single, unworn lamella of the third molar (M^3) present in the Sunggu elephant mandible. The $\delta^{13}C$ values of the serial samples range between -13.4‰ and -12.0‰ (Figure 4.16), suggesting that the diet of this individual was constantly dominated by C_3 plants in a densely vegetated environment. The narrow difference between the minimum and maximum values indicates non-significant shifts of food resources over the growth period covered by the samples. While the $\delta^{13}C$ values display no clear seasonal pattern, the $\delta^{18}O$ values provide stronger seasonal variation. The $\delta^{18}O$ values of this individual range between -6.6‰ and -3.9‰, indicating that this animal experienced a considerable seasonal fluctuation in surface water isotopic composition. The serial $\delta^{18}O$ values of the molar show a series of low $\delta^{18}O$ values between sub-sample 1 and 8, indicating wetter conditions during the earlier stage of molar development. A sharp increase occurs at the sub-sample 9, and remains high up to sub-sample 19, suggesting a drier period. The high $\delta^{18}O$ values between sample number 9 and 19 followed by a decrease in the remaining samples, suggest a change to wetter conditions. Sudden decreases occur at sub-samples 20, 21 and 23, indicating the possibility of an unstable seasonal transition

between dry to wet conditions. Nine dry peaks are identified from the $\delta^{13}C$ values (sample number: 2, 6, 9, 13, 19, 22, 24, 27 and 29), which tend to correspond with eight peaks identified in the $\delta^{18}O$ values (sample number: 2, 6, 9, 13, 17-19, 22, 24 and 29).

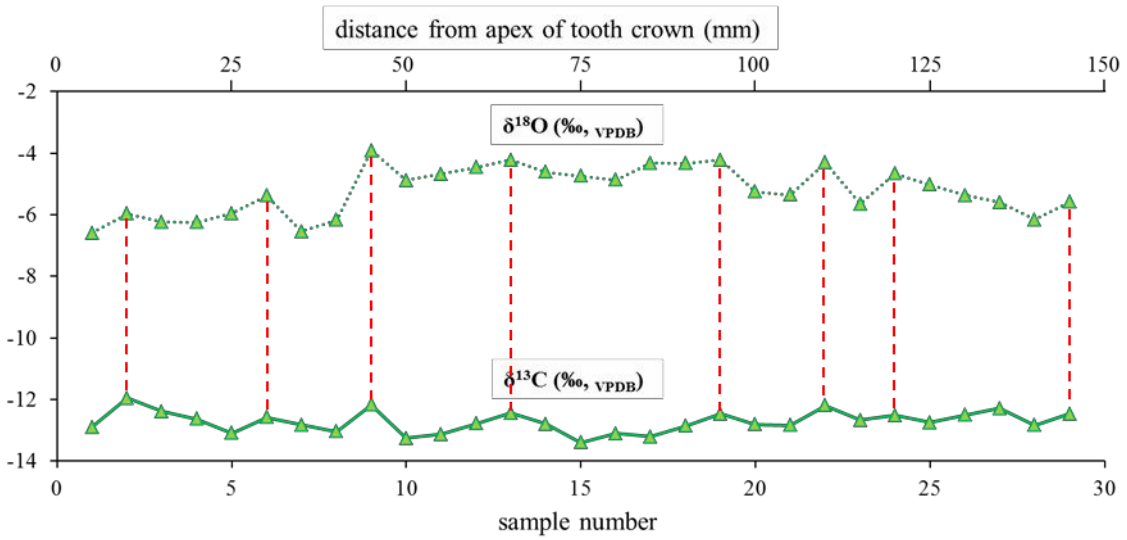

Figure 4.16 Serial $\delta^{13}C$ and $\delta^{18}O$ values of the Elephas hysudrindicus molar from the Sunggu locality. Sub-sample numbers start at the tip of the crown (No. 1, earliest enamel formation) to the base of the crown (No. 29, last formed). Red dashed lines indicate corresponded dry peaks between $\delta^{13}C$ and $\delta^{18}O$ values.

4.4.3.3 The Late Pleistocene-Recent assemblages

The Late Pleistocene-Recent assemblages are represented by nine Elephas maximus individuals from three different localities: Cipeundeuy, Karangbolong (represents cave fauna), and Sumatra (represents Recent Fauna). Individual values and ranges plotted for E. maximus are presented in Figure 4.13D.

Carbon isotope values from the Cipeundeuy and Holocene cave assemblages (-15.08 to -8.7‰) are consistent with a range for predominant C_3 feeding in a closed canopy to more open vegetation. The $\delta^{13}C$ values of wild individuals from Sumatra (range between -16.2 and -14.8‰, after correction factor of 1.5‰) also suggest a feeding habitat of dense vegetation, which closely reflects their actual natural habitat. Likewise, the $\delta^{13}C$ value of a captive individual (-11.1‰, after correction factor of 1.5‰) is plotted in the expected range of C_3 feeding in a more open environment, which is also consistent with its habitat in the national park. The $\delta^{18}O$ values of all E. maximus (between -7.2 and -5.2‰) are significantly lower than all other analysed species, except

for Stegoloxodon indonesicus. The values of individuals from Cipeundeuy are relatively lower than for Karang Bolong and Sumatra. However, there is no significant difference in both $\delta^{13}C$ and $\delta^{18}O$ values among all three assemblages (Kruskal-Wallis test p for $\delta^{13}C = 0.3012$ and for $\delta^{18}O = 0.0948$).

4.5 Discussion

4.5.1 Palaeoenvironment reconstruction of mainland Asia and Java

Despite spanning a shorter time range, the stratigraphy and numerical dating of the terrestrial fauna sequence of Java is much better understood compared to other fossil-bearing sequence of mainland Asia. With the currently available dataset, Java would play an important role in any regional hypothesis regarding Quaternary faunal migration and isolation, environmental change and faunal adaptation of mainland Asia and Sundaland. The data from other fossil bearing sites in mainland Asia are still rather limited to permit firm conclusions, but can be considered as supplementary data prior to the colonisation of fauna in Java, as well as serving as a comparison of the faunal adaptation in response to environmental change in two geographical settings.

The palaeoenvironmental reconstruction of the Middle Miocene mainland is solely based on the analysis of Platybelodon individuals from China. Due to the unavailability of reliable stratigraphic and age data of the locality, speculation on the feeding ecology of this species and its palaeoenvironmental condition is rather limited. A C_3 dominated diet can be assumed from the Platybelodon cf. grangeri individuals from the Middle Miocene sediment of west China. The $\delta^{13}C$ values for this species are consistent with the $\delta^{13}C$ values for herbivore foraging in a more open to a mesic woodland environment, rather than a closed canopy environment. The feeding habitat of Platybelodon during the Middle Miocene was presumably more woody than the present habitat of the Linxia Basin, which consist of shrubland/grassland with patchy woodland (Chang, 1981). The climatic condition might be also warmer and less monsoons during the Middle Miocene. Consumption of aquatic plants could be another reason for ^{13}C enrichment in the species, since Platybelodon has been reconstructed as a semi-aquatic animal that preferred a wet prairie habitat (Lambert, 1992), and thus their diet might include a considerable amounts of aquatic plants with relatively higher $\delta^{13}C$ values than

terrestrial C_3 plants. The $\delta^{13}C$ values of Platybelodon support palynological analysis of the Middle-Late Miocene sediments from the Linxia Basin and surrounding area, which shows a higher proportion of fossil pollen from non-woody C_3 plants, as well as a significant proportion of aquatic herbs and ferns (Ma et al., 1998, Fan et al., 2007, Hui et al., 2011).

In contrast, the $\delta^{18}O$ values of Platybelodon are low in comparison with other species that have similar or lower $\delta^{13}C$ values. The low $\delta^{18}O$ values of Platybelodon may correspond with warm and humid conditions that lasted from the Miocene to ~8.5 Ma (Fan et al., 2007, Wang et al., 2012b, Hou et al., 2014). Or the low values could be caused by the geography of the palaeohabitat at the Linxia basin, which is located in a high latitude and far inland, and thus the ^{18}O depletion in precipitation would reflect the "continental effect".

Subsequently, the $\delta^{13}C$ values of Late Miocene to Early Pliocene taxa (Sinomastodon sp., Stegolophodon cf. stegodontoides, Stegolophodon intermediate form, Stegodon cf. zdanskyi and Stegodon cf. elephantoides) indicate that most individuals are consistent with a range expected for C_3 browsers in both closed canopy forest and woodland vegetation. Mixed feeders are absent from the Tha Chang locality throughout the Miocene. The low $\delta^{13}C$ values of Elephantoidea taxa from the Tha Chang locality is consistent with an abundance of woody fossils and a high proportion of arboreal pollen in the sediment, which reflect closed canopy forests and woodland habitat (Sepulchre et al., 2010). The feeding ecology of Late Miocene Elephantoidea taxa closely resembles the Late Miocene mammalian fauna from the Siwalik Group (Nelson, 2007), suggesting that feeding habitats of mammalian faunas in the mainland during the Late Miocene were varied from densely vegetated forest to a more open woodland vegetation. Furthermore, Elephantoidea taxa from the Late Miocene in Tha Chang co-occurred with Khoratpithecus piriyai. The feeding habitat of these Elephantoidea might also resemble the habitat of the hominoid species, which is thought to be a forested habitat.

The generally low $\delta^{18}O$ values of the Late Miocene–Early Pliocene taxa may reflect Late Miocene enhancement of the Asian monsoon and seasonality (Dettman et al., 2001, Zheng et al., 2004). Alternatively, the low $\delta^{18}O$ values might have been caused by the "continental effect", since all fossil sites were located far inland. The different $\delta^{18}O$ values among the Tha Chang, Irrawaddy and Siwalik localities is inferred to reflect

differences in moisture source and air mass circulation that operating at these localities (Aggarwal et al., 2004). The differences can also be explained as different degrees of aridity occurring at these localities, where the Siwaliks appears to be drier than Tha Chang and Irrawaddy, as it is today. The wider ranges of $\delta^{18}O$ values in the Siwaliks compared to Tha Chang and Irrawaddy may reflect stronger and seasonal difference more intense in the Siwaliks than in the two other localities. A more subtle increase in $\delta^{18}O$ values observed in the Late Miocene to Early Pliocene corresponding with an increase in $\delta^{13}C$ values, signalling a gradual increase of aridity in the region.

The $\delta^{13}C$ values of the Late Pliocene to Early Pleistocene species from the Siwaliks and Irrawaddy (Stegodon insignis, Archidiskodon planifrons and Elephas hysudricus) generally show more positive values than species from previous periods, indicating that they consumed increasing proportions of C_4 vegetation. All individuals yielded $\delta^{13}C$ values of between -6.9 and 1.2‰ indicating that they were either mixed feeders or grazer, while pure browser values are absent at this stage. These values overlap with the expected ranges for animals living in a C_4-dominated vegetation and with mixed C_3-C_4 feeding habitats, such as open woodland and savannah. The dominance of mixed feeder and grazer species in this period suggests a further C_4 biomass increase in the Siwaliks and Irrawaddy, consistent with the observed increase in $\delta^{13}C$ values of pedogenic carbonate (Behrensmeyer et al., 2007) and an increase in the proportion of C_4 plant pollen (Phadtare et al., 1994, Patnaik, 2003) in the Upper Siwalik Group sediment.

Unfortunately, samples of Elephantoidea taxa from the Late Pliocene to Early Pleistocene of Thailand were not available for this study, leaving an incomplete regional mainland SE Asian palaeoenvironmental reconstruction for this interval. Located in the longitude between Irrawaddy and Tha Chang, the diet of the Late Pliocene-Early Pleistocene mammalian fauna from Yunnan, Southern China was evenly distributed within the mixed feeders and grazers ranges (Biasatti et al., 2012). The wide range of $\delta^{13}C$ values covering C_4-dominated and mixed C_3-C_4 vegetation indicates the occurrence of heterogeneous habitats in the mainland of SE Asia. Presumably C_4 grasses invaded the drier portions of the ecosystem, while C_3 plants persisted in more humid landscapes.

As mentioned above, the increasing $\delta^{13}C$ values of species in mainland Asia occurred during the Early Pliocene to Middle Pliocene as compared to earlier taxa. This increase

in $\delta^{13}C$ is associated with an increase in $\delta^{18}O$ values. The more positive $\delta^{18}O$ values suggest drier conditions throughout the Pliocene to Early Pleistocene. Moreover, the spreading of $\delta^{18}O$ values of each taxon represented from this age group is smaller compared to taxa from older ages, which may reflect a weakening of the monsoon due to prolonged periods of glaciation associated with lowered of sea-levels. Taken together, the increasing $\delta^{13}C$ and $\delta^{18}O$ values suggest a general drying of the regional climate over time and a slight transition from a largely woodland-forested environment to a more open environment (woody-grassland and grasslands) during the Late Pliocene to Middle Pleistocene in mainland SE Asia. The onset of the increase of $\delta^{13}C$ and $\delta^{18}O$ values of fauna, of $\delta^{13}C$ values of pedogenic carbonate and of the proportion of C_4 pollen taxa coincides with the onset of lowered global eustatic sea-levels and rapid glacial-interglacial cycles around the transition between the Late Pliocene to Early Pleistocene. In the same period, large portion of Java started to emerge during this stage (van Bemmelen, 1949, Hall, 1998, 2009, 2012a, 2013). However, due to the scarcity of data from the Pre-Pleistocene, the chronology of the species from is largely based on asumption, and thus the conclusion of climate driven trends for this period potentially means a large error.

In Java, the first recorded island colonization by terrestrial fauna is recorded only during the latest Early Pleistocene, as represented by the Satir Fauna. Data on the interpretation of the local palaeoenvironment during this early Pleistocene stage are rather limited. This is due to a limited number of available specimens, as well as poor stratigraphic and geochronological control. The isotopic results of the presumably earliest taxon, Stegoloxodon indonesicus, suggest that the initial climatic conditions of Java following its emergence were humid and that the habitat was dominated by a densely vegetated forest. Considering that the palaeogeography of Java during this period was presumably consisting of significantly smaller isolated island(s) than at present, the vegetation such as lowland rainforest may have been dominant. The dense vegetated feeding habitat as deducted from the $\delta^{13}C$ range of Sl. indonesicus is consistent with the low $\delta^{18}O$ values. This isotopic result is also consistent with palynological data of Sundaland, in which during the late Pliocene to Early Pleistocene, the composition of fossil flora was dominated by coastal and lowland rainforest elements (Sémah et al., 2010, Sémah, 1997, Morley and Morley, 2013).

The humid forested palaeohabitat of Stegoloxodon indonesicus in Java during the Early Pleistocene certainly differs from the palaeoenvironment of the mainland during the same period. This condition is thought to be due to the difference of regional geographical setting and climatic conditions between the mainland and Java, as it is occurring in the present. Alternatively, the samples of Stegoloxodon indonesicus from Java may represent a brief interglacial period in the Early Pleistocene, while samples from the mainland cover wider time frames. Nevertheless, due to the lack of accurate dating, any inferences regarding the differences in the Early Pleistocene feeding habitat in the mainland and Java remain tentative.

Some Sinomastodon bumiajuensis individuals had a similar C_3 dietary preference as their Early Pliocene Sinomastodon sp. relatives from the mainland. However, most of the $\delta^{13}C$ values of the analysed samples show distinct dietary preferences, either as mixed feeder or grazer. The wide range of $\delta^{13}C$ values of Sinomastodon bumiajuensis samples (-12.1 to 1.7‰) suggests that this species was a flexible feeder, which was adaptable to various types of vegetation. The wide range of the S. bumiajuensis diet may indicate occurrence of mixed types of vegetation in their feeding habitat, or a temporal change from dense vegetation to open grassland habitat. Accordingly, the carbon isotopic values of the subsequent fauna (including S. bumiajuensis and Stegodon trigonocephalus originating from the Sangiran Formation), indicate that they were pure grazers, implying that a dry and open environment dominated the habitat coverage during the later stage of the Early Pleistocene. Hence, the data seem to indicate that a transition from dense forested vegetation habitat into more open grassland vegetation must have occurred, at least before the minimum age of the Satir Fauna at 1.5 Ma.

The domination of forested vegetation during the earliest Pleistocene in Java as suggested by the isotopic results is consistent with the palynological study of the Early Pleistocene sediments of the Kaliglagah and Sangiran Formations (Polhaupessy, 1990, Sémah et al., 2010, Sémah and Sémah, 2012). These studies suggest that the earliest terrestrial Pleistocene habitats of Java were characterised by alternating mangrove and rain forests. Additional support is provided by the pedo-sedimentary analysis of the Sangiran Formation, which displays characteristics of coastal marshes and mangrove environments (Brasseur et al., 2014). Both pollen and pedo-sediment records indicate

episodic marine influence which may correlate to the sea-level fluctuations during the earliest Pleistocene.

The vegetation turnover from closed canopy-dominated vegetation to a drier and more open vegetation during the later stage of the Early Pleistocene on Java as suggested by the isotopic result, is also marked by a significant increase in grassland and riparian fossil pollen taxa in the upper part of the Sangiran Formation (Polhaupessy, 1990, Suedy and Jumari, 2004, Sémah et al., 2010, Sémah and Sémah, 2012), particularly below the T9 layer (dated at 1.49 Ma; Tokunaga et al., 1985, Sémah et al., 2010) . These results are also consistent with a transition of the pedo-sedimentary facies from a wet swampy sequence to a dry pedoclimate with a strong signal of seasonality (Brasseur et al., 2014). Since the timing of this vegetation turnover coincided with the faunal turnover from the low diversity Satir Fauna to the more balanced Cisaat (Sangiran) Fauna that has more herbivores, the new arrival of a substantial new megaherbivore species may also be one of the key factors of this vegetation change. With greater diversity and in larger population numbers, these megaherbivores might have aggravated the canopy disclosure by uprooting small trees and maintaining canopy clearance. Alternatively, this change may have been caused by a shift from insular (during warmer climate) to continental (colder/drier) conditions during a glacial phase. To further investigate the onset of the change of proboscidean diet due to the vegetation turnover from a dense vegetated habitat to a more open vegetation, which also marked an early C_4 expansion on Java, additional samples from a detailed stratigraphic records along the Kaliglagah and Mengger Formations are needed.

Considering that the C_4 expansion in east Java only occurred after ~1.5 Ma stage of the Early Pleistocene and the uplift of the east part of Java only occurred later than in west Java, the occurrence of grazer pygmy Stegodon sp. from Sambungmacan might not be older than 1.49 Ma. Another possibility that is the pygmy Stegodon may be older than 1.5 Ma, yet its grazing diet may be because it lived in a small isolated island (van den Bergh, 1999). With more limited resources of plant on a small island, the older population/individuals of this pygmy species may have consumed C_3 plant and left only grasses for the younger population/individuals. Apart from that, to plot the individual from Cirebon in the sequence of chronological occurrence is more difficult due to poor stratigraphic context. In either case, discovery of more specimens along with reliable

stratigraphy and geochronology data are needed to confirm the occupation of this pygmy Stegodon sp. on Java.

The isotopic results of all proboscidean samples originating from the upper part of the Sangiran Formation ("black clay") up to the top of the Bapang Formation and the Kabuh Formation (Kedung Brubus), and most non-Proboscidean taxa from unknown stratigraphic levels in Sangiran analysed by Janssen et al. (2016), strongly suggest the continuous predominant occurrence of open grassland vegetation since the Early to Middle Pleistocene. Other evidence in support of this are the identification of substantial number of vertisols (clay-rich soils that shrink and swell with changes in moisture content and that form under semi-arid seasonal climatic conditions) in the upper Sangiran and Bapang Formations (Brasseur et al., 2014). The predominance of open vegetation on the landscape may be related to prolonged periods of dry climate during glacial periods, became more prominent since MIS 22 (Sémah et al., 2010). The addition of more herbivorous taxa into the Kedung Brubus + Bapang Fauna may also have caused a bigger effect on canopy clearance by fauna.

A small proportion of predominant browser suids from unknown stratigraphic level in Sangiran might have either been derived from older strata, when the habitat in Sangiran was still dominated by woody vegetation, or alternatively, patches of woody vegetation may have been covering the landscape in scattered pattern. Considering that predominant browser individuals only occupy a small proportion of the sample assemblage, the rain forest may have undergone severe fragmentation, being restricted to locally humid patches among an open landscape with extensive grasslands. Niche separation seems to have occurred to some extent among analysed taxa from Sangiran, of which elephantoids, most cervids, bovids and hominin preferred to forage on savannah vegetation, while suids were seemingly more flexible as their isotopic values cover a broad range of feeding habitats. A similar palaeocological pattern during the Middle Pleistocene emerges from the pollen records from the associated sediments, in which grassland and riparian pollen taxa are present in a substantial proportion, while a smaller proportion is occupied by rainforest and mangrove pollen taxa, suggesting that the habitat was dominated by grassland vegetation, with patches of woody vegetation occurring in the vicinity (Tokunaga et al., 1985). However, the palaeoenvironmental interpretation based on the isotopic result of the samples from Kedung Brubus does not

match with a reconstruction of habitat allocation of the Kedung Brubus Fauna by Louys and Meijaard (2010) based on a synecological method (community-based comparison with medium to large mammalian faunal structure of modern faunal assemblages). Their model predicted that the palaeoecosystem of the Kedung Brubus Fauna was densely forested habitat based on the constituent taxa of the Kedung Brubus fauna. Nevertheless, the assemblage of fauna in Kedung Brubus may represent a mixed woodland-grassland environment, whilst the elephants only occupied the open biome niches. However, due to the low number of taxa analysed, it is difficult to establish a more detailed interpretation.

Remarkably, the isotopic results of analysed specimens from the Trinil H.K. layer are all consistent with a C_4-dominated feeding habitat during a drier climate stage. The homogeneity of the isotopic results is due to relatively narrow stratigraphical interval from which the samples originate. Janssen et al., (2016) suggest that the climatic stage of the Trinil Fauna most likely correlated with glacial cycles during either MIS 12, 14 or 16. The dominance of C_4 feeders in the Trinil Fauna corresponds well with the palaeoenvironmental fauna classification of Trinil as open woodland vegetation (de Vos et al., 1982, de Vos, 1985, Louys and Meijaard, 2010). Due to the prevalence of C_4 grasses during the period of the Trinil Fauna, the majority of herbivores might have been forced to consume grasses, including cervids (Axis lydekkeri) that are otherwise commonly adapted to a mixed feeding pattern (Kitchener, 1990; Oka, 2000). However, in the Trinil H.K. fauna the cervids are all grazers. The occurrence of outlying C_3 feeder cervid and suid individuals may suggest that closed canopy vegetation was within the vicinity. Although the Trinil H.K. Fauna indicating a glacial climate conditions, the absence of Elephas hysudrindicus, the low species diversity and high endemism of the Trinil Fauna suggests isolated island conditions. This suggests that glacial periods did not always result in absolute connectivity between the Asian continent and Java.

The isotopic result of Stegodon trigonocephalus and Elephas hysudrindicus derived from the Middle Pleistocene sediments of west Java are also suggests open vegetation with possibly some patchy woodland as their feeding habitat. This palaeoenvironment interpretation for west Java suggests that dry climates and the expansion of grasslands during the Middle Pleistocene seemingly occurred throughout the island of Java.

Unfortunately, due to the poor age control of Pleistocene sediments in West Java, a more precise timing of grassland expansion in West Java cannot be ascertained.

A wide range of isotope values was obtained from the Ngandong Fauna. There is a large gap between the minimum and maximum age constraints of the Ngandong terrace (between 546 and 143 ka; Indriati et al., 2011). Collection of the Ngandong Fauna may have been excavated from different stratigraphic intervals, or representing an admixture of material from strata with a different ages and palaeoclimatic backgrounds. Nevertheless, a change from drier climate conditions throughout the Middle Pleistocene to a more humid condition is recorded in the fossils originating from the Ngandong terrace, dated from the later stages of the Pleistocene. In general, a notable decline of $\delta^{13}C$ values from the Trinil to Ngandong Fauna suggests a change of feeding ecology towards the latest Middle Pleistocene. The lower $\delta^{13}C$ values in mixed feeder individuals from the Ngandong Fauna is interpreted as an increasing proportion of C_3 plants in their diet as a result of increasing wooded vegetation in the landscape. Nevertheless, the occurrence of pure C_4 grazers indicates that a considerable proportion of C_4 plants and open vegetation were still available in the habitat. Given that the carbon isotopic range of the late Early to Middle Pleistocene faunas is consistent with mixed C_3/C_4 to C_4 dominated habitats, it is suggested that the late Early to Middle Pleistocene habitats of Java were rather diverse, with dominant extensive grasslands habitats and nearby varying proportion of evergreen forests, shrubby or woodland vegetation, within a tropical dry climate. Other than that, the diverse diet range of the Ngandong Fauna may also reflect contrasting floral differences between glacial and interglacial cycles. Although the age range given by Indriati et al. (2011) seems to be too large, it is still possible that the Ngandong Fauna elements include animals from a single glacial-interglacial cycle, e.g. covering MIS 6-5.

From mainland Asia, the available data for the Middle Pleistocene are only represented by cf. Palaeoloxodon namadicus (n = 4) and Stegodon cf. orientalis (n = 4) samples from Tha Chang and Laos. The $\delta^{13}C$ values of these individuals (-12.7‰ to -5.8‰) records only browsers and mixed feeder signatures from these sites, while pure grazer Proboscidea are completely absent from the sediment. The variability of $\delta^{13}C$ values suggests that the feeding habitats of these individuals are consistent with the expected ranges expected for animals foraging in closed canopy forest and woodland/woody

grassland environments. The absence of pure grazer species from the Tha Chang sediment since the Miocene may indicate that open vegetation was less prominent in the eastern part compared to the western part of mainland Asia and Java. However, due to the limited sample size from Tha Chang and unavailability of samples from other parts of mainland Asia, it is difficult to draw any firm conclusion concerning the Middle Pleistocene palaeohabitat in the continental area.

A change of diet preference of Proboscidean taxa in mainland Asia is observed during the latest Middle Pleistocene, as the diet of both Elephas maximus samples that represented this period is significantly different from the diets of species from the Late Pliocene to early Middle Pleistocene. The $\delta^{13}C$ values (range between -13.1 and -9.5‰) of all analysed individuals from this time range (n = 4) indicate a pure C_3 diet preference. The variability of $\delta^{13}C$ values suggests that the feeding habitats of these individuals are consistent with ranges expected for animals foraging in closed canopy forest environments. Along with the more negative values of $\delta^{13}C$, the $\delta^{18}O$ values are also decreasing, which suggests a warmer and more humid climate. A comparative isotopic result of cave fauna dated at 169-300 ka from the Tham Wiman Nakhin Cave, Kon San district of Chaiyaphum Province, Northeastern Thailand is presented in Pushkina et al. (2010), which suggested that the range of habitats during the Middle to Late Pleistocene became dominated by dense-canopy forest and woodland, with minor or seasonal occurrence of C_4 grasses.

Similar pattern of habitat change from grassland/open woodland dominated vegetation to denser forest vegetation in Sundaland is suggested by the stable isotope values of the only Elephas hysudrindicus individual from this time interval, which utilized a diet primarily composed of C_3 vegetation in a closed canopy vegetation. The analysis of the pollen assemblage (undertaken by Sanders van der Kaars) and leaf fossils contained in a clay lens associated with the elephant fossil skeleton, suggests that the habitat of this individual was a dense tropical evergreen forest, most likely a lowland forest. This floral analysis is in an agreement with the isotopic data from the elephant, which strongly support the former presence of a humid closed canopy forest associated with the Sunggu elephant. Providing the age, isotopic value and habitat reconstruction, the palaeoenvironment surrounding the Sunggu elephant may be associated with climatic conditions during the end of MIS 7 or the beginning of the MIS 5 interglacial cycle.

Meanwhile, the seasonal change recorded in the molar serial sample of the same E. hysudrindicus individual indicates that the molar lamella (150 mm-long) had mineralized over a period of between 8 and 9 years, during which only C_3 plants were consumed. The timing of the lamellar development of E. hysudrindicus estimated in this study is assumed to be close to the timing of lamellar development of a single plate (measured at 180.9 mm height) in Mammuthus columbi (Dirks et al., 2011). The slight change between the dry and wet peaks identified in the $\delta^{13}C$ values may be due to feeding on different part of the plants/different browsing proportion during successive wet and dry seasons.

The low $\delta^{13}C$ and $\delta^{18}O$ values of all analysed recent E. maximus individuals from Java and Sumatra are consistent with the feeding habitat of humid and densely vegetated forest. Consistency in low isotopic values of both the recent and the Late Pleistocene-Holocene individuals suggests that this species in Java was a specialized browser, at least since its occurrence in the Cipeundeuy Fauna. The radiocarbon ages of the Cipeundeuy Fauna suggest that the humid period was associated with the MIS 3 interglacial, while the remaining samples are associated with the present isotopic stage. Similar to the isotopic results from Tha Chang and Java, the observations of the modern wild Elephas maximus feeding indicates that this species substantially or exclusively exploited C_3 vegetation and inhabited dense vegetated forest to woodland (Wing and Buss, 1970, Field and Ross, 1976, Sukumar, 1990, Cerling et al., 1999). Interestingly, only the samples from the latest Elephantoidea lineages from Holocene and Recent show extremely negative $\delta^{13}C$ values, which are absent from Pleistocene samples analysed in this study. The result is intriguing, given that MIS 5 and 11 are thought to be warmer than the present interglacial, yet samples from those stages (Ngandong and Sunggu) are not showing any more negative values than the present interglacial samples. Other than reduction of C_4 grasslands, the migration of the last Elephantoidea lineages back to forested habitats may relate to inter-specific competition with other large herbivores. Alternatively, the movement to forested habitats may be to avoid predation by humans, since most lowland/grassland area were converted to agricultural lands during the Holocene (Taylor, 2003). The migration of elephants to forested habitats may also reduce the chance to grass foraging, resulting in more negative $\delta^{13}C$ values as compared to the preceding lineages.

As previously suggested, the foraging activities of megaherbivores, especially Proboscidean, may have a role in controlling the distribution of vegetation. The behaviour of megaherbivores, such as uprooting small trees might have maintain their habitat clear from canopy coverage and kept their habitat as more open. However, this case only seems to apply when the climate is in a drier state. During more humid conditions (i.e. the Late Miocene to Early Pliocene and the Late Pleistocene), the indicated feeding habitat in both mainland SE Asia and Java were dominated by C_3 vegetation. Thus on a larger scale, climate must have played a bigger role in controlling vegetation distribution, as it sets the limits to potential plant growth and vegetation depending on temperature and moisture for growth (Bond, 2005), while herbivorous activities must have affected the vegetation on a smaller scale. Additionally, fire, especially during drier stages, may also have affected the dynamic between woody and grassy vegetation. However, the implication of fire cannot be ascertained from isotopic results alone and other lines of evidence would be required to test this influence.

Of the $\delta^{18}O$ values of samples from Java, no significant differences are observed among any of the faunal assemblages. Despite their arrangement in chronological order, the $\delta^{18}O$ values display no clear climatic or environmental trend. However, significant differences within $\delta^{18}O$ values are generally observed between different taxa. The $\delta^{18}O$ values of Sinomastodon bumiajuensis and Elephas hysudrindicus, as well as bovids and cervids are mostly higher than other analysed taxa, even when those taxa have the same $\delta^{13}C$ values. This significant difference may suggest that bovids and cervids were more drought tolerant than other taxa. However, for S. bumiajuensis and E. hysudrindicus this may be not the case, as Elephantoidea are obligate drinkers. S. bumiajuensis and E. hysudrindicus might have had an oxygen water metabolism that differed from other proboscidean taxa. Alternatively, they might have preferred feeding on plant organs that are more enriched in ^{18}O (such as roots and fruits), which is less likely due to the insignificant to no difference in their $\delta^{13}C$ values. In either case, further study is needed to test those possibilities.

Although less prominent, the relatively high $\delta^{18}O$ values of taxa from the Sangiran, Kedung Brubus, Bapang, Trinil, Ngandong and West Java depict dry conditions on Java or weakening of monsoonal strength due to the prolonged glacial periods occurred since the late Early to Middle Pleistocene. Despite their predominant grazing behaviour, the

range of $\delta^{18}O$ values for Stegodontidae are always lower in comparison to other analysed proboscidean taxa. However, the $\delta^{18}O$ values of Stegodon trigonocephalus from four successive assemblages show a changing pattern, consistent with the shifting of their $\delta^{13}C$ values. Comparatively, the $\delta^{18}O$ values of Elephantidae taxa more prominently resemble their diet and palaeoenvironmental condition. The browser Stegoloxodon indonesicus and Elephas maximus have consistently low $\delta^{18}O$ values, which represent a humid palaeoenvironment, while the $\delta^{18}O$ values of E. hysudrindicus individuals are uniformly compatible with their $\delta^{13}C$ values.

4.5.2 Temporal changes in stable isotope values: adaptation and extinction of Proboscidean taxa

The oldest taxa included in the study, the low-crowned Gomphotheriidae and earliest Stegodontidae, including Platybelodon, Stegolophodon, Sinomastodon sp., and earlier Stegodon were strict C_3 feeders. They all tend to have fewer plates per-molar, low hypsodonty index and thick double layered enamel. Platybelodon along with many other gomphotheres genera went extinct from the faunal record in the Tibetan Plateau and other parts of China after the Late Miocene. Their disappearance coinciding with aridification of central Asia noted by the onset of aeolian red clay deposition in the later part of the Late Miocene (Liu et al., 2009).

Since ~8 Ma, a gradual increase in the $\delta^{13}C$ values of carbonate palaeosols were recorded from the sediments of the Siwalik Group coincided with an increase of Poaceae/Graminae pollen record and indicating displacement of C_3-dominated vegetation by C_4-grassland (Quade et al., 1989, Quade and Cerling, 1995, Behrensmeyer et al., 2007). Mixed C_3-C_4 feeder individuals started to appear in the Siwaliks aequence since ~ 8 Ma (Morgan et al., 1994). In the Irrawaddy, a few mixed feeders individuals (n = 3) only appeared after ~7 Ma, represented by Stegolophodon cf. stegodontoides (CCZ 386, this study) and Stegodon spp. (Zin-Maung-Maung-Thein et al., 2011). The low-crowned Stegolophodon and earlier Stegodon (S. zdansky and S. elephantoides) were also extinct from Tha Chang approximately after the Late Miocene. The increase in $\delta^{13}C$ values of the fauna following the increase in $\delta^{13}C$ values of carbonate palaeosols suggest that some fauna elements responded to the change of

vegetation by changing their diet. However, a diet change did not apply for all taxa. From the Chaingazuk Fauna (~6-5 Ma), Elephantoidea, Rhinocerotidae and smaller mammals (Hystricidae, Tragulidae and Suidae) remained predominantly browsers or mixed feeders, while Hippopotamidae, Bovidae, and Ursidae became predominantly grazers (Zin-Maung-Maung-Thein et al., 2011). The co-occurrence of browsers, mixed feeders and grazers at the same time in Irrawaddy suggests a varied and of vegetation during the Miocene to Pliocene transition. In the Siwaliks, by contrast, predominant and obligate browser taxa such as several Suidae and Tragulidae are presumed to have become extinct after the vegetation turnover at ~8 Ma (Barry et al., 2002, Badgley et al., 2008), suggesting that the change to more open vegetation was more intense in the Siwaliks.

While mixed feeder and grazer taxa started to appear in the Siwaliks and Irrawaddy between ~8 and 6 Ma, some taxa from Tha Chang maintained their browsing diet until approximately the Early Pliocene. From the isotopic results, it can be seen that mixed feeder individuals only appeared in Tha Chang after the Early Pleistocene or most likely earlier. However, due to the absence of Pliocene-Early Pleistocene samples from Tha Chang and other relevant areas, the initial appearance of mixed feeder/grazers for this region remains unknown.

Based on the isotopic result from mainland Asia, only the genus Stegodon is known to adapt to the change of vegetation by changing its diet from browser to mixed feeder and grazer. Following this diet change, the morphological characters that support grazing behaviour, started to appear in the more advanced Stegodon species. These characters include plate addition per molar, from a maximum 8 ridges in the third molar of the primitive forms of Stegodon, such as Stegodon zdanskyi and S. elephantoides, to 10+ ridges in the third molars of more advanced species such as Stegodon insignis and S. orientalis (see Appendix I). The addition of plates is simultaneous with an increase of hypsodonty index (maximum unworn height of individual ridges divided by maximum crown width), from around 0.5 in S. zdanskyi to ~0.7 to 0.8 in S. trigonocephalus, as well enamel thinning from 3.5 to 5.0 mm in M3s of Stegodon zdanskyi and S. elephantoides to only 2.0 to 3.0 mm in M3s in Stegodon insignis/ganesa, S. trigonocephalus and S. orientalis. These modification of tooth morphology are

considered as adaptations to increase tooth-life of chewing the more abrasive C_4 grasses (Lister, 2013).

The members of Elephantidae are not found in mainland Asia before the Pliocene, and only radiated there from the Pliocene onward, especially after the expansion of C_4-dominated vegetation. The radiation of Elephantidae may be related to the morphology of their molars that generally have a larger number of plates per molar, high hypsodonty and a thin enamel layer, which are more suited for a grassy diet.

The diet of the earliest recorded proboscidean inhabitants of Java, Stegoloxodon indonesicus (C_3-dominant), was very different to its closest relative from the mainland, Archidiskodon planifrons (C_4-dominant). This result suggests that Archidiskodon/Stegoloxodon lineages initially could adapt to different environments. Despite being a grazer specialist, A. planifrons, went extinct from the Siwaliks after 2.6 Ma (Barry et al., 1985, Hussain et al., 1992, Basu, 2004, Patnaik and Nanda, 2010), when the climatic conditions were more suitable for the growth of grassy vegetation (Dam et al., 2001). Their extinction coincides with the first appearance of Elephas hysudricus and several Cervus taxa in the Siwaliks (Hussain et al., 1992, Nanda, 2002, Basu, 2004, Patnaik and Nanda, 2010). Therefore, the extinction of A. planifrons from the Siwaliks may be due to their inability to compete with Elephas and Cervus. In contrast, Sl. indonesicus on Java is not documented from the lower part of the Lower Pleistocene sequence, coinciding with the onset of C_4 expansion on the island or change from warmer/humid to cooler/dry climate. Therefore, the C_4 expansion that change the habitat coverage from rainforest dominated to more open biomes at the Early Pleistocene might have led to the extinction of Sl. indonesicus, which is a highly specialized browser. Additionally, the arrival of larger and more diverse herbivores (Sinomastodon bumiajuensis, cervids and bovids) as well as predator species on the island, potentially could have added up the determining factors that caused the extinction of Sl. indonesicus.

In mainland Asia, the last occurrence of Sinomastodon is recorded from the Late Pliocene-Early Pleistocene fauna in Sanhe and Juyuan karst Caves, South China (Wang et al., 2012c, 2014a, 2015) and from the Early Pleistocene Renzidong Cave in eastern China (Wang et al., 2014b). So far, their occurrence has never been recorded from the Late Pliocene-Early Pleistocene sequence in Thailand, Myanmar and the Siwaliks.

Based on dental microwear texture analysis of samples from previously mentioned localities in China, (Zhang et al., 2016) suggest that the Early Pleistocene Sinomastodon were browsers. On the other hand, in Java, the diet of the Sinomastodon bumiajuensis changed from predominantly browser in the mainland to predominantly grazer. The Javanese lineage of Sinomastodon may have represented a remnant insular lineage of Sinomastodon that evolved under the insular conditions. This result suggests that Sinomastodon lineages were flexible feeders and could initially cope with changes in vegetation.

Despite having low-crowned molar, apparently Sinomastodon bumiajuensis was able to adapt to the change of environment during the Early Pleistocene, and survived as the dominant herbivore in an insular Java during the Early Pleistocene. This species does not occur anymore in the later part of Early Pleistocene, following the invasion of a range of herbivores, including Stegodon. In mainland Asia, Sinomastodon went extinct after the earliest Pleistocene, earlier than their relative from Java. The extinction of Sinomastodon in mainland Asia happened when they co-occurred and shared the same dietary preference as a browser with Stegodon, and before the vegetation change from a forested to a more open grassland habitat as suggested by Zhang et al. (2016). Therefore, the extinction of Sinomastodon lineages both in Mainland Asia and Java presumably was not caused by environmental change, but most likely caused by the inability to compete with other herbivores, notably Stegodon. Molars of Stegodon were better adapted to grazing as their masticatory mechanism with larger, more derived lophodont and higher hypsodonty index than Sinomastodon. These characteristics are more efficient for processing abrasive vegetation, may have allowed Stegodon to outcompete Sinomastodon and become the dominant megaherbivore both in the mainland and island conditions. However, this suggestion needs to be evidenced by the in situ co-occurrence between Sinomastodon and Stegodon in the same faunal unit, which is still absent for both mainland and Java.

The Stegodon lineage had been a specialised grazer since the Pliocene in mainland Asia. Correspondingly, the earliest record of Stegodon in Java also shows a strong grazing signal. Stable isotope analysis of Elephas hysudrindicus co-occurring in the same faunal stage with Stegodon (Kedung Brubus + Bapang, west Java and Ngandong Faunas) suggests the two species shared the same niches and food sources. The result showing

that all co-occurring herbivores (Stegodon, Elephas, cervids and bovids) in the late Early-Middle Pleistocene were predominantly grazer suggest that grassland vastly covered the landscape and became the main food source of the herbivores. The timing of Stegodon trigonocephalus extinction at the latest stage of the Middle Pleistocene in Java coincides with climate change from a prolonged dry to more humid conditions and vegetation turnover from a C_4-dominated/mixed C_3-C_4 vegetation to a C_3-dominated vegetation. As a specialized grazer, the change in available food resources to predominantly C_3 vegetation might have caused the demise of Stegodon trigonocephalus. Otherwise, inter-specific competition with Elephas and other herbivores that better adapted to C_3 diet and hunting by hominins might also lead to the extinction of this species, which requiring further studies. Alternatively, it may have been a combination of all factors. In contrast, the youngest lineage of Stegodon from mainland Asia, S. orientalis, adapted to climatic and vegetation change during the Late Pleistocene. Schepart et al. (2003, 2005) suggest that the extinction of the latest Stegodon species from Asia was probably a result of hominin activities, either hunting or scavenging, since the assemblages of S. orientalis from the latest Middle Pleistocene to the earliest Late Pleistocene are associated with artefacts and other evidence for human use of Proboscidean skeletal material.

Since the isotopic results suggested that Elephas (mainland Asia and Sundaland) and Palaeoloxodon (only mainland Asia) lineages were able to adapt to the vegetation turnover from C_4 to C_3 dominated in the latest Middle Pleistocene, the extinction of these taxa was most likely caused by other factor, presumably overhunting by human. Their occurrence in the sediment is commonly associated with remains of human activities. Similarly, the disappearance of E. maximus from Java was most likely attributable to hunting and habitat loss due to the modern human activities, especially since its occurrence was associated with Homo sapiens. However, none of the sites analysed in this study has a direct association of Elephas-H. erectus/H. sapiens, making it difficult to confirm the cause of extinction for both species. Additionally, the retreat of the latest surviving lineage of Elephantoidea to forested vegetation might also have been an attempt to avoid human predation.

4.6 Conclusions

The early Proboscidean species (Gomphotheriidae, Stegolophodon and primitive Stegodon) from the Middle to Late Miocene sediments of mainland Asia mostly consumed C_3 plants with none to a very minor proportion of C_4 plants in their diet. The range of their $\delta^{13}C$ values suggests that the feeding habitats of early Proboscidea were predominantly consisting of mesic woodland and wooland-forested habitat. The medium to low $\delta^{18}O$ values suggests humid climate conditions. Two vegetation turnovers can be proposed, which took place after the Late Miocene-Early Pliocene. The first vegetation turnover is marked by a diet transition of Proboscidean taxa, from a C_3 dominated diet to C_4 enriched diet, which is interpreted as corresponding with an expansion of C_4 biomass. The onset of the C_4 expansion differs between Asian regions, recorded approximately between ~8 (Siwaliks) and 6-4 Ma (Chaingazuk, Irrawaddy). The vegetation turnover in mainland Asia is slightly delayed compared to the initial C_4 expansion in Africa (between 10 and 9 Ma). The occurrence of habitats with mixed C_3-C_4 to C_4-dominated vegetation was further intensified during the Pliocene and was predominant in mainland SE Asia until the Middle Pleistocene. Although the transition to C_4-dominated vegetation appeared to be abrupt, the turnover could have been occurred as gradual change at any point during the Middle-Late Pliocene. However, the data obtained for this study do not allow to estimate when the transition occurred, as not sufficient data are available for this interval.

Of the earliest terrestrial fauna record of Java, the feeding ecology of Stegoloxodon indonesicus was restricted to a closed canopy rainforest during the earliest Pleistocene, while Sinomastodon bumiajuensis was highly adaptable to different or increasingly drier grassy habitats that occurred during the Early Pleistocene. C_4 expansion on the island took place since the later part of the Early Pleistocene (before 1.5 Ma) and continued until the Middle Pleistocene, as suggested by the carbon and oxygen isotope composition of assemblages of proboscidean taxa from the Sangiran, Kedung Brubus, Trinil, and west Java, which also predominantly displayed the expected range of C_4-dominant feeders. However, the occurrence of mixed C_3/C_4 feeder Proboscidea in the Ngandong Fauna suggests that fragmented evergreen forests, shrubby or woodland vegetation were reappearing towards the end of the Middle Pleistocene. Stegodon, which was apparently well-adapted to C_4 grazing, dominated the habitat during this

prolonged dry interval. Elephas hysudrindicus, which commonly co-occurred with S. trigonocephalus, also seems to have been well adapted for C_4 plant resources. The absence of Elephas hysudrindicus in the Trinil H.K. Fauna suggests that this species might have been a temporary species that occasionally migrated to Java when Java connected to the mainland. It is also suggest that glacial periods did not always result in absolute connectivity between the Asian continent and Java. The variability in the onset of increasing $\delta^{13}C$ and $\delta^{18}O$ values between different localities in mainland Asia and Java suggests that the expansion of C_4 vegetation was neither as simultaneous nor as prevalent as generally thought.

The second vegetal/environmental shift is detected in the later stage of the Middle Pleistocene, both on mainland Asia and Java, as the dietary preference of all analysed samples from individuals from this age shifted back from a C_4-dominated into a C_3-dominated diet, which suggests a change from a dry to more humid climate conditions. The humid, closed canopy-dominated vegetation persisted in Java, Sumatra and some parts of mainland Asia until present.

The Proboscidean taxa from the mainland and Sundaland have a different respons on environmental change. Most of the older taxa that were exclusively C_3 plant browsers went extinct after the onset of C_4 vegetation expansion at ~8 Ma in the mainland and only after the earliest Pleistocene in Java. Most taxa that appear after the onset of vegetation turnover from C_3-dominant to C_4-dominant during the Pliocene in the mainland are mixed feeders and/or C_4 grazers, while in Java the earliest appearance of mixed feeders and C_4 grazers is recorded in the Early Pleistocene. The delay of C_4 vegetation expansion on Java may be due to the late emergence of Java, which fully uplifted above the sea-level only after the Pliocene. Grazer and mixed feeder taxa, exclusively Stegodon and Elephas, dominated until the latest Middle Pleistocene. Following the onset of a more humid climate conditions and intensification of monsoon since the latest Middle Pleistocene, grazers went extinct and were replaced by browsers. Some genera appear to have been flexible feeders, i.e. Sinomastodon bumiajuensis and Elephas hysudrindicus, and their estimated extinction timing did not coincide with major vegetation change. Therefore, the causes of the extinction of these genera are most likely due to their inability to compete with newcomer taxa or due to human activity, especially after the arrival of humans.

Additionally, the serial analysis of the sample of the E. hysudrindicus molar from Sunggu recorded seasonal changes of wet and dry periods, in accordance with the assumption that the molar lamella had mineralized over a period of approximately 8-9 years.

Chapter 5. Sulawesi, Sangihe and Luzon

5.1 Geological context

5.1.1 Geology of Sulawesi, Sangihe and Luzon

Sulawesi and the northern part of Wallacea are renowned for their complex geology and biogeography. Islands included in this region (Fig. 5.1.) have been formed by the collision of fragments from the Eurasian Plate and the Australian Plate, with island arcs part of the Pacific Plate (Sukamto, 1975, Sukamto and Simandjuntak, 1983, Hamilton, 1979, Metcalfe and Irving, 1990, Audley-Charles, 1991, van Leeuwen et al., 1994, Hall, 2012b, Hall, 2013). Due to its complex origin, the islands have undergone major deformation by faults and folds. Part of the history of earlier terrestrial mammals is recorded in the Quaternary deposits of the Sengkang Basin, in caves within the Maros-Pangkep karst complex in the Southwest part of Sulawesi, in the island of Sangihe and in the Cagayan Valley in Luzon (Philippines).

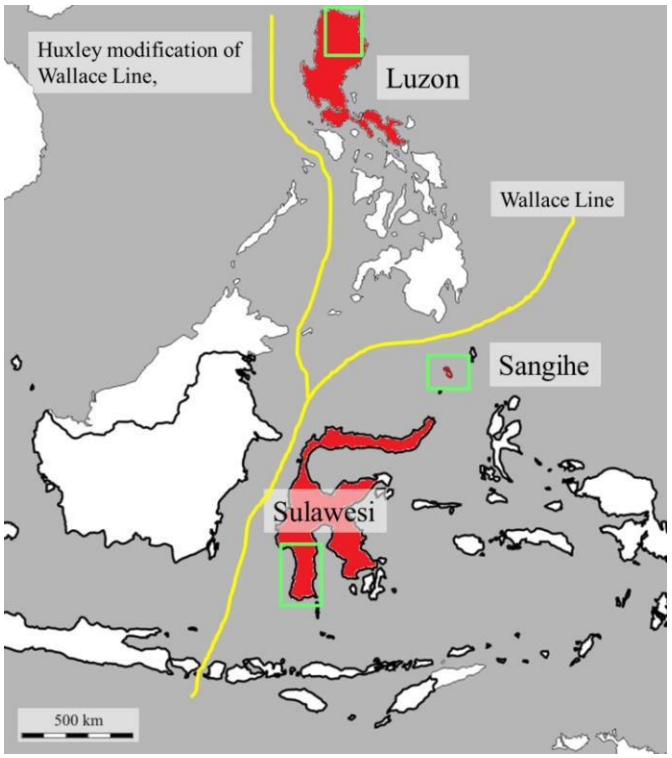

Figure 5.1 Map of the islands from which fossil samples were analysed: Sulawesi, Sangihe and Luzon. Green rectangles indicate studied areas; yellow line indicates the Wallace Line, the major biogeographic boundary recognized in the region.

5.1.1.1 Sulawesi

As a consequence of complex tectonic origins and history, Sulawesi has an irregular shape with its four peninsulas arranged around a relatively narrow centre. Sulawesi and its surrounding islands are formed by the collision of terranes from the Eurasian Plate (forming the west and southwest part of Sulawesi), terranes from the Australian Plate (forming the southeast part of Sulawesi and Banggai), with island arcs that are part of the Pacific Plate (forming the north and east peninsulas). The area with fossiliferous deposits is located in the southwestern part of this island (Figure 5.2). The lithology of this area consists of thick Palaeogene-Neogene sedimentary and volcanic sequences overlying pre-Palaeogene tectonically intercalated metamorphic, ultrabasic and marine sedimentary lithologies (Sukamto, 1975, van Leeuwen, 1981).

The metamorphic basement of southwest Sulawesi is thought to represent old continental crust with an Australian origin (Coffield et al., 1993, Priadi et al., 1993, Bergman et al., 1996), which accreted to the Sundaland during the Early Cretaceous. This basement is covered by Middle to Late Cretaceous deep marine sediments (Sukamto, 1975, van Leeuwen, 1981, Sukamto and Simandjuntak, 1983, Wakita et al., 1996). Early volcanism, characterised by andesitic composition, occurred between the Palaeocene and Late Oligocene, and crops out to the north and east of the Sengkang Basin (Sukamto, 1975, Sukamto and Simandjuntak, 1983). In the west part, a marginal marine coal-bearing deposit (Malawa Formation) formed during the Early to Middle Eocene. A carbonate platform (Tonasa Formation) developed in the Middle Eocene to Early Miocene to the west of the Maros limestone cave sites discussed in this chapter. A formation of coal-bearing deposit and carbonate platform marked the separation of Sulawesi from the Sundaland Platform due to spreading of the Makassar Strait (Sukamto, 1982, Bergman et al., 1996, Wilson and Bosence, 1996, Wilson and Moss, 1999). Volcanic activity resumed in the Middle Miocene and affected the entire part of the southwestern Sulawesi peninsula. This volcanic activity was related to the formation of a north-south trending subduction system to the east (Sukamto, 1982) and brought an abrupt end to the limestone deposition (Wilson & Bosence, 1996). These volcanic products, grouped as the Camba Formation, cover most of older formations. The Sengkang Basin and Walanae Fault Zone (WFZ) developed during the late Middle Miocene and the basin filling has continued up to now in the West Sengkang Basin.

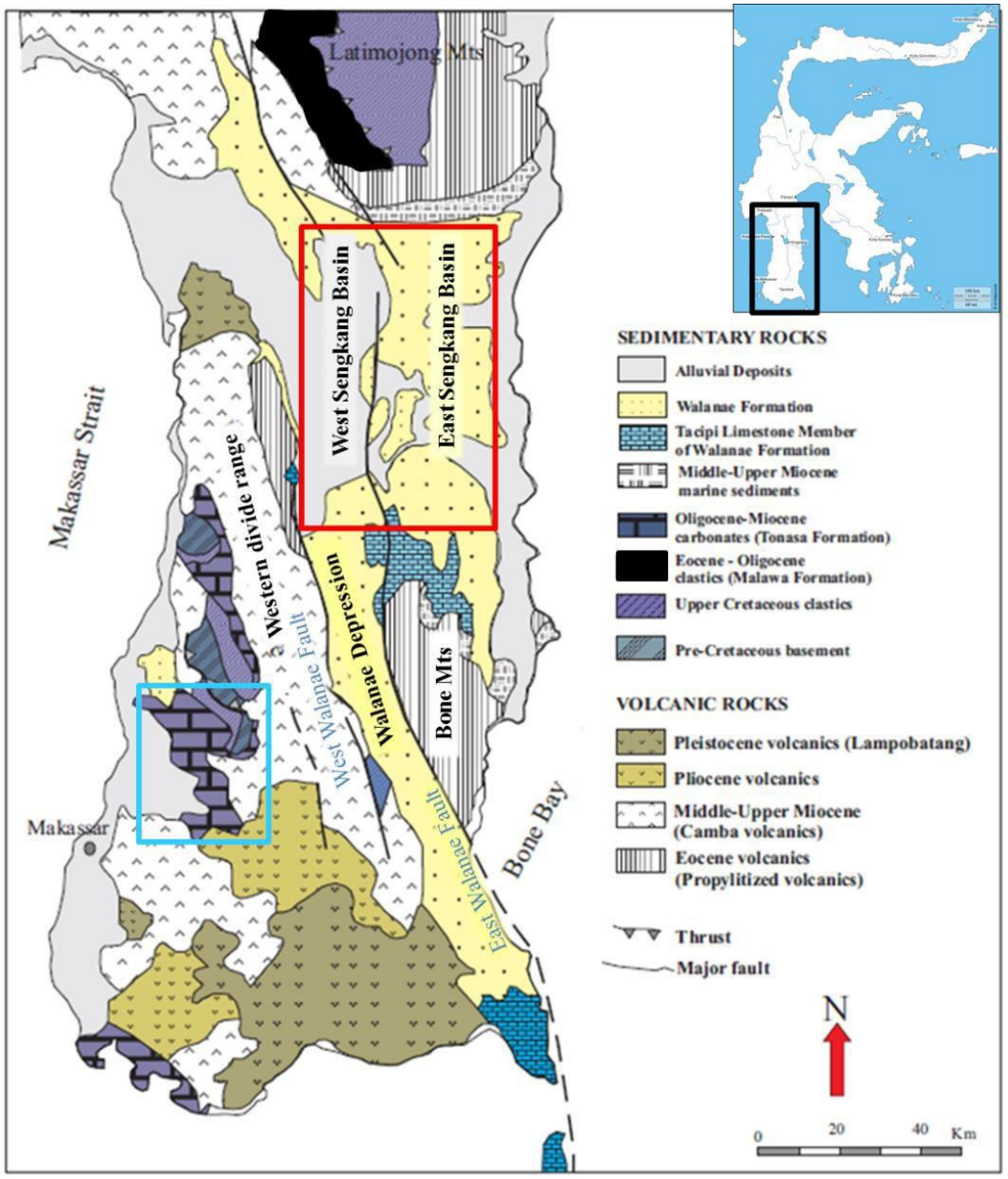

Figure 5.2 Schematic geological map of southwest Sulawesi. The Walanae Fault Zone covers an arc between the West and East Walanae Faults. Red rectangle indicates the Early to Late Pleistocene localities of the Sengkang Basin and the blue rectangle indicates the Maros-Pangkep karst with the Late Pleistocene fossil cave deposits (Modified from Wilson and Bosence, 1996).

5.1.1.1.1 The Sengkang Basin

The Sengkang Basin area is a low lying area close to sea level with a large shallow lake, Danau Tempe, covering the western part of the basin. The basin is a northern extension of the Walanae depression that developed since the Miocene (Grainge and Davies, 1983), bordered by the Latimojong Mountains in the north, the Bone Mountains in the

South and Bone Bay in the east (Figure 5.2). The Walanae Fault Zone (WFZ) is a major NNW-SSE trending fault that separates the West Sengkang Basin (WSB) from the East Sengkang Basin (ESB; Grainge and Davies, 1983). The fault zone covers a distance of almost 200 km and influenced deposition of both basins since the Late Miocene to recent. Van Leeuwen (1981) divided the WFZ into two major fault zones: the West Walanae Fault (WWF) and East Walanae Fault (EWF). He suggests that the WWF influenced the uplift of the ESB during the Middle Miocene. Rapid subsidence of the West Sengkang Basin as a deep marine trough took place during the early Late Miocene (Grange & Davies, 1983). The Sengkang Basin was soon filled with continuous and uninterrupted marine sediments of the Walanae Formation up to the Pliocene. The Late Pliocene-Pleistocene uplift caused the full emergence of southwest Sulawesi and changed the depositional environment from marine to fully terrestrial (van den Bergh, 1999). Since the island is surrounded by steeply dipping slopes, eustatic sea level fluctuations during the Pleistocene did not greatly affected the extension of island surface area. However, sea-level fluctuations may have caused a number of transgressive-regressive cycles within the Sengkang Basin.

5.1.1.1.2 Leang Bulu Bettue, Maros Karst

The Maros karst was developed in the Eocene to middle Miocene limestone of the Tonasa Formation and covers an area of ~450 km^2 in a southwest-to-northwest direction. Rivers are dissecting the volcanic highlands in the east and have eroded down into the basal limestone to form an extensive network of caves, some of which are filled with Late Pleistocene-Holocene sediments. Leang Bulu Bettue (LBB) is a small cave with an adjoining rock-shelter situated at the foot of a plateau-like karst tower in the Tompobalang area of the Maros karsts. This cave forms the southern entrance to what appears to be a relict river chamber through the ~260 m long karst tower in a southwest-to-northeast direction and connects to another cave at the northern side of the tower, named Leang Samalea. LBB is formed in homogeneous limestone, which outcrops below massive coral carbonates. The cave-deposit comprises a relatively flat and level surface that is generally free of large roof-fall blocks and other obstructions and which slopes gently upwards towards the back of the cave. The present cave floor of LBB is

elevated ~5m above the adjacent alluvial plain and is capped by a layer of cemented flowstone (van den Bergh, 2015a, Brumm et al., in prep.).

5.1.1.2 Sangihe and Luzon

Sangihe Island forms a part of a volcanic arc located between the northern Sulawesi magmatic arc and Mindanao (Morrice et al., 1983). Volcanism in Sangihe was caused by an active arc-arc collision consuming the Molucca Sea Plate by two tectonic microplates: the Halmahera Plate towards the west and the Sangihe Plate towards the east. The collision has been active since the Neogene (Macpherson et al., 2003). Volcanic rocks exposed in Sangihe are (Figure 5.3): the Pliocene-Early Pleistocene Sahendaruman andesitic-basaltic breccia and lava (Morrice et al., 1983, Samodra, 1994), Late Pliocene-Early Pliocene dioritic and andesitic intrusions (Samodra, 1994) and Late Pleistocene-Present Hawu volcanics (Samodra, 1994). The only sedimentary rock exposed in Sangihe is the Pintareng Formation, where the Stegodon fossils originate from (Samodra, 1994).

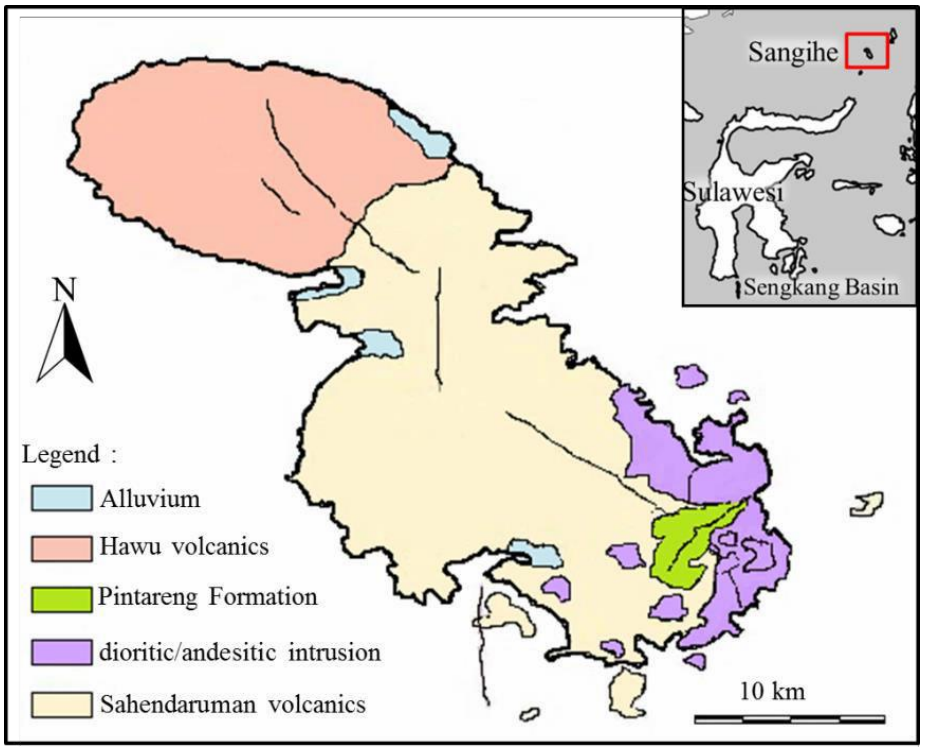

Figure 5.3 Geological map of Sangihe (modified after Samodra, 1994)

The island of Luzon is a part of the volcanic arc developed due to the east-dipping collision between the east-heading South China Sea Plate and the northwest-heading Luzon terrane (Acharya and Aggarwal, 1980, Defant et al., 1989, Richard et al., 1986). The oldest lithology that comprises the basement of Luzon is composed of Cretaceous ophiolites and Palaeogene basalt, schists and cherts. This basement is overlain by a variety of Neogene marine deposits (Acharya and Aggarwal, 1980). Terrestrial Pliocene and Quaternary sediments infilling the depression of the Cagayan Valley (Fig 5.4).

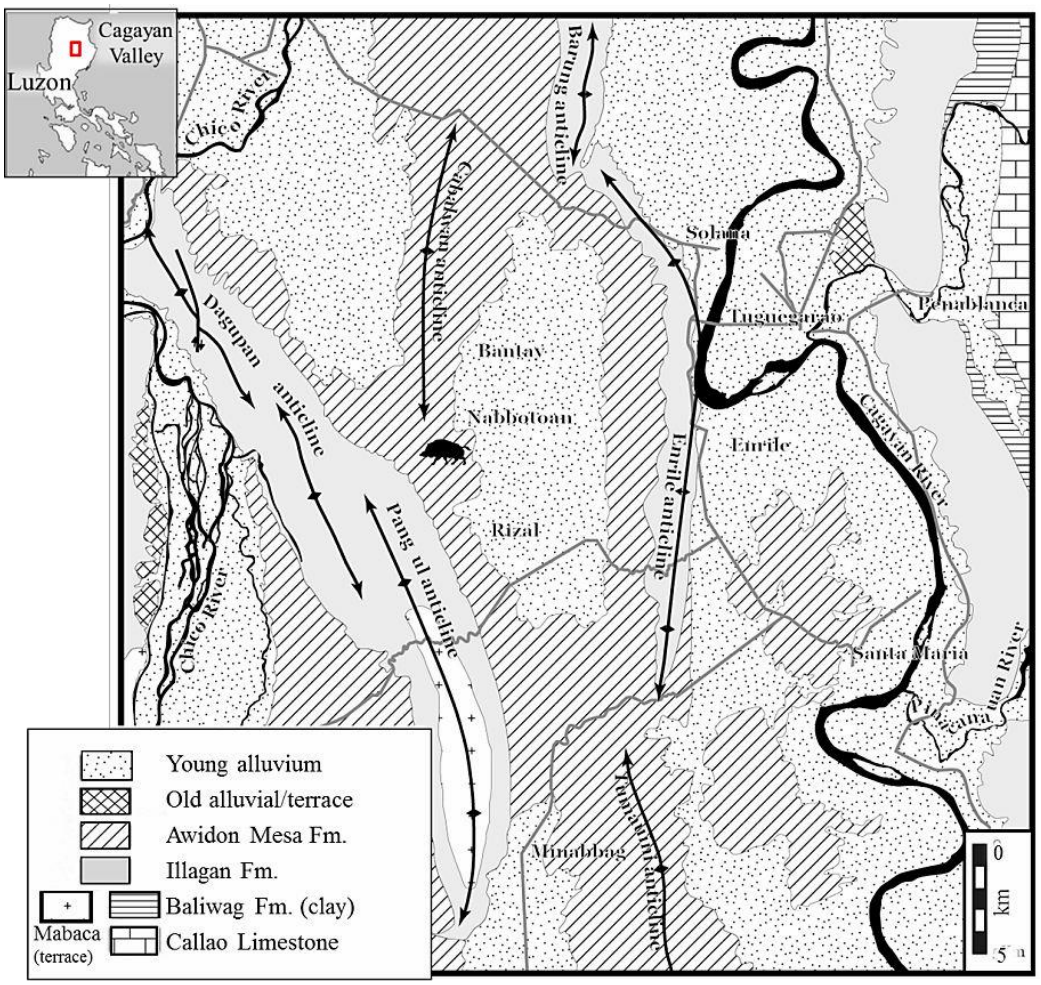

Figure 5.4 Geological map of the Cagayan Valley in Luzon Island, Philippines (modified after Ingicco et al., 2016).

5.1.2 Quaternary stratigraphy of vertebrate fossil localities

Two successive Quaternary vertebrate fossil areas were studied: 1. a number of Early to Late Pleistocene localities in the Sengkang Basin and 2. Late Pleistocene-Holocene cave

sediments from Liang Bulu Bettue, a cave/rockshelter in the Maros karst area. The fossil vertebrates from the first group originate from the upper part of the Walanae Formation and the Tanrung Formation (Figure 5.5).

5.1.2.1 Sengkang Basin

5.1.2.1.1 Walanae Formation

The Walanae Formation comprises four members, from oldest to youngest (Figure 5.5, Grainge and Davies, 1983, van den Bergh, 1999):

- The Tacipi Member, which constitutes the base of the Walanae Formation, is exposed along the southern margin of the ESB and south and southeast of the Sengkang Anticline. This member consists of small carbonate reefs intercalated with or conformably overlain by marine claystones. The Tacipi Member was deposited in shallow water during the Middle Miocene and drowned during the Late Miocene to Early Pliocene (Grange & Davies, 1983).
- The Burecing Member consists of marine marls of Late Miocene to the Early Pliocene in the WSB and possibly extending to the Late Pliocene in the ESB. In the WSB, the base of the Burecing Member is intercalated with the Tacipi Member, while in the ESB the top of this member is intercalated with the Samaoling Member.
- The Samaoling Member consists of an intercalation of shallow marine silty mudstones and fine to medium-grained well-sorted sandstone, dated to Early to Late Pliocene. It is exposed in the west flank of the Sengkang Anticline and in large parts of the WSB and ESB. A transitional zone between the Samaoling Member and the Beru Member was recorded in the eastern flank of the Sengkang Anticline near Sompe, as suggested by the occurrence of terrestrial vertebrate remains encrusted with shallow marine invertebrates.
- The Beru Member consists of fluvio-estuarine sandstones, lagoonal claystones and fluvial conglomerates from the late Pliocene to the Late Pleistocene. A terrestrial vertebrate fossil fauna is found in this member and is the focus in this study.

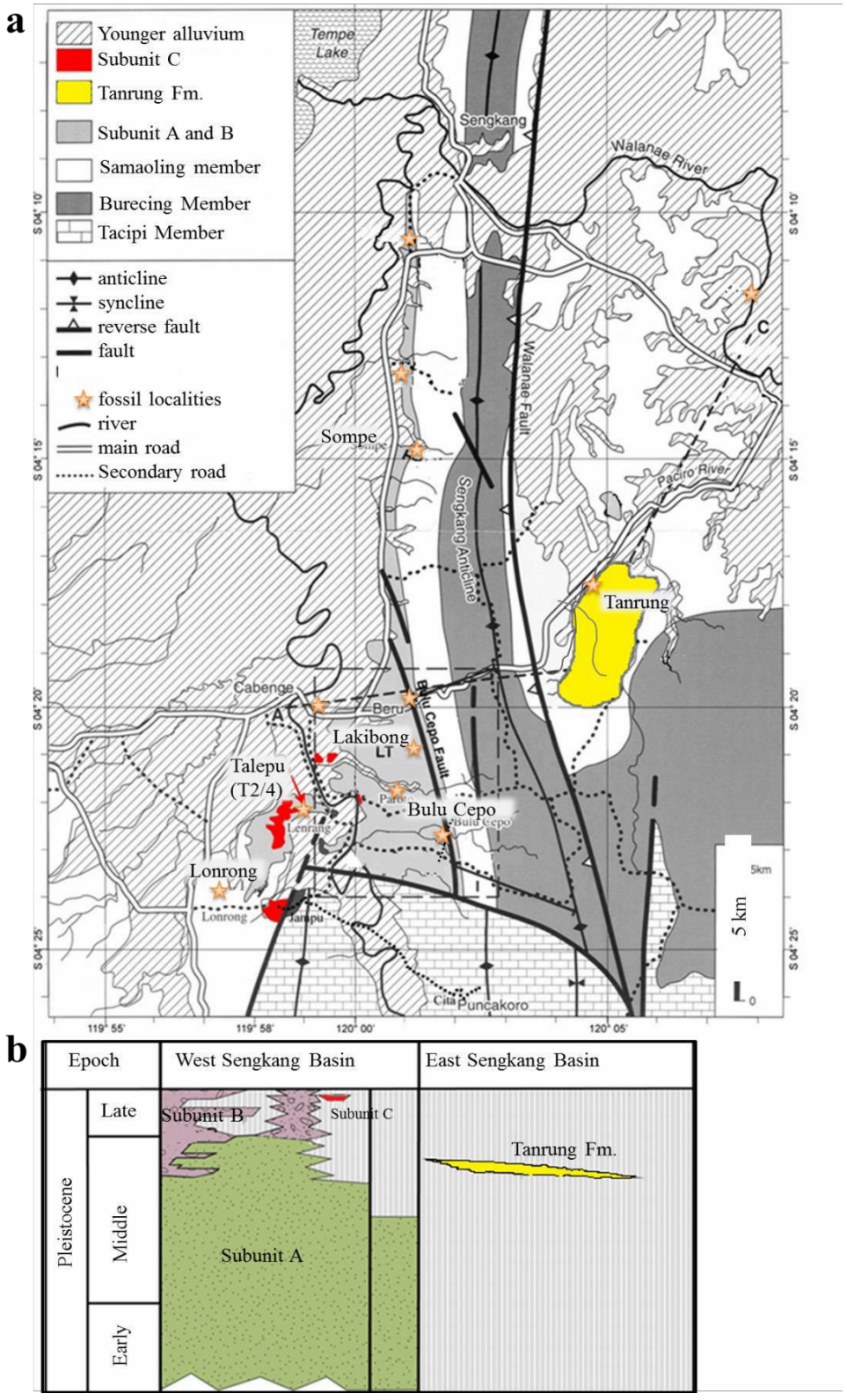

Figure 5.5 a. Geological map of the Sengkang Basin (modified after van den Bergh, 1999), showing the distribution of the Walanae Formation, Tanrung Formation and younger alluvium. The Tacipi, Burecing and Samaoling Members of the Walanae Formation represent the marine depositional environment, while the Subunits A-C indicate the subdivisions of the terrestrial Beru Member of the Walanae Formation; **b.**stratigraphic correlation between West and East Sengkang Basin (modified after van den Bergh et al., 2016). Stars indicate fossil localities included in this study.

Sartono (1979) initially addressed the Beru Member as a formation (Beru Formation), thought to be formed as Late Pleistocene fluvial deposits that were tilted in the west flank of the Sengkang Anticline; deposited into several terraces. However, since this lithology is not continuous, van den Bergh (1999) classified the youngest member of the Walana Formation as the Beru Member and divided this member into two subunits: A and B. Subunit C, which was previously referred to as the 'Old Alluvial Fan Gravel' (van den Bergh, 1999), is added here as a new subunit of the Beru Member. The Beru Member is only well developed in WSB, while in the ESB it might have been eroded or not have been deposited. In the ESB, horizontal-bedded layers of the Tanrung Formation unconformably overlie sediments of the Samaoling Member with a gentle dipping (5-15°).

Subunit A is exposed in the WSB along the west flank of the Sengkang Anticline, east of the Bulu Cepo Fault (BCF), between the BCF and the Walanae River, and in the Talepu-Lonrong Ridge, west of the Walanae River (Figure 5.5). The lithology of this subunit comprises sandstones, claystones and siltstones. Alternating fluvial fine-grained sandstones with mud drape structures occur in the western flank of the Sengkang Anticline. The occurrence of terrestrial vertebrate fossils together with shark teeth and benthic foraminifers was reported by Sartono (1979). Molluscs and pollen assemblages from the lower part of Subunit A along the Lakibong River, suggest that the area was a transitional zone between lagoonal-estuarine and fluvio-lacustrine environments. Fossils analysed from this subunit originate from various fossiliferous layers located near Sompe, Lonrong, and Bulu Palece. Two fossiliferous layers were found to occur near Sompe, which are a sandstone interval overlain by a 12 m-thick interval of claystone and sandy-siltstone. The fossiliferous layers near Sompe are thought to be older because those layers represent the depositional environment around the first marine-terrestrial transition, which is the characteristic of the lower part of the Beru Member (van den Bergh, 1999). However, the notion that Sompe contains older deposit might be erroneous, due to the lack of dating control. Meanwhile three fossil layers were found in Lonrong and Bulu Palece: sandstone interval (marine-terrestrial transition), silty claystone and fluvial.

In the area west of the BCF and east of the Walanae River (referred to as the 'Lakibong Triangle' and following van den Bergh, 1999), Subunit A is covered by Subunit B.

Tidally influenced clastics with sand/mud and marine fossils are absent from Subunit B, indicating that the depositional environment of this member was fully terrestrial. Subunit B consists of fluvial coarse and cross-bedded sandstones and conglomerates. The conglomerates contain pebbles dominated by volcanic rock fragments. This subunit is exposed largely near Lakibong and Bulu Cepo. The large-sized Stegodon sp. B occurs only in the upper part of the Beru Member.

Based on the foraminiferal assemblage from a sample collected from the base of the Beru Member, which presumably corresponds to the Samaoling Member, Sartono (1979) concluded that the age of the sediment is N19 or N20 (of Blow, 1969) or Late Pliocene. The palaeomagnetic analysis at the transition between the Samaoling and Beru Members shows a transition from Normal to Reversed magnetic polarity (van den Bergh, 1999). The Gauss-Matuyama transition at 2.58 Ma or Olduvai at 1.8 Ma are the most likely interpretation for the maximum age of the Beru Member, since this age fits well with the ESR dating of Stegoloxodon celebensis and Celebochoerus heekereni from Bulu Cepo and Lonrong that gave relatively old ESR ages of ~2.1 Ma (van den Bergh, 1999). However, this age assessment was calculated based on estimated average background radiation values (Reese et al., 1996) and should be considered with caution. Subsequently recorded in situ measurements of background radiation indicated relatively high dose-rate values of 4-5 Gy/year (van den Bergh et al., 2016), and therefore the calculated age of ~2.1 Ma might be too old. Meanwhile, ESR dating of a Celebochoerus heekereni molar from Subunit A (Lakibong-2 excavation locality) resulted an age of 0.5 Ma, which probably can be considered as a minimum age.

Subunit C is locally developed on top of a series of hills aligned in an elongated NNE-SSW Talepu-Lonrong Ridge, covering the eroded Subunit A over a scattered area within ±5 km north-south and ±3 km east-west (Figure 5.5). The deposit exposed along this ridge comprises a coarsening-upward sequence of sub-horizontal fluvio-estuarine sand and silt layers overlain by alluvial cobble gravels (van den Bergh et al., 2016b). The gravels are dominated by heavily weathered volcanic rocks and silicified limestone (Figure 5.6). The volcaniclastic unit has more variability in source rock types and tends to be much coarser-grained than the conglomerates from Subunit B (van den Bergh, 1999). The uranium-series dating of excavated teeth and bones from the lowest part resulted in a maximum faunal age of >350 ka, while the OSL (post-IR IRSL or MET-

pIRIR) dating undertaken on five potassium-rich feldspar from the entire sequence resulted in ages between ~200 and 100 ka (van den Bergh et al., 2016b). Palaeomagnetic samples from the upper, middle and lower part of the fan gravels indicate Normal polarity, which correlates with the Bruhnes Chron.

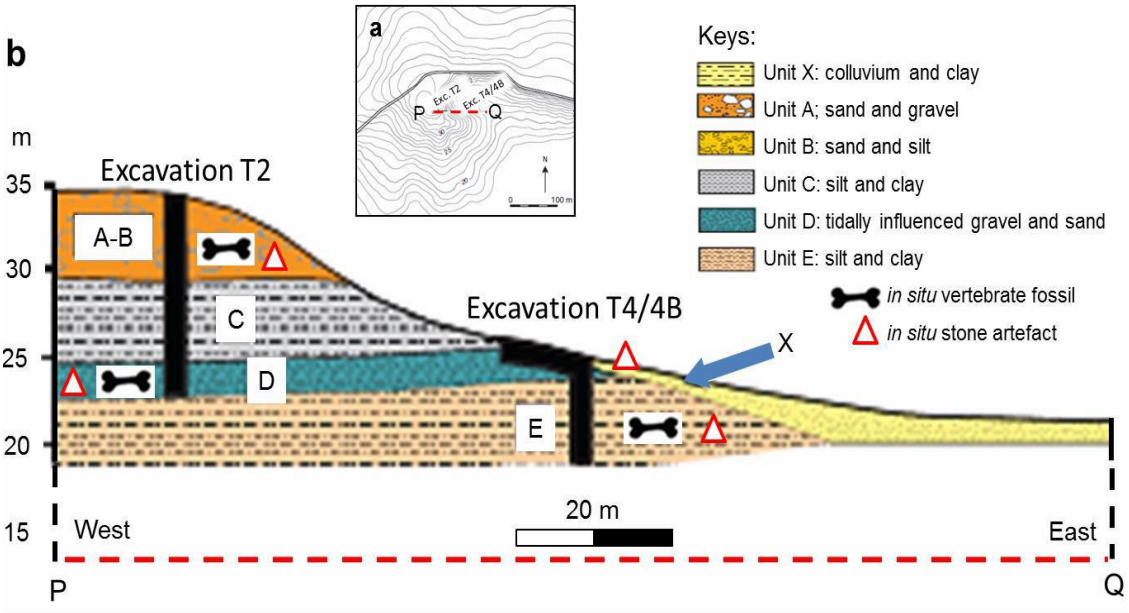

Figure 5.6 a. Site map showing position of Excavation 2 and 4 (labelled as T2/4 in Fig. 5.5), dashed line (PQ) indicate profile shown in **b**; Schematic stratigraphy of W-E cross section (P-Q) along the Talepu Excavation 2 and 4, showing fossil and stone artefact occurrences (modified after van den Bergh et al., 2016b). Fossil Celebochoerus analysed in this study originates from Unit E.

Along the eastern flank of the Sengkang Anticline, the clastic members are steeply folded and the Beru Member is heavily eroded. Along the depocentral axis of the WSB some isolated pockets of colluvium and younger alluvial deposits unconformably overlie the clastic members of the Walanae Formation. The colluvium deposited west of Ciangkangke, and south of the Cabenge-Pampanua Road, consists of a loose mixture of sand, caliche nodules, small pebbles and angular clasts in a poorly sorted muddy matrix, as well as fossil vertebrate remains that are considered as the youngest fossiliferous unit. The small pebbles and angular clasts are derived from the underlying Beru Member sediments. This deposit is unstratified and unconformably overlies steeply westward dipping sandstone layers of the Beru Member.

The youngest alluvium deposit consists of the floodplain deposits of the Walanae River, and represents the youngest deposit of the WSB. The deposit consists of unconsolidated

sands, silts, clay and gravels bars, which represents the recent Walanae floodplain and channel deposits. Accumulation of fine-grained lacustrine sediments continues in and around Lake Tempe. These sediments are dominated by organic clays and silts, with minor intercalations of sands up to a depth of 150 m (Kusbini and Najamuddin, 1991), which indicates that lacustrine and fluvial deposition has continued for a long period in this area in response to continuous basin subsidence (van den Bergh, 1999).

5.1.2.1.2 Tanrung Formation

In the ESB, the eroded and folded marine members of the Walanae Formation (indicated as layer 1 in Figure 5.7) are unconformably overlaid by the Tanrung Formation and more recent alluvial deposits. The Tanrung Formation consists of sub-horizontally bedded conglomeratic deposits unconformably overlying slightly folded marine strata of the Walanae Formation along the Tanrung River (Figure 5.7). Initially, Sukamto (1975) and Bartstra (1994) included the lithology of this formation in the top of the Walanae Formation. However, van den Bergh (1999) specified that the characteristic and distinct conglomeratic fluvio-estuarine deposits are only developed in the ESB as a separate formation. The composition of the conglomerate consists exclusively of limestone and caliche clasts, whereas the vertebrate faunal content is different as compared to the vertebrate fauna from the Beru Member of the Walanae Formation. The thickness of the Tanrung Formation is limited to a maximum of 10 m.

The conglomerates of the Tanrung Formation (indicated as layer 2 in Figure 5.7) contain abundant fragmented and rounded calcareous clasts and oysters, which seem to be reworked from the underlying marine part of the Walanae Formation. The sandy matrix of the carbonate clasts contains abundant quartz grains. Consolidated fine-grained siliciclastic lenses are locally intercalated in the conglomerates. The Tanrung Formation is well cemented with sparitic calcite, and is different from the most common cement type in the Walanae Formation, which consists of siderite. The sedimentary structure of the Tanrung Formation indicates a small-scale meandering channel system. The top of the Tanrung Formation has been eroded and is unconformably overlain by younger and unconsolidated ‘Older Alluvium’, ‘Younger Alluvium’ and ‘Recent Alluvium’ deposits, respectively (van den Bergh, 1999, layer 4, 5 and 6 in Figure 5.7).

No palaeomagnetic and radiometric dating has been conducted on the Tanrung Formation. The assumed late Middle Pleistocene age of this formation is derived from the fauna, which contains an advanced, high-crowned Elephantini (a tribe including genera Elephas, Palaeoloxodon and Mammuthus).

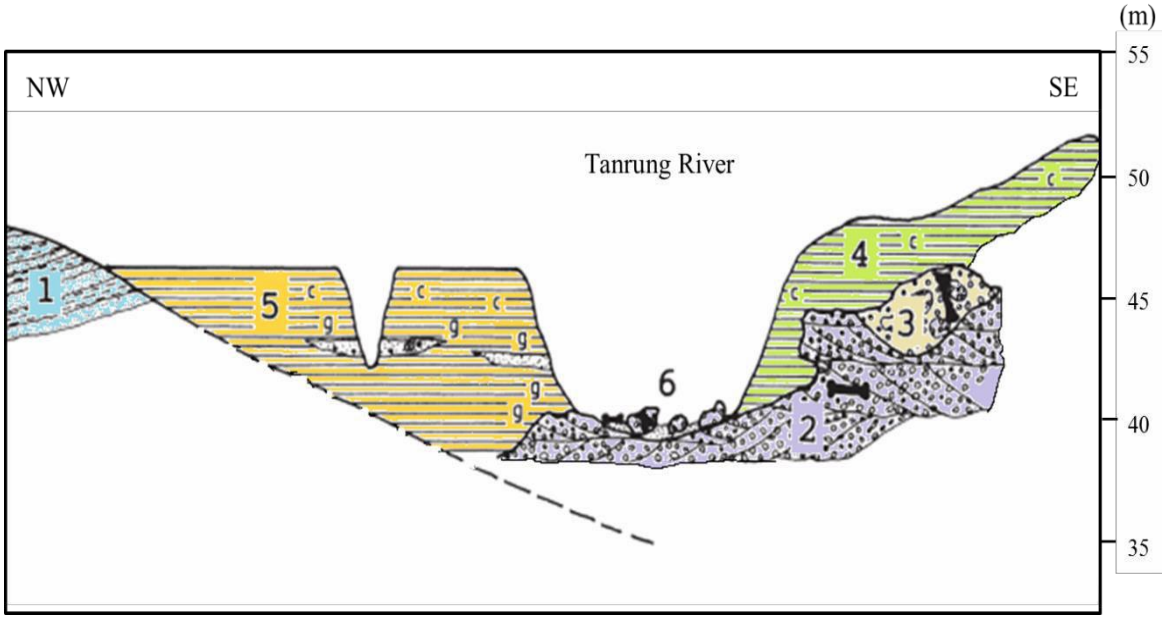

Figure 5.7 Schematic NW-SE cross section along the Tanrung River showing the spatial relationships between the lithology of the Tanrung Formation and other lithological units cropping out in the East Sengkang Basin. Scale on the right indicates the elevation above sea level. 1: folded marine layers of the Walanae Formation; 2: Tanrung Formation; 3: redeposited calcareous gravel eroded from the Tanrung Formation; 4: Older Alluvium unconformably overlying the Tanrung Formation; 5: Younger Alluvium; 6: Recent Alluvium of the Tanrung River containing eroded blocks of the Tanrung Formation. Bone symbols indicate the occurrence of Elephantoidea fossils, which occur in situ in the Tanrung Formation (primary deposition) and in reworked deposits containing eroded material of the Tanrung Formation (modified from van den Bergh, 1999).

5.1.2.2 Late Pleistocene cave deposits of the Maros-Pangkep karst: Liang Bulu Bettue

Due to long term and complex karstification, extensive networks of caves were formed around the base of the limestone towers in the Maros-Pangkep karst. These caves are known for their artefacts, better-known as the Toalian culture (Glover, 1977, Glover, 1981) and the Late Pleistocene cave art recorded in nine different caves (Aubert et al., 2014). However, the fauna of the Late Pleistocene cave deposits for this area is still understudied.

An excavation was undertaken in the Liang Bulu Bettue cave between 2013 and 2015 by Adam Brumm and the Balai Arkeologi Makassar joint team. Excavation trenches exposed the undisturbed stratigraphic sequence of the cave. Pits were excavated to 6.5 and 8 m-deep (excavation pit A and B) and revealed a succession of 13 recognisable layers (Brumm et al., in prep), as shown in Figure 5.8.

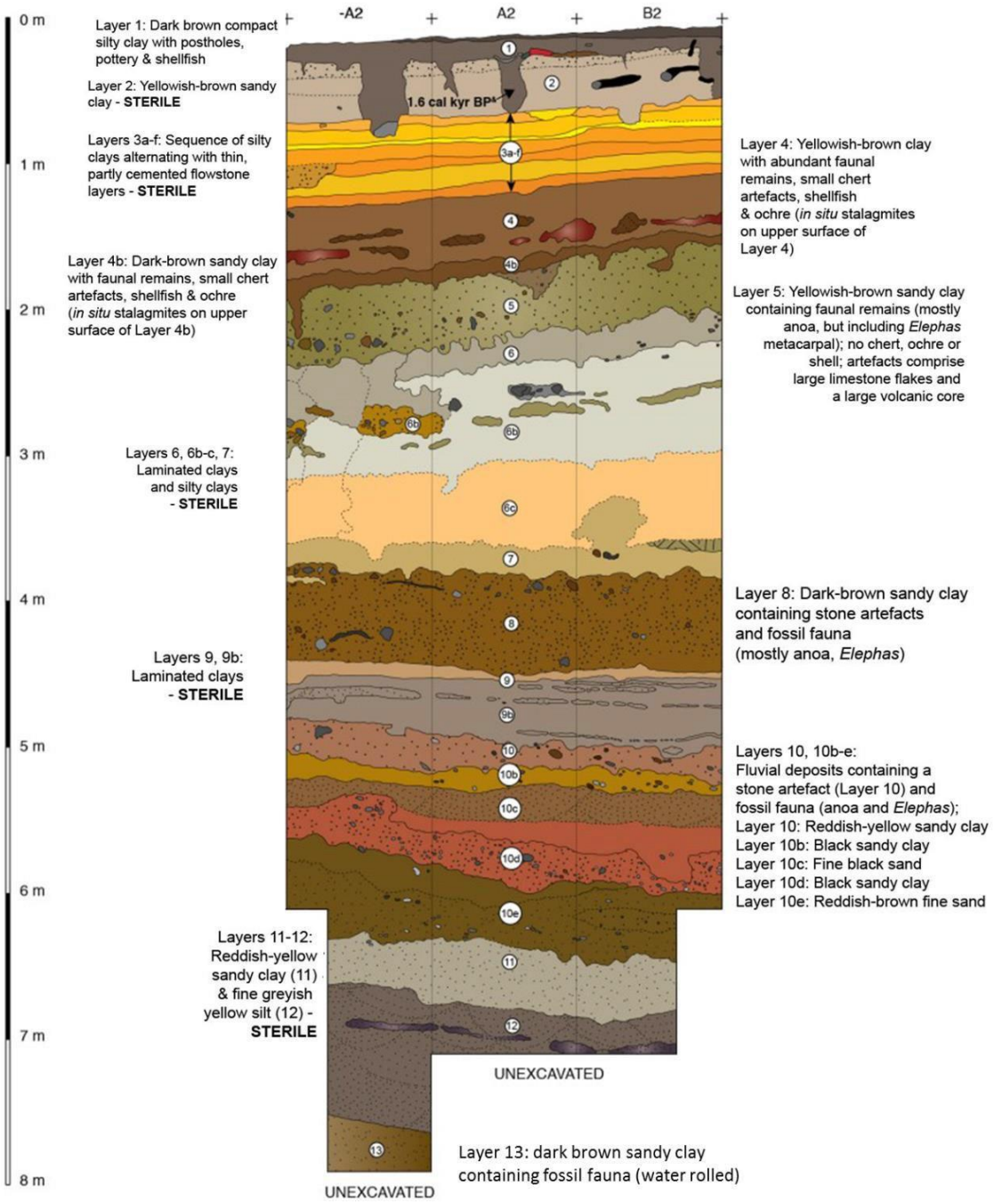

Figure 5.8 Stratigraphic profiles and layers (no vertical exaggeration) of the excavation wall in Leang Bulu Bettue as recorded during the 2015 fieldwork (modified after Brumm et al., in prep.).

The lowermost layer (Layer 13, Figure 5.8) comprises sandy silt with faunal remains (not yet identified), while the overlying layers (Layer 11 and 12, Figure 5.8) are culturally sterile sandy fluvial deposit. An OSL IRSL date from feldspar from Layer 11 yielded a minimum date of ~187 ka (Brumm et al., in prep). An up to 150-cm-thick sequence of bedded fluviatile deposits comprising fine to coarse sands and clayey gravels (Layer 10, Fig. 5.8) yielded fossils and artefacts. Layer 10 is topped by an up to 85-cm-thick laminated clays layer that contains no fossil fauna or artefacts (Layer 9). Layer 8 is an up to 55-cm-thick sandy clay containing volcanic cobbles, fossil Bubalus and stone artefacts, which is overlain by an up to 170 cm thick sequence of culturally-sterile laminated clays and silty clays (Layers 6 and 7). Layer 5 is yellowish-brown sandy clay up to 50 cm thick with fragments of limestone rubble and a Late Pleistocene fossil fauna. The OSL (feldspar IRSL) dating of Layers 10, 8 and 5 yielded ages between ~42 and 102 ka (Brumm et al., in prep.). The four uppermost layers (Layers 1 to 4) consist of alternating clays, sandy clay and thin laminated silty clay layers, with a thickness up to ~2 m. Layer 4 contains abundant faunal remains and artefacts, while Layers 2 and 3 are sterile. The top Layer 1 contains shellfish and pottery. In situ stalagmites formed on the exposed upper surface of Layer 4, while the upper portion formed during the deposition of overlying Layer 3. Compiled radiocarbon, OSL (feldspar IRSL) and uranium-series (in situ stalagmites and faunal remains) dating of this interval obtained an age range of between 1.6 and ~27.5 ka (Brumm et al., in prep.).

5.1.2.2 Sangihe and Luzon

The only sedimentary rock on Sangihe is the Pintareng Formation (Fig. 5.3), outcropping along the Pintareng River and overlying the Sahendaruman volcanics and the intrusive rocks. It consists of conglomerate, pebbly sandstone, sand, silt and black clay, minor intercalated layers of tuff derived from the surrounding volcanic rocks. The conglomerate contains Stegodon fossils and wood fragments. The age of the Pintareng Formation is estimated to be Middle to Late Pleistocene (Samodra, 1989, 1994).

The fossils studied from Luzon originate from Rizal, Kalinga District in the Cagayan Valley (Fig. 5.4). The Cagayan Basin is a 250 x 80 km^2 depression located along the subduction zone infilled by approximately 10 km of sediments. The upward-coarsening volcaniclastics reflect the tectonic and volcanic evolution of the adjacent Cordillera Central volcanic arc. The fossil fauna originate from the upper Awidon Mesa Formation. This formation consists of lahar, pyroclastic flow, and ash-fall deposits that have been redeposited by a large fluvial system (Mathisen and Vondra, 1983). Based on the widespread distribution of tektites (australites), the age of the sediments is estimated to be younger than 800 ka, since the occurrence of tektites is thought to correspond with an impact event at ~800 ka (Glass and Koeberl, 2006). Based on its faunal content, the age of this deposit is estimated to be Middle Pleistocene (Wasson and Cochrane, 1979). Palaeomagnetic samples taken in a silty layer of the Awidon Mesa Formation near the fossil locality have a Normal polarity, which would be in accordance with an age younger than 782 ka or within the Brunhess Chron (van den Bergh, 2015b).

5.2 Palaeogeography and faunal succession

5.2.1 Palaeogeography and present environment

Sulawesi, in contrast to most of the other islands in the biogeographical region of Wallacea, is not truly oceanic. The southwest part of Sulawesi was formerly attached to Sundaland as the continental margin that became separated from Sundaland by the opening of the Makassar Strait separating West Sulawesi from Sundaland in the Late Eocene (Moss and Wilson, 1998, Wilson and Moss, 1999). Exposed land areas probably existed during the Middle Oligocene as deduced from unconformities recognized throughout the area. However, the size, continuity and connection of this palaeo-island are uncertain. Another possibility of limited land connection may have occurred during the Middle Miocene, when the regional extensional tectonic regime changed into a compressive regime related to the collision of East Sulawesi, which also caused volcanism in the area (Sukamto, 1975, Wilson and Bosence, 1996, Wilson and Moss, 1999). The local presence of Middle Miocene ignimbritic rocks in the southern part of South Sulawesi (van Leeuwen, 1981) may indicate that one or more small N-S aligned volcanic islands were intermittently exposed in the area during the Middle Miocene

(Moss and Wilson, 1998, Wilson and Moss, 1999, Hall, 2009). However, a form of complete land connection is unlikely, as shallow marine deposition was widespread throughout the area, including in south Sulawesi itself. A connection with Sundaland, in particular with Java is very unlikely because shallow marine deposition along the northern part of Java continued until the Late Pliocene. The Makassar Strait was fully established as a deep marine basin during the Pliocene, thus creating an effective marine barrier between Sulawesi and Kalimantan. Moreover, major parts of the shallow carbonate shelf extending into the Flores Sea adjacent to the southwest arm of Sulawesi, rapidly subsided during the Pliocene, increasing the extend of the marine barriers between Sulawesi and the Lesser Sunda Islands as well. Therefore, the colonization by mainland terrestrial vertebrates most likely occurred by means of overseas sweepstake dispersal (van den Bergh, 1999, Aziz, 2000). Full emergence of south Sulawesi must have happened during the Late Pliocene and Early Pleistocene, as recorded in the Walanae Formation.

Unlike the large islands in the Sundaland Platform, Pleistocene sea level fluctuations did not affect the connectivity of Sulawesi with mainland Southeast Asia. The glacio-eustatic changes may affect the increasing/decreasing distance between Sundaland and Sulawesi to some degree, yet Sulawesi and Sundaland would never have been connected, as both landmasses are separated by the deep Makassar Strait. After its full development as a deep marine basin since the Pliocene, the Makassar Strait has widened up to ~100 km since its formation and has water depths varying between 200 to 2000 m (Guntoro, 1999). However, glacioeustatic fluctuations might have determined island surface area expansion from time to time, as well as local climate and vegetation. Tectonic activity probably had a bigger influence in shaping the exposed land area of Sulawesi and its past connectivity to the mainland.

Incorporating the stratigraphy, sedimentology, seismology and chronostratigraphy, van den Bergh (1999) reconstructed the palaeogeographic history of the Sengkang Basin area between the Early Pleistocene and Quaternary. After its full emergences as an island, the palaeogeographic reconstruction of the island is as follows: during the Early Pleistocene the Sengkang Basin was a transitional area between shallow marine and terrestrial environment, with a delta formed by the palaeo-Walanae River prograding into a marine gulf. From the Early Pleistocene onwards the area was uplifted and

became gradually fully terrestrial, with alluvial fans forming along the Western dividing range.

Similarly, Luzon and Sangihe are two oceanic islands that were never connected to the Sunda Shelf since their emergence. Prior to the Quaternary, as many Wallacean islands, Luzon Island was submerged during the Cenozoic and the emergence only occurred after the Late Pliocene (Durkee and Pederson, 1961). The emergence of Sangihe probably happened slightly later during the Early Pleistocene (Morrice et al., 1983). Due to the absence of Late Pliocene/Early Pleistocene fauna in both islands, nothing is known about the insular fauna.

5.2.2 Faunal succession and age of the faunas

In the 1990s, a joint Dutch-Indonesian team recovered vertebrate fossils remains from 31 localities in the Sengkang Basin. Based on their findings and earlier fossil faunal reports (Hooijer, 1948a, 1948b, 1948c, 1949, 1950, 1953a, 1953b, 1953c, 1954c, 1954b, 1954d, 1954e, 1954a, 1964b, 1969a, 1972a, van Heekeren, 1949), van den Bergh (1999) proposed three successive fauna stages for Sulawesi, from oldest to youngest: Walanae Fauna, Tanrung Fauna and Sub-recent to Recent Fauna (Figure 5.9). In addition to these three successive faunal stages, the Talepu site was excavated between 2007 and 2012. Talepu contains an in situ fauna and artefacts dated to the Late Pleistocene. A reliable faunal succession of Luzon and Sangihe cannot be established at present, because data of fossil context and stratigraphic context are insufficient. Morphological descriptions and related information for the analysed Proboscidean taxa are presented in Appendix I.

5.2.2.1 Walanae Fauna

The Walanae Fauna comprises all the fossil land vertebrates derived from the Beru Member of the Walanae Formation. This faunal assemblage occurs in Subunits A and B of the Beru Member (van den Bergh, 1999). The in situ fossil fauna excavated from the lowest part of Subunit A near the Sompe locality comprises Stegoloxodon celebensis, Celebochoerus heekereni, Geochelone atlas, Trionychidae sp. and two crocodile taxa. These taxa are present in the upper layers of Subunit A, and continue into Subunit B.

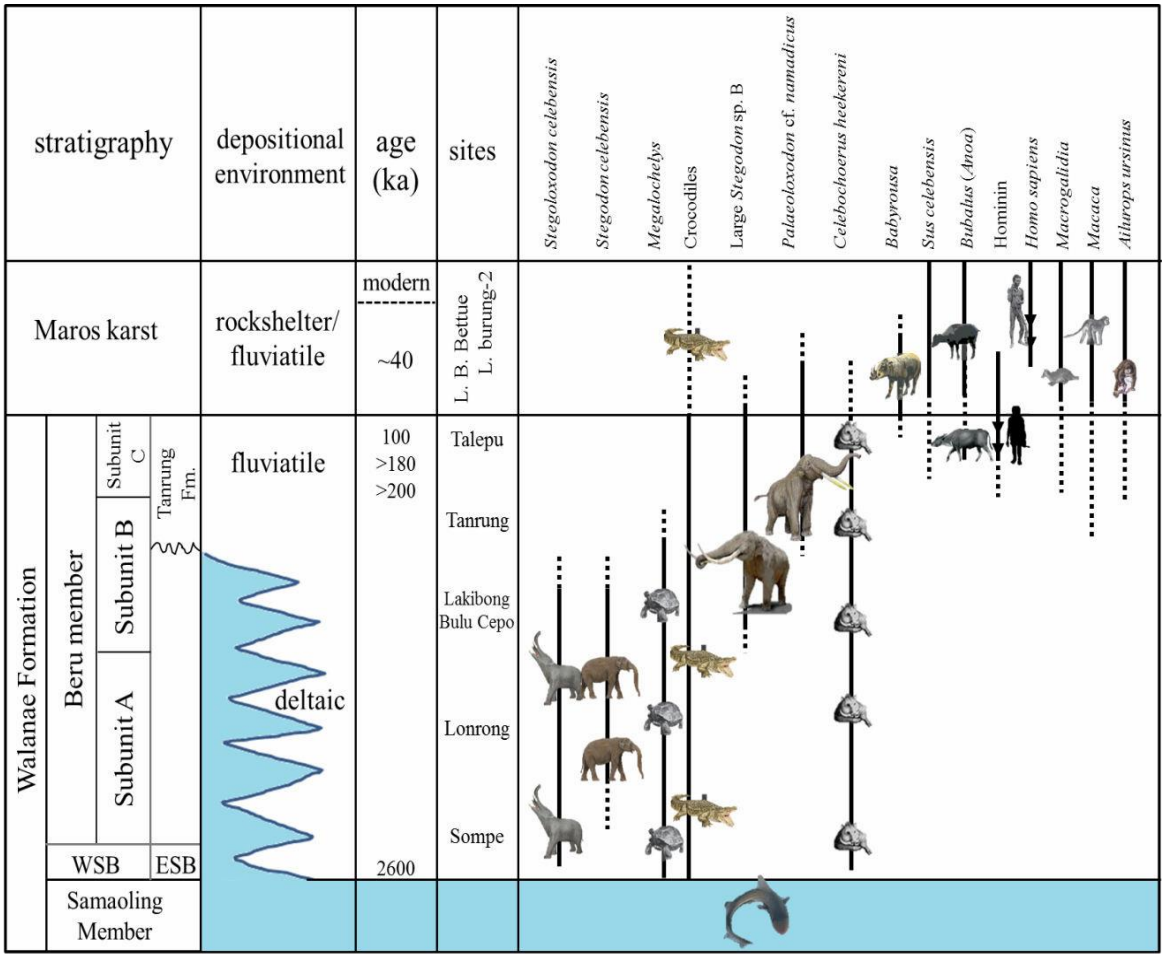

Figure 5.9 Faunal succession of Sulawesi (modified after van den Bergh, 2001)

The pygmy Stegodon sompoensis has not been found in the lowermost layers of Subunit A. In the excavation, this species only appears in the upper part of Subunit A and continues in Subunit B. The confusion over the occurrence of S. sompoensis in the Sompe locality as recorded in the van Heekeren collection (Hooijer, 1964) and in the MGB collection is explained by van den Bergh (van den Bergh, 1999, van den Bergh et al., 2001) as mixing specimens from younger deposits. This explanation is plausible, because S. sompoensis specimens from this locality were collected from the surface.

Celebochoerus heekereni is the most abundant element of the Walanae Fauna. This species seems to have evolved towards a short-legged variety during the timespan covered by the Beru Member (van den Bergh, 1999), based on a single shortened metapodial surface collected in the upper reaches of the Beru Member. Large-sized Stegodon fossil remains have been found only in the upper part of Subunit B. However,

the large-sized Stegodon specimens are not represented by in situ findings. Nevertheless, fossil remains of this species have only been found in the areas where Subunit B is exposed, and no indication for transport from younger deposits was observed. So far there is no in situ artefact found in the sediment associated with the Walanae Fauna in Subunits A and B. Therefore, the Walanae Fauna presumably did not interact with hominins.

The oldest exposed layer that contained the first group of the Walanae Faunal assemblage is in the base of the Beru Member, dated to around 2.5 Ma. However, the timing of the onset of S. sompoensis in the sediment remains uncertain, since there is no palaeomagnetic or radiometric dating for the upper part of Subunit A of the Beru Member. The first appearance and the upper constraint of the large Stegodon sp. occurrence also remains uncertain, since no radiometric dates for the lower part of Subunit B of the Beru Member are unavailable. Hence, the upper limit of the Walanae Fauna is drawn from the ESR dating result on a Celebochoerus heekereni teeth from the Lakibong site, which shows an age of 0.5 Ma, albeit of uncertain accuracy.

5.2.2.2 Tanrung Fauna

The early faunal assemblage stability in south Sulawesi only prevailed until the Middle Pleistocene. During the Middle Pleistocene new immigrants started to arrive and most elements from the Walanae Fauna apparently became extinct, resulting in a faunal turnover. This faunal turnover is marked by the Tanrung Fauna, which originates from the Tanrung Formation. The constituent taxa of the Tanrung Fauna are clearly distinct from the Walanae Fauna due to the absence of Stegoloxodon celebensis and Stegodon sompoensis. The occurrence of a large Stegodon sp. continued in this assemblage. Another faunal element that differentiates the Tanrung Fauna from the Walanae Fauna is the occurrences of cf. Palaeoloxodon namadicus. Molar fragments and two metacarpals of cf. Palaeoloxodon namadicus were found on the surface at the Tanrung River. Based on the attached matrix, it was inferred that the specimens were derived from the Tanrung Formation.

Celebochoerus also occurs in situ in the Tanrung Formation, but fragments of this species in this sediment are rounded and may have been reworked. Celebochoerus

specimens from the Tanrung Fauna are relatively smaller compared to the remains from the Walanae Formation (van den Bergh, 1999, van den Bergh et al., 2001). Additionally, teeth of Bubalus (Anoa) sp. and Sus celebensis were found on the surface at the Tanrung River and its confluent, the Paciro River. However, the association of Bubalus and Sus in the Tanrung Fauna is debatable, since those taxa only occur in the younger deposits that are exposed along the Tanrung and Paciro River, and have a distinct fossilisation, and have never been found in situ in the Tanrung Formation. Furthermore, no artefacts were found in the Tanrung Formation or Tanrung River, but this could be due to a lack of suitable source materials in that area. Additionally, an in situ giant tortoise humerus was found in the Tanrung Formation more recently during a survey in 2007 (van den Bergh, pers. comm.).

The lack of available palaeomagnetic, micropalaeontological or radiometric dating results for the Tanrung Formation makes it difficult to estimate the age of this fauna. Thus the relative age of the Tanrung Fauna can only be estimated from its faunal content. The age determining element of this fauna is the cf. Palaeoloxodon namadicus, which has high hypsodont molars. From elsewhere in Eurasia, including Java, such high-crowned Elephantini, like Elephas hysudrindicus from Java and Palaeoloxodon namadicus from mainland Southeast Asia have their first appearance during the Middle Pleistocene (Maglio, 1973, Sondaar, 1984, de Vos, 1985, Hong et al., 2013, Louys et al., 2007). Interpolating the first occurrence of the similar taxa from mainland Southeast Asia and Java with the occurrence of cf. Palaeoloxodon namadicus from the Tanrung Fauna, van den Bergh (van den Bergh, 1999, van den Bergh et al., 2001) suggested a maximum age constraint for the Tanrung Fauna as Middle Pleistocene.

Fossil fauna excavated from Subunit C in the Talepu site includes taxa yielded in the older fauna, such as: molars and lower canine of Celebochoerus cf. heekereni and a Stegodon sp. molar ridge fragment. The fragmented nature of the Stegodon molar ridge fragment attribution to a large or small-bodied Stegodon is uncertain. Fossil Bubalus depressicornis were also found in the sediment. Due to the close resemblance to the Tanrung Fauna, taxa recovered from this site are included in the Tanrung Fauna. The stone artefact found in this subunit indicates that hominin has been occurred during this interval.

Although more limited in number, the fauna originating from Talepu is relatively better dated. A uranium-series dates obtained from Celebochoerus between 0.2-0.5 m below the deepest stone artefact in the same lithology indicates that the fossil samples are older than ~200 ka (between 200 and 780 ka, van den Bergh et al, 2016), which is older than dated sediment (between 200 and 100 ka). Hence, the minimum age of the sediment in Talepu (~100 ka) is used as a minimum age constraint for the Tanrung Fauna. Moreover, this sediment is important since the earliest in situ stone artefacts are found that mark the first immigration of humans into Sulawesi. Thus, unlike the older faunas, the fauna yielded in this sediment may have been the first to be interacting with humans.

5.2.2.3 Late Pleistocene, Sub-recent and recent faunas

The late Pleistocene fauna of Sulawesi was mostly excavated from the sediments in Leang Bulu Bettue (LBB). Remains of Stegodon occur in layer 8, 10 and 13 in LBB (van den Bergh, 2015a); however, these specimens possibly derived from older sediments. cf. Palaeoloxodon namadicus occur in Layer 10 and continued up to layer 4. A large-sized suid upper canine fragment could possibly belong to Celebochoerus. Bubalus quarlesi, Bubalus (Anoa) depressicornis, Babyrousa babyrousa and Sus celebensis also occur up to Layer 4. Phalanger, Macaca, Tarsius, Macrogalidia, Repitilia, Macrochiroptera and Rodentia first appeared in Layer 5 or 4. However, these taxa might have colonized Sulawesi earlier than this date. Additionally, Bubalus (Anoa) and Sus celebensis were also found in the younger alluvial deposits of the Walanae Basin. The fossils of cf. Palaeoloxodon namadicus originate from the cave deposit mark the last occurrence of Proboscidean taxa in Sulawesi. The age of Layer 5 of Leang Bulu Bettue (~42 ka) is assumed to be the last occurrence datum of Proboscidea in Sulawesi.

A list of recent fauna of Sulawesi is presented in Cranbrook (1981). The recent fauna recovered from the uppermost part of the cave sediment include: bird, pig, bovid, cuscus, Soricidae (mole), squirrel, murine rodents, snake, frog, and deer (van den Bergh, 2015a). Other than the island's native species, the recent fauna also includes several introduced mammalian species (Cervus timorensis, Paradoxurus hermaphroditus, Sus scrofa). Faunal assemblages from the cave sediments occur

alongside stone artefacts, suggesting an interaction between humans with the faunal assemblages. Various taphonomic characteristics, such as signs of burning, bone breakage, presence of cut and chop marks, and polished bone/dental surfaces as potential signs of use-wear occur in some bones (van den Bergh et. al., 2015).

5.2.2.4 Fossil fauna north of Sulawesi

In Sangihe, a partial skeleton of a single Stegodon individual was incidentally found in the Pintareng Formation by a local resident while excavating a gold placer (Samodra, 1989). Further fossil collection and inspection of the locality were carried out by Aziz and Tatsuo Shibasaki (Aziz, 1990). This specimen was referred to as Stegodon sp. B cf. trigonocephalus. Van den Bergh (1999) suggested that the elements belongs to a single individual and that the tooth morphology of the Sangihe specimen is very similar to the Stegodon from the Tanrung Formation (Stegodon sp. B) and tentatively attributed it to the same species. The age of the Sangihe Stegodon is estimated as Middle Pleistocene (van den Bergh, 1999).

The fossil fauna from the Middle Pleistocene sediment of Luzon comprises Stegodon luzonensis, Elephas sp., Rhinoceros philippinensis, Bubalus sp., Celebochoerus sp./Sus sp. and Cervus sp. (Bautista, 1991). This fauna seemed to be associated with stone artefacts and tektites (von Koenigswald, 1956, Bautista, 1991). Due to scarce fossil records and and unclear stratigraphic context, a reliable biostratigraphy of the early terrestrial faunal occupation of Luzon cannot be established. Additionally, a molar of primitive dwarf Stegodon from unknown stratigraphic level is stored in the National Museum of Philippines. Due to its primitive form (see Appendix II for brief description of molar), and extrapolated from the occurrence of similar form from other island (Sulawesi, Java and Flores), it may be older than 1 Ma.

A Late Pleistocene fossil fauna of Luzon is recorded from cave deposits. The faunal assemblage comprises a large number of Cervus and Muridae, primates, Tarsius and Varanus specimens. So far, there is no record of Elephantoidea from the Late Pleistocene deposits of Luzon. Therefore the Elephantoidea taxa presumably only lasted on the island until the late Middle Pleistocene or the early Late Pleistocene.

5.2.3 Dispersal of mainland taxa to the Wallacean islands

Due to the lack of former land connections between Sundaland/mainland Southeast Asia and Sulawesi/Luzon, ancestors of all other large mammals, fossil and extant, must have reached these islands by crossing ocean barriers between the Sunda Shelf and these islands. There is an unresolved debate on the origins of the fauna of Sulawesi, whether its fauna migrated from the Sundaland via Philippines Archipelago or crossing the Makassar Strait.

As the characteristics of the palaeogeography and fossil fauna of Sulawesi and the Philippines, especially Luzon, are relatively similar (e.g., Luzon and Sulawesi are the only islands with evidence for the former occurrence of the genus Celebochoerus, see Ingicco et al., 2016), there is a possibility that the fauna found in Sulawesi might have migrated via the Philippines Archipelago. Faunal assemblages in both islands contain many endemic taxa, are impoverished, lack carnivores and contain pygmy Proboscidea. Even so, the Middle Pleistocene fossil fauna of Luzon has more mainland taxa elements than Sulawesi (Tougard, 2001). The distance between mainland Southeast Asia and Luzon, especially during periods of lower sea levels, must have been much smaller (Kealy et al., 2016). Additionally, other processes such as strong currents between Sundaland and Sulawesi may have favoured north-south dispersal to Sulawesi from the Phillipines. Therefore it is thought that smaller mainland taxa such as Cervus and Rhinocheros could have migrated to Luzon through Palawan and Mindoro. According to De Terra (1943), a migration route from mainland Asia via Taiwan to the Philippines and on to Sulawesi could have been an alternative, but not as an exclusive Pleistocene route. Hooijer (1975) also considered the Philippine islands as an important link in the dispersal route of Pleistocene Asiatic faunal elements to Sulawesi. The recent find of a Celebochoerus upper canine fragment in the Cagayan Valley (Ingicco et al., 2016) further adds to this presumed link.

On the other hands, based on its faunal elements, Groves (1976, 1985) concluded that the Pleistocene faunal elements from Sulawesi bear close relationships with fauna from the Middle Siwaliks. He thought it most likely that this fauna had immigrated to Sulawesi via the Makassar Strait. Although not too wide (~50 km during the lowest sea

level stands, i.e. during the LGM; Voris, 2000), this strait is relatively deep and has strong surface currents. Thus the Makassar Strait represents the primary selective factor of migration to Sulawesi. Only mammals that have large body mass can deliberately cross this sea barrier, while smaller mammals might have been carried by currents. Alternatively, large mammals with better swimming ability would have a better chance to survive the possibility of unexpectedly being swept out to the sea by a tsunami. Van den Bergh (1999) added that an unlikely possibility for overseas dispersal between Sulawesi and the Philippines islands may be related to insufficient chronostratigraphic and tectonic data and the poorly known fossil record from the Philippines.

Although very limited, the presence of Stegodon in Sangihe, allows the possibility of overseas faunal dispersal during the Middle Pleistocene, especially during low sea levels of the Middle Pleistocene. Comparing the recent mammalian fauna of Sangihe with faunas from Sulawesi and the Philippines, van den Bergh (1999) suggests that the Stegodon originated from Sulawesi. Besides some more widespread mammals, Phalanger celebensis, Callosciurus leucomus, and Tarsius spectrum, all endemic species that occur on Sangihe also occur on Sulawesi (Groves, 1976). In contrast, Sangihe has no non-flying mammals in common with the Philippines, suggesting that its fauna originated entirely from Sulawesi. Combining glacioeustatic sea level lowering of maximum 120 m and the present-day bathymetry, a distance of 175 km of sea would have to be crossed to reach Sangihe from the southernmost tip of Mindanao. From northern Sulawesi also a total distance of 170 km would have to be crossed, but 5 small islands in between could have been used as stepping stones, so that the largest overseas distance would be no more than ~35 km. Therefore migration out from Sulawesi to Sangihe is more likely than from Mindanao.

As for the southward dispersal to the Lesser Sunda Islands (LSI), Hooijer (1972a, 1975, 1982) and Audley-Charles and Hooijer (1973) postulated a land connection between Sulawesi, Flores and Timor called “Stegoland”. These land connections would have disappeared subsequently during the Middle to Late Pleistocene. Simpson (1977), Sondaar (1981), van den Bergh (1999) and Morwood and van Oosterzee (2007) rejected this concept and argued that the southern dispersal of fauna to the LSI would have been by means of overseas crossing. In more detail, van den Bergh (1999) suggests that this overseas crossing from Sulawesi to the LSI was only carried out by large-sized

Stegodon from the Middle Pleistocene and not by the Early Pleistocene pygmy Stegodon. Based on molar similarities, there may be a link between S. florensis from Flores and Stegodon sp. B. from Sulawesi. S. florensis may have arrived from South Sulawesi through Selayar and the Bonerate islands.

5.3 Analysed materials

A total of 66 enamel samples of six different Elephantoidea taxa and Celebochoerus from Sulawesi, Sangihe and Luzon were selected for stable isotope analysis. Analysed specimens comprise: Stegoloxodon celebensis (n = 19), Stegodon sompoensis (n = 13), Stegodon sp. B (n = 14), cf. Palaeoloxodon namadicus (Sulawesi, n = 4), dwarf Stegodon sp. (Luzon, n = 1), Stegodon cf. luzonensis (n = 1), Elephas sp. (Luzon, n = 2), Celebochoerus heekereni from the Walanae Fauna (n = 11) and Celebochoerus sp. from Talepu (n = 1). Samples cover a time span between the Early Pleistocene and the Late Pleistocene. Although not included in the Proboscidean taxa, Celebochoerus was also included in the analysis in order to investigate possible niche segregation and diet differentiation among the various island mammals in the palaeoecosystem of Sulawesi. Moreover, Celebochoerus is the dominant faunal element in the Walanae Fauna. The palaeodiet and palaeoenvironmental analysis will be discussed for each taxon throughout their occurrence in different ages to explore any changes in their feeding preference and the overall faunal assemblage to test whether any niche differentiation occurred between faunal elements.

The Walanae Fauna samples are further divided into those originating from Subunit A and those from Subunit B. Distinction between Subunits A and B is carried out due to different depositional environments and the occurrence of Stegodon sp. B only in Subunit B. The Walanae Fauna in Subunit A includes fossil fauna collected from fossil localities east of the Bulu Cepo Fault: Sompe and Bulu Cepo, as well as fossil localities west of the Lakibong Triangle: Lonrong and Paroto. Subunit B fossils include all samples originating from fossil localities within the Lakibong Triangle and Bulu Cepo. The Tanrung fauna includes all fossils derived from the Tanrung Formation, the one and only Stegodon sp. B individual from Sangihe, as well as Celebochoerus from Talepu

and cf. Palaeoloxodon namadicus from Leang Bulu. However, different labels are given to these samples in the graphs to distinguish the distinct origin of these samples.

Four enamel samples obtained from the Cagayan Valley (Luzon), belongs to dwarf Stegodon sp. (n = 1), Stegodon cf. luzonensis (n = 1) and Elephas sp. (n = 2) were also included in the analysis. The dwarf Stegodon sp. specimen is a third lower molar (M_3, see Appendix II for description of the specimen), while the Stegodon cf. luzonensis and Elephas sp. specimens each comprises only a plate/lamella fragment. Due to the fragmented nature and very limited information of Stegodon cf. luzonensis and Elephas sp. specimens, descriptions of these specimens are not included in the appendix. Since the number of samples originating from Sangihe and Luzon is very limited, thus the conclusion drawn for these locations should be treated as preliminary.

5.4 Isotopic analysis results

A list of individual isotopic values of analysed samples is given in Appendix II. Individual and range of $\delta^{13}C$ (‰, $_{VPDB}$) and $\delta^{18}O$ (‰, $_{VPDB}$) values of all analysed samples, which are grouped by faunal assemblages is presented in Figure 5.10, followed by individual and range of isotopic values for each faunal assemblage (Fig 5.11 A-D). The individual $\delta^{13}C$ and $\delta^{18}O$ values and ranges (in ‰, $_{VPDB}$), grouped by taxa are presented in Figure 5.12 A-D. In Figure 5.13, individual $\delta^{13}C$ and $\delta^{18}O$ values of all taxa from Sulawesi are arranged in chronological order, based on the estimated age of faunal assemblages. Due to the lack of firm age control, the age of species may be speculative, and therefore reconstruction of palaeoenvironmental change is limited.

Table 5.1 reports descriptive statistic of measured $\delta^{13}C$ and $\delta^{18}O$ values of analysed samples, which are grouped based on faunal assemblages (A) and species (B), respectively. Matrices of pairwise probability Benferroni corrected p values of Mann-Whitney post hoc test to determine significant differences among taxa are presented in Table 5.2.

Table 5.1 Descriptive statistic for $\delta^{13}C$ and $\delta^{18}O$ values of: (**A)** faunal assemblages and (**B)** species from Sulawesi, Sangihe and Luzon.

A. faunal assemblage	n	$\delta^{13}C$ (‰, VPDB)					$\delta^{18}O$ (‰, VPDB)				
		mean	median	std. dev	std. error	range	mean	median	std. dev	std. error	range
Tanrung Fauna + cave deposit	14	-4.8	-0.8	7.2	1.9	-14.9 to 1.8	-5.6	-5.7	1.0	0.3	-7.5 to -3.2
1. Stegodon sp. B (Sulawesi)	8	0.3	0.0	1.2	0.4	-1.1 to 1.8	-5.3	-5.6	1.0	0.3	-6.2 to -3.2
Stegodon sp. B (Sangihe)	1	-	1.8	-	-	1.8	-	-6.4	-	-	-6.4
2. cf. Palaeoloxodon namadicus (incl. LBB)	4	-14.2	-14.2	0.6	0.3	-14.9 to-13.6	-6.4	-6.2	0.8	0.4	-7.5 to -5.6
3. Celebochoerus heekereni	1	-	-13.5	-	-	-13.5	-	-5.7	-	-	-5.7
Walanae Fauna B	22	-3.0	-1.4	4.6	1.0	-14.9 to 1.1	-4.6	-4.8	1.1	0.2	-6.6 to -2.7
1. Stegoloxodon celebensis	4	-6.9	-6.8	7.6	3.8	-14.9 to 0.9	-4.6	-4.8	0.9	0.5	-5.4 to -3.3
2. Stegodon sompoensis	9	-3.3	-2.2	4.3	1.4	-12.3 to 1.1	-4.7	-4.8	1.2	0.4	-6.6 to -2.8
3. Stegodon sp. B	5	-1.4	0.1	2.5	1.1	-4.5 to 0.7	-5.4	-5.4	0.6	0.3	-6.4 to -4.8
4. Celebochoerus heekereni	4	-0.4	-0.5	0.6	0.3	-1.0 to 0.4	-3.5	-3.4	0.9	0.5	-4.6 to -2.7
Walanae Fauna A	26	-3.0	-0.9	4.7	0.9	-14.1 to 1.3	-4.6	-4.25	1.4	0.3	-8.9 to -1.7
1. Stegoloxodon celebensis	15	-4.0	-1.0	5. 9	1.5	-14.1 to 1.3	-4.7	-4.50	0.9	0.2	-6.1 to -3.69
2. Stegodon sompoensis	4	-4.0	-3.8	1.1	0.5	-5.3 to -3.1	-6.4	-5.80	1.7	0.9	-8.9 to -4.99
3. Celebochoerus heekereni	7	-0.4	-0.7	0.5	0.2	-0.9 to 0.2	-3.2	-3.30	0.8	0.3	-4.2 to -1.7
Pleistocene Luzon	4	-2.7	-2.4	2.8	1.4	-6.2 to -0.0	-5.3	-5.1	1.3	0.7	-7.2 to -4.0
1. Stegodon cf. luzonensis	1	-	0.0	-	-	0.0	-	-5.2	-	-	-5.2
2. Elephas sp.	2	-2.3	-2.3	-	-	-3.6 and -1.1	-4.5	-4.5	-	-	-5.0 and -4.0
3. dwarf Stegodon sp.	1	-	-6.2	-	-	-6.2	-	-7.2	-	-	-7.2

B. species	n	$\delta^{13}C$ (‰, VPDB)					$\delta^{18}O$ (‰, VPDB)				
		mean	median	std. dev	std. error	range	mean	median	std. dev	std. error	range
Stegoloxodon celebensis	19	-4.6	-1.9	6.2	1.4	-14.9 to 1.31	-4.7	-4.7	0.9	0.2	-6.1 to -3.3
Stegodon sompoensis	13	-3.5	-3.2	3.6	1.0	-12.31 to 1.1	-5.2	-5.0	1.6	0.4	-8.9 to -2.8
Stegodon sp. B	14	-0.3	0.1	1.9	0.5	-4.5 to -1.8	-5.3	-5.4	0.8	0.2	-6.4 to -3.2
cf. Palaeoloxodon namadicus	4	-14.2	-14.2	0.6	0.3	-14.9 to -13.6	-6.4	-6.2	0.8	0.4	-7.5 to -5.6
dwarf Stegodon sp. (Luzon)	1	-	-6.2	-	-	-6.2	-	-7.2	-	-	-7.2
Stegodon cf. luzonensis	1	-	0.0	-	-	0.0	-	-5.2	-	-	-5.2
Elephas sp. (Luzon)	2	-2.3	-2.3	-	-	-3.6 and -1.1	-4.5	-4.5	-	-	-5.0 and -4.0
Celebochoerus heekereni (Walanae fauna)	11	-0.4	-0.7	0.5	0.2	-1.0 to 0.4	-3.3	-3.3	0.8	0.2	-4.6 to -1.7
Celebochoerus heekereni (Talepu)	1	-	-13.5	-	-	-13.5	-	-5.7	-	-	-5.7

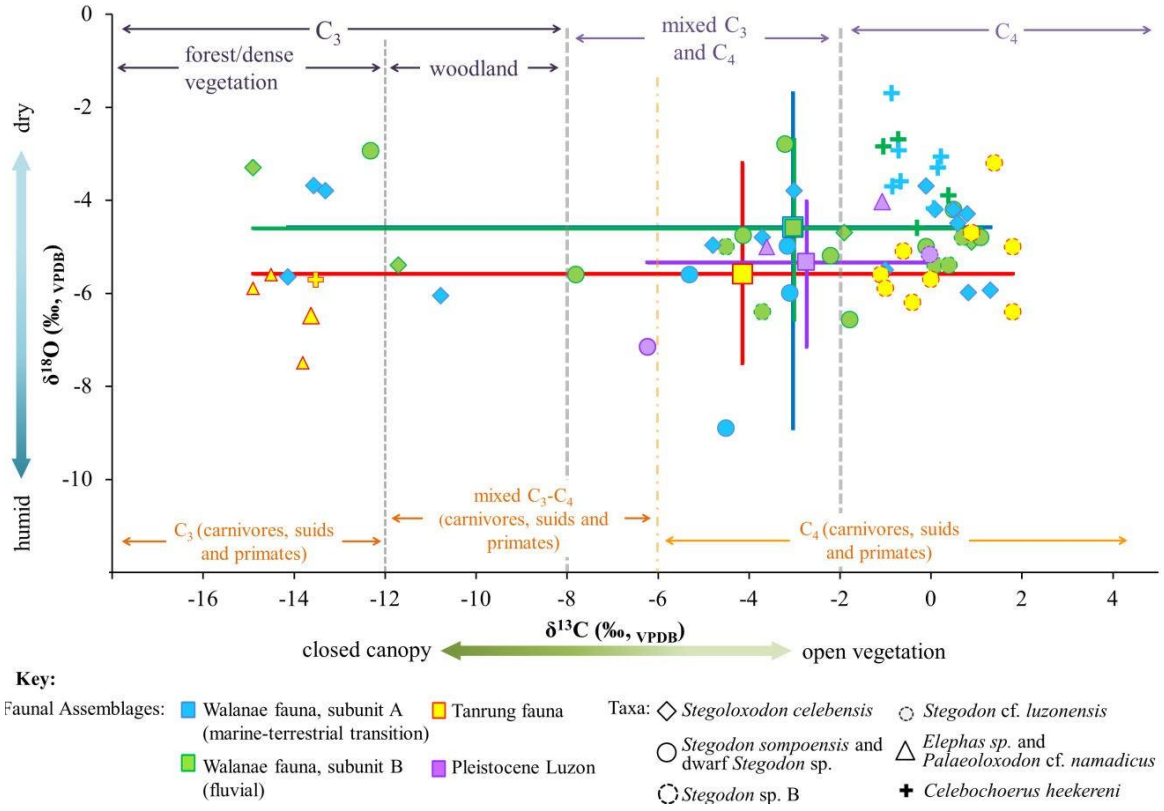

Figure 5.10 Mean $\delta^{13}C$ and $\delta^{18}O$ values and ranges separated by stratigraphic interval, for all analysed samples. Different colours represent the faunal assemblages, while different shapes indicate taxa. Dashed lines represent boundaries between vegetation diet types (Cerling et al., 1997a, 1999, MacFadden et al., 1999, Passey et al., 2002, Feranec, 2007). Mean values are designated by the crossing of the range bars.

Table 5.2 Matrices of pairwise probabilities of mean difference in $\delta^{13}C_{enamel}$ and $\delta^{18}O_{enamel}$ values. Values shown in red indicate significant p values ($\alpha \leq 0.05$) using Mann-Whitney test.

5.2.1 among faunal assemblages (**A**) and among co-occurred species within each faunal assemblage (**B, C, D**).

A	**faunal assemblage**	**1**		**2**		**3**	
		$\delta^{13}C$	$\delta^{18}O$	$\delta^{13}C$	$\delta^{18}O$	$\delta^{13}C$	$\delta^{18}O$
1	Walanae Fauna A	-	-				
2	Walanae Fauna B	0.9835	1				
3	Tanrung Fauna	0.9322	**0.0441**	0.9871	**0.0219**		
4	Pleistocene Luzon	0.4829	1	0.6441	1	0.7905	1

B	**Walanae Fauna Subunit**	**1**		**2**	
		$\delta^{13}C$	$\delta^{18}O$	$\delta^{13}C$	$\delta^{18}O$
1	Stegoloxodon celebensis	-	-		
2	Stegodon sompoensis	1	0.1529		
3	Celebochoerus heekereni	1	**0.0035**	**0.0322**	**0.0322**

C	Walanae Fauna Subunit B	1		2		3	
		$\delta^{13}C$	$\delta^{18}O$	$\delta^{13}C$	$\delta^{18}O$	$\delta^{13}C$	$\delta^{18}O$
1	Stegoloxodon celebensis	-	-				
2	Stegodon sompoensis	0.5892	1				
3	Stegodon sp. B	0.5403	1	0.5938	1		
4	Celebochoerus heekereni	0.3123	0.6741	0.3159	0.4559	0.903	0.1167

D	Tanrung Fauna	1	
		$\delta^{13}C$	$\delta^{18}O$
1	Stegodon sp. B	-	-
2	Palaeoloxodon cf. namadicus	**0.0069**	0.1042

5.2.2 among species (**A**) and specified for each species occurs in more than one successive faunal assemblages (**B, C, D, E**)

A	species	1		2		3		4		5	
		$\delta^{13}C$	$\delta^{18}O$	$\delta^{13}C$	$\delta^{18}O$	$\delta^{13}C$	$\delta^{18}O$	$\delta^{13}C$	$\delta^{18}O$	$\delta^{13}C$	$\delta^{18}O$
1	Sl. celebensis	-	-								
2	S. sompoensis	0.7882	1								
3	Stegodon sp. B	0.0657	0.5913	**0.0101**	1						
4	Palaeoloxodon cf. namadicus	**0.0094**	0.1998	**0.0039**	1	**0.0035**	0.7330				
5	Elephas sp. (Luzon)	0.7019	1	0.7879	1	0.0507	1	0.0518	1		
6	C. heekereni	0.3437	**0.0079**	**0.0150**	**0.0263**	0.3663	**0.0017**	**0.0050**	0.0750	**0.0127**	0.4391

B	Stegoloxodon celebensis	1		2	
		$\delta^{13}C$	$\delta^{18}O$	$\delta^{13}C$	$\delta^{18}O$
1	Sompe (subunit A, base)	-	-		
2	Lonrong (subunit A, top)	0.9758	0.1274		
3	Lakibong (subunit B)	1	1	1	0.4691

C	Stegodon sompoensis	1	
		$\delta^{13}C$	$\delta^{18}O$
1	Walanae Subunit A	-	-
2	Walanae Subunit B	0.3961	0.0892

D	Stegodon sp. B	1	
		$\delta^{13}C$	$\delta^{18}O$
1	Walanae Fauna	-	-
2	Tanrung Fauna	0.3501	0.8936

E	Celebochoerus. Heekereni	1	
		$\delta^{13}C$	$\delta^{18}O$
1	Walanae Subunit A	-	-
2	Walanae Subunit B	0.9247	0.9247

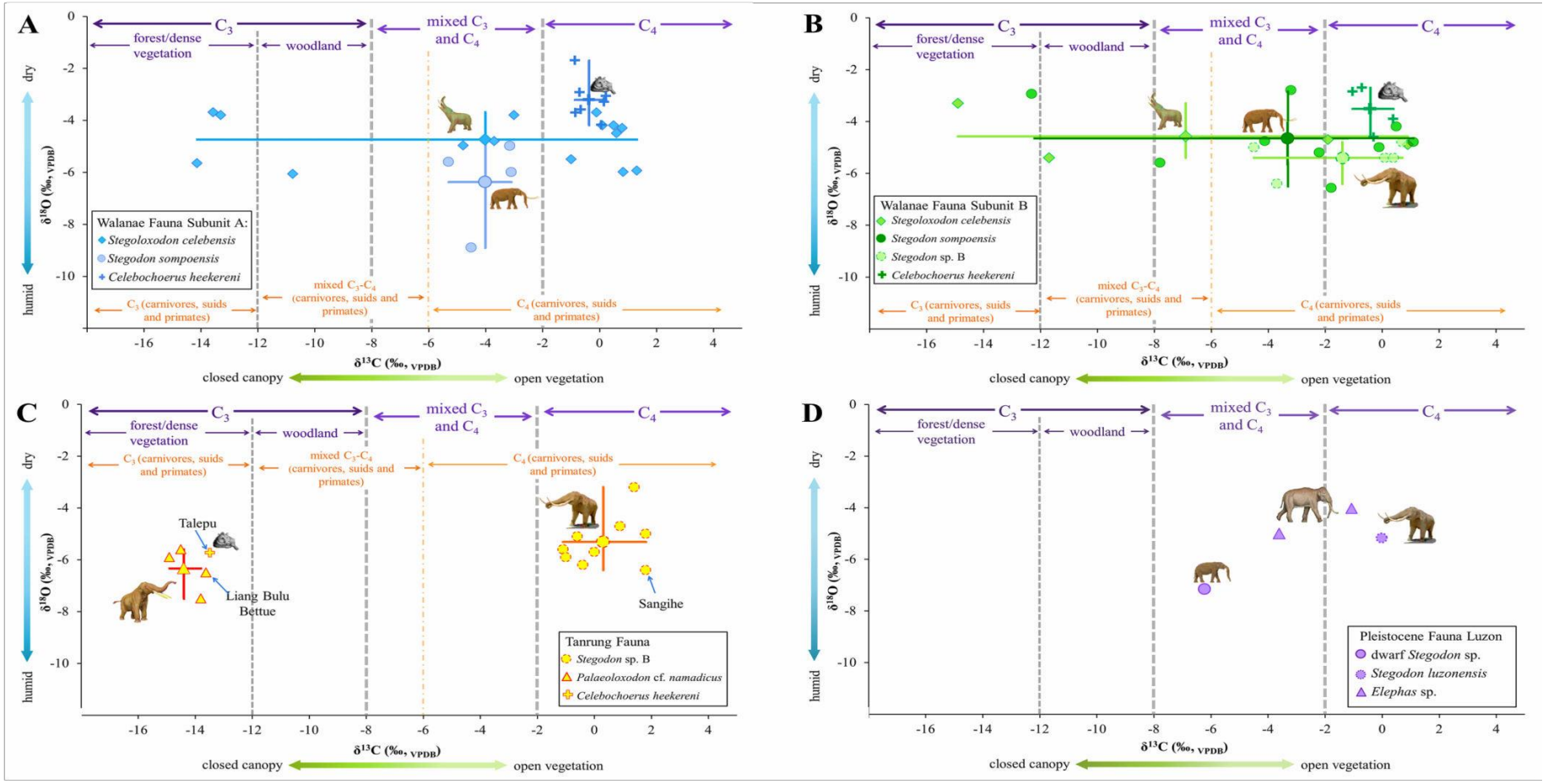

Figure 5.11 Mean $\delta^{13}C$ and $\delta^{18}O$ values and ranges for all samples included in: **A)** the Walanae Fauna from the Subunit A of the Beru Member, **B)** theWalanae Fauna from the Subunit B of the Beru Member, **C)** the Tanrung Fauna from the Tanrung Formation, Sangihe, Talepu and Liang Bulu Bettue, and **D)** all samples from Luzon. Dashed lines represent boundaries between vegetation and diet types (Cerling et al., 1997a, 1999, MacFadden et al., 1999, Passey et al., 2002, Feranec, 2007). Means are indicated by the crossing of the range bars.

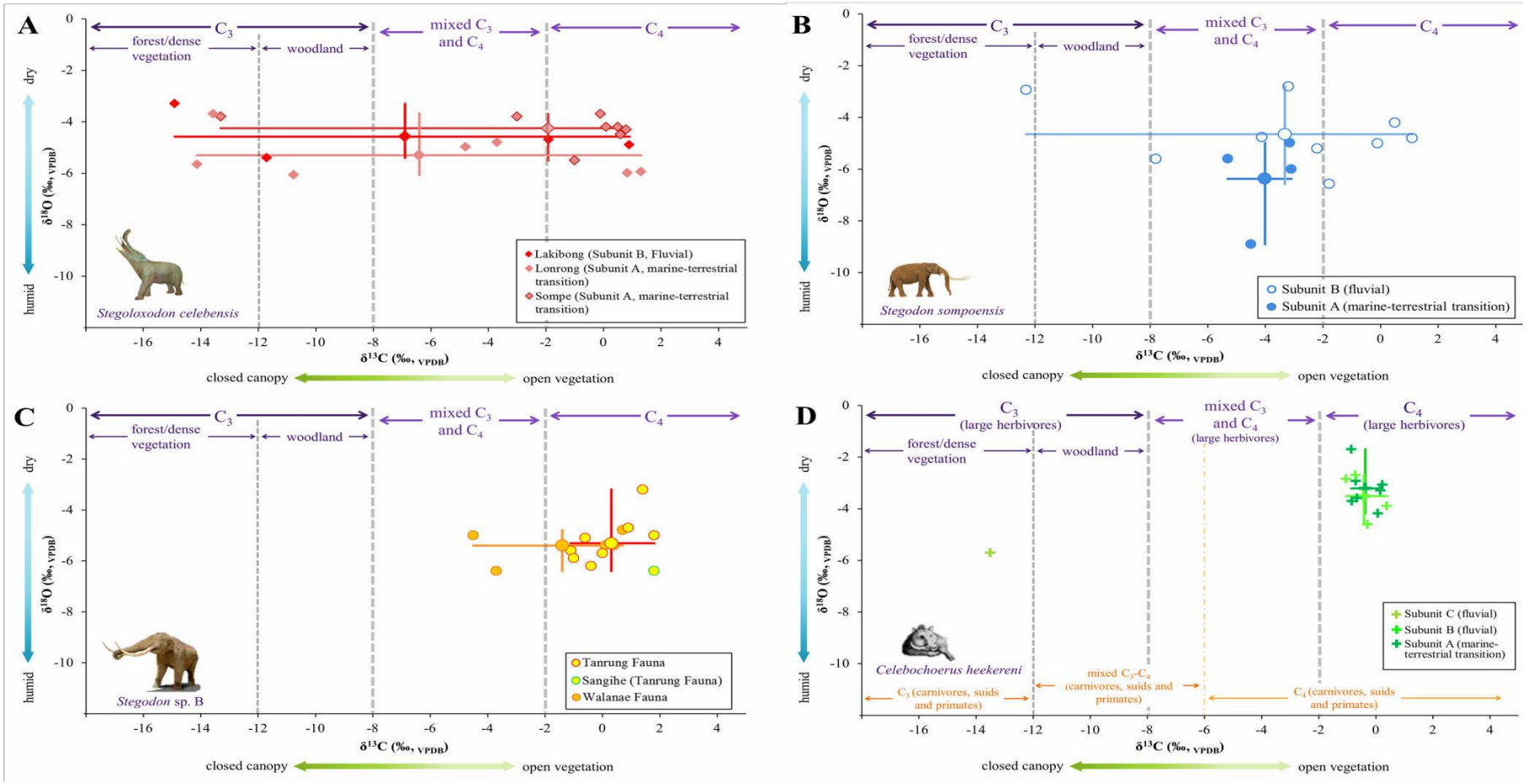

Figure 5.12 Mean $\delta^{13}C$ and $\delta^{18}O$ values and ranges for: **A.** Stegoloxodon celebensis from Sompe, Lonrong and Lakibong, **B.** Stegodon sompoensis from the Subunit A and B, **C.** Stegodon sp. B from the Walanae Fauna, the Tanrung Fauna and Sangihe, and **D.** Celebochoerus hekeereni from Subunit A, B and C. Dashed lines represent boundaries between vegetation and diet types (Cerling et al., 1997a, 1999, MacFadden et al., 1999, Passey et al., 2002, Feranec, 2007). Means are designated by the crossing of the range bars.

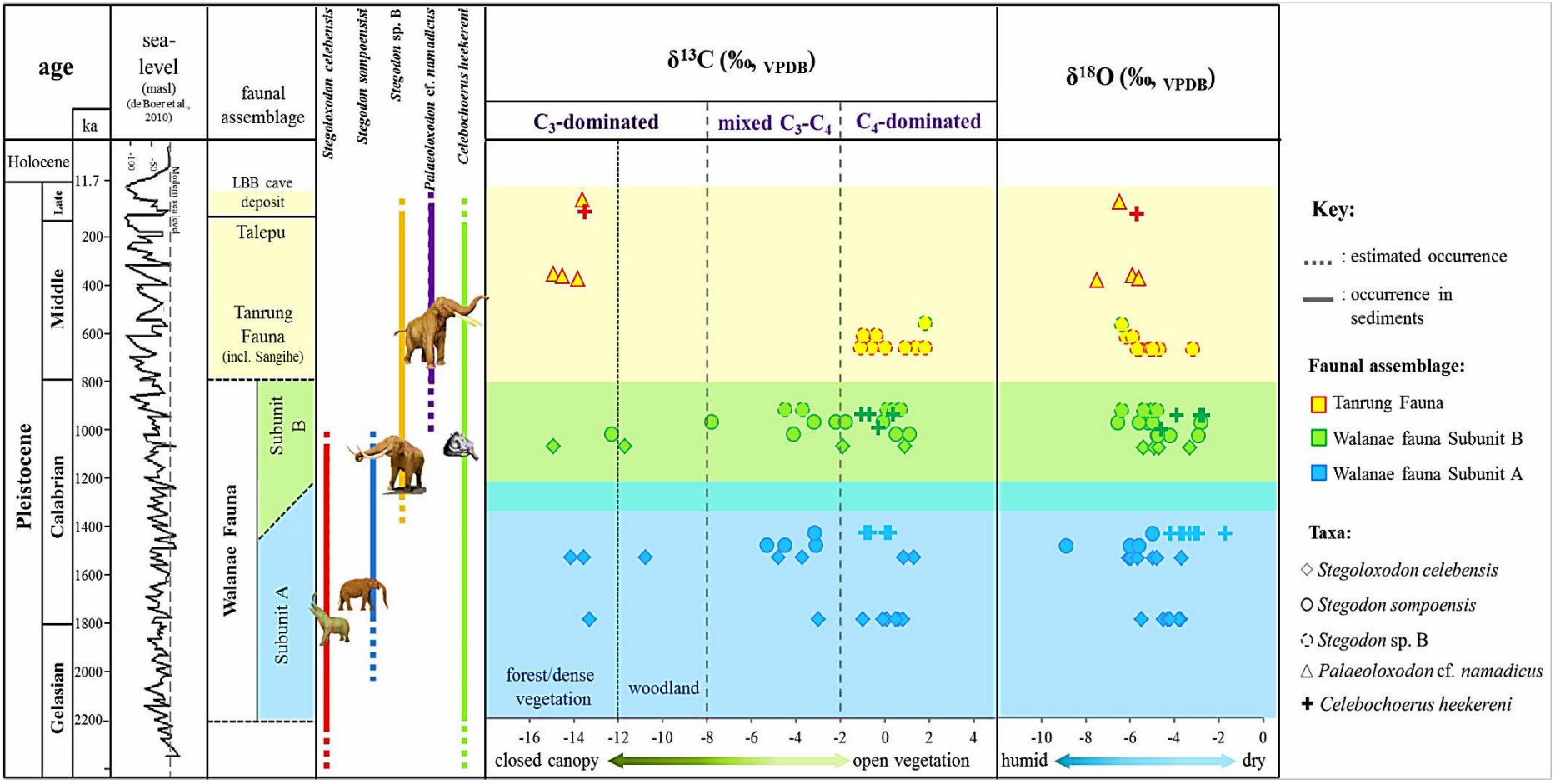

Figure 5.13 $\delta^{13}C$ and $\delta^{18}O$ values of analysed taxa of Sulawesi in estimated chronological sequence. Different colours indicate the faunal assemblages while different shapes indicate taxa. Dashed lines in the $\delta^{13}C$ column represent boundaries between vegetation and diet types (Cerling et al., 1997a, 1999, MacFadden et al., 1999, Passey et al., 2002, Feranec, 2007). The age distribution for taxa from different localities was slightly separated in this graph. The age separation does not depict the real age/stratigraphic position and is simply intended to show the isotopic distribution for each taxa found in different localities, as many of the isotopic values are overlapping, especially in Walanae Fauna.

5.4.1 Faunal assemblages

The $\delta^{13}C$ values of all samples cover a wide interval between -14.9 and 1.8‰, while $\delta^{18}O$ values range between -8.9 and -1.7‰ (Table 5.1). The $\delta^{13}C$ values of Walanae faunal elements cover C_3, mixed and C_4 diets, whereas the Tanrung faunal elements are divided into strictly C_3 browsers and C_4 grazers, without the occurrence of mixed feeders. The limited samples from Luzon plot in the mixed feeders and C_4 grazer ranges. There are no significant differences in $\delta^{13}C$ among faunal assemblages (Kruskal Wallis test p = 0.9481), while the $\delta^{18}O$ values of the Tanrung fauna is significantly lower than for the Walanae Fauna (Kruskal Wallis test p = 0.01629, Table 5.2.1A), for both from Subunit A (Mann-Whitney test Benferroni corrected p = 0.0441) and Subunit B (p = 0.0219, Mann-Whitney test).

5.4.1.1 Walanae Fauna, Subunit A

For the Walanae Fauna from Subunit A (Figure 5.11A and Table 5.1A), the $\delta^{13}C$ values of Stegoloxodon celebensis range between -14.1 and 1.3‰, suggesting flexible C_3, mixed C_3-C_4 and C_4 diets. The $\delta^{13}C$ values of Stegodon sompoensis are between -5.3 and -3.1‰, plot in the mixed C_3-C_4 and C_4 diets. The $\delta^{13}C$ values of Celebochoerus heekereni are between -0.9 and 0.2‰, suggesting that they had a specific C_4 dietary preference. All taxa from Subunit A have $\delta^{13}C$ values that are consistent with the expected ranges for closed canopy to open vegetation, suggesting that various types of vegetation coverage existed. From the graph (Fig. 5.11A), it can be seen that there are two distinct cluster of Stegoloxodon celebensis. However, these clusters do not represent any difference of localities. Despite of the widespread in their $\delta^{13}C$ values of Sl. celebensis, this group is statistically indistinguishable from S. sompoensis and C. heekereni (Kruskal-Wallis test p = 0.174, Mann-Whitney test Benferroni corrected p are 1 for both pairings), while the $\delta^{13}C$ values of C. heekereni are significantly higher compared to S. sompoensis (Benferroni corrected p = 0.0322).

The $\delta^{18}O$ values of Sl. celebensis (-6.1 ‰ to -3.7‰) and S. sompoensis (-8.9 to -2.9‰) are high to moderate and only one S. sompoensis individual has a very low $\delta^{18}O$ value. Statistically, only the $\delta^{18}O$ values of C. heekereni (–4.6 to -1.7‰) are significantly

higher than the two proboscidean species (Kruskal-Wallis test p = 0.001, Mann-Whitney test Benferroni corrected p for each pairing displayed in Table 5.2.1B).

5.4.1.2 Walanae Fauna, Subunit B

Similar to Subunit A, all analysed taxa in the Walanae Fauna found in Subunit B (Figure 5.11B and Table 5.1) have $\delta^{13}C$ values that correspond with all dietary ranges and habitats. The range of $\delta^{13}C$ values for both Stegoloxodon celebensis (-14.9 to 0.9‰) and Stegodon sompoensis (-12.3 to 1.1‰) correspond with expected ranges for C_3 browsers, mixed feeders and C_4 grazers. Again, this suggests that the two species were flexible feeders. However, there is no mixed feeder individual present among the analysed Sl. celebensis samples. The $\delta^{13}C$ values of the newcomer, the large Stegodon sp. B ranges between -4.5 and 0.7‰, suggesting a higher consumption of C_4 grasses and coinciding with an expected range for species foraging in open vegetation haitats. Similarly, the $\delta^{13}C$ values of C. heekereni individuals (-1.0 to 0.4‰) fall in the range of a C_4 dominant diet, like the C. heekereni specimens from Subunit A.

Among all analysed taxa from Subunit B, the $\delta^{18}O$ values of Stegodon sp. B (-6.4 to -4.8‰) has the lowest range, C. heekereni (-4.6 to -2.7‰) in higher range, while Sl. celebensis (-5.4 to -3.3‰) and S. sompoensis (between -6.6 and -2.8‰) have intermediate $\delta^{18}O$ values partly overlapping with Stegodon sp. B and C. heekereni. The $\delta^{18}O$ values of fauna from Subunit B are statistically indistinguishable from those of Subunit A. Although there is a high variability of dietary types and $\delta^{18}O$ values for each species, no significant differences for both $\delta^{13}C$ and $\delta^{18}O$ values occur among species within Subunit B (p for $\delta^{13}C$ = 0.6147 and $\delta^{18}O$ = 0.0504, Kruskal-Wallis test).

5.4.1.3 Tanrung Fauna

In the Tanrung Fauna, the $\delta^{13}C$ values of analysed taxa are divided into two opposite feeding preferences (Figure 5.11C and Table 5.1). The $\delta^{13}C$ values of Stegodon sp. B (-1.1 to 1.8‰) are consistent with the expected range for a pure C_4 dominated diets in open grassland vegetation. In contrast, the $\delta^{13}C$ values of cf. Palaeoloxodon namadicus from the Tanrung Formation (-14.9 to -13.8‰) and the cave deposit of Liang Bulu

Bettue (-13.6‰), as well as the single Celebochoerus heekereni individual from Talepu (-13.5‰) are all indicative of C_3 browsers in a dense vegetated habitat.

In accordance with the high $\delta^{13}C$ values of Stegodon sp. B, their $\delta^{18}O$ values (-6.4 to -3.2‰) also correspond with a higher range compared to the $\delta^{18}O$ values of cf. Palaeoloxodon namadicus (between -7.5 and -5.6‰ for individuals from the Tanrung Formation and -6.5‰ for the individual from LBB) and C. heekereni (-5.7‰). With regard to the dietary preferences of the two groups, significant differences occur between individuals of the grazer Stegodon sp. B and the browser Palaeoloxodon (Kruskal-Wallis test p =0.0054, Mann-Whitney test Benferroni corrected p = 0.0068, Table 5.2D). Although the $\delta^{18}O$ values of grazer and browser taxa can be roughly separated in lower and higher ranges, apparently both groups are statistically indistinguishable (p = 0.08875, Kruskal-Wallis test).

5.4.1.4 Pleistocene Luzon

Within the Pleistocene fauna of Luzon (Fig 5.11D, Table 5.1), the $\delta^{13}C$ value of dwarf Stegodon sp. (-6.2‰), the $\delta^{13}C$ values of two individuals of Elephas sp. (-3.6‰ and -1.1‰, respectively) correspond with the expected range for a mixed C_3-C_4 feeder and C_4 grazer, while the $\delta^{13}C$ value Stegodon cf. luzonensis (-0.0‰) suggest a predominant C_4 diet. In general, their diet suggests a diverse amount of C_4 plant consumption. The individual $\delta^{18}O$ values of all samples from Luzon (-7.2 to -4.0‰) are linearly correlated with their $\delta^{13}C$ values. The $\delta^{18}O$ value of dwarf Stegodon sp. (-7.2‰), which presumably from older horizon, is the lowest among all specimens, suggesting a more humid condition. Although their $\delta^{13}C$ values of the two Elephas sp. are higher than Stegodon cf. luzonensis, their $\delta^{18}O$ values are higher. However, the $\delta^{18}O$ values of Elephas sp. and Stegodon cf. luzonensis suggest a dry condition at some point during the Middle Pleistocene. Statistical analysis cannot be applied for this assemblage due to the small sample size.

5.4.2 Temporal variation in feeding ecology of analysed taxa

Although the results of the isotopic measurements of species/taxa within the faunal assemblages has been mentioned in the previous sections, a qualitative and statistical analysis for each species/taxa group from successive units/stages is provided in this section. This analysis (Table 5.1B and 5.2.2) was performed to explore temporal changes in feeding palaeoecology for each taxon, except for Luzon, for which the sample was too small to draw meaningful conclusions.

5.4.2.1 Stegoloxodon celebensis

The Stegoloxodon celebensis samples that are derived from the Sompe and Lonrong localities (Subunit A) are analysed separately, because of a suspected difference in age, where Lonrong is supposedly younger than Sompe, since only the lower part of the Subunit A exposed at Sompe (van den Bergh, 1999). These specimens are divided into three groups: Sompe (base Subunit A), Lonrong (top Subunit A) and other localities (Subunit B, Figure 5.12A). The individual $\delta^{13}C$ values of the Sompe (-13.3 to 0.8‰) and Lonrong (-14.1 to 1.3‰) groups plotted in expected range for all types of diet and habitats. Meanwhile, only C_3 browsers and a C_4 grazer are present in the Lakibong population (ranges between -14.9 and 0.9‰), and mixed feeder individuals are not present among the analysed samples. Moreover, there is no significant difference in the $\delta^{13}C$ values among these populations ($p = 0.51$, Kruskal-Wallis test). However, a shift to more negative values in the younger age sample is observed in the $\delta^{13}C$ values. The $\delta^{18}O$ values of all samples occupy a narrow range between -6.1 and -3.3‰, which is relatively higher compared to other Elephantoidea taxa and only significantly lower than Celebochoerus heekereni (Mann-Whitney test Benferroni corrected $p = 0.0079$). There is no significant difference for $\delta^{18}O$ values among different age groups of Sl. celebensis ($p = 0.0736$, Kruskal-Wallis test).

5.4.2.2 Stegodon sompoensis

The $\delta^{13}C$ and $\delta^{18}O$ values of Stegodon sompoensis (Figure 5.12B) from the Subunit B population (mixed feeder) are slightly more positive than those from the Subunit A

population (C_3, mixed C_3-C_4 and C_4 feeders). However, both $\delta^{13}C$ and $\delta^{18}O$ values of Subunit A are not significantly different from the Subunit B population (Kruskal-Wallis test p values for $\delta^{13}C$ = 0.3545 and $\delta^{18}O$ = 0.7558). The $\delta^{13}C$ values of S. sompoensis are significantly lower compared to Stegodon sp. B (Mann-Whitney test Benferroni corrected p = 0.0101) and Celebochoerus heekereni (Mann-Whitney test Benferroni corrected p = 0.0150), but significantly higher than cf. Palaeoloxodon (Mann-Whitney test Benferroni corrected p = 0.0039). The $\delta^{18}O$ values are only significantly lower than C. heekereni (Mann-Whitney test Benferroni corrected p = 0.0263), but statistically indistinguishable from other taxa.

5.4.2.3 Stegodon sp. B

The $\delta^{13}C$ values of Stegodon sp. B (Figure 5.12C, Table 5.1) suggest that their diet shifted from mixed C_3-C_4 and C_4-dominated in the Walanae Fauna to a pure C_4 diet in the Tanrung Fauna. The ranges of $\delta^{13}C$ values for both faunas suggest that the feeding habitat of this species is open vegetation. Only the $\delta^{13}C$ values show an increase between Walanae and Tanrung faunas, while the $\delta^{18}O$ values remain similar. However, there is no significant difference for the $\delta^{13}C$ and $\delta^{18}O$ values (p for $\delta^{13}C$ = 0.3168, p for $\delta^{18}O$ = 0.841, Kruskal-Wallis test) between both faunas. The $\delta^{13}C$ values of Stegodon sp. B are significantly higher than Stegodon sompoensis and cf. Palaeoloxodon namadicus, while the $\delta^{18}O$ values are only significantly lower than Celebochoerus heekereni but relatively similar with other taxa (Table 5.2.2A). In particular, the $\delta^{13}C$ value of the Sangihe individual is among the highest, yet its $\delta^{18}O$ value is the lowest among all analysed Stegodon sp. B. As shown in Figure 5.11C, the $\delta^{18}O$ values of Stegodon sp. B from the Tanrung Fauna increase as the increasing of the $\delta^{13}C$ values. However a positive correlation between $\delta^{13}C$ and $\delta^{18}O$ values is statistically unreliable (Regression analysis, R square = 0.157, F = 0.33, P = 7.77E-6).

5.4.2.4 cf. Palaeoloxodon namadicus

The cf. Palaeoloxodon namadicus from Tanrung and Liang Bulu Bettue is the only taxon that is restricted to a C_3-dominated diet, and foraging in the expected range of closed canopy forest. Individuals for both sites do not show any difference in their

isotopic values. In general, the $\delta^{18}O$ values of cf. Palaeoloxodon namadicus are also relatively lower compared to other species found in Sulawesi, but it is statistically indistinguishable from other taxa.

5.4.2.5 Celebochoerus heekereni

The $\delta^{13}C$ values suggest that all individuals from Subunit A and B (Figure 5.12D) were preferred C_4 feeders or consumed small animals that feed on C_4 plants in an open grassland. The $\delta^{13}C$ and $\delta^{18}O$ values of populations from Subunit A and B are statistically indistinguishable (p for $\delta^{13}C$ and $\delta^{18}O$ are both 0.8501, Kruskal-Wallis test), suggesting that the feeding preference of C. heekerenii did not change from the Early Pleistocene to Middle Pleistocene. In contrast, the youngest Celebochoerus heekereni specimen excavated from Talepu suggests a significant change to a C_3 dominated diet. In comparison with other analysed taxa, the $\delta^{13}C$ values of C. heekereni Subunit A, and B, in general, are higher than for other taxa, but only statistically significant for S. sompoensis, cf. Palaeoloxodon namadicus, and Elephas sp., while their $\delta^{18}O$ values are significantly higher than for Stegoloxodon celebensis and Stegodon sp. B (Mann-Whitney test Benferroni corrected p values in Table 5.2.2A).

5.5 Discussion

The results of stable isotope analyses of the Walanae Fauna from Subunit A and B of the Beru member suggest that during the earliest inhabitation of Sulawesi by terrestrial mammals, the habitats were covered by heterogeneous vegetation types, from closed canopy forest and woodlands dominated by C_3 plants to mixed C_3-C_4 and C_4-dominated grassland. As mentioned before, the isotopic values of Stegoloxodon celebensis samples are roughly divided into two clusters: C_3-dominated diet and mixed-C_4 dominated diet. Since the fossils from Subunit A of the Beru Member are derived from multiple fossil layers and might cover a large time span of possibly more than 1 Ma with a poor temporal resolution, the wide range of vegetation types might have existed during the entire period covered by these samples or possibly depict an accumulation of samples from several periods with different climatic conditions (glacial versus interglacial).

Since the palaeogeography of the area was a deltaic environment throughout the Early Pleistocene, the transgression and regression transitions due to sea level fluctuations (Bintanja et al., 2005) might be taken to correspond with glacial and interglacial conditions during the Quaternary, the glacial periods corresponding with drier conditions and here forcing the Proboscidea to shift to a more C_4 dominated diet. It is possible that at sea-level high stands, shorelines extended inland and wetland estuarine/brackish or lowland forest environment prevailed and C_3-dominated vegetation was more prevalent. In contrast, more extensive coastal plains were exposed during periods of lower sea-level during glacial cycles, thus increasing land area with expansion of C_4 plants. In contrast to the wide range of Proboscidean diet, Celebochoerus heekereni in this assemblage are consistent with C_4-dominated diet. As most C. heekereni fossils analysed in this study were surface collected, it is difficult to confirm whether these fossils originated from the same fossil layer (and lived during the same age/climatic condition) or rather covered several different ages. Nevertheless, the specific diet of C. heekereni indicates that open C_4-dominated vegetation type present on the island, and C. heekereni were consistent with the grassy diet, while Proboscidea shifted between a C_3-dominated to a C_4-dominated diet.

Notwithstanding the repeated transitions of habitat during the time span of the Walanae Fauna, both Stegoloxodon celebensis and Stegodon sompoensis show that they are generally flexible in their feeding behaviour. Throughout their occurrence, their $\delta^{13}C$ values are distributed over all diet types, suggesting that they were well-adapted to vegetation transitions. With an assumption that Sl. celebensis and S. sompoensis co-existed during the same period, the data suggest that diet segregation between both taxa did not occur and that both species potentially shared the same habitat. However, the conclusion drawn based on this assumption is rather tentative, as all specimens were treated as representing a single time unit. The lack of intermediate $\delta^{13}C$ apatite values between -6 and -11‰ in Sl. celebensis samples is intriguing, especially given the tighter ranges in S. sompoensis and C. heekereni. It is possible that some age ranges when the transition from C_3-dominated to C_4-dominated diet (or the other way around) occurred were not covered by the samples analysed in this study.

Celebochoerus, supposedly is an omnivore like most suids, andtheir carbon isotope ranges are expected to be different from a large-sized herbivore. Omnivores, including

the Suidae, consuming C_4 plants and small animals in C_4 habitats are expected to have $\delta^{13}C$ apatite values above -6‰ and in C_3 habitats below -12‰ (Cerling et al., 1997a, 1999, MacFadden et al., 1999, Passey et al., 2002, Feranec et al., 2007). However, Celebochoerus heekereni was exclusively adapted to a grassy diet and seems to have been less flexible in its choice of food, suggesting that this species was an open vegetation dweller rather than a forest dwelling species. The comparatively high $\delta^{13}C$ values of C. heekereni are possibly a result of consumption of roots and bulbs of grassy plants. The diet of the C. heekereni population from Subunit B does not seem to change with time. It is interesting to note that the African warthog (Phacochoerus africanus), which is the only living Suids that is specialized in feeding on grasses (Treydte et al., 2006), has enlarged upper canines very similar to those of Celebochoerus. Although these both taxa are not closely related, it is possible that the enlarged upper canines served a similar function and are the result of parallel evolution (Herring, 1972, Harris and White, 1979). In both the living and the extinct species both females and males had enlarged upper canines (Hooijer, 1948a, Herring, 1972, Treydte et al., 2006). The enlarged upper canine of warthog functions mainly to dig up the roots and bulbs of C_4 plants that are more nutritious than the leaves (Herring, 1972, Chen et al., 2008). Unlike Phacochoerus, the dentition of Celebochoerus does not show an increase in the size of the M3 as an adaptation to a grassy diet.

The variability of the feeding ecology of the analysed taxa suggests niche segregations of plant diet and habitat did occur between both Elephantoidea species combined, and C. heekereni. As their isotopic results suggest that C. heekereni was a dominant grazer, it seemed that this species was a constant grassland-dweller. During periods when grasses were preferable, Sl. Celebensis, S. sompoensis presumably shifted their diet to one that contained more grasses and thus shared the same food sources and habitat with C. heekereni. Meanwhile during periods when C_3 plants were more available, both Elephantoidea species moved to a forested habitat, while C. heekereni stayed in the open habitat. Yet again, this scenario must be treated as tentative, as the data are not sufficient to demonstrate such a niche segregation.

Interpolated from the occurrence of grazer large Stegodon domination in Java and Flores, the timing of the Tanrung Fauna is possibly earlier than 400 ka, as previously proposed by van den Bergh (1999). The timing for the onset of the Tanrung Fauna

probably corresponds with the prolonged low sea level during the Middle Pleistocene (Bintanja et al., 2005). However, a reliable radiometric dating for the Tanrung Fauna is needed to confirm this speculation. Meanwhile, the finding of fossils of this species in the Bettue Village, Central Sulawesi and Sangihe suggests that large Stegodon sp. B not only inhabited southwest Sulawesi but was also distributed northward. The distribution of large Stegodon sp. B may be a suggestion of a northward migration of Stegodon sp. B from southwest Sulawesi to Sangihe or a southward dispersal of large Stegodon from the Philippines via Sangihe.

The dietary preference cf. Palaeoloxodon namadicus (browser) derived from the Tanrung Formation and Leang Bulu Bettue (LBB) was different from Stegodon sp. B. The complementary diet preferences of Stegodon sp. B and Palaeoloxodon in the Tanrung Fauna could have been a niche separation during a relatively short interval of time between the two species, suggesting that both densely vegetated forest and grassland were available at their habitat. Alternatively, the two species did not co-occur and may have lived during different periods. In this case, the grassy feeding habitat of Stegodon sp. B probably related to dry conditions during glacial periods, while the forested feeding habitat of Palaeoloxodon possibly corresponds with prolonged wet periods. Prolonged wet periods are recorded in speleothem samples from the Maros-Pangkep karst complex. These samples show significant peaks in stalagmite growth in Sulawesi at 425–400 ka, 385–370 ka and 345–335 ka (Scroxton et al., 2014, 2016), which roughly correspond with MIS 11 and MIS 9, respectively. However, it is difficult to determine whether the two species were co-occurring in the Tanrung Fauna, since other than TR12 (which was not found in situ with Stegodon sp. B), other Palaeoloxodon fossils have not been found in situ in the Tanrung Formation (see Appendix I for information related to Palaeoloxodon findings in the Tanrung Formation). Nevertheless, it is unexpected that the form with the lower hypsodonty index (Stegodon sp. B) was a grazer, while Palaeoloxodon with its high-crowned teeth was a browser.

Although very limited, the isotopic results of the browser Celebochoerus heekereni from the youngest site, Talepu, suggests that this lineage had shifted its dietary preferences prior to the late Middle Pleistocene-Late Pleistocene. Associated with the dating data of the cave deposit, the browser C. heekereni from Talepu and cf.

Palaeoloxodon namadicus of the cave deposit probably correspond with an increase in monsoonal rainfall in southwest Sulawesi during MIS 7 (Scroxton et al., 2013, Scroxton et al., 2014) or the penultimate interglacial MIS 5 (~125 ka). Although, given the age constraints of the sequence at Talepu (between 780 and 200 ka), the C. heekereni fossils may also equate to MIS 7, 9, 11, 13, 15 and 17.

The extinction of Sl. celebensis and S. sompoensis presumably occurred during the later stages of the Early Pleistocene, since these small-sized species do not occur in the successive faunal assemblage of the Tanrung Fauna. Their extinction is presumably not caused by the change of habitat coverage due to the expansion of C_4 grasses on the island, as their stable isotope results indicate that they had versatile and flexible feeding behaviours. Moreover, Sulawesi seems to have been covered by a variety of vegetation types during the Early Pleistocene. It is more likely that their extinction is related to an incapability to compete with the larger-sized newcomers Stegodon sp. B. The occurrence of Stegodon sp. B may not only have affected the ecosystem simply as a herbivore that consumed vegetation, but due to their large size, their feeding behaviour may have had an impact on reducing canopy coverage and keeping the habitat open, as documented by recent influences of megaherbivores on vegetation (Dublin, 1995, Dublin et al., 1990, Midgley et al., 2005). Sl. celebensis and S. sompoensis were probably also cropping plant materials, yet due to their smaller size, their feeding behaviour probably did not generate an impact on vegetation as significant as the larger-sized Proboscidea. Subsequently, Stegodon sp. B individuals from the successive Tanrung Fauna, which were entirely C_4 grazer, which might be due to a prolonged aridification period, probably due to weakened monsoon strength during multiple glacial periods during the deposition of the Subunit B in the Middle Pleistocene. Or alternatively, the occurrence of large Stegodon also led to canopy clearing from the landscape and their behaviour of cropping plant in large scale kept the habitat open.

The timing and cause of extinction of the large Stegodon sp. B is more uncertain, since records of the last appearance of the species are Leang Bulu Bettue. Nevertheless, considering that the large Stegodon sp. tended to be a specialized grazer, and the fact that a change of habitat coverage into a more closed canopy vegetation, it can be concluded that the extinction of this species was probably due to their incapacity to adapt with a change of food resource. Alternatively, since the last appearance of

Stegodon sp. B and cf. Palaeoloxodon namadicus happened after the arrival of humans, as documented by the association in the sediments with the stone tools, their extinction could be related to the arrival of modern humans into the island. The role of more advanced hunting activity employed by modern humans is the likely cause of megafaunal extinction from the island, as has been proposed for other areas where the arrival of modern humans may led to the extinction of megafauna (Johnson, 2002, Wroe et al., 2004, Bulte et al., 2006, Brook et al., 2007, Pushkina and Raia, 2008, Johnson et al., 2016, Saltré et al., 2016).

In Flores and Java, where time constraints are clearer, a shift to a more grass-dominated vegetation type occurred between 1.2 Ma and 1 Ma, as recorded in shifting dietary patterns of Stegodon taxa present on these islands (Chapters 4 and 6), while C_4 vegetation remained dominant on the islands during the Middle Pleistocene. It is possible that a similar shift deduced from the Stegodon data from Sulawesi, correlates with the observed shift around 1 Ma in the aforementioned islands. The presence of the predominantly C_3 browser (Sl. celebensis) and mixed feeder (Sl. celebensis, S. sompoensis and Stegodon sp. B) individuals in the Walanae Fauna suggests that closed canopy habitats were present. Alternatively, the wide ranges in diet may reflect temporal climatic fluctuations and vegetation changes. The C_4 vegetation expansion during the Middle Pleistocene on Sulawesi appears not to have been as drastic as in Java and Flores, since grazers and browsers individuals (and mixed feeders for the Walanae Fauna) always co-occurred in all faunal assemblages, although the proportion of predominant grazers are slightly more dominant during the latest Early to Middle Pleistocene.

The feeding preferences of Palaeoloxodon cf. namadicus, as well as Elephas hysudrindicus from the Late Pleistocene sediment of Java and E. maximus from mainland SE Asia, and modern Sumatra and Java, which are all pure browsers, are quite remarkable, since these high-crowned Elephantoidea seem to have the best adapted molars for grinding tough and abrasive grasses. Similarly, Celebochoerus with its brachiodont molars appeared to be a grazer, once again showing that care must be taken in interpreting dietary preferences from tooth morphology alone (Harris and Cerling, 2002, Rivals and Semprebon, 2006, Cerling et al., 2015).

Due to the limitations of the poor stratigraphic control, and the low number of analysed samples, the interpretation of the proboscidean feeding ecology and palaeoenvironment for Luzon is highly speculative. The isotopic values of dwarf Stegodon sp. ($\delta^{13}C$ = -6.2‰, $\delta^{18}O$ = -7.2‰), which may be older than 1 Ma, suggest a mixed vegetated and humid feeding habitat. Subsequently, the $\delta^{13}C$ values of presumably younger taxa, Stegodon cf. luzonensis (-3.6 and -1.1‰) and Elephas sp. (0.0‰) suggest a mixed C_3-C_4 feeding pattern and specialized C_4 grazer individuals suggests that the Middle Pleistocene habitat of Luzon was mostly covered by open canopy biome, supposedly woodland or grassland with a considerable proportion of C_4 plants. Their $\delta^{18}O$ values (-5.2 and -4.3‰), which higher than the dwarf Stegodon sp., suggest a drier condition during the Middle Pleistocene.

The large variation of $\delta^{18}O$ in the Walanae Fauna is presumably caused by the long time frame that is covered by the sediments of Subunit A and B of the Beru Member. Therefore, the $\delta^{18}O$ interval actually represents multiple climatic changes that affect meteoric water, as well as different drinking water sources. Although statistically not significant, segregation of both $\delta^{18}O$ values between the grazer Stegodon sp. B and the browser cf. Palaeoloxodon namadicus. can still be observed in the Tanrung Fauna. This result amplifies the indication that the two species are niche-separated, either temporally or spatially. Generally, there is no significant difference in $\delta^{18}O$ values between Proboscidean species, although based on mean values of each species, it can be seen that Sl. celebensis has the highest $\delta^{18}O$ mean value, followed by S. sompoensis, Stegodon sp. B, Elephas sp. of Luzon and the lowest value is occupied by cf. Palaeoloxodon namadicus. Slight differences in the measured $\delta^{18}O$ values among proboscidean species may not only have occurred due to different climatic conditions and drinking water sources. A notable difference of measured $\delta^{18}O$ values can be recognised between Celebochoerus heekereni and all Proboscidean taxa. This difference most likely occurs because the majority of its diet consisted of food items dug from the ground (rhizomes, roots, tubers and bulbs). Celebochoerus may also have scavenged on burrowing animals that are more enriched in ^{18}O.

5.6 Conclusions

The wide range of carbon and oxygen isotope values in all analysed faunal assemblages suggests that different vegetation types provided the habitat in Sulawesi, reflecting climatic fluctuations and vegetation changes during the time span covered by the Walanae and the Tanrung Faunas. The co-occurrence of grazers, browsers and/or mixed feeders in all faunal assemblages suggests that the C_4 vegetation expansion during the late Early to Middle Pleistocene on Sulawesi did not seem to be as pronounced as in Java (Chapter 4) and Flores (Chapter 6). A more humid and closed canopy habitat seems to be prevalent during the Late Pleistocene, as represented by samples from Talepu and Liang Bulu Bettue. However, the number of samples is too limited to produce further speculation of the Late Pleistocene palaeoenvironment.

Carbon isotope data suggest that Stegoloxodon celebensis and Stegodon sompoensis were flexible feeders and were able to adapt to different niches, from closed canopy forest to open vegetation, while the diets of Stegodon sp. B, Celebochoerus heekereni and cf. Palaeoloxodon namadicus suggest that they were more specialized. Stegodon sp. B was predominantly a grazer, whereas cf. Palaeoloxodon namadicus analysed in this study shows a predominantly browsing diet. In the earlier population (Early to Middle Pleistocene), the dietary preference of C. heekereni was C_4-dominated, while the diet of a single C. heekereni individual from the Late Pleistocene (Talepu) was dominated by C_3 plants. However, due to the limited sample number, the sample from Talepu is insufficient to represent the Late Pleistocene C. heekereni population. When co-occurring in the Walanae Fauna, Sl. celebensis and S. sompoensis seem to have shared the same niches. Both species possibly shared the same niches with C. heekereni and Stegodon sp. B in the grassland only when grasses were more prevalent. In contrast, the diet separation between the grazer Stegodon sp. B and browser cf. Palaeoloxodon namadicus were more unequivocal in the Tanrung Fauna. The occurrence of Stegodon sp. B. north of the Sengkang Basin, to Sangihe, suggests a northward distribution of the species, or vice versa. The extinction of Sl. celebensis and S. sompoensis recorded around the upper part of Subunit B deposition seemingly did not occur due to a change in vegetation, but by their inability to compete with two larger immigrants Stegodon sp. B and Palaeoloxodon, whilst the extinction of Stegodon sp B and Palaeoloxodon sp. seems to correspond with the arrival of modern humans.

Additionally, the limited isotopic result of the dwarf Stegodon sp., Elephas sp. and Stegodon cf. luzonensis from the Pleistocene sediment of the Cagayan Valley gives a glimpse of a Pleistocene habitat within Luzon predominantly covered by woodland and grassland with a substantial proportion of C_4 vegetation.

Chapter 6. Lesser Sunda Islands: Flores, Timor and Sumba

6.1 Geological context

6.1.1 Geology of the LSI

The Lesser Sunda Islands (LSI) or Nusa Tenggara is a volcanic island chain situated east of Java and west of the Banda Arc (Figure 6.1). The subduction of the Australian Plate beneath the Eurasian Plate actively caused the uplift of oceanic crust, emergence of a string of volcanic and non-volcanic islands, as well as the formation of deep sea straits within the LSI (Simandjuntak and Barber, 1996, Hall, 2001). Flores is one of the islands that is volcanic and it forms part of the inner arc of the subduction complex, while Sumba and Timor are of non-volcanic origin and are part of the outer arc of the subduction system (Audley-Charles, 1981, Simandjuntak and Barber, 1996, Hall, 2011, 2012b).

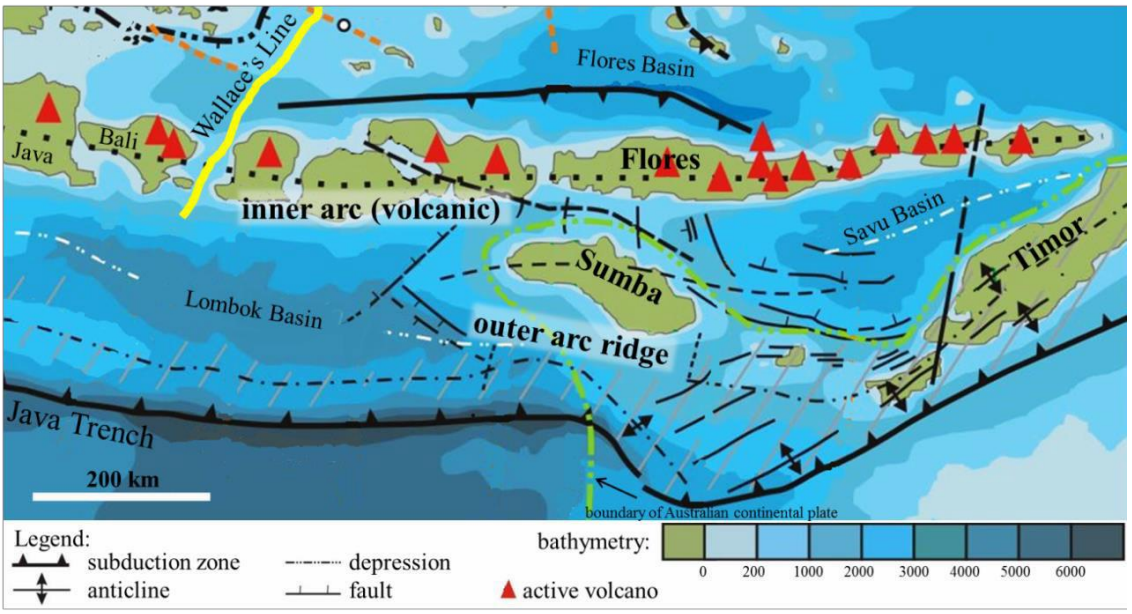

Figure 6.1 Schematic map of the Lesser Sunda Islands, showing the main tectonic units (modified after Darman, 2014).

The volcanism in the inner arc of the LSI only formed after the Early Miocene, initially as submarine volcanism (Burrett et al., 1991). Shallow-water magmatism continued in

the Pliocene-Early Pleistocene (van Bemmelen, 1949, Koesoemadinata et al., 1994, Muraoka et al., 2002), and became fully sub-aerial after the uplift of the islands since the Early Pleistocene (Muraoka et al., 2002).

The islands of the outer arc overlie the margin of the Pre-Cambrian craton that is associated with the northern margin of the Australian Plate and has been uplifted by the Australia-Eurasia collision (Hamilton, 1979, Abbott and Chamalaun, 1981, de Smet et al., 1990, Audley-Charles, 1991, Charlton et al., 1991, Charlton, 2002, Kaneko et al., 2007). The outer arc stretches between Savu and Kai, and includes Timor. The basement underlying Quaternary sediments in this area consists of a wide range of lithological formations dated between the late Palaeozoic and Neogene (Sawyer et al., 1993). Sumba represents a Mesozoic micro-continental fragment or terrane, of which the origin remains under debate (Audley-Charles, 1975, Hamilton, 1979, Norvick, 1979, Otofuji et al., 1981, Chamalaun and Sunata, 1982, Rangin et al., 1990, Simandjuntak, 1993, Wensink, 1994, Fortuin et al., 1997, Metcalfe, 1998, 2011, Abdullah et al., 2000). Sumba has occupied approximately its present position since the Miocene, but emerged above sea level only after the Early Pleistocene (Pirazzoli et al., 1993, Wensink and van Bergen, 1995, Abdullah et al., 2000, Rutherford et al., 2001).

Prior to their emergence in the Early Pleistocene, most islands of the LSI were submerged (Hall, 2013), thus the Pre-Quaternary lithology mostly consist of marine sediments (deep and shallow marine) and/or submarine volcaniclastics. Terrestrial deposition started due to further uplift of the area since the Early Pleistocene (Abbott and Chamalaun, 1981, Audley-Charles, 1981). The uplift process has been continuous since the Early Pleistocene allowing the emergence of islands and the colonization of the island by terrestrial fauna.

6.1.2 Quaternary stratigraphy of fossil vertebrate localities

6.1.2.1 Flores

From Flores, two Quaternary vertebrate fossil sites were studied: 1) a number of Early to Middle Pleistocene localities in the So'a Basin, and 2) the Late Pleistocene cave sediments from Liang Bua (Figure 6.2).

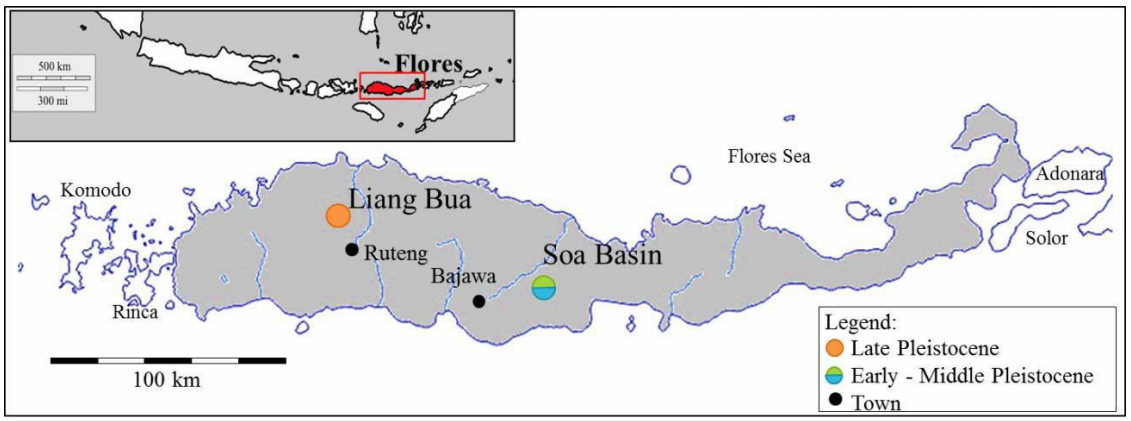

Figure 6.2 Schematic map of Flores showing the two studied Quaternary vertebrate fossil sites.

6.1.2.1.1 So'a Basin

The So'a Basin is an intramontane basin located to the northeast of Bajawa, the capital of the Ngada Regency, Central Flores. The basin is at an elevation between 300-370 m above sea level, and is surrounded by active and non-active volcanoes and drained by the Ae Sissa River and its tributaries. Fossil vertebrate remains from the So'a Basin occur in the Ola Bula Formation. At least 17 fossil localities are known, as shown in Figure 6.3. The basement of the So'a Basin consists of a >100 m thick sequence of massive volcaniclastics dominated by andesitic breccia with minor intercalations of tuffaceous siltstone, sandstone and lava flow intervals, named the Ola Kile Formation. This type of lithology was deposited as a lahar-dominated volcanic apron and does not contain any fossils. The upper part of the formation is fission track dated at 1.86 Ma (O'Sullivan et al., 2001).

The Ola Kile Formation is unconformably overlain by the Ola Bula Formation. The Ola Bula Formation represents an up to 120 m thick sequence of undistorted volcanics, fluvial and lacustrine sediments. The Ola Bula Formation is divided into three members, from bottom to top: the Tuff Member, Sandstone Member and Gero Limestone Member (O'Sullivan et al., 2001, Suminto et al., 2009). This formation contains several fossils and stone tool-bearing layers, and is the focus of this study.

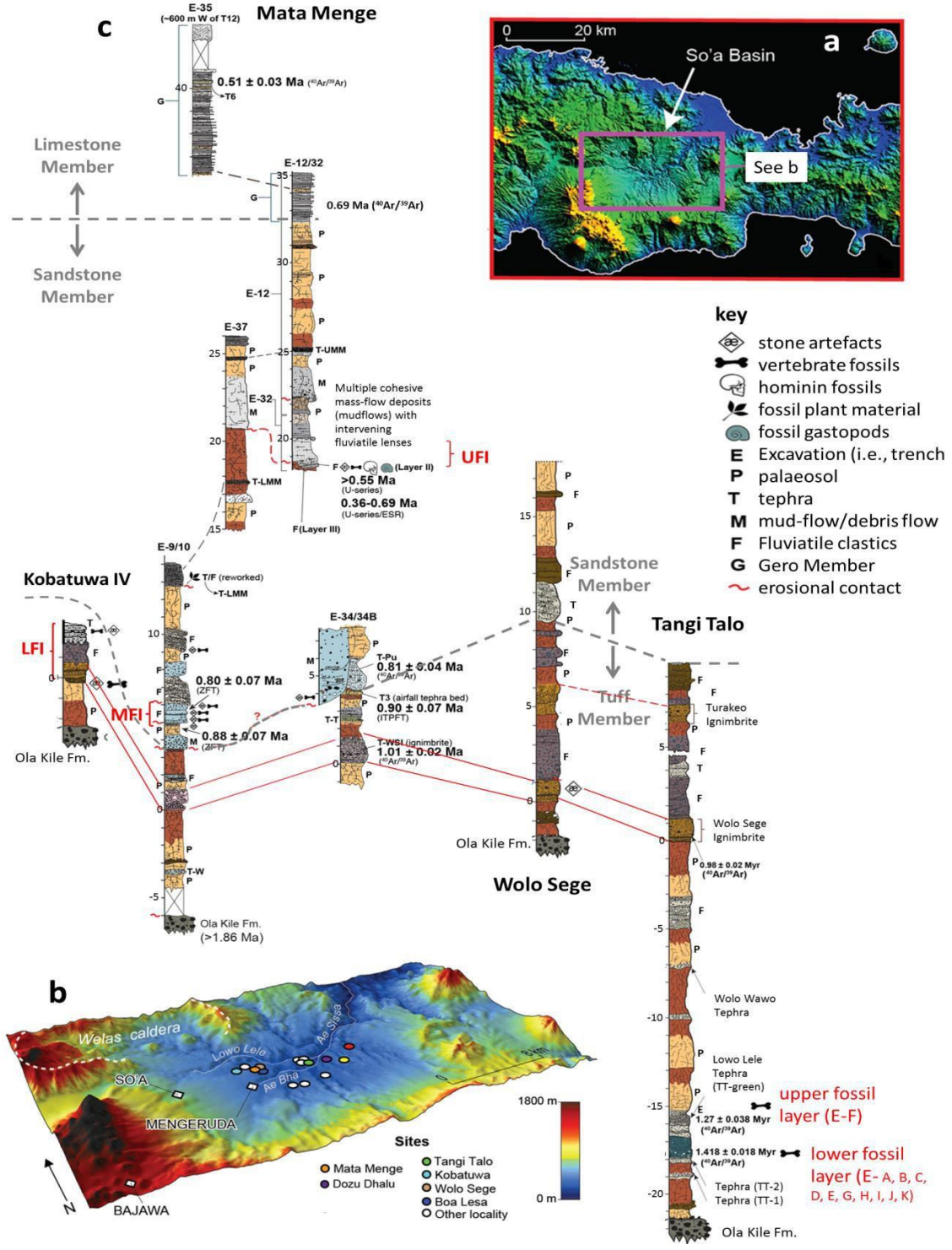

Figure 6.3 Context and chronology of the So'a Basin. **a,** location of the So'a Basin; **b**, digital elevation map of the So'a Basin, showing the location of sites mentioned in the text, **c**, Stratigraphy of key sections within the So'a Basin, showing the stratigraphic positions of silicic volcaniclastic deposits and associated faunal remains and stone artefacts, the relevant $^{40}Ar/^{39}Ar$, zircon fission-track (ZPT), isothermal plateau fission-track (ITPFT), Electron spin resonance (ESR), and U-series age determinations, lower and upper fossil layer within the Tuff Member at Tangi Talo, as well as the Lower fossil interval (LFI, at Kobatuwa), and the Middle Fossil Interval (MFI) and Upper Fossil Interval (UFI) at Mata Menge within the Sandstone Member. Sections are shown according to their real elevation; scales are in metres (modified after van den Bergh, 2014 and Brumm et al., 2016).

Tuff Member

The Tuff Member comprises prominent layers of white pumiceous volcanic tuff interbedded with tuffaceous silts, minor sand layers and conglomerate lenses. Some of the pumice layers show characteristics of ignimbritic flows. Volcaniclastics of this member are dominated by rhyolitic components, and a smaller proportion of andesitic tuffs. This member appears thick (50-60 m) in the So'a Basin depocentre near Tangi Talo (Fig. 6.3) and thins towards the west near Mata Menge (maximum 12 m at Mata Menge excavations). Massive fine-grained layers with a few large pumice fragments occur in the esst part of the basin, deposited under a lacustrine condition near the distal part of a volcanic apron (Suminto et al., 2009).

The basal part of the Tuff member can only be found in the central part of the basin. The lithology here is dominated by palaeosols, interbedded with pyroclastic airfall tuffs and clay-rich lahar deposits. At Tangi Talo, two fossil layers occur in this member. The two fossil layers were excavated during fieldwork in 1994, 1997, and 2012 - 2014. The lower fossil layer (Figure 6.3) was exposed in a series of 11 excavations, indicated with the letters A-E and G-L, and located at the southern side of a hill. The fossil-bearing layer represents a mudflow rich in pumice clasts with undulating basal contact and appears to have filled a pre-existing depression with well-developed palaeosols. The upper fossil layer (Excavation F, excavated in 2012) is located to the north of the same hill, and represents a small muddy pit filled with tuffaceous mud. The upper part of the Tuff Member consists predominantly of palaeosols alternating with cross stratified tuffaceous sandstones and conglomerates. Finer grained clastics comprise interbedded silty palaeosols, pyroclastic airfalls, tuffaceous sandstone and siltstones (Suminto et al., 2009, van den Bergh, 2014).

A highly distinctive ignimbrite layer, which was formed by a pyroclastic density current and known as the Wolo Sege Ignimbrite (WSI), appears in the upper part of the Tuff Member. The WSI, along with other marker beds have been identified at a number of sites within the So'a Basin by Brent Alloway and Ruly Setiawan. As this particular layer can be observed in many areas, it has become an important stratigraphic marker for correlating stratigraphic sections throughout the So'a Basin. The $^{40}Ar/^{39}Ar$ dating of hornblende from the WSI indicates an age of 1.01 ± 0.02 Ma (Brumm et al., 2010).

Previously, the age of the fossil-bearing layer at Tangi Talo was thought to be around 900 ka, based on fission track analysis (Morwood et al., 1998, O'Sullivan et al., 2001). However, in 2012, the WSI was recognized to occur at stratigraphically 18 m above the fossil-bearing layer at Tangi Talo, implying that one of the dates, either the age of the WSI or of the fossil layer at Tangi Talo should be wrong. Hence, during the following years, an attempt to obtain robust age for Tangi Talo was pursued. New $^{40}Ar/^{39}Ar$ dating results showed that the age of the Lowo Lele Tephra (LWL), positioned above the Tangi Talo fossil layers but below the WSI, had an age of 1.27 ± 0.038 Ma. Dating result of a pyroclastic density current layer covering the lower fossil-bearing layer has provided an age of 1.418 ± 0.018 Ma (Storey, unpublished data). The palaeomagnetic analysis supported these dating results, as it shows that the Tuffaceous Member has a reverse polarity below the WSI, associated with the Matuyama Chron. These results indicate that the lower fossil-bearing layer at Tangi Talo is half a million years older than initially thought.

Sandstone Member

The Sandstone Member comprises alternation of pyroclastic airfall tephras, clay-rich lahars and associated mass-flow deposits and fluvio-volcaniclastics, interspersed by well-developed palaeosols and pedogenically altered fine-grained fluviatile deposits. The volcaniclastics of this member are dominated by andesitic components with a few basaltic interbeds. Cross bedding appears in the fluvio-volcaniclastic sandstones and pebbly sandstone layers. This member was deposited predominantly under fluvial influence. The deposits were incised by erosional gullies during periods without volcanic activity, but became sites of rapid accretion following major volcanic influxes (Brumm et al., 2016, Appendix III). Two zircon fission track (ZFT) samples taken from just below and near the top of the ~2 m thick main fossil-bearing interval at Mata Menge have ages of 0.88 ± 0.07 Ma and 0.80 ± 0.07 Ma, respectively (O'Sullivan et al., 2001). The Isothermal Plateau Fission-Track (ITPFT) dating of glass shards of a tephra marker (T3) and a $^{40}Ar/^{39}Ar$ of hornblende from the Pu Maso Ignimbrite (T-Pu), $^{40}Ar/^{39}Ar$ of hornblende identified at several So'a Basin localities, including at Mata

Menge (Excavation 34), resulted in weighted means ages of 0.90 ± 0.07 Ma and 0.81 ± 0.04 Ma, respectively (Fig. 6.3), which is consistent with the earlier ZFT ages.

Brumm et al. (2016) also dated a fossil-bearing interval containing hominin fossils at Mata Menge (Excavation 32, excavated between 2012 and 2016). This excavation is located ±12.5 m higher in the stratigraphic sequence than the 0.8 Ma old ZFT layer. Based on U-series dating of the hominin tooth root and combined U-series/ESR dating of Stegodon molars from this fossil-bearing interval, as well as $^{40}Ar/^{39}Ar$ dating on tephra layers above the fossil-bearing interval, the age of the hominin-bearing layer (Fig. 6.3) is concluded to be ~0.70 Ma old (Brumm et al., 2016).

Multiple fossil-bearing layers can be found in the Sandstone Member. Based on their stratigraphic position, these layers can be grouped into three fossil-bearing intervals: lower, middle and upper (Fig. 6.3). The lower fossil-bearing interval (subsequently referred as LFI), includes all fossil layers between the WSI and T3, which bracketed the age of this interval at between 1.01 and 0.9 Ma. The lithology of this interval is actually included in the Tuff Member, but for practical purposes, the explanation of this interval is included in this section. All samples of this interval originate from five fossiliferous layers (Layer J to F, Figure 6.4) exposed in excavations in Kobatuwa. Kobatuwa is the most northwestern locality at the tuff member is condensed here to a few meters-thick. Eleven distinctive layers (from bottom to top, Layer K to A) were recognized during the excavation. These layers directly overlie the Ola Kile Formation. Lithological description of these layers is presented in Figure 6.4.

The Middle Fossil-bearing Interval (MFI) includes all fossil layers between the lower ZFT layer, or associated T3 and T-Pu (Fig 6.3), giving an age limit of between 0.9 and 0.8 Ma. Samples included in this interval were excavated from the main fossil layer at the Dozu Dhalu, Boa Leza localities, as well as Excavation 14, 21, 22, 23, 24, 25, 26, 30 and 31 at Mata Menge. The lithology of this fossil-bearing interval is dominated by fine to coarse-grained fluvial sediments, mass-flow associated deposits, silty tuffs and palaeosols. Abundant cross-bedding structures, erosional scours and silty clay drapes and lenses occur in this fluvial interval, suggesting a strong fluvial influence.

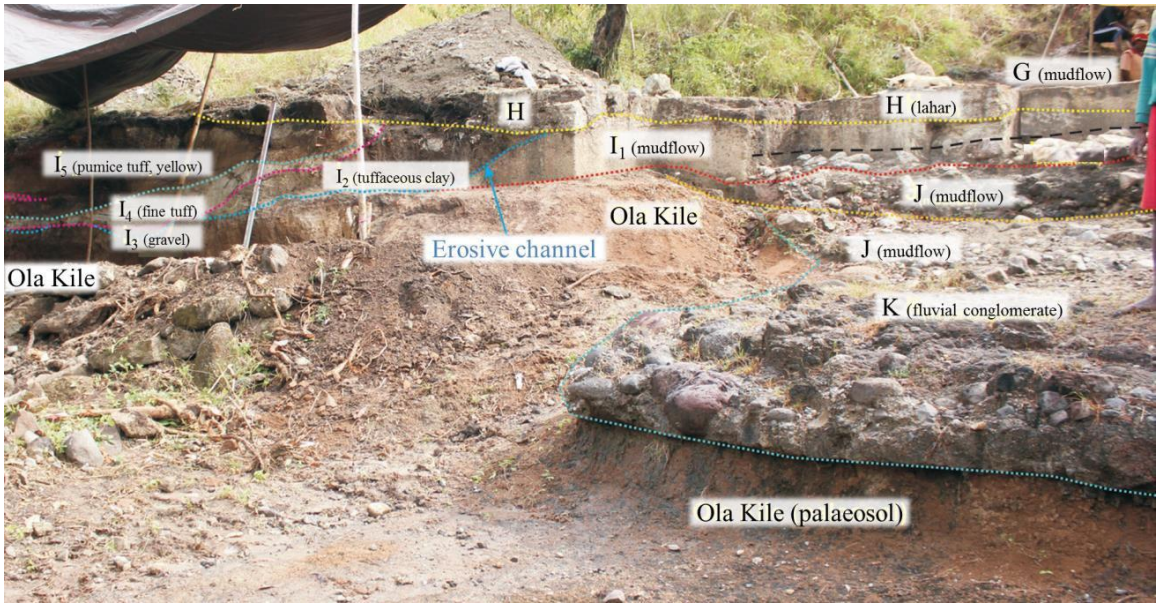

Figure 6.4 Stratigraphy of Kobatuwa, as developed in the south wall of excavation KI-II (Photo by G. van den Bergh). From bottom to top: Layer K is a 2-m thick poorly-sorted fluvial conglomerate lens with rounded pebbles, Stegodon florensis fossil found in this layer; Layer J is a mudflow deposit, characterized by well-sorted and massive brown sandy silt, with a few fossil; Layer I (I_1 to I_5) is a series of fine-grained deposits, mainly consisting tuffaceous clayey silt with rounded polymict boulders floating in matrix with a few fossil fragments. I_4 is a reworked pumice tuff corresponding in composition with the WSI; Layer H and G are mudflow deposits comprise very poorly sorted tuffaceous conglomerate with abundant pumice clasts, fine sandy silt matrix and fossil content. Both layers are separated by a sharp undulous non-erosive contact and distinguished by their colours (Layer H is light grey while Layer G is brownish green); Layer F (not shown in the picture) is a mudflow deposit consisting of well-sorted massive grey clayey tuffaceous sand with abundant wood and plant fragments.

The Upper Fossil-bearing Interval (UFI) has so far only been exposed at Mata Menge in Excavation 32 A-F, which corresponds with the hominin fossil-bearing layers (Fig 6.3). The lithology of this interval consists of a series of 2.5 m thick massive tuffaceous mudflows (Layer I in Brumm et al., 2016), overlying two distinct sandstone units (Unit II and III in Brumm et al., 2016). The upper sandstone unit (Unit II) has a maximum thickness of 30 cm. The lower unit (Unit III) was excavated up to a maximum of 40 cm thick, yet the base of this layer was not exposed. Contacts between units are erosional. The characteristics of the sediments from this interval suggest that these sediments were deposited in a small stream valley.

Gero Limestone Member and sub-recent sediments

The Sandstone Member is conformably overlain by the Gero Limestone Member (GLM), which reaches up to 14 m in thickness. This member consists of thin-bedded micritic freshwater limestones intercalated with basaltic crystal-rich airfall tuffs, and siltstones. Locally, the limestones show parallel laminations and may contain freshwater algae (Oogonia) and diatoms. The top of some limestone layers show polygonal shrinkage cracks, indicating fluctuating water levels. In the northern part of the basin, the tuff and sandstones members are commonly absent, and the Gero Limestone unconformably overlies the Ola Kile Formation. Along the western basin margin, the limestone member is thinner and mostly alternating with fine-grained clastics, as well as tuff layers. A $^{40}Ar/^{39}Ar$ date on tephra layer T6 from the top of the GLM has an age of 0.51 ± 0.03 Ma. No mammalian fossil has so far been found in this member.

The Ola Bula Formation is unconformably overlain by sub-recent volcanic products and alluvium along the western, southern and eastern basin margins. The subrecent volcanics primarily consists of andesitic and basaltic lavas interbedded with sandstone and conglomerate layers with volcanic fragments originating from the surrounding volcanoes (Suminto et al., 2009).

6.1.2.1.2 Liang Bua

Liang Bua Cave is located approximately 13 km north-west of Ruteng, the capital of the Manggarai Regency. This cave started to develop by rapid karstification processes and tectonic uplift ~400 ka (Morwood et al., 2004, Westaway et al., 2009b) and was filled by sediment since 200 ka (Westaway et al., 2009b). The cave sediments have yielded numerous vertebrate fossils of a limited number of genera from the Late Pleistocene and Holocene, and most importantly, a diminutive hominin species, Homo floresiensis (Brown et al., 2004, Morwood et al., 2004).

Within the cave, so far 27 sectors have been excavated between 2001 and 2014, varying in size between 2 x 2 and 3 x 3 m^2 surface areas. The different sectors were excavated to various depths down to bedrock, with a maximum depth of approximately 11 m. The

sediments can be divided into two sequences, separated by an erosional surface (Fig. 6.5). The lower section of the cave sediment consists of a sequence of several alternating layers of clayey silt that were produced by the weathering of limestone, flowstones, conglomerate, cross bedded lenses, and cave-wall debris layers. A sequence of tephra layers (T1-T5) occur at the top of this sequence. An erosional phase sets in after the T1-T5 layers were deposited, and erosional contact locally incises up to 5 m into the sequence. This erosional surface is unconformably overlain by the upper sequence, which consists of alternating clayey silt and sandy silt layers (Fig. 6.5). Fragments of cave wall debris are commonly found in the silt. The deposition of the upper sequence is interrupted by three tephra layers (T6-T8; Sutikna et al., 2016).

The $^{40}Ar/^{39}Ar$ dating of hornblende crystals from T1 gave an age range between 103 and 55 ka, which is consistent with the luminescence and $^{234}U/^{230}Th$ ages for the underlying tephra layers. Sediments between T2 and T3 in Sector XXI yielded a weighted mean IRSL age of 63 ± 6 ka from two samples and a TL age of 58 ± 13 ka. Five samples taken from interbedded flowstones and a small stalagmite in the same Sector gave $^{234}U/^{230}Th$ ages of between 66.1 ± 0.3 and 54.4 ± 0.3 ka, while a flowstone immediately underlying T3 in Sector XII, near the cave centre, was dated to 49.6 ± 0.5 ka.

The weighted mean $^{234}U/^{230}Th$ age of three flowstone samples from the coarse gravel layer above T4 is at 46.6 ± 0.5 ka, and charcoal from immediately above the upper surface of T5 yielded a ^{14}C age of ~44 ka cal. BP. The majority of Pleistocene fauna fossils, including Homo floresiensis, Stegodon florensis subsp. insularis, several small-mammals and avian taxa, were recovered from multiple siltstone layers (Meijer and Due, 2010, Meijer et al., 2013, Meijer et al., 2010, van den Bergh et al., 2008, van den Bergh et al., 2009, van den Hoek Ostende et al., 2006), right below T1. Stegodon florensis is found just below T3, previously referred as the "black tuff" layer. The radiocarbon dating of charcoal samples obtained from layers overlying the erosional surface, giving an age range between 19.2 and 13 ka cal. BP (Sutikna et al., 2016).

The S. florensis insularis samples analysed in this study were mostly excavated from the H. floresiensis fossil layer (indicated as LB1, LB4, LB6 and LB8 in Figure 6.5), below the T1 Layer. Only one sample was recovered from the T3 Layer.

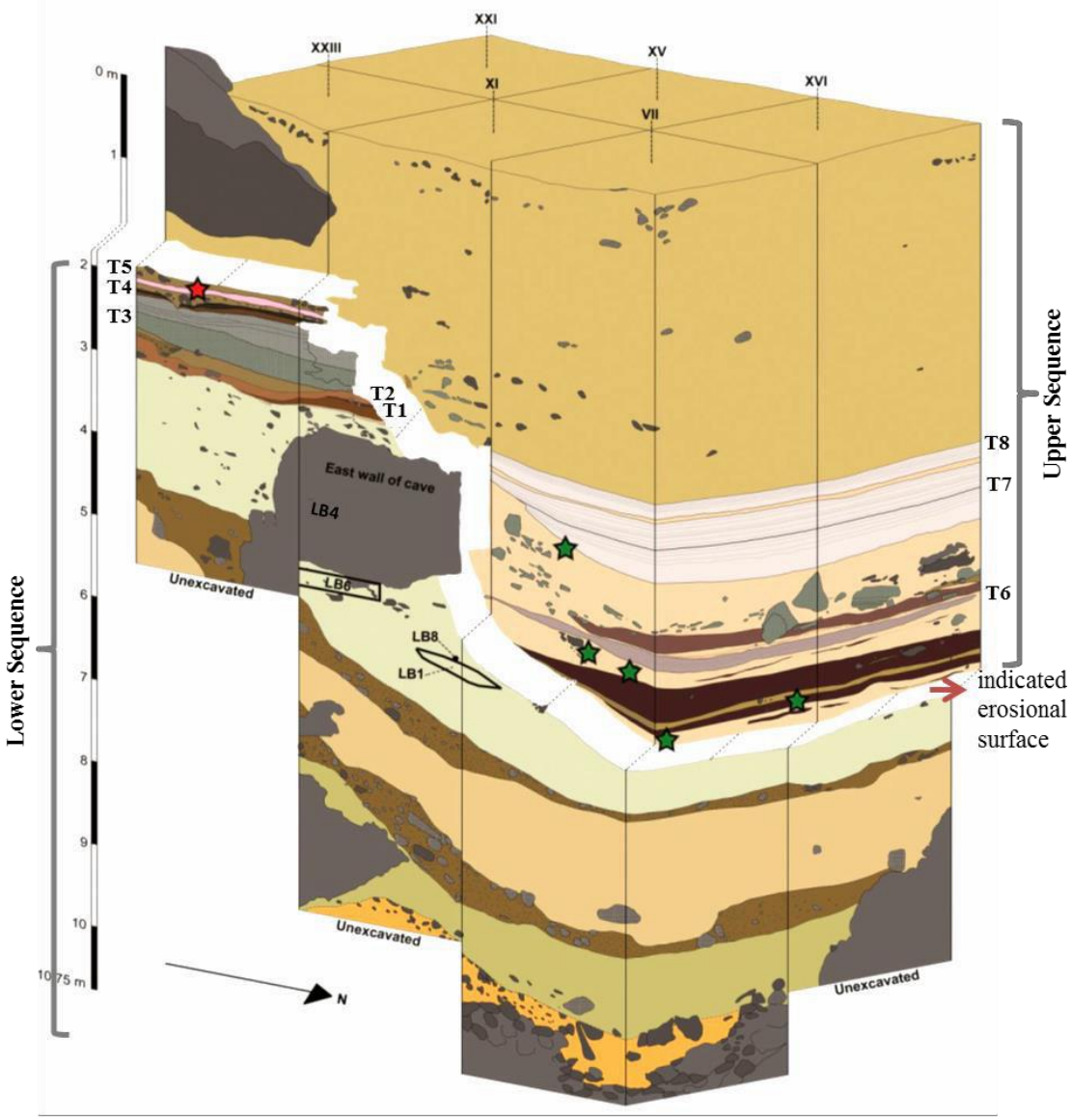

Figure 6.5 Stratigraphy of excavated sectors near the eastern wall of the cave (Sutikna et al., 2016), showing the position of multiple specimens of Homo floresiensis (LB1, LB4, LB6 and LB8). The sediments containing H. floresiensis and Stegodon florensis insularis analysed in this study directly underlie a sequence of five tephras (T1–T5). A single S. f. insularis molar sample originates from T3 and interstratified deposits. The charcoal sample denoted by the red star at ~2 m depth indicates remnant deposits form a pedestal, which is dated to ~46 ka cal. bp. The overlying section represents deposits (including three additional tephras, T6–T8) that rest unconformably on the steeply sloping erosional surface of the pedestal. The green stars mark the respective locations (from top to bottom) of the charcoal samples which were previously used erroneously to infer the age of LB1 (Morwood et al., 2004, Morwood et al., 2005, Roberts et al., 2009).

6.1.2.2 Timor

The Quaternary fossil-bearing sequence in Timor is located in the intramontane Atambua Basin (Fig. 6.6). The basin emerged and was raised to altitudes of 1500 m

above sea-level due to rapid post-collisional uplift phases of Timor, which took place during the Early Pleistocene (2.2 to 2 Ma) and at 0.2 Ma (de Smet et al., 1990). The analysed fossils from Timor were recovered from the Noele Formation and unconformably overlying alluvial terraces.

6.1.2.2.1 Noele Formation

In the Atambua Basin, the basal unit of the Noele Formation comprises a minimum 100 m-thick sequence of blue clays and marls containing molluscs that are of shallow marine origin. The marl interval alternates with several coarse-grained conglomeratic mass-flow deposits, grading upwards into shallow marine marls locally interbedded with in situ coral. The foraminifer assemblage of the marine clays and the marine interval of the Central Noele Basin further south indicates an age corresponding with biozones N18-N22, Pliocene-Pleistocene (Rosidi et al., 1979). A coral sample from the top of the marine interval of the Noele Formation provided a minimum U-Th age of 500 ka (van den Bergh, pers. comm.).

The upper unit of the Noele Formation consists of a ~600 m thick sequence (Figure 6.7) of terrestrial origin. The sequence comprises predominantly fine-grained deposits, mostly consisting of clayey silts and minor intervals of laminated clays. Poorly preserved mollusc remains and plant fossils occur in some clayey intervals. Palaeosols and caliche concretions commonly occur in the fine-grained deposits. The deposits alternate with sheets and ribbons of conglomerate up to 4 m thick. The conglomerate clasts are dominated by sub-angular to sub-rounded pebbles and consist almost entirely of green-coloured ultramafic and metamorphic fragments, which have been derived from the Atapupu Peridotite Complex to the north. The sedimentary structures indicate that the conglomerates were deposited in a small fluviatile channel, entering a swamp or lake environment. In situ and surface-collected vertebrate remains invariably originate from such conglomerate layers at various stratigraphic levels (van den Bergh, 2007, van den Bergh et al., in prep.). The base of the Noele Fm. is not exposed but the upper fluvio-lacustrine interval has been folded since its deposition. The folding, uplift and erosion of the formation corresponds with the second uplift phase that took place during the last 0.2 Ma (de Smet et al., 1990).

Deposition of the upper part of the Noele Formation was occasionally interrupted by the accumulation of white vitreous tuff. Three tuff layers occur in the upper part of the Noele Formation, named as the Lower Tuff, Raebia Middle Tuff and Raebia Upper Tuff (Figure 6.6e). A U-Th-Sm/He age on apatite crystals contained in the Middle Tuff was dated at 810 ± 50 ka. A fossil-bearing conglomerate containing in situ vertebrate fossils is stratigraphically located above the Middle Tuff. This layer was excavated (Excavation II) in 2007 (van den Bergh, 2007).

6.1.2.2.2 Alluvial terraces

The Noele Formation in the Atambua Basin is unconformably overlain by horizontal alluvial deposits with an erosional base. Alluvial terraces developed in the Atambua Basin likely formed during pulsed tectonic uplift at 0.2 Ma, triggering river downcutting and the abandonment of older floodplains.

Based on their elevation and lithology, at least three alluvial terraces can be distinguished in the study area (van den Bergh et al., 2007). The lithology of the terraces comprises clastic alluvial deposits, such as conglomerates intercalated with cross-bedded sands and silts that have been deposited in a braided river system. The silts contain abundant caliche concretions and grey mottling, suggesting relatively dry conditions.

The highest and oldest terrace is developed near Hula Menahu village, and was named as the Hulamenahu High Terrace Complex (HHTC), with a maximum thickness of the terrace fill of 40 m. This terrace, reaching an elevation between 390 and 414 m above sea-level is heavily dissected and crops out in the southeastern part of the study area (Figure 6.6). It consists of consolidated cross-bedded pebbly sandstones, conglomerate lenses, and minor siltstones. Calcite cemented concretions and lenses are developed in the fluvial deposits. An OSL dating sample was taken from this terrace, which yielded an age of 66 ± 5 ka (van den Bergh et al., in prep).

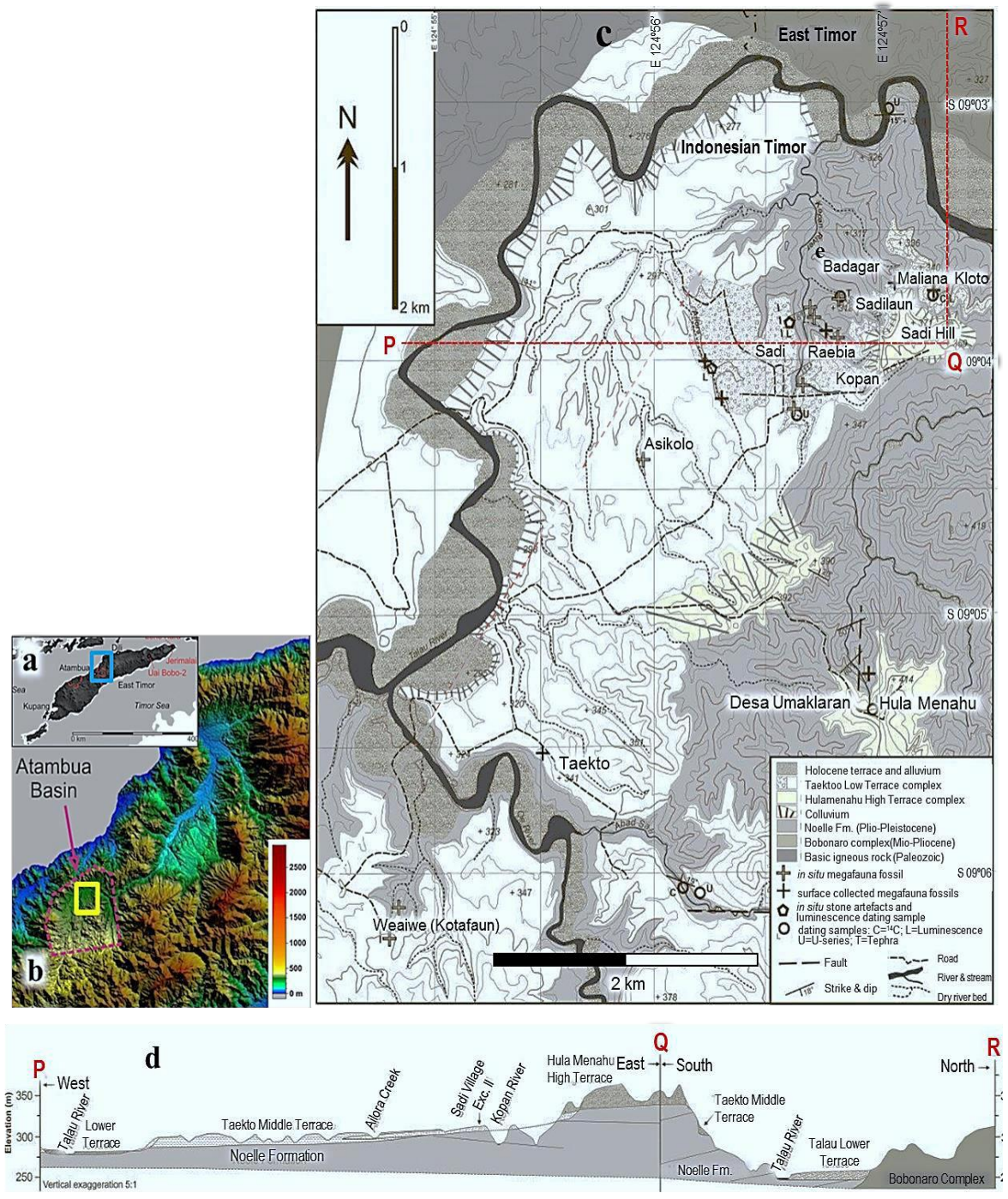

Figure 6.6 Context and stratigraphy of the Atambua Basin, Timor: **a,** The Island of Timor, with the blue rectangle enclosing the area on the border between Indonesian Timor and Timor l'Este shown in: **b,** digital elevation map of the Atambua Basin (enclosed by red dashed line) and adjacent areas, yellow rectangle encloses the study area in the Atambua Basin shown in: **c,** detailed geological map of studied area; dashed red lines (P-Q-R) indicate the profile shown in: **d,** cross section of the studied area, showing the distribution of the Quaternary Noele Formation and alluvial terraces (vertical exaggeration 5:1)**.**

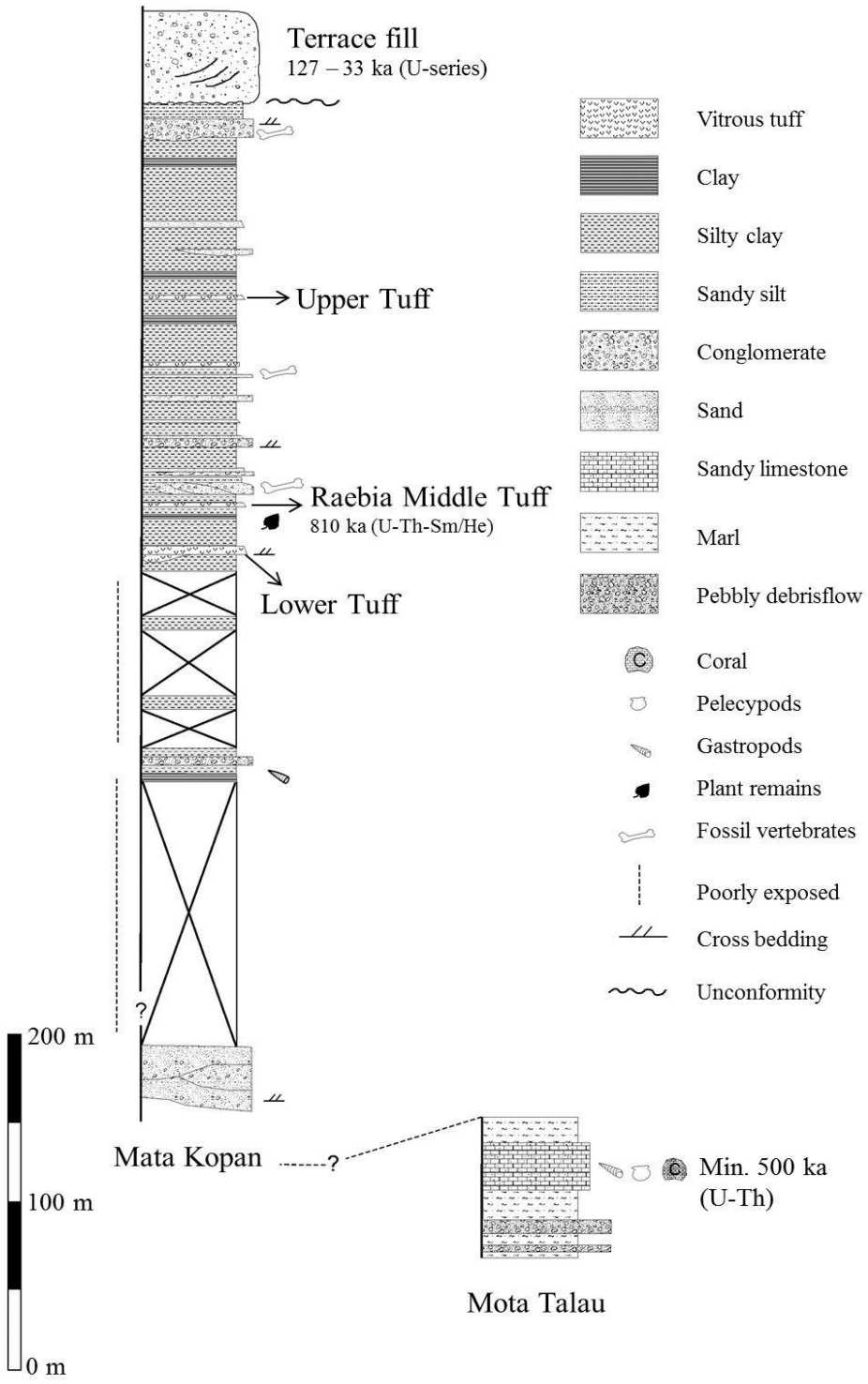

Figure 6.7 Lithostratigraphic sections recorded in the upper part of the Noele Formation along the Mota Talau and Mata Kopan rivers in the northern part of the Atambua Basin. The lower marine interval was measured along the Mota Talau River, and the fluvial interval was measured along the Mata Kopan River. The two sections are possibly separated by a fault (modified after van den Bergh 2007, van den Bergh et al., in prep.).

The most extensive terrace developed in the study area was named the Taektoo Middle Terrace Complex (TMTC), covering most of the western part of Atambua basin (van den Bergh, 2007, van den Bergh et al., in prep.). The lower part of TMTC is dominated by massive siltstones with caliche concretions and mottling, formed during relatively dry soil conditions and deposited in a floodplain environment. Locally, lenses of conglomerate and pebbly sandstones are embedded in the finer-grained siltstones. The basal contact locally cuts down steeply into shallow dipping layers of the Noele Formation. The upper part of the terrace mainly consists of conglomerates embedded in siltstones.

Another terrace fill, dominated by massive cross-bedded sandstones, is developed in the northern area near Maliana Kloto, with an elevation of between 275 m and 340 m. It may represent the lateral equivalent of the TMTC. The youngest terrace developed adjacent to the modern braided rivers extensive gravel terraces, is named the Talau Terrace (Figure 6.6). The terrace flanks the Talau and Oe Rivers and is still periodically flooded. It consists of unconsolidated coarse gravels and gravel lenses similar in size and composition to the gravel in the modern river bedding, grading upwards in loosely consolidated coarse sands and silts at the top (van den Bergh, 2007). No fossils were recovered from this unit.

Two U-series ages on travertine samples provide an age estimate for the terrace formation between 126.8 ± 4.3 ka and 33.8 ± 1.1 ka. Travertine samples were obtained from basal travertine exposures along the terrace exposure at the Kopan and Abad Sali Rivers, respectively (Fig. 6.7; van den Bergh et al., in prep.). The oldest age provides a minimum age for the uplift and doming phase of Timor in this region, and indicates a hiatus between deposition of the uppermost part of the Noele Formation and the unconformably overlying Sadi terrace fills, as well as their respective fossil assemblages (van den Bergh et al., in prep). Additionally, a U-Th dating of a Stegodon tusk recovered from the Ainaro Gravels in East Timor, which may associate with the alluvial terrace in Atambua, resulted in a weighed mean age of ~130 ka (Louys et al., 2016).

6.1.2.3 Sumba

In Sumba, the Quaternary fossil-bearing sediments sampled are located near the Watumbaka and Lewapaku villages (Figure 6.8). The type specimen of Stegodon sumbaensis mandible was found in a Quaternary coastal terrace near Watumbaka by Sartono (1979), but no details about stratigraphy were given. No additional fossils were reportedly found at this site. In 2012 a team from GSI/UOW investigated the original site. The sediment in Watumbaka consists of a 2 m high erosional cliff face exposed along the south slope of a shallow dry river valley eroded into the lowest coral-reef terrace complex at 3 - 20 m above sea-level. The lithology comprises beach deposits and alluvial sediments in contact with coral reef terraces. Sequentially from bottom to top, it consists of fine-grained sandstone, and parallel laminated poorly sorted pebbly sandstones, which are made up of limestone clasts and reworked fossil shells, as well as limestones fragments with marine molluscs at the top of the sequence. The deposits represent a transitional zone that experienced a regressive trend (van den Bergh, 2011).

The second site, Lewapaku, is located in a small basin at an elevation of 500 to 520 m above sea-level. To the East, North and West, the basin is bordered by coralline limestone hills. The basin has an SW-NE oriented elongated shape and is roughly 6 x 14 km wide. The floor of the basin has a very faint but overall flat relief and is barelydissected by river valleys (van den Bergh, 2011). The base of the basin is made up of marine sandy marls, referred to as the Late Miocene-Pliocene Waikabubak Formation (Effendi and Apandi, 1993). Near Lewapaku, the Waikabubak Formation is unconformably overlain by a thin layer between 2.2 and 2.4 m-thick sequence of Quaternary sediments containing fossil terrestrial vertebrate remains, and then by homogeneous clay layers covered with humic topsoils (Fig. 6.8). The basal sandy marl layer is groundwater-bearing, which hindered further excavation. The fossil-bearing layer (Layer 4 in Fig. 6.8) consists of a silty lacustrine/paludrine clay matrix containing poorly-sorted coarse sandy material consisting exclusively of carbonate fragments with a local origin, and pebbles up to 8 cm in diameter. This layer rests unconformably on top of the horizontal marl, but there is no angular unconformity evident; contact with the overlying clay layer is gradational (van den Bergh, 2011, Turvey et al., in prep).

.

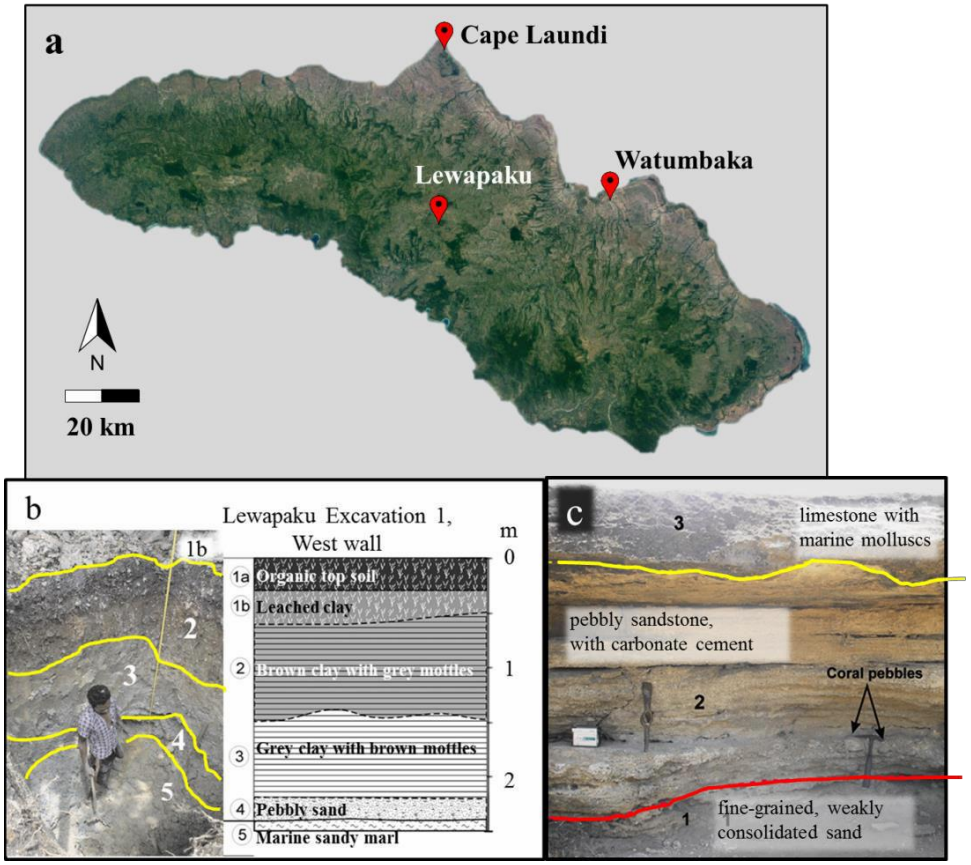

Figure 6.8 a: Map of Sumba, showing fossil vertebrate sites mentioned in the text; b: view towards the northeast corner and stratigraphic profile of the West wall of excavation 1 near Lewapaku, fossil vertebrate remains are concentrated in Layer 4; c: beach rock deposits at the alleged Stegodon site near Watambuka, fossil Stegodon possibly associated with Layer 2, or the fluvial valley deposits that cut down into this sequence (Figure b and c were modified after van den Bergh, 2011).

6.2 Palaeogeography and faunal succession

6.2.1 Palaeogeography and present environment

The emergence of the LSI above sea level as volcanic islands might have started in the Miocene (Ehrat, 1925, Nishimura et al., 1981). However, only after the Early Pleistocene, have the basins in the LSI area been fully uplifted and the newly-formed islands eventually became habitable for fauna. Due to the occurrence of the deep ocean barriers between islands, the LSI remains physically remote and separated from the mainland, even when the eustatic sea-level was at its lowest during glacial phases of the Pleistocene.

Volcanism and tectonic uplifts rates primarily determined sediment accumulation and erosion throughout the Pleistocene. Since the So'a Basin is located in the far inland in an intra-montane basin, Pleistocene sea-level fluctuations associated with glacial-interglacial cycles probably did not cause significant base-level adjustments of the Ae Sissa River system (Suminto et al., 2009).

According to Westaway et al. (2009a, 2009b), both tectonic uplift and sea-level fluctuations played an important role in the alluvial down-cutting of the Wae Racang River, controlling the pace of karstification and exposure at Liang Bua since ~600 ka. Similarly, the post-collisional uplift has periodically raised bedrock at the sites Lewapaku and Watumbaka in Sumba, as well as in the Atambua Basin in Timor, to form land and to create its present relief (Jouannic et al., 1988, Fortuin et al., 1994, Bard et al., 1996, 1997).

The Quaternary uplift is evidenced by a series of geomorphologically well-preserved coral-reef terraces, recording uplift on Sumba, Timor, Atauro, and Alor. These coral terraces provide the most reliable proxy for estimating uplift rates, which can be used to estimate the age of the Quaternary vertebrate fossil sites that have not been directly dated. In Sumba, the coral-reef terraces developed near Cape Laundi (Fig. 6.8). These coral terraces are developed between an elevation of 475 m and present day sea-level. Coral samples from these terraces have been dated with Electron Spin Resonance (ESR) and uranium-series methods. Based on elevation and dating results, an average long-term uplift rate could be estimated of between 0.2 and 0.5 mm/year (Pirazzoli et al., 1991, 1993, Bard et al., 1996).

An estimated uplift based on dated raised coral terraces of 0.03-0.5 mm/year has been documented in numerous areas on Timor (Chappell and Veeh, 1978, Hamilton, 1979, Jouannic et al., 1988, Vita-Finzi and Hidayat, 1991, Kaneko et al., 2007), and 0.47 mm/yr for Atauro (Abbott and Chamalaun, 1981).

The tectonic, uplift and volcanic activity throughout the history of the islands' formation generated a variability of landscape within the present LSI. In Flores, a chain of volcanoes occur in the southern part; scant coastal lowland areas are located at Lembor, Mbay and Maumere, while the rest of the island is occupied by hilly terrains. The topography of Sumba and Timor is also similar to Flores, with predominantly hilly

topography and scant coastal lowland areas, except that there are no volcanoes on either island. The ecoregion of Flores, Sumba and Timor fall in the tropical dry climate zone (Peel et al., 2007)and receive less rainfall than many parts of island Southeast Asia. With an average annual rainfall of 800 to 1,400 mm (Jones and Harris, 2013), this region represents the driest but also the most seasonal in island Southeast Asia (Wikramanayake, 2002). The modern ecosystems in these islands consist of markedly seasonally dry monsoonal vegetation (Dennis, 1999), with 62% of the islands' landscape are covered by grassland and scrubland with a low tree density. The rest of the landscape is covered by semi-deciduous monsoon lowland forest (29%, including moist deciduous forest, dry deciduous forest, dry thorn forest, and dry evergreen forest), sub-montane and montane rainforest (6%), coastal forest, mangroves, and riparian vegetation (Monk et al., 2013). However, many of the forest areas are declining due to natural fire associated with major El Nino Southern Oscillation (ENSO) drought events (Dennis, 1999) and deliberate burning practices (Russell-Smith et al., 2007).

6.2.2 Faunal succession and age of the faunas

6.2.2.1 Flores

A summary of the faunal sequence of Flores, including stratigraphy and the most recent dating results, is presented in Figure 6.9. The earliest recorded island fauna of Flores is represented by taxa found in the excavation of the Tuff Member of the Ola Bula Formation at Tangi Talo, including Excavation A-L. The assemblage comprises the pygmy Stegodon sondaari, giant tortoise Colossochelys sp., Varanus komodoensis and incisor fragments and tibia of an undetermined species of giant rat. The sediment does not contain any stone tools, suggesting that the Tangi Talo Fauna did not interact with hominins. The arrival of taxa in this assemblage must have taken place before 1.4 Ma. The minimum age of this fauna derived from the age Lowo Lele Tephra (LWL), at 1.27 Ma, since so far this assemblage has not been found in the overlying strata.

The earliest occurrence of subsequent faunal assemblage is recorded from a fluvial conglomerate layer (Layer K), at the base of the Lower fossil interval (LFI) at Kobatuwa. Stegodon florensis made its first appearance in this interval. Stegodon sondaari and Colossochelys sp. are no longer occur in this interval, but Varanus

komodoensis and murine rodent continues in this interval. The base of the LFI (Layer K) is laid below the Wolo Sege ignimbrite (WSI), suggesting that the minimum date of this fauna is 1.02 Ma. The WSI contains no vertebrate fossils yet abundant in situ artefacts were recovered during the 2010 excavations from a conglomerate layer directly underlying the WSI (Brumm et al., 2010).

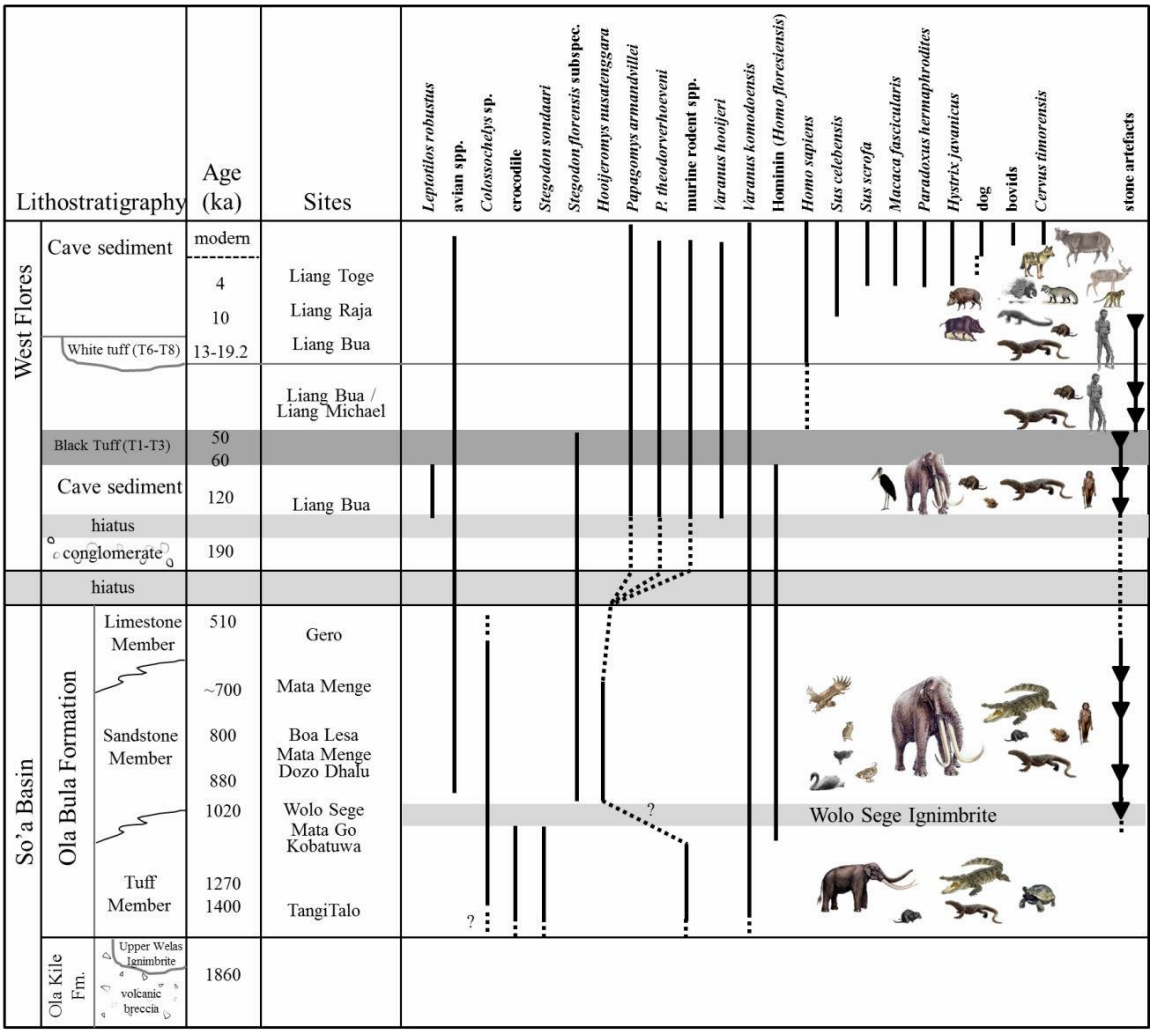

Figure 6.9 Faunal succession of Flores (modified after van den Bergh, et al., 2009 and Meijer et al., 2015)

Additional fossil taxa are recovered from multiple fossil-bearing layers within the Middle Fossil-bearing Interval (MFI) and Upper Fossil-bearing Interval (UFI, the Sandstone Member, Ola Bula Formation). Fossils from the MFI and UFI were mostly recovered from Mata Menge. Other localities containing fossil from the MFI are: Ola Bula, Dozu Dhalu and Boa Lesa. The age of the faunal assemblage contained in the MFI and the UFI is limited to between 1 and 0.7 Ma (Brumm et al., 2010, 2016). This

assemblage includes Stegodon florensis florensis, murine rodents (Hooijeromys nusatenggara), Varanus komodoensis, freshwater crocodiles, frogs, and birds (Cygnus sp., Bubo sp., Anas cf. gibberifrons, cf. Gallinula/Fulica, Vanellus sp., cf. Hieraaetus; Brumm et al., 2010, 2016, Meijer et al., 2015).

Hominin fossils (van den Bergh et al., 2016a) and the only articulated Stegodon bones (a series of vertebrae) ever excavated at Mata Menge were recovered from the UFI (Excavation 32 at Mata Menge, Brumm et al., 2016). Freshwater molluscs, plant remains and stone tools are associated. In the Limestone Member, only aquatic flora and fauna such as fish, ostracods, diatoms and molluscs are locally present (Hartono, 1961, Suminto et al., 2009).

There is no fossil vertebrate fauna record covering the period between the Upper Fossil Interval (UFI, ~700 ka) of the So'a Basin deposit and the cave deposit of Liang Bua (oldest fauna is ~100 ka). The fossil fauna in Liang Bua can be divided into the Late Pleistocene and the Holocene to modern faunas. The Late Pleistocene Fauna of Liang Bua consists of Homo floresiensis, Stegodon florensis insularis, Varanus komodoensis, V. hooijeri, six giant and small murine rodent taxa, and birds (van den Hoek Ostende et al., 2006, van den Bergh et al., 2008, 2009, Locatelli et al., 2012, Meijer and Due, 2010, Meijer et al., 2010, Meijer et al., 2013). Based on the latest dating results, the age of this fauna is estimated between 100 and 50 ka (Sutikna et al., 2016). The Holocene fauna recovered from the cave sediments consists of Sus celebensis, Macaca fascicularis, Paradoxurus hermaphroditus, Hystrix javanica, dog, bovids and cervids, which were introduced by Homo sapiens during the Neolithic (van den Bergh et al., 2009).

6.2.2.2 Timor

Stegodon timorensis, Varanus sp. nov. and remains of giant tortoise attributed to Geochelone atlas (= Colossochelys) are recorded from various localities in Timor (Hooijer, 1969b, 1971, 1972b, Hocknull et al., 2009). During a reconnaissance survey in 2007, van den Bergh (2007) recorded remains of Stegodon timorensis and giant tortoise, found in situ and on the surface of the Noele Formation and alluvial terraces. In situ and surface artefacts were found near Sadi Hill, on top of dissected terrace-fill

deposits, but were absent from the Noele Formation. The age of the fossil fauna associated with the Noele Formation, thus can be considered as ~810 ka, based on the dated Raebia Middle Tuff, and is overlapping with the age of the Middle Fossil Interval of the sandstone Member of the Ola Bula Formation (So'a Basin, Flores). The age of the fossil assemblage collected from the alluvial terraces is presumably younger than 130 ka, and overlaps with the Stegodon florensis insularis fauna from Liang Bua in Flores.

6.2.2.3 Sumba

Sumba's Quaternary faunal and human history is extremely poorly understood as little mammal research has been conducted on this island (Dammerman, 1928, Musser, 1972, Coates et al., 1997, Olsen et al., 2009). The Quaternary fossil fauna of Sumba comprises the Pleistocene and Holocene Fauna. The Pleistocene Fauna recorded in the Lewapaku site consists of Stegodon sumbaensis, Varanus komodoensis, an undetermined giant murine rodent, and undetermined avian fauna (van den Bergh, 2011, Turvey et al., in prep). Given that this fossil assemblage was found at an elevation of ~500 m, and in absence of any numerical dating results, the age of the fossil fauna can be estimated by extrapolating this site's elevation with the mean uplift rate, assuming that accumulation of the fossil-bearing strata started shortly following emergence above sea-level. This provides a maximum age estimation of ~1 Ma. The age of the Watumbaka Site is extrapolated from the age of Terrace complex I at Cape Laundi, which has similar elevation as the Watumbaka Terrace. The published U-Th dates obtained from this terrace complex shows that this terrace was formed during MIS 5, with coral ages corresponding with the three main high sea-levels at ~86 ka BP, 105 ka BP and 125 ka BP (Pirazzoli et al., 1991, Pirazzoli et al., 1993). The limited information from the outcrop at Watumbaka does not provide a more specific age for the Stegodon fossil other than that it likely has an age corresponding with the Last Interglacial. Thus, the Stegodon from Watumbaka seems to partly overlap in time with Stegodon florensis insularis from Liang Bua in Flores, of which the oldest remains are ~100 - 95 ka (van den Bergh et al., 2009).

6.3 Analysed materials

A total of 114 enamel samples from four different Stegodon species and two subspecies from the LSI were used for stable isotope analysis. The sampled species include: Stegodon sondaari (n = 22), Stegodon florensis, including two subspecies: S. f. florensis (n= 47) and S. f. insularis (n = 29), Stegodon timorensis (n = 13) and Stegodon sumbaensis (n = 1). Samples cover the time span between the Early Pleistocene and the Late Pleistocene.

Stegodon sondaari specimens are grouped based on their stratigraphic position: the lower fossil layer (obtained from Excavations A, B, G, H; dated at 1.4 Ma; n = 23) and the upper fossil layer (obtained from Excavation F; dated slightly younger than 1.27 Ma). Due to the limited number of molar specimens of adult individuals retrieved from Exc. F, only three enamel samples were included in the analysis from this site.

Stegodon florensis florensis samples from the So'a Basin are grouped by stratigraphic position: the LFI (n = 7), the MFI (n = 31) and the UFI (n = 9). All LFI samples originate from Kobatuwa. The MFI samples originate from three localities: Mata Menge (n = 22), Boa Leza (n = 4) and Dozo Dhalu (n = 5). The UFI samples were recovered from the Excavation 32 at Mata Menge. In addition, crocodiles (n = 5: MFI = 1, UFI = 4) and murine rodents (n = 7: MFI = 2, UFI = 5) from Mata Menge were also included in the analysis, especially because this site has yielded hominin fossils. The analysis of the whole faunal assemblage of Mata Menge was carried out in order to investigate the various island mammals associated with the hominins in more detail.

Due to a limited number of available adult Stegodon florensis insularis individuals from the Liang Bua deposits, samples of juvenile individuals were also included in the analysis, but have been separated from the adult specimens. This was also to test if juveniles might have had different feeding habits compared to adults. Therefore, the grouping of Stegodon florensis insularis individuals is divided according to the ontogenic age, which grouped based on their dental elements: dI^2-dp2-dp3 (n = 12) that represent pre-natal dental development, dp4-M1 (n = 14) that were formed around the weaning to post-weaning period, and M2-M3 (n =3) that represent pre-adult to adult dental development (Shoshani, 1996, Kozawa et al., 2001, Dirks et al., 2012).

Specimens of Stegodon timorensis were collected from the Noele Formation and the younger, unconformably overlying Terrace deposits. However, since most of the specimens of Stegodon timorensis were not collected in situ, the stratigraphic provenance of seven samples could not be determined with certainty. From a total of thirteen samples, the stratigraphic provenance of six samples is known. A single molar ridge (either M1, M2 or M3) of Stegodon sumbaensis from Lewapaku, Sumba, estimated to be of Early-Middle Pleistocene age, was also included in the analysis.

6.4 Isotopic analysis results

A list of individual isotopic values of all analysed samples from the LSI is given in Appendix II. The range of isotopic values and statistics of all analysed samples are listed in Table 6.1, while Table 6.2 reports matrices of pairwise probability Benferroni corrected p values of Mann-Whitney post hoc tests to determine significant differences among taxa.

6.4.1. Stegodon from the LSI

Compared to mainland Asia, Java and Sulawesi samples, the carbon isotope values ($\delta^{13}C$) of individual samples from the LSI covers a less wide range of between -8.3‰ and 3.2‰, while the $\delta^{18}O$ values cover a range between -8.8‰ and -0.8‰. A plot of individual, mean and range values of $\delta^{13}C$ (‰, $_{VPDB}$) and $\delta^{18}O$ (‰, $_{VPDB}$) values of all analysed Stegodon samples is presented in Figure 6.10. In Figure 6.11 individual $\delta^{13}C$ and $\delta^{18}O$ values of all Stegodon taxa from Flores and Sumba are arranged in chronological order, based on the estimated ages of faunal assemblages, while for Timor, only the specimens from known origins were included in this this graph. The age determinations of species occurrence of Flores are more accurate due to the substantial availability of chronological data. However, the age of species occurrences is less accurate for Timor and Sumba.

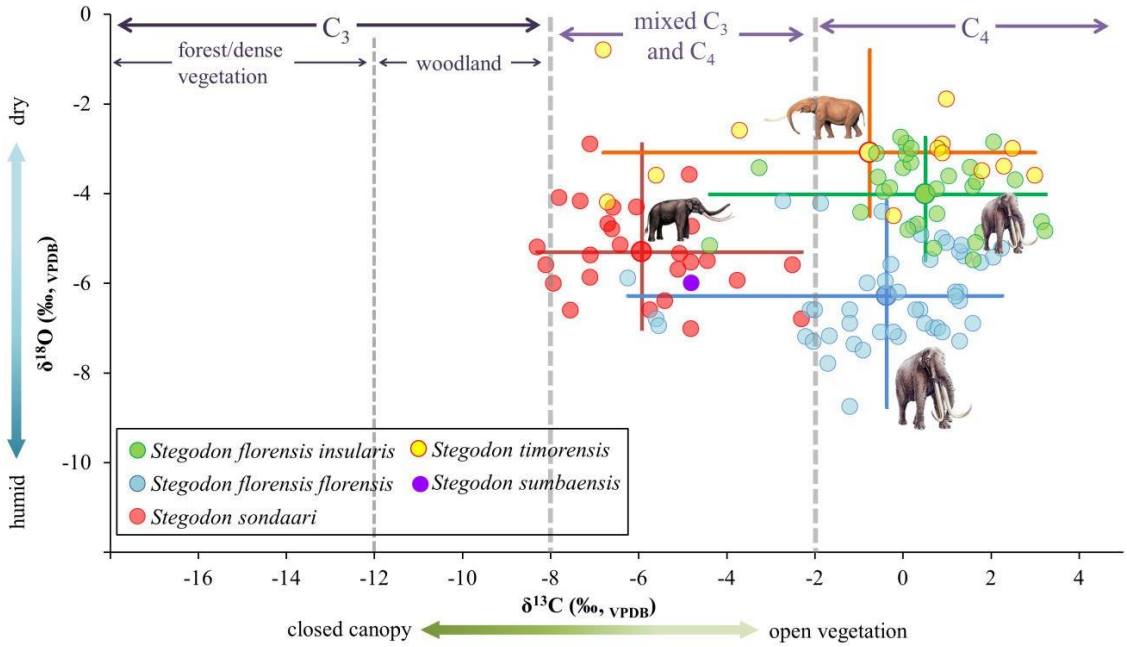

Figure 6.10 Mean $\delta^{13}C$ and $\delta^{18}O$ values and ranges of all analysed Stegodon samples from the LSI, grouped by species and sub species. Dashed lines represent boundaries between vegetation and diet types (Cerling et al., 1997a, 1999, MacFadden et al., 1999, Passey et al., 2002, Feranec et al., 2007). Means are designated by the crossing of the range bars.

The $\delta^{13}C$ values of all Stegodon florensis (subspecies florensis and insularis) and Stegodon timorensis indicate that these species were predominantly C_4 grazers, with the exception of a few individuals from the LFI and Liang Bua with a mixed feeding isotopic signature. The $\delta^{13}C$ values of S. sondaari individuals plot in a narrower range that is entirely consistent with mixed C_3-C_4 feeders, except for two individuals that just fall within the range of a C_3-dominant diet in a forested open canopy environment. A significant difference in $\delta^{13}C$ values occurs between Stegodon sondaari and the three other groups: S. f. florensis, S. f. insularis and S. timorensis (Kruskal-Wallis test p = 2.061E-11, see Table 6.2A for Mann-Whitney test Benferroni corrected p for each pairing). The $\delta^{18}O$ values of S. sondaari (-7.0‰ to -2.9‰) and S. florensis florensis (-8.8‰ to -4.2‰) are comparatively lower than S. florensis insularis (-5.5‰ to -2.8‰) and S. timorensis (-4.5‰ to -0.8‰). Significant differences of $\delta^{18}O$ values occur among all pairings of groups (Kruskal-Wallis test p =1.243E-13, see Table 6.2A for Mann-Whitney test Benferroni corrected p values for all pairings). The significant differences between all pairings suggest different conditions of drinking water sources and/or climatic differences for each island and or assemblages.

Table 6.1 Descriptive statistic for $\delta^{13}C$ and $\delta^{18}O$ values of taxa examined from the LSI.

faunal assemblage	n	$\delta^{13}C$ (‰, VPDB)					$\delta^{18}O$ (‰, VPDB)				
		mean	median	std. dev	std. error	range	mean	median	std. dev	std. error	range
FLORES											
Liang Bua											
1. Stegodon florensis insularis	29	0.5	0.3	1.6	0.3	-4.4 to 3.2	-4.0	-3.8	0.8	0.2	-5.5 to -2.8
a. dI^2, dp2 and dp3	12	-0.2	0.3	1.9	0.6	-4.4 to 1.8	-4.1	-3.9	0.7	0.2	-5.2 to -3.3
b. dp4 and M1	14	0.8	0.2	1.2	0.3	-0.6 to 3.2	-4.0	-3.7	1.0	0.3	-5.5 to -2.8
c. M2 and M3	3	2.0	2.1	1.2	0.7	0.8 to 3.2	-3.8	-3.9	0.9	0.5	-4.6 to -2.9
Kobatuwa, Mata Menge, Dozo Dhalu, Boa Leza											
1. Stegodon florensis florensis	47	-0.4	-0.1	1.9	0.3	-6.2 to 2.3	-6.3	-6.6	1.0	0.2	-8.8 to -4.2
a. UFI (~0.7 Ma)	9	0.3	0.4	1.8	0.6	-2.7 to 2.3	-4.9	-4.9	0.5	0.2	-5.6 to -4.2
b. MFI (0.9-0.8 Ma)	31	0.0	0.4	1.2	0.2	-2.2 to 1.6	-6.6	-6.6	0.7	0.1	-7.8 to -5.0
- Mata Menge	22	-0.0	0.1	1.1	0.2	-2.0 to 1.6	-6.8	-6.9	0.5	0.1	-7.8 to -5.5
- Boa Leza	4	1.1	1.1	0.2	0.1	0.9 to 1.3	-5.9	-5.8	0.9	0.5	-7.1 to -5.1
- Dozo Dhalu	5	-0.7	-1.7	1.7	0.8	-2.2 to 1.4	-6.3	-6.6	1.0	0.5	-7.2 to -5.0
c. LFI (1-0.9 Ma)	7	-2.9	-1.2	2.7	1.0	-6.2 to -0.3	-6.3	-6.0	0.7	0.3	-7.4 to -5.6
2. murine rodents	7	0.2	0.3	1.3	0.5	-2.0 to 1.6	-7.1	-7.2	0.9	0.3	-8.2 to -5.8
a. UFI (~0.7 Ma)	5	0.5	0.3	1.0	0.5	-0.5 to 1.6	-6.9	-6.6	1.0	0.4	-8.2 to -5.8
b. MFI (0.9-0.8 Ma)	2	-0.6	-0.6	2.0	1.4	-2.0 and 0.9	-7.6	-7.6	0.6	0.5	-8.1and -7.2
3. crocodiles	5	-1.0	-0.4	1.8	0.8	-3.7 to 0.9	-8.2	-6.6	2.6	1.2	-11.4 to -6.0
a. UFI (~0.7 Ma)	4	-0.3	-0.2	1.2	0.6	-2.0 to 0.9	-8.7	-8.6	2.7	1.4	-11.4 to -6.0
b. MFI (0.9-0.8 Ma)	1	-	-3.7	-	-	-3.7	-	-6.5	-	-	-6.5
Tangi Talo											
1. Stegodon sondaari	26	-5.9	-6.2	1.6	0.3	-8.1 to -2.3	-5.3	-5.5	1.0	0.2	-7.0 to -2.9
a. upper interval (1.27 Ma)	3	-7.7	-7.8	0.6	0.4	-8.3 to -7.1	-4.1	-4.1	1.2	0.7	-5.2 to -2.9
b. lower interval (1.4 Ma)	23	-5.7	-5.7	1.6	0.3	-8.1 to -2.3	-5.5	-5.5	0.9	0.2	-7.2 to -3.6
TIMOR											
1. Stegodon timorensis	13	-0.8	0.9	3.6	1.0	-6.8 to 3	-3.1	-3.1	1.0	0.3	-4.5 to -0.8
SUMBA											
1. Stegodon sumbaensis	1	-	-4.8	-	-	-4.8	-	-6.0	-	-	-6.0

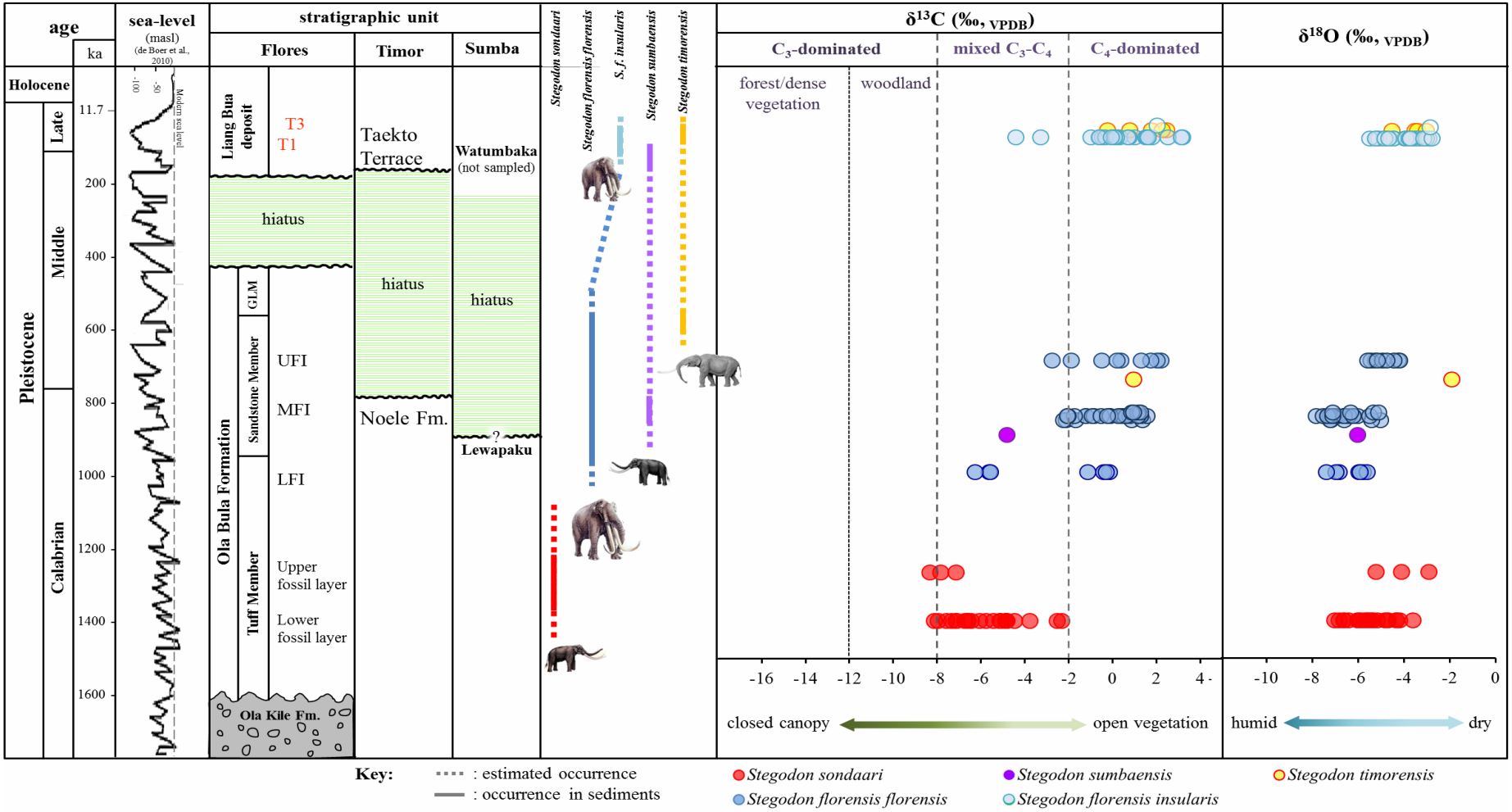

Figure 6.11 $\delta^{13}C$ and $\delta^{18}O$ values of analysed Stegodon taxa from the LSI in chronological order. Dashed lines in the $\delta^{13}C$ column represent boundaries between vegetation and diet types (Cerling et al., 1997a, 1999, MacFadden et al., 1999, Passey et al., 2002, Feranec et al., 2007). For Stegodon florensis insularis, juvenile samples are included.

Table 6.2 Matrices of pairwise probabilities of mean differences in $\delta^{13}C_{enamel}$ and $\delta^{18}O_{enamel}$ values. Values shown in red indicate significant Benferroni corrected p values ($\alpha \leq 0.05$) using Mann-Whitney test.

A	Elephantoidea taxa	1		2		3	
		$\delta^{13}C$	$\delta^{18}O$	$\delta^{13}C$	$\delta^{18}O$	$\delta^{13}C$	$\delta^{18}O$
1	Stegodon sondaari	-	-				
2	Stegodon florensis florensis	**1.86E-10**	**0.01**				
3	Stegodon florensis insularis	**4.72E-9**	**2.11E-4**	0.3915	**3.28E-9**		
4	Stegodon timorensis	**0.0018**	**5.40E-5**	1	**9.53E-7**	1	**0.0145**

B	Stegodon sondaari	1	
		$\delta^{13}C$	$\delta^{18}O$
1	lower fossil layer (1.4 Ma)	-	-
2	upper fossil layer (1.27 Ma)	**1.86E-10**	**0.01**

C	Stegodon florensis florensis	1		2	
		$\delta^{13}C$	$\delta^{18}O$	$\delta^{13}C$	$\delta^{18}O$
1	LFI (1.0-0.9 Ma)	-	-		
2	MFI (0.9-0.8 Ma)	**0.0386**	1		
3	UFI (~0.7 Ma)	0.1028	**0.0031**	1	**1.31E-4**

D	S. f. florensis of the MFI	1		2	
		$\delta^{13}C$	$\delta^{18}O$	$\delta^{13}C$	$\delta^{18}O$
1	Mata Menge	-	-		
2	Boa Leza	0.1773	0.3253		
3	Dozo Dhalu	1	1	0.6562	1

E	Stegodon florensis insularis	1		2	
		$\delta^{13}C$	$\delta^{18}O$	$\delta^{13}C$	$\delta^{18}O$
1	dI^2, dp2 and dp3	-	-		
2	dp4 and M1	1	0.6996		
3	M2 and M3	0.2136	0.718	0.3452	0.8501

F	Mata Menge Fauna	1		2		3	
		$\delta^{13}C$	$\delta^{18}O$	$\delta^{13}C$	$\delta^{18}O$	$\delta^{13}C$	$\delta^{18}O$
1	S. florensis MFI	-	-				
2	S. florensis UFI	0.3492	**1.27E-4**				
3	crocodiles	0.3026	1	0.1824	**0.0201**		
4	murine rodents	0.5747	1	0.672	**0.0062**	0.4168	1

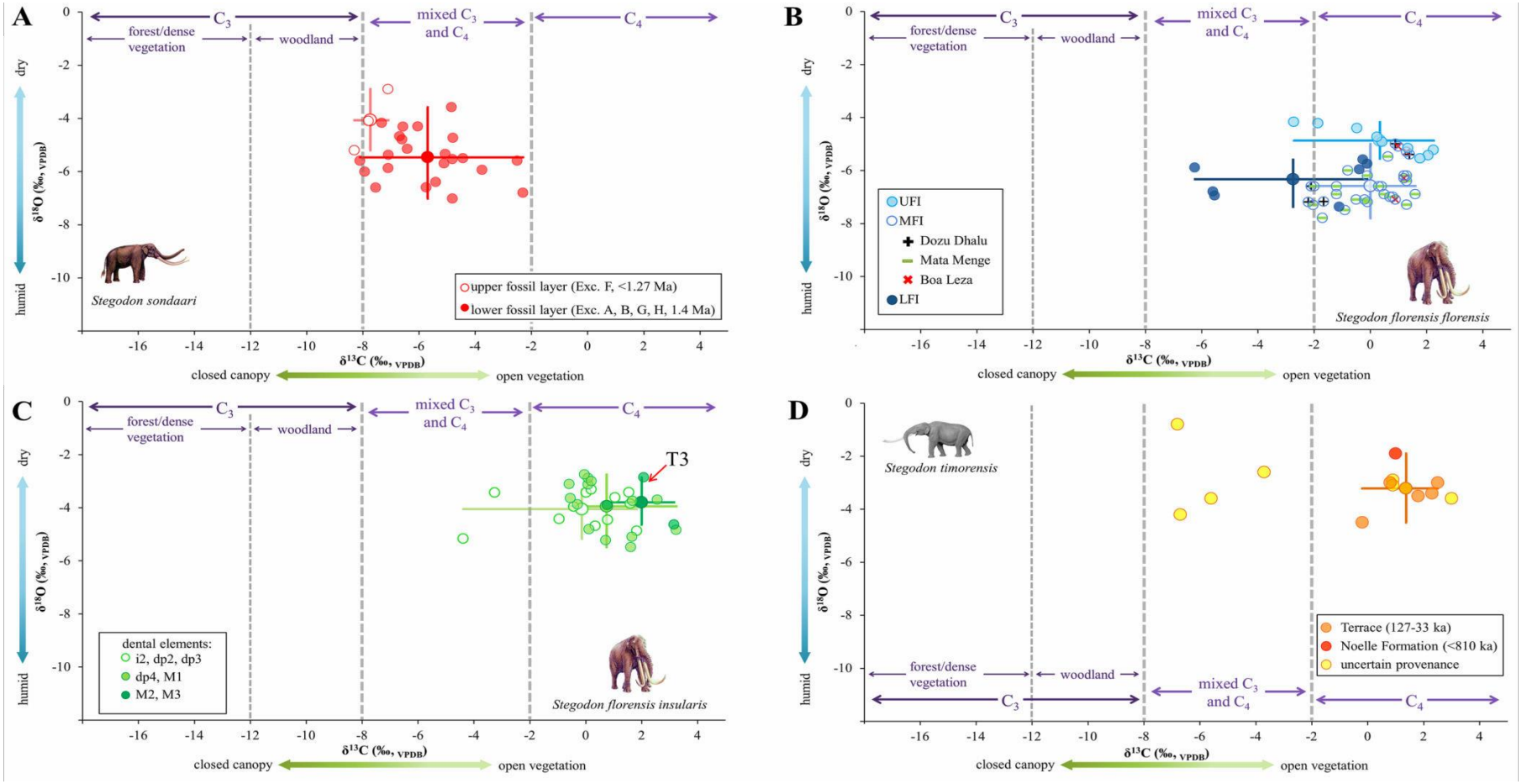

Figure 6.12 Mean $\delta^{13}C$ and $\delta^{18}O$ values and ranges of: **A,** Stegodon sondaari, grouped by provenance layers; **B,** Stegodon florensis from the So'a Basin, grouped by fossil-bearing intervals. For all fossils from the MFI, samples from Boa Lesa, Dozu Dhalu and Mata Menge are marked differently; **C,** Stegodon florensis insularis, grouped by dental elements. The only individual from layer T3 is indicated a by red arrow; and **D.** Stegodon timorensis, grouped by provenance stratigraphy. Dashed lines represent boundaries between vegetation and diet types (after Cerling et al., 1997a, 1999, MacFadden et al., 1999, Passey et al., 2002, Feranec et al., 2007). Means are designated by the crossing of the range bars.

6.4.2 Stegodon sondaari

A plot of individual, mean and ranges of $\delta^{13}C$ (‰, $_{VPDB}$) and $\delta^{18}O$ (‰, $_{VPDB}$) values is presented in Figure 6.12A. All $\delta^{13}C$ values of individuals from the lower fossil layer (between -8.1 and -2.3‰) and the upper fossil layer (between -8.3 and 7.1‰) fall within the range expected for a mixed C_3-C_4 diet, except for a single individual in both groups that have $\delta^{13}C$ values slightly below the standard minimum value for the mixed C_3-C_4 diet. The difference between the two groups is significant, with the $\delta^{13}C$ values of the individuals from the upper fossil layer having lower values than for the lower fossil layer (Kruskal-Wallis test p = 0.02458, Benferroni corrected p = 1.86E-10).

The $\delta^{18}O$ values of S. sondaari samples from two fossil layers are evenly distributed across a wide range between -7.0 and -2.9‰. Unlike their $\delta^{13}C$ values, the median $\delta^{18}O$ value of the individuals from the lower fossil layer (-5.5‰) is significantly lower than for the upper fossil layer (-4.1‰; Kruskal-Wallis test p = 0.04067, Benferroni corrected p = 0.01).

6.4.3 Stegodon florensis

6.4.3.1 Stegodon florensis florensis

A plot of individual, mean and range of $\delta^{13}C$ and $\delta^{18}O$ values of this group are presented in Figure 6.12B. Univariate analysis was applied to the S. florensis groups from the three different stratigraphic intervals (Table 6.2C), as well as from the three different localities included in the MFI (Table 6.2D).

The average of carbon isotope values for the LFI samples falls within the range expected for mixed feeders. Three individuals have $\delta^{13}C$ values below -2‰ and four individuals have $\delta^{13}C$ values above -2‰. As the values between mixed feeder and grazer individuals differ greatly, the two groups are also statistically distinguishable (p = 0.03389, Kruskal-Wallis test). However the difference in isotopic values does not correspond to different stratigraphic origins of the specimens, as mixed feeder and grazer individuals co-occur in the same layers (Layer H and I, see Fig. 6.4).

All of the S. florensis samples from the MFI fall within a narrow range of $\delta^{13}C$ values between -2.2 to 1.6‰, reflecting a C_4-dominant diet. Although two samples plot in the mixed feeder range, their values are very close to the C_4-diet boundary, suggesting that all individuals relied on a more prominent proportion of C_4 plants as their food sources. Additionally, both the $\delta^{13}C$ and $\delta^{18}O$ values of individuals from Mata Menge, Dozo Dhalu and Boa Leza are statistically indistinguishable (p for $\delta^{13}C$ = 0.1213 and p for $\delta^{18}O$ = 0.2258, Kruskal-Wallis test). Subsequently, the $\delta^{13}C$ values of the samples from the UFI (-2.7 to 2.3‰) generally correspond with pure a C_4 diet, except for one individual that has a $\delta^{13}C$ value slightly below the standard minimum value for C_4 diet.

Significant differences of the $\delta^{13}C$ and $\delta^{18}O$ values occur among the three stratigraphic interval groups (p for $\delta^{13}C$ = 0.02497 and p for $\delta^{18}O$ = 8.52 E-5, Kruskal-Wallis test). Of the Stegodon florensis obtained from the Sandstone Member, the individuals from the MFI have significantly higher $\delta^{13}C$ values compared to the individuals from the LFI (Benferroni corrected p = 0.0386), while the UFI group is statistically indistinguishable from the LFI and MFI groups. As for the $\delta^{18}O$, the median value of the individuals of the UFI are significantly higher than the LFI and UFI, while the LFI and MFI groups are statistically indistinguishable (Table 6.2C for pairwise matrices).

6.4.3.2 Stegodon florensis insularis

A plot of individual, mean and range of $\delta^{13}C$ and $\delta^{18}O$ values of this group are presented in Figure 6.12C. All individual $\delta^{13}C$ values, including the only individual from T3, fall in the range expected for C_4 feeders (-4.4 to 3.2‰), except for two juvenile (dp3s) samples that plot in the mixed feeder range. The $\delta^{13}C$ and $\delta^{18}O$ values of pre-natal, weaning and post-weaned dental development groups are statistically indistinguishable (p for $\delta^{13}C$ = 0.1344 and p for $\delta^{18}O$ = 0.8652, Kruskal-Wallis test, Table 6.3E for matrices pairwise). However, a weak trend of increasing $\delta^{13}C$ values from younger to older individual occurs within the analysed samples.

The $\delta^{13}C$ values of Stegodon florensis insularis are statistically indistinguishable from the S. f. florensis population from the So'a Basin (Benferroni corrected p = 0.3915, Mann-Whitney test). However, Liang Bua $\delta^{18}O$ values (-5.5‰ to -2.8‰) are

significantly higher than those of their predecessor population from the So'a Basin (Benferroni corrected p = 3.28E-9, Mann-Whitney test, Table 6.2A).

6.4.4 Local fauna of Mata Menge

A plot of individual, mean and range of $\delta^{13}C$ and $\delta^{18}O$ values of taxa from Mata Menge are displayed in Figure 6.13. All samples except for one S. florensis from the UFI plot in the expected range for C_4 diet, suggesting that the herbivores (S. florensis and murine rodents) were grazers, while the carnivores (crocodile) preyed on grazer herbivores. No significant difference occurs in the $\delta^{13}C$ values among analysed taxa from the two stratigraphically separated populations (p = 0.4632, Kruskal-Wallis test), while the $\delta^{18}O$ values of S. florensis from the UFI are significantly higher than S. florensis of the MFI, crocodiles and murine rodents (p =9.79E-5, Kruskal-Wallis test, Table 6.2F for matrices pairwise). Although not detected in statistical analysis, the $\delta^{18}O$ values of crocodile samples (-11.4‰ to -6.0‰) are noticeably lower than S. florensis and murine rodents. Moreover, the $\delta^{18}O$ values of crocodile have a large variance of 7.53.

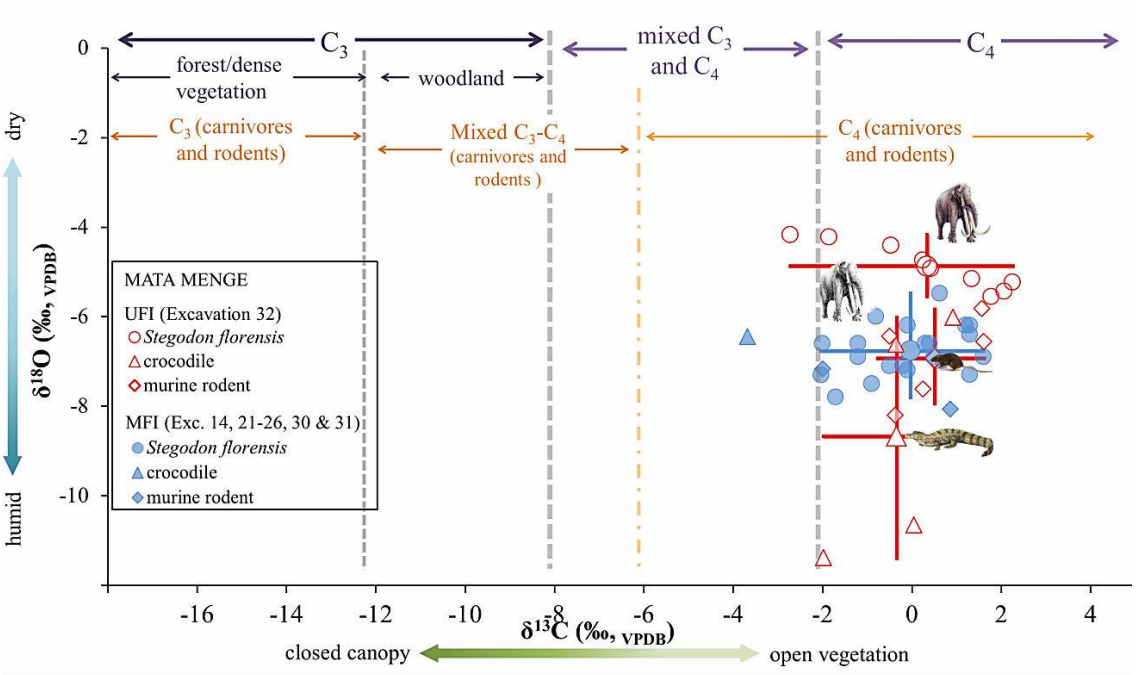

Figure 6.13 Mean $\delta^{13}C$ and $\delta^{18}O$ values and ranges of all analysed samples from the Middle Fossil-bearing Interval (MFI) and the Upper Fossil-bearing Interval (UFI) in Mata Menge. Dashed lines represent boundaries between vegetation and diet types (after Cerling et al., 1997a, 1999, MacFadden et al., 1999, Passey et al., 2002, Feranec et al., 2007). Means are designated by the crossing of the range bars.

6.4.5 Stegodon timorensis

A plot of individual, mean and ranges of $\delta^{13}C$ and $\delta^{18}O$ values of this group is presented in Figure 6.12D. The $\delta^{13}C$ and $\delta^{18}O$ values of the single specimen known to originate from the Noele Formation are 1.0‰ and -1.9‰, respectively. The measured $\delta^{13}C$ values of individuals known to originate from the fluvial terraces range between -0.2 and 2.5‰, while the measured $\delta^{18}O$ values range between -4.5 and -1.9‰ (mean = -3.2‰). All carbon isotope values of individuals from known stratigraphic position and three samples from unknown position plot in the expected range of a C_4-dominated diet. Four mixed feeder individuals occur among analysed samples. Unfortunately their stratigraphic origins are uncertain, making it difficult to reconstruct the timing of vegetation change. Regardless, the $\delta^{18}O$ values are constantly high, moreover, are significantly higher compared to other islands, suggesting an overall drier climate on Timor.

6.4.6 Stegodon sumbaensis

The measured $\delta^{13}C$ and $\delta^{18}O$ values of this specimen are -4.8‰ and -6.0‰, respectively. Its $\delta^{13}C$ value indicates that this individual was a mixed C_3-C_4 feeder, foraging in an open canopy environment. The isotopic values of this specimen cannot be statistically analysed.

6.5 Discussion

With the availability of stratigraphy and dating data, the terrestrial sequence of Flores is now much better understood compared to the other Wallacean islands and the Asian mainland. With the currently available dataset, Flores should thus play an important role in any regional hypothesis regarding Quaternary environmental change. The data from the adjacent islands of Sumba and Timor are still rather limited to draw any firm conclusions, but can be considered as supplementary to Flores.

The carbon isotope values ($\delta^{13}C$) of individual samples from the LSI cover a less wide range in comparison to other regions analysed in this study, which may be due to the more limited time constraint covered by the samples (1.4 to 0.1 Ma). None of the specimens from the LSI represents an individual feeding in a closed canopy environment, even among the lowest isotopic values, which similarly depicts the present vegetation coverage of the LSI. This suggests that C_4 plants were always available, if not dominating, because food resources in the habitat and closed canopy forest/woodland were never dominating the habitat in the LSI, at least during the periods covered by the samples.

Of the oldest insular faunal record of Flores, the range of carbon isotopic values of Stegodon sondaari (1.4 to 1.27 Ma) suggest that this species was capable of both grazing and browsing, implying that both C_3 and C_4 plant were available in the habitat through the indicated period. The period covered by the S. sondaari fossil record from the So'a Basin, coincides with a prolonged interglacial period (~MIS 45 to MIS 37, Fig. 2.1, Ehlers and Gibbard, 2007). The climate during this interglacial period was warmer and more humid, with stronger monsoon and seasonal differences compared to the present (Clemens and Tiedemann, 1997). Therefore the availability of both C_3 and C_4 plants is associated with a distinctive wet-dry seasonal change and intensified monsoon during the interglacial period. In this case, the C_3:C_4 proportion in S. sondaari's diet might have changed seasonally, as observed in mixed feeder modern elephants with a mixed diet of grasses and leaves/barks (Sukumar, 1993). The new growth of grasses during the wet seasons might have promoted the consumption of a substantial proportion of grass (C_4 plant), while the ratio of C_3 plant consumption might have been higher during the dry seasons. Additionally, the wide range of $\delta^{18}O$ values may also reflect variations in the isotopic composition of drinking water due to seasonal differences. Nevertheless, isotopic data from serial enamel sampling would be required to test this speculation concerning seasonality.

Since the changing proportions between C_3 and C_4 plants can only occur in a habitat where both types of plant are present, the suggested habitat of the So'a Basin during the time range covered by S. sondaari would include deciduous forest, woodland, or a mosaic of woodland and grassland. Alternatively, the vegetation cover during the occupation of S. sondaari may have been similar to the present conditions of the So'a

Basin, where C_4 plant dominate the open plains (grassland and wooded grassland), while the C_3 plant prevail in the wetter parts adjacent to rivers and on mountain slope areas. Due to its small body size, the population of S. sondaari might not have been able to clear the canopy coverage from the landscape, and thus the vegetation cover of the So'a Basin during this stage was possibly not as markedly cleared from trees as in dry areas where modern African savannah elephants roam (Laws, 1970, Dublin et al., 1990, Dublin, 1995, Midgley et al., 2005, Campos-Arceiz and Blake, 2011).

The statistical difference observed between mean $\delta^{13}C$ values in older and younger S. sondaari population may reflect the smaller sample size of the Upper fossil layer, rather than a true feeding behavioural difference, as these samples are largely encompassed by the range in $\delta^{13}C$ values observed in specimens from the lower fossil layer. It is difficult to speculate what caused the extinction of S. sondaari by only relying on the isotopic data, as additional data that support the regional palaeoclimate during the Early Pleistocene are not available. It is interesting that the $\delta^{13}C$ values of the upper fossil layer show a stronger browser signal, while their $\delta^{18}O$ values fall to the drier end of the $\delta^{18}O$ range. This result suggests that S. sondaari was preferentially feeding on C_3 plants despite the dry condition. While the age of the upper fossil layer does not necessarily correspond with any minor/major glaciation cycle, the higher $\delta^{18}O$ values of samples from the upper fossil layer may be correlated to a seasonal signal. If this is the case, the feeding preference of S. sondaari might make them more susceptible to drier conditions, which commenced not long after 1.27 Ma, when seasonal resources of C_3 plants became more limited. Furthermore, since there is a large time gap of more than 200,000 years between its youngest occurrence and the faunal assemblage from the LFI, it is likely that hominins and larger Stegodon florensis arrived during this interval. The arrival of new taxa into the island led to increasing competition among taxa to obtain the available food resources, and thus adds up the factors that may have caused the extinction of S. sondaari. However, this explanation may remain speculative for the time being, since the in situ co-occurrence of Stegodon sondaari with hominins and/or S. florensis has not been recorded so far.

In comparison to the S. sondaari population, the carbon isotopic composition of Stegodon florensis from the Lower fossil interval (LFI), Middle Fossil Interval (MFI) and Upper Fossil Interval (UFI) have more positive values, with most of the analysed

samples corresponding with the range of a dominant C_4 diet. The pronounced shift of $\delta^{13}C$ values from the mixed feeder S. sondaari population to the earliest record of grazer/mixed feeder Stegodon florensis originating from the LFI implies a change of vegetation cover occurred around the earliest record of Stegodon florensis at ~1 Ma. and may have taken a while for S. florensis to shift to a more C_4-dominated diet.

The predominant grazing diet through the temporal range covered by of S. florensis (~1-0.7 Ma) implies that grassland and wooded grassland were the prevalent vegetation covers in the So'a Basin. An additional indication that a dry-climate habitat was dominant in the early Middle Pleistocene So'a Basin is provided by palynological data from the MFI and UFI. The fossil pollen and phytolith from these intervals are dominated by C_4 taxa, such as: Poaceae, Cyperaceae and Restionaceae (van der Kars, pers. comm. to van den Bergh, Brumm et al., 2016). Nevertheless, the occurrence of mixed C_3-C_4 feeder individuals in all fossil intervals, particularly in the LFI, and minor proportions of fossil pollen of tree and shrub elements (van der Kaars, pers. comm. to van den Bergh, Brumm et al., 2016) further indicate the presence of fragmented patches of woodland or more closed canopy vegetation in the surrounding habitat. The type of habitat suggested by the isotopic result also accords with the avian assemblage from Mata Menge and Boa Leza, which is indicative of an open environment with a strong open, freshwater component and nearby grasslands, and with forests at a distance (Meijer et al., 2015).

All of the murine rodent samples from the MFI and UFI, yielded individual $\delta^{13}C$ values indicating a C_4 dominated diet. Crocodiles have similar $\delta^{13}C$ range, indicating that they primarily predated on C_4 grazers. This result amplifies the indication that the habitat coverage during the late Early Pleistocene to the early Middle Pleistocene on Flores was dominated by open grassland. Due to the fact that the $\delta^{13}C$ values of Stegodon and murine rodents from the MFI and the UFI all overlap in the range of a C_4-dominant diet range, a niche separation between both taxa seemingly did not happen.

The prevalence of C_4-dominated vegetation during the late Early Pleistocene to Middle Pleistocene in the So'a Basin could be associated with several factors. Notably, climate is the primary determinant as it sets the limits to potential plant growth and vegetation, by providing variation of humidity, temperature and precipitation (Whittaker and Klomp, 1975). The expansion of C_4-dominated vegetation through the temporal range

covered by S. florensis (~1-0.7 Ma) in the So'a Basin may be correlated to the climate through the glacial cycles, since the age of the three intervals coincide with several Early-Middle Pleistocene glacial cycles. The age range of the LFI (~1 Ma) might correspond with the minor glaciation during MIS 30 (1.07-1.03 Ma) or MIS 26 (0.97 - 0.96 Ma, see Fig 2.1 for the timeline of glaciations). The age range of the MFI (0.88-0.80 Ma) is equivalent with the onset of major glaciation during MIS 22 (~0.88-0.87 Ma), while the UFI (~0.7 Ma) may correspond with the major glaciation during MIS 16 (0.68-0.63 Ma). Proxy records covering glacial periods from the Timor Sea and Sundaland have been interpreted as indicating a drier climate with a substantial reduction in precipitation (van der Kaars, 1991, 1998, van der Kaars et al., 2000, De Deckker et al., 2003, Hesse et al., 2004). The impact of glacial climate might be equated with the impact of periodic drought driven by El Niño–Southern Oscillation (ENSO) in modern tropical vegetation, although occurring for a prolonged period of time. Lower precipitation, humidity and a weaker monsoon strength at a periodic drought have restricted forest expansion by reducing tree growth as well as providing more room for grassy vegetation to expand (Lehmann et al., 2011, Lehmann et al., 2014).

Not only causing higher rates of tree mortality and biomass loss (Phillips et al., 2009), drought driven by prolonged drying climate also increases the susceptibility of vegetation to fire (Dennis, 1999, Cochrane, 2003). Reciprocally, the occurrence of grassy vegetation may also invade a heathland promoting fires (Bond, 2005). Therefore fires can also be considered as a control on vegetation. Fire controls the distribution of forest and savannah vegetation by removing large amounts of plant biomass unselectively, including parts that are not consumed by herbivores, as well as changing soil moisture and nutrition (Bond, 2005). Under dry climate, grasses would be more likely to succeed vegetation regimes in the ecosystem following fire. In this case, the presence of fire could have promoted the persistence of grassy vegetation on the landscape. Many present-day fires are induced by human activity. However, it is difficult to prove whether the insular hominins that inhabited the So'a Basin through the indicated period also played the same role in inducing fire as modern humans do. Furthermore, it is implausible to examine the presence of fire during the Early-Middle Pleistocene ecosystem in the So'a Basin relying on the isotopic and palynological data

alone. Additional analysis (i.e. charcoal and elemental carbon) is needed to examine the temporal shifts in the occurrence of fire in this context.

Additionally, the feeding behaviour of Stegodon florensis as a megaherbivore might have contributed to the dominance of grassy vegetation in the past So'a Basin landscape. S. florensis might have had a similar feeding behaviour as its modern megaherbivore equivalent, such as Asian and African elephants. Modern elephants commonly uproot small trees and bushes, which on a large scale can regulate tree population at a low density (Dublin et al., 1990, Sukumar, 1990, Dublin, 1995, Cumming et al., 1997, Blake, 2003, Midgley et al., 2005, Campos-Arceiz and Blake, 2011). With a large body mass and a large population, S. florensis could have had a palaeoecological role in maintaining the landscape cleared from the canopy, moreover, due to the small roaming area on the island.

For the earliest S. florensis record from the LFI at ~1 Ma, both mixed feeder and grazer individuals were present. This time might represent the vegetation turnover from a habitat of mixed C_3-C_4 plant, to a more grass-dominated habitat. The mixed feeder individuals may represent earliest insular S. florensis population, which uproot small C_3 trees and bushes, when C_3 plants were more abundant might have subsequently kept the landscape clear of canopy coverage, while the grazer individuals may already have adapted to a full grassy diet. However, it is difficult to test this speculation for the early fossil record from the LFI, since the distinction between mixed feeder and grazer individuals does not correspond to different stratigraphic positions of the specimens.

The analysis of avifauna (Meijer et al., 2015), mollusc content (Brumm et al., 2016) as well as pollen and phytolith content (van der Kaars, pers. comm. to van den Bergh) of the late Early to early Middle Pleistocene So'a Basin suggest the presence of a strong open, freshwater component in a savannah-type biome. The lithology of the Sandstone Member is indicative of a fluvio-lacustrine environment (Suminto et al., 2009, Brumm et al., 2016). The result of oxygen isotope analysis does not necessarily indicate the type of water-body as a source of drinking water, yet it provides the information that the conditions affecting drinking water changed over the time period covered by S. florensis.

The $\delta^{18}O$ values of the S. f. florensis did not significantly change for ~200 ka during their occupation in the LFI and MFI, suggesting that conditions affecting the $\delta^{18}O$ values of drinking water remained relatively stable for the time covered by the two populations. Alternatively, their source of drinking water did not change, which is less likely. However, the values significantly increase in both S. florensis and murine rodent fossils from the UFI. Again, climate factor could be one of the causes of this significant change, since the timing of this fossil interval coincides with the onset of the change of the Earth's orbital perturbation from the 41 ka obliquity to the 100-ka eccentricity prolonged glaciation cycles, which marked an increase in prolonged glaciation and a dry climate (Clemens and Tiedemann, 1997, Raymo et al., 1997). Markedly, enrichment of ^{18}O in the source of drinking water would be more intense under a prolonged drier climate. The increasing $\delta^{18}O$ values of S. florensis from the UFI is similar to the S. sondaari population from the lower fossil layer, which despite the change in $\delta^{18}O$ values, their feeding behaviour does not change. As for the S. florensis population, which preferred a C_4-dominated food, the shift into a dryer climate might not be a problem, since the availability of their preferred food sources was still sustained.

The postulated existence of a lake within the Welas Caldera, following the eruptive activity, as interpreted from the lithology of the fossil-bearing layers within Excavation 32 (Brumm et al., 2016), might have also contributed to the enrichment of ^{18}O in the potential drinking water. The presence of the lake would have increased the $\delta^{18}O$ values, as evaporation in hot tropical environments causing water to become enriched in ^{18}O, especially when it occurred during a dry glacial period. If the ^{18}O-enriched caldera lake water inundated the river that flowed passing the So'a basin and became a principal source of herbivore drinking water, the $\delta^{18}O$ values in the mammal tissues and teeth would increase correspondingly. As the $\delta^{18}O$ values of two mammalian taxa (S. florensis and murine rodents) found in the UFI are increasing in comparison to the MFI, the $\delta^{18}O$ data may provide additional support for the postulated existence of a lake in the caldera.

Lower $\delta^{18}O$ values in semi-aquatic crocodiles compared to fully terrestrial fauna elements are as expected, since their bioapatite oxygen isotopic values were not enriched much from the actual isotopic values of the water bodies in which they live (Bocherens et al., 1996, Clementz et al., 2008). In addition, a wide range of $\delta^{18}O$ values

in crocodiles is explained as due to the faster regeneration of teeth during shorter time periods as compared to mammals. Hence, teeth growing during different seasons would give different isotopic values. This wide range also suggests that the seasonal variation in rainfall, like the present, also occurred in the past.

From the Late Pleistocene sediments in Liang Bua, based on the diversity of avifauna, Meijer et al. (2013) suggested that the surrounding environment of the cave was floristically diverse and included several habitat types, from wetland and forested habitats to drier grassland and scrubland. The age of the sediment containing S. florensis insularis corresponds with penultimate interglacial (MIS 5), which is expected to have been warmer, more humid, and more suitable for the growth of more dense vegetation. However, based on the $\delta^{13}C$ values, the overall feeding behaviour of Stegodon florensis insularis from below Layer T1 in Liang Bua indicates a C_4-dominant diet, with an exception of two juvenile individuals that correspond with a mixed C_3-C_4 diet. This implies that S. florensis insularis by this time was a highly specialized grazer and much preferred feeding on C_4 plant, although softer and more nutritious C_3 plant were also available in their habitat.

Westaway et al. (2009b) and Meijer et al. (2013) are in agreement that freshwater bodies, such as a river, a lake and/or marshes/swamps, were present in the habitat. As the age of the sediment containing Stegodon florensis insularis corresponds with the penultimate interglacial (MIS 5), the significantly higher $\delta^{18}O$ values of the Liang Bua population compared to the predecessor population from the So'a Basin does not necessarily indicate that more arid conditions occurred during this period. The high $\delta^{18}O$ values of S. florensis insularis may indicate that this population primarily relied on more evaporated lake or swamp water as their drinking water source.

The single adult individual from the Black Tuff Layer, which marks the last recorded occurrence of S. florensis, is expected to have higher $\delta^{13}C$ value since its age corresponds with a collapse in vegetation around ~68 ka (Scroxton et al., 2016). However, this sample does not show any significant difference in $\delta^{13}C$ and $\delta^{18}O$ values compared to samples originating from the underlying layers. Since the age of the horizon corresponds with the assumed arrival of modern humans in the region it is possible that the extinction was caused by modern humans, but as yet no definitive proof exists for this hypothesis (Sutikna et al., 2016).

As shown in the result of ontogenic age-based analysis, despite no significant difference in measured $\delta^{13}C$ values among ontogenic age-based groups of S. f. insularis, there appears to be a slight increase in the ranges of $\delta^{13}C$ with increasing ontogenic age to more positive values. So far, to my knowledge, there is no study available of ontogenic age-related carbon isotope ratios in large terrestrial mammals. However, an explanation for carbon isotope offsets can be compared with the isotopic fractionation between females and their offspring for marine and small mammals. In these groups, the lowest $\delta^{13}C$ values are observed in those dental elements that developed prior to birth. This is due to a depletion of ^{13}C carbon in the offspring compared to the mother's tissue, as suggested by Sare et al. (2005) based on the isotopic measurements in Clethrionomys gapperi. In dental elements growing after birth, the intermediate $\delta^{13}C$ values in the molars that developed during the lactation/pre-weaning period are caused by the mixing of isotopic signals of milk from the mother and of the individual's own forage. As suggested by Habran et al. (2010), the carbon isotope value in Mirounga angustirostris (elephant seals) breast milk is depleted by ~5.6‰ relative to other tissues in the mother's body. Molars that develop after weaning reflect the adult diet. Therefore, the presence of a few individuals with lower $\delta^{13}C$ values is not indicative of a mixed C_3-C_4 diet, since these specimens were dp3s, which mineralized while still in utero.

In the case of Timor, it is difficult to produce a high resolution environmental reconstruction, due to poor stratigraphic control of most specimens. All individuals from known stratigraphic positions correspond to a C_4 diet, while the stratigraphic provenance of all individuals from the mixed feeder population is unknown, as some were obtained from locals and could be from anywhere. Morphologically, there is no difference between the in situ and unprovenanced specimens, suggesting a stable lineage. It is possible that there was a change of feeding behaviour from a mixed C_3-C_4 to a C_4 diet, corresponding with a change in habitat on Timor similar to that observed on Flores. In that case, the unprovenanced specimens are likely from the lower terrestrial interval of the Noele Formation. However, the timing of this change remains unknown. The available data suggest that after 0.8 Ma, the landscape was dominated by grassy savannah like on Flores.

Extrapolating the change in feeding behaviour of Stegodon populations in Flores to Timor, it is possible that the unprovenanced mixed feeder individuals originated from

the older sedimentary strata of the Noele Formation below the Raebia Middle Tuff at 0.81 Ma. Because the only individual known to originate from the Noele Formation (fossil layer dated younger than 0.81 Ma) is included in the C_4 grazer diet group, it can be speculated that S. timorensis had switched to a C_4 diet by this time. Since only a single specimen known to originate from the Noele Formation shows a C_4 dietary isotopic value, this might be unrepresentative. Yet another possibility could be that the change from a mixed diet to a C_4 diet on Timor was not a single transition, but could have fluctuated through time. Clearly, more local palaeoclimatic records and fossil data are required to test the various possible explanations of the observed data.

One aspect in which the Timor specimens differ in their isotopic composition from all other groups is that the measured $\delta^{18}O$ range of S. timorensis is the highest among all the species analysed. This could be the result of the geographic location of Timor, which has lower rainfall compared to other islands in this study (Jones and Harris, 2013). The relatively high $\delta^{18}O$ values correspond with both the mixed feeder and the grazer individuals, unrelated to their different ages. This suggests that relatively dry conditions prevailed on the island throughout the period covered by the sampled specimens.

The ancestor of S. sumbaensis is probably similar to S. sondaari, or could have been S. sondaari that migrated from Flores. The timing of the first immigration to the island is unknown. The first occurrence of this species is estimated from the extrapolated age of the Lewapaku site, and is thought to be around 1 Ma. The Sumba pygmy Stegodon seemingly survived until the Late Pleistocene, as suggested by the age estimate of the S. sumbaensis type mandible from the Watumbaka Site. Since the isotopic data for pygmy Stegodon sumbaensis was measured from a single specimen, any inferences regarding its feeding habits need to remain tentative. It is interesting to note however, that the isotopic value of this Early Pleistocene individual falls within the S. sondaari $\delta^{13}C$ range, also of Early Pleistocene age. This adds further support to the hypothesis that a regional change towards drier climatic conditions and a more open vegetation may have occurred around 1Ma.

Based on the overall dietary isotopic results, it can be proposed that generally open vegetation dominated habitats within the LSI over the period covered by the analysed samples. Savannah-type vegetation also covers a substantial proportion of the modern

LSI landscape (Dennis, 1999). Canopy coverage sporadically occurs in certain periods on each island, especially during the Early Pleistocene to early Middle Pleistocene, as suggested by the presence of mixed feeder populations and/or individuals. However, closed canopy forest habitat never become dominant in the LSI at least during the period covered by the analysed samples. Unlike Java and probably Sulawesi, where closed canopy forest dominated the habitat during the Early Pleistocene and Late Pleistocene-Holocene, the climatic conditions in the LSI were relatively dry throughout the late Early to the Late Pleistocene. The driest conditions prevailed in Timor. The last appearance of any Stegodon species in the LSI is dated to ~100-60 ka (MIS 5-4). The timing of Stegodon species extinction corresponds with the early immigration of modern humans to the LSI, at least for Flores. Therefore, the arrival of modern humans could be one of, if not the main cause of the Stegodon extinction in the LSI.

6.6 Conclusion

The earlier proboscidean occupants of the LSI are represented by pygmy Stegodon species (S. sondaari, S. sumbaensis and S. timorensis). The timing of the first immigration and colonization are unknown for each island, but it is likely that the ancestral population of these pygmy Stegodon arrived much earlier than their first appearance in the fossil record. The oldest well-secured occurrence is known from the Soa Basin, Flores, dated at 1.4 Ma. The last occurrence of the pygmy Stegodon sondaari in Flores is dated at 1.27 Ma, after which it is replaced by a medium-sized species, Stegodon florensis sometime between 1.27 and 1 Ma. The S. florensis record continues up to ~50 ka. Its youngest occurrence is documented in Liang Bua. The latest known population from Liang Bua had become reduced in size compared to its ancestor from the So'a Basin. The oldest Stegodon occurrence on Timor is recorded from the Noele Formation, which dated at ~0.81 Ma, while its last occurrence is known from the unconformably overlying alluvial terrace, which are presumably younger than 130 ka. The Stegodon recorded from Sumba is of a pygmy size. Its first and last occurrence extrapolated from the sites' elevations and the mean uplift rate, providing an age estimation of ~1 Ma and ~125 ka, respectively.

The carbon isotopic values of Stegodon sondaari show it as a mixed feeder, suggesting that between 1.4 and 1.27 Ma, variety of vegetation types, ranging from woodland to wooded grassland might have covered the palaeohabitat of the So'a Basin. The wide range of $\delta^{18}O$ values suggests a strong seasonality during the time range covered by S. sondaari.

The earlier population of S. florensis from ~1.0 to 0.9 Ma intervals show a range of mixed C_3-C_4 to pure C_4 diets, suggesting a more open vegetation feeding habitat such as woodland to savannah. A significant increase in the $\delta^{13}C$ values of the subsequent population indicate reduction of C_3 vegetation and greater C_4 consumption, which could be tied to increasingly arid conditions towards the Middle Pleistocene. S. florensis remained predominantly a grazer up to its last recorded occurrence in the So'a Basin. A significant increase of the $\delta^{18}O$ values for the S. florensis population from the UFI suggests either further drier conditions between 725 and 650 ka, or a shift in main drinking water source from fluvial to lacustrine source during the later development of the basin, or a combination of both. The postulated nearby lake in the Welas Caldera may have been their dominant water source during the UFI. The population of fauna yielded from the UFI marked the last occurrence of the vertebrate fossil fauna in the Soa Basin. Due to the unavailability of fossil findings from the younger interval, it is uncertain whether vertebrate fauna stayed or migrated out from the Soa Basin following the changes in palaeoenvironment. The younger occurrence of S. florensis is represented by the S. f. insularis from Liang Bua, aged between 120 and 50 ka. The even smaller bodied successive sub-species S. f. insularis from Liang Bua remained predominantly grazers.

The isotopic analysis of different ontogenic age groups of Stegodon florensis insularis from Liang Bua shows a slight increase in the ranges of $\delta^{13}C$ with increasing ontogenic age to more positive values. The lower $\delta^{13}C$ values of pre-adult individuals may be caused by the mixing of isotopic signals of milk from the mother, which is more depleted in ^{13}C, and of the individual's own forage.

All Stegodon timorensis individuals from known stratigraphic positions correspond with a C_4 diet, while the stratigraphic provenance of all individuals with mixed-feeder isotope signatures is unknown. The occurrence of the two feeding ranges suggests that a change in feeding behaviour from a mixed C_3-C_4 to a C_4 diet might have occurred,

corresponding with a change in habitat on Timor around the same time as the one observed on Flores after ~1 Ma. The consistently high $\delta^{18}O$ values of S. timorensis suggest that the driest conditions of all the studied islands occurred in Timor. The carbon and oxygen isotopes of the only S. sumbaensis specimen suggest a mixed feeding behaviour for this species. The inferred age of the specimen is thought to be ~1 Ma, suggesting that on Sumba conditions were more humid around that time, as is documented for Flores.

Chapter 7. $^{87}Sr/^{86}Sr$ analysis (An indicator for migratory movements and size of roaming area: preliminary result)

7.1 Fossil materials and bedrock geology of studied areas

The island of Java and Flores were selected in this preliminary study of $^{87}Sr/^{86}Sr$ analysis due to the availability of more comprehensive stratigraphic and dating data. For selected species from Java and Flores, the usefulness of the $^{87}Sr/^{86}Sr$ values of fossil bioapatite to estimate the migratory movements and size of roaming area was investigated. An individual that has the $^{87}Sr/^{86}Sr$ ratio similar to its surrounding lithology, most likely did not travel long distances to get its food, and vice versa. By the same token, small mammals as well as invertebrates are better in representing the locally bioavailable $^{87}Sr/^{86}Sr$ ratio, since these taxa normally have limited roaming areas (Hoppe et al., 1999, Bentley, 2006, Tütken and Vennemann, 2009, Maurer et al., 2012, Tütken, 2014).

The $^{87}Sr/^{86}Sr$ ratio in the substrate lithology is distinguished by lithological type and geologic age. The older the rock, the higher the $^{87}Sr/^{86}Sr$ would be, and vice versa. As an example, old crustal rocks have a high $^{87}Sr/^{86}Sr$ of 0.711 and young mantle-derived volcanic rocks have ratios around 0.703. Meanwhile, marine carbonates have intermediate values of 0.707 to 0.709 depending on their geological age (McArthur et al., 2001. See Chapter 2 for further explanation of $^{87}Sr/^{86}Sr$ ratios).

From Java, samples analysed for Sr isotope ratios are: Stegoloxodon indonesicus (n = 2) and Sinomastodon bumiajuensis (n = 2) from the Kaliglagah Formation in Semedo, Stegodon trigonocephalus (n = 2) and Elephas hysudrindicus (n = 2) from the Bapang Formation in Sangiran and an Elephas hysudrindicus from a terrace deposit in Sunggu. The exact stratigraphic position of Sl. indonesicus and Sm. bumiajuensis are unknown. However, based on biostratigraphic grounds these specimens most likely originated from the Lower Pleistocene. The S. trigonocephalus and E. hysudrindicus specimens from Sangiran were recovered from the fossil layers in the Bapang Formation, while

another E. hysudrindicus specimen was recovered from a late Middle Pleistocene terrace deposit in Sunggu (see Chapter 4).

From Flores, ten enamel samples for strontium analysis were taken from four successive fossil localities: Tangi Talo (~1.4 Ma), Kobatuwa (~1 Ma) and Mata Menge (~0.7-0.8 Ma) from the So'a Basin and Liang Bua (~60 ka). The enamel samples consist of Stegodon sondaari (n = 2) from Tangi Talo, Stegodon florensis florensis from Mata Menge (n=1) and Kobatuwa (n=1); crocodile (n = 2) and murine rodents (n = 2) from Mata Menge, as well as Stegodon florensis insularis (n = 2) from Liang Bua. In addition, a soil sample from the Middle Fossil-bearing Interval (MFI, ~0.88 to 0.8 Ma) at Mata Menge was analysed for local $^{87}Sr/^{86}Sr$ bioavailability of the So'a Basin.

The lithology of all fossil-bearing sediments selected for strontium isotope analysis in Java consists of terrestrial deposits derived from, or a mixture of carbonate and volcaniclastic sediments deposited in marine-terrestrial transitional environments, overlying older marine sediments (Fig. 7.1). The lithology of fossil-bearing sediments at Semedo (the Kaligagah Formation, see Chapter 4 for description of the lithostratigraphy of Semedo) comprises a sequence of fine-grained lithologies deposited under a fluvio-lacustrine, near-shore environment. It is thought that during the occupation of Stegoloxodon indonesicus and Sinomastodon bumiajuensis, vegetation covered the weathered Kalibiuk, Halang, Kumbang and Tapak Formations, which comprise carbonate sediments and submarine volcaniclastics (Djuri et al., 1998), or on emerged parts of the Kaliglagah Formation itself.

In Sangiran, Stegodon trigonocephalus and Elephas hysudrindicus are two Elephantoidea species that commonly co-occurred in the faunal assemblage during the Middle Pleistocene. The analysed specimens were recovered from the fossil layers located between the Middle Tuff and Upper Tuff layers of the Bapang Formation, thus the age of the sediment is estimated at between 0.78 and 0.71 Ma (Suzuki et al., 1985, Hyodo et al., 1993). The underlying lithology of the Middle Pleistocene of Sangiran and its surrounding areas is alternated between volcaniclastic and marine-terrestrial transitional lithologies (Sangiran and Bapang Formations), while the lithology of the Pre-Middle Pleistocene is dominated by marine marls and limestones that were deposited before the emergence of Java above sea level (i.e. Puren and Kerek Formations). South of Sangiran, the lithology is dominated by Quaternary

volcaniclastics, as well as Neogene volcaniclastic and various marine sediments (Surono et al., 1992). The nearest dominant calcareous marine lithology sources are located more than 50 km to the north and northeast (Sukardi and Budhitrisna, 1992).

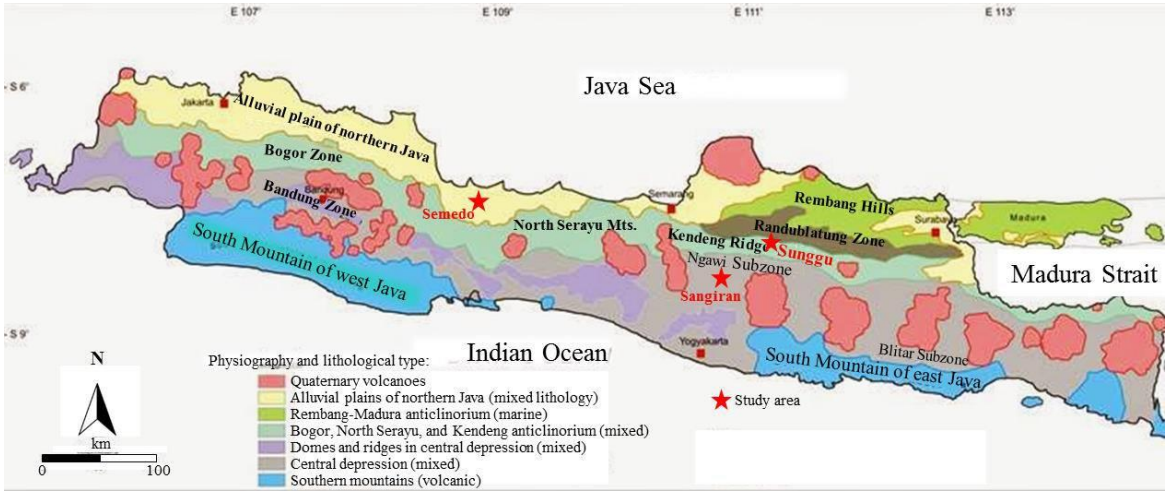

Figure 7.1 Map of physiography and indicated lithological type of Java (modified after Darman, 2014). Physiographic zones are based on van Bemmelen (1949).

Considering the lithological characteristics of Semedo and Sangiran, the local $^{87}Sr/^{86}Sr$ bioavailability of both localities during the occupation of the faunas is expected to be a mixture between the volcanic and marine ratios. Since the location of carbonate-dominated areas are either further north or south, while volcanic bedrock sources (Old Andesite) located further south from the investigated fossil localities, individuals with low or high $^{87}Sr/^{86}Sr$ ratios would be considered to have a wider roaming area.

The fossil-bearing layer at Sunggu is a terrace deposits that consists of unconsolidated sandstone and conglomerate with mixed volcaniclastic-limestone fragments, dated at 165 ka, and unconformably overlying marine marls of the Kalibeng Formation. Due to the uplift of the Kendeng Hills during the Middle Pleistocene, various sediments dominated by marine carbonate lithology, such as the Tambakromo/Lidah, Selorejo, Mundu, Kalibeng, and Ledok Formations, are exposed at the surface up to 60 km to the north of the fossil locality. The nearest volcaniclastic bedrock at the time probably formed part of exposures of the Pucangan and Kabuh Formations ~15 km to the south (Datun et al., 1996). Old rivers, either in West Java and East Java, which may be

potential sources of drinking water of the studied faunas of Java, were flowing through diverse types of lithologies, thus the strontium isotope ratios from drinking water would be somewhat between those of the marine carbonate and volcanic signals.

The two fossil localities in Flores have distinct lithologies (Fig. 7.2; see Chapter 6 for a more detailed stratigraphy of the analysed localities). The lithology of the So'a Basin is dominated by Early-Middle Pleistocene volcaniclastics and primary volcanics. The source area of marine carbonate that was probably exposed during the Early to Middle Pleistocene is located north and east of the So'a Basin. Therefore, local dwellers are expected to have low $^{87}Sr/^{86}Sr$ ratios that reflect local volcanic bedrocks, while individuals that roamed further away from the taphonocoenosis would have yielded higher strontium isotope composition from the marine carbonate lithologies. In contrast, the underlying lithology of cave sediments and the surrounding areas of Liang Bua consists of the Late Miocene-Pliocene marine carbonates (the Waihekang Formation), thus the local bioavailable $^{87}Sr/^{86}Sr$ ratio is expected to show a high value that reflects this marine carbonate. However, areas underlain by the Miocene to Early Pleistocene Nangapada Formation, Kiro Formation and quartz diorites surround the fossil locality (Koesoemadinata et al., 1994), so that animals did not have to travel far to engage a lower $^{87}Sr/^{86}Sr$ ratio from the weathering of volcanic rocks.

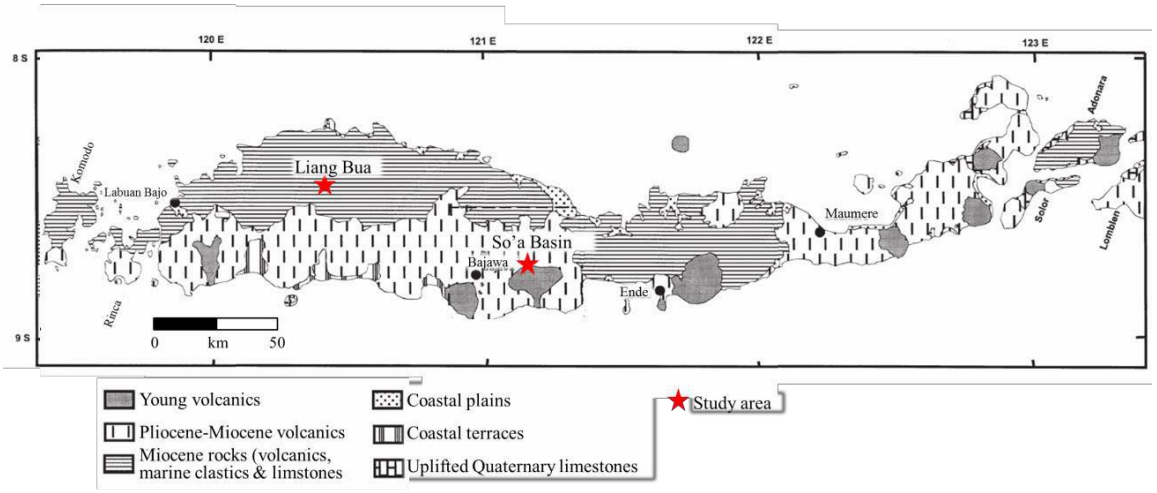

Figure 7.2 Simplified geological map of Flores, showing types of lithology of study areas and their surrounding (modified from van den Bergh, 1999)

As a part of Sundaland, the floor of the Java Sea would have been exposed during the Quaternary low sea-level stands, thus a higher $^{87}Sr/^{86}Sr$ ratio might also occur due to

feeding on plants that had grown on the now-drowned Java Sea bottom. Flores on the contrary, is surrounded by deep oceanic basins, and sea-level fluctuations would have less influenced $^{87}Sr/^{86}Sr$ ratios in terrestrial herbivores. The oldest lithologies exposed in Java and Flores are predominantly from the Neogene, thus the change in $^{87}Sr/^{86}Sr$ ratios due to different geological ages ^{87}Sr ingrowth can be ignored (see explanation of $^{87}Sr/^{86}Sr$ ratios for different age in the Chapter 2).

7.2 Results

The $^{87}Sr/^{86}Sr$ ratios of all analysed samples are presented in Table 7.1 and Figure 7.3. In Figure 7.4, the $^{87}Sr/^{86}Sr$ ratios of all samples are coupled with their $\delta^{13}C$ values to detect whether the individuals' roaming areas were affected by a difference in diet. All $^{87}Sr/^{86}Sr$ ratios of samples from Java cover a narrow range between 0.70611 and 0.70737. The lowest ratio was measured in both Stegodon trigonocephalus samples from Sangiran. Interestingly, the two Sinomastodon bumiajuensis samples from Semedo show the largest difference, as their bioapatite $^{87}Sr/^{86}Sr$ ratios are the lowest and highest among all analysed samples from Java (0.70731 and 0.70611, respectively). The strontium isotope compositions of all three Elephas hysudrindicus samples correspond with the upper range of Java samples (between 0.70685 and 0.70734), suggesting a strong influence of marine carbonate. The $^{87}Sr/^{86}Sr$ ratios of the two Stegoloxodon indonesicus samples are in the intermediate range of all Java samples (0.70638 and 0.70653).

The carbonate concretion from Mata Menge has a low $^{87}Sr/^{86}Sr$ ratio of 0.70527, representing the local bedrock of the So'a Basin. Bioapatite $^{87}Sr/^{86}Sr$ ratios of all vertebrate taxa originating from the So'a Basin cover a range between 0.70509 and 0.70567 (Table 7.1 and Figure 7.1), which closely resembles the ratio of the local strontium bioavailability. The crocodile and murine rodent individuals excavated from the upper fossil-bearing interval (Excavation 32) have $^{87}Sr/^{86}Sr$ ratios that are slightly lower than the soil sample. The $^{87}Sr/^{86}Sr$ ratios of the two crocodile individuals have similar ratios of 0.70510 and 0.70509, while the $^{87}Sr/^{86}Sr$ of the two murine rodents are practically identical (0.70507 and 0.70509). The Stegodon florensis florensis excavated from the same fossil layer as the crocodile and murine rodents yielded a slightly higher

$^{87}Sr/^{86}Sr$ ratio of 0.70524, although not significantly distinct. A slightly lower $^{87}Sr/^{86}Sr$ ratio of 0.70504 was obtained from the S. f. florensis individual excavated from the lower fossil-bearing interval (LFI) at Kobatuwa. The two Stegodon sondaari samples from Tangi Talo yielded $^{87}Sr/^{86}Sr$ ratios of 0.70567 and 0.70513, which also closely resembles the ratio of local Sr from the overlying sediments. In contrast, the $^{87}Sr/^{86}Sr$ ratios of the two specimens from Liang Bua (0.70612 and 0.70774), are higher than all samples from the So'a Basin.

Table 7.1 Strontium isotope composition ($^{87}Sr/^{86}Sr$) of analysed samples

sample number	taxon	material	locality	age	$^{87}Sr/^{86}Sr$	$\delta^{13}C$
Blora-17	Elephas hysudrindicus	enamel	Sunggu	165 ka	0.70734	-12.7
Nge 2	Elephas hysudrindicus	enamel	Sangiran	~700 ka	0.70716	-2.6
Nge 3	Elephas hysudrindicus	enamel	Sangiran	~700 ka	0.70685	0.1
Myr 1	Stegodon trigonocephalus	enamel	Sangiran	~700 ka	0.70621	0.1
Nge 1	Stegodon trigonocephalus	enamel	Sangiran	~700 ka	0.70613	0.2
DK 145	Sinomastodon bumiajuensis	enamel	Semedo	Early Pleistocene	0.70737	-1.0
DK 146	Sinomastodon bumiajuensis	enamel	Semedo	Early Pleistocene	0.70611	-1.9
SMD 1050	Stegoloxodon indonesicus	enamel	Semedo	Early Pleistocene	0.70653	-12.8
SMD 1063	Stegoloxodon indonesicus	enamel	Semedo	Early Pleistocene	0.70638	-13.8
LB04/XI/46/456	Stegodon florensis insularis	enamel	Liang Bua	100-50 ka	0.70774	2.1
LB08/XVI/70/3631	Stegodon florensis insularis	enamel	Liang Bua	100-50 ka	0.70612	0.8
KBT11-T1/II	Stegodon florensis	enamel	Kobatuwa	1020-880 ka	0.70510	-5.5
MM14-32B-74	Stegodon florensis	enamel	Mata Menge	~700 ka	0.70524	1.3
MM13-32-237	crocodile	tooth	Mata Menge	~700 ka	0.70510	-2.0
MM13-32-266	crocodile	tooth	Mata Menge	~700 ka	0.70509	0.1
MM13-32-222	murine rodent	incisor	Mata Menge	~700 ka	0.70507	1.6
MM13-32-240	murine rodent	incisor	Mata Menge	~700 ka	0.70509	1.6
SC5	-	concretion	Mata Menge	880-800 ka	0.70527	n/a
TT13-H-71	Stegodon sondaari	enamel	Tangi Talo	1.4 Ma	0.70567	-6.4
TT13-H-91	Stegodon sondaari	enamel	Tangi Talo	1.4 Ma	0.70513	-7.3

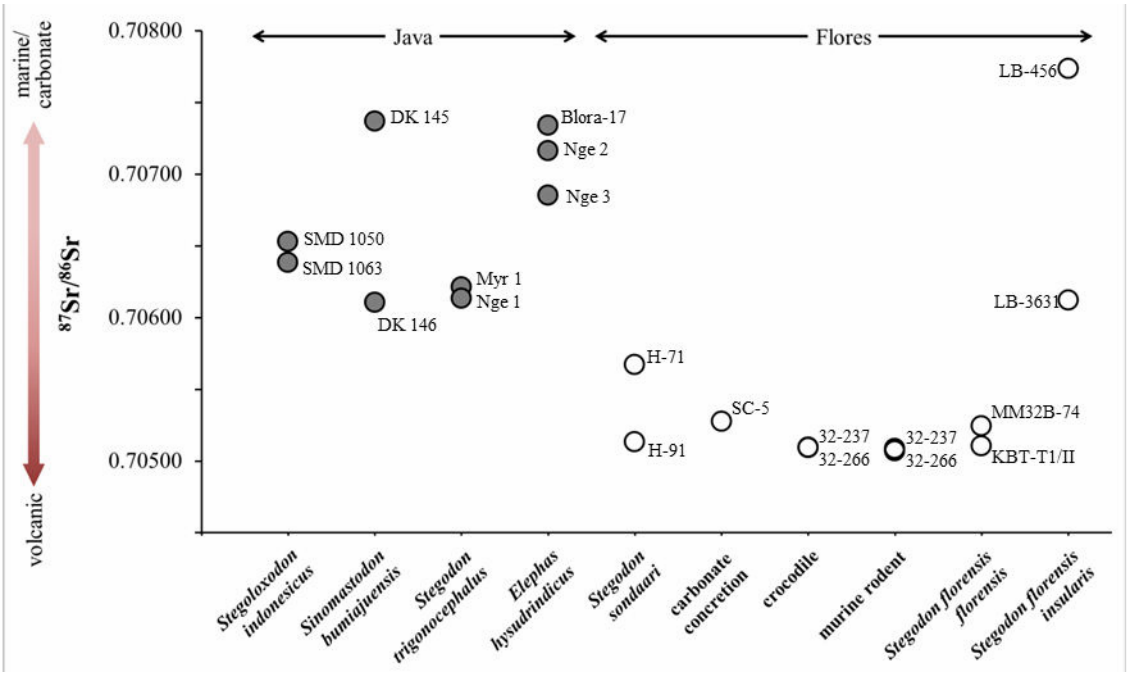

Figure 7.3 $^{87}Sr/^{86}Sr$ isotope composition of analysed samples from Java and Flores.

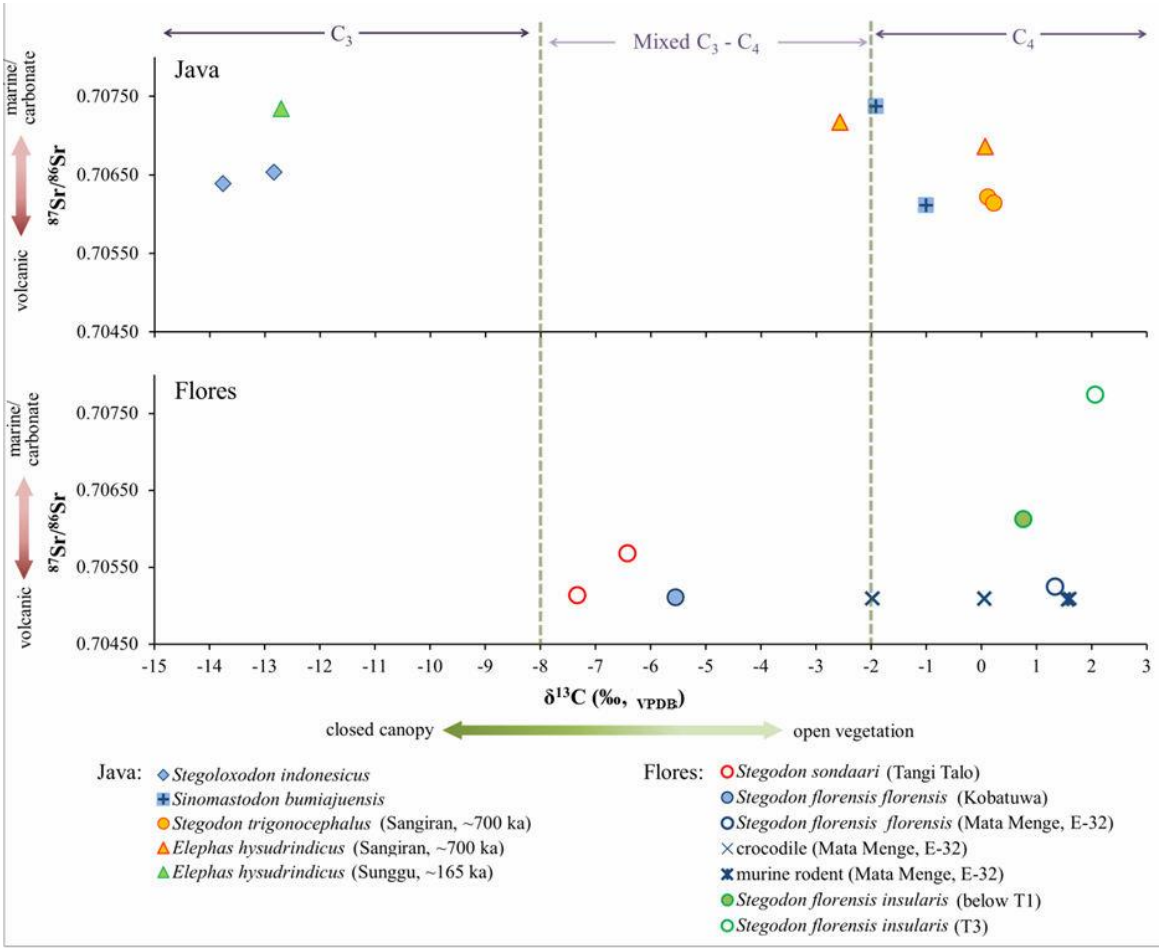

Figure 7.4 $\delta^{13}C$ (‰, VPDB) and $^{87}Sr/^{86}Sr$ values of fossils and a carbonate concretion from Java and Flores.

7.3 Discussion

7.3.1 Java

All samples from Java have $^{87}Sr/^{86}Sr$ ratios that are consistent with an expected ratio for herbivores that foraged on vegetation overlying a mixture of volcanic and marine carbonate bedrocks, or on carbonate dominated bedrocks. Even the lowest $^{87}Sr/^{86}Sr$ ratios among the analysed samples from Java are still too high for a strontium isotope composition indicative solely of volcanic bedrocks.

The $^{87}Sr/^{86}Sr$ of Stegoloxodon indonesicus would be indicative for mixed marine and volcanic substrates. Hence, at the time S. indoncesicus dwelled in the forested landscape around Semedo, its range included both marine and volcanic substrates. During the occupation of this species in the Early Pleistocene, Java was probably smaller than at present, and thus the roaming area of his species probably was more limited.

The high $^{87}Sr/^{86}Sr$ of one Sinomastodon bumiajuensis individual (DK 145) from Semedo corresponds with the value expected for predominantly marine carbonate lithology, suggesting that the individual foraged specifically over carbonate substrates. In contrast, the lower $^{87}Sr/^{86}Sr$ ratio of DK 146 is indicative for mixed volcanic and carbonate lithologies, which is consistent with the presumable exposed substrate of the thanatocoenosis. The large difference of the $^{87}Sr/^{86}Sr$ ratios between the two S. bumiajuensis individuals suggests that these two individuals probably lived on different exposed bedrocks during different periods. Alternatively, the individual with the higher $^{87}Sr/^{86}Sr$ ratio probably migrated further away from the taphonocoenosis. Possibly, the individual with the higher $^{87}Sr/^{86}Sr$ ratio could have lived during a period of low sea-level when the Java Sea floor was exposed, allowing the herbivores to roam and feed over the exposed sea floor while picking up the strontium signal from marine sediments. However, the distinct Sr isotope composition between the two Sinomastodon bumiajuensis individuals is not positively correlated with a distinct dietary preference, which was C4 grass for both individuals (Figure 7.2). The distinct $^{87}Sr/^{86}Sr$ ratio between the two individuals suggests that the open grassland environments prevailed on Java during the Early Pleistocene, regardless of the exposed bedrocks.

The two Stegodon trigonocephalus samples from Sangiran have similar $^{87}Sr/^{86}Sr$ ratios of 0.70613 and 0.70621, suggesting that the individuals were also foraging over both volcanic and marine carbonate lithologies. Like Sinomastodon, these individuals possibly were local residents that did not migrate far from the taphonocoenosis. On the other hand, the $^{87}Sr/^{86}Sr$ ratios of E. hysudrindicus, originating from the same fossil-bearing interval, are 0.70685 and 0.70715, which is slightly higher than the assumed local bioavailability of Sangiran. This result suggests that the individuals presumably migrated and roamed to the areas dominated by marine carbonate substrates. Considering that the amount of Stegodon fossil findings outnumbers those of Elephas, Stegodon must have been more dominant in the palaeohabitat at around Sangiran. Thus, suggesting that E. hysudrindicus was probably migrating further away from its taphonocoenosis and roaming more widely to avoid competition with S. trigonocephalus over the same food resource. However, they might occasionally remigrate to Sangiran during more favourable seasons.

The time interval during which the Bapang Formation sediments were deposited included a low sea-level stand of to 100 m below present day sea-level between 800 and 720 ka, and up to 90 m at 750 ka (Bintanja et al., 2005, de Boer et al., 2010), when the floor of the Java Sea must have been exposed. The Kendeng Hills that contain marine lithologies were not yet uplifted during this stage. Therefore, herbivores, including these E. hysudrindicus individuals, probably roamed further away up to carbonate substrates on the exposed floor of the Java Sea and acquired a partly marine signal from their food. The difference in strontium isotope composition in both species that share similar feeding preferences as C_4 grazers (Figure 7.2) further suggests that open vegetation seemed to dominate the habitats during the Middle Pleistocene, regardless of the difference in substrate.

In addition, the E. hysudrindicus specimen from Sunggu, which –as a C_3 browser– had a different feeding preference than its predecessor from the Bapang Formation, was also analysed. The $^{87}Sr/^{86}Sr$ of this specimen is 0.70734, which is highest among all samples from Java. This ratio is indicative for feeding on marine carbonate substrates. Since the taphonocoenosis of this individual is surrounded by marl of marine origin, the Sr isotopic ratio of the Sunggu specimen could easily represent the direct surroundings during the Late Pleistocene.

7.3.2 Flores

The value of local $^{87}Sr/^{86}Sr$ ratio bioavailability is represented directly by one soil sample and indirectly by an aquatic vertebrate (crocodile) and small mammals (murine rodent) all originating from the site Mata Menge. The low $^{87}Sr/^{86}Sr$ of these samples reflects Sr input from the weathering of the Early Pleistocene andesitic breccias of the Ola Kile Formation and volcaniclastics of the andesitic/rhyolitic Tuff Member and andesitic/basaltic Sandstone Member of the Ola Bula Formation (see Chapter 6 for lithological description). The $^{87}Sr/^{86}Sr$ ratio of the underlying Tuff Member and the overlying layers of the Sandstone Member would have given more or less similar values, since these lithologies are derived from the same tectonic and volcanic source. The $^{87}Sr/^{86}Sr$ ratios of two Stegodon florensis individuals are consistent with the values of local dwellers and the overlying sediment (represented by the soil sample), although both have slightly different ages. This result suggests that the S. f. florensis individuals were rather local dwellers of the So'a Basin and its surrounding areas, or at least only roamed on the area with volcanic bedrock surfaces and not the marine lithologies to the North of the So'a Basin.

The two Stegodon sondaari samples also have low $^{87}Sr/^{86}Sr$ ratios that are consistent with the locally derived soil sample and all analysed vertebrate samples from the overlying sediments, suggesting that these individuals foraged on the bedrock surface composed of local volcanic lithologies. A slightly higher value compared to the overall So'a Basin specimens was obtained from one of the S. sondaari individuals (TT-H-71). This could signal that the individual acquired a minor marine signature from the exposed marine-volcanic lithologies further north and east of the taphonocoenosis.

In contrast, the enamel samples of Stegodon florensis insularis derived from the cave deposit of Liang Bua yielded higher values compared to the So'a Basin specimens. The measured ratios of the two analysed specimens are 0.70612 and 0.70774, respectively. The value of 0.70774 would be consistent with animals foraging on a purely marine carbonate bedrock surface with more elevated bioavailable $^{87}Sr/^{86}Sr$, thus this individual can be considered as a local inhabitant, at least during the period of development of the analysed molar, which lasted for approximately a year. However, the ratio of the second individual is too low to be considered as an individual that foraged on purely marine carbonate, and is rather consistent with a mixture of volcanic and carbonate lithologies.

Therefore, this individual might have travelled further up to the surrounding area where the Miocene Nangapada Formation, Kiro Formation and quartz diorites intrusion were exposed.

Apparently, diet preferences of these individuals did not show a strong correlation with migratory behaviour and roaming area of the analysed individuals, and appear to be related to their age. In the case of S. f. florensis individuals derived from different ages (the LFI of Kobatuwa and the UFI of Mata Menge) have different diet preferences yet similar $^{87}Sr/^{86}Sr$ ratios. In contrast, the S. f. florensis and S. f. insularis from different ages have different $^{87}Sr/^{86}Sr$ ratios yet have similar diet preferences. A close similarity of $^{87}Sr/^{86}Sr$ ratios between samples and the expected ratio of the local lithology suggests that Stegodon species of Flores in general were local dwellers, or had a relatively small roaming area. The different $^{87}Sr/^{86}Sr$ ratios of grazer individuals from different ages and locations suggest that the C_4 dominated vegetation occurred multiple times in different areas on the island. However, these results should be considered as preliminary, until more $^{87}Sr/^{86}Sr$ ratios of bedrock became available.

7.4 Conclusions

The preliminary study based on the analysis of the strontium isotope composition of a number of Proboscidean species from Java and Flores, as well as reptilian and small mammals from Flores, suggests different migratory behaviour and roaming areas among individuals of analysed taxa. The result of this preliminary $^{87}Sr/^{86}Sr$ analysis is promising as it has been able to distinguish local feeders from species or individuals with wider roaming areas.

It can be concluded that migratory behaviour and roaming area are likely not correlated with diet preference of individuals. Besides, similar diet preferences, especially of grazers, of individuals that have different migratory behaviour and roaming areas suggest that C_4 expansion not only occurred locally in the taphonocoenosis, but also within the roaming areas of individuals. $^{87}Sr/^{86}Sr$ analysis of bedrocks of each fossil-bearing locality and a larger number of samples from fossil taxa would be required to provide a better reconstruction of migratory movements and the size of roaming areas of proboscidean taxa.

Chapter 8. Synthesis and recommendations for future research

8.1 Synthesis of palaeoenvironment and dietary-related evolution of Proboscidea

The aim of this research was to reconstruct the interactions between past environmental changes and the evolution of the fossilized and living Proboscidean taxa in mainland and island Southeast Asia, by analysing feeding ecology, dietary preferences and habitat preferences, utilizing stable isotope records ($\delta^{13}C$, $\delta^{18}O$ and $^{87}Sr/^{86}Sr$) from fossil and living Proboscidean tooth enamel as the main focus of this study. With an integration of the isotopic results with dental morphology, stratigraphy, as well as available geochronology and palaeoclimate data of mainland and island Southeast Asia, the reconstruction of dietary-related evolution of analysed Proboscidea taxa and palaeoenvironment of the mainland and insular Southeast Asia are synthetized below.

8.1.1 Linking the diet shift of Proboscidea with vegetation and climatic change in mainland and insular Southeast Asia

In chronological order, the stable isotope analyses from proboscidean enamel samples of mainland and insular Southeast Asia gives hints at two major vegetation changes between the Middle Miocene and present. The Middle Miocene-Early Pliocene taxa in this study substantially or exclusively exploited C_3 vegetation and inhabited dense vegetated forest to more open woodland, except for Platybelodon cf. grangeri that exclusively lived in a more open woody habitat, probably wooded grassland. Mixed C_3-C_4 feeders, started to appear only after the latest Miocene (~8 Ma), and marked an early shift of C_4 vegetation expansion in mainland Asia. The recorded time of this shift differs from ~8 in the Siwaliks to 6.5 to 4 Ma for Myanmar and Thailand regions. Subsequently, mixed C_3-C_4 and C_4 grazer taxa became dominant between the Late Pliocene and Middle Pleistocene in the analysed regions of mainland Asia. The timing of the dietary shift of proboscidean taxa from C_3-dominated to C_4-dominated plant at

mainland Asia in the latest Miocene to Early Pliocene coincided with C_4 vegetation expansion in mainland Asia (Cerling et al., 1997b, Ma et al., 1998, Sanyal et al., 2004, Jiang and Ding, 2009, (Sepulchre et al., 2010), which is thought to be mainly linked to the Asian monsoon intensification and aridification of Central Asia due to the Himalayan uplift (Zhisheng et al., 2001, Zheng et al., 2004).

In island Southeast Asia, which emerged only after the Late Pliocene/Early Pleistocene, the pattern and timing of the dietary shifts of proboscidean lineages appear differently from island to island. Java, which was intermittently connected to mainland Asia, a similar pattern of dietary change for the proboscidean lineage with those of the mainland can be recognised. The Proboscidea of the earliest Pleistocene taxa of Java exclusively consumed C_3 plants in dense forest vegetation. The occurrence of exclusive browser taxa does not seem to last long in Java, as these browsers were rapidly succeeded by mixed feeders and grazers before 1.5 Ma, which may be related to the C_4 vegetation expansion in Java, which started later than in mainland Asia, perhaps due to the delay of the island's emergence.

In contrast to mainland Asia and Java, regardless of the species and faunal assemblages, the two Early Pleistocene Proboscidean taxa of Sulawesi were either browsers, mixed feeders and grazers. Owing to poor chronological control, the results suggest that a variety of vegetation types co-occurred in the palaeohabitat of Sulawesi and the shift between C_3 and C_4 vegetation is not as pronounced as in mainland Asia, Java and Flores. In the LSI, the earliest recoded taxa (dated between 1.4 and 1.27 Ma on Flores) foraged on both C_3 and C_4 plants in a habitat covered by a variety of vegetation types, ranging from woodland to wooded grassland. In Luzon, the possibly earliest Proboscidea (dwarf Stegodon sp.) was also a mixed feeder. The occurrence of mixed feeders and grazers in Sulawesi, Luzon and Flores suggests that the C_4 expansion took place since the earliest recorded faunal occupation in both islands. Prolonged lowering of sea-level and drier conditions due to rapid glaciation cycles between the Late Pliocene and Middle Pleistocene may have intensified the distribution of grassland in mainland Asia and in later-emerged insular Southeast Asia. This may have forced the existing Proboscidea taxa to become grazers or mixed feeders with a larger proportion of grass consumption. Approximately after 1 Ma, all Elephantoidea of insular Southeast Asia exclusively or substantially incorporate C_4 vegetation in their diet, suggesting that

the feeding habitat was dominated by open vegetation (woodland, wooded grassland and grassland). The domination of a C_4 diet lasted in insular Southeast Asia until the latest Middle Pleistocene.

A second dietary shift for Proboscidea is observed during the latest Middle Pleistocene. The isotopic result suggests a turnover from C_4-dominated to C_3-dominated diet, occurring almost simultaneously in both mainland and insular Southeast Asia. In mainland Asia and Java, a decrease in carbon isotopic values ($\delta^{13}C$) appears to be gradual. The predominant browsing diet in surviving Elephantoidea taxa continues until the present. This latest dietary shift of Elephantoidea from C_4-dominated back to C_3-dominated coincides with the humid climate during several interglacial cycles (MIS 7, MIS 5, MIS 3 and present). Unfortunately, samples dated from the Last Glacial Maximum are not available. Therefore, whether the humid condition was temporary due to the interglacial cycle or lasted throughout the Late Pleistocene to the present remains unknown.

In East Africa, previous evidence exists for the transition from C_3-dominated to C_4-dominated vegetation since 10 Ma, and completed by 8 Ma (Cerling et al., 1999). Within mainland Asia, the first appearance of C_4 plant feeders (either mixed feeders or grazers) is recorded in the isotopic result only after 8 Ma for the Siwaliks, then continued to Irrawaddy at about 6-4 Ma and around the onset of the Pliocene in Tha Chang, and in the Early Pleistocene in Java (dated before 1.5 Ma), Sulawesi (dated after 2.1 Ma) and Flores (~1.4 Ma). The progressive onset of the mixed C_3-C_4 feeder/grazer appearance across each area suggests that floral transition from C_3-dominated to C_4-dominated vegetation did not occur simultaneously as previously thought. By tracing the pattern of first C_4 occurrence, which started in Africa, continued into the Siwaliks and the Irrawaddy, it can be suggested that the expansion of C_4 plants started in Africa and spread eastward along mainland Southeast Asia. While in insular Southeast Asia the delay was due to the indication that most of this area was still submerged before the Late Pliocene/Late Pleistocene. However, C_4 vegetation expanded rapidly as these islands emerged and became fully sub-aerial.

The foraging of Proboscidea and other herbivores may have a role in controlling the distribution of woody and grassy vegetation. The behaviour of Proboscidea, such as their uprooting small trees might have maintained an open habitat clear from canopy

coverage and kept their habitat as an open grass dominated vegetation. However, the impact of this herbivory seems to be more pronounced during drier climates and particularly in a smaller ecosystem, such as on an island.

8.1.2 Inter- and intra-specific competition of Proboscidea and associations with other taxa

In this study (Chapters 4 to 6), in situ co-occurrences of Elephantoidea was recorded in the Upper Siwalik sediment (Stegodon insignis - Archidiskodon planifrons), the upper part of the Sangiran Fm. (Sinomastodon bumiajuensis - Stegodon trigonocephalus), the Middle Pleistocene assemblages: Kedung Brubus + Bapang, Ngandong and West Java (Stegodon trigonocephalus - Elephas hysudrindicus), the Walanae Fauna Subunit A (Stegoloxodon celebensis - Stegodon sompoensis) and the Walanae Fauna Subunit B (Stegoloxodon celebensis - Stegodon sompoensis - large Stegodon sp. B). Additionally, although Stegodon orientalis and Elephas maximus in this study were not found in the same assemblage, in situ co-occurrences of these species was reported from various other localities (de Vos and Ciochon, 1996, Wang et al., 2007a, Rink et al., 2008). When co-occurring, these taxa pairings appear to compete over the same food resources, as all co-occurring taxa signal similar dietary preferences with overlapping isotopic values. The Late Miocene-Early Pliocene genera in Tha Chang (Stegolophodon stegodontoides, Stegolophodon int. form, Stegodon zdanskyi and Sinomastodon sp.) might have share the same niche types, since these taxa occurred at about the same age range and had similar dietary signals.

An indication for partial niche separation in Sulawesi was observed only in the Walanae Fauna Subunit B between the large Stegodon sp. B on one side and Sl. celebensis - S. sompoensis on the other side, in which the two older species were flexible feeders, while the new immigrant large Stegodon was more in the grazing range. Conversely, if large Stegodon sp. B (grazer) and cf. Palaeoloxodon namadicus (browser) in the Tanrung Fauna and Liang Bulu Bettue co-occurred, the two species underwent niche separation. However, due to the lack of in situ findings of Palaeoloxodon in the Tanrung Fauna, the co-occurrence of these taxa remains open to question.

The isotopic results from the Sangiran and Trinil Faunas suggest that niche partitioning did not occur within the co-occurring Elephantoids, bovids and cervids. In the Sangiran and Trinil Faunas (Chapter 4), co-occurring Homo erectus and Elephantoidea also shared the same feeding habitat. Niche separation did not occur between murine rodent and Stegodon florensis in the Middle Pleistocene So'a Basin. Partial diet separation is observed where Elephantoidea co-occurred with Suidae in the Walanae Fauna (Elephantoidea as flexible feeder and unexpectedly, Celebochoerus heekereni as a pure grazer), Sangiran and Trinil H.K. Faunas (Elephantoidea, cervids and bovids as grazers and other suids as mixed feeders), as well as with other taxa in Chaingazuk. The partial dietary distinction of Suidae from Elephantoidea and other herbivores suggests that Suidae were able to avoid competition with these herbivores.

Additionally, there was no indication of diet separation between juvenile and adult individuals, as exemplified by the Stegodon florensis insularis population in Liang Bua. A slight difference of carbon isotopic values between juvenile and adult individuals is explained as a mixing of isotopic signals between milk from the mother, which is more depleted in ^{13}C, and the individuals' own forage.

The $^{87}Sr/^{86}Sr$ analysis on Stegodon trigonocephalus and Elephas hysudrindicus (Chapter 7) gives a first glimpse that co-occurring taxa with similar dietary signal might not share the same habitat. When co-occurring, the less dominant genera probably migrated further away from its taphonocoenosis and were roaming in much wider areas, possibly to avoid competition with more dominant genera, yet remigrated to the taphonocoenosis during more favourable seasons or periods. Meanwhile, the similarity of their diet suggests that grassy vegetation was widely distributed in the palaeohabitat, regardless of the difference in substrate.

8.1.3 Palaeoenvironmental change and adaptation/extinction of the Proboscidea

Following the vegetation changes that occurred between the Middle Miocene and present, a change in feeding behaviour of proboscidean taxa is observed, which either forced them to adapt to new food resources or become extinct. Following the change of habitat to a drier grassy-dominated vegetation since the latest Miocene in mainland Asia

or in the earliest Pleistocene in insular Southeast Asia, many low crowned Proboscidea that were adapted to C_3 browsing (i.e. Platybelodon, Stegolophodon, primitive Stegodon and Stegoloxodon indonesicus) went extinct. Their successive lineages adapted by incorporating a larger proportion of C_4-vegetation in their diet and later descendants even specialised as grazers. In response to the change of diet to more abrasive grazing, most of the adapted genera (i.e. later Stegodon and Elephantidae) developed dental characters that better fitted a grassy diet: more distinct horizontal displacement of molars, larger molars, more lophids/ridge per molar, a higher hypsodonty index and thinner enamel. On the mainland, the Early Pleistocene Sinomastodon was predominantly browser (Tha Chang and Irrawaddy, Chapter 4). It maintained its browsing diet up to its youngest occurrence during Early Pleistocene at south and east China (Zhang et al., 2016). By contrast, the Sinomastodon lineage on Java changed to a grassy diet yet maintained its low hypsodonty. The Javanese lineage of Sinomastodon may have represented a remnant insular lineage of Sinomastodon that evolved under the insular conditions. This result suggests that Sinomastodon lineages were flexible feeders and could initially cope with changes in vegetation.

In island Southeast Asia, the earliest recorded taxa have smaller size and are generally more flexible feeders. Following the intensification of C_4-dominated vegetation in the Early Pleistocene, large-sized Stegodon and Elephas/Palaeoloxodon became more dominant on insular palaeoecosystems. Compared to mainland taxa, the development of dental morphology appears less distinguishable for insular taxa. Here, we are dealing with a different scale of evolutionary change. On islands, the evolutionary changes are smaller (microevolution), since even the earliest insular taxa were already advanced forms in dental morphology compared to those from the mainland. In contrast, the taxa on the mainland tend to be larger (macroevolution), as the mainland taxa experienced longer periods of evolution.

Following the second vegetation change from C_4-dominated to C_3-dominated during the latest Middle Pleistocene, grazing specialist large Stegodon in Java, Sulawesi and Flores became extinct, while Stegodon orientalis in mainland Asia adapted to a browsing diet. By contrast, the genus Elephas fully abandoned the abrasive C_4 diet, although their high-crowned teeth had become extremely specialised for grazing, which may be not only related to vegetation change, but also increasing competition/predation with other

taxa, especially humans. The C_3-dominant diet continued in Elephas maximus until the present, although some populations in India are known to be mixed feeders, and apparently are opportunistic feeders.

When the extinction of genera did not related to vegetation changes, competition with other taxa, predation and eventually habitat loss, could become the major cause of their disappearance from the palaeoecosystem. Despite having been flexible feeders that were well-adapted to a variety of vegetation changes, smaller-sized Stegoloxodon, Stegodon and Sinomastodon went extinct from mainland Asia (Zhang et al., 2016), Java, Sulawesi and presumably Flores after the arrival of larger Stegodon species and later, Elephas. Thus, their extinction of Sinomastodon in mainland and island may be caused by their incapability to compete with other herbivores, notably Stegodon and Elephas. The dentition of Stegodon and Elephas are better adapted for grazing diet, which became more dominant in palaeoenvironment of mainland and island Southeast Asia after the Early Pleistocene.

In case of co-occurrence with humans and possibly also large carnivores, the interaction of these taxa was closely associated with predation. It is notable that Stegodon trigonocephalus and Elephas hysudrindicus in Java and Stegodon florensis in Flores co-existed with pre-modern humans for almost a million years, but there is no indication that the existence of pre-modern humans caused the extinction of these species. However, only after the arrival of Homo sapiens, some species that were well-adapted to the vegetation change (i.e. Stegodon orientalis in mainland Asia, Elephas hysudrindicus and Elephas maximus in Java, and cf. Palaeoloxodon namadicus in Sulawesi) went extinct. Thus in this case, their extinction may be linked to modern human over-exploitation. Moreover, as the population density of modern humans is higher than pre-modern humans, their activities may have caused habitat loss and eventually led to the extinction of elephants. The retreat of the latest lineage of Elephantoidea to forested vegetation might also be an attempt to avoid human predation.

8.2 Recommendations for future research

Stable isotope analysis conducted on tooth enamel of vertebrate fauna has contributed to knowledge on the terrestrial palaeoenvironment in mainland and insular Southeast Asia, which was previously scarce. The focus of using Proboscidea in this study provides a better understanding of how a single taxonomical lineage adjusted to their feeding habitat and how each genus responded to the change in terrestrial environment. The stratigraphic position and geochronological data of fossil-bearing sediments are critical to establish a reliable timeline and to link palaeoenvironmental dynamics with regional/global climate and geological history. If available, an adequate number of samples, at least sufficient for statistical analysis, are also important to determine whether the dietary signal indicated by isotopic values is indeed part of a general trend for the population or rather represents an anomaly in the population. Additional information on palaeogeography, palaeoclimate and palaeovegetation of the region are also required to produce a better reconstruction of palaeohabitat. In this case a better resolution of geochronological data is critically needed, especially for the Early Pleistocene sediments at Java and Sulawesi, and localities in mainland Asia in general. Data for the associated faunal assemblage are also necessary to provide of their role and trophic level in the palaeoecosystem. Future analysis of serial sampling for each taxon is needed to test the seasonal feeding shift. Especially for smaller-sized mixed feeder species, an analysis with laser ablation method would be required to provide data for better reconstruction of seasonality and diet change in Proboscidea. Additionally, dental morphology data are useful to provide additional support for the reconstruction of dietary-related evolution.

In this study, data from mainland taxa are rather scattered and often lack chronostratigraphic control, has made the reconstruction of palaeoenvironment rather limited. Chronological details for the stratigraphy of Java and Sulawesi prior the Middle Pleistocene is also still lacking. Moreover, the time interval between the Late Pleistocene and recent, when faunas were commonly associated with humans is still poorly covered. Thus, further analysis of these points is recommended to produce a higher resolution palaeoenvironment and the influence of human activities to the faunas.

The preliminary study based on the analysis of the $^{87}Sr/^{86}Sr$ of a number of Proboscidean, reptilian and small mammal species from Java and Flores provides a

glimpse of different migratory behaviours and roaming areas among individuals. Further study using this this type analysis, particularly for Sundaland, has the potential use to reveal migratory pattern of the faunas and humans within Sundaland, especially during lowered sea level periods when the floor of the Java Sea was exposed. For such research, analysis of substrate lithology and faunas are equally important.

Bibliography

Abbott, M. J., Chamalaun, F. H. 1981. Geochronology of some Banda Arc volcanics. The Geology and Tectonics of Eastern Indonesia, 2**,** 253-268.

Abdullah, C., Rampnoux, J.-P., Bellon, H., Maury, R., Soeria-Atmadja, R. 2000. The evolution of Sumba Island (Indonesia) revisited in the light of new data on the geochronology and geochemistry of the magmatic rocks. Journal of Asian Earth Sciences, 18**,** 533-546.

Acharya, H., Aggarwal, Y. 1980. Seismicity and tectonics of the Philippine Islands. Journal of Geophysical Research: Solid Earth, 85**,** 3239-3250.

Adams, G. J. 1910. Geologic reconnaissance of southwestern Luzon. Philippines Journal of Science, 5(A)**,** 57–117.

Aggarwal, P. K., Fröhlich, K., Kulkarni, K. M., Gourcy, L. L. 2004. Stable isotope evidence for moisture sources in the asian summer monsoon under present and past climate regimes. Geophysical Research Letters, 31**,** L08203, 4pp.

Aiglstorfer, M., Bocherens, H., Böhme, M. 2014. Large mammal ecology in the late Middle Miocene Gratkorn locality (Austria). Palaeobiodiversity and Palaeoenvironments, 94**,** 189-213.

Aimi, M., Aziz, F. 1985. Vertebrate fossils from the Sangiran Dome, Mojokerto, Trinil and Sambungmacan areas. In: Watanabe, N.,Kadar, D. (eds.) Quaternary Geology of the Hominid Fossil Bearing Formations in Java. Bandung: GRDC, Special Publication, 4, 156-197.

Alcover, J. A., Campillo, X., Macias, M., Sans, A. 1998. Mammal species of the world: additional data on insular mammals. American Museum Novitates, 3248**,** 18 pp.

Amiot, R., Lécuyer, C., Escarguel, G., Billon-Bruyat, J.-P., Buffetaut, E., Langlois, C., Martin, S., Martineau, F., Mazin, J.-M. 2007. Oxygen isotope fractionation between crocodilian phosphate and water. Palaeogeography, Palaeoclimatology, Palaeoecology, 243**,** 412-420.

An, Z., Clemens, S. C., Shen, J., Qiang, X., Jin, Z., Sun, Y., Prell, W. L., Luo, J., Wang, S., Xu, H. 2011. Glacial-interglacial Indian summer monsoon dynamics. Science, 333**,** 719-723.

An, Z., Kutzbach, J. E., Prell, W. L., Porter, S. C. 2001. Evolution of Asian monsoons and phased uplift of the Himalaya–Tibetan plateau since Late Miocene times. Nature, 411**,** 62-66.

Araguás-Araguás, L., Froehlich, K., Rozanski, K. 1998. Stable isotope composition of precipitation over southeast Asia. Journal of Geophysical Research: Atmospheres, 103**,** 28, 721-28, 742.

Arppe, L., Karhu, J. A., Vartanyan, S. L. 2009. Bioapatite $^{87}Sr/^{86}Sr$ of the last woolly mammoths - Implications for the isolation of Wrangel Island. Geology, 37**,** 347-350.

Aubert, M., Brumm, A., Ramli, M., Sutikna, T., Saptomo, E. W., Hakim, B., Morwood, M., van den Bergh, G. D., Kinsley, L., Dosseto, A. 2014. Pleistocene cave art from Sulawesi, Indonesia. Nature, 514**,** 223-227.

Audley-Charles, M. G. 1975. The Sumba fracture: a major discontinuity between eastern and western Indonesia. Tectonophysics, 26**,** 213-228.

Audley-Charles, M. G. 1981. Geological history of the region of Wallace's Line. In: Whitmore, T. C. (ed.) Wallace's Line and Plate Tectonics. Oxford: Clarendon Press, 24-35.

Audley-Charles, M. G. 1991. Tectonics of the New Guinea area. Annual Review of Earth and Planetary Sciences, 19**,** 17-41.

Audley-Charles, M. G., Ballantyne, P. D., Hall, R. 1988. Mesozoic-Cenozoic rift-drift sequence of Asian fragments from Gondwanaland. Tectonophysics, 155**,** 317-330.

Audley-Charles, M. G., Hooijer, D. A. 1973. Relation of Pleistocene migrations of pygmy stegodonts to island arc tectonics in eastern Indonesia. Nature, 241**,** 197-198.

Ayliffe, L. K., Chivas, A. R. 1990. Oxygen isotope composition of the bone phosphate of Australian kangaroos: potential as a palaeoenvironmental recorder. Geochimica et Cosmochimica Acta, 54**,** 2603-2609.

Ayliffe, L. K., Chivas, A. R., Leakey, M. G. 1994. The retention of primary oxygen isotope compositions of fossil elephant skeletal phosphate. Geochimica et Cosmochimica Acta, 58**,** 5291-5298.

Aziz, F. 1990. Pleistocene Mammal Faunas of Sulawesi and Their Bearings to Paleozoogeography. Unpublished PhD thesis, Kyoto University, 106 pp.

Aziz, F. 2000. The Pleistocene endemic fauna of the Indonesian archipelago. Tropics.

Aziz, F., van den Bergh, G. D., van Hinte, J. E. 1995. A dwarf Stegodon from Sambungmacan (Central Java, Indonesia). Proceedings of the Royal Netherlands Academy of Sciences-Biological Chemical Geological, 98 (3)**,** 229-242.

Badgley, C., Barry, J. C., Morgan, M. E., Nelson, S. V., Behrensmeyer, A. K., Cerling, T. E., Pilbeam, D. 2008. Ecological changes in Miocene mammalian record show impact of prolonged climatic forcing. Proceedings of the National Academy of Sciences, 105**,** 12145-12149.

Badoux, D. M. 1959. Fossil Mammals from Two Fissure Deposits at Punung (Java): with some remarks on migration and evolution of mammals during the Quaternary in South East Asia. PhD thesis, University of Utrecht, 151 pp.

Bard, E., Jouannic, C., Hamelin, B. 1997. Pleistocene sea levels and tectonic uplift based on dating of corals from Sumba Island, Indonesia. Oceanographic Literature Review, 1 (44)**,** 1-32.

Bard, E., Jouannic, C., Hamelin, B., Pirazzoli, P., Arnold, M., Faure, G., Sumosusastro, P. 1996. Pleistocene sea levels and tectonic uplift based on dating of corals from Sumba Island, Indonesia. Geophysical Research Letters, 23**,** 1473-1476.

Barrick, R. E., Fischer, A. G., Showers, W. J. 1999. Oxygen isotopes from turtle bone: applications for terrestrial paleoclimates? Palaios, 14**,** 186-191.

Barry, J. C., Johnson, N. M., Raza, S. M., Jacobs, L. L. 1985. Neogene mammalian faunal change in southern Asia: Correlations with climatic, tectonic, and eustatic events. Geology, 13**,** 637-640.

Barry, J. C., Lindsay, E., Jacobs, L. 1982. A biostratigraphic zonation of the middle and upper Siwaliks of the Potwar Plateau of northern Pakistan. Palaeogeography, Palaeoclimatology, Palaeoecology, 37**,** 95-130.

Barry, J. C., Morgan, M. E., Flynn, L. J., Pilbeam, D., Behrensmeyer, A. K., Raza, S. M., Khan, I. A., Badgley, C., Hicks, J., Kelley, J. 2002. Faunal and environmental change in the late Miocene Siwaliks of northern Pakistan. Paleobiology, 28**,** 1-71.

Bartek, L. R., Vail, P., Anderson, J., Emmet, P., Wu, S. 1991. Effect of Cenozoic ice sheet fluctuations in Antarctica on the stratigraphic signature of the Neogene. Journal of Geophysical Research: Solid Earth, 96**,** 6753-6778.

Bartstra, G. J., Hooijer, D. A., Kallupa, B., Akib, M. A. 1994. Notes on fossil vertebrates and stone tools from Sulawesi, Indonesia, and the stratigraphy of the Northern Walanae Depression. Palaeohistoria, 33**,** 1-18.

Bartstra, G. J., Soegondho, S., van der Wijk, A. 1988. Ngandong man: age and artifacts. Journal of Human Evolution, 17**,** 325-337.

Basu, P. K. 2004. Siwalik mammals of the Jammu Sub-Himalaya, India: an appraisal of their diversity and habitats. Quaternary International, 117**,** 105-118.

Bautista, A. P. 1991. Recent zooarchaeological researches in the Philippines. Jurnal Arkeologi Malaysia, 4**,** 45–58.

Bautista, A. P. 1995. Fossil remains of Rhinoceros from the Philippines. National Museum Papers, 5**,** 1-15.

Beard, B. L., Johnson, C. M. 2000. Strontium isotope composition of skeletal material can determine the birth place and geographic mobility of humans and animals. Journal of Forensic Sciences, 45**,** 1049-1061.

Beaufort, L., de Garidel-Thoron, T., Mix, A. C., Pisias, N. G. 2001. ENSO-like forcing on oceanic primary production during the late Pleistocene. Science, 293**,** 2440-2444.

Behrensmeyer, A. K., Quade, J., Cerling, T. E., Kappelman, J., Khan, I. A., Copeland, P., Roe, L., Hicks, J., Stubblefield, P., Willis, B. J. 2007. The structure and rate of late Miocene

expansion of C_4 plants: evidence from lateral variation in stable isotopes in paleosols of the Siwalik Group, northern Pakistan. Geological Society of America Bulletin, 119**,** 1486-1505.

Bender, F. 1983. Geology of Burma, Berlin, Gebrüder Borntraeger, VIII, 293 pp.

Bender, M. M. 1971. Variations in the $^{13}C/^{12}C$ ratios of plants in relation to the pathway of photosynthetic carbon dioxide fixation. Phytochemistry, 10**,** 1239-1244.

Bentley, R. A. 2006. Strontium isotopes from the earth to the archaeological skeleton: a review. Journal of Archaeological Method and Theory, 13**,** 135-187.

Bergman, S. C., Coffield, D. Q., Talbot, J. P., Garrard, R. A. 1996. Tertiary tectonic and magmatic evolution of western Sulawesi and the Makassar Strait, Indonesia: evidence for a Miocene continent-continent collision. Geological Society, London, Special Publications, 106**,** 391-429.

Bertrand, G., Rangin, C. 2003. Tectonics of the western margin of the Shan plateau (central Myanmar): implication for the India–Indochina oblique convergence since the Oligocene. Journal of Asian Earth Sciences, 21**,** 1139-1157.

Bettis, E. A., Zaim, Y., Larick, R. R., Ciochon, R. L., Rizal, Y., Reagan, M., Heizler, M. 2004. Landscape development preceding Homo erectus immigration into Central Java, Indonesia: the Sangiran formation lower lahar. Palaeogeography, Palaeoclimatology, Palaeoecology, 206**,** 115-131.

Beyer, H. O. 1949. Outline review of Philippine archaeology by islands and provinces. Philippine Journal of Science, 77**,** 205-347.

Biasatti, D., Wang, Y., Gao, F., Xu, Y., Flynn, L. 2012. Paleoecologies and paleoclimates of late Cenozoic mammals from Southwest China: evidence from stable carbon and oxygen isotopes. Journal of Asian Earth Sciences, 44**,** 48-61.

Bintanja, R., van de Wal, R. S., Oerlemans, J. 2005. Modelled atmospheric temperatures and global sea levels over the past million years. Nature, 437**,** 125-128.

Bird, M. I., Taylor, D., Hunt, C. 2005. Palaeoenvironments of insular Southeast Asia during the Last Glacial Period: a savanna corridor in Sundaland? Quaternary Science Reviews, 24**,** 2228-2242.

Blake, S. 2003. The ecology of forest elephant distribution and its implications for conservation. PhD thesis, University of Edinburgh, 307 pp.

Blasco, F., Bellan, M., Aizpuru, M. 1996. A vegetation map of tropical continental Asia at scale 1: 5 million. Journal of Vegetation Science, 7**,** 623-634.

Blow, W. H. 1969. Late Middle Eocene to Recent planktonic foraminiferal biostratigraphy. Proceedings of the first international conference on planktonic microfossils, 1**,** 199-422. Blum, J. D., Taliaferro, E. H., Weisse, M. T., Holmes, R. T. 2000. Changes in Sr/Ca, Ba/Ca and $^{87}Sr/^{86}Sr$ ratios between trophic levels in two forest ecosystems in the northeastern USA. Biogeochemistry, 49**,** 87-101.

Bocherens, H., Drucker, D. G. 2007. Carbonate stable isotope: terrestrial teeth and bones. Encyclopedia of Quaternary Sciences. Elsevier. 309-317.

Bocherens, H., Koch, P. L., Mariotti, A., Geraads, D., Jaeger, J. 1996. Isotopic biogeochemistry (^{13}C, ^{18}O) of mammalian enamel from African Pleistocene hominid sites. Palaios, 11**,** 306-318.

Bocherens, H., Sandrock, O., Kullmer, O., Schrenk, F. 2011. Hominin palaeoecology in Late Pliocene Malawi: First insights from isotopes (^{13}C, ^{18}O) in mammal teeth. South African Journal of Science, 107**,** 1-6.

Bocherens, R., Ambrose, S., Katzenberg, A. 2000. Isotopic Signals (^{13}C; ^{15}N) in Pleistocene Mammals. Biogeochemical Approches to Paleodietary Analysis, 5**,** 65-84.

Bohlin, B. 1942. The Fossil Mammals from the Tertiary Deposit of Taben-buluk, Western Kansu: Insectivora and Lagomorpha, Aktiebolaget Hasse W. Tullberg.

Bohlin, B. 1945. Palaeontological and geological researches in Mongolia and Kansu 1929-1933. Swedish Expedition Publication, 26**,** 257–325.

Bohlin, B. 1946. The Fossil Mammals from the Tertiary Deposit of Taben-buluk, Western Kansu: Simplicidentata, Carnivora, Artiodactyla, Perissodactyla and Primates, Aktiebolaget Hasse W. Tullberg.

Bohlin, B. 1953. Fossil reptiles from Mongolia and Kansu. Reports from the scientific expedition to the north-western provinces of China under leadership of Dr. Sven Hedin. The Sino-Swedish Expedition. Publication 37, VI. Vertebrate palaeontology, 113 pp.

Bohlin, B., Hedin, S. A. 1937. Eine Tertiäre säugetier-fauna aus Tsaidam. In: Wong, H., Chow, T., Grabau, A. W., Lee, J., Sun , Y., Young, C.,Yin, T. (eds.) Palaeontologica Sinica. Beijing: The Geological Survey of China, I, 111 pp.

Bond, W. J. 2005. Large parts of the world are brown or black: a different view on the 'Green World'hypothesis. Journal of Vegetation Science, 16**,** 261-266.

Borissiak, A. A. 1928. On a new mastodon from the Chokrak Beds (Middle Miocene) of the Kuban region, Platybelodon danovi, n. gen., n. sp. Annual of the Paleontological Society Russie, 7**,** 105-120.

Borissiak, A. A. 1929. On a new direction in the adaptive radiation of mastodonts. Palaeobiologica, 2**,** 19-33.

Braches, F., Shutler, R. 1984. Von Koenigswald's Cijulang fauna reconsidered. Proceedings of the Sixth International Symposium on Asian Studies, 1**,** 831-848.

Brasseur, B., Sémah, F., Sémah, A.-M., Djubiantono, T. 2014. Pedo-sedimentary dynamics of the Sangiran dome hominid bearing layers (Early to Middle Pleistocene, central Java, Indonesia): A palaeopedological approach for reconstructing 'Pithecanthropus' (Javanese Homo erectus) palaeoenvironment. Quaternary International, 376**,** 84-100.

Brook, B. W., Bowman, D. M. J. S., Burney, D. A., Flannery, T. F., Gagan, M. K., Gillespie, R., Johnson, C. N., Kershaw, P., Magee, J. W., Martin, P. S., Miller, G. H., Peiser, B., Roberts, R. G. 2007. Would the Australian megafauna have become extinct if humans had never colonised the continent? Comments on "A review of the evidence for a human role in the extinction of Australian megafauna and an alternative explanation" by S. Wroe and J. Field. Quaternary Science Reviews, 26**,** 560-564.

Brown, P., Sutikna, T., Morwood, M. J., Soejono, R. P., Saptomo, E. W., Due, R. A. 2004. A new small-bodied hominin from the Late Pleistocene of Flores, Indonesia. Nature, 431**,** 1055-1061.

Brumm, A., Aubert, M., Ramli, M., Sutikna, T., van den Bergh, G. D., Morwood, M. J. in prep. Age and context of Leang Bulu Bettue, Sulawesi.

Brumm, A., Jensen, G. M., van den Bergh, G. D., Morwood, M. J., Kurniawan, I., Aziz, F., Storey, M. 2010. Hominins on Flores, Indonesia, by one million years ago. Nature, 464**,** 748-752.

Brumm, A., van den Bergh, G. D., Storey, M., Kurniawan, I., Alloway, B. V., Setiawan, R., Setiabudi, E., Grün, R., Moore, M. W., Yurnaldi, D., Puspaningrum, M. R., Wibowo, U. P., Insani, H., Sutisna, I., Westgate, J. E., Pearce, N. J. G., Duval, M., Meijer, H. J. M., Aziz, F., Sutikna, T., van der Kaars, S., Morwood, M. J. 2016. Stratigraphic context and age of hominin fossils from Middle Pleistocene Flores. Nature, 534**,** 249-253.

Bulte, E., Horan, R. D., Shogren, J. F. 2006. Megafauna extinction: A paleoeconomic theory of human overkill in the Pleistocene. Journal of Economic Behavior & Organization, 59**,** 297-323.

Bunopas, S., Vella, P. 1992. Geotectonics and geologic evolution of Thailand. Proceeding of Geological Resources of Thailand: Potential for Future Development**,** 209-228.

Burrett, C., Duhid, N., Berry, R., Varne, R. 1991. Asian and south-western Pacific continental terranes derived from Gondwana, and their biogeographic significance. Australian Systematic Botany, 4**,** 13-24.

Bush, A. B., Philander, S. G. H. 1998. The role of ocean-atmosphere interactions in tropical cooling during the Last Glacial Maximum. Science, 279**,** 1341-1344.

Campos-Arceiz, A., Blake, S. 2011. Megagardeners of the forest–the role of elephants in seed dispersal. Acta Oecologica, 37**,** 542-553.

Cande, S. C., Kent, D. V. 1995. Revised calibration of the geomagnetic polarity timescale for the Late Cretaceous and Cenozoic. Journal of Geophysical Research, 100**,** 6093-6095.

Cerling, T. E., Andanje, S. A., Blumenthal, S. A., Brown, F. H., Chritz, K. L., Harris, J. M., Hart, J. A., Kirera, F. M., Kaleme, P., Leakey, L. N., Leakey, M. G., Levin, N. E., Manthi,

F. K., Passey, B. H., Uno, K. T. 2015. Dietary changes of large herbivores in the Turkana Basin, Kenya from 4 to 1 Ma. Proceedings of the National Academy of Sciences, 112**,** 11467-11472.

Cerling, T. E., Harris, J. M. 1999. Carbon isotope fractionation between diet and bioapatite in ungulate mammals and implications for ecological and paleoecological studies. Oecologia, 120**,** 347-363.

Cerling, T. E., Harris, J. M., Ambrose, S. H., Leakey, M. G., Solounias, N. 1997a. Dietary and environmental reconstruction with stable isotope analyses of herbivore tooth enamel from the Miocene locality of Fort Ternan, Kenya. Journal of Human Evolution, 33**,** 635-650.

Cerling, T. E., Harris, J. M., Leakey, M. G. 1999. Browsing and grazing in elephants: the isotope record of modern and fossil proboscideans. Oecologia 120**,** 364-374.

Cerling, T. E., Harris, J. M., MacFadden, B. J., Leakey, M. G., Quade, J., Eisenmann, V., Ehleringer, J. R. 1997b. Global vegetation change through the Miocene/Pliocene boundary. Nature, 389**,** 153-158.

Cerling, T. E., Sharp, Z. D. 1996. Stable carbon and oxygen isotope analysis of fossil tooth enamel using laser ablation. Palaeogeography, Palaeoclimatology, Palaeoecology, 126**,** 173-186.

Cerling, T. E., Wynn, J. G., Andanje, S. A., Bird, M. I., Korir, D. K., Levin, N. E., Mace, W., Macharia, A. N., Quade, J., Remien, C. H. 2011. Woody cover and hominin environments in the past 6 million years. Nature, 476**,** 51-56.

Chaimanee, Y., Suteethorn, V., Jintasakul, P., Vidthayanon, C., Marandat, B., Jaeger, J.-J. 2004. A new orang-utan relative from the Late Miocene of Thailand. Nature, 427**,** 439-441.

Chaimanee, Y., Yamee, C., Tian, P., Chavasseau, O., Jaeger, J. J. 2006. Khoratpithecus piriyai, a Late Miocene hominoid of Thailand. American Journal of Physical Anthropology, 131**,** 311-323.

Chamalaun, F., Sunata, W. 1982. The paleomagnetism of the Western Banda Arc System - Sumba. Proceeding of Workshop Palaeomagnetic research in Southeast and East Asia 162-194.

Chang, D. H. S. 1981. The vegetation zonation of the Tibetan Plateau. Mountain Research and Development, 1**,** 29-48.

Chappell, J., Shackleton, N. J. 1986. Oxygen isotopes and sea level. Nature, 324**,** 137 - 140.

Chappell, J., Veeh, H. 1978. Late Quaternary tectonic movements and sea-level changes at Timor and Atauro Island. Geological Society of America Bulletin, 89**,** 356-368.

Charles, C., Hunter, D., Fairbanks, R. G. 1997. Interaction between the ENSO and the Asian monsoon in a coral record of tropical climate. Science, 277**,** 925-928.

Charlton, T. 2002. The structural setting and tectonic significance of the Lolotoi, Laclubar and Aileu metamorphic massifs, East Timor. Journal of Asian Earth Sciences, 20**,** 851-865. Charlton, T., Barber, A., Barkham, S. 1991. The structural evolution of the Timor collision complex, eastern Indonesia. Journal of Structural Geology, 13**,** 489-500.

Cheema, M. R., Raza, S. M., Ahmad, H. 1977. Cainozoic. Stratigraphy of Pakistan, 12**,** 56-98.

Chen, P., Lin, A., Lin, Y., Seki, Y., Stokes, A. G., Peyras, J., Olevsky, E. A., Meyers, M. A., McKittrick, J. 2008. Structure and mechanical properties of selected biological materials. Journal of the Mechanical Behavior of Biomedical Materials, 1**,** 208-226.

Clemens, S. C., Tiedemann, R. 1997. Eccentricity forcing of Pliocene–early Pleistocene climate revealed in a marine oxygen-isotope record. Nature, 385**,** 801-804.

Clementz, M. T., Holroyd, P. A., Koch, P. L. 2008. Identifying aquatic habits of herbivorous mammals through stable isotope analysis. Palaios, 23**,** 574-585.

Coates, B., Bishop, K., Gardner, D. 1997. A field guide to the birds of Wallacea, Dove Publications, Queensland, Australia, 535 pp.

Cobb, K. M., Adkins, J. F., Partin, J. W., Clark, B. 2007. Regional-scale climate influences on temporal variations of rainwater and cave dripwater oxygen isotopes in northern Borneo. Earth and Planetary Science Letters, 263**,** 207-220.

Cochrane, M. A. 2003. Fire science for rainforests. Nature, 421**,** 913-919.

Coffield, D. Q., Bergman, S. C., Garrard, R. A., Guritno, N., Robinson, N. M., Talbot, J. 1993. Tectonic and stratigraphic evolution of the Kalosi PSC area and associated development of a Tertiary petroleum system, South Sulawesi, Indonesia. Proceedings of the 22nd Annual Convention of the Indonesian Association of Geologists, 1**,** 679-706.

Colbert, E. H., Brown, B., Granger, W., Gregory, W. K. 1938. Fossil mammals from Burma in the American Museum of Natural History. Bulletin of the AMNH, 74**,** 255-436.

Copeland, S. R., Sponheimer, M., de Ruiter, D. J., Lee-Thorp, J. A., Codron, D., le Roux, P. J., Grimes, V., Richards, M. P. 2011. Strontium isotope evidence for landscape use by early hominins. Nature, 474**,** 76-78.

Coplen, T. B., Herczeg, A. L., Barnes, C. 2000. Isotope engineering - using stable isotopes of the water molecule to solve practical problems. In: Cook, P. G.,Herczeg, A. L. (eds.) Environmental Tracers in Subsurface Hydrology. Boston: Kluwer Academic Publishers, 79-110.

Cramer, B. S., Miller, K. G., Barrett, P. J., Wright, J. D. 2011. Late Cretaceous–Neogene trends in deep ocean temperature and continental ice volume: Reconciling records of benthic foraminiferal geochemistry ($\delta^{18}O$ and Mg/Ca) with sea level history. Journal of Geophysical Research: Oceans, 116 (12)**,** 1-23.

Cranbrook, E. o. 1981. The vertebrate faunas. In: Whitmore, T. C. (ed.) Wallace's Line and Plate Tectonics. Oxford: Cladendron Press, 57-69.

Cranbrook, E. o., Payne, J., Leh, C. 2008. Origin of the elephants Elephas maximus of Borneo. Sarawak Museum Journal, 63**,** 1-25.

Croft, D. A., Heaney, L. R., Flynn, J. J., Bautista, A. P. 2006. Fossil remains of a new, diminutive Bubalus (Artiodactyla: Bovidae: Bovini) from Cebu island, Philippines. Journal of Mammalogy, 87 (5)**,** 1037-1051.

Cumming, D., Fenton, M., Rautenbach, I., Taylor, R., Cumming, G., Cumming, M., Dunlop, J., Ford, A., Hovorka, M., Johnston, D. 1997. Elephants, woodlands and biodiversity in southern Africa. South African Journal of Science, 93**,** 231-236.

Dam, M. A. C. 1994. The Late Quaternary Evolution of the Bandung Basin, West Java, Indonesia. PhD thesis, Universiteit Amsterdam, 240 pp.

Dam, M. A. C., van der Kaars, S., Kershaw, A. P. 2001. Quaternary environmental change in the Indonesian region. Palaeogeography, Palaeoclimatology, Palaeoecology, 171**,** 91-95.

Dammerman, K. W. 1928. On the mammals of Sumba. Treubia, 10**,** 299-315.

Dansgaard, W. 1964. Stable isotopes in precipitation. Tellus A, 16**,** 436-468.

Darlington, P. J. 1957. Zoogeography: the Geographical Distribution of Animals, New York, John Willey and Sons, 676 pp.

Darman, H. 2014. Seismic expression of tectonic features in the Lesser Sunda Islands, Indonesia [Online]. http://geoseismic-seasia.blogspot.com.au/2013/06/the-lesser-sunda-islands.html: FOSI Special Publication. [Accessed 10 June 2016].

Datun, M., Rumidi, S., Hermanto, B., Suwarna, N. 1996. Geological Map of the Ngawi Quadrangle. Bandung: Geological Research and Development Centre.

de Boer, B., van de Wal, B. R., Lourens, L. J., Tuetter, E. 2010. Cenozoic global ice-volume and temperature simulations with 1-D ice-sheet models forced by benthic $\delta^{18}O$ records. Annals of Glaciology, 51**,** 23-33.

De Deckker, P., Tapper, N. J., van der Kaars, S. 2003. The status of the Indo-Pacific Warm Pool and adjacent land at the Last Glacial Maximum. Global and Planetary Change, 35**,** 25-35.

de Garidel-Thoron, T., Rosenthal, Y., Bassinot, F., Beaufort, L. 2005. Stable sea surface temperatures in the western Pacific warm pool over the past 1.75 million years. Nature, 433**,** 294-298.

de Rosayro, R. A. 1974. Vegetation of humid tropical Asia. Natural Resources of Humid Tropical Asia. Paris: UNESCO. 179-195.

de Smet, M. E. M., Fortuin, A. R., Troelstra, S. R., van Marle, L. J., Karmini, M., Tjokrosapoetro, S., Hadiwasastra, S. 1990. Detection of collision-related vertical movements in the Outer Banda Arc (Timor, Indonesia), using micropaleontological data. Journal of Southeast Asian Earth Sciences, 4**,** 337-356.

de Terra, H. 1943. Pleistocene Geology and Early Man in Java. Transactions of the American Philosophical Society, 32**,** 437-464.

de Vos, J. 1983. The Pongo faunas from Java and Sumatra and their significance for biostratigraphical and paleo-ecological interpretations. Proceedings of the Koninklke Nederlandse Akademie van Wetenschappen Series B: palaeontology, geology, physics and chemistry, 86**,** 417-425.

de Vos, J. 1985. Faunal stratigraphy and correlation of the Indonesian hominid sites. Ancestors: the Hard Evidence**,** 215-20.

de Vos, J., Ciochon, R. L. 1996. The fossil mammal fauna of the Lang Trang caves, Vietnam, compared with Southeast Asian fossil and recent mammal faunas: the geographical implications. Bulletin of the Indo-Pacific Prehistory Association, 14**,** 101-109.

de Vos, J., Elias, S. 2007. Mid Pleistocene of southern Asia. Encyclopaedia of Quaternary Sciences, 4**,** 3232-3249.

de Vos, J., Sartono, S., Hardjasasmita, S., Sondaar, P. 1982. The fauna from Trinil, type locality of Homo erectus - a reinterpretation. Geologie en Mijnbouw, 61**,** 207-211.

de Vos, J., Sondaar, P. Y., van den Bergh, G. D., Aziz, F. 1994. The Homo bearing deposits of Java and its ecological context. Courier Forschungsinstitut Senckenberg, 171**,** 129-140.

de Vos, J., van den Hoek Ostende, L. W., van den Bergh, G. D. 2007. Patterns in insular evolution of mammals: a key to island palaeogeography. In: Renema, W. (ed.) Biogeography, Time, and Place: Distributions, Barriers, and Islands. Springer, 29, 315-345.

de Vos, J., Vu, T. L. 2001. First settlements: relations between continental and Insular Southeast Asia. Origine des peuplements et chronologie des Cultures paléolithiques dan le Sud-est Asiatique, I**,** 225-249.

DeCelles, P. G. 2011. Foreland basin systems revisited: Variations in response to tectonic settings. In: Busby, C.,Azor, A. (eds.) Tectonics of Sedimentary Basins: Recent Advances. New York: John Wiley & Sons, 405-426.

Defant, M. J., Jacques, D., Maury, R. C., de Boer, J., Joron, J.-L. 1989. Geochemistry and tectonic setting of the Luzon arc, Philippines. Geological Society of America Bulletin, 101**,** 663-672.

Deng, T. 2004. Establishment of the middle Miocene Hujialiang Formation in the Linxia Basin of Gansu and its features. Journal of Stratigraphy, 28**,** 307-312.

Deng, T. 2006. Chinese Neogene mammal biochronology. Vertebrata PalAsiatica, 44**,** 143-163.

Deng, T., Hanta, R., Jintasakul, P. 2013a. A new species of Aceratherium (Rhinocerotidae, Perissodactyla) from the late Miocene of Nakhon Ratchasima, northeastern Thailand. Journal of Vertebrate Paleontology, 33**,** 977-985.

Deng, T., Qiu, Z.-X., Wang, B., Wang, X., Hou, S., Wang, X., Flynn, L., Fortelius, M. 2013b. Late Cenozoic biostratigraphy of the Linxia Basin, northwestern China. Fossil Mammals of Asia: Neogene Biostratigraphy and Chronology. Columbia University Press, New York**,** 243-273.

Deng, T., Wang, X., Ni, X., Liu, L. 2004. Sequence of the Cenozoic mammalian faunas of the Linxia Basin in Gansu, China. Acta Geologica Sinica, 78**,** 8-14.

DeNiro, M. J., Epstein, S. 1978. Influence of diet on the distribution of carbon isotopes in animals. Geochimica et Cosmochimica Acta, 42**,** 495-506.

Dennell, R., Coard, R., Turner, A. 2006. The biostratigraphy and magnetic polarity zonation of the Pabbi Hills, northern Pakistan: an upper Siwalik (Pinjor stage) upper Pliocene–Lower Pleistocene fluvial sequence. Palaeogeography, Palaeoclimatology, Palaeoecology, 234**,** 168-185.

Dennis, R. 1999. A review of fire projects in Indonesia, 1982-1998, CIFOR, 105 pp.

Dettman, D. L., Fang, X., Garzione, C. N., Li, J. 2003. Uplift-driven climate change at 12 Ma: a long $\delta^{18}O$ record from the NE margin of the Tibetan plateau. Earth and Planetary Science Letters, 214**,** 267-277.

Dettman, D. L., Kohn, M. J., Quade, J., Ryerson, F., Ojha, T. P., Hamidullah, S. 2001. Seasonal stable isotope evidence for a strong Asian monsoon throughout the past 10.7 my. Geology, 29**,** 31-34.

Dietrich, W. O. 1926. Zur Altersbestimmung der Pithecanthropus Schichten. Sitzungsberichte der Gesellschaft Naturforschender Freunde zu Berlin for 1924**,** 134-139.

Dirks, W., Bromage, T. G., Agenbroad, L. D. 2012. The duration and rate of molar plate formation in Palaeoloxodon cypriotes and Mammuthus columbi from dental histology. Quaternary International, 255**,** 79-85.

Djuri, M., Samodra, H., Amin, T. C., Gafoer, S. 1998. Geological map of the Purwokerto and Tegal Quadrangles, Jawa. Bandung: Geological Resarch and Development Centre.

Domingo, L., Koch, P. L., Fernández, M. H., Fox, D. L., Domingo, M. S., Alberdi, M. T. 2013. Late Neogene and early Quaternary paleoenvironmental and paleoclimatic conditions in southwestern Europe: isotopic analyses on mammalian taxa. PloS ONE, 8(5)**,** 1-15.

Dowsett, H., Barron, J., Poore, R. 1996. Middle Pliocene sea surface temperatures: a global reconstruction. Marine Micropaleontology, 27 (1)**,** 13-25.

Dowsett, H. J., Robinson, M. M. 2009. Mid-Pliocene equatorial Pacific sea surface temperature reconstruction: a multi-proxy perspective. Philosophical Transactions of the Royal Society of London A: Mathematical, Physical and Engineering Sciences, 367(1886)**,** 109-125. Driak, F. 1937. Anatomical and histological examination of the structure and development of the elephant molar. Journal of Dental Research, 16**,** 73-80.

Duangkrayom, J., Ratanasthien, B., Jintasakul, P., Carling, P. 2014. Sedimentary facies and paleoenvironment of a Pleistocene fossil site in Nakhon Ratchasima province, northeastern Thailand. Quaternary International, 325**,** 220-238.

Dublin, H. T. 1995. Vegetation dynamics in the Serengeti-Mara ecosystem: the role of elephants, fire, and other factors. In: Sinclair, A. R. E.,Arcese, P. (eds.) Serengeti II: Dynamics, Management, and Conservation of an Ecosystem. Chicago: University of Chicago Press, 71-90.

Dublin, H. T., Sinclair, A. R., McGlade, J. 1990. Elephants and fire as causes of multiple stable states in the Serengeti-Mara woodlands. The Journal of Animal Ecology, 59**,** 1147-1164.

Dubois, E. 1908. Das geologische Alter der Kendeng-oder Trinil-fauna. Tijdschrift van het Koninklijk Nederlandsch Aardrijkskundig Genootschap, 2 (25)**,** 1235-1270.

Dudley, J. P., Criag, G., Gibson, D., Haynes, G., Klimowicz, J. 2001. Drought mortality of bush elephants in Hwange National Park, Zimbabwe. African Journal of Ecology, 39**,** 187-194.

Durkee, E. F., Pederson, S. L. 1961. Geology of northern Luzon, Philippines. AAPG Bulletin, 45**,** 137-168.

Dwyer, G. S., Chandler, M. A. 2009. Mid-Pliocene sea level and continental ice volume based on coupled benthic Mg/Ca palaeotemperatures and oxygen isotopes. Philosophical Transactions of the Royal Society of London A: Mathematical, Physical and Engineering Sciences, 367**,** 157-168.

Ecker, M., Bocherens, H., Julien, M. A., Rivals, F., Raynal, J. P., Moncel, M. H. 2013. Middle Pleistocene ecology and Neanderthal subsistence: Insights from stable isotope analyses in Payre (Ardèche, southeastern France). Journal of Human Evolution, 65**,** 363-373.

Ehleringer, J. R., Cerling, T. E. 2002. C_3 and C_4 photosynthesis. Encyclopedia of Global Environmental Change, The Earth System: biological and ecological dimensions of global environmental change, 2**,** 186-190.

Ehleringer, J. R., Cerling, T. E., Helliker, B. R. 1997. C_4 photosynthesis, atmospheric CO_2, and climate. Oecologia 112**,** 285-299.

Ehlers, J., Gibbard, P. L. 2007. The extent and chronology of Cenozoic global glaciation. Quaternary International, 164**,** 6-20.

Ehrat, H. 1925. Geologische mijnbouwkundige onderzoekingen op Flores. Jaarboek van het Mijnwezen in NOI, Verhandelingen, 2**,** 208-226.

Eichinger, L., Rauert, W., Stichler, W., Bertleff, B., Egger, R. 1983. Comparative study of different aquifer types in Central Europe, using environmental isotopes. Isotope Hydrology**,** 271-289.

Falconer, H. 1868. Fauna antiqua sivalensis, R. Hardwicke, 1, 1-556.

Fan, M., Dettman, D. L., Song, C., Fang, X., Garzione, C. N. 2007. Climatic variation in the Linxia basin, NE Tibetan Plateau, from 13.1 to 4.3 Ma: the stable isotope record. Palaeogeography, Palaeoclimatology, Palaeoecology, 247**,** 313-328.

Fang, X., Garzione, C., Van der Voo, R., Li, J., Fan, M. 2003. Flexural subsidence by 29 Ma on the NE edge of Tibet from the magnetostratigraphy of Linxia Basin, China. Earth and Planetary Science Letters, 210**,** 545-560.

FAO 2001. Global forest resources assessment 2000. Main Report. Food and Agriculture Organization of the United Nations. Rome, PAO Forestry Paper.

Farquhar, G. D., Ehleringer, J. R., Hubick, K. T. 1989. Carbon isotope discrimination and photosynthesis. Annual Review of Plant Biology, 40**,** 503-537.

Feranec, R. S. 2007. Stable carbon isotope values reveal evidence of resource partitioning among ungulates from modern C_3-dominated ecosystems in North America. Palaeogeography, Palaeoclimatology, Palaeoecology, 252**,** 575-585.

Feranec, R. S., Hadly, E. A., Paytan, A. 2007. Determining landscape use of Holocene mammals using strontium isotopes. Oecologia, 153**,** 943-950.

Feranec, R. S., MacFadden, B. J. 2000. Evolution of the grazing niche in Pleistocene mammals from Florida: evidence from stable isotopes. Palaeogeography, Palaeoclimatology, Palaeoecology, 162**,** 155-169.

Fernando, P., Vidya, T. N. C., Payne, J., Stuewe, M., Davison, G., Alfred, R. J., Andau, P., Bosi, E., Kilbourn, A., Melnick, D. J. 2003. DNA analysis indicates that Asian elephants are native to Borneo and are therefore a high priority for conservation. PLoS Biol, 1 (1)**,** 110-115.

Field, C., Ross, I. 1976. The savanna ecology of Kidepo Valley National park. African Journal of Ecology, 14**,** 1-15.

Flower, B. P., Kennett, J. P. 1993. Middle Miocene ocean- climate transition: High- resolution oxygen and carbon isotopic records from Deep Sea Drilling Project Site 588A, southwest Pacific. Paleoceanography, 8**,** 811-843.

Flower, B. P., Kennett, J. P. 1994. The middle Miocene climatic transition: East Antarctic ice sheet development, deep ocean circulation and global carbon cycling. Palaeogeography, Palaeoclimatology, Palaeoecology, 108 (3-4)**,** 537-555.

Flynn, L. J., Jacobs, L. L. 1982. Effects of changing environments on Siwalik rodent faunas of northern Pakistan. Palaeogeography, Palaeoclimatology, Palaeoecology, 38**,** 129-138.

Fortuin, A. R., Sumosusastro, P. A., Berghuis, H. W. K., Roep, T. B. Uplifted Pleistocene coral-limestone terraces interfingering with fandeltas and fluviatile conglomerates—a record of sealevel highstands and low-stands between c. 550 and 100 ka (isotopic stages 14 to 5); Waingapu area, Sumba, Indonesia. UNESCO-IUGS Congress Climates of the Past, 1994 Denpasar, Bali. 15.

Fortuin, A. R., Van der Werff, W., Wensink, H. 1997. Neogene basin history and paleomagnetism of a rifted and inverted forearc region, on-and offshore Sumba, Eastern Indonesia. Journal of Asian Earth Sciences, 15**,** 61-88.

Foster, G. L., Lear, C. H., Rae, J. W. 2012. The evolution of pCO_2, ice volume and climate during the middle Miocene. Earth and Planetary Science Letters, 341**,** 243-254.

Friedli, H., Lötscher, H., Oeschger, H., Siegenthaler, U., Stauffer, B. 1986. Ice core record of the $^{13}C/^{12}C$ ratio of atmospheric CO_2 in the past two centuries. Nature, 324**,** 237-238.

Gagan, M., Ayliffe, L., Beck, J., Cole, J., Druffel, E., Dunbar, R., Schrag, D. 2000. New views of tropical paleoclimates from corals. Quaternary Science Reviews, 19**,** 45-64.

Garzione, C. N., Ikari, M. J., Basu, A. R. 2005. Source of Oligocene to Pliocene sedimentary rocks in the Linxia Basin in northeastern Tibet from Nd isotopes: Implications for tectonic forcing of climate. Geological Society of America Bulletin, 117**,** 1156-1166.

Gat, J. R. 1996. Oxygen and hydrogen isotopes in the hydrologic cycle. Annual Review of Earth and Planetary Sciences, 24**,** 225-262.

Ghosh, P., Padia, J., Mohindra, R. 2004. Stable isotopic studies of palaeosol sediment from Upper Siwalik of Himachal Himalaya: evidence for high monsoonal intensity during late Miocene? Palaeogeography, Palaeoclimatology, Palaeoecology, 206**,** 103-114.

Glass, B. P., Koeberl, C. 2006. Australasian microtektites and associated impact ejecta in the South China Sea and the Middle Pleistocene supereruption of Toba. Meteoritics & Planetary Science, 41**,** 305-326.

Glover, I. C. 1977. The late stone age in eastern Indonesia. World Archaeology, 9**,** 42-61.

Glover, I. C. 1981. Leang Burung 2: an upper palaeolithic rock shelter in South Sulawesi, Indonesia. Modern Quaternary Research in Southeast Asia, 6**,** 1-38.

GmbH, H. 2011. Groundwater Analysis: Further information, Stable isotopes oxygen-18 und deuterium (Figure 10) [Online]. Schweitenkirchen. Available: http://www.hydroisotop.de/en/further-information-6 [Accessed 27 October 2015].

Grainge, A. M., Davies, K. G. 1983. Reef exploration in the East Sengkang Basin, Sulawesi. Marine and Petroleum Geology, 2**,** 142-155.

Groves, C. P. 1976. The origin of the mammalian fauna of Sulawesi (Celebes). Zeitschrift für Säugetierkunde, 41**,** 201-216.

Groves, C. P. 1985. Plio-pleistocene mammals in island Southeast Asia. Modern Quaternary Research in Southeast Asia, 9**,** 43-54.

Guntoro, A. 1999. The formation of the Makassar Strait and the separation between SE Kalimantan and SW Sulawesi. Journal of Asian Earth Sciences, 17**,** 79-98.

Habran, S., Debier, C., Crocker, D. E., Houser, D. S., Lepoint, G., Bouquegneau, J. M., Das, K. 2010. Assessment of gestation, lactation and fasting on stable isotope ratios in northern elephant seals (Mirounga angustirostris). Marine Mammal Science, 26**,** 880-895.

Haines, P. W., Howard, K. T., Ali, J. R., Burrett, C. F., Bunopas, S. 2004. Flood deposits penecontemporaneous with ~0.8 Ma tektite fall in NE Thailand: impact-induced environmental effects? Earth and Planetary Science Letters, 225 (1)**,** 19-28.

Hall, R. 1996. Reconstructing Cenozoic SE Asia. Geological Society, London, Special Publications, 106 (1)**,** 153-184.

Hall, R. 1998. The plate tectonics of Cenozoic SE Asia and the distribution of land and sea. Biogeography and Geological Evolution of SE Asia**,** 99-131.

Hall, R. 2001. Cenozoic reconstructions of SE Asia and the SW Pacific: changing patterns of land and sea. Faunal and Floral Migrations and Evolution in SE Asia–Australasia**,** 35-56.

Hall, R. 2009. Southeast Asia's changing palaeogeography. Blumea-Biodiversity, Evolution and Biogeography of Plants, 54**,** 148-161.

Hall, R. 2011. Australia–SE Asia collision: plate tectonics and crustal flow. Geological Society, London, Special Publications, 355**,** 75-109.

Hall, R. 2012a. Late Jurassic–Cenozoic reconstructions of the Indonesian region and the Indian Ocean. Tectonophysics, 570**,** 1-41.

Hall, R. 2012b. Sundaland and Wallacea: geology, plate tectonics and palaeogeography. Biotic Evolution and Environmental Change in Southeast Asia**,** 32-78.

Hall, R. 2013. The palaeogeography of Sundaland and Wallacea since the Late Jurassic. Journal of Limnology, 72 (s2)**,** 1-15.

Hall, R., Smyth, H. R. 2008. Cenozoic arc processes in Indonesia: identification of the key influences on the stratigraphic record in active volcanic arcs. Geological Society of America Special Papers, 436**,** 27-54.

Hamilton, W. B. 1979. Tectonics of the Indonesian region, Washington, US Goverment Printing Office, 1078 pp.

Hammer, Ø., Harper, D.A.T., Ryan, P.D. 2001. PAST: Paleontological statistics software package for education and data analysis. Palaeontologia Electronica, 4(1)**,** 1-9.

Hansen, D. M., Galetti, M. 2009. The forgotten megafauna. Science, 324**,** 42-43.

Hanta, R., Ratanasthien, B., Kunimatsu, Y., Saegusa, H., Nakaya, H., Jintasakul, P., Wannakao, L., Srisuk, K., Youngme, W., Lertsirivorakol, R. Description of the Tha Chang Merycopotamus and its preserved condition. Proceedings of the International Conference

on Geology, Geotechnology and Mineral Resources of Indochina, Khon Kean, Thailand, 2005. 28-30.

Hanta, R., Ratanasthien, B., Kunimatsu, Y., Saegusa, H., Nakaya, H., Nagaoka, S., Jintasakul, P. 2008. A new species of Bothriodontinae, Merycopotamus thachangensis (Cetartiodactyla, Anthracotheriidae) from the late Miocene of Nakhon Ratchasima, northeastern Thailand. Journal of Vertebrate Paleontology, 28**,** 1182-1188.

Haq, B. U., Hardenbol, J., Vail, P. R. 1987. Chronology of fluctuating sea levels since the Triassic. Science, 235**,** 1156-1167.

Harris, J. M., Cerling, T. E. 2002. Dietary adaptations of extant and Neogene African suids. Journal of Zoology, 256**,** 45-54.

Harris, J. M., White, T. D. 1979. Evolution of the Plio-Pleistocene African Suidae. Transactions of the American Philosophical Society, 69**,** 1-128.

Hartono, H. M. S. 1961. Geological investigations at Ola Bula, Flores. Unpublished field report. Bandung: Djawatan Geologi, 41 pp.

Hatch, M. D. 2002. C_4 photosynthesis: discovery and resolution. Photosynthesis Research, 73 (1-3)**,** 251-256.

Haug, G. H., Tiedemann, R., Zahn, R., Ravelo, A. C. 2001. Role of Panama uplift on oceanic freshwater balance. Geology, 29**,** 207-210.

Hauptvogel, D. W., Passchier, S. 2012. Early–Middle Miocene (17–14Ma) Antarctic ice dynamics reconstructed from the heavy mineral provenance in the AND-2A drill core, Ross Sea, Antarctica. Global and Planetary Change, 82**,** 38-50.

Haynes, C. V. 1991. Geoarchaeological and paleohydrological evidence for a Clovis-age drought in North America and its bearing on extinction. Quaternary Research, 35**,** 438-450.

Heaney, L. R. 1986. Biogeography of mammals in SE Asia: estimates of rates of colonization, extinction and speciation. Biological Journal of the Linnean Society, 28**,** 127-165.

Heaney, L. R., Piper, P. J., Mijares, A. S. 2011. The first fossil record of endemic murid rodents from the Philippines: A late Pleistocene cave fauna from northern Luzon. Proceedings of the Biological Society of Washington, 124**,** 234-247.

Hedges, S., Tyson, M. J., Sitompul, A. F., Kinnaird, M. F., Gunaryadi, D. 2005. Distribution, status, and conservation needs of Asian elephants (Elephas maximus) in Lampung Province, Sumatra, Indonesia. Biological conservation, 124 (1)**,** 35-48.

Helliker, B. R., Ehleringer, J. R. 2002. Differential ^{18}O enrichment of leaf cellulose in C_3 versus C_4 grasses. Functional Plant Biology, 29**,** 435-442.

Herring, S. W. 1972. The role of canine morphology in the evolutionary divergence of pigs and peccaries. Journal of Mammalogy, 53**,** 500-512.

Hertler, C., Rizal, Y. 2005. Excursion guide to the Pleistocene hominid sites in Central and East Java, Joint Excursion July–August 2005, JWG University, Frankfurt (Germany), and ITB, Bandung (Indonesia). 1-35.

Hesse, P. P., Magee, J. W., van Der Kaars, S. 2004. Late Quaternary climates of the Australian arid zone: a review. Quaternary International, 118**,** 87-102.

Higgins, P., MacFadden, B. J. 2004. "Amount Effect" recorded in oxygen isotopes of Late Glacial horse (Equus) and bison (Bison) teeth from the Sonoran and Chihuahuan deserts, southwestern United States. Palaeogeography, Palaeoclimatology, Palaeoecology, 206**,** 337-353.

Hillson, S. 2005. Teeth, Cambridge University Press, 373 pp.

Hintong, C., Pholprasit, C., Polachan, S. 1984. Geologic Map, Changwat Nakhon Ratchasima, sheet ND 48-5, scale 1: 250,000. Bangkok, Thailand: Department of Mineral Resources (DMR).

Hocknull, S. A., Piper, P. J., van den Bergh, G. D., Due, R. A., Morwood, M. J., Kurniawan, I. 2009. Dragon's paradise lost: palaeobiogeography, evolution and extinction of the largest-ever terrestrial lizards (Varanidae). PloS One, 4 (9)**,** e7241, 1-15.

Hoffmann, G., Heimann, M. 1997. Water isotope modeling in the Asian monsoon region. Quaternary International, 37**,** 115-128.

Hong, A., Dekkers, M. J., Qi, W., Qiang, X., Xiao, G. 2013. New evidence for early presence of hominids in North China. Scientific Reports, 3 (2403)**,** 5 pp.

Hooijer, D. A. 1948a. Pleistocene Vertebrates from Celebes. I. Celebochoerus heekereni nov. gen. nov. spec. Proceedings of the Koninklijke Nederlandse Akademie van Wetenschappen Series B, 51(8)**,** 1024-1032.

Hooijer, D. A. 1948b. Pleistocene Vertebrates from Celebes. II. Testudo margae nov. spec. Koninklijke Nederlandse Akademie van Wetenschappen, 51 (9)**,** 1169-1182.

Hooijer, D. A. 1948c. Pleistocene Vertebrates from Celebes. III. Anoa depressicornis (Smith) subsp., and Babyrousa babyrussa beruensis nov. subspec. Koninklijke Nederlandse Akademie van Wetenschappen, 51 (9)**,** 1322-1330.

Hooijer, D. A. 1949. Pleistocene Vertebrates from Celebes. IV. Archidiskodon celebensis nov.spec. Zoologische Mededelingen, 30**,** 205-226.

Hooijer, D. A. 1950. Man and other mammals from Toalian sites in south-western Celebes. Verhandelingen der Koninklijke Nederlandsche Akademie van Wetenschappen Afdeling Natuurkunde, tweede sectie, 46**,** 1-164.

Hooijer, D. A. 1953a. Pleistocene Vertebrates from Celebes. V. Lower molars of Archidiskodon celebensis Hooijer. Zoologische Mededelingen, 31**,** 311-318.

Hooijer, D. A. 1953b. Pleistocene Vertebrates from Celebes. VI. Stegodon spec. Zoologische Mededelingen, 32**,** 107-112.

Hooijer, D. A. 1953c. Pleistocene Vertebrates from Celebes. VII. Milk molars and premolars of Archidiskodon celebensis Hooijer. Zoologische Mededelingen, 32**,** 221-230.

Hooijer, D. A. 1954a. Crocodilian remains from the Pleistocene of Celebes. Copeia, 4**,** 263-266.

Hooijer, D. A. 1954b. Pleistocene Vertebrates from Celebes. IX. Elasmobranchii. Koninklijke Nederlandse Akademie van Wetenschappen series B, 57**,** 475-485.

Hooijer, D. A. 1954c. Pleistocene Vertebrates from Celebes. VIII. Dentition and skeletton of Celebochoerus heekereni. Zoologische Verhandelingen, 24**,** 3-46.

Hooijer, D. A. 1954d. Pleistocene Vertebrates from Celebes. X. Testudinata. Koninklijke Nederlandse Akademie van Wetenschappen series B, 57**,** 486-489.

Hooijer, D. A. 1954e. Pleistocene Vertebrates from Celebes. XI. Molars and a tusked mandible of Archidiskodon celebensis Hooijer. Zoologische Mededelingen, 33**,** 103-122.

Hooijer, D. A. 1954f. A pygmy Stegodon from the Middle Pleistocene of eastern Java. Zoologische Mededelingen, 33**,** 91-102.

Hooijer, D. A. 1955. Fossil Proboscidea from the Malay archipelago and the Punjab. Zoölogische Verhandelingen, 28**,** 1-146.

Hooijer, D. A. 1957. A Stegodon from Flores. Treubia, 24**,** 119-29.

Hooijer, D. A. 1964a. On two milk molars of a pygmy stegodont from Ola Bula, Flores. Bulletin Geological Survey of Indonesia, 1**,** 49-52.

Hooijer, D. A. 1964b. Pleistocene Vertebrates from Celebes. XII. Notes on pygmy Stegodonts. Zoologische Mededelingen, 40**,** 37-44.

Hooijer, D. A. 1969a. Pleistocene vertebrates from Celebes. XIII. Sus celebensis Mueller et Schlegel, 1845. Beaufortia, 222**,** 215-218.

Hooijer, D. A. 1969b. The Stegodon from Timor. Proceedings of the Koninklke Nederlandse Akademie van Wetenschappen Series B: palaeontology, geology, physics and chemistry, 72**,** 201-210.

Hooijer, D. A. 1971. A giant land tortoise, Geochelone atlas (Falconer et Cautlay), from the Pleistocene of Timor. I&II. Proceedings of the Koninklijke Nederlandse Akademie van Wetenschappen Series B, 74**,** 504-525.

Hooijer, D. A. 1972a. Pleistocene vertebrates from Celebes. XIV. Additions to the Archidiskodon - Celebochoerus fauna. Zoologische Mededelingen, 46**,** 1-16.

Hooijer, D. A. 1972b. Varanus (Reptilia, Sauria) from the Pleistocene of Timor. Zoologische Mededelingen, 47**,** 445-448.

Hooijer, D. A. 1974. Elephas celebensis (Hooijer) from the Pleistocene of Java. Zoologische Mededelingen, 48 (11)**,** 85-93.

Hooijer, D. A. 1975. Quaternary mammals west and east of Wallace's line. Netherlands Journal of Zoology, 25**,** 46-56.

Hooijer, D. A. 1982. The extinct giant land tortoise and the pygmy stegodont of Indonesia. Modern Quaternary Research of Southeast Asia, 7**,** 171-176.

Hoppe, K. A., Koch, P. L., Carlson, R. W., Webb, S. D. 1999. Tracking mammoths and mastodons: reconstruction of migratory behavior using strontium isotope ratios. Geology, 27**,** 439-442.

Hopwood, A. T. 1935. Fossil Proboscidea from China. Palaeontologia Sinica. C9, 1-108.

Hou, Z., Li, J., Song, C., Zhang, J., Hui, Z., Chen, S., Xian, F. 2014. Understanding Miocene climate evolution in Northeastern Tibet: Stable carbon and oxygen isotope records from the Western Tianshui Basin, China. Journal of Earth Science, 25**,** 357-365.

Howard, K., Haines, P., Burrett, C., Ali, J., Bunopas, S. Sedimentology of 0.8 Ma log-bearing flood deposits in northeast Thailand and mechanisms for pre-flood deforestation. Proc. 8th Inter. Conf. Pacific Neogene Strat., 2003. Chaing Mai, Thailand. 46-49.

Huang, Y., Clemens, S. C., Liu, W., Wang, Y., Prell, W. L. 2007. Large-scale hydrological change drove the late Miocene C_4 plant expansion in the Himalayan foreland and Arabian Peninsula. Geology, 35**,** 531-534.

Hui, Z., Li, J., Xu, Q., Song, C., Zhang, J., Wu, F., Zhao, Z. 2011. Miocene vegetation and climatic changes reconstructed from a sporopollen record of the Tianshui Basin, NE Tibetan Plateau. Palaeogeography, Palaeoclimatology, Palaeoecology, 308**,** 373-382.

Hussain, S. T., van den Bergh, G. D., Steensma, K. J., de Visser, J. A., de Vos, J., Arif, M., van Dam, J., Sondaar, P. Y., Malik, S. B. 1992. Biostratigraphy of the Plio-Pleistocene continental sediments (Upper Siwaliks) of the Mangla-Samwal Anticline, Azad Kashmir, Pakistan. Proceedings of the Koninklijke Nederlandse Akademie van Wetenschappen Series B, 95**,** 65-80.

Hutchison, C. S. 1989. Geological evolution of South-east Asia, Oxford Monographs on Geology and Geophysics, Clarendon Press Oxford, 13, 376 pp.

Hyodo, M., Matsu'ura, S., Kamishima, Y., Kondo, M., Takeshita, Y., Kitaba, I., Danhara, T., Aziz, F., Kurniawan, I., Kumai, H. 2011. High-resolution record of the Matuyama–Brunhes transition constrains the age of Javanese Homo erectus in the Sangiran dome, Indonesia. Proceedings of the National Academy of Sciences, 108**,** 19563-19568.

Hyodo, M., Watanabe, N., Sunata, W., Susanto, E. E., Wahyono, H. 1993. Magnetostratigraphy of hominid fossil bearing formations in Sangiran and Mojokerto, Java. Anthropological Science, 101**,** 157-186.

Iacumin, P., Bocherens, H., Mariotti, A., Longinelli, A. 1996. Oxygen isotope analyses of co-existing carbonate and phosphate in biogenic apatite: a way to monitor diagenetic alteration of bone phosphate? Earth and Planetary Science Letters, 142**,** 1-6.

Indriati, E., Swisher III, C. C., Lepre, C., Quinn, R. L., Suriyanto, R. A., Hascaryo, A. T., Grün, R., Feibel, C. S., Pobiner, B. L., Aubert, M. 2011. The age of the 20 meter Solo River terrace, Java, Indonesia and the survival of Homo erectus in Asia. PLoS One, 6 (6)**,** e21562, 1-10.

Ingicco, T., van den Bergh, G. D., de Vos, J., Castro, A., Amano, N., Bautista, A. 2016. A new species of Celebochoerus (Suidae, Mammalia) from the Philippines and the paleobiogeography of the genus Celebochoerus Hooijer, 1948. Geobios, 49(4)**,** 285-291.

Janensch, W. 1911. Die Proboscidier-Schädel der Trinil-Expeditions-sammlung. Die Pithecanthropusschichten auf Java. Herausg. von ML Selenka und M. Blanckenhorn**,** 151-195.

Janssen, R., Joordens, J. C. A., Koutamanis, D. S., Puspaningrum, M. R., de Vos, J., van der Lubbe, J. J. L., Vonhof, H. B. 2016. Tooth and bone stable isotope ratios of fossil faunas reveal the glacial-interglacial paleoenvironments of hominins on Java, Indonesia. Quaternary Science Reviews, 144**,** 145-154.

Jiang, H., Ding, Z. 2009. Spatial and temporal characteristics of Neogene palynoflora in China and its implication for the spread of steppe vegetation. Journal of Arid Environments, 73**,** 765-772.

Jin, C., Qin, D., Pan, W., Tang, Z., Liu, J., Wang, Y., Deng, C., Zhang, Y., Dong, W., Tong, H. 2009. A newly discovered Gigantopithecus fauna from Sanhe Cave, Chongzuo, Guangxi, South China. Chinese Science Bulletin, 54**,** 788-797.

Johnson, B. J., Miller, G. H., Fogel, M. L., Magee, J. W., Gagan, M. K., Chivas, A. R. 1999. 65,000 years of vegetation change in central Australia and the Australian summer monsoon. Science, 284**,** 1150-1152.

Johnson, C. N. 2002. Determinants of loss of mammal species during the Late Quaternary 'megafauna'extinctions: life history and ecology, but not body size. Proceedings of the Royal Society of London. Series B: Biological Sciences, 269**,** 2221-2227.

Johnson, C. N., Alroy, J., Beeton, N. J., Bird, M. I., Brook, B. W., Cooper, A., Gillespie, R., Herrando-Pérez, S., Jacobs, Z., Miller, G. H. 2016. What caused extinction of the Pleistocene megafauna of Sahul? Proceedings of the Royal Society of London. Series B: Biological Sciences, 283 (1824)**,** 1-8.

Johnson, N. M., Opdyke, N. D., Johnson, G. D., Lindsay, E. H., Tahirkheli, R. 1982. Magnetic polarity stratigraphy and ages of Siwalik Group rocks of the Potwar Plateau, Pakistan. Palaeogeography, Palaeoclimatology, Palaeoecology, 37**,** 17-42.

Jones, P., Harris, I. 2013. CRU TS3. 20: Climatic Research Unit (CRU) Time-Series (TS) Version 3.20 of High Resolution Gridded Data of Month-by-Month Variation in Climate (January 1901–December 2011). NCAS British Atmospheric Data Centre, digital media. (Available online at http://badc.nerc.ac.uk/view/badc.nerc.ac.uk__ATOM__ACTIVITY_3ec0d1c6-4616-11e2-89a3-00163e251233.).

Joordens, J. C., d'Errico, F., Wesselingh, F. P., Munro, S., De Vos, J., Wallinga, J., Ankjærgaard, C., Reimann, T., Wijbrans, J. R., Kuiper, K. F. 2015. Homo erectus at Trinil on Java used shells for tool production and engraving. Nature, 518**,** 228-231.

Jouannic, C., Hoang, C.-T., Hantoro, W. S., Delinom, R. M. 1988. Uplift rate of coral reef terraces in the area of Kupang, West Timor: preliminary results. Palaeogeography, Palaeoclimatology, Palaeoecology, 68**,** 259-272.

Kalb, J. E., Froehlich, D. J., Bell, G. L. 1996a. Palaeobiogeography of late Neogene African and Eurasian Elephantoidea. In: Shoshani, J.,Tassy, P. (eds.) The Proboscidea: Evolution and Palaeoecology of Elephants and Their Relatives. Oxford: Oxford University Press, 101-116.

Kalb, J. E., Froehlich, D. J., Bell, G. L. 1996b. Phylogeny of African and Eurasian Elephantoidea of the late Neogene. In: Shoshani, J.,Tassy, P. (eds.) The Proboscidea: Evolution and Palaeoecology of Elephants and their Relatives. Oxford: Oxford University Press, 101-116.

Kaneko, Y., Maruyama, S., Kadarusman, A., Ota, T., Ishikawa, M., Tsujimori, T., Ishikawa, A., Okamoto, K. 2007. On-going orogeny in the outer-arc of the Timor–Tanimbar region, eastern Indonesia. Gondwana Research, 11**,** 218-233.

Katili, J. A. 1975. Volcanism and plate tectonics in the Indonesian island arcs. Tectonophysics, 26**,** 165-188.

Kealy, S., Louys, J., O'Connor, S. 2016. Islands under the sea: a review of early modern human dispersal routes and migration hypotheses through Wallacea. The Journal of Island and Coastal Archaeology, 11**,** 364-384.

Keast, A. 2001. The vertebrate fauna of the Wallacean Island Interchange Zone: the basis of inbalance and impoverishment. In: Metcalfe, I., Smith, J. M. B., Morwood, M. J.,Davidson, I. (eds.) Faunal and Floral Migrations and Evolution in SE Asia-Australasia. Lisse: Balkema, 287-310.

Keeley, J. E., Rundel, P. W. 2003. Evolution of CAM and C_4 carbon- concentrating mechanisms. International Journal of Plant Sciences, 164**,** S55-S77.

Kershaw, A. P., Penny, D., van der Kaars, S., Anshari, G., Thamotherampillai, A. 2001. Vegetation and climate in lowland Southeast Asia at the Last Glacial Maximum. Faunal and Floral Migrations and Evolution in SE Asia-Australasia. Lisse: Balkema, 227-236.

Khin, A., Win, K. 1969. Geology and hydrocarbon prospects of the Burma Tertiary Geosyncline. Journal of Science and Techonology, 2 (1), 52–73.

Klotz, S., Fauquette, S., Combourieu-Nebout, N., Uhl, D., Suc, J.P. , Mosbrugger, V. 2006. Seasonality intensification and long-term winter cooling as a part of the Late Pliocene climate development. Earth and Planetary Science Letters, 241 (1), 174-187.

Koch, P. L. 1998. Isotopic reconstruction of past continental environments. Annual Review of Earth and Planetary Sciences, 26, 573-613.

Koch, P. L., Tuross, N., Fogel, M. L. 1997. The effects of sample treatment and diagenesis on the isotopic integrity of carbonate in biogenic hydroxylapatite. Journal of Archaeological Science, 24, 417-429.

Koesoemadinata, S., Noya, Y., D., K. 1994. Geological map of the Ruteng Quadrangle, Nusatenggara. Bandung: Geological Research and Development Centre.

Kohn, M. J. 1996. Predicting animal $\delta^{18}O$: accounting for diet and physiological adaptation. Geochimica et Cosmochimica Acta, 60, 4811-4829.

Kohn, M. J., Cerling, T. E. 2002. Stable isotope compositions of biological apatite. Reviews in Mineralogy and Geochemistry, 48 (1), 455-488.

Kohn, M. J., Schoeninger, M. J., Valley, J. W. 1996. Herbivore tooth oxygen isotope compositions: effects of diet and physiology. Geochimica et Cosmochimica Acta, 60, 3889-3896.

Kohn, M. J., Schoeninger, M. J., Valley, J. W. 1998. Variability in oxygen isotope compositions of herbivore teeth: reflections of seasonality or developmental physiology? Chemical Geology, 152, 97-112.

Kopp, H., Flueh, E. R., Petersen, C. J., Weinrebe, W., Wittwer, A., Scientists, M. 2006. The Java margin revisited: Evidence for subduction erosion off Java. Earth and Planetary Science Letters, 242, 130-142.

Köppen, W., Geiger, R. 1930. Handbuch der klimatologie, Gebrüder Borntraeger Berlin, Germany.

Kozawa, Y., Mishima, H., Suzuki, K., Ferguson, M. Dental formula of elephant by the development of tooth germ. Proceedings of the first International Congress: The World of Elephants, Rome, 2001. 639-642.

Kretzoi, M. 1950. Stegoloxodon nov. gen., a loxodonta elefantok estleges azsiai ose. Foldtani Kozlony, 80, 405-108.

Krigbaum, J. 2005. Reconstructing human subsistence in the West Mouth (Niah Cave, Sarawak) burial series using stable isotopes of carbon. Asian Perspectives, 44, 73-89.

Kruskal, W. H., Wallis, W. A. 1952. Use of ranks in one-criterion variance analysis. Journal of the American Statistical Association, 47 (260), 583-621.

Kumaravel, V., Sangode, S. J., Kumar, R., Siddaiah, N. S. 2005. Magnetic polarity stratigraphy of Plio-Pleistocene Pinjor Formation (type locality), Siwalik Group, NW Himalaya, India. Current Science, 88 (9), 1453-1461.

Kunimatsu, Y., Ratanasthien, B., Nakaya, H., Saegusa, H., Nagaoka, S. 2005. Hominoid fossils discovered from Chiang Muan, northern Thailand: the first step towards understanding hominoid evolution in Neogene Southeast Asia. Anthropological Science, 113, 85-93.

Kusbini, Najamuddin 1991. Ringkasan laporan penyelidikan airtanah dengan metoda pendugaan geolistrik dan pemboran eksplorasi Kapupaten Dati II Wajo. Makassar: Bidang Geologi Sumberdaya Mineral Kanwil Departemen Pertambangan Energi Provinsi Sulawesi Selatan, Internal Report. 1-15.

Lambeck, K., Esat, T. M., Potter, E.-K. 2002. Links between climate and sea levels for the past three million years. Nature, 419, 199-206.

Lambert, W. D. 1992. The feeding habits of the shovel-tusked gomphotheres: evidence from tusk wear patterns. Paleobiology, 18, 132-147.

Laws, R. M. 1970. Elephants as agents of habitat and landscape change in East Africa. Oikos, 1-15.

Lee-Thorp, J. A., Sealy, J. C., van der Merwe, N. J. 1989. Stable carbon isotope ratio differences between bone collagen and bone apatite, and their relationship to diet. Journal of Archaeological Science, 16**,** 585-599.

Lee-Thorp, J. A., Sponheimer, M. 2003. Three case studies used to reassess the reliability of fossil bone and enamel isotope signals for paleodietary studies. Journal of Anthropological Archaeology, 22**,** 208-216.

Lee-Thorp, J. A., van der Merwe, N. J. 1987. Carbon isotope analysis of fossil bone apatite. South African Journal of Science, 83**,** 712-715.

Lehmann, C. E., Anderson, T. M., Sankaran, M., Higgins, S. I., Archibald, S., Hoffmann, W. A., Hanan, N. P., Williams, R. J., Fensham, R. J., Felfili, J. 2014. Savanna vegetation-fire-climate relationships differ among continents. Science, 343**,** 548-552.

Lehmann, C. E., Archibald, S. A., Hoffmann, W. A., Bond, W. J. 2011. Deciphering the distribution of the savanna biome. New Phytologist, 191**,** 197-209.

Leinders, J. J. M., Aziz, F., Sondaar, P. Y., de Vos, J. 1985. The age of hominid-bearing deposits of Java: State of the art. Geologie en Mijnbouw, 64 (2)**,** 167-173.

Leloup, P. H., Arnaud, N., Lacassin, R., Kienast, J., Harrison, T., Trong, T., Replumaz, A., Tapponnier, P. 2001. New constraints on the structure, thermochronology, and timing of the Ailao Shan- Red River shear zone, SE Asia. Journal of Geophysical Research: Solid Earth, 106 (B4)**,** 6683-6732.

Levin, N. E., Brown, F. H., Behrensmeyer, A. K., Bobe, R., Cerling, T. E. 2011. Paleosol carbonates from the Omo Group: Isotopic records of local and regional environmental change in East Africa. Palaeogeography, Palaeoclimatology, Palaeoecology, 307**,** 75-89.

Levin, N. E., Cerling, T. E., Passey, B. H., Harris, J. M., Ehleringer, J. R. 2006. A stable isotope aridity index for terrestrial environments. Proceedings of the National Academy of Sciences, 103**,** 11201-11205.

Li, J., Fang, X., Zhu, J., Zhong, W., Cao, J., Wang, J., Zhang, Y., Wang, J., Kang, S. 1995. Paleomagnetic chronology and type sequence of the Cenozoic stratigraphy of the Linxia Basin in Gansu Province of China. Annual Study on Formation, Evolution, Environmental Change and Ecology of Tibetan Plateau**,** 41-54.

Lim, Y. K., Kim, K. Y., Lee, H. S. 2002. Temporal and spatial evolution of the Asian summer monsoon in the seasonal cycle of synoptic fields. Journal of Climate, 15**,** 3630-3644.

Lister, A. M. 2013. The role of behaviour in adaptive morphological evolution of African proboscideans. Nature, 500**,** 331-334.

Lister, A. M. 2014. Behavioural leads in evolution: evidence from the fossil record. Biological Journal of the Linnean Society, 112**,** 315-331.

Locatelli, E., Due, R. A., van den Bergh, G. D., Van Den Hoek Ostende, L. W. 2012. Pleistocene survivors and Holocene extinctions: the giant rats from Liang Bua (Flores, Indonesia). Quaternary International, 281**,** 47-57.

Lomolino, M. V., Sax, D. F., Palombo, M. R., Van Der Geer, A. A. 2012. Of mice and mammoths: evaluations of causal explanations for body size evolution in insular mammals. Journal of Biogeography, 39**,** 842-854.

Longinelli, A. 1984. Oxygen isotopes in mammal bone phosphate: a new tool for paleohydrological and paleoclimatological research? Geochimica et Cosmochimica Acta, 48**,** 385-390.

Lopez, S. M. 1972. Contribution to the Pleistocene Geology of Cagayan Valley, Philippines. Seminar on Southeast Asian Prehistory and Archaeology. Manila: National Museum of the Philippines. 1-16.

Louys, J., Curnoe, D., Tong, H. 2007. Characteristics of Pleistocene megafauna extinctions in Southeast Asia. Palaeogeography, Palaeoclimatology, Palaeoecology, 243**,** 152-173.

Louys, J., Meijaard, E. 2010. Palaeoecology of Southeast Asian megafauna-bearing sites from the Pleistocene and a review of environmental changes in the region. Journal of Biogeography, 37**,** 1432-1449.

Louys, J., Price, G. J., O'Connor, S. 2016. Direct dating of Pleistocene stegodon from Timor Island, East Nusa Tenggara. PeerJ, 4**,** e1788, 1-16.

Luz, B., Cormie, A. B., Schwarcz, H. P. 1990. Oxygen isotope variations in phosphate of deer bones. Geochimica et Cosmochimica Acta, 54**,** 1723-1728.

Luz, B., Kolodny, Y. 1985. Oxygen isotope variations in phosphate of biogenic apatites, IV. Mammal teeth and bones. Earth and Planetary Science Letters, 75**,** 29-36.

Luz, B., Kolodny, Y., Horowitz, M. 1984. Fractionation of oxygen isotopes between mammalian bone-phosphate and environmental drinking water. Geochimica et Cosmochimica Acta, 48**,** 1689-1693.

Ma, Y., Li, J., Fan, X. 1998. Pollen-based vegetational and climatic records during 30.6 to 5.0 My from Linxia area, Gansu. Chinese Science Bulletins, 43**,** 301-304.

MacArthur, R. H., Wilson, E. O. 1967. The Theory of Island Biogeography, Princeton University Press, 1, 1-216.

MacFadden, B. J., Higgins, P. 2004. Ancient ecology of 15-million-year-old browsing mammals within C_3 plant communities from Panama. Oecologia, 140**,** 169-182.

MacFadden, B. J., Solounias, N., Cerling, T. E. 1999. Ancient diets, ecology, and extinction of 5-million-year-old horses from Florida. Science, 283**,** 824-827.

Macpherson, C. G., Forrde, E. J., Hall, R., Thirlwall, M. F. 2003. Geochemical evolution of magmatism in an arc-arc collision: The Halmahera and Sangihe arcs, eastern Indonesia. Geological Society, London, Special Publications, 219**,** 207-220.

Maglio, V. J. 1973. Origin and evolution of the Elephantidae. Transactions of the American Philosophical Society, 63**,** 1-149.

Maloney, B. K. 1995. Evidence for the Younger Dryas climatic event in Southeast Asia. Quaternary Science Reviews, 14**,** 949-958.

Mann, H. B., Whitney, D. R. 1947. On a test of whether one of two random variables is stochastically larger than the other. The Annals of Mathematical Statistics**,** 50-60.

Marino, B. D., McElroy, M. B. 1991. Isotopic composition of atmospheric CO_2 inferred from carbon in C_4 plant cellulose. Nature, 349**,** 127-131.

Markov, G. N., Saegusa, H. 2008. On the validity of Stegoloxodon Kretzoi, 1950 (Mammalia: Proboscidea). Zootaxa, 1861**,** 55-56.

Martin, K. 1883. Palaeontologische Ergebnisse von Tiefbohrungen auf Java, nebst allgemeineren Studien ueber das Tertiaer von Java, Timor und einiger anderer Inseln. Sammlungen des Geologischen Reichs-Museums in Leiden. Serie 1, Beiträge zur Geologie Ost-Asiens und Australiens, 3**,** 1-380.

Martin, K. 1884. Ueberreste vorweltlicher Proboscidier von Java und Bangka. *Jaarboek van het mijnwegen in Nederlandsch-Indië,* 1884**,** 285-308.

Martin, K. 1887. Fossile Saugethierreste von Java und Japan. *Jaarboek van het mijnwegen in Nederlandsch Oost Indië, Wet. Ged, XVI, Palaeontologie Nederlandsch- Indië,* 21**,** 1-45.

Martin, K. 1888. Neue Wirbelthierreste vom Pati-Ajam auf Java-Leiden. Sammlungen des Geologischen Reichs-Museums, 4**,** 1884-1889.

Martin, K. 1890. Ueber neue Stegodon-Reste auf Java. Verhehandelingen Koninklijke Nederlandsche Akademie van Wetenschappen, afdeeling Natuurkunde, 28**,** 1-13.

Martin, P. S. 1984. Prehistoric overkill: the global model. Quaternary Extinctions: a Prehistoric Revolution**,** 354-403.

Martin, P. S. 1990. Who or what destroyed our mammoths. In: Agenbroad, L. D., Mead, J. I.,Nelson, L. W. (eds.) Megafauna and Man: Discovery of America's Heartland. Hot Springs, The Mammoth Site of Hot Springs, South Dakota, 109-117.

Marwick, B., Gagan, M. K. 2011. Late Pleistocene monsoon variability in northwest Thailand: an oxygen isotope sequence from the bivalve Margaritanopsis laosensis excavated in Mae Hong Son province. Quaternary Science Reviews, 30 (21)**,** 3088-3098.

Mathisen, M., Vondra, C. 1983. The fluvial and pyroclastic deposits of the Cagayan Basin, northern Luzon, Philippines—An example of non- marine volcaniclastic sedimentation in an interarc basin. Sedimentology, 30 (3)**,** 369-392.

Matsu'ura, S. 1985. A consideration of the stratigraphic horizons of hominid finds from Sangiran by the fluorine method. In: Watanabe, N.,Kadar, D. (eds.) Quaternary Geology of

the Hominid Fossil Bearing Formations in Java. Bandung: GRDC, Special Publication, 4, 359-366.

Maung, H. 1987. Transcurrent movements in the Burma–Andaman Sea region. Geology, 15**,** 911-912.

Maurer, A. F., Galer, S. J., Knipper, C., Beierlein, L., Nunn, E. V., Peters, D., Tütken, T., Alt, K. W., Schöne, B. R. 2012. Bioavailable $^{87}Sr/^{86}Sr$ in different environmental samples - Effects of anthropogenic contamination and implications for isoscapes in past migration studies. Science of the Total Environment, 433**,** 216-229.

Mayr, E. 2000. The biological species concept. Species Concepts and Phylogenetic Theory: a Debate. New York: Columbia University Press, 17-29.

Medina-Elizalde, M., Lea, D. W. 2005. The mid-Pleistocene transition in the tropical Pacific. Science, 310**,** 1009-1012.

Medlicott, H. B. 1879. Manual of the geology of India. Geological Survey of India Publication, 2**,** 1-524.

Meesook, A., Suteethorn, V., Chaodumrong, P., Teerarungsigul, N., Sardsud, A., Wongprayoon, T. Mesozoic rocks of Thailand: a summary. Proceedings of the Symposium on Geology of Thailand. Department of Mineral Resources, Bangkok, Thailand, 2002. 82-94.

Meijaard, E. 2003. Mammals of southeast Asian islands and their Late Pleistocene environments. Journal of Biogeography, 30**,** 1245-1257.

Meijer, H. J., Due, R. A. 2010. A new species of giant marabou stork (Aves: Ciconiiformes) from the Pleistocene of Liang Bua, Flores (Indonesia). Zoological Journal of the Linnean Society, 160**,** 707-724.

Meijer, H. J., Kurniawan, I., Setiabudi, E., Brumm, A., Sutikna, T., Setiawan, R., van den Bergh, G. D. 2015. Avian remains from the Early/Middle Pleistocene of the So'a Basin, central Flores, Indonesia, and their palaeoenvironmental significance. Palaeogeography, Palaeoclimatology, Palaeoecology, 440**,** 161-171.

Meijer, H. J., Sutikna, T., Saptomo, E. W., Awe, R. D., Jatmiko, Wasisto, S., James, H. F., Morwood, M. J., Tocheri, M. W. 2013. Late Pleistocene-Holocene non-Passerine Avifauna of Liang Bua (Flores, Indonesia). Journal of Vertebrate Paleontology, 33**,** 877-894.

Meijer, H. J., van den Hoek Ostende, L. W., van den Bergh, G. D., de Vos, J. 2010. The fellowship of the hobbit: the fauna surrounding Homo floresiensis. Journal of Biogeography, 37**,** 995-1006.

Metcalfe, I. 1988. Origin and assembly of South-east Asian continental terranes. Geological Society, London, Special Publications, 37**,** 101-118.

Metcalfe, I. 1998. Palaeozoic and Mesozoic geological evolution of the SE Asian region: multidisciplinary constraints and implications for biogeography. Biogeography and Geological Evolution of SE Asia**,** 25-41.

Metcalfe, I. 2011. Tectonic framework and Phanerozoic evolution of Sundaland. Gondwana Research, 19**,** 3-21.

Metcalfe, I., Irving, E. 1990. Allochthonous terrane processes in Southeast Asia [and discussion]. Philosophical Transactions of the Royal Society of London A: Mathematical, Physical and Engineering Sciences, 331**,** 625-640.

Metcalfe, J. Z., Longstaffe, F. J. 2012. Mammoth tooth enamel growth rates inferred from stable isotope analysis and histology. Quaternary Research, 77**,** 424-432.

Meyer, B., Tapponnier, P., Bourjot, L., Metivier, F., Gaudemer, Y., Peltzer, G., Shunmin, G., Zhitai, C. 1998. Crustal thickening in Gansu-Qinghai, lithospheric mantle subduction, and oblique, strike-slip controlled growth of the Tibet Plateau. Geophysical Journal International, 135**,** 1-47.

Meyer, M., Palkopoulou, E., Baleka, S., Stiller, M., Penkman, K. E., Alt, K. W., Ishida, Y., Mania, D., Mallick, S., Meijer, T. 2017. Palaeogenomes of Eurasian straight-tusked elephants challenge the current view of elephant evolution. eLife, 6.

Midgley, J. J., Balfour, D., Kerley, G. I. 2005. Why do elephants damage savanna trees?: commentary. South African Journal of Science, 101 (5-6)**,** 213-215.

Miller, K. G., Fairbanks, R. G., Mountain, G. S. 1987. Tertiary oxygen isotope synthesis, sea level history, and continental margin erosion. Paleoceanography, 2**,** 1-19.

Miller, K. G., Kominz, M. A., Browning, J. V., Wright, J. D., Mountain, G. S., Katz, M. E., Sugarman, P. J., Cramer, B. S., Christie-Blick, N., Pekar, S. F. 2005. The Phanerozoic record of global sea-level change. Science, 310 (5752)**,** 1293-1298.

Mishra, S., Gaillard, C., Hertler, C., Moigne, A.-M., Simanjuntak, T. 2010. India and Java: contrasting records, intimate connections. Quaternary International, 223**,** 265-270.

Molnar, P., England, P., Martinod, J. 1993. Mantle dynamics, uplift of the Tibetan Plateau, and the Indian monsoon. Reviews of Geophysics, 31**,** 357-396.

Morgan, M. E., Kingston, J. D., Marino, B. D. 1994. Carbon isotopic evidence for the emergence of C_4 plants in the Neogene from Pakistan and Kenya. Nature, 367**,** 162-165.

Morley, R. J., Morley, H. P. 2013. Mid Cenozoic freshwater wetlands of the Sunda region. Journal of Limnology, 72 (s2)**,** 18-35.

Morrice, M. G., Jezek, P. A., Gill, J. B., Whitford, D. J., Monoarfa, M. 1983. An introduction to the Sangihe arc: Volcanism accompanying arc—arc collision in the Molucca Sea, Indonesia. Journal of Volcanology and Geothermal Research, 19 (1)**,** 135-165.

Morris, S., Humphreys, D., Reynolds, D. 2006. Myth, Marula, and Elephant: An Assessment of Voluntary Ethanol Intoxication of the African Elephant (Loxodonta africana) Following Feeding on the Fruit of the Marula Tree (Sclerocarya birrea)*. Physiological and Biochemical Zoology, 79**,** 363-369.

Morwood, M. J., Brown, P., Sutikna, T., Saptomo, E. W., Westaway, K. E., Due, R. A., Roberts, R. G., Maeda, T., Wasisto, S., Djubiantono, T. 2005. Further evidence for small-bodied hominins from the Late Pleistocene of Flores, Indonesia. Nature, 437**,** 1012-1017.

Morwood, M. J., O'Sullivan, P. B., Aziz, F., Raza, A. 1998. Fission-track ages of stone tools and fossils on the east Indonesian island of Flores. Nature, 392**,** 173-176.

Morwood, M. J., Soejono, R. P., Roberts, R. G., Sutikna, T., Turney, C. S., Westaway, K. E., Rink, W. J., Zhao, J.-X., Van Den Bergh, G. D., Due, R. A. 2004. Archaeology and age of a new hominin from Flores in eastern Indonesia. Nature, 431**,** 1087-1091.

Morwood, M. J., van Oosterzee, P. 2007. A new human: the discovery of the Hobbits of Flores, Washington, Smithsonian Books.

Moss, S. J., Wilson, M. E. 1998. Biogeographic implications of the Tertiary palaeogeographic evolution of Sulawesi and Borneo. Biogeography and Geological Evolution of SE Asia**,** 133-163.

Mubroto, B., Suminto, Kimura, J. 1995. Paleomagnetic analysis of sediments of the Kedung Brubus area. Geology of Quaternary Environment of the Solo-Madiun Area, Central-East Java, Geological Research and Development Centre Bandung, Special Publication, 17**,** 100-104.

Mudelsee, M., Stattegger, K. 1997. Exploring the structure of the mid-Pleistocene revolution with advanced methods of time-series analysis. Geologische Rundschau, 86**,** 499-511.

Muraoka, H., Nasution, A., Urai, M., Takahashi, M., Takashima, I., Simanjuntak, J., Sundhoro, H., Aswin, D., Nanlohy, F., Sitorus, K., Takahashi, H., Koseki, T. 2002. Tectonic, volcanic and stratigraphic geology of the Bajawa geothermal field, central Flores, Indonesia. Bulletin of the Geological Survery of Japan, 53 (2)**,** 109-138.

Musser, G. G. 1972. Identities of taxa associated with Rattus rattus (Rodentia, Muridae) of Sumba Island, Indonesia. Journal of Mammalogy, 53**,** 861-865.

Nakaya, H., Saegusa, H., Ratanasthien, B., Kunimatsu, Y., Nagaoka, S., Suganuma, Y. 2002. Neogene mammalian biostratigraphy of Thailand. Journal of Vertebrate Paleontology, 22 (supplementary issue)**,** 91A.

Nanda, A. 1977. A new Pentalophodon (Mammalia, Gomphotheriidae) from the Tatrot Formation of Ambala, India. Recent Researches in Geology, 3**,** 44-51.

Nanda, A. C. 2002. Upper Siwalik mammalian faunas of India and associated events. Journal of Asian Earth Sciences, 21**,** 47-58.

Nanda, A. C. 2008. Comments on the Pinjor Mammalian Fauna of the Siwalik Group in relation to the post-Siwalik faunas of Peninsular India and Indo-Gangetic Plain. Quaternary International, 192**,** 6-13.

Nanson, G. C., Price, D. M., Short, S. A. 1992. Wetting and drying of Australia over the past 300 ka. Geology, 20**,** 791-794.

Nelson, S. J. 2015. Wheeler's Dental Anatomy, Physiology and Occlusion, 10th ed., Missouri, Saunders, 1-392.

Nelson, S. V. 2005. Paleoseasonality inferred from equid teeth and intra-tooth isotopic variability. Palaeogeography, Palaeoclimatology, Palaeoecology, 222**,** 122-144.

Nelson, S. V. 2007. Isotopic reconstructions of habitat change surrounding the extinction of Sivapithecus, a Miocene hominoid, in the Siwalik Group of Pakistan. Palaeogeography, Palaeoclimatology, Palaeoecology, 243**,** 204-222.

Nishimura, S., Otofuji, Y., Ikeda, T., Abe, E., Yokoyama, T., Kobayashi, Y., Hadiwasastra, S., Sopaheluwakan, J., Hehuwat, F. 1981. Physical geology of the Sumba, Sumbawa and Flores islands. The Geology and Tectonics of Eastern Indonesia, 2**,** 105-114.

Norvick, M. 1979. The tectonic history of the Banda Arcs, eastern Indonesia: a review. Journal of the Geological Society, 136**,** 519-526.

O'Leary, M. H. 1981. Carbon isotope fractionation in plants. Phytochemistry, 20**,** 553-567.

O'Leary, M. H. 1988. Carbon isotopes in photosynthesis. Bioscience**,** 328-336.

O'Sullivan, P. B., Morwood, M., Hobbs, D., Suminto, F. A., Situmorang, M., Raza, A., Maas, R. 2001. Archaeological implications of the geology and chronology of the Soa basin, Flores, Indonesia. Geology, 29**,** 607-610.

Olsen, J., Trost, S., Myers, S. D. 2009. Owls on the island of Sumba, Indonesia. Australian Field Ornithology, 26 (1/2)**,** 2-14.

Opdyke, N. D., Lindsay, E., Johnson, G. D., Johnson, N., Tahirkheli, R. A. K., Mirza, M. A. 1979. Magnetic polarity stratigraphy and vertebrate paleontology of the Upper Siwalik Subgroup of northern Pakistan. Palaeogeography, Palaeoclimatology, Palaeoecology, 27**,** 1-34.

Osborn, H. F. 1936. Proboscidea: A Monograph of the Discovery, Evolution, Migration and Extinction of the Mastodonts and Elephants of the World. Moeritherioidea, Deinotherioidea, Mastodontoidea, American Museum Press.

Osborn, H. F., Granger, W. 1931. The shovel-tuskers, Amebelodontinae, of Central Asia. American Museum Novitates, 470**,** 1-12.

Otofuji, Y.-I., Sasajima, S., Nishimura, S., Yokoyama, T., Hadiwisastra, S., Hehuwat, F. 1981. Paleomagnetic evidence for the paleoposition of Sumba Island, Indonesia. Earth and Planetary Science Letters, 52**,** 93-100.

Owen-Smith, R. N. 1992. Megaherbivores: the Influence of Very Large Body Size on Ecology, Cambridge University Press, 1-369.

Palombo, M. R. 2007. How can endemic proboscideans help us understand the "island rule"? A case study of Mediterranean islands. Quaternary International, 169**,** 105-124.

Parkash, B., Sharma, R. P., Roy, A. K. 1980. The Siwalik Group (molasses) sediments shed by collision of continental plates. Sedimentary Geology, 25**,** 127-159.

Passey, B. H., Cerling, T. E. 2006. In situ stable isotope analysis ($\delta^{13}C$, $\delta^{18}O$) of very small teeth using laser ablation GC/IRMS. Chemical Geology, 235**,** 238-249.

Passey, B. H., Cerling, T. E., Perkins, M. E., Voorhies, M. R., Harris, J. M., Tucker, S. T. 2002. Environmental change in the Great Plains: an isotopic record from fossil horses. The Journal of Geology, 110**,** 123-140.

Passey, B. H., Robinson, T. F., Ayliffe, L. K., Cerling, T. E., Sponheimer, M., Dearing, M. D., Roeder, B. L., Ehleringer, J. R. 2005. Carbon isotope fractionation between diet, breath CO_2, and bioapatite in different mammals. Journal of Archaeological Science, 32**,** 1459-1470.

Patnaik, R. 2003. Reconstruction of Upper Siwalik palaeoecology and palaeoclimatology using microfossil palaeocommunities. Palaeogeography, Palaeoclimatology, Palaeoecology, 197**,** 133-150.

Patnaik, R. 2013. Indian Neogen Siwalik Mammalian biostratigraphy: an overview. In: Wang, X. F., Lawrence J; Fortelius, Mikael (ed.) Fossil Mammals of Asia: Neogene Biostratigraphy and Chronology. New York: Columbia University Press, 423-444.

Patnaik, R., Nanda, A. C. 2010. Early Pleistocene Mammalian faunas of India and evidence of connections with other parts of the world. In: Fleagle, J., Shea, J., Grine, F. E., Baden, A. L.,Leakey, R. (eds.) Out of Africa I: The Hominin Colonization of Eurasia. New York: Springer, 129-143.

Peel, M. C., Finlayson, B. L., McMahon, T. A. 2007. Updated world map of the Köppen-Geiger climate classification. Hydrology and Earth System Sciences Discussions, 4 (2)**,** 439-473.

Phadtare, N. R., Kumar, R., Ghosh, S. K. 1994. Stratigraphic palynology, floristic succession and the Tatrot/Pinjor boundary in upper Siwalik sediments of Haripur Khol area, district Sirmaur (HP), India. Himalayan Geology, 15**,** 69-82.

Phillips, O. L., Aragão, L. E., Lewis, S. L., Fisher, J. B., Lloyd, J., López-González, G., Malhi, Y., Monteagudo, A., Peacock, J., Quesada, C. A. 2009. Drought sensitivity of the Amazon rainforest. Science, 323**,** 1344-1347.

Pilbeam, D., Barry, J., Meyer, G. E., Shah, E. M. I., Pickford, M. H. L., Bishop, W. W., Thomas, H., Jacobs, L. L. 1977. Geology and paleontology of Neogene strata of Pakistan. Nature, 270**,** 684-689.

Pilgrim, G. E. 1913. The correlation of the Siwaliks with mammal horizons of Europe. Record of Geological Survey India, 43**,** 264-326.

Pillans, B., Williams, M., Cameron, D., Patnaik, R., Hogarth, J., Sahni, A., Sharma, J. C., Williams, F., Bernor, R. L. 2005. Revised correlation of the Haritalyangar magnetostratigraphy, Indian Siwaliks: implications for the age of the Miocene hominids Indopithecus and Sivapithecus, with a note on a new hominid tooth. Journal of Human Evolution, 48**,** 507-515.

Pirazzoli, P. A., Radtke, U., Hantoro, W. S., Jouannic, C., Hoang, C. T., Causse, C., Best, M. B. 1991. Quaternary raised coral-reef terraces on Sumba Island, Indonesia. Science, 252**,** 1834-1836.

Pirazzoli, P. A., Radtke, U., Hantoro, W. S., Jouannic, C., Hoang, C. T., Causse, C., Best, M. B. 1993. A one million-year-long sequence of marine terraces on Sumba Island, Indonesia. Marine Geology, 109**,** 221-236.

Polachan, S., Pradidtan, S., Tongtaow, C., Janmaha, S., Intarawijitr, K., Sangsuwan, C. 1991. Development of Cenozoic basins in Thailand. Marine and Petroleum Geology, 8**,** 84-97.

Polhaupessy, A. A. 1990. Late Cenozoic Palynological Studies on Java. PhD thesis, University of Hull.

Poore, R. Z., Sloan, L. C. 1996. Introduction climates and climate variability of the Pliocene. Marine Micropaleontology, 27**,** 1-2.

Poussart, P. F., Evans, M. N., Schrag, D. P. 2004. Resolving seasonality in tropical trees: multi-decade, high-resolution oxygen and carbon isotope records from Indonesia and Thailand. Earth and Planetary Science Letters, 218**,** 301-316.

Priadi, B., Polve, M., Maury, R., Soeria-Atmadja, R., Bellon, H. 1993. Geodynamic implications of Neogene potassic calc-alkaline magmatism in Central Sulawesi: geochemical and isotopic constraints. Proceedings of the 22nd Annual Convention of the Indonesian Association of Geologists, 1**,** 59-81.

Price, T. D., Burton, J. H., Bentley, R. A. 2002. The characterization of biologically available strontium isotope ratios for the study of prehistoric migration. Archaeometry, 44**,** 117-135.

Pushkina, D., Bocherens, H., Chaimanee, Y., Jaeger, J.-J. 2010. Stable carbon isotope reconstructions of diet and paleoenvironment from the late Middle Pleistocene Snake Cave in Northeastern Thailand. Naturwissenschaften, 97**,** 299-309.

Pushkina, D., Raia, P. 2008. Human influence on distribution and extinctions of the late Pleistocene Eurasian megafauna. Journal of Human Evolution, 54**,** 769-782.

Quade, J., Cerling, T. E. 1995. Expansion of C_4 grasses in the Late Miocene of Northern Pakistan: evidence from stable isotopes in paleosols. Palaeogeography, Palaeoclimatology, Palaeoecology, 115**,** 91-116.

Quade, J., Cerling, T. E., Barry, J. C., Morgan, M. E., Pilbeam, D. R., Chivas, A. R., Lee-Thorp, J. A., van der Merwe, N. J. 1992. A 16-Ma record of paleodiet using carbon and oxygen isotopes in fossil teeth from Pakistan. Chemical Geology, 94**,** 183-192.

Quade, J., Cerling, T. E., Bowman, J. R. 1989. Development of Asian monsoon revealed by marked ecological shift during the latest Miocene in northern Pakistan. Nature, 342**,** 163-166.

Raia, P., Meiri, S. 2006. The island rule in large mammals: paleontology meets ecology. Evolution, 60**,** 1731-1742.

Rangga Rao, A., Agarwal, R. P., Sharma, U. N., Bhalla, M. S., Nanda, A. C. 1988. Magnetic polarity stratigraphy and vertebrate paleontology of the Upper Siwalik Subgroup of Jammu Hills, India. Journal of Geological Society of India, 31**,** 361-385.

Rangga Rao, A., Nanda, A. C., Sharma, U. N., Bhalla, M. S. 1995. Magnetic polarity stratigraphy of the Pinjor Formation (Upper Siwalik) near Pinjor, Haryana. Current Science, 68**,** 1231-1236.

Rangin, C., Jolivet, L., Pubellier, M. 1990. A simple model for the tectonic evolution of Southeast Asia and Indonesia region for the past 43 My. Bulletin de la Société Géologique de France, 6 (6)**,** 889-905.

Ratnam, J., Bond, W. J., Fensham, R. J., Hoffmann, W. A., Archibald, S., Lehmann, C. E., Anderson, M. T., Higgins, S. I., Sankaran, M. 2011. When is a 'forest'a savanna, and why does it matter? Global Ecology and Biogeography, 20**,** 653-660.

Ravelo, A. C., Andreasen, D. H. 2000. Enhanced circulation during a warm period. Geophysical Research Letters, 27**,** 1001-1004.

Raven, J. A., Edwards, D. 2001. Roots: evolutionary origins and biogeochemical significance. Journal of Experimental Botany, 52**,** 381-401.

Raymo, M. E., Ganley, K., Carter, S., Oppo, D. W., McManus, J. 1998. Millennial-scale climate instability during the early Pleistocene epoch. Nature, 392**,** 699-702.

Raymo, M. E., Oppo, D. W., Curry, W. 1997. The mid- Pleistocene climate transition: A deep sea carbon isotopic perspective. Paleoceanography, 12**,** 546-559.

Reese, D. S., Belluomini, G., Ikeya, M. 1996. Absolute dates for the Pleistocene fauna of Crete. In: Reese, D. S. (ed.) Pleistocene and Holocene Fauna of Crete and its First Settlers. Philadelphia: James A. Knight. 47-52.

Replumaz, A., Tapponnier, P. 2003. Reconstruction of the deformed collision zone between India and Asia by backward motion of lithospheric blocks. Journal of Geophysical Research: Solid Earth, 108 (B6)**,** 1-24.

Richard, M., Bellon, H., Maury, R., Barrier, E., Wen-Shing, J. 1986. Miocene to recent calc-alkalic volcanism in eastern Taiwan: K-Ar ages and petrography. Tectonophysics, 125**,** 87-102.

Rind, D., Perlwitz, J. 2004. The response of the Hadley circulation to climate changes, past and future. The Hadley Circulation: Present, Past and Future. Springer. 399-435.

Rink, W. J., Wei, W., Bekken, D., Jones, H. L. 2008. Geochronology of Ailuropoda–Stegodon fauna and Gigantopithecus in Guangxi Province, southern China. Quaternary Research, 69 (3)**,** 377-387.

Rivals, F., Semprebon, G. M. 2006. A comparison of the dietary habits of a large sample of the Pleistocene pronghorn Stockoceros onusrosagris from the Papago Springs Cave in Arizona to the modern Antilocapra americana. Journal of Vertebrate Paleontology, 26**,** 495-500.

Rizal, Y. 1998. die Straßen Entlang des Solo-Flusses in Mittel- und Ost-Java. Unpublished PhD thesis, Universität zu Köln.

Roberts, R. G., Westaway, K. E., Zhao, J.-x., Turney, C. S., Bird, M. I., Rink, W. J., Fifield, L. K. 2009. Geochronology of cave deposits at Liang Bua and of adjacent river terraces in the Wae Racang valley, western Flores, Indonesia: a synthesis of age estimates for the type locality of Homo floresiensis. Journal of Human Evolution, 57**,** 484-502.

Rodolfo, K. S. 1975. The Irrawaddy Delta: tertiary setting and modern offshore sedimentation. In: Bruzzard, M. L. (ed.) Delta: Models for Exploration. Houston: Houston Geological Society. 339-356.

Rosidi, H. M. D., Tjokrosapoetro, S., Gafoer, S., Suwitodirdjo, K. 1979. Geologic map of the Kupang-Atambua Quadrangles, Timor (1:250.000). Geological Research and Development Centre, Indonesia.

Rozanski, K., Araguás-Araguás, L., Gonfiantini, R. 1992. Relation between long-term trends of oxygen-18 isotope composition of precipitation and climate. Science, 258**,** 981-985.

Rozanski, K., Araguás - Araguás, L., Gonfiantini, R. 1993. Isotopic patterns in modern global precipitation. Climate Change in Continental Isotopic Records**,** 1-36.

Ruddiman, W. F., Cline, R. M. L., Hays, J. D., Prell, W. L., Moore, T. C., Kipp, N. G., Molfino, B. E., Denton, G. H., Hughes, T. J. 1984. The last interglacial ocean. Quaternary Research, 21**,** 123-224.

Rutherford, E., Burke, K., Lytwyn, J. 2001. Tectonic history of Sumba Island, Indonesia, since the Late Cretaceous and its rapid escape into the forearc in the Miocene. Journal of Asian Earth Sciences, 19**,** 453-479.

Saegusa, H. Phylogenetic relationships of Stegodon and Sinomastodon (Proboscidea, Mammalia) of the mainland of East Asia. Abstract International Symposium Biogeogriogeography Vertebrates in Indonesian Islands and adjacent Area & Comparative Anatomy of Early Hominids and other Mammals, 1995 Kashiwa, Japan.

Saegusa, H. 1996. Stegodontidae: evolutionary relationships. In: Shoshani, J.,Tassy, P. (eds.) The Proboscidea; Evolution and Palaeoecology of Elephants and Their Relatives. Oxford: Oxford University Press, 178-190.

Saegusa, H., Thasod, Y., Ratanasthien, B. 2005. Notes on Asian stegodontids. Quaternary International, 126**,** 31-48.

Saltré, F., Rodríguez-Rey, M., Brook, B. W., Johnson, C. N., Turney, C. S., Alroy, J., Cooper, A., Beeton, N., Bird, M. I., Fordham, D. A. 2016. Climate change not to blame for late Quaternary megafauna extinctions in Australia. Nature Communications, 7**,** 1-7.

Samodra, H. 1994. Geological map of the Sangihe and Siau Sheets, Sulawesi 1:250,000. Bandung: Geological Research and Development Centre.

Sano, M., Xu, C., Nakatsuka, T. 2012. A 300- year Vietnam hydroclimate and ENSO variability record reconstructed from tree ring $\delta^{18}O$. Journal of Geophysical Research: Atmospheres, 117 (D12)**,** 1-11.

Sanyal, P., Bhattacharya, S., Kumar, R., Ghosh, S., Sangode, S. 2004. Mio–Pliocene monsoonal record from Himalayan foreland basin (Indian Siwalik) and its relation to vegetational change. Palaeogeography, Palaeoclimatology, Palaeoecology, 205**,** 23-41.

Sare, D. T. J., Millar, J. S., Longstaffe, F. J. 2005. Nitrogen-and carbon-isotope fractionation between mothers and offspring in red-backed voles (Clethrionomys gapperi). Canadian Journal of Zoology, 83**,** 712-716.

Sartono, S. 1969. Stegodon timorensis: a pygmy species from Timor (Indonesia). Proceedings of the Koninklijke Nederlandse Akademie van Wetenschappen Series B, 72**,** 192-202.

Sartono, S. 1976. Genesis of the Solo terraces. Modern Quaternary Research in Southeast Asia, 2**,** 1-21.

Sartono, S. 1979. The discovery of a pygmy Stegodon from Sumba, East Indonesia: an announcement. Modern Quaternary Research in SE Asia, 5**,** 57-63.

Satarugsa, P., Youngmee, W., Meesawat, S. New regional boundary of Maha Sarakham Formation in the Northeastern Thailand: results from 2D seismic mapping. Proceedings on International Conference on Geology, Geotechnology and Mineral Resources of Indochina, 2005. 28-30.

Sawyer, R. K., Sani, K., Brown, S. 1993. The stratigraphy and sedimentology of West Timor, Indonesia. AAPG 22nd Annual Convention Proceedings, 1**,** 533-574.

Schepartz, L. A., Bakken, D. A., Miller-Antonio, S., Paraso, C. K., Karkanas, P. 2003. Faunal approaches to site formation processes at Panxian Dadong. Current Research in Chinese Pleistocene Archaeology, 1179**,** 99-110.

Schepartz, L. A., Stoutamire, S., Bekken, D. A. 2005. Stegodon orientalis from Panxian Dadong, a Middle Pleistocene archaeological site in Guizhou, South China: taphonomy,

population structure and evidence for human interactions. Quaternary International, 126**,** 271-282.

Schüle, W. 1992. Vegetation, megaherbivores, man and climate in the Quaternary and the genesis of closed forests. In: Goldammer, J. G. (ed.) Tropical Forests in Transition. Birkhäuser Basel: Springer, 45-76.

Scroxton, N., Gagan, M., Ayliffe, L., Hellstrom, J., Cheng, H., Edwards, R., Zhao, J., Hantoro, W., Rifai, H., Scott-Gagan, H. Speleothem carbon isotopes in the tropics: a proxy for vegetation and what they reveal about the demise of Homo floresiensis. AGU Fall Meeting Abstracts, 2013. 1935.

Scroxton, N., Gagan, M., Dunbar, G., Ayliffe, L., Hantoro, W., Shen, C., Hellstrom, J., Zhao, J., Cheng, H., Edwards, R. Stalagmite Survival: 500kyr of Cyclical Growth and Natural Attrition of Stalagmites in Sulawesi. AGU Fall Meeting Abstracts, 2014. 1141.

Scroxton, N., Gagan, M. K., Dunbar, G. B., Ayliffe, L. K., Hantoro, W. S., Shen, C.-C., Hellstrom, J. C., Zhao, J.-x., Cheng, H., Edwards, R. L. 2016. Natural attrition and growth frequency variations of stalagmites in southwest Sulawesi over the past 530,000 years. Palaeogeography, Palaeoclimatology, Palaeoecology, 441**,** 823-833.

Sémah, A.-M., Sémah, F. 2012. The rain forest in Java through the Quaternary and its relationships with humans (adaptation, exploitation and impact on the forest). Quaternary International, 249**,** 120-128.

Sémah, A.-M., Sémah, F., Djubiantono, T., Brasseur, B. 2010. Landscapes and Hominids' environments: changes between the Lower and the Early Middle Pleistocene in Java (Indonesia). Quaternary International, 223**,** 451-454.

Sémah, F. 1997. Plio-Pleistocene reference sections in Indonesia. The Pleistocene Boundary and the Beginning of the Quaternary, 1 (9)**,** 264-272.

Sepulchre, P., Jolly, D., Ducrocq, S., Chaimanee, Y., Jaeger, J.-J., Raillard, A. 2010. Mid-Tertiary paleoenvironments in Thailand: pollen evidence. Climate of the Past, 6**,** 461-473.

Sharp, Z. D., Cerling, T. E. 1998. Fossil isotope records of seasonal climate and ecology: straight from the horse's mouth. Geology, 26**,** 219-222.

Shimizu, Y., Mubroto, B., Siagian, H., Untung, M. 1985. A paleomagnetic study in the Sangiran area. In: Watanabe, N.,Kadar, D. (eds.) Quaternary Geology of the Hominid Fossil Bearing Formations in Java. Bandung: GRDC, Special Publication, 4, 275-307.

Shoshani, J. 1996. Skeletal and other basic anatomical features of elephants. In: Shoshani, J.,Tassy, P. (eds.) The Proboscidea: Evolution and Palaeoecology of Elephants and Their Relatives. Oxford: Oxford University Press, 8-20.

Shoshani, J. 1998. Understanding proboscidean evolution: a formidable task. Trends in Ecology and Evolution, 13**,** 480-487.

Shoshani, J., Tassy, P. (eds.) 1996a. The Proboscidea: Evolution and Palaeoecology of Elephants and their Relatives, Oxford: Oxford University Press, 472 pp.

Shoshani, J., Tassy, P. 1996b. Summary, conclusions, and a glimpse into the future. In: Shoshani, J.,Tassy, P. (eds.) The Proboscidea: Evolution and Palaeoecology of Elephants and Their Relatives. Oxford: Oxford University Press, 335-348.

Simandjuntak, T. O. 1993. Tectonic origin of Sumba platform. Jurnal Geologi dan Sumberdaya Mineral, 3**,** 10-19.

Simandjuntak, T. O. 2004. Tectonostratigraphy of Jawa. Stratigrafi Pulau Jawa, 30**,** 14.

Simandjuntak, T. O., Barber, A. J. 1996. Contrasting tectonic styles in the Neogene orogenic belts of Indonesia. Geological Society, London, Special Publications, 106**,** 185-201.

Simpson, G. G. 1977. Too many lines; the limits of the Oriental and Australian zoogeographic regions. Proceedings of the American Philosophical Society**,** 107-120.

Singh, B. P. 2013. Evolution of the Paleogene succession of the western Himalayan foreland basin. Geoscience Frontiers, 4**,** 199-212.

Smyth, H. R., Hall, R., Nichols, G. J. 2008. Cenozoic volcanic arc history of East Java, Indonesia: the stratigraphic record of eruptions on an active continental margin. Geological Society of America Special Papers, 436**,** 199-222.

Sondaar, P. Y. 1977. Insularity and its effect on mammal evolution. In: Hecht, M. K., Goody, P. C.,Hecht, B. M. (eds.) Major Patterns in Vertebrate Evolution. Springer US, 607-707. Sondaar, P. Y. 1981. The Geochelone faunas of the Indonesian Archipelago and their paleogeographical and biostratigraphical significance. Modern Quaternary Research of SE Asia, 6**,** 111-120.

Sondaar, P. Y. 1984. Faunal evolution and the mammalian biostratigraphy of Java. Courier Forschungsinstitut Senckenberg, 69**,** 219-235.

Sondaar, P. Y. 1987. Pleistocene man and extinctions of island endemics. Mémoires de la Société Géologique de France NS, 150**,** 159-165.

Sondaar, P. Y., van den Bergh, G. D., Mubroto, B., FACHROEL, A., de Vos, J., Batu, U. L. 1994. Middle Pleistocene faunal turnover and colonization of Flores (Indonesia) by Homo erectus. Comptes rendus de l'Académie des sciences. Série 2. Sciences de la terre et des planètes, 319**,** 1255-1262.

Stamp, L. D. 1922. An outline of the Tertiary geology of Burma. Geological Magazine, 59**,** 481-501.

Stephens, M., Rose, J. 2005. Modern stable isotopic ($\delta^{18}O$, $\delta^{2}H$, $\delta^{13}C$) variation in terrestrial, fluvial, estuarine and marine waters from north- central Sarawak, Malaysian Borneo. Earth Surface Processes and Landforms, 30**,** 901-912.

Stibig, H.-J., Belward, A., S., Roy, P. S., Rosalina-Wasrin, U., Agrawal, S., Joshi, P. K. Beuchle, R. 2014. A land-cover map for South and Southeast Asia derived from SPOT-VEGETATION data. Journal of Biogeography, 34**,** 625-637.

Storm, P., Aziz, F., de Vos, J., Kosasih, D., Baskoro, S., van den Hoek Ostende, L. W. 2005. Late Pleistocene Homo sapiens in a tropical rainforest fauna in East Java. Journal of Human Evolution, 49**,** 536-545.

Storm, P., de Vos, J. 2006. Rediscovery of the Late Pleistocene Punung hominin sites and the discovery of a new site Gunung Dawung in East Java. Senckenbergiana lethaea, 86**,** 271-281.

Storm, P., Wood, R., Stringer, C., Bartsiokas, A., de Vos, J., Aubert, M., Kinsley, L., Grün, R. 2013. U-series and radiocarbon analyses of human and faunal remains from Wajak, Indonesia. Journal of Human Evolution, 64**,** 356-365.

Stott, L., Poulsen, C., Lund, S., Thunell, R. 2002. Super ENSO and global climate oscillations at millennial time scales. Science, 297**,** 222-226.

Suedy, S. W. A., Jumari, J. 2004. Rekonstruksi Vegetasi dan Bentang Alam Daerah Bumiayu pada Masa Pliosen-Plistosen Berdasarkan Bukti-bukti Palinologi. Semarang: Universitas Diponegoro, 18 pp.

Suganuma, Y., Hamada, T., Tanaka, S., Okada, M., Nakaya, H., Kunimatsu, Y., Saegusa, H., Nagaoka, S., Ratanasthien, B. 2006. Magnetostratigraphy of the Miocene Chiang Muan Formation, northern Thailand: Implication for revised chronology of the earliest Miocene hominoid in Southeast Asia. Palaeogeography, Palaeoclimatology, Palaeoecology, 239**,** 75-86.

Sukamto, R. 1975. The structure of Sulawesi in the light of plate tectonics. Proceedings of the Regional Conference on the Geology and Mineral Resources of Southeast Asia. Jakarta. 1, 4-7.

Sukamto, R. 1982. Geologic Map of the Pangkajene and Western Part of Watampone Quadrangles, Sulawesi, and its Explanatory Note, 1: 250.000 Series. Bandung: GRDC, 27 pp.

Sukamto, R., Simandjuntak, T. 1983. Tectonic relationship between geologic provinces of western Sulawesi, eastern Sulawesi and Banggai-Sula in the light of sedimentological aspects. Bulletin Geological Research and Development Centre, Bandung, 7**,** 1-12.

Sukardi, Budhitrisna, T. 1992. Geological Map of the Salatiga Quadrangle, Jawa. Bandung: Geological Research and Development Centre.

Sukumar, R. 1990. Ecology of the Asian elephant in southern India. II. Feeding habits and crop raiding patterns. Journal of Tropical Ecology, 6**,** 33-53.

Sukumar, R. 1993. The Asian elephant: ecology and management, Cambridge University Press.

Sukumar, R. 2006. A brief review of the status, distribution and biology of wild Asian elephants Elephas maximus. International Zoo Yearbook, 40**,** 1-8.

Suminto, Morwood, M. J., Kurniawan, I., Aziz, F., van den Bergh, G. D., Hobbs, D. R. 2009. Geology and fossil sites of the Soa Basin, Flores, Indonesia. Pleistocene Geology, Palaeontology and Archaeology of the Soa Basin, Central Flores, Indonesia**,** 19-40.

Suraprasit, K., Chaimanee, Y., Bocherens, H., Chavasseau, O., Jaeger, J.-J. 2014. Systematics and phylogeny of middle Miocene Cervidae (Mammalia) from Mae Moh Basin (Thailand) and a paleoenvironmental estimate using enamel isotopy of sympatric herbivore species. Journal of Vertebrate Paleontology, 34**,** 179-194.

Surono, Toha, B., Sudarno, I. 1992. Geological Map of the Surakarta-Giritontro Quadrangles, Jawa. Bandung: Geological Research and Development Centre.

Suteethorn, V., Chaimanee, Y., Khansupa, S. 1997. Preliminary Report on the Tertiary Vertebrate Fossil of Khorat Basin, Thailand. Annual Meeting and Presentation of Geological Survey Division**,** 111-113.

Sutikna, T., Tocheri, M. W., Morwood, M. J., Saptomo, E. W., Awe, R. D., Wasisto, S., Westaway, K. E., Aubert, M., Li, B., Zhao, J.-x. 2016. Revised stratigraphy and chronology for Homo floresiensis at Liang Bua in Indonesia. Nature, 532**,** 366-369.

Suyono, Kusnama 2010. Stratigraphy and tectonics of the Sengkang Basin, South Sulawesi. Jurnal Geologi Indonesia, 5**,** 1-11.

Suzuki, M., Wikarno, B., Saefudin, I., Itihara, M. 1985. Fission track ages of pumice tuff, tuff layers and javites of Hominid fossil bearing formations in Sangiran area, Central Java. In: Watanabe, N.,Kadar, D. (eds.) Quaternary Geology of the Hominid Fossil Bearing Formations in Java. Bandung: GRDC, Special Publication, 4, 309-311.

Swe, W. 1981. Tectonic evolution of the Western Ranges of Burma. Contributions to Burmese Geology, 1**,** 45-46.

Swisher, C. C., Rink, W. J., Antón, S. C., Schwarcz, H. P., Curtis, G. H., Widiasmoro, A. S. 1996. Latest Homo erectus of Java: potential contemporaneity with Homo sapiens in Southeast Asia. Science, 274**,** 1870-1874.

Takai, M., Saegusa, H., Thaung-Htike, Zin Maung Maung, T. 2006. Neogene mammalian fauna in Myanmar. Asian Paleoprimatology, 4**,** 143-172.

Tapper, N. 2002. Climate, climate variability and atmospheric circulation patterns in the maritime continent region. In: Kershaw, P. (ed.) Bridging Wallace's Line: the Environmental and Cultural History and Dynamics of the Australian-Southeast Asian region. Reiskirchen, Germany: Catena Verlag GMBH, 5-28.

Tapponnier, P., Peltzer, G., Armijo, R. 1986. On the mechanics of the collision between India and Asia. Geological Society, London, Special Publications, 19**,** 113-157.

Tapponnier, P., Peltzer, G., Le Dain, A., Armijo, R., Cobbold, P. 1982. Propagating extrusion tectonics in Asia: new insights from simple experiments with plasticine. Geology, 10**,** 611-616.

Tapponnier, P., Zhiqin, X., Roger, F., Meyer, B., Arnaud, N., Wittlinger, G., Jingsui, Y. 2001. Oblique stepwise rise and growth of the Tibet Plateau. Science, 294**,** 1671-1677.

Tassy, P. 1983. Les Elephantoidea Miocènes du plateau du Potwar, groupe de Siwalik, Pakistan. Annales de Paléontologie, 69 (2-4)**,** 99-136, 235-297, 317-354.

Tassy, P. 1986. Nouveaux Elephantoidea (Proboscidea, Mammalia) dans le Miocène du Kenya: essai de réévaluation systématique. Cahiers de Paléontologie Travailer Paléontologique Est-africaine, Éditions du CNRS**,** 43-65.

Tassy, P. 1988. The classification of Proboscidea: how many cladistic classifications? Cladistics, 4**,** 43-57.

Tassy, P. 1996a. Dental homologies and nomenclature in the Proboscidea. In: Shoshani, J.,Tassy, P. (eds.) The Proboscidea: Evolution and Palaeoecology of Elephants and Their Relatives. Oxford: Oxford University Press, 21-25.

Tassy, P. 1996b. Who is who among the Proboscidea? In: Shoshani, J.,Tassy, P. (eds.) The Proboscidea: Evolution and Palaeoecology of Elephants and Their Relatives. Oxford: Oxford University Press, 39-48.

Tassy, P., Anupandhanant, P., Ginsburg, L., Mein, P., Ratanasthien, B., Sutteethorn, V. 1992. A new Stegolophodon (Proboscidea, Mammalia) from the early Miocene of northern Thailand. Geobios, 25**,** 511-523.

Taylor, J. G. 2003. Indonesia: Peoples and Histories, New Heaven and London, Yale University Press. pp. 8-9.

ter Haar, C. 1934. Toelichting bij Blaad 58 (Boemiajoe). Geologische Kaart van Java Schaal, 1.

Thasod, Y. 2007. Miocene Mastodonts in Thailand and Paleoenvironment. PhD thesis, Chiang Mai University, 368 pp.

Thasod, Y., Jintasakul, P., Ratanasthien, B. 2012. Proboscidean Fossil from the Tha Chang Sand Pits, Nakhon Ratchasima Province, Thailand. Journal of Science and Technology MSU, 1**,** 33-44.

Theunissen, B., de Vos, J., P.Y., S., Aziz, F. 1990. The establishment of a chronological framework for the hominid-bearing deposits of Java; a historical survey. Geological Society of America Special Papers, 242**,** 39-53.

Thunell, R., Anderson, D., Gellar, D., Miao, Q. 1994. Sea-surface temperature estimates for the tropical western Pacific during the last glaciation and their implications for the Pacific warm pool. Quaternary Research, 41**,** 255-264.

Tian, J., Wang, P., Cheng, X. 2004. Development of the East Asian monsoon and Northern Hemisphere glaciation: oxygen isotope records from the South China Sea. Quaternary Science Reviews, 23**,** 2007-2016.

Tiedemann, R., Sarnthein, M., Shackleton, N. J. 1994. Astronomic timescale for the Pliocene Atlantic $\delta^{18}O$ and dust flux records of Ocean Drilling Program Site 659. Paleoceanography, 9**,** 619-638.

Tipple, B. J., Pagani, M. 2007. The early origins of terrestrial C_4 photosynthesis. Annual Review of Earth and Planetary Sciences, 35**,** 435-461.

Tobien, H. 1973. On the Evolution of Mastodonts (Proboscidea, Mammalia). Part 1: The bunodont trilophodont Groups. Notizbl. Hessisches Landesamt Bodenforsch, 101**,** 202-276.

Tobien, H., Chen, G., Li, Y. 1986. Mastodonts (Proboscidea, Mammalia) from the late Neogene and early Pleistocene of the People's Republic of China. Mainzer Geowiss. Mitt., 15**,** 119-181.

Todd, N. E., Roth, V. L. 1996. Origin and radiation of the Elephantidae. In: Shoshani, J.,Tassy, P. (eds.) The Proboscidea: Evolution and Palaeoecology of Elephants and Their Relatives. . Oxford: Oxford University Press, 193-202.

Tokunaga, S., Oshima, H., Polhaupessy, A. A., Ito, Y. 1985. A palynological study of the Pucangan and Kabuh Formations in the Sangiran area. In: Watanabe, N.,Kadar, D. (eds.) Quaternary Geology of the Hominid Fossil Bearing Formations in Java. Bandung: GRDC, Special Publication, 4, 199-207.

Tougard, C. 2001. Biogeography and migration routes of large mammal faunas in South–East Asia during the Late Middle Pleistocene: focus on the fossil and extant faunas from Thailand. Palaeogeography, Palaeoclimatology, Palaeoecology, 168**,** 337-358.

Trevena, A. S., Varga, R. J., Collins, I. D., Nu, U. Tertiary tectonics and sedimentation in the Salin (fore-arc) Basin, Myanmar. Proceeding of the Annual meeting of AAPG, 1991 Dallas, Texas, USA, 75 (3), 683.

Treydte, A. C., Bernasconi, S. M., Kreuzer, M., Edwards, P. J. 2006. Diet of the common warthog (Phacochoerus africanus) on former cattle grounds in a Tanzanian savanna. Journal of Mammalogy, 87 (5)**,** 889-898.

Tudhope, A. W., Chilcott, C. P., McCulloch, M. T., Cook, E. R., Chappell, J., Ellam, R. M., Lea, D. W., Lough, J. M., Shimmield, G. B. 2001. Variability in the El Niño-Southern Oscillation through a glacial-interglacial cycle. Science, 291**,** 1511-1517.

Turney, C. S. M., Kershaw, A. P., Clemens, S. C., Branch, N., Moss, P. T., Fifield, L. K. 2004. Millennial and orbital variations of El Niño-Southern Oscillation and high-latitude climate in the last glacial period. Nature, 428 (6980)**,** 306-310.

Turvey, S. T., Crees, J. J., Hansford, J., Jeffree, T. E., Setiyabudi, E., Kurniawan, I., Paranggarimu, U., van den Bergh, G. D. in prep. Pleistocene and Holocene vertebrate faunas from Sumba, Indonesia: implications for Quaternary biogeography and evolution in Wallacea.

Tütken, T. 2014. Isotope compositions (C, O, Sr, Nd) of vertebrate fossils from the middle Eocene oil shale of Messel, Germany: implications for their taphonomy and palaeoenvironment. Palaeogeography, Palaeoclimatology, Palaeoecology, 416**,** 92-109.

Tütken, T., Furrer, H., Walter Vennemann, T. 2007. Stable isotope compositions of mammoth teeth from Niederweningen, Switzerland: implications for the Late Pleistocene climate, environment, and diet. Quaternary International, 164**,** 139-150.

Tütken, T., Kaiser, T. M., Vennemann, T., Merceron, G. 2013. Opportunistic feeding strategy for the earliest old world hypsodont equids: Evidence from stable isotope and dental wear proxies. PLoS One, 8 (9)**,** e74463, 1-14.

Tütken, T., Vennemann, T. 2009. Stable isotope ecology of Miocene large mammals from Sandelzhausen, southern Germany. Paläontologische Zeitschrift, 83**,** 207-226.

Tütken, T., Vennemann, T., Janz, H., Heizmann, E. 2006. Palaeoenvironment and palaeoclimate of the Middle Miocene lake in the Steinheim Basin, SW Germany: a reconstruction from C, O, and Sr isotopes of fossil remains. Palaeogeography, Palaeoclimatology, Palaeoecology, 241**,** 457-491.

van Bemmelen, R. W. 1949. The Geology of Indonesia, Government Printing Office, The Hague.

van den Bergh, G. D. 1999. The Late Neogene elephantoid-bearing faunas of Indonesia and their palaeozoogeographic implications. Scripta Geologica, 117**,** 1-419.

van den Bergh, G. D. 2007. Report on palaeontological/archaeological fieldwork in the Atambua region, Belu District, West Timor, Indonesia. Unpublished field report,University of Wollongong, 53 pp.

van den Bergh, G. D. 2011. Field Report, Sumba, Indonesia. Unpublished field report, University of Wollongong, 20 pp.

van den Bergh, G. D. 2014. In search of the first Asian hominins: large-scale excavations at Mata Menge, So'a Basin, Flores, NTT. Bandung: unpublished field report of the collaboration between the Geological Agency of Indonesia and the University of Wollongong, 41 pp.

van den Bergh, G. D. 2015a. Preliminary report on the faunal remains of the 2013-2015 excavations at Leang Bulu Bettue, South Sulawesi, Indonesia. Unpublished field report, University of Wollongong. 39 pp.

van den Bergh, G. D. 2015b. Sedimentology of the Rizal excavation sites 2014-2015. Unpublished field report, National Museum of the Philippines, 21 pp. .

van den Bergh, G. D., Awe, R. D., Morwood, M. J., Sutikna, T., Wahyu Saptomo, E. 2008. The youngest stegodon remains in Southeast Asia from the Late Pleistocene archaeological site Liang Bua, Flores, Indonesia. Quaternary International, 182**,** 16-48.

van den Bergh, G. D., Aziz, F., Sondaar, P., Hussain, S. 1992. Taxonomy, stratigraphy, and paleozoogeography of Plio-Pleistocene Proboscideans from the Indonesian Islands. Bulletin of Geological Research and Development Centre, Paleontology Serie, 7**,** 28-58.

van den Bergh, G. D., Aziz, F., Sondaar, P. Y., de Vos, J. 1994. The first Stegodon fossils from Central Sulawesi and a new advanced Elephas species from South Sulawesi (Indonesia). Geological Research and Development Center Bandung Bulletin, 17**,** 22-39.

van den Bergh, G. D., Brumm, A., Puspaningrum, M. R., Setiabudi, E., Kurniawan, I., Prasetyo, U. W. Taphonomy of Stegodon florensis remains from the early Middle Pleistocene archaeological site Mata Menge, Flores, Indonesia. the VIth International Conference on Mammoths and their Relatives, 2014. 207-208.

van den Bergh, G. D., de Vos, J., Sondaar, P. Y. 2001. The Late Quaternary palaeogeography of mammal evolution in the Indonesian Archipelago. Palaeogeography, Palaeoclimatology, Palaeoecology, 171**,** 385-408.

van den Bergh, G. D., Kaifu, Y., Kurniawan, I., Kono, R. T., Brumm, A., Setiyabudi, E., Aziz, F., Morwood, M. J. 2016a. Homo floresiensis-like fossils from the early Middle Pleistocene of Flores. Nature, 534**,** 245-248.

van den Bergh, G. D., Kurniawan, I. 2010. A partial elephant skeleton and skull from the Menden Alluvial Terrace near Sunggu village, Solo River valley, east Central Java. University of Wollongong.

van den Bergh, G. D., Li, B., Brumm, A., Grün, R., Yurnaldi, D., Moore, M. W., Kurniawan, I., Setiawan, R., Aziz, F., Roberts, R. G. 2016b. Earliest hominin occupation of Sulawesi, Indonesia. Nature, 529**,** 208-211.

van den Bergh, G. D., Meijer, H., Awe, R. D., Morwood, M. J., Szabó, K., van den Hoek Ostende, L., Sutikna, T., Saptomo, E., Piper, P., Dobney, K. M. 2009. The Liang Bua faunal remains: a 95k. yr. sequence from Flores, East Indonesia. Journal of Human Evolution, 57**,** 527-537.

van den Bergh, G. D., Westaway, K. E., Morwood, M. J., Kurniawan, I., Moore, M. W., Setiawan, R., Zhao, J., Kohn, B., Turney, C. S. M., Suyono, Aziz, F. in prep. Hominin colonisation of Timor, East Indonesia: evidence from the Atambua Basin.

van den Hoek Ostende, L., van den Bergh, G. D., Due, R. A. 2006. First fossil insectivores from Flores. Hellenic journal of geosciences, 41**,** 67-72.

van der Geer, A. A. E., van den Bergh, G. D., Lyras, G. A., Prasetyo, U. W., Due, R. A., Setiyabudi, E., Drinia, H. 2016. The effect of area and isolation on insular dwarf proboscideans. Journal of Biogeography, 43**,** 1656–1666.

van der Kaars, S. 1998. Marine and terrestrial pollen records of the last glacial cycle from the Indonesian region: Bandung Basin and Banda Sea. Palaeoclimates, 3**,** 209-219.

van der Kaars, S., Wang, X., Kershaw, P., Guichard, F., Setiabudi, D. A. 2000. A Late Quaternary palaeoecological record from the Banda Sea, Indonesia: patterns of vegetation, climate and biomass burning in Indonesia and northern Australia. Palaeogeography, Palaeoclimatology, Palaeoecology, 155**,** 135-153.

van der Kaars, W. A. 1991. Palynology of eastern Indonesian marine piston-cores: a Late Quaternary vegetational and climatic record for Australasia. Palaeogeography, Palaeoclimatology, Palaeoecology, 85**,** 293-302.

van der Maarel, F. H. 1932. Contributions to the knowledge of the fossil mammalian fauna of Java. Dienst van den Mijnbouw in Nederlandsch-Indië, 15**,** 1-208.

van der Merwe, N. J., Medina, E. 1989. Photosynthesis and $^{13}C/^{12}C$ ratios in Amazonian rain forests. Geochimica et Cosmochimica Acta, 53**,** 1091-1094.

van Heekeren, H. 1949. Early man and fossil vertebrates on the island of Celebes. Nature, 163**,** 492.

van Leeuwen, T. M. 1981. The geology of southwest Sulawesi with special reference to the Biru area. The Geology and Tectonics of Eastern Indonesia, 2**,** 277-304.

van Leeuwen, T. M., Taylor, R., Coote, A., Longstaffe, F. J. 1994. Porphyry molybdenum mineralization in a continental collision setting at Malala, northwest Sulawesi, Indonesia. Journal of Geochemical Exploration, 50**,** 279-315.

van Oosterzee, P. 2000. Where worlds collide: the Wallace Line. Journal of the History of Biology, 33 (1)**,** 202-205

Vandenberghe, J., Lu, H., Sun, D., van Huissteden, J. K., Konert, M. 2004. The late Miocene and Pliocene climate in East Asia as recorded by grain size and magnetic susceptibility of the Red Clay deposits (Chinese Loess Plateau). Palaeogeography, Palaeoclimatology, Palaeoecology, 204**,** 239-255.

Vasishat, R. N., Gaur, R., Chopra, S. R. K. 1978. Community structure of Middle Śivalik vertebrates from Haritalyangar (H.P.), India. Palaeogeography, Palaeoclimatology, Palaeoecology, 23**,** 131-140.

Vidya, T., Sukumar, R., Melnick, D. J. 2009. Range-wide mtDNA phylogeography yields insights into the origins of Asian elephants. Proceedings of the Royal Society B: Biological Sciences, 276**,** 893-902.

Visser, K., Thunell, R., Stott, L. 2003. Magnitude and timing of temperature change in the Indo-Pacific warm pool during deglaciation. Nature, 421**,** 152-155.

Vita-Finzi, C., Hidayat, S. 1991. Holocene uplift in West Timor. Journal of Southeast Asian Earth Sciences, 6**,** 387-393.

Vogel, J. C. 1980. Fractionation of the carbon isotopes during photosynthesis, Berlin, Springer-Verlag, 1-29.

von Koenigswald, G. H. R. 1933. Beitrag zur Kenntnis der fossilen Wirbeltiere Javas, Wetenschappelijke mededeelingen, dienst van den mijnbouw in Nederlandsch-Indie, 23, 184 pp.

von Koenigswald, G. H. R. 1934. Zur stratigraphie des Javanischen Pleistocän. De Ingenieur in Nederlandsch-Indië, 11**,** 1985-201.

von Koenigswald, G. H. R. 1935a. Bemerkungen zur fossilen Säugetierfauna Javas I. De Ingenieur in Nederlandsch - Indië, 2**,** 67-70.

von Koenigswald, G. H. R. 1935b. Bemerkungen zur fossilen Säugetierfaunas Javas. II. De Ingenieur Nederlandsch - Indië, 10**,** 85-88.

von Koenigswald, G. H. R. 1956. Fossil mammals from the Philippines. National Research Council of the Philippines, University of the Philippines**,** 1-24.

von Koenigswald, W., Martin, T., Pfretzschner, H. U. 1993. Phylogenetic interpretation of enamel structures in mammalian teeth: possibilities and problems. Mammal Phylogeny, 2**,** 303-314.

Voris, H. K. 2000. Maps of Pleistocene sea levels in Southeast Asia: shorelines, river systems and time durations. Journal of Biogeography, 27**,** 1153-1167.

Vrba, E. S., Denton, G. H., Prentice, M. L. 1989. Climatic influences on early hominid behavior. Ossa, 14**,** 127-156.

Wakita, K., Sopaheluwakan, J., Miyazaki, K., Zulkarnain, I. 1996. Tectonic evolution of the Bantimala complex, south Sulawesi, Indonesia. Geological Society, London, Special Publications, 106**,** 353-364.

Wallace, A. R. 1876. The Geographical Distribution of Animals: With a Study of the Relations of Living and Extinct Faunas as Elucidating the Past Changes of the Earth's Surface, Macmillan. London.

Wandrey, C. J. 2006. Eocene to Miocene composite total petroleum system, Irrawaddy-Andaman and north Burma geologic provinces, Myanmar. No. 2208-E: U. S. Geological Survey, VI, 1-26.

Wang, S., He, W., Chen, S. 2012a. The gomphotheriid mammal Platybelodon from the Middle Miocene of Linxia Basin, Gansu, China. Acta Palaeontologica Polonica, 58**,** 221-240. Wang, W., Potts, R., Baoyin, Y., Huang, W., Cheng, H., Edwards, R. L., Ditchfield, P. 2007a. Sequence of mammalian fossils, including hominoid teeth, from the Bubing Basin caves, South China. Journal of Human Evolution, 52**,** 370-379.

Wang, X., Qiu, Z., Li, Q., Wang, B., Qiu, Z., Downs, W. R., Xie, G., Xie, J., Deng, T., Takeuchi, G. T. 2007b. Vertebrate paleontology, biostratigraphy, geochronology, and paleoenvironment of Qaidam Basin in northern Tibetan Plateau. Palaeogeography, Palaeoclimatology, Palaeoecology, 254**,** 363-385.

Wang, Y., Fang, X., Zhang, T., Li, Y., Wu, Y., He, D., Gao, Y., Meng, P., Wang, Y. 2012b. Distribution of biomarkers in lacustrine sediments of the Linxia Basin, NE Tibetan Plateau, NW China: Significance for climate change. Sedimentary Geology, 243**,** 108-116.

Wang, Y., Jin, C., Deng, C., Wei, G., Yan, Y. 2012c. The first sinomastodon (Gomphotheriidae, Proboscidea) skull from the Quaternary in China. Chinese Science Bulletin, 57 (36)**,** 4726-4734.

Wang, Y., Jin, C., Mead, J. I. 2014a. New remains of Sinomastodon yangziensis (Proboscidea, Gomphotheriidae) from Sanhe karst cave, with discussion on the evolution of Pleistocene Sinomastodon in South China. Quaternary International, 339**,** 90-96.

Wang, Y., Jin, C., Pan, W., Qin, D., Yan, Y., Zhang, Y., Liu, J., Dong, W., Deng, C. 2015. The Early Pleistocene Gigantopithecus-Sinomastodon fauna from Juyuan karst cave in Boyue Mountain, Guangxi, South China. Quaternary International.

Wang, Y., Wei, G., Mead, J. I., Jin, C. 2014b. First mandible and deciduous dentition of juvenile individuals of Sinomastodon (Proboscidea, Mammalia) from the Early Pleistocene Renzidong Cave of eastern China. Quaternary International, 354**,** 131-138.

Wasson, R., Cochrane, R. 1979. Geological and geomorphological perspectives on archaeological sites in the Cagayan valley, Northern Luzon, The Philippines. Modern Quaternary Research in Southeast Asia, 5**,** 1-26.

Watzel, R., Heidinger, M. 2006. Isotope response of hydrological systems to long term exploitation in the Singen aquifer system, Germany. Isotopic Assessment of Long Term Groundwater Exploitation. Vienna, Austria, 273-285.

Wensink, H. 1994. Paleomagnetism of rocks from Sumba: tectonic implications since the late Cretaceous. Journal of Southeast Asian Earth Sciences, 9**,** 51-65.

Wensink, H., van Bergen, M. J. 1995. The tectonic emplacement of Sumba in the Sunda-Banda Arc: paleomagnetic and geochemical evidence from the early Miocene Jawila volcanics. Tectonophysics, 250**,** 15-30.

Westaway, K., Morwood, M. J., Roberts, R., Rokus, A., Zhao, J.-x., Storm, P., Aziz, F., Van Den Bergh, G., Hadi, P., de Vos, J. 2007. Age and biostratigraphic significance of the Punung Rainforest Fauna, East Java, Indonesia, and implications for Pongo and Homo. Journal of Human Evolution, 53**,** 709-717.

Westaway, K., Sutikna, T., Saptomo, W., Morwood, M. J., Roberts, R. G., Hobbs, D. 2009a. Reconstructing the geomorphic history of Liang Bua, Flores, Indonesia: a stratigraphic interpretation of the occupational environment. Journal of Human Evolution, 57**,** 465-483.

Westaway, K. E., Roberts, R. G., Sutikna, T., Morwood, M. J., Drysdale, R., Zhao, J.-x., Chivas, A. 2009b. The evolving landscape and climate of western Flores: an environmental context for the archaeological site of Liang Bua. Journal of Human Evolution, 57**,** 450-464.

Westaway, M. 2002. Preliminary observations on the taphonomic processes at Ngandong and some implications for a late Homo erectus survivor model. Tempus, 7**,** 189-193.

Whitmore, T. C. (ed.) 1981. Wallace's Line and Plate Tectonics, Oxford: Clarendon Press, 1-91.

Whitmore, T. C. 1984. A vegetation map of Malesia at scale 1: 5 million. Journal of Biogeography**,** 461-471.

Whittaker, R. H., Klomp, H. 1975. The design and stability of plant communities. Unifying Concepts in Ecology. Springer Netherlands, 169-183.

Wilson, M. E., Bosence, D. W. 1996. The Tertiary evolution of South Sulawesi: a record in redeposited carbonates of the Tonasa Limestone Formation. Geological Society, London, Special Publications, 106**,** 365-389.

Wilson, M. E. J., Moss, S. J. 1999. Cenozoic palaeogeographic evolution of Sulawesi and Borneo. Palaeogeography, Palaeoclimatology, Palaeoecology, 145**,** 303-337.

Wing, L. D., Buss, I. O. 1970. Elephants and forests. Wildlife monographs**,** 3-92.

WMO IAEA, WMO WMO 2006. Global network of isotopes in precipitation. The GNIP database.

Wright, J. D., Miller, K. G., Fairbanks, R. G. 1992. Early and middle Miocene stable isotopes: implications for deepwater circulation and climate. Paleoceanography, 7**,** 357-389.

Wroe, S., Field, J., Fullagar, R., Jermin, L. S. 2004. Megafaunal extinction in the late Quaternary and the global overkill hypothesis. Alcheringa, 28**,** 291-331.

Xu, C., Sano, M., Nakatsuka, T. 2011. Tree ring cellulose $\delta^{18}O$ of Fokienia hodginsii in northern Laos: A promising proxy to reconstruct ENSO? Journal of Geophysical Research: Atmospheres, 116.

Yin, A., Rumelhart, P., Butler, R., Cowgill, E., Harrison, T., Foster, D., Ingersoll, R., Qing, Z., Xian-Qiang, Z., Xiao-Feng, W. 2002. Tectonic history of the Altyn Tagh fault system in northern Tibet inferred from Cenozoic sedimentation. Geological Society of America Bulletin, 114**,** 1257-1295.

Yoshikawa, S., Suminto 1985. Tuff layers and pumice tuff beds of the Pliocene and Pleistocene sediments in the Sangiran area. In: Watanabe, N.,Kadar, D. (eds.) Quaternary Geology of the Hominid Fossil Bearing Formations in Java. Bandung: GRDC, Special Publication, 4, 97-104.

You, Y., Huber, M., Müller, R., Poulsen, C., Ribbe, J. 2009. Simulation of the middle Miocene climate optimum. Geophysical Research Letters, 36 (4), L04702, 1-5.

Yuyen, W., Sirinavin, T. 1985. Geologic Map, Changwat Chaiyaphum, sheet ND 48-1, scale 1: 250,000. Bangkok, Thailand: Department of Mineral Resources (DMR).

Zachos, J. C., Breza, J. R., Wise, S. W. 1992. Early Oligocene ice-sheet expansion on Antarctica: Stable isotope and sedimentological evidence from Kerguelen Plateau, southern Indian Ocean. Geology, 20, 569-573.

Zachos, J. C., Flower, B. P., Paul, H. 1997. Orbitally paced climate oscillations across the Oligocene/Miocene boundary. Nature, 388, 567-570.

Zaim, Y. 2010. Geological evidence for the earliest appearance of hominins in Indonesia. In: Fleagle, J., Shea, J., Grine, F. E., Baden, A. L.,Leakey, R. (eds.) Out of Africa I: The Hominin Colonization of Eurasia. New York: Springer, 97-110.

Zaim, Y., Larick, R., Ciochon, R. L., Suminto, Rizal, Y., Sujatmiko 1999. Karakteristik satuan Lahar Bawah dari formasi Pucangan di Sangiran, Jawa Tengah. Buletin Geologi, Jurusan Teknik Geologi ITB, 31, 67-84.

Zazzo, A., Balasse, M., Passey, B. H., Moloney, A. P., Monahan, F. J., Schmidt, O. 2010. The isotope record of short- and long-term dietary changes in sheep tooth enamel: Implications for quantitative reconstruction of paleodiets. Geochimica et Cosmochimica Acta, 74, 3571-3586.

Zhang, C., Wang, Y., Deng, T., Wang, X., Biasatti, D., Xu, Y., Li, Q. 2009. C_4 expansion in the central Inner Mongolia during the latest Miocene and early Pliocene. Earth and Planetary Science Letters, 287, 311-319.

Zhang, H., Wang, Y., Janis, C. M., Goodall, R. H., Purnell, M. A. 2016. An examination of feeding ecology in Pleistocene proboscideans from southern China (Sinomastodon, Stegodon, Elephas), by means of dental microwear texture analysis. Quaternary International.

Zheng, H., Powell, C. M., Rea, D. K., Wang, J., Wang, P. 2004. Late Miocene and mid-Pliocene enhancement of the East Asian monsoon as viewed from the land and sea. Global and Planetary Change, 41, 147-155.

Zin-Maung-Maung-Thein, Takai, M., Tsubamoto, T., Egi, N., Thaung-Htike, Nishimura, T., Maung-Maung, Zaw-Win 2010. A review of fossil rhinoceroses from the Neogene of Myanmar with description of new specimens from the Irrawaddy Sediments. Journal of Asian Earth Sciences, 37, 154-165.

Zin-Maung-Maung-Thein, Takai, M., Uno, H., Wynn, J. G., Egi, N., Tsubamoto, T., Thaung-Htike, Aung-Naing-Soe, Maung-Maung, Nishimura, T., Yoneda, M. 2011. Stable isotope analysis of the tooth enamel of Chaingzauk mammalian fauna (late Neogene, Myanmar) and its implication to paleoenvironment and paleogeography. Palaeogeography, Palaeoclimatology, Palaeoecology, 300, 11-22.

Appendix I: Description of Proboscidea taxa

I.1 Gomphotheriidae I.1.1

Genus Platybelodon I.1.1.1

Platybelodon cf. grangeri

The genus Platybelodon is distinguished from other Proboscidea for having an elongated, well developed shovel-like symphysis with two strong flattened lower incisors and the occurrence of dentinal tubules in the lower tusk (Borissiak, 1928, 1929, Tassy, 1986). The original diagnosis of the genus was presented in Osborn and Granger (1931).

Molar analysed in this study (n=6: PRY 74, PRY 75, PRY 77, PRY 79, PRY 80 and PRY 85) are an upper and five lower isolated third molars (M3, Plate I.a-d). Molars are of bunolophodont type and each upper and lower molars are narrow in posterior direction. The upper molar (M^3) possesses 5 lophids, while the lower molars (M_3) contain 5 to 5½ lophids. Measured length and width of the upper molar are 181.3 mm and 72.2 mm, respectively. The length of lower molars ranges between 139 and 190.4+ mm, while the width varies between 61.4 and 69.4 mm. Molars have well-developed cementum, with the presence of small enamel conules in the interlophids and median sulcus. Both anterior and posterior cingula are present. The worn anterior pretrite and posttrite half−lophs specific enamel wear pattern called trefoils, comprising mesoconelets and posterior accessory central conules, and the first anterior pretrite accessory central conule being linked to the anterior cingulum. The first and second anterior lophs of the M3s have well−developed trefoils pattern in their pretrites and postrites. Posterior accessory central conules only present in 3 anterior pretrites. The first anterior pretrite accessory central conule is linked to the anterior cingulum. The anterior pretrite accessory central conules are only developed on the third and fourth lophs, and tend to become smaller from the anterior to the more posterior lophs, or are absent altogether. The posterior posttrite only consists of mesoconelets. The posterior cingulum composes of one large pretite cusps and two small postrite cusps.

The characteristics of the analysed molar are in a close affinity of two common Platybelodon species found in Asia: Platybelodon danovi and Platybelodon grangeri. However, the sizes of the specimens fit within the range of P. grangeri and too large for the range of P. danovi (L= 130-133 mm, W= 65 mm, Osborn and Granger, 1931).

I.1.2 Genus Sinomastodon

I.1.2.1 Sinomastodon sp.

The genus Sinomastodon is characterised by a mandible with a transverse section of the ramus horizontal is widened buccally, and a protruding angular to round coronoid processes. Lower tusks are absent. The molars are bunodont, with trilophodont intermediates (m1 and m2), which are combined with an elephantiod-like mandible, lacking lower incisors and with a reduced symphysis with narrow gutter. This combination of features can be summarized as bunodont-trilophodont-dibelodont-brevirostrine mastodonts (Tobien, 1973). Due to the fragmented nature of the specimens, further identification at the species level could not be made.

I.1.1.3 Sinomastodon bumiajuensis

Earlier findings of dental materials of Sinomastodon reported from the 1930s excavation in Bumiayu (Kaliglagah Formation, van der Maarel, 1932) and in Sangiran, in the "black clay" of the Sangiran Formation (Watanabe and Kadar, 1985). A total of five dental specimens were reported from these earlier findings and all are identified as M3s. This species is described from the holotype from the Kaliglagah Formation: a fragmentary right mandibular ramus with M_3 from Bumiayu (Kaliglagah Excavation 8, Fig.4.9), a fragmentary upper jaw with injured left and right M^3, a fragment of cranium with left and right M^3 and a detached upper incisive tusk that probably belongs to the same individual (the latter two are from Kaliglagah Excavation 1-4, Fig. 4.9).

The specific characters of the genus Sinomastodon are the brevirostrine (shortened) mandible lacking tusk (dibelodont), the bunodont molar with trilophodont intermediate molars (Saegusa, 1995). The holotype of S. bumiajuensis are that the third inferior

molars (labelled as WM-15, K135, and K462), which now stored in the MGB. The third molars have five transverse lophs and are narrowing posteriorly. Three anterior lophs of approximately equal width have prominent trefoils pattern on worn pretrite but not on postrite, 5^{th} lophid bearing four conelets, anterior and posterior cingulum are present, posterior cingulum consists of three rudimentary conelets (van der Maarel, 1932).

Only recently, six Sinomastodon bumiajuensis fossil molars were surface collected from the Early Pleistocene sediments in the Semedo Village, Central Java reported by Fitriawati (2009), while two other specimens recognised during this study from local museum collection (labelled as SMD 1 and SMD 2). In her thesis, Fitriawati (2009) has only given measurement of the specimens and attributed the specimens as intermediate molars (M2), while detailed description was not given. However, her report is giving new additional information of the size M2s of this species, as the previous description of S. bumiajuensis is only based on M3s. Due to importance of these specimens, the morphological description of the molars from Semedo will be given as follows.

All specimens are attributed to inferior (lower) molars. Both, D1/SS-18 (Plate I.e) and DK 144 (Plate I.f) are complete isolated left M_2, DK 145 (Plate I.g) is an anterior fragment of a left M_2 with two lophs remaining, while DK 146 (Plate I.h) is an anterior fragment of a right M_3 with remains of the first and broken second ridges. SMD 1 and SMD 2 (Plate I.i) are unworn third lophs of the third molars. Each molar are slightly narrowing posteriorly. Lophid numbers of complete M2 are 3, with maximum width measured at 41 and 52 mm, while maximum length measured at 62 and 70.45 mm. Molars in particular have less-developed cementum and small enamel conules in the interlophids, median sulcus present, anterior cingulum is prominent, while posterior cingulum is relatively weak. Anterior and posterior accessory central conules present in all three lophids, but posteriorly diminished in size. The worn molars show trefoil pattern in all lophs (1 to 3), which appear more prominent in their pretrite, and weak in postrite.

Sinomastodon bumiajuensis is the only Gomphotheriidae that has been found in Java and in the Indonesian Archipelago so far. The bumiajuensis is assigned as the specific epithet because the holotype of the species originated from the Bumiayu area. The species was then placed in the genus Tetralophodon by van der Maarel (1932) and in the genus Mastodon (von Koenigswald, 1933). As proposed by Saegusa (1995) the

Bumiayu mastodon should be placed in the genus Sinomastodon (Tobien et al., 1986). The skull and dental morphologies of S. bumiajuensis shows close similarity with Chinese sinomastodonts (S. hanjiangensis, S. jiangnanensis and S. yangziensis) from the Early Pleistocene cave in the southern China (Wang et al., 2012), but more derived compared to the Pliocene Sinomastodon from Japan and North China.

The first occurrence this species is derived from specimens from Kaliglagah (van der Maarel, 1932) can be assigned as older than 1.5 Ma, since all specimens were excavated from the Kaliglagah Formation, which its stratigraphic position is placed below the Mengger Formation ($^{40}Ar/^{39}Ar$ dated at 1.53 Ma, Storey, pers. comm. to van den Bergh, 2013). The last occurrence is derived from the specimen from Sangiran that was found below the T10 layer, which fission track dated at 1.16 Ma (Suzuki et al., 1985). In contrast, the age of the specimens from Semedo is harder to estimate, since all specimens are surface collected and the sediments in Semedo lack of dating control. However, the lithology of the outcrops in the vicinity of the discovery site of SMD 1 and 2 is comparable with the Kaliglagah Formation (personal observation). Hence, interpolated from the age of Kaliglagah Formation in Bumiayu, the age of S. bumiajuensis specimens from Semedo is estimated as older than 1.5 Ma.

I.2 Stegodontidae

I.2.1 Genus Stegolophodon

I.2.1.1 Stegolophodon cf. stegodontoides

A group of primitive Stegolophodon were surface collected from the Irrawaddy Group and Tha Chang sandpits. Molars analysed in this study includes the second and third molars (M2 and M3, Plate I. j, k, l). The second molar has a consistent width from anterior to posterior, while the width of third molars is decreasing posteriorly. The numbers of lophids in the upper and lower second molars varies between x4x and x5, while the third molars consist x5x to x6x lophids. A median sulcus is present. Each lophids contains 4-6 conules, which are large, rounded and blunt. Conules separated by a shallow grove. Accessory anterior and/or posterior central conules are usually developed in the pretrite of the first to second or third anterior lophids, while the

posterior lophids do not have accessory conules. The anterior cingulum contains a variable number of small conules that may or may not be present, and if present it connected to the accessory anterior central conule. Enamel is relatively thick (0.4-0.55 mm). A weak trefoil pattern is shown in half worn first and second lophids. Enamel folding shows a weak pattern when half worn and no folding when heavily worn. Posterior cingulum usually contains 3-4 small conules.

The described specimens are comparable to Stegolophodon cf. stegodontoides, diagnosed by Pilgrim (1913) and Tassy (1983). Detailed descriptions of molars found in the Tha Chang sandpit are presented by Thasod (2007). Saegusa (2005) includes the Tha Chang species in the Stegolophodon group 4, which is generally characterised by large molars, with a width of ~10 cm or more. Osborn (1936) and Tassy et al. (1992) considered that Stegolophodon stegodontoides represents a progressive Stegolophodon species, which is proposed to be a transitional between Stegolophodon and Stegodon. To the contrary, Saegusa et al. (2005) consider this species to be more primitive than other Stegolophodon species that are included in Stegolophodon groups 1, 2 and 3 from the northern Thailand and Japan, based on the stronger distal displacement of the main pretrite cusp on their lophids.

I.2.1.2 Stegolophodon intermediate form

Specimens of a morphologically intermediate form between advanced Stegolophodon and primitive Stegodon were recovered from the Tha Chang sandpits, seven of them were analysed in this study. This unnamed form is distinguished from other known Stegolophodon species by having x7x lophids in the M3s. Molars are generally large (complete M^3 are 200 to 273+ mm long and 96 to 130 mm wide; M_3s range between 284+ to 306 mm in length and between 100 to 116 mm in width).There are four conules in each lophid with occurrence of strong posterior central conules, yet the development of a median sulcus is not evident (Plate I.m). Accessory anterior and posterior central conules are present in the pretrite of the first to second or third anterior lophids. The fourth and fifth lophids may or may not have posterior central conules, but these are always absent in the most posterior two lophids. The structure of the posttrite is the mirror image of that of pretrite. Anterior and posterior cingulums are similar to

Stegolophodon cf. stegodontoides. Enamel is relatively thick (0.4-0.55 mm). Weak trefoil pattern is only shown in half worn first to third worn lophids. Enamel folding in the analysed specimens is stronger than it is in the Stegolophodon stegodontoides specimens. These characteristics represent a mixture between more archaic Stegolophodon species with 6 or less lophids and primitive Stegodon molars.

This intermediate form is proposed in Saegusa et al. (2005) as Stegolophodon group 5 and in Thasod et al. (2012) as Stegolophodon intermediate form. However, this form has not yet been given a formal species name, since most candidates for syntypes of such a new species are kept in private collections instead of public institution. Nevertheless, it is no doubt that this form is a distinct species.

I.2.2 Genus Stegodon

I.2.2.1 Stegodon cf. zdanskyi

Specimens of Stegodon originated from the Tha Chang sandpits are showing a primitive molar structure intermediate between Stegolophodon and Stegodon. The analysed molars consist of 4 upper third molars (M^3) and a lower third molar (M_3). A complete M^3 consist of x6x ridges (Plate II.a), while the M_3 is represented by a worn posterior fragment of the right side with -5x ridges remaining. The anterior lophid contains four conules, but subsequent lophids tend to be subdivided into six or more conules. Enamel folding is weakly and irregularly folded with a well-developed stufenbildung. The strong sulcus in the upper M^3s is distinct throughout the lophs but is heavily displaced buccally. Cement covering the crown is very thin, and the sulcus between cusps is very shallow. The character and number of lophid of these specimens are comparable to the description of Stegodon zdanskyi (Hopwood, 1935).

This species is considered as a primitive Stegodon due to the small lophids number per molar, few conules and conelets number and distinct median sulcus throughout the lophs but heavily displaced buccally, which is commonly seen in primitive Stegodon. Saegusa (in Saegusa, 1996 and Saegus et al., 2005) proposed that this species may be the ancestral form of S. orientalis and S. trigonocephalus, due to the irregular enamel folding and strong stufenbildung.

I.2.2.2 Stegodon cf. elephantoides

A group of incomplete molars surface collected from the Tha Chang Sandpits were sampled for stable isotope analysis. All analysed molars (n =11) are fragmented, thus the number of total ridges of complete molar cannot be identified. The most complete specimen, a M^3 of the left side, is shown in Plate II.b. This worn M^3 has -7½ ridges left, so that presumably each third molar at least contained more than 7 ridges. Specimens are upper and lower third molars with their maximum width varying between 93 and 107 mm, with width of ridges decreasing posteriorly. Molar crowns are robust and widening towards the base. Each ridge is subdivided into six to eight conules with blunt rounded tips. Worn ridges show coarse folding on the enamel-dentine junction. Cement occurs in the inter-valleys of posterior lophids. The enamel thickness varies between 0.35 and 0.45 mm. Worn enamel are showing small weak folding forming an irregular pattern. The enamel folding of these specimens is more complicated than in the Stegodon n sp. 1 figured by Thasod (2007, p. 172-178).

The size and ridge characteristics of these specimens are comparable to Stegodon elephantoides. However, the size of the mammillae is smaller and the enamel folding pattern is coarser than those of S. elephantoides from the Irrawaddy beds. This group might represent a primitive form of S. elephantoides, therefore in this study this group will be assigned as Stegodon cf. elephantoides.

I.2.2.3 Stegodon cf. insignis/ganesa

A group of analysed Stegodon molars (n = 5) showing advanced characters were recovered from Irrawaddy and the Siwalik Group in the vicinity of Haripur. Descriptions of specimens from the Siwalik (Dubois coll. No. 3041+3099, 3051 and 3053) are given by Hooijer (1955). The specimens from the Irrawaddy Beds represent both upper and lower third molars and bear close similarities to those from Siwalik. A complete M_3 from Irrawaddy contains x11x ridges, while a complete M^3 contains x10x ridges (Plate II.c). Widths of lower and upper molars from Irrawaddy are 93 and 98 mm, respectively, while length measured at 250 mm (M^3) and 276 mm (M_3). Molars are only

slightly narrowing in posterior direction. Ridges are relatively tall and each ridge contains 8-10 small conules. Thick cement occurs between ridges. Worn ridges are showing fine and strong enamel folding. Size of specimens and described characters are comparable to Stegodon insignis and S. ganesa from the upper Siwalik deposits. However, both species are difficult to distinguish only by their molar, thus these specimens attributed as S. insignis/ganesa. The age of this species is estimated at Late Pliocene-Early Pleistocene (Opdyke et al., 1979).

I.2.2.4 Stegodon cf. orientalis

An advanced form of Stegodon molars were surface collected from the upper part of the Tha Chang Sandpits (n = 3) and from an unknown locality in Laos (n =1). The most complete specimen, a left M_2 from Tha Chang, is shown in Plate II.d. Analysed specimens comprise a lower first molar (M_1), a lower second molar (M_2), an upper third molar (M^3) and a fragmented $M^{2/3}$(?). The M_2 contains 10½ lophs, with a length and width measured at 226 mm and 76mm, respectively. The second and third molars are incomplete (fragmented molars contain -6-, x7- and x8- ridges). Width varies between 108 and 115, and length must have exceeded 200-268 mm. Ridges are subdivided into more than 10 fine and pointed conules. Worn ridges are showing fine and irregular enamel folding, enamel thickness ranges between 0.15 and 0.3 mm. Cement is weakly-developed between lophs. Worn ridges show fine, strong and asymmetrical enamel folding. The size and characteristics of these specimens are comparable to Stegodon orientalis from the late Middle to Upper Pleistocene deposits of northern and southern China as well as from Japanese localities.

I.2.2.5 pygmy Stegodon sp.

A small-sized Stegodon reported from Sambungmacan, Central Java and from Ranji Kares in Cirebon, West Java (Aziz et al., 1995, van den Bergh, 1999). The only specimen found in Sambungmacan is a right mandibular ramus with M_1. The specimen from Sambungmacan was found embedded in the limestone matrix, presumably from the base of the Pucangan Formation. While the specimen from Cirebon is a fragment of

a right lower M_3 from unknown stratigraphic position. The main differences of the pygmy Stegodon species compared to molars of Stegodon trigonocephalus are it has significantly smaller size and lower ridge numbers (ridge formula of M_3 of the pygmy Stegodon sp = x9x and Stegodon trigonocephalus = 13). The molar of pygmy Stegodon sp. is very similar to another molar from an unknown locality, and also to von Koenigswald's subspecies Stegodon trigonocephalus praecursor. Van den Bergh (1999) suggested that the pygmy Stegodon sp. is diminutive insular form of one of the earliest Stegodon invaders of Java and represents the existence of one or more separate palaeo-islands in the area at the onset of the Pleistocene, inhabited by dwarf Stegodon. He also suggested that dwarf Stegodon maybe occurred simultaneously in isolated areas. Its position in the faunal succession scheme (Figure 4.10) is estimated from the evidence that it was found in the Early Pleistocene sediments, but was not recorded in the Satir Fauna, and neither in the sedimentary units that contain the Kedung Brubus and younger faunas.

I.2.2.6 Stegodon trigonocephalus

Due to a large number of collections, wide distributions and continuous occurrence in the Pleistocene sediments of Java, Stegodon trigonocephalus is comparatively better studied than other proboscidean taxa in Java. Descriptions of this species have been done by various authors (Martin, 1887, 1888, 890, Dubois, 1908, Janensch, 1911, Dietrich, 1926, van der Maarel, 1932, von Keonigswald, 1933, 1935a, 1935b, Hooijer, 1955, van den Bergh, 1999), while occurrence of these species are vastly reported from various Pleistocene fossil localities in western and eastern parts of Java. Different scientific names had been given to this species due to morphological variability of Stegodon specimens: Stegodon javanoganesa and S. ganesa var. javanicus (Dubois, 1908), S. airawana (Janensch, 1911), S. bondolensis (van der Maarel, 1932) and Crytomastodon martini (von Koenigswald, 1933). However, Hooijer (1955) concluded that all specimens belong to single species Stegodon trigonocephalus and treated other names as junior synonym. Sub-grouping of Stegodon trigonocephalus into subspecies has been done by von Koenigswald (1933) and van den Bergh (1999) based on increase of the average number of ridges per molar that can be recognised through the time, from

primitive to advance: Stegodon trigonocephalus praecursor, S. t. trigonocephalus, and S. t. ngandongensis.

Molars of Stegodon trigonocephalus (e.g. Plate II.n) included in advance form, since it lacks of median sulcus, has large number of ridge per molar (6-7 in dP3, 7-9 in dP4, 7-9+ in M1, 9-10 in M2 and 11-13 in M3; van den Bergh, 1999), thin enamel, fine and complex enamel folding, high hypsodonty index (0.5-0.8), and large number of cusps lined in parallel arrangement. This species is distinguished from other Stegodon species after the triangular outline of the (juvenile) skull Martin (1887).

The possible oldest occurrence of S. trigonocephalus represents by primitive form (S. t. praecursor) from the excavation in Kali Glagah area, presumably from the upper part of Kaliglagah or Mengger formations (?). However, with the lack of detailed stratigraphic data and age assessments of these isolated findings it is hard to estimate the first appearance datum of this species. Similar primitive form of this species was found in the black clay layer of Sangiran, dated older than 1.16 Ma (Suzuki et al., 1985), thus this date is used in this study to estimate the early occurrence of S. trigonocephalus. Its occurrence continued in most Early to Middle Pleistocene fossil localities of Java. Last occurrence of S. trigonocephalus is recorded in the sediment in Ngandong terraces; with minimum age of 143 ka. The S. trigonocephalus analysed in this study found in Sangiran (both Bapang and Sangiran formations), Kedung Brubus, Trinil, Ngandong and West Java (Bumiayu and Subang from unknown age, most likely from the Middle Pleistocene).

I.2.2.7 Stegodon sompoensis

The specimen of Stegodon sompoensis, a fragmentary molar from the Sompe locality, was first mentioned by Hooijer (1953b), in which he still doubted whether to address this fossil material as a pygmy or normal-sized Stegodon (Plate II.e). Subsequent finding of new fossil materials allowed Hooijer to give a more detailed description of the species and he concluded that all Stegodon material from Sulawesi so far belonged to a pygmy species.

Stegodon sompoensis has a body mass estimation of 350 kg (van den Bergh, 1999). The sizes of M1s to M3s are half to two-thirds smaller than in Stegodon trigonocephalus. Its M_3s have10 ridges per molar while the M^3s have 8-9 ridges per molar. Molar hypsodonty index is relatively low, with a range between 0.6 and 0.75 for adult upper molars, and 0.7 to 0.85 for lower molars, with lack median pillars and a median sulcus. Each ridge possess 4 to10 cusps, usually the 4 median cusps are larger and separated by a shallow sulcus of about equal size, except in milk molars, where a deeper median sulcus may be developed. The two median cusps usually widen toward the base and lead to weakly expanded double enamel wear patterns upon wear, especially in the anterior side of the anterior two wear figures. Enamel is very thick, up to 5.5 mm in the M3. Its thickness decreases toward base, showing Stufenbildung at the occlusal surface. Enamel folding is moderate and gets weaker toward the base. A more detailed description of dental and post cranial elements and taxonomical assessment of S. sompoensis are given in Hooijer (1964b) and van den Bergh (1999).

Stegodon sompoensis fossil remains was collected from many localities, yet most specimens were found in the structural block of the Lakibong Triangle, west of the Bulu Cepo Fault. Stratigraphically all the localities are placed in the Beru Member of the Walanae Formation. The first in situ appearance of this species is in the upper part of Subunit A of the Beru Member. Therefore, the arrival of this species into the island may have happened later than the arrival of Stegoloxodon celebensis during the Early Pleistocene. The occurrence of the species presumably continued into the early Middle Pleistocene, since fossil remains still occur in Subunit B of the Beru Member. This species co-occurs with Sl. celebensis and C. heekereni, and maybe also co-occurred with the large Stegodon species. From the upper part of Subunit C of the Beru Member, it is not known if the single molar fragment from the Talepu excavation belongs to S. sompoensis or the large Stegodon sp. B.

I.2.2.8 Large Stegodon sp. B

A large Stegodon attributed to Stegodon sp. B (Plate II.f) was first mentioned in Aziz (1990) and van den Bergh et al. (1992), then fully described in van den Bergh (1999) based on dental and postcranial material remains originating from the Tanrung

Formation. The molar size of Stegodon sp. B is larger than in S. sompoensis. Molars are more hypsodont and comparatively narrow for their length. Enamel is less thick than in S. sompoensis (varying between 2 and 3.5 mm in M3s) and regularly folded, showing a scalloped pattern. Complete ridge numbers of M3s cannot be determined due to the fragmented nature of the material. Description of dental materials and comparison of materials with other Stegodon species are presented in van den Bergh (1999). The relatively narrow molars suggest that it may have close links with S. florensis from Flores or with S. trigonocephalus ngandongensis from Java. Due to a lack of data, possible links with Philippine Stegodon remains uncertain (van den Bergh, 1999).

Based on stratigraphic data, the species first appeared on the island during the Early Middle Pleistocene, based on the finding of this species in Subunit B of the Beru Member. The occurrence of this species was thought to continue throughout the Middle Pleistocene, as recorded in the Tanrung Formation. Two molar fragments of a large Stegodon sp. found in the Napu Formation near Bettue Village in Central Sulawesi, initially identified as Stegodon cf. trigonocephalus (van den Bergh et al., 1994), suggest a former distribution to the northern part of the island. In addition, the occurrence on the island of Sangihe suggests an overseas dispersal of this species.

Only a molar ridge fragment was recovered from the Talepu excavation. Additionally, a number of Stegodon molar fragments were excavated from Liang Bulu Bettue, restricted to the basal fluvial layers (Layer 8, 10, 13, Brumm et al., in prep.). Thus, the last occurrence of the species is derived from the minimum age of the fluvial layers in Liang Bulu Bettue (~100 ka). However, fossil remains from Liang Bulu Bettue are rather fragmented and heavily water-rolled and therefore it is possible that these remains were reworked from older strata.

I.2.2.9 dwarf Stegodon sp. (Luzon)*

***Description and measurement of the single specimen are provided by Gert van den Bergh.**

A primitive dwarf Stegodon molar from unknown stratigraphic layer in Luzon is stored in National Museum of Philippines (Plate II.g). The specimen is a sinistral lower third molar (M_3) with x10x ridges, a brachidont. The anterior halfridge developed on lingual half, posterior halfplate consists of single conule, low. Only 10, or actually 9 ridges if

the posterior one is considered as halfridge. In ridge 1 the median cleft is shifted towards the buccal side; details enamel wear figure obliterated by black crust. heavy cement covers ridges 3-5, but is broken around the conules of the posterior ridges, where only cement between the ridges remains but the ridges are largely exposed on medial and lateral side. There is possibility that it is an upper molar. The crownbase is convex apically on the buccal side and flat to slightly concave at anterior 3 ridges lingually. The wear surface is quite steep, more typical for upper molar, but may be pathological. The maximum length of this specimen is 19.6 cm, with maximum width of 8.9 cm and maximum height of 7 cm. The hypsodonty index of this specimen is 0.7.

The size of this single specimen is comparable to Stegodon sompoensis and pygmy Stegodon sp. from Java, but larger than Stegodon sondaari from Flores and Stegodon sumbaensis from Sumba. Extrapolating the occurrence of the pygmy species from other islands and the primitive traits of the molar (low ridge number and low hypsodonty) the age of this taxon is estimated as older than 1 Ma.

I.2.2.10 Stegodon sondaari

Prior to 1980 the dwarf Stegodon from Flores was only known from a pair of isolated milk molars from unknown stratigraphic position and referred to as pygmy Stegodon (Hooijer, 1964a, 1972c, 1975) or Stegodon sompoensis (Hooijer, 1975). Between1980 and 1994, through a more detailed geological survey, the dwarf Stegodon remains collected from Tangi Talo by GSI-Dutch joint team. Based on this collection, this species was referred as dwarf Stegodon (Sondaar, 1987), Stegodon species C (van den Bergh et al., 1992) and pygmy Stegodon (Sondaar et al., 1994). Van den Bergh (1999) named the species Stegodon sondaari and assigned as holotype a partial mandible with M1s, M_2s and an incomplete sinistral M_3 (collection number: GRDC TT-3837), excavated in 1992. Based on the estimated length of an adult femur of S. sondaari, this species was thought to have stood about 1.2 m at the shoulder and weighted around 350 kg (van den Bergh, 1999). A complete femur excavated in 2012 from the Excavation F confirmed the earlier body mass estimation (van den Geer et al., 2016).

The cranial and molar elements of S. sondaari (e.g. Plate II.h, l) are considered as among the smallest of all recorded pygmy Stegodon species, as its size range is only

superior to (juvenile) S. sumbaensis. Unlike the other primitive Stegodon forms, the mandibular symphysis is rather short and lacks a protruding rostrum. The molars of S. sondaari exhibit a mixture of primitive and advanced traits. It has a low number of ridges yet has a relatively high unworn crown. Molars of S. sondaari are rather hypsodont and relatively large in proportion to the jaws, and the anterior region of the horizontal ramii is enlarged and thickened, providing space for an anteriorly expanded molar root. Upper molars are relatively wider than the lower. The largest width of the ridges occurs at the base, while lateral and median borders are only weakly tapering in apical direction. A detailed description of the molars of S. sondaari is given in the van den Bergh (1999).

Between 2010 and 2014, more S. sondaari molar specimens were found. These new specimens have provided additional information on the dental variation of the species. Summary measurements of S. sondaari molars from Tangi Talo are provided in the Table Appendix I.1, while additional data of the ridge crest formula added to previous descriptions is presented in Table Appendix I.2.

Table Appendix I.1 Summary measurements of Stegodon sondaari molars from Tangi Talo

element	H	W	L/W
dI[1]	11	6.5	0.7846154

element		P	P	L	W	H	LF	L/W	ET	h/w
dP[2]	average	x1x/2	1.67	7.53	7.63	7.4	-	0.98		70.37
sup.	min		1	6.3	6.9	7.4	-	0.91	1.25	-
	max		2	8.4	8.1	7.4	-	1.06	1.45	-
	SD		0.58	1.10	0.64	-	-	0.08		-
	CV		37.53	15.77	9.12	-	-	8.31		-
	n		3	3	3	1	-	3		1
dP[3] sup.	average	x4x/5x/x 5x/ 6/6x/x6x	5.33	30.38	19.10	9.19	18.97	1.57	1.41	57.43
	min		4	27.50	18.10	5.70	16.06	1.44	1.00	48.32
	max		6	35.00	21.50	11.90	22.92	1.71	2.00	62.14
	SD		0.65	2.36	1.04	1.90	1.90	0.09	0.33	4.46
	CV		12.47	7.93	5.55	21.17	10.26	5.79	23.85	7.98
	n		12	12	11	10	11	11	10	9
dP$_3$ inf.	average	x7x	7	37.60	19.60	15.01	17.16	1.92	1.2	76.58
	n		1	1	1	1	1	1	1	1

element		P	P	L	W	H	LF	L/W	ET	h/w
dP^4	average	x5x/6x/x6x	5.90	48.22	26.06	17.69	15.14	1.88	1.80	70.83
sup.	min		5.00	42.00	22.40	16.00	13.85	1.69	1.60	65.93
	max		6.00	51.70	29.25	19.20	16.85	2.13	2.00	75.80
	SD		0.32	3.24	2.41	1.00	1.03	0.14	0.23	3.99
	CV		5.49	6.90	9.48	5.83	6.99	7.54	13.63	5.81
	n		10	9	10	8	10	9	4	8
dP$_4$	average	x7x/8x	6.40	54.15	24.07	17.90	14.38	2.33	1.70	77.43
inf.	min		5.00	52.40	22.30	17.10	13.03	2.16	1.40	75.00
	max		7.00	55.90	25.60	18.60	16.31	2.51	2.00	79.22
	SD		0.89	2.47	1.66	0.75	1.28	0.25	0.42	2.18
	CV		14.67	5.14	7.48	4.57	9.32	12.06	28.08	3.05
	n		5	2	3	3	5	2	2	3
M^1	average	x4-/x6x	6.00	62.13	29.20	22.83	13.37	2.13	1.83	88.64
sup.	min		6.00	61.55	29.20	19.60	11.52	2.11	1.70	86.17
	max		6.00	62.70	29.20	24.60	15.30	2.15	2.00	91.11
	SD		-	0.81	0.00	2.80	1.64	0.03	0.13	3.49
	CV		-	1.47	0.00	13.30	13.07	1.49	7.33	4.43
	n		1	2	2	3	4	2	4	2
M$_1$	average	-x5/x5	5.00	38.7+	26.57	22.70	12.17	-	1.82	90.16
inf.	min		5.00	35+	26.10	21.30	9.49	-	1.60	86.93
	max		5.00	43.7+	27.40	24.10	15.00	-	2.00	93.39
	SD		-	-	0.72	1.98	1.97	-	0.15	4.57
	CV		-	-	2.95	9.81	16.96	-	8.56	5.70
	n		1	3	3	2	5	-	5	2
M^2	average	x6-/-6x/x8	8.00	87.40	44.43	37.15	8.07	2.31	3.20	85.98
sup.	min		8.00	-	37.80	33.60	6.43	-	2.60	77.31
	max		8.00	-	52.50	40.70	10.12	-	3.80	94.64
	SD			-	6.07	5.02	1.74	-	0.52	12.25
	CV			-	14.52	15.20	22.98	-	17.15	16.03
	n		1	1	4	2	4	1	4	2
M$_2$	average	x8x/x9x/10	9	109.83	43.08	37.30	8.58	2.55	3.14	86.96
inf.	min		8	104.20	41.10	34.00	7.30	2.48	2.70	85.46
	max		10	119.60	45.90	40.60	9.65	2.61	3.60	88.45
	SD			8.49	2.09	4.67	1.06	0.07	0.34	2.11
	CV			8.38	5.15	14.08	12.95	2.77	11.24	2.74
	n			3	4	2	5	3	5	2
M^3	average	-7x/x8x/-9x	8.33	99.60	40.40	30.70	10.44	2.47	3.10	92.91
sup.	min		8	98.20	39.70	29.20	9.59	2.46	3.00	91.73
	max		9	101.00	41.10	32.20	11.48	2.47	3.20	94.08
	SD		0.58	1.98	0.99	2.12	0.87	0.01	0.14	1.66
	CV		7.51	2.24	2.76	7.77	8.87	0.32	5.13	2.01
	n		3	2	2	2	4	2	2	2
M$_3$	average	x7-/x8-	-	-	39.83	-	15.24	-	3.15	-
inf.	min		-	74+	36.35	19+	-	-	3.00	-
	max		-	84+	43.30	23+	-	-	3.30	-
	SD		-	-	4.91	-	-	-	0.21	-
	CV		-	-	13.88	-	-	-	7.58	-
	n		-	2	2	2	1	-	2	-

Table Appendix I.2 Additional data of ridge crest formula of Stegodon sondaari (new data are written in bold)

Element	dP2	dP3	dP4	M1	M2	M3
superior	**x1x/2**	**x4x/5x/x5x/6x/x6x**	x6x/x7/7x	x6x/**7x**	x6x/x7/x7x/**x8**	**8x/9/9x**
inferior	-	6/**x7**	**7x/x7x/8x**	-5	x8/x8x/**x9x/10**	x8/**9x/10**

The first occurrence of Stegodon sondaari is recorded from a 1.4 Ma-old fossil-bearing layer at Tangi Talo. Van den Bergh (1999) assumed that the ancestor of S. sondaari is from Sulawesi, which migrated out to Flores through oceanic crossing during a low sea-stand of the Early Pleistocene (~1.6-1.5 Ma), when the crossing distance was smaller. Meanwhile, the last occurrence of S. sondaari is recorded at 1.27 Ma.

Van den Bergh et al. (2014) have been determined the minimum number of individuals (MNI) and age structure of the Stegodon sondaari death assemblages from the lower fossil layer and upper fossil layer analysed based on all material excavated between 2010 and 2013. From a minimum number of individuals (MNI) of 40, the death assemblage of the lower fossil-bearing layer resembles that of a living population, with relatively 30% of the assemblage consisting of juveniles, and successively smaller percentage for higher age groups. This death assemblage suggests that the entire population died at the site without age-selective mortality of specific age groups. A natural-caused of death or a volcanic eruption might have been a likely cause of death at this fossil layer. Of 31 individuals in the Tangi Talo upper fossil layer, the death assemblage is dominated by juvenile individuals (~90%), which resembles a common signature of selective death assemblage related to predation or drought (Haynes, 1991, Dudley et al., 2001). Due to the absence of evidence for hominins in this layer, in this case, the predators could have possibly been Komodo dragons and/or crocodiles.

I.2.2.11 Stegodon florensis

Stegodon florensis (e.g. Plate II.k) was initially described as a subspecies of S. trigonocephalus that was thought to have migrated eastward from Java (1957). However, additional fossil finds from the So'a Basin, collected between 1992 and 1994,

justified its classification as a distinct species, S. florensis (van den Bergh, 1999). The weight of adult individuals of this species is estimated to have been between 1017 and 1713 kg, based on lengths of femur and humeri. The average body weight of S. florensis is still smaller than S. trigonocephalus, although the largest S. florensis individuals tend to overlap in size with the smallest S. trigonocephalus individuals from Trinil (van den Bergh, 1999). Van den Bergh (1999) suggests that the ancestor of S. florensis may have arrived from the north via Sulawesi.

This species is distinguished from other Stegodon species by having the highest number of molar ridges in the M_3, and a generally higher hypsodonty index compared to most other insular Stegodon, except for pygmy Stegodon, which have smaller size. This species differ significantly from the S. sondaari by its size and by the having relatively thinner and more wrinkled enamel. S. florensis differs from S. trigonocephalus in being slightly smaller, having relatively narrower and more hypsodont molars, and more ridges per molar (Hooijer, 1957, van den Bergh, 1999).

The oldest occurrence of Stegodon florensis in the So'a Basin is recorded from the excavations in Kobatuwa. Its occurrence continued throughout the Sandstone Member of the So'a Basin. This species is no longer found in the Limestone Member, probably due to the shift of environment from fluvial to lacustrine during the later stage of basin development (Brumm et al., 2016). A younger population of S. florensis is recorded from Liang Bua. S. florensis findings in Liang Bua also mark the last occurrence of this species in the island at 50 ka (Sutikna et al., 2016). So far, no remains of this species have been found that are intermediate in age between of the upper part of Sandstone Member in the So'a Basin and the oldest Liang Bua records.

The Liang Bua population is assigned as a different subspecies from the So'a Basin population due to their smaller size, ~30% smaller in linear direction than the So'a Basin population and only weight ~60% of the So'a Basin population's body mass (van der Geer et al., 2016). This subspecies also has more advanced plate formula (one additional ridge in the dP3 and dP4), and relatively thinner, more folded enamel. S. f. insularis (e.g. Plate II.h) was given a subspecies name and thus, S. florensis of the So'a Basin is referred to as the subspecies S. f. florensis (van den Bergh et al., 2008). The size diminution of S. florensis with time suggests that the reduction in body size was due to the island effect to the species.

The minimum number of individuals (MNI) and age structure of the S. florensis death assemblages from the So'a Basin and Liang Bua have been determined based on material excavated between 20010 and 2012. An age profile based on an MNI of 136 S. f. florensis individuals excavated from the MFI at Mata Menge, shows a non-selective death pattern resembling that of a living population. This suggests that an entire population died at the site without age-selective mortality of specific age groups. The death assemblage of S. f. insularis (MNI = 48) shows selective death of juveniles, which suggests predatory factors related to the bone accumulation. The predation could have been done either by hominin or other island predators (i.e.: Komodo dragon), since those species both co-occur with S. f. insularis.

I.2.2.12 Stegodon sumbaensis

Very little is known about Stegodon sumbaensis due to the scanty material. The original diagnosis was presented in Sartono (1979) based on the adult mandible from Watumbaka. Additional specimens obtained from 2011 GSI-UOW reconnaissance survey comprises a molar fragment, a tusk fragment, a metapodial, a humerus fragment and a juvenile mandible with worn dP_3s, slightly worn dP_4s, and the M_1s still under formation inside the alveoli. Preliminary description of these additional materials was given by van den Bergh (2011) and Turvey et al. (in prep.).

The juvenile mandible of S. sumbaensis from Lewapaku (Plate II.m) has similar characteristic as Stegodon sondaari, its symphysis is very short, even shorter than S. sondaari, and it lacks a protruding rostrum. The anterior region of the horizontal ramus is enlarged and thickened. The molar also has a low number of ridges yet has a relatively high crown and is relatively large in proportion to the mandible, but slightly less hypsodont compared to S. sondaari. The larger width of the ridges occurs at the crown base, while lateral and median borders are weakly tapering in apical direction. The dP_3 of this species does not exhibit the typical anterior constriction usually developed in other Stegodon dP_3s. However, this might represents variation since only one specimen could be examined. The entire wear-surface has a pear shaped outline and in occlusal view the wear figures of the ridges are folded in V-shaped patterns, pointing in anterior direction. Based on measurements given by van den Bergh (2011), the size

of the mandible is very small. It falls below the size range of homologue elements of Stegodon sondaari from Tangi Talo, Flores. Thus, make the juvenile of this species as the smallest known Stegodon species. The body mass of this juvenile specimen is estimated at 252 kg (van der Geer et al., 2016) based on its mandible size.

I.2.2.13 Stegodon timorensis

Stegodon timorensis was first described by Sartono (1969) from a third molar fossil collected in Atambua by Verhoeven. Hooijer (1969) made a revision of the species description and described additional material collected by Verhoeven. Hooijer (1972c) also described a larger-sized species and assigned it to Stegodon cf. trigonocephalus florensis, as he thought that the LSI's Stegodon are thought to be derived from S. trigonocephalus (Martin) from Java, and later postulated that there were two Stegodon species occured in Timor (Hooijer, 1972b). However, Hooijer's view of occurrence of two successive species in Timor has been challenged by van den Bergh (2007), due to the fragmentary nature and unknown stratigraphic level of the larger form, and uncertainties about the stratigraphic context and size differences due to sexual dimorphism. Therefore, most, if not all specimens originating from the Atambua Basin in Timor, and certainly all material used in this study, belong to S. timorensis (e.g. II.j).

S. timorensis differs from other Stegodon species by its small size and high crown. The size range of this species is only slightly superior to S. sondaari and S. sumbaensis. S. timorensis has a protruding symphysis and does not have an anteriorly thickened and enlarged horizontal ramus. In addition, it tends to have more prominently developed and congested perikymata as compared to the other Stegodon species from surrounding islands. The average weight of adult S. timorensis individual is estimated at ~760 kg, based on its mandible size (van der Geer et al., 2016). Fossils of S. timorensis are found in the Noele Formation and older alluvial terraces. However, most of the specimen were collected from the surface or brought in by local farmers. Thus the exact provenance of many specimens could be determined.

I.3 Elephantidae

I.3.1 Genus Archidiskodon and Stegoloxodon

I.3.1.1 Archidiskodon planifrons

Analysed Archidiskodon planifrons specimens from the Early Pleistocene Siwalik sediments located near Haripur. Both specimens are upper third molar fragments. Measurements and descriptions of the two specimens (Dubois 1714 and 3106, Plate III.a) are given in Hooijer (1954). The occurrence of this species in the vicinity of Haripur is estimated between 3.3 and 2.6 Ma (Hussain et al., 1992).

I.3.1.2 Stegoloxodon indonesicus

Until recently, the occurrence of Stegoloxodon indonesicus on Java was evidenced by a right first upper molar (M^1, with a lamella formula of x7x) from Ci Panglosoran, near Bumiayu. This species was initially identified as Archidiskodon (Elephas) planifrons (van der Maarel, 1932), while it's present name was introduced by Kretzoi (1950). Additionally, the morphology of molar fragments from Jetis and Perning, East Java that have been identified as Stegodon hysilophus (Hooijer, 1954b), bear closer resemblance to a Stegoloxodon than Stegodon. No further support for the occurrence of this species from other localities. There are indications that this genus was found in several places of unknown stratigraphic level in Java (Braches and Shutler, 1984)and near Sangiran (Hooijer, 1982), thought to be belong to the A. planifrons. Since the whereabouts of those rare and poorly known specimens can no longer be tracked, the occurrence of this species in other localities cannot be confirmed.

Recently five molar fragments were surface collected in Semedo by local villagers and stored in the local museum. Identification, description and measurement of these specimens (labelled as SMD 1050, SMD 1063, SMD 1082, SMD 1085 and SMD 3) were conducted during the sampling process. This finding is important, since it gives additional information of dental morphology and the occurrence of Sl. indonesicus in Java, which was very limited. Since all of the specimens were surface collected, the exact stratigraphic position remains unknown. The estimated age of these specimens is considered older or similar to Sinomastodon bumiajuensis specimens from the same

area. The estimation of its occurrence in the faunal succession scheme (Fig. 4.10) is derived from position of the Ci Panglosoran specimen, which is considered to be older than the occurrence of Sinomastodon bumiajuensis.

Molars of Stegoloxodon indonesicus from Semedo (Plate III.b-e) are identified as follows: SMD 1050 is an anterior fragment of right first or second upper molar (M^1/M^2?) with x4- lamellas, SMD 1082 is a posterior fragment of right third lower molar (M_3) with -5x lamellas, Semedo 1085 is an anterior fragment of right third lower molar (M_3) with 5- lamellas, SMD 3 is a posterior fragment of right third upper molar (M^3) with -4x lamellas, and Semedo 1063 is a lamella plate fragment (not shown in the picture). Estimated from its width (71.11 mm), Semedo 1063 can be assigned as ridge fragment from second or third molar. Morphometric measurement of these specimens is presented in Table Appendix I.3.

Table Appendix I.3 dental morphometry of newly reported Stegoloxodon indonesicus from Semedo

tag	element	ridge no.	L	W	H	LF	L/W	ET_{min}	ET_{max}	Min h/w	Max h/w
Semedo 1050	M^1, dex	x4-	67.9+	55.60	56.00	7.44	-	-	-	95.87	102.75
Semedo 1082	M_3, dex	-5x	110.5+	62.40	57.20	7.26	-	-	-	89.43	93.64
Semedo 1085	M^3, dex	-5-	108.5+	74.9c	-	4.93	-	3.80	4.60	-	-
SMD 3	M_3, dex	x4-	78.5+	56.30	62.90	5.21	-	-	-	101.40	111.72

Due to the incomplete nature of specimens, the total of ridge number in each stage of molars is remaining uncertain. The width of ridges in M^1/M^2(?) are approximately equal, while the M3s are narrowing posteriorly. The molars have relatively low hypsodonty index for Elephantidae (1.0 for $M^{1/2?}$, 0.9 for M_3 and 1.1 for M^3). Each lamella comprises 4-6 cusps with the two prominent median cusps, except for most posterior lamella in M3s that only has 3 cusps. Each cusp separated by shallow grooves. Lamellas are slightly narrowing toward occlusal, forming a triangular shape, which are more noticeable in posterior lamellas of M3. Anterior and posterior median pillars appear prominent below the apex of the lamellae, producing pronounced rhomboidal middle sinuses upon further wear. Enamel is thick (2.6-3.8 mm measured in worn

occlusal surface of SMD 1085), very weakly or not folded except for irregular folds at the median pillars and lacks of Stufenbildung. Molar morphology of Sl. indonesicus shows a close similarity to Archidiskodon planifrons from Siwalik and Sl. celebensis from Sulawesi. However, the sizes of the analysed specimens are smaller than mainland A. planifrons but slightly larger than Sl. celebensis.

I.3.1.3 Stegoloxodon celebensis

Fossil of Stegoloxodon celebensis was first described by Hooijer (1949) based on the collection recovered from the Sompe locality by van Heekeren. The species was described based on fragments of a posterior M^2 and a posterior M^3, which he attributed to a new species Archidiskodon celebensis. Subsequent findings of fossil material from different localities allowed Hooijer (1953a, 1953c, 1954a, 1955, 1972a) to establish a more complete description of the species. Maglio (1973), in his revision of Elephantoidae, placed this species under the genus Elephas, a classification subsequently followed by Hooijer (1974). Markov and Saegusa (2008) revised the the classification this taxon, of such similarity with a molar from Java, named Stegoloxodon was noted by van den Bergh (1999) and he employed the existing genus name Stegoloxodon (Kretzoi, 1950) for the Sulawesi form.

The cranium and dental element of Stegoloxodon celebensis (e.g. III.f) has both apomorphic and primitive Elephantoidea characters (see Kretzoi, 1950, van den Bergh, 1999, Markov and Saegusa, 2008). The most prominent primitive trait is the downturned mandibular symphysis, provided with functional mandibular tusk, probably only in males, as well as the development of premolars. The M_3 has x10x or x11x lamellae, with hypsodonty indexes of lower molars are generally around 1.1, while for upper molars hypsodonty index are between 0.9 and 1. Each lamella has 4-6 cusps with the two prominent median cusps, each separated by shallow grooves. Anterior and posterior median pillars appear prominent at two-third below the apex of the lamellae, which produce pronounced rhomboidal middle sinuses upon further wear. Enamel is thick (2-2.2 mm in M3) and very weakly or not folded, except for irregular folds at the median pillars. Molars of Stegoloxodon celebensis have a similar size as equivalent molars of Stegodon sompoensis, which also co-occurs in the upper part of Subunit A of

the Beru Member. However, Sl. celebensis molar differs from the pygmy Stegodon in lacking Stufenbildung at the worn enamel surfaces and has weaker enamel folding. A more detailed description of dental and post cranial elements and taxonomical assessment of S. celebensis are presented in Hooijer (1955) and van den Bergh (1999).

Stegoloxodon celebensis molars bear great similarity with Archidiskodon planifrons molars from Mainland SE Asia and Stegoloxodon indonesicus from Java. However, molars of Sl. celebensis are only half the size of A. planifrons, and only slightly smaller than Sl. indonesicus. Additionally, the genus Stegoloxodon is restricted to the Early Pleistocene strata of both islands and never reached the Lesser Sunda Islands.

Stegoloxodon celebensis specimens were found at several localities, but only samples from Sompe, Lonrong, Paroto, Bulu Cepo and in the surroundings of the Lakibong River were analysed. These localities are mostly situated in the Sengkang Anticline area west of the East Walanae Fault within the WSB. The Sl. celebensis occurs since the early deposition of the Beru Member (base of Subunit A) and its occurrence is continuous into the upper reaches of the Beru Member (Subunit B), but has not been recorded from the Tanrung Formation or Subunit C of the Beru Member. Therefore it can be estimated that this species occurred in Sulawesi between the Early to the Middle Pleistocene. In Subunit B, Sl. celebensis co-occurs with Stegodon sompoensis, Celebochoerus heekereni and probably a large-sized Stegodon species.

I.3.2 Genus Elephas and Palaeoloxodon

I.3.2.1 Elephas hysudricus

Specimens of Elephas hysudricus (n = 2) analysed in this study are all derived from the Upper Siwalik sediment located near Haripur. Analysed specimens are a lower second molar (Dubois coll. 3102) and a third molar fragment (Dubois coll. 3103, Plate III.g, h). Description of these specimens is given in Hooijer (1955). The occurrence of this species is estimated between 2.7 and 0.8 Ma (Hussain et al., 1992, Dennel et al., 2006).

I.3.2.2 cf. Palaeoloxodon namadicus

Four fragmented molars of Elephantini were found in the upper part of the Tha Chang Sandpits (Plate III.i, j; IV.c). Due to the fragmented nature of specimens, recognition of morphological features and measurement of biometrical parameters is limited. The measured incomplete width ranges between 62 and 73 mm. On the lateral view, the lamellas are showing a curved shape near the base. The widest part of individual lamellae is located slightly above the root.

All lamellas are slightly to half worn and the worn occlusal part shows a weak irregular enamel folding pattern. Measured enamel thickness ranges between 1.5 and 2 mm. Based on measurement of slightly worn lamella, the hypsodonty index measured from the most complete lamella is 1.8. Characteristics of these specimens are comparable with Palaeoloxodon (Elephas) namadicus and Elephas hysudrindicus of Java (Hoooijer, 1955). Moreover their hypsodonty index is higher than E. hysudricus of Punjab (Hooijer, 1955). Since Tha Chang locality is within mainland, hence four fragmented molars from Tha Chang attributed as cf. Palaeoloxodon namadicus.

Although all specimens originate from the Tanrung Formation are rare and very fragmented, the molar fragments clearly show high hypsodonty, an apomorphic character of the tribe Elephantini. Molar fragments from the Tanrung Formation are representing adult molars, either M2 or M3. Molars are high-crowed, no unworn lamellas were found, but measurements of all worn lamella are resulting in hypsodonty indeces of between 1.7 and 2. The lateral sides of the lamellae are strongly curved near the base and straight toward the occlusal surface, suggesting that the fragment is part of the posterior end of a molar, which is usually more curved than the anterior or intermediate portion. The lamellae widen near the base of the crown. Most of the occlusal surface is covered by matrix. On the exposed anterior surface it can be observed that the enamel is considerably wrinkled and that a median pillar or expansion is absent. Enamel is relatively thin compared to other Proboscidean species from Sulawesi, with the enamel thickness of the molars measured at about 2 mm. Van den Bergh (1999) considered that the species of this molar fragment is closely resembled to the Middle Pleistocene Palaeoloxodon (=Elephas) namadicus from mainland Southeast Asia, hence these high hypsodonty molar from southwest Sulawesi also attributed as cf. Palaeoloxodon namadicus

Additional specimen of cf. Palaeoloxodon namadicus are a molar fragment from the Tanrung River, surface collected during a geological survey in 2007, and a molar fragment (with some sediment of the Tanrung Formation attached) that was recovered during excavation survey in the Tanrung River in 2012. Its occurrence in the Tanrung Formation marks the earlier occurrence of this species. Meanwhile the last appearance datum for this species is derived based on the recent findings of cf. Palaeoloxodon namadicus in the LBB cave deposit, which is dated at ~100 ka (van den Bergh, 2015). During archaeological excavations at Leang Bulu Bettue between 2013 and 2015, more materials were collected from cave deposits, including a right mandible with M_1 and an isolated left M_1, besides several smaller molar plate and enamel fragments. This material awaits a detailed description (Brumm et al., in prep.)

I.3.2.3 Elephas hysudrindicus

Most of Elephas hysudrindicus specimens used in this study are isolated molar fragments. The molars of this species are identified by the sub-parallel border of opposite lamellar flanks. The widest part of individual lamellae is located right above the root (Plate IV.a, b). Enamel folding pattern of E. hysudrindicus worn molars are close resembles of those of Elephas maximus, as both species have double-layered and heavily wrinkled enamel. The E. hysudrindicus has relatively thick enamel (ranges between 2.5 and 4.5 in analysed specimens) and has a slightly low hypsodonty index (ranges between 1.5 and 1.8 in analysed specimens).

Elephas hysudrindicus occurs in the Kedung Brubus fauna, Ngandong fauna and fluvial sediment in Sunggu, but absent in Trinil Fauna and no longer occurs in Punung fauna. The E. hysudrindicus specimens analysed in this study were obtained from fossil localities in Sangiran (Bapang Formation), Kedung Brubus, Ngandong, Sunggu and West Java (Bumiayu and Subang from unknown age). Thus the occurrence range of this species in Java of this species is estimated between 0.9 and 0.16 Ma.

I.3.2.4 Elephas maximus

Molars of advanced Elephas form from the Late Pleistocene to recent sediments from Tha Chang, Java and Sumatra. Due to the fragmented nature of most of the specimens, the dental stage of each specimen is unrecognisable. The most complete specimen (Plate III.k, l) recognised as a posterior M^3 fragment with -16- remaining lamellas. The lateral part of individual lamella is straight and the widest part of individual lamella is located in the middle. Lamellar frequencies range between 5.8 and 7.7. Worn occlusal surfaces exhibit strongly folded enamel with an irregular pattern lacking a median expansion or sinus. The enamel folding of this form is stronger than Palaeoloxodon namadicus and Elephas hysudrindicus. The thickness of the enamel ranges between 0.1-0.17 mm. The hypsodonty index measured from the complete lamella of the upper molar ranges between 1.8 and 2.3. Molars of this species are distinguished from Palaeoloxodon namadicus and Elephas hysudrindicus by the largest width of the individual lamellae is not directly above the roots, but approximately halfway the heights and above (Plate IV.d). These characteristics, in particular the thin strongly folded enamel, the lack of median expansions of the wear-figures, and the high hypsodonty indices, allow attribution to Elephas maximus.

First record of Elephas maximus in Java was reported based on a molar fragment found in the Upper Pleistocene sediment in Punung. Its occurrence is continuous in Cipeundeuy faunal assemblage and in the Holocene cave composite. In Java, this species probably went extinct in during historical times, but still extant in nearby islands: Sumatra and in a small area in the northeast Borneo, as well as in the mainland SE Asia.

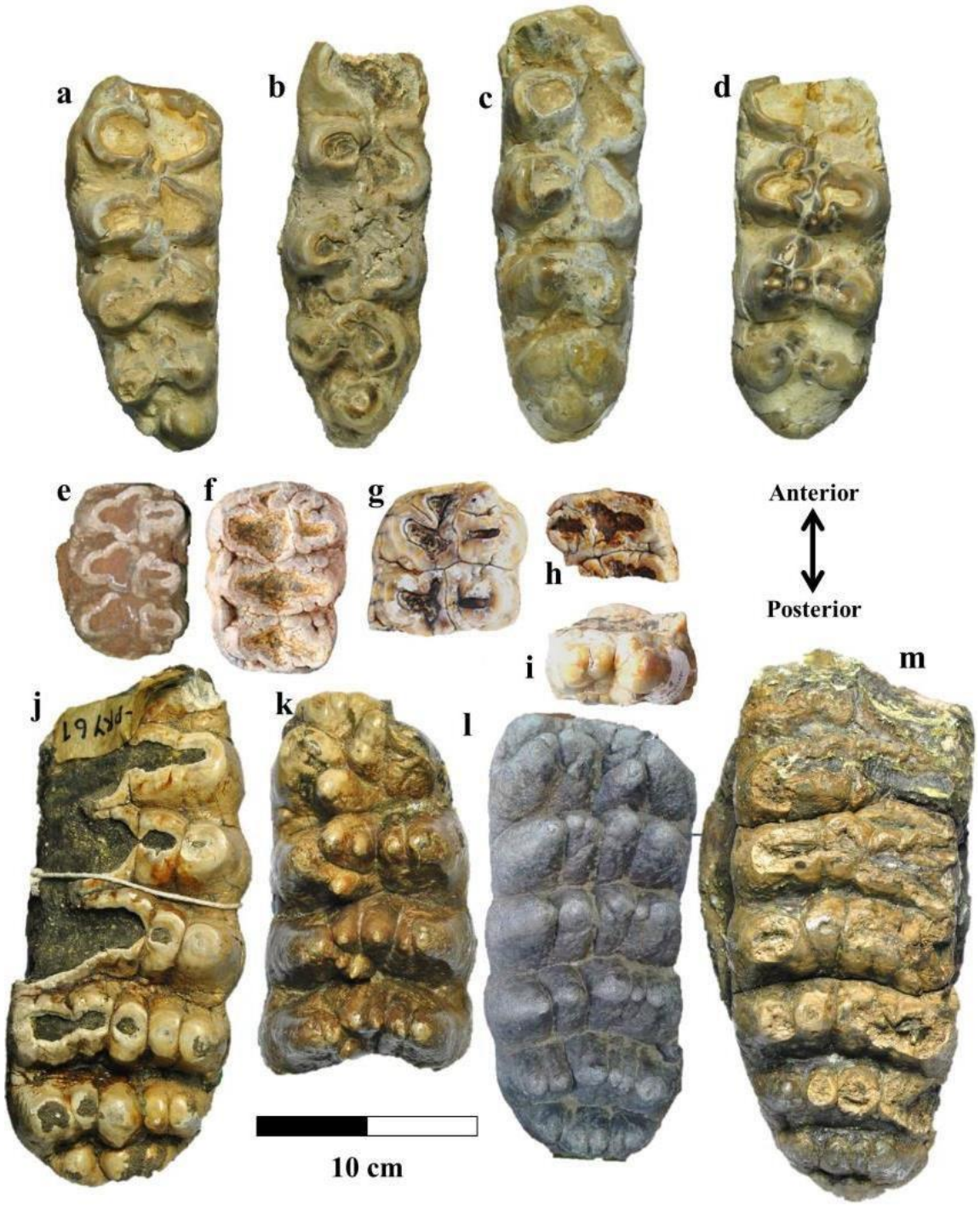

Plate I Occlusal view of: Platybelodon cf. grangeri from the Linxia Basin: **a**) PRY 74 (dex M^3), **b**) PRY 75 (dex M_3), **c**) PRY 79 (dex M_3), **d**) PRY 80 (sin M^3); Sinomastodon bumiajuensis from Semedo, Java: **e**) D1/SS-18 (sin M_2, taken from Fitriawati, 2009), **f**) DK 144 (sin M_2), **g**) DK 145 (sin anterior M_2 fragment), **h**) DK 146 (dex anterior M_3 fragment with remains of the first and broken second lophids), **i**) SMD 2 (unworn third lophid of M3); Stegolophodon cf. stegodontoides: **j**) NRRU PRY 61 (posterior sin M^3 fragment from Tha Chang), **k**) RIN 43 (anterior dex M_2 fragment from Tha Chang), **l**) CCZ 490 (dex M^2 from the Irrawaddy beds); Stegolophodon intermediate form: **m)** RIN 63 (sin M^3, Tha Chang).

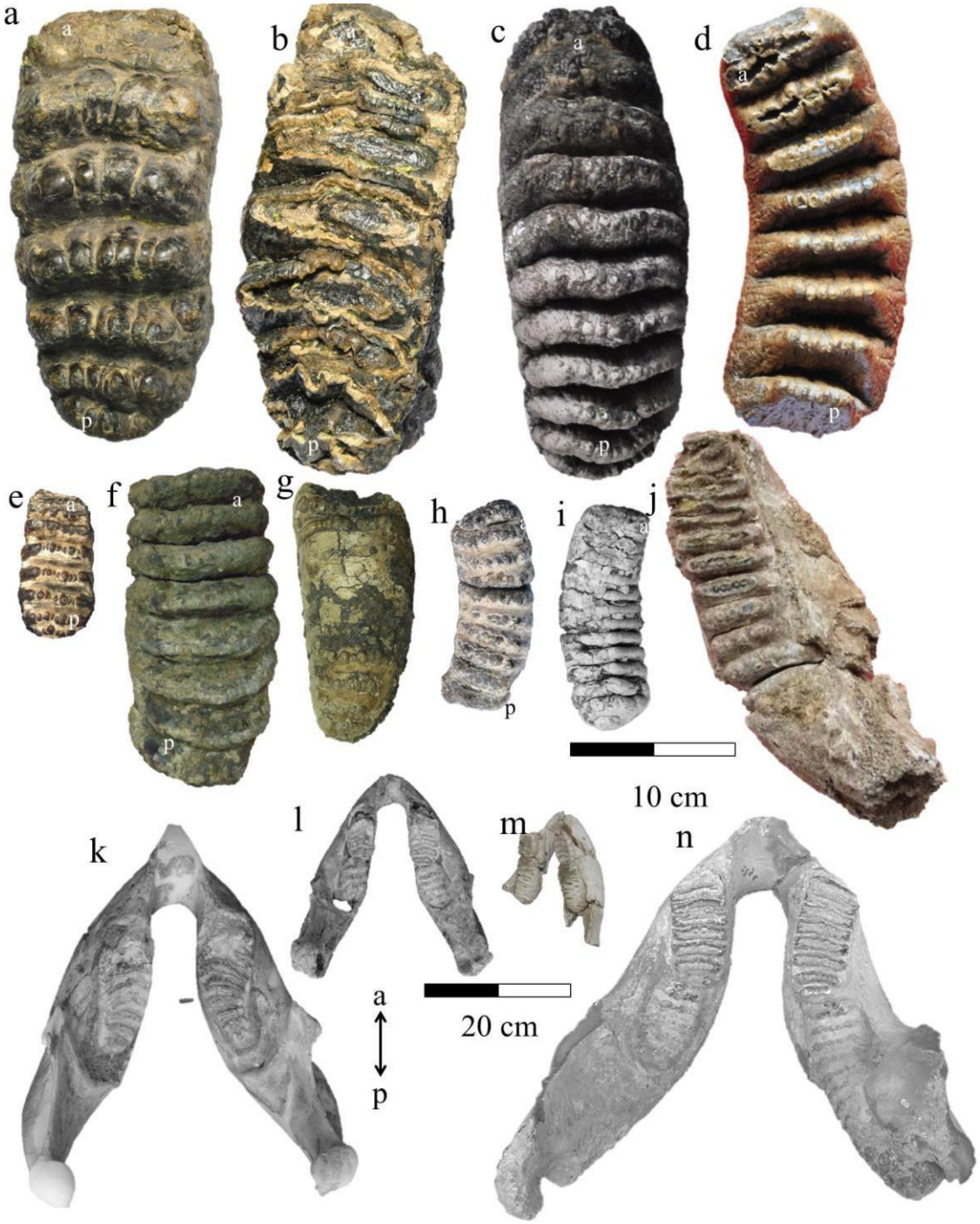

Plate II Occlusal view of: **a)** Stegodon cf. zdanskyi (RIN 50, sin M^3, Tha Chang); **b**) Stegodon cf. elephantoides (NRRU 1002-78, sin M^3, Tha Chang); **c**) Stegodon cf. insignis/ganesa (CCZ 402, dex M^3, Irrawaddy); **d**) Stegodon cf. orientalis (RIN 14 sin, M_2, Tha Chang); **e**) Stegodon sompoensis (PA-3730, sin dp^3, Paroto); **f**) large Stegodon sp. (no label, Lonrong, sin M^1); **g**); dwarf Stegodon sp. (NMP-239, sin M_3, Luzon); **h**) Stegodon sondaari (TT13-TG-F984, sin M^2, So'a Basin); **i**) Stegodon florensis insularis (ICA29.7.03-1, dex dp^4, Liang Bua, taken from van den Bergh et al., 2008); **j**) Stegodon timorensis (ATB 07-2, dex mandibular ramus with M_3, Noele Formation, taken from van den Bergh, 2007). Size comparison of mandibula: **k**) Stegodon florensis (adult mandibula with M_3, Mata Menge); **l**) Stegodon sondaari (adult mandibula with M_3, Tangi Talo); **m**) Stegodon sumbaensis (juvenile mandibula with dp_3 and dp_4, Lewapaku); **n)**. Stegodon trigonocephalus (adult mandibula with M_2 and M_3, Kedung Brubus). Scale 10 cm is applied for **a-j**, while 20 cm for **k-n**. Key: a = anterior, p = posterior.

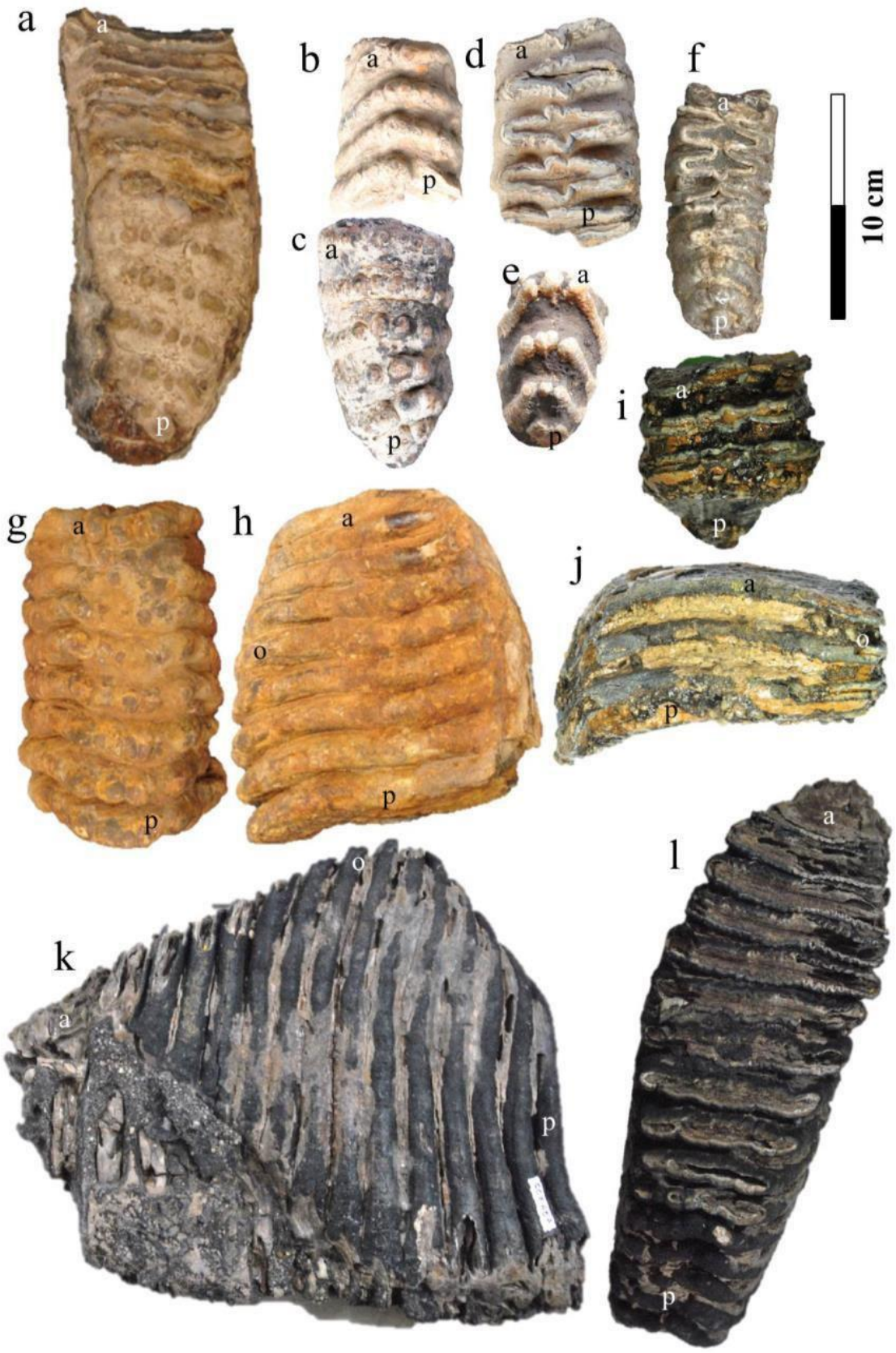

Plate III a) Archidiskodon planifrons (DUB-3106, occlusal view, dex M^3, Punjab); occlusal view of Stegoloxodon indonesicus from Semedo: **b**) SMD 1050 (anterior dex M^1 frg.), **c**) SMD 1082 (posterior dex M_3 frg.), **d**) SMD 1085 sin, (anterior dex M^3 frg.), **e**) SMD 3(posterior dex

M^3 frg.); **f**) Stegoloxodon celebensis (LR 3517, occlusal view,dex M_3, Lonrong); Elephas hysudricus, DUB-3103, M^3 frg. from Punjab: **g**) occlusal view, **h**) lateral view; cf. Palaeoloxodon namadicus, NRRU 1002-88, M^1 (?) lamellas frg., Tha Chang: **i**)occlusal view, **j**) lateral view; Elephas maximus, CCZ-408, sin M^3, Tha Chang: **k**) occlusal view, **l**) lateral view. Key: a = anterior, p = posterior, o = occlusal.

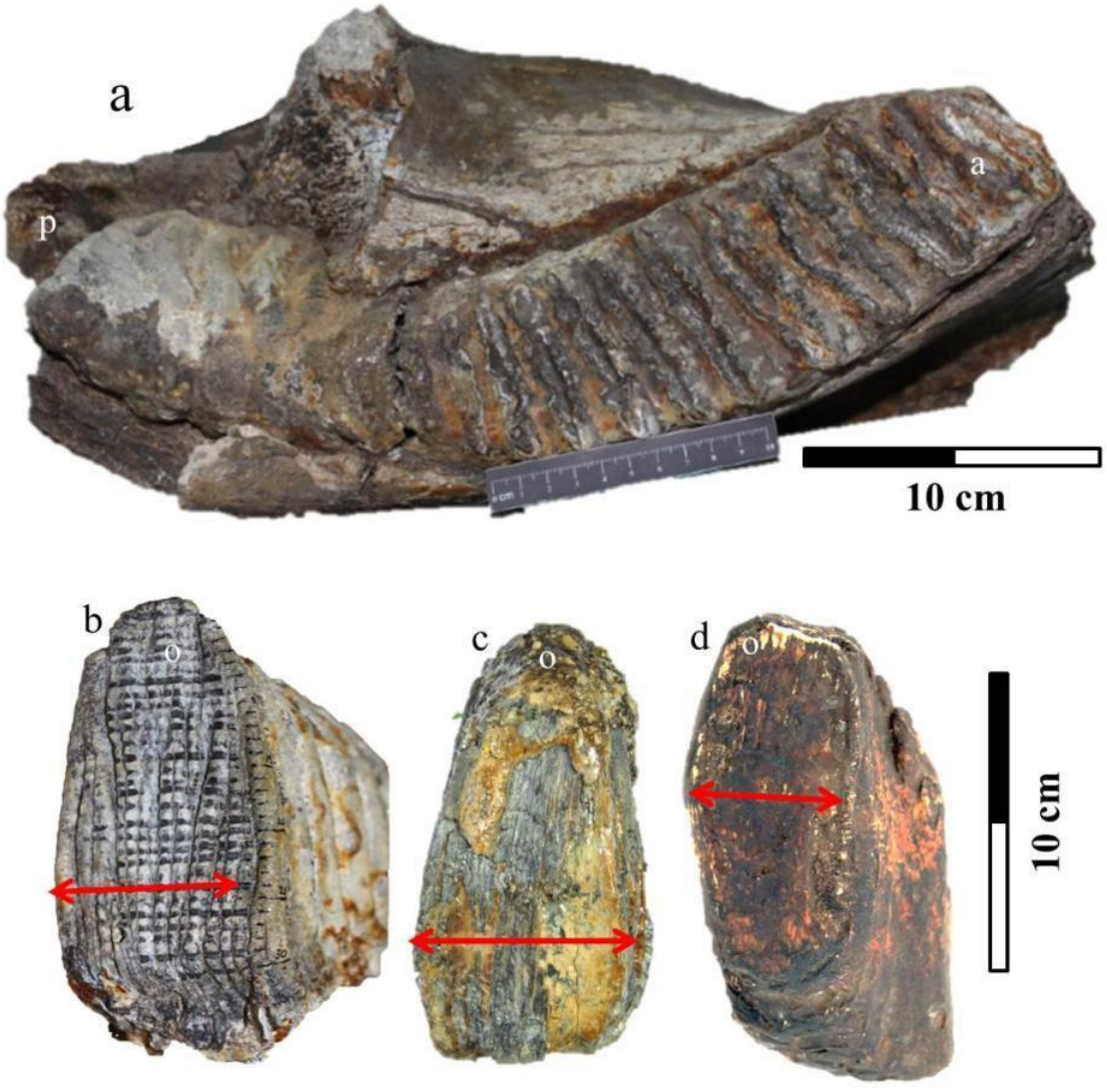

Plate IV a) Elephas hysudrindicus, occlusal view, sin mandibular with M_3, form Sunggu (Blora). Frontal view of : **b**) Elephas hysudrindicus, **c**) cf. Palaeoloxodon namadicus, **d**) Elephas maximus; red arrows indicate the widest part of individual lamellae.

Appendix II. $\delta^{13}C$ and $\delta^{18}O$ values of analysed samples

II.1 Bulk samples

locality	collec-tion	collection number	taxon	dental rank and status	collection remark	Faunal assemblage	isotopic value	
							$\delta^{13}C$ (‰, VPDB)	$\delta^{18}O$ (‰, VPDB)
Linxia Basin, China	NRIPM	NRRU PRY-74	Platybelodon cf. grangeri	dex M^3 frg	surface coll.	Hujialiang	-9.7	-6.6
Linxia Basin, China	NRIPM	NRRU PRY-75	Platybelodon cf. grangeri	dex M_3 frg	surface coll.	Hujialiang	-8.8	-6.3
Linxia Basin, China	NRIPM	NRRU PRY-77	Platybelodon cf. grangeri	dex M_3 frg	surface coll.	Hujialiang	-9.3	-9.3
Linxia Basin, China	NRIPM	NRRU PRY-79	Platybelodon cf. grangeri	dex M_3 frg	surface coll.	Hujialiang	-8.8	-6.4
Linxia Basin, China	NRIPM	NRRU PRY-80	Platybelodon cf. grangeri	dex M_3 frg	surface coll.	Hujialiang	-9.1	-5.8
Linxia Basin, China	NRIPM	NRRU PRY-85	Platybelodon cf. grangeri	dex M^3 frg	surface coll.	Hujialiang	-9.3	-8.6
Ta Chang, Thailand	NRIPM	NRRU 1002-35	Sinomastodon sp.	M3 frg	surface coll.	undetermined	-12.2	-6.3
Irrawaddy, Myanmar	CV	CCZ 24	Sinomastodon sp.	M3 frg	surface coll.	Lower Irrawaddy	-12.8	-7.2
Irrawaddy, Myanmar	CV	CCZ Sino 2	Sinomastodon sp.	M2 frg	surface coll.	Lower Irrawaddy	-11.3	-5.6
Ta Chang, Thailand	NRIPM	NRRU PRY-61	Stegolophodon cf. stegodontoides	dex M_3 frg	surface coll.	undetermined	-11.0	-5.5
Ta Chang, Thailand	NRIPM	RIN-3	Stegolophodon cf. stegodontoides	dex M_3 frg	surface coll.	undetermined	-11.5	-6.1
Ta Chang, Thailand	NRIPM	RIN-7	Stegolophodon cf. stegodontoides	dex M^3 frg	surface coll.	undetermined	-12.2	-7.1
Ta Chang, Thailand	NRIPM	RIN-43	Stegolophodon cf. stegodontoides	M_3 frg	surface coll.	undetermined	-11.9	-5.7
Ta Chang, Thailand	NRIPM	RIN-55	Stegolophodon cf. stegodontoides	M_3 frg	surface coll.	undetermined	-11.9	-5.8
Ta Chang, Thailand	NRIPM	RIN-66	Stegolophodon cf. stegodontoides	M_2/M_3 frg	surface coll.	undetermined	-11.1	-6.5
Irrawaddy, Myanmar	CV	CCZ 338	Stegolophodon cf. stegodontoides	dex M_3	surface coll.	Lower Irrawaddy	-11.8	-6.8
Irrawaddy, Myanmar	CV	CCZ 339	Stegolophodon cf. stegodontoides	dex M_3 frg	surface coll.	Lower Irrawaddy	-12.3	-6.1
Irrawaddy, Myanmar	CV	CCZ 386	Stegolophodon cf. stegodontoides	sin M^3 frg	surface coll.	Lower Irrawaddy	-6.1	-7.7
Irrawaddy, Myanmar	CV	CCZ 388	Stegolophodon cf. stegodontoides	sin M_3 frg	surface coll.	Lower Irrawaddy	-12.4	-7.0
Irrawaddy, Myanmar	CV	CCZ 490	Stegolophodon cf. stegodontoides	M_2/M_3 frg	surface coll.	Lower Irrawaddy	-11.9	-8.0
Irrawaddy, Myanmar	CV	CCZ 491	Stegolophodon cf. stegodontoides	sin M^2	surface coll.	Lower Irrawaddy	-11.1	-8.8
Ta Chang, Thailand	NRIPM	RIN-62	Stegolophodon intermediate form	dex M_3 frg	surface coll.	undetermined	-12.2	-8.1
Ta Chang, Thailand	NRIPM	RIN-63	Stegolophodon intermediate form	sin M^3 frg	surface coll.	undetermined	-10.7	-4.9
Ta Chang, Thailand	CV	CCZ 02	Stegolophodon intermediate form	dex dP_4	surface coll.	undetermined	-12.8	-7.1

Ta Chang, Thailand	CV	CCZ 03	Stegolophodon intermediate form	sin M^3	surface coll.	undetermined	-12.7	-8.1
Ta Chang, Thailand	CV	CCZ 401	Stegolophodon intermediate form	sin M_3	surface coll.	undetermined	-11.6	-7.6
Ta Chang, Thailand	CV	CCZ 403	Stegolophodon intermediate form	dex M^3	surface coll.	undetermined	-12.5	-6.8
Ta Chang, Thailand	CV	CCZ 404	Stegolophodon intermediate form	sin M^3	surface coll.	undetermined	-10.9	-7.2
Ta Chang, Thailand	NRIPM	NRRU PRY-63	Stegodon cf. zdansky	dex M^3 frg	surface coll.	undetermined	-11.7	-7.9
Ta Chang, Thailand	NRIPM	RIN-1	Stegodon cf. zdansky	sin M^3	surface coll.	undetermined	-12.4	-7.9
Ta Chang, Thailand	NRIPM	RIN-32	Stegodon cf. zdansky	sin M_3 frg	surface coll.	undetermined	-12.6	-7.3
Ta Chang, Thailand	NRIPM	RIN-48	Stegodon cf. zdansky	M^3 frg	surface coll.	undetermined	-12.9	-7.6
Ta Chang, Thailand	NRIPM	RIN-50	Stegodon cf. zdansky	sin M^3 frg	surface coll.	undetermined	-11.9	-6.4
Ta Chang, Thailand	NRIPM	NRRU 1002-37	Stegodon cf. elephantoides	sin M^3 frg	surface coll.	undetermined	-12.6	-7.3
Ta Chang, Thailand	NRIPM	NRRU 1002-40	Stegodon cf. elephantoides	sin M^3 frg	surface coll.	undetermined	-12.8	-6.5
Ta Chang, Thailand	NRIPM	NRRU 1002-42	Stegodon cf. elephantoides	dex M^3 frg	surface coll.	undetermined	-11.6	-5.0
Ta Chang, Thailand	NRIPM	NRRU 1002-44	Stegodon cf. elephantoides	dex M^3 frg	surface coll.	undetermined	-12.2	-4.0
Ta Chang, Thailand	NRIPM	NRRU 1002-59	Stegodon cf. elephantoides	sin M_3 frg	surface coll.	undetermined	-11.8	-6.4
Ta Chang, Thailand	NRIPM	NRRU 1002-62	Stegodon cf. elephantoides	dex M^3 frg	surface coll.	undetermined	-12.7	-7.1
Ta Chang, Thailand	NRIPM	NRRU 1002-64	Stegodon cf. elephantoides	dex M^3 frg	surface coll.	undetermined	-10.0	-6.5
Ta Chang, Thailand	NRIPM	NRRU 1002-69	Stegodon cf. elephantoides	sin M^3 frg	surface coll.	undetermined	-12.5	-7.8
Ta Chang, Thailand	NRIPM	NRRU 1002-78	Stegodon cf. elephantoides	sin M^3 frg	surface coll.	undetermined	-12.8	-5.5
Ta Chang, Thailand	NRIPM	NRRU 1002-36	Stegodon cf. elephantoides	dex M^3 frg	surface coll.	undetermined	-12.4	-6.1
Ta Chang, Thailand	NRIPM	NRRU 1002-41	Stegodon cf. elephantoides	sinM^3 frg	surface coll.	undetermined	-11.1	-5.9
Irrawaddy, Myanmar	CV	CCZ 402	Stegodon insignis/ganesa	dex M^3	surface coll.	Upper Irrawaddy	-6.9	-6.9
Irrawaddy, Myanmar	CV	CCZ 406	Stegodon insignis/ganesa	dex M^3	surface coll.	Upper Irrawaddy	-0.8	-5.5
Irrawaddy, Myanmar	CV	CCZ 407	Stegodon insignis/ganesa	dex M^2	surface coll.	Upper Irrawaddy	-1.9	-6.1
Haripur, India	NBC	DUB-3041+3099	Stegodon insignis/ganesa	M3 frg	in situ	Upper Siwalik	1.2	-5.0
Haripur, India	NBC	DUB-3051	Stegodon insignis/ganesa	M^1/M^2 frg	in situ	Upper Siwalik	-2.2	-6.0
Haripur, India	NBC	DUB-3053	Stegodon insignis/ganesa	dP_4 + mandible frg	in situ	Upper Siwalik	-0.8	-6.4
Ta Chang, Thailand	NRIPM	RIN-14	Stegodon cf. orientalis	M_2 frg	surface coll.	undetermined	-12.8	-7.5
Ta Chang, Thailand	CV	CCZ 360	Stegodon cf. orientalis	dex M^3	surface coll.	undetermined	-11.7	-6.7
Ta Chang, Thailand	CV	CCZ 405	Stegodon cf. orientalis	dex M^2/M^3 frg	surface coll.	undetermined	-7.7	-6.8
unknown, Laos	CV	CCZ 409	Stegodon cf. orientalis	dex M_1	surface coll.	undetermined	-12.4	-9.5
Haripur, India	NBC	DUB-17??	Archidiskodon (Elephas) planifrons	dex M^3	in situ	Upper Siwalik	-0.2	-5.4
Haripur, India	NBC	DUB-3106	Archidiskodon (Elephas) planifrons	M^3	in situ	Upper Siwalik	1.1	-2.2
Haripur, India	NBC	DUB-3102	Elephas hysudricus	mandible + sin M_2	in situ	Upper Siwalik	-2.8	-6.8
Haripur, India	NBC	DUB-3103	Elephas hysudricus	M^3 frg	in situ	Upper Siwalik	0.1	-4.5
Ta Chang, Thailand	NRIPM	NRRU 1002-87	cf. Palaeoloxodon namadicus	molar frg	surface coll.	undetermined	-5.8	-5.9
Ta Chang, Thailand	NRIPM	NRRU 1002-88	cf. Palaeoloxodon namadicus	M1(?) frg	surface coll.	undetermined	-5.8	-3.1
Ta Chang, Thailand	NRIPM	NRRU 1002-89	cf. Palaeoloxodon namadicus	molar frg	surface coll.	undetermined	-6.0	-3.0
Ta Chang, Thailand	CV	CCZ 410	cf. Palaeoloxodon namadicus	molar frg	surface coll.	undetermined	-7.8	-4.9
Ta Chang, Thailand	NRIPM	NRRU 1002-85	Elephas maximus	molar frg	surface coll.	undetermined	-9.5	-5.6

Ta Chang, Thailand	NRIPM	NRRU 1002-86	Elephas maximus	molar frg	surface coll.	undetermined	-9.9	-4.4
Ta Chang, Thailand	CV	CCZ 84	Elephas maximus	molar frg	surface coll.	undetermined	-12.6	-4.5
Ta Chang, Thailand	CV	CCZ 408	Elephas maximus	dex M_2	surface coll.	undetermined	-13.1	-6.1
Semedo, Java	DKR	1050/SMD/P.26/13	Stegoloxodon indonesicus	dex M^1	surface coll.	older than Satir(?)	-12.8	-5.0
Semedo, Java	DKR	1063/SMD/P.26/13	Stegoloxodon indonesicus	molar frg	surface coll.	older than Satir(?)	-13.8	-6.5
Semedo, Java	DKR	1082/SMD/P.27/S/43	Stegoloxodon indonesicus	dex M_3 frg	surface coll.	older than Satir(?)	-13.5	-5. 8
Semedo, Java	DKR	1085/SMD/P.27/S/13	Stegoloxodon indonesicus	dex M^3 frg	surface coll.	older than Satir(?)	-14.1	-5.8
Semedo, Java	DKR	SMD Pr 3	Stegoloxodon indonesicus	dex M^3 frg	surface coll.	older than Satir(?)	-14.1	-5.5
Semedo, Java	DKR	DK 145	Sinomastodon bumiajuensis	sin M_2 frg	surface coll.	Satir	-1.0	-4.7
Semedo, Java	DKR	DK 146	Sinomastodon bumiajuensis	dex M_2 frg	surface coll.	Satir	-1.9	-4.2
Semedo, Java	DKR	SMD 2	Sinomastodon bumiajuensis	M_3 frg	surface coll.	Satir	-0.2	-4.3
Semedo, Java	DKR	SMD 1	Sinomastodon bumiajuensis	M^3 frg	surface coll.	Satir	-12.1	-5.5
Bumiayu, Java	MGB	WM 15	Sinomastodon bumiajuensis	maxilla frg with M^3	in situ	Satir	0.3	-4.9
Bumiayu, Java	MGB	K135	Sinomastodon bumiajuensis	mandible wi ı M_2	in situ ing B lyrIX/X	Satir	-7.8	-4.6
Bumiayu, Java	MGB	K462	Sinomastodon bumiajuensis	M^3 frg	surface coll.	Satir	0.9	-7.9
Sangiran, Java	MGB	K-311	Sinomastodon bumiajuensis	M_3 frg	surface coll., JICA	Satir	1.7	-3.7
Cirebon, Java	MGB	K 391	pygmy Stegodon sp.	sin M^1	surface, von Koenigswald coll	Satir (Early Pleistocene)	0.3	-4.9
Sambungmacan, Java	MGB	SM 9207-4	pygmy Stegodon sp.	dex mandible frg with M_1	in situ	Satir (Early Pleistocene)	0.0	-5.5
Bumiayu, Java	MGB	WM 15/M 36	Stegodon trigonocephalus	dex M_1	surface Kaliglagah Fm.	Cisaat (Sangiran)	-0.9	-6.2
Bumiayu, Java	MGB	MA?	Stegodon trigonocephalus	M_2 frg	surface Kaliglagah/ Mengger Fm.	Cisaat (Sangiran)	-2.4	-7.2
Bumiayu, Java	MGB	830618-4	Stegodon trigonocephalus	M_2 frg	surface Kaliglagah/ Mengger Fm.	Cisaat (Sangiran)	1.3	-5.7
Bumiayu, Java	MGB	CS 830616-I (BA 93)	Stegodon trigonocephalus	sin M_1 frg	in situ, Cisaat Rvr. conglomeratic sandstone	Cisaat (Sangiran)	0.5	-5.5
Sangiran, Java	MGB	SB-B2	Stegodon trigonocephalus	sin dP_4 frg	"black clay" layer	Cisaat (Sangiran)	-0.9	-6.0
Sangiran, Java	MGB	SA 200578, Ngr 19	Stegodon trigonocephalus	molar frg	Grenzbank	Cisaat (Sangiran)	-0.6	-7.1
Sangiran, Java	MGB	SA 290178, Ngr 1	Stegodon trigonocephalus	molar frg	below Grenzbank, Kali Brangkal	Cisaat (Sangiran)	1.4	-5.1
Sangiran, Java	MGB	SA 280178, Ngr 3	Stegodon trigonocephalus	M^2 frg	below Grenzbank, Kali Brangkal	Cisaat (Sangiran)	-0.1	-6.3
Sangiran, Java	MGB	SA 190578, Tjk 3	Stegodon trigonocephalus	molar frg	upper cengklik, "black clay"	Cisaat (Sangiran)	-0.3	-6.9

Sangiran, Java	MGB	SA 250378, Ngr 2	Stegodon trigonocephalus	molar frg	below Grenzbank, Kali Brangkal	Cisaat (Sangiran)	-0.8	-6.4
Sangiran, Java	MGB	SA 280578, Pu 4	Stegodon trigonocephalus	M_3 fragment	above Grenzbank	Kedung Brubus (+ Bapang)	0.7	-5.9
Sangiran, Java	MGB	SA 280178, Krt 2	Stegodon trigonocephalus	molar frg	above pinkish tuff	Kedung Brubus (+ Bapang)	1.4	-5.3
Sangiran, Java	MGB	SA 230578, Nge 1	Stegodon trigonocephalus	molar frg	triangulation point	Kedung Brubus (+ Bapang)	0.1	-5.8
Sangiran, Java	BPSMPS	Myr 1	Stegodon trigonocephalus	dex M^3	in situ	Kedung Brubus (+ Bapang)	0.2	-5.2
Sangiran, Java	BPSMPS	Myr 2	Stegodon trigonocephalus	M^3 frg	in situ	Kedung Brubus (+ Bapang)	-0.1	-4.8
Sangiran, Java	BPSMPS	Myr 3	Stegodon trigonocephalus	molar frg	in situ	Kedung Brubus (+ Bapang)	0.5	-5.1
Sangiran, Java	BPSMPS	37/Elp/0276	Stegodon trigonocephalus	mandible sin with M_3	surface coll.	Kedung Brubus (+ Bapang)	-0.7	-5.4
Sangiran, Java	BPSMPS	0430/Elp	Stegodon trigonocephalus	dex M_3 frg	surface coll.	Kedung Brubus (+ Bapang)	1.3	-4.4
Sangiran, Java	BPSMPS	ELP 157	Stegodon trigonocephalus	maxilla with M^2 frg	surface coll.	Kedung Brubus (+ Bapang)	-0.3	-5.3
Sangiran, Java	BPSMPS	ELP 1196	Stegodon trigonocephalus	mandible with M_1	surface coll.	Kedung Brubus (+ Bapang)	0.7	-5.3
Sangiran, Java	BPSMPS	ELP 1223	Stegodon trigonocephalus	maxilla with M^3	surface coll.	Kedung Brubus (+ Bapang)	0.3	-5.7
Sangiran, Java	MGB	Pu 85-54	Stegodon trigonocephalus	sin M^2	surface coll.	Kedung Brubus (+ Bapang)	0.9	-6.9
Sangiran, Java	MGB	SA 250178, GK 25	Stegodon trigonocephalus	molar frg	above pinkish tuff	Kedung Brubus (+ Bapang)	-0.3	-6.4
Sangiran, Java	MGB	SA 240378, GK 5	Stegodon trigonocephalus	molar frg	surface coll.	Kedung Brubus (+ Bapang)	0.2	-9.8
Kedung Brubus, Java	MGB	KB1	Stegodon trigonocephalus	sin M^2 frg	surface coll.	Kedung Brubus (+ Bapang)	-1.1	-6.0
Kedung Brubus, Java	NBC	DUB-14052	Stegodon trigonocephalus	molar frg	in situ, Dubois collection	Kedung Brubus (+ Bapang)	-0.2	-5.4
Kedung Brubus, Java	NBC	DUB-2428	Stegodon trigonocephalus	M^2	in situ, Dubois collection	Kedung Brubus (+ Bapang)	0.7	-5.6
Kedung Brubus, Java	NBC	DUB-3443+3444	Stegodon trigonocephalus	M_2	in situ, Dubois collection	Kedung Brubus (+ Bapang)	1.0	-5.8
Kedung Brubus, Java	NBC	DUB-2444	Stegodon trigonocephalus	M_+	in situ, Dubois collection	Kedung Brubus (+ Bapang)	-0.6	-6.4

Kedung Brubus, Java	NBC	DUB-3357	Stegodon trigonocephalus	M^2	in situ, Dubois collection	Kedung Brubus (+ Bapang)	0.9	-6.9
Kedung Brubus, Java	NBC	DUB 2?06	Stegodon trigonocephalus	M_1/M_2	in situ, Dubois collection	Kedung Brubus (+ Bapang)	-0.7	-6.1
Trinil, Java	MGB	K 390	Stegodon trigonocephalus	molar frg	in situ, von Koenigswald collection	Trinil H.K.	1.4	-5.7
Trinil, Java	MGB	K 399	Stegodon trigonocephalus	sin dP^4/M^1	in situ, von Koenigswald collection	Trinil H.K.	-1.8	-5.7
Trinil, Java	NBC	DUB-2895	Stegodon trigonocephalus	M^3	in situ, Dubois collection	Trinil H.K.	0.7	-6.7
Trinil, Java	NBC	DUB-2225	Stegodon trigonocephalus	M_2/M_3	in situ, Dubois collection	Trinil H.K.	0.1	-6.1
Trinil, Java	NBC	DUB-379	Stegodon trigonocephalus	M^2	in situ, Dubois collection	Trinil H.K.	0.3	-5.5
Trinil, Java	NBC	DUB-389	Stegodon trigonocephalus	M^3	in situ, Dubois collection	Trinil H.K.	1.0	-6.3
Trinil, Java	NBC	DUB-3491	Stegodon trigonocephalus	M_1	in situ, Dubois collection	Trinil H.K.	-0.3	-6.4
Trinil, Java	NBC	DUB-3253	Stegodon trigonocephalus	dP_4	in situ, Dubois collection	Trinil H.K.	-2.7	-5.6
Trinil, Java	NBC	DUB-1803A	Stegodon trigonocephalus	dP_3	in situ, Dubois collection	Trinil H.K.	-2.3	-6.2
Trinil, Java	NBC	DUB-2896	Stegodon trigonocephalus	M_2	in situ, Dubois collection	Trinil H.K.	-0.3	-6.7
Ngandong, Java	MGB	11309 (K363)	Stegodon trigonocephalus	dex M^1	ingr IB block F lyr IV, von Koenigswald coll.	Ngandong	0.6	-6.8
Ngandong, Java	MGB	13322 (K351)	Stegodon trigonocephalus	dex mandible frg with dP_3+dP_4	ing Ib block 9,von Koenigswald coll.	Ngandong	-1.6	-6.4
Ngandong, Java	MGB	K 323	Stegodon trigonocephalus	sin dP_4	in situ, von Koenigswald coll	Ngandong	0.0	-6.3
Ngandong, Java	MGB	9875 (k320)	Stegodon trigonocephalus	sin M_1	ing Ib bl. E lyr III, von Koenigswald coll	Ngandong	-2.0	-6.5
Ngandong, Java	MGB	5667 (K440a)	Stegodon trigonocephalus	$M^{2/3}$ frg	in situ, von Koenigswald coll	Ngandong	-5.9	-7.6
Ngandong, Java	MGB	383 (K318)	Stegodon trigonocephalus	dex dP^4 frg	ing VIII lyr III, von Koenigswald coll	Ngandong	-5.3	-6.7

Ngandong, Java	MGB	K316	Stegodon trigonocephalus	sin M_1 frg	in situ, von Koenigswald coll	Ngandong	-3.2	-6.6
Ngandong, Java	MGB	K329	Stegodon trigonocephalus	mandible sin +dP^3	in situ, von Koenigswald coll	Ngandong	-3.5	-7.4
Ngandong, Java	MGB	1075 (K307)	Stegodon trigonocephalus	abnormal M3 frg	ing VIII Lyr II, von Koenigswald coll	Ngandong	0.7	-7.2
Watualang, Java	MGB	2205 (K387)	Stegodon trigonocephalus	upper $M^2/^3$ frg	ing 1N lyr II, von Koenigswald coll	Ngandong	2.3	-6.3
Subang, Java	MGB	Sbg 10-2	Stegodon trigonocephalus	M^1 frg	surface coll	West Java	-0.3	-4.7
Subang, Java	MGB	Sbg 10-4	Stegodon trigonocephalus	M_2 frg	surface coll	West Java	0.4	-5.8
Subang, Java	MGB	Sbg 10-7	Stegodon trigonocephalus	$M_2/_3$ frg	surface coll	West Java	0.1	-5.1
Subang, Java	MGB	Sbg 10-9	Stegodon trigonocephalus	M_2 frg	surface coll	West Java	-3.0	-5.1
Sangiran, Java	MGB	SA 180578, Nge 2	Elephas hysudrindicus	molar frg	triangulation point, N. Ngebung lower	Kedung Brubus (+ Bapang)	-2.6	-2.3
Sangiran, Java	MGB	SA 230578	Elephas hysudrindicus	molar frg	triangulation point, N. Ngebung lower	Kedung Brubus (+ Bapang)	0.1	-2.3
Sangiran, Java	BPSMPS	ELP 642	Elephas hysudrindicus	molar frg	surface coll	Kedung Brubus (+ Bapang)	0.9	-4.0
Sangiran, Java	BPSMPS	ELP 545	Elephas hysudrindicus	molar frg	surface coll	Kedung Brubus (+ Bapang)	1.8	-3.4
Sangiran, Java	BPSMPS	ELP 1378	Elephas hysudrindicus	molar frg	surface coll	Kedung Brubus (+ Bapang)	1.4	-4.4
Kedung Brubus, Java	NBC	DUB-2265	Elephas hysudrindicus	molar frg	in situ, Dubois collection	Kedung Brubus (+ Bapang)	0.3	-5.3
Kedung Brubus, Java	NBC	DUB-2230	Elephas hysudrindicus	molar frg	in situ, Dubois collection	Kedung Brubus (+ Bapang)	0.2	-3.9
Kedung Brubus, Java	NBC	DUB-14341	Elephas hysudrindicus	molar frg	in situ, Dubois collection	Kedung Brubus (+ Bapang)	0.6	-5.6
Ngandong, Java	MGB	5667 (K440b)	Elephas hysudrindicus	dP_4 frg	ing 5 lyr III, von Koenigswald coll	Ngandong	-2.9	-5.0
Brebes, Java	MGB	KS	Elephas hysudrindicus	molar frg	surface coll	West Java	1.0	-6.4
Bumiayu, java	MGB	BUM 05	Elephas hysudrindicus	molar frg	surface coll	West Java	0.1	-7.3
Sunggu, Blora, Java	MGB	B	Elephas hysudrindicus	sin M_3	in situ	Sunggu	-12.7	-5.2
Cipendeuy, Java	MGB	Cpd 2	Elephas maximus	molar frg	in situ	Cipeundeuy	-8.7	-6.7
Cipendeuy, Java	MGB	Cpd 3	Elephas maximus	molar frg	in situ	Cipeundeuy	-14.9	-7.8
Cipendeuy, Java	MGB	Cpd 119	Elephas maximus	molar frg	in situ	Cipeundeuy	-13.4	-7.3
Karang Bolong, Java	MGB	K436	Elephas maximus	molar frg	surface coll.	Holocene Cave Composite	-15.0	-5.3
Way Kambas, Sumatra	MGB	WK*	Elephas maximus	mandible with M_1+M_2 frg	surface coll.	modern	-12.6	-5.2

unknown, Sumatra	MGB	ELP 2	Elephas maximus	dP_4	surface coll.	modern	-17.4	-6.4
unknown, Sumatra	MGB	ELP 3	Elephas maximus	M_1	surface coll.	modern	-17.7	-5.9
unknown, Sumatra	MGB	ELP 4	Elephas maximus	M_1	surface coll.	modern	-16.3	-5.6
unknown, Sumatra	MGB	ELP 5	Elephas maximus	M_2	surface coll.	modern	-17.1	-7.2
Lakibong, Sulawesi	MGB	LK1327	Stegoloxodon celebensis	molar frg	surface coll.	Walanae B	-11.7	-5.4
Lakibong, Sulawesi	MGB	L-2356	Stegoloxodon celebensis	M2/M3 frg	surface coll.	Walanae B	0.9	-4.9
Lakibong, Sulawesi	MGB	890602-2-13	Stegoloxodon celebensis	molar frg	surface coll.	Walanae B	-14.9	-3.3
Lakibong, Sulawesi	MGB	LKB 2-1	Stegoloxodon celebensis	molar frg	surface coll.	Walanae B	-1.9	-4.7
Sompe, Sulawesi	MGB	SP2410	Stegoloxodon celebensis	ridge frg	surface coll.	Walanae A	0.6	-4.5
Sompe, Sulawesi	MGB	SP2412	Stegoloxodon celebensis	molar frg	surface coll.	Walanae A	-13.3	-3.8
Sompe, Sulawesi	MGB	SP2413	Stegodon sompoensis	molar frg	surface coll.	Walanae A	0.1	-4.2
Sompe, Sulawesi	MGB	SP2414	Stegodon sompoensis	maxilla+M^3 frg	surface coll.	Walanae A	-1.0	-5.5
Sompe, Sulawesi	MGB	SP2415	Stegoloxodon celebensis	molar frg	surface coll.	Walanae A	-0.1	-3.7
Sompe, Sulawesi	MGB	SP2417	Stegoloxodon celebensis	molar frg	surface coll.	Walanae A	0.8	-4.3
Sompe, Sulawesi	MGB	SP2418	Stegoloxodon celebensis	dP_4/M_1 frg	surface coll.	Walanae A	-3.0	-3.8
Sompe, Sulawesi	MGB	SP3964	Stegoloxodon celebensis	molar frg	surface coll.	Walanae A	0.5	-4.2
Lonrong, Sulawesi	MGB	LR-2737	Stegoloxodon celebensis	molar frg	surface coll.	Walanae A	1.3	-5.9
Lonrong, Sulawesi	MGB	LR-2738	Stegoloxodon celebensis	molar frg	surface coll.	Walanae A	-10.8	-6.1
Lonrong, Sulawesi	MGB	LR-2743	Stegoloxodon celebensis	molar frg	surface coll.	Walanae A	0.8	-6.0
Lonrong, Sulawesi	MGB	LR-2752	Stegoloxodon celebensis	molar frg	surface coll.	Walanae A	-4.8	-5.0
Lonrong, Sulawesi	MGB	LR-2756	Stegoloxodon celebensis	molar frg	surface coll.	Walanae A	-13.6	-3.7
Lonrong, Sulawesi	MGB	LR-3513	Stegoloxodon celebensis	molar frg	in situ	Walanae A	-3.7	-4.8
Lonrong, Sulawesi	MGB	LR-3517	Stegoloxodon celebensis	post dex M_3	in situ	Walanae A	-14.1	-5.7
Lakibong, Sulawesi	MGB	LK 890602-3-12	Stegodon sompoensis	molar frg	surface coll.	Walanae B	-2.2	-5.2
Lakibong, Sulawesi	MGB	LK 890603-1	Stegodon sompoensis	molar frg	surface coll.	Walanae B	-1.8	-6.6
Lakibong, Sulawesi	MGB	LK coll 90	Stegodon sompoensis	upper molar fragment	surface coll.	Walanae B	-0.1	-5.0
Lakibong, Sulawesi	MGB	L2-2370	Stegodon sompoensis	sin dP_2	surface coll.	Walanae B	-3.2	-2.8
Lakibong, Sulawesi	MGB	L-3985	Stegodon sompoensis	molar frg	surface coll.	Walanae B	-7.8	-5.6
Bulu Cepo, Sulawesi	MGB	BC-2959	Stegodon sompoensis	M^3	surface coll.	Walanae B	0.5	-4.2
Bulu Cepo, Sulawesi	MGB	BC2945	Stegodon sompoensis	molar frg	surface coll.	Walanae B	-12.3	-2.9
Bulu Cepo, Sulawesi	MGB	BC2957	Stegodon sompoensis	molar frg	surface coll.	Walanae B	1.1	-4.8
Bulu Palece, Sulawesi	MGB	BP 10-5	Stegodon sompoensis	dex mandible frg with post M_3	surface coll.	Walanae A	-3.1	-6.0
Paroto, Sulawesi	MGB	PA-3730	Stegodon sompoensis	sin dp^3	surface coll.	Walanae A	-3.2	-5.0
Lonrong, Sulawesi	MGB	LR2752	Stegodon sompoensis	ridge frg	surface coll.	Walanae A	-5.3	-5.6
Lakibong, Sulawesi	MGB	L2-2736	large Stegodon sp. B	ridge frg	surface coll.	Walanae B	-3.7	-6.4
Lakibong, Sulawesi	MGB	LK1324	large Stegodon sp. B	molar frg	surface coll.	Walanae B	-4.5	-5.0

Lakibong, Sulawesi	MGB	LK1325	large Stegodon sp. B	molar frg	surface coll.	Walanae B	0.1	-5.4
Lakibong, Sulawesi	MGB	LK1326	large Stegodon sp. B	molar frg	surface coll.	Walanae B	0.4	-5.4
Lakibong, Sulawesi	MGB	LK-1	large Stegodon sp. B	molar frg	surface coll.	Walanae B	0.7	-4.8
Bulu Cepo, Sulawesi	MGB	BC-3990	Stegodon sompoensis	molar frg	surface coll.	Walanae B	-4.1	-4.8
Lonrong, Sulawesi	MGB	LR-3999	Stegodon sompoensis	dex M^1 frg	surface coll.	Walanae A	-4.5	-8.9
Sangihe	MGB	Sangihe	large Stegodon sp. B	dex M^3	surface coll.	Tanrung	1.8	-6.4
Lakibong, Sulawesi	MGB	LK-1036	Celebochoerus heekereni	M_3	surface coll.	Walanae B	-0.7	-2.7
Lakibong, Sulawesi	MGB	LK-1629	Celebochoerus heekereni	dex mandible frg+M_3,	surface coll.	Walanae B	0.4	-3.9
Lakibong, Sulawesi	MGB	LK-3041	Celebochoerus heekereni	dex maxilla with M^2+M^3	surface coll.	Walanae B	-1.0	-2.0
Bulu Cepo, Sulawesi	MGB	BC-3989	Celebochoerus heekereni	molar frg	surface coll.	Walanae B	-0.3	-4.6
Lonrong, Sulawesi	MGB	LR-2536	Celebochoerus heekereni	maxilla frg with M^2+M^3	surface coll.	Walanae A	-0.9	-1.7
Lonrong, Sulawesi	MGB	LR-2543	Celebochoerus heekereni	dex maxilla frg with M^3	surface coll.	Walanae A	0.2	-3.3
Lonrong, Sulawesi	MGB	LR-2577	Celebochoerus heekereni	dex mandible frg with M_3	surface coll.	Walanae A	4.7	-8.7
Lonrong, Sulawesi	MGB	LR-2578	Celebochoerus heekereni	dex mandible frg with M_2+M_3	surface coll.	Walanae A	-0.7	-3.6
Lonrong, Sulawesi	MGB	LR-2715	Celebochoerus heekereni	sin maxilla frg with M^2+M^3	surface coll.	Walanae A	0.1	-4.2
Lonrong, Sulawesi	MGB	LR-2716	Celebochoerus heekereni	dex mandible with M_3	surface coll.	Walanae A	0.2	-3.1
Lonrong, Sulawesi	MGB	LR-07-03	Celebochoerus heekereni	M_3	surface coll.	Walanae A	-0.7	-2.9
Lonrong, Sulawesi	MGB	LR-07-21	Celebochoerus heekereni	M^3	surface coll.	Walanae A	-0.8	-3.7
Tanrung, Sulawesi	MGB	TA 07-1	Large Stegodon sp. B	post. lower molar frg	surface coll.	Tanrung	-0.6	-5.1
Tanrung, Sulawesi	MGB	TA 07-2	Large Stegodon sp. B	post. upper sin molar frg	surface coll.	Tanrung	1.4	-3.2
Tanrung, Sulawesi	MGB	TA 07-61	Large Stegodon sp. B	molar fragment	surface coll.	Tanrung	-0.4	-6.2
Tanrung, Sulawesi	MGB	TA 07-62	Large Stegodon sp. B	molar fragment	surface coll.	Tanrung	0.9	-4.7
Tanrung, Sulawesi	MGB	TA3711	Large Stegodon sp. B	sin M_1 frg	in situ	Tanrung	-1.1	-5.6
Tanrung, Sulawesi	MGB	TA3712	Large Stegodon sp. B	maxilla with dP^4+M^1 frg	in situ	Tanrung	-1.0	-5.9
Tanrung, Sulawesi	MGB	TA3723	Large Stegodon sp. B	dex mandible frg with M_3	in situ	Tanrung	0.0	-5.7
Tanrung, Sulawesi	MGB	TA-3070	Large Stegodon sp. B	molar fragment	surface coll.	Tanrung	1.8	-5.0

Tanrung, Sulawesi	MGB	TR12-F2	cf. Palaeoloxodon namadicus	upper molar frg, 3½ plates	in situ	Tanrung	-14.9	-5.9
Tanrung, Sulawesi	MGB	TA3920	cf. Palaeoloxodon namadicus	molar frg	surface coll.	Tanrung	-13.8	-7.5
Tanrung, Sulawesi	MGB	TA07-35	cf. Palaeoloxodon namadicus	molar frg	surface coll.	Tanrung	-14.5	-5.6
Talepu, Sulawesi	MGB	TLP10-16	Celebochoerus heekereni	M_3	in situ	Tanrung	-13.5	-5.7
Leang Bulu Bettue, Sulawesi	Arkenas	LBB-S42-B2-L8-610	cf. Palaeoloxodon namadicus	molar frg	in situ	Tanrung	-13.6	-6.5
Rizal, Luzon, Philippines	NMP	NMP-239*	dwarf Stegodon sp.	M_3 frg	surface	Pleistocene Luzon	-6.2	-7.2
Rizal, Luzon, Philippines	NMP	P1 (no label)*	Elephas sp.	molar frg	surface, tag: R2-2014-JI-004	Pleistocene Luzon	-3.6	-5.0
Rizal, Luzon, Philippines	NMP	P2 (no label)*	Elephas sp.	molar frg	Surface, found June 2014, waypoint: tusk (GPS Paul), N17°33.606', E121°33.549'	Pleistocene Luzon	-1.1	-4.0
Rizal, Luzon, Philippines	NMP	P3 (no label)*	Stegodon cf. luzonensis	molar frg	surface coll.	Pleistocene Luzon	-0.0	-5.2
Tangi Talo, Flores	MGB	TT4040	Stegodon sondaari	sin M^1 frg	in situ	Tangi Talo	-5.4	-6.4
Tangi Talo, Flores	MGB	TT4262	Stegodon sondaari	sin M^1 frg	in situ	Tangi Talo	-5.1	-5.7
Tangi Talo, Flores	MGB	TT new site	Stegodon sondaari	dP_4 frg	surface coll.	Tangi Talo	-2.5	-5.6
Tangi Talo, Flores	MGB	TT new site	Stegodon sondaari	M^1 frg	surface coll.	Tangi Talo	-2.3	-6.8
Tangi Talo, Flores	MGB	TT new site large	Stegodon sondaari	M^1 frg	surface coll.	Tangi Talo	-8.1	-5.6
Tangi Talo, Flores	MGB	TTTT	Stegodon sondaari	tusk tip	surface coll.	Tangi Talo	-11.9	-5.3
Tangi Talo, Flores	MGB	TT12-TG-F57	Stegodon sondaari	molar frg	in situ	Tangi Talo	-7.1	-5.9
Tangi Talo, Flores	MGB	TT12-TG-F208	Stegodon sondaari	M_1 frg	in situ	Tangi Talo	-4.4	-5.5
Tangi Talo, Flores	MGB	TT12-TG-F600	Stegodon sondaari	molar frg	in situ	Tangi Talo	-4.8	-4.7
Tangi Talo, Flores	MGB	TT12-TG-F705	Stegodon sondaari	molar frg	in situ	Tangi Talo	-7.9	-6.0
Tangi Talo, Flores	MGB	TT12-TG-F838	Stegodon sondaari	sin $M_2/_3$ frg	in situ	Tangi Talo	-6.6	-4.8
Tangi Talo, Flores	MGB	TT13-TG-F871	Stegodon sondaari	dex M_2 frg	in situ	Tangi Talo	-4.8	-7.0
Tangi Talo, Flores	MGB	TT13-TG-F872	Stegodon sondaari	dex M_2	in situ, TT13-TG-F984's pair	Tangi Talo	-6.7	-4.7
Tangi Talo, Flores	MGB	TT13-TG-F873A	Stegodon sondaari	dex M_1 frg	in situ	Tangi Talo	-6.0	-4.3
Tangi Talo, Flores	MGB	TT13-TG-F873B	Stegodon sondaari	dex M^1 frg	in situ	Tangi Talo	-5.1	-5.3
Tangi Talo, Flores	MGB	TT13-TG-F876	Stegodon sondaari	molar frg	in situ	Tangi Talo	-3.8	-5.9
Tangi Talo, Flores	MGB	TT13-TG-F897	Stegodon sondaari	sin M^1	in situ	Tangi Talo	-4.8	-5.5
Tangi Talo, Flores	MGB	TT13-TG-F966	Stegodon sondaari	dex M^1	in situ	Tangi Talo	-5.7	-6.6
Tangi Talo, Flores	MGB	TT13-TG-F984	Stegodon sondaari	sin M_2	in situ, TT13-TG-F872's pair	Tangi Talo	-7.5	-6.6

Tangi Talo, Flores	MGB	TT13-TG-F985	Stegodon sondaari	sin M^2 frg	in situ	Tangi Talo	-4.8	-3.6
Tangi Talo, Flores	MGB	TT13-TG-F1013	Stegodon sondaari	sin M^2 frg	in situ	Tangi Talo	-7.1	-5.4
Tangi Talo, Flores	MGB	TT13-TH-F71	Stegodon sondaari	sin M^3	in situ	Tangi Talo	-6.4	-5.1
Tangi Talo, Flores	MGB	TT13-TH-F91	Stegodon sondaari	sin M^3 frg	in situ	Tangi Talo	-7.3	-4.2
Tangi Talo, Flores	MGB	TT13-TH-F100	Stegodon sondaari	sin M^3 frg	in situ	Tangi Talo	-6.6	-4.3
Tangi Talo, Flores	MGB	TT12-TF -F110	Stegodon sondaari	sin M^2 frg	in situ	Tangi Talo	-7.1	-2.9
Tangi Talo, Flores	MGB	TT12-TF-F147	Stegodon sondaari	dex M_2 frg	in situ	Tangi Talo	-7.8	-4.1
Tangi Talo, Flores	MGB	TT12-TF-F148	Stegodon sondaari	sin M^2 frg	in situ	Tangi Talo	-8.3	-5.2
Kobatuwa, Flores	Arkenas	KBT12-42	Stegodon florensis	molar frg	in situ	Mata Menge, LFI	-5.6	-6.8
Kobatuwa, Flores	Arkenas	KBT11-T1/II	Stegodon florensis	M^3	in situ	Mata Menge, LFI	-5.5	-7.0
Kobatuwa, Flores	Arkenas	KBT11-T1/T2/K3/F	Stegodon florensis	molar frg	in situ	Mata Menge, LFI	-1.2	-8.8
Kobatuwa, Flores	Arkenas	KBT11-T1/T2/K2	Stegodon florensis	posterior M_3 frg	in situ	Mata Menge, LFI	-1.1	-7.4
Kobatuwa, Flores	Arkenas	KBT 2013 1	Stegodon florensis	molar frg	surface coll.	Mata Menge, LFI	-0.8	-5.5
Kobatuwa, Flores	Arkenas	KBT 2013 2	Stegodon florensis	molar frg	surface coll.	Mata Menge, LFI	-1.5	-7.4
Kobatuwa, Flores	Arkenas	KBTI/II T2/K3	Stegodon florensis	M_1 frg	in situ	Mata Menge, LFI	-0.4	-6.0
Kobatuwa, Flores	Arkenas	KBTI/12 T2/K14	Stegodon florensis	M_2 frg	in situ	Mata Menge, LFI	-0.3	-5.6
Kobatuwa, Flores	Arkenas	KBTI/III T2/K15	Stegodon florensis	M_2 frg	in situ	Mata Menge, LFI	-6.2	-5.9
Dozo Dhalu, Flores	MGB	DD4207	Stegodon florensis	molar frg	in situ	Mata Menge, MFI	-2.1	-6.6
Dozo Dhalu, Flores	MGB	DD B5	Stegodon florensis	molar frg	in situ	Mata Menge, MFI	-1.7	-7.2
Dozo Dhalu, Flores	MGB	DD 4200	Stegodon florensis	dex M^3 frg	in situ	Mata Menge, MFI	0.9	-5.0
Dozo Dhalu, Flores	MGB	DD 4201	Stegodon florensis	molar frg	in situ	Mata Menge, MFI	1.4	-5.4
Dozo Dhalu, Flores	MGB	DD 4234	Stegodon florensis	$M^{2/3}$ frg	in situ	Mata Menge, MFI	-2.2	-7.2
Boa Leza, Flores	MGB	BL12-T1-F54	Stegodon florensis	molar frg	in situ	Mata Menge, MFI	1.2	-6.3
Boa Leza, Flores	MGB	BL12-T1-F418	Stegodon florensis	molar frg	in situ	Mata Menge, MFI	1.3	-5.3
Boa Leza, Flores	MGB	BL12-T1-F428	Stegodon florensis	molar frg	in situ	Mata Menge, MFI	0.9	-7.1
Boa Leza, Flores	MGB	BL12-T1-F504	Stegodon florensis	molar frg	in situ	Mata Menge, MFI	1.0	-5.1
Mata Menge, Flores	MGB	MM05-4	Stegodon florensis	tusk tip	in situ	Mata Menge, MFI	-13.0	-5.2
Mata Menge, Flores	MGB	MM06-02	Stegodon florensis	Sin M_3 frgt	in situ	Mata Menge, MFI	0.4	-6.6
Mata Menge, Flores	MGB	MM11-T14a-93	Stegodon florensis	molar frg	in situ	Mata Menge, MFI	-1.2	-6.6
Mata Menge, Flores	MGB	MM11-T14b-171	Stegodon florensis	molar frg	in situ	Mata Menge, MFI	0.7	-7.0
Mata Menge, Flores	MGB	MM11-T21-F231	Stegodon florensis	dex M^3 frg	in situ	Mata Menge, MFI	1.3	-6.2
Mata Menge, Flores	MGB	MM11-T22-F150	Stegodon florensis	M_3 frg	in situ	Mata Menge, MFI	-0.1	-6.2
Mata Menge, Flores	MGB	MM11-T22-F164	Stegodon florensis	molar frg	in situ	Mata Menge, MFI	-1.2	-6.9
Mata Menge, Flores	MGB	MM11-T23C-F750	Stegodon florensis	milk tusk	in situ	Mata Menge, MFI	-3.4	-7.2
Mata Menge, Flores	MGB	MM11-T24B-F172	Stegodon florensis	M^3 frg	in situ	Mata Menge, MFI	-1.7	-7.8
Mata Menge, Flores	MGB	MM11-T24B-F272	Stegodon florensis	molar frg	in situ	Mata Menge, MFI	1.6	-6.9
Mata Menge, Flores	MGB	MM11-T25-F23	Stegodon florensis	molar frg	in situ	Mata Menge, MFI	-0.8	-6.0
Mata Menge, Flores	MGB	MM11-T25-F209	Stegodon florensis	molar frg	in situ	Mata Menge, MFI	1.3	-6.4
Mata Menge, Flores	MGB	MM11-T25-F227	Stegodon florensis	sin mandible frg with M_2	in situ	Mata Menge, MFI	0.5	-6.9

Mata Menge, Flores	MGB	MM11-T26-148	Stegodon florensis	molar frg	in situ	Mata Menge, MFI	0.8	-7.0
Mata Menge, Flores	MGB	MM11-T30-F618	Stegodon florensis	dP^3 frg	in situ	Mata Menge, MFI	-2.0	-6.6
Mata Menge, Flores	MGB	MM12-T23A-F780	Stegodon florensis	molar frg	in situ	Mata Menge, MFI	-0.9	-7.5
Mata Menge, Flores	MGB	MM12-T23A-F1438	Stegodon florensis	dex dP_3 frg	in situ	Mata Menge, MFI	-0.5	-7.1
Mata Menge, Flores	MGB	MM12-T23D-F569	Stegodon florensis	sin M_2 frg	in situ	Mata Menge, MFI	-0.1	-7.2
Mata Menge, Flores	MGB	MM12-T23D-F851	Stegodon florensis	molar frg	in situ	Mata Menge, MFI	0.6	-5.5
Mata Menge, Flores	MGB	MM12-T23D-F855	Stegodon florensis	molar frg	in situ	Mata Menge, MFI	0.3	-6.6
Mata Menge, Flores	MGB	MM12-T31-F69	Stegodon florensis	M3 frg	in situ	Mata Menge, MFI	1.3	-7.3
Mata Menge, Flores	MGB	MM12-T31-F172	Stegodon florensis	M3 frg	in situ	Mata Menge, MFI	1.2	-6.2
Mata Menge, Flores	MGB	MM12-T31-F257	Stegodon florensis	sin dP_3 frg	in situ	Mata Menge, MFI	-2.0	-7.3
Mata Menge, Flores	MGB	MM12-T31-F902	Stegodon florensis	sin M^3 frg	in situ	Mata Menge, MFI	-0.2	-7.1
Mata Menge, Flores	MGB	MM13-T32-F168	Stegodon florensis	molar frg	in situ	Mata Menge, UFI	2.3	-5.2
Mata Menge, Flores	MGB	MM13-T32-F198	Stegodon florensis	sin M^3	in situ	Mata Menge, UFI	2.1	-5.4
Mata Menge, Flores	MGB	MM13-T32-F247	Stegodon florensis	molar frg	in situ	Mata Menge, UFI	1.8	-5.6
Mata Menge, Flores	MGB	MM13-T32-F913	Stegodon florensis	sin $M^2/^3$ frg	in situ	Mata Menge, UFI	-1.9	-4.2
Mata Menge, Flores	MGB	MM13-T32-F923	Stegodon florensis	molar frg	in situ	Mata Menge, UFI	-2.7	-4.2
Mata Menge, Flores	MGB	MM13-T32-F1016	Stegodon florensis	molar frg	in situ	Mata Menge, UFI	0.4	-4.9
Mata Menge, Flores	MGB	MM13-T32-F1050	Stegodon florensis	molar frg	in situ	Mata Menge, UFI	-0.5	-4.4
Mata Menge, Flores	MGB	MM13-T32-F1077	Stegodon florensis	molar frg	in situ	Mata Menge, UFI	0.2	-4.7
Mata Menge, Flores	MGB	MM14-T32B-F74	Stegodon florensis	M_1 frg	in situ	Mata Menge, UFI	1.3	-5.2
Mata Menge, Flores	MGB	MM10-T11-F142	Crocodilus	tooth	in situ	Mata Menge, MFI	-3.7	-6.5
Mata Menge, Flores	MGB	MM13-T32-F202	Crocodilus	tooth	in situ	Mata Menge, UFI	0.9	-6.0
Mata Menge, Flores	MGB	MM13-T32-F237	Crocodilus	tooth	in situ	Mata Menge, UFI	-2.0	-11.4
Mata Menge, Flores	MGB	MM13-T32-F266	Crocodilus	tooth	in situ	Mata Menge, UFI	0.1	-10.7
Mata Menge, Flores	MGB	MM13-T32-F311	Crocodilus	tooth	in situ	Mata Menge, UFI	-0.4	-6.6
Mata Menge, Flores	MGB	MM11-T24B-151	Muridae	incisor	in situ	Mata Menge, MFI	-2.0	-7.2
Mata Menge, Flores	MGB	MM11-T27-562	Muridae	incisor	in situ	Mata Menge, MFI	0.9	-8.1
Mata Menge, Flores	MGB	MM13-T32-211	Muridae	incisor	in situ	Mata Menge, UFI	0.3	-7.6
Mata Menge, Flores	MGB	MM13-T32-222	Muridae	incisor	in situ	Mata Menge, UFI	1.6	-5.8
Mata Menge, Flores	MGB	MM13-T32-238	Muridae	incisor	in situ	Mata Menge, UFI	-0.4	-8.2
Mata Menge, Flores	MGB	MM13-T32-240	Muridae	incisor	in situ	Mata Menge, UFI	1.6	-6.6
Mata Menge, Flores	MGB	MM13-T32-244	Muridae	incisor	in situ	Mata Menge, UFI	-0.5	-6.4
Liang Bua, Flores	Arkenas	LB04-SXI-Sp37-1	Stegodon florensis insularis	Milk tusk frg	in situ	Liang Bua	-1.0	-4.4
Liang Bua, Flores	Arkenas	LB04-SXI-Sp38b-2	Stegodon florensis insularis	dex dP_3 frg	in situ	Liang Bua	-3.3	-3.4
Liang Bua, Flores	Arkenas	LB04-SXI-Sp40-3	Stegodon florensis insularis	milk tusk frg	in situ	Liang Bua	1.8	-4.9
Liang Bua, Flores	Arkenas	LB04-SXI-Sp41-4	Stegodon florensis insularis	dP4/M1 frg	in situ	Liang Bua	1.7	-5.1
Liang Bua, Flores	Arkenas	LB04-SXI-Sp42-6a	Stegodon florensis insularis	M2 frg	in situ	Liang Bua	3.2	-4.6
Liang Bua, Flores	Arkenas	LB04-SXI-Sp42-6b	Stegodon florensis insularis	dP_3 frg	in situ	Liang Bua	0.0	-3.4
Liang Bua, Flores	Arkenas	LB04-SXI-Sp44-7	Stegodon florensis insularis	dP_3	in situ	Liang Bua	0.3	-4.7

Liang Bua, Flores	Arkenas	LB04-SXI-Sp49-12-669g	Stegodon florensis insularis	dex M^1 frg	in situ	Liang Bua	3.2	-4.8
Liang Bua, Flores	Arkenas	LB04-SXI-Sp52-14-803a	Stegodon florensis insularis	molar frg	in situ	Liang Bua	1.6	-5.5
Liang Bua, Flores	Arkenas	LB04-SXI-Sp79-15	Stegodon florensis insularis	tusk frg	in situ	Liang Bua	-3.4	-5.5
Liang Bua, Flores	Arkenas	LB08-SXVI-Sp59-16	Stegodon florensis insularis	dP_3 frg	in situ	Liang Bua	1.6	-3.9
Liang Bua, Flores	Arkenas	LB08-SXVI-Sp64-17-3495	Stegodon florensis insularis	M1	in situ	Liang Bua	-0.6	-3.6
Liang Bua, Flores	Arkenas	LB08-SXVI-Sp70-18-3613	Stegodon florensis insularis	dP4/M1 frg	in situ	Liang Bua	0.7	-5.2
Liang Bua, Flores	Arkenas	LB08-XV-Sp57-2056B	Stegodon florensis insularis	sin dP_3	redish brown clay	Liang Bua	-0.4	-4.0
Liang Bua, Flores	Arkenas	LB04-SXI-Sp46-456	Stegodon florensis insularis	dex M_2	brown sandy clay frg limestone	Liang Bua	2.1	-2.9
Liang Bua, Flores	Arkenas	LB09-SXIX-Sp33	Stegodon florensis insularis	sin dP_3	flowstone+silt	Liang Bua	0.2	-3.3
Liang Bua, Flores	Arkenas	LB04-SXI-Sp45-449B	Stegodon florensis insularis	post. dex dP^4	in situ	Liang Bua	0.1	-3.1
Liang Bua, Flores	Arkenas	LB04-SXI-Sp45-453	Stegodon florensis insularis	dP^4 frg	in situ	Liang Bua	-0.3	-3.9
Liang Bua, Flores	Arkenas	LB04-SXI-Sp49	Stegodon florensis insularis	dP^4 frg	in situ	Liang Bua	1.7	-3.7
Liang Bua, Flores	Arkenas	LB08-SXV-Sp49	Stegodon florensis insularis	ridge frg (dP4/M1)	redish brown clay	Liang Bua	2.6	-3.7
Liang Bua, Flores	Arkenas	LB09-SXV-Sp68	Stegodon florensis insularis	dP_3 frg	redish brown clay below conglmrt I	Liang Bua	-4.4	-5.2
Liang Bua, Flores	Arkenas	LB07-SXII-Sp41	Stegodon florensis insularis	dex M^1	pale brown soil	Liang Bua	0.1	-2.9
Liang Bua, Flores	Arkenas	LB04-SXI-Sp49-669F	Stegodon florensis insularis	ant. sin. M^1 frg	humid brown clay, coarse frg,limestone pebble	Liang Bua	0.2	-3.0
Liang Bua, Flores	Arkenas	LB08-SXV-Sp55-2042A	Stegodon florensis insularis	dP^3 sin	redish brown clay	Liang Bua	1.1	-3.6
Liang Bua, Flores	Arkenas	LB04-SXI-Sp48-608	Stegodon florensis insularis	M_1 sin	in situ	Liang Bua	0.1	-4.8
Liang Bua, Flores	Arkenas	LB08-SXV-Sp65	Stegodon florensis insularis	dP^4 ridge frg	redish brown clay	Liang Bua	0.8	-4.5
Liang Bua, Flores	Arkenas	LB09-SXV-Sp62	Stegodon florensis insularis	dP_3 ridge frg	redish brown clay inside conglmrt I	Liang Bua	1.5	-3.4
Liang Bua, Flores	Arkenas	LB08-SXVI-Sp70-3631	Stegodon florensis insularis	maxilla frg with M^3	redish brown clay	Liang Bua	0.8	-3.9
Liang Bua, Flores	Arkenas	LB04-SXI-Sp47-521F	Stegodon florensis insularis	M^1 frg	in situ	Liang Bua	-0.6	-3.1
Liang Bua, Flores	Arkenas	LB04-SXI-Sp47-521F	Stegodon florensis insularis	dP^4 frg	in situ	Liang Bua	-0.0	-2.8
Klobor Makerek, Timor	MGB	ATB 06-1	Stegodon timorensis	sin M_1 frg	Raebia Exc. II, surface	Noele Fm.	1.0	-1.9
Sadi, Timor	MGB	ATB 07-11A	Stegodon timorensis	sin dP_4/M_1 frg	surface coll.	undetermined	-5.6	-3.6
Sadi, Timor	MGB	ATB 07- 11B	Stegodon timorensis	sin $dP_3/_4$ frg	surface coll.	undetermined	-6.8	-0.8
Sadi, Timor	MGB	ATB 07-12	Stegodon timorensis	sin M^3 frg	surface coll.	undetermined	0.9	-2.9
Sadi, Timor	MGB	ATB07-13	Stegodon timorensis	molar frg	surface coll.	undetermined	-3.7	-2.6
Sadi, Timor	MGB	ATB 07-14A	Stegodon timorensis	dex M^1 frg	surface coll.	undetermined	-6.7	-4.2
Ailora, Timor	MGB	ATB 07-17	Stegodon timorensis	dex M^3 frg	surface coll., most likely terrace	terrace	2.5	-3.0

Asikolo, Raebia, Timor	MGB	ATB 07-31A	Stegodon timorensis	dex M_3 frg	Taektoo Terrace in situ	terrace	1.8	-3.5
Ailora, Timor	MGB	ATB 09-2	Stegodon timorensis	sin M_3 frg	Taektoo Terrace in situ	terrace	2.3	-3.4
Ailora, Timor	MGB	ATB 09-3	Stegodon timorensis	dex M_2(?)frg	Taektoo Terrace in situ	terrace	0.8	-3.0
Ailora, Timor	MGB	ATB 09-5	Stegodon timorensis	dex M_3 frg	Taektoo Terrace in situ	terrace	-0.2	-4.5
Ailora, Timor	MGB	RB-07	Stegodon timorensis	dex maxilla frg with ant M^3	surface coll.	undetermined	3.0	-3.6
Sadi, Timor	MGB	WPT 032	Stegodon timorensis	molar and tusk frg	surface coll.	undetermined	0.9	-3.1
Lewa Paku, Sumba	MGB	Sumba	Stegodon sumbaensis	ridge frg (dP4/M1)	in situ	undetermined	-4.8	-6.0

* = Specimens that were not sampled according to the standard method along the entire height of a lamella due to the rareness of the sample. Enamel samples obtaine from small enamel fragments that were crushed.

II.2 Serial samples of the Elephas hysudrindicus M_3 from Sunggu, Java

sample no.	$\delta^{13}C$ (‰, VPDB)	$\delta^{18}O$ (‰, VPDB)	sample no.	$\delta^{13}C$ (‰, VPDB)	$\delta^{18}O$ (‰, VPDB)	sample no.	$\delta^{13}C$ (‰, VPDB)	$\delta^{18}O$ (‰, VPDB)
B-2.2	-12.9	-6.6	**B-11**	-13.3	-4.9	**B-21**	-12.8	-5.3
B-3	-12.0	-6.0	**B-12**	-13.1	-4.7	**B-22**	-12.8	-5.4
B-4	-12.4	-6.2	**B-13**	-12.8	-4.5	**B-23**	-12.2	-4.3
B-5	-12.6	-6.2	**B-14**	-12.4	-4.2	**B-24**	-12.7	-5.7
B-6	-13.1	-6.0	**B-15**	-12.8	-4.6	**B-25**	-12.5	-4.7
B-7	-12.6	-5.4	**B-16**	-13.4	-4.7	**B-26**	-12.7	-5.0
B-8	-12.8	-6.6	**B-17**	-13.1	-4.9	**B-27**	-12.5	-5.4
B-9	-13.0	-6.2	**B-18.2**	-13.2	-4.3	**B-28**	-12.3	-5.6
B-10	-12.2	-3.9	**B-19.2**	-12.9	-4.3	**B-29**	-12.8	-6.2
			B-20	-12.5	-4.2	**B-30**	-12.5	-5.6

Appendix III: Publications

The following papers have been peer-reviewed and have been included as they are presented in this thesis.

1. Brumm, et al.. 2016. Stratigraphic context and age of hominin fossils from Middle Pleistocene Flores. Nature, 534, 249-253.
2. Janssen, et al. 2016. Tooth and bone stable isotope ratios of fossil faunas reveal the glacial-interglacial paleoenvironments of hominins on Java, Indonesia. Quaternary Science Reviews, 144, 145-154.

Item 1 removed due to Copyright reasons

Quaternary Science Reviews 144 (2016) 145e154

Contents lists available at ScienceDirect

Quaternary Science Reviews

journal homepage: www.elsevier.com/locate/quascirev

Tooth enamel stable isotopes of Holocene and Pleistocene fossil fauna reveal glacial and interglacial paleoenvironments of hominins in Indonesia

Renée Janssen [a, *], Josephine C.A. Joordens [b, a], Dafne S. Koutamanis [b], Mika R. Puspaningrum [c], John de Vos [d], Jeroen H.J.L. van der Lubbe [a], John J.G. Reijmer [a], Oliver Hampe [e], Hubert B. Vonhof [a, f]

[a] Faculty of Earth and Life Sciences, VU University Amsterdam, The Netherlands
[b] Faculty of Archaeology, Leiden University, The Netherlands
[c] School of Earth and Environmental Sciences, University of Wollongong, New South Wales, Australia
[d] Naturalis Biodiversity Center, Leiden, The Netherlands
[e] Museum für Naturkunde, Leibniz-Institut für Evolutions- und Biodiversitätsforschung, Berlin, Germany
[f] Max Planck Institut für Chemie, Mainz, Germany

article info

Article history:
Received 20 August 2015
Received in revised form
19 February 2016
Accepted 29 February 2016
Available online 3 June 2016

Keywords:
Sundaland
C_3
C_4
Vegetation
Sea-level
Paleoclimate
Diet
Homo erectus
Trinil
Sangiran

abstract

The carbon ($\delta^{13}C$) and oxygen ($\delta^{18}O$) isotope compositions of fossilized animal tissues have become important proxies of paleodiet and paleoenvironment, but such stable isotope studies have not yet been extensively applied to the fossil assemblages of Sundaland (the biogeographical region comprising most of the Indonesian Archipelago). Here, we use the isotope composition of tooth enamel to investigate the diet and habitat of bovids, cervids, and suids from several Holocene and Pleistocene sites on Java and Sumatra. Our carbon isotope results indicate that individual sites are strongly dominated by either C_3-browsers or C_4-grazers. Herbivores from the Padang Highlands (Sumatra) and Hoekgrot (Java) cave faunas were mainly C_3-browsers, while herbivores from Homo erectus-bearing sites Trinil and Sangiran (Java) utilized an almost exclusive C_4 diet. The suids from all sites show a wide range of $\delta^{13}C$ values, corroborating their omnivorous diet. For the dataset as a whole, oxygen and carbon isotope values are positively correlated. This suggests that isotopic enrichment of rainwater and vegetation $\delta^{18}O$ values coincides with an increase of C_4-grasslands. We interpret this pattern to mainly reflect the environmental contrast between glacial (drier, more C_4) and interglacial (wetter, more C_3) conditions. Intermediate herbivore $\delta^{13}C$ values indicating mixed C_3/C_4 feeding is relatively rare, which we believe to reflect the abruptness of the transition between glacial and interglacial precipitation regimes in Sundaland. For seven Homo erectus bone samples we were not able distinguish between diagenetic overprint and original isotope values, underlining the need to apply this isotopic approach to Homo erectus tooth enamel instead of bone. Importantly, our present results on herbivore and omnivore faunas provide the isotopic framework that will allow interpretation of such Homo erectus enamel isotope data.

1. Introduction

Sundaland, a biogeographical region comprising Malaysia and the western part of Indonesia, is a well-studied biodiversity hotspot (e.g. Myers et al., 2000; den Tex et al., 2010; Lim et al., 2010). To a large extent, climate controls biodiversity dynamics in this region (Woodruff, 2010). Glacial-interglacial cycles generate eustatic sea-level fluctuations, periodically turning the western islands of the Indonesian Archipelago into mountain ranges on the sub-aerially exposed Sunda Shelf (Hutchison, 1989; Voris, 2000, Fig. 1). The recurring land connection and greater extent of more open vegetation during glacial periods enabled repeated biotic migrations from mainland Asia into Sundaland. Subsequent isolation during interglacial periods encouraged genetic divergence and speciation of these faunas (von Koenigswald, 1935; Hanebuth et al., 2011; Slik

* Corresponding author.
E-mail address: r2.janssen@vu.nl (R. Janssen).

http://dx.doi.org/10.1016/j.quascirev.2016.02.028
0277-3791/

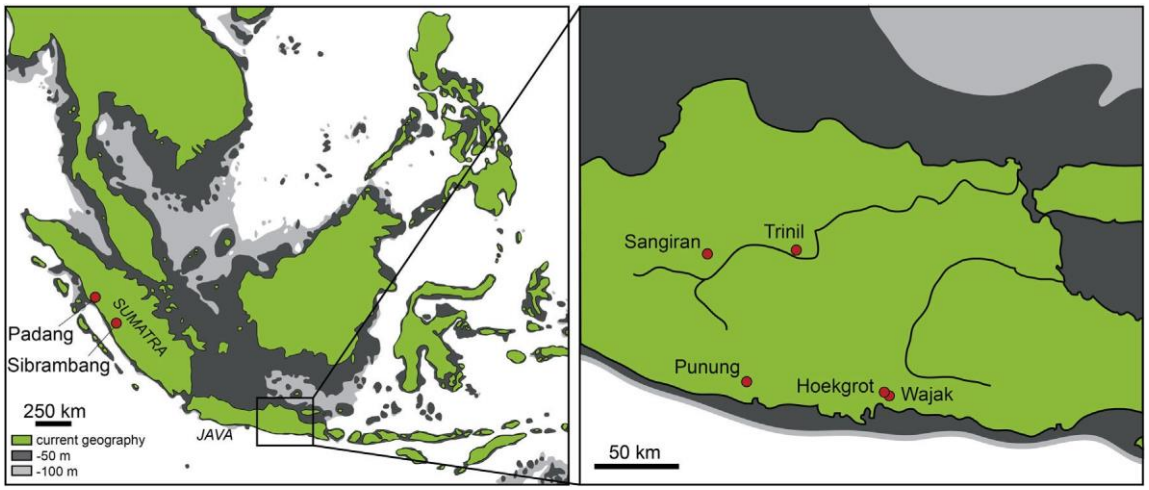

Fig. 1. Map of Sundaland (left) and central Java (right), adapted from Voris (2000) and Sathiamurthy and Voris (2006), showing the extent of the Sunda plains sub-aerially exposed during glacial periods when the sea drops to respectively −50 and −100 m below its current level. The red dots indicate locations from which material sampled in this study originates, see Table 1.

et al., 2011; Leonard et al., 2015).

A long history of paleontological research in the Indonesian Archipelago has captured the resulting biodiversity changes in rich and well-documented faunal collections (e.g. Van den Bergh et al., 2001). Arguably among the most iconic discoveries are specimens of the hominin Homo erectus found at Trinil, Sangiran, and several other locations on Java (e.g. Dubois, 1894, 1896; Sartono, 1968, 1971; Kaifu et al., 2005a,b; Huffman et al., 2006; Kaifu, 2006; Indriati and Antǒn, 2008; Huffman et al., 2010; Zaim et al., 2011; Antǒn, 2013). Altogether the Indonesian fossil collections contain a wealth of Pleistocene and Holocene terrestrial faunas, with taxonomic compositions suggesting diverse paleohabitat conditions.

In this study, we aim to further expand our knowledge of available resources and ecological niches in Sundaland paleohabitats, and examine what this reveals about the climatic background of these environments inhabited by early humans. To achieve this we use carbon and oxygen isotope ratios in tooth enamel of seven Sundaland fossil fauna sites as a proxy for paleodiet and paleoecology of the faunas under study. This is the first time that such an extensive isotopic approach is applied to fossil faunas from Sundaland sites.

2. Background

The carbon isotopic composition ($\delta^{13}C$) in mammalian bones and teeth records dietary $\delta^{13}C$ values, with a fixed fractionation factor of ~13‰ for the tooth enamel of most large mammalian herbivores (Lee-Thorp et al., 1989; Passey et al., 2005) and ~14.1‰ for the tooth enamel of ungulates (hoofed animals) in particular (Cerling and Harris, 1999). For enamel there is limited, if any $\delta^{13}C$ fractionation as one moves to the carnivores higher up the food chain (Lee-Thorp and Sponheimer, 2006). The $\delta^{13}C$ of animal tissue thus ultimately records the $\delta^{13}C$ value of the vegetation at the base of the food chain (DeNiro and Epstein, 1978). Trees and shrubs utilize the C_3 photosynthetic pathway, whereas many tropical grasses and sedges are C_4-type photosynthesizers (Calvin and Bassham, 1962; Hatch and Slack, 1966). The $\delta^{13}C$ ranges of C_3 plants and C_4 grasses differ by on average ~14‰ and do not overlap (Smith and Epstein, 1971; Cerling et al., 1997). The $\delta^{13}C$ values of C_3 plants are considerably influenced by environmental factors: water stress results in higher $\delta^{13}C$ values (Ehleringer and Cooper, 1988; Farquhar et al., 1989; Stewart et al., 1995; Abram et al., 2009; Kohn, 2010), whereas a closed canopy environment shifts $\delta^{13}C$ to very low values (Medina and Minchin, 1980; van der Merwe and Medina, 1991; Cerling et al., 1997; Kohn, 2010). More positive $\delta^{13}C$ values in vegetation and animal tissues can thus be taken to indicate a habitat with more open vegetation. For this reason, tooth enamel $\delta^{13}C$ has become an increasingly important paleodietary and paleoenvironmental proxy in southern and eastern African paleoanthropological studies (Lee-Thorp et al., 1994; Sponheimer et al., 2003; Sponheimer and Lee-Thorp, 2006; Levin et al., 2008; Cerling et al., 2013, 2015).

Previous studies suggest that the cycling between colder and drier glacials and warmer and more humid interglacials affect the relative abundance of open habitats on Sundaland. For instance, leaf wax records from Sulawesi in central Indonesia record a shift to more positive $\delta^{13}C$ values during the Last Glacial Maximum (LGM), an indication of an increasingly open habitat and possibly an increase in C_4 grasses (Russell et al., 2014; Wicaksono et al., 2015). Palynological evidence from Java indicates an increase of open swamp vegetation and grasslands in this time period (van der Kaars and Dam, 1997; van der Kaars et al., 2000). Leaf wax and palynological records from northwestern Sumatra do not show this LGM-Holocene vegetation contrast, which is likely due to the fact that this particular area remains relatively wet during glacial periods (Maloney, 1980; Morley, 1982; Newsome and Flenley, 1988; Niedermeyer et al., 2014). Paleoclimate simulations suggest that tropical rainforests in other parts of Sumatra and the adjacent shelf were significantly reduced during the LGM, with the glacial increase in open vegetation and C_4 grasses taking place in a geographically delimited 'savanna corridor' (Bird et al., 2005; Cannon et al., 2009). Overall the available data suggest that, although local microclimatic effects deserve careful consideration, the larger part of the region comprising Java, Sumatra and Sulawesi experiences significant vegetation changes during glacial interglacial transitions.

The oxygen isotopic composition ($\delta^{18}O$) in animal tissue is largely determined by $\delta^{18}O$ values in food and drinking water (Longinelli, 1984; Luz and Kolodny, 1989), which are in turn dependent on ecological, climatic and geographical factors (Craig, 1961; Dansgaard, 1964). The $\delta^{18}O$ value of rainwater decreases with increasing distance from the moisture source, increasing altitude, decreasing temperature, and high intensity precipitation (Dansgaard, 1964). Arid conditions enrich leaf water and surface

water $d^{18}O$ values due to greater evaporation (Gonfiantini et al., 1965). And under similar conditions, C_4 plants have higher $d^{18}O$ values than C_3 plants (Sternberg, 1989; Helliker and Ehleringer, 2000). Fossil bone and teeth $d^{18}O$ values are thus controlled by a complex interplay of environmental parameters, but its interpretation is commonly generalized as a proxy for aridity (e.g. Longinelli, 1984; Koch et al., 1989; Fricke et al., 1998; Stanton Thomas and Carlson, 2004; Levin et al., 2006; Bernard et al., 2009).

For Sundaland, flooding of the Sunda Shelf in the late glacial to Holocene transition shifted the moisture source and intensified summer monsoon rainfall. Together with the increase in local sea surface temperatures and the decrease in ocean water $d^{18}O$, this resulted in a ~1.5e2.0‰ drop in precipitation $d^{18}O$ values on Flores, as is documented in speleothem records by Griffiths et al. (2009, 2010, 2013) and Westaway et al. (2007a). Conversely, in glacial periods we can expect decreased rainfall, at relatively high $d^{18}O$ values. The related glacial-interglacial shift in the abundance of C_4 vegetation may further exacerbate this $d^{18}O$ contrast.

3. Material and methods

For this study, we sampled tooth and bone material from seven Holocene and late Pleistocene fossil fauna sites on Java and Sumatra (Table 1; see Appendix A for full sample list).

The analyzed specimens include 46 bovids, 27 cervids, and 28 suids from the Dubois Collection and the Von Koenigswald Collection curated at the Naturalis Biodiversity Center (Leiden, The Netherlands) and 9 bovids, 5 cervids, and one tiger (Panthera tigris) from the Selenka collection at the Museum für Naturkunde (Berlin, Germany). The Trinil samples (except the tiger tooth fragment) from the Selenka Collection all feature the original Selenka field book number, showing that they derive from excavated layers at Trinil which to the best of our present knowledge are the equivalent of the Trinil HK as excavated by Dubois (Selenka, 1906e1907; Selenka and Blanckenhorn, 1911; Paul Albers, pers. comm.). The tiger tooth fragment derives from a jawbone that has the chocolate brown color and heavy fossilization typical of the Trinil HK.

For the stable isotope analyses we targeted tooth enamel, as it is less susceptible to diagenetic alteration than dentin or bone (Kolodny and Raab, 1988; Wang and Cerling, 1994; Picard et al., 1998; Sharp et al., 2000; Lécuyer et al., 2003; Pucéat et al., 2003; Stanton Thomas and Carlson, 2004). As post-depositional alteration is most commonly present as overgrowth of diagenetic carbonate, we mechanically removed a thin top layer of enamel, and specifically sampled from areas of intact enamel that showed no conspicuous cracks or signs of overgrowth. Sampling was done using a handheld dentist drill with a diamond coated drill bit, which was carefully cleaned between samples. The majority of specimens was subjected to growth-incremental sampling, obtaining two or three samples over the full growth range from near the root to the top of the crown. A subset of enamel samples from all sites was leached with 2e3% NaOCl and 1 M acetic-Ca acetate buffer (Bocherens et al., 1996) to detect possible diagenetic offsets comparing isotope values to untreated samples.

In addition, we analyzed available powdered bone samples from 6 Homo erectus specimens from Sangiran, originally prepared for bone fluorine analysis (Bergman and Karsten, 1952), and a fragment of bone belonging to Trinil Femur III originally used for SEM analysis by Day and Molleson (1973) (see Table 2). Splits were made of all Homo erectus bone samples. One split was left untreated, the other split was leached with 2e3% NaOCl and 1 M acetic-Ca acetate buffer to remove contingent organic matter and exogenous carbonate before isotope analysis (Bocherens et al., 1996).

To measure stable isotope ratios, sample powders of ~0.3 mg were placed in exetainer vials and flushed with pure helium (5.0) gas. At a constant temperature of 45 °C, 100% anhydrous orthophosphoric acid (H_3PO_4) was added and sample powders were left to dissolve for 24 h. Subsequently, the liberated CO_2 gas was analyzed using a Thermo Finnigan GasBench II preparation device interfaced with a Thermo Finnigan Delta Plus mass spectrometer. Standard procedure involves the analysis of a total of 20 aliquots of two different calcite lab standard (normalized to international reference materials NBS 18, NBS 19 and NBS 20) per series of 60 samples. These standards are subjected to the same digestion procedure as the samples. The 10 aliquots of one of these standards serve to correct for sample size fractionation effects common to continuous-flow mass spectrometry, and the 10 aliquots of the other standard, subsequently quantify the precision and accuracy of the corrected isotope data. Reproducibility of lab standards after sample size correction typically is better than 0.10‰ for $d^{13}C$ and 0.15‰ for $d^{18}O$ (1s). We have not corrected for possible fractionation factor differences between pure calcite (our standards) and structural carbonate (our samples). All $d^{13}C$ and $d^{18}O$ data are reported relative to the Vienna-Peedee Belemnite (V-PDB) standard.

To assess potential diagenetic alteration, we thin-sectioned several specimens for analysis with a transmitted light microscope and a cathodoluminescence microscope (~20 kV, 400-mA). We also examined fresh fractures and polished sections of tooth and bone samples by scanning electron microscopy (SEM). The SEM specimens were etched for 2e5 s with 34% (v/v) phosphoric acid, sputter-coated with gold-palladium, and viewed with JEOL JSM 6301F and JEOL NeoScope JCM-6000 scanning electron microscopes.

4. Preservation of stable isotope values in tooth enamel

Macroscopic inspection of the outer surface of the teeth selected for sampling showed no clear signs of dissolution or extensive overgrowth. Thin sections of a Trinil, Sangiran and Wajak tooth showed no signs of bacterial invasion or secondary mineral ingrowth in dentin or enamel, and only minimal cracking of the enamel (Appendix B, Fig. B1). Scanning electron microscopy (SEM)

Table 1
Age and setting for the sampled sites. Padang refers to one or several unknown caves in the Padang Highlands on Sumatra. The Trinil samples derive from the hominin-bearing Hauptknochenschicht (HK) excavated by E. Dubois and nearby excavations by M.L. Selenka. The exact stratigraphic origin of the Early Pleistocene Sangiran specimens analyzed in this study is uncertain.

Site	Age estimate	Setting
Hoekgrot, Java	around ~2.6, 3.3 ka (Shutler et al., 2004)	Cave
Wajak, Java	around ~6.5, 10.6 ka (Shutler et al., 2004) min. 28.5e37.4 ka (Storm et al., 2013)	Cave
Punung, Java	min. 118 ± 3 ka and max. 128 ± 15 ka (Westaway et al., 2007b)	Cave
Padang, Sumatra	~115e158 ka, based on correlation with Punung (De Vos, 1983)	Cave
Sibrambang, Sumatra	~115e158 ka, based on correlation with Punung (De Vos, 1983)	Cave
Trinil, Java	min. 0.43 ± 0.05 Ma and max. 0.54 ± 0.1 Ma (Joordens et al., 2015)	Open air
Sangiran, Java	between <1.51 and 0.8 Ma (Larick et al., 2001; Hyodo et al., 2011)	Open air

Table 2
Homo erectus specimens analyzed in this study, with their original sample names and nomenclature. Formation (Fm) of origin according to von Koenigswald (1940); Day (1986).

Specimen	Bone type	Sample material	Origin
Femur III (Trinil 7)	femur	fragment	Trinil HK
Sangiran 1b ('Pithecanthropus B')	mandible	powdered	surface find Bapang or Sangiran Fm., Sangiran
Sangiran 2 ('Pithecanthropus II')	cranium	powdered	surface find Bapang or Sangiran Fm., Sangiran
Sangiran 3 ('Pithecantropus III')	cranium	powdered	surface find Bapang Fm., Sangiran
Sangiran 4 ('Pithecanthropus IV')	cranium	powdered	surface find Sangiran Fm., Sangiran
Sangiran 5 ('Pithecanthropus dubius')	mandible	powdered	surface find Sangiran Fm., Sangiran
Sangiran 6a ('Meganthropus A')	mandible	powdered	surface find Sangiran Fm., Sangiran

inspection showed the parallel prismatic structure typical of mammalian enamel to be intact in all three teeth (Appendix B, Fig. B2). We observed no obvious difference in structural preservation between the outer margin of the enamel and the deeper layers. Areas of discoloration in the enamel were not correlated with poor structural preservation. Cathodoluminescence examination showed the dentin in these teeth to be luminescent, likely indicating substitution of elements in the calcium sites of the crystal lattice (Mariano, 1988; Mason and Mariano, 1990). In contrast, the enamel (including the outer margin) is non-luminescent, suggesting minimal alteration.

Fig. 2 shows the isotope composition for a selection of untreated versus pre-leached enamel samples (pre-leached samples are represented by diamonds). The observed differences are small when compared to the total range of isotope values; generally 1e2‰ for $\delta^{13}C$ and 1‰ for $\delta^{18}O$ versus a total range of 21‰ for $\delta^{13}C$ and 10‰ for $\delta^{18}O$ (Fig. 3). For the Hoekgrot and Punung samples, the offset is <1.0‰ for $\delta^{13}C$ and $\delta^{18}O$. The majority of untreated Wajak, Padang, and Sangiran samples show an offset up to several permille towards intermediate $\delta^{13}C$ and $\delta^{18}O$ values when compared to leached samples, although not all samples from these sites conform to this pattern. These results suggest that some amount of diagenetic alteration on Wajak, Padang, and Sangiran enamel specimens may be present, although not sufficiently large to compromise paleodietary and paleoenvironmental interpretations made on the basis of these data. For Trinil and Sibrambang the offsets are non-systematic. Since treatment intended to remove organic matter and exogenous carbonate potentially induces unintended chemical artefacts and isotopic fractionation in the original compounds (Koch et al., 1997; Lee-Thorp, 2002), it is not evident that the leached Trinil and Sibrambang sample splits give a better representation of the original isotope values than the untreated splits. Given the documented good preservation of the tooth material understudy, and the risk of introducing isotopic artefacts due to pre-treatment, we prefer to base our interpretations in this study primarily on isotope data from untreated tooth enamel.

5. Stable isotope patterns in well-preserved tooth enamel from Sundaland

Bovid, cervid and suid tooth enamel isotope data are provided in Appendix A, and given in Fig. 3 as cross plots with incremental samples averaged per specimen. The range of more than 20‰ in $\delta^{13}C$ values covers the entire spectrum from pure C_3 feeders to pure C_4 feeders. Carbon isotope values of growth-incremental intra-tooth samples span an average range of only 1.2‰, indicating that seasonal variability is not an important contributor to the broad $\delta^{13}C$ range observed.

The herbivore $\delta^{13}C$ values of most sites cluster around values indicative of either C_3-dominated or C_4-dominated values, with few specimens showing intermediate values. The suid $\delta^{13}C$ values lack this strong C_3 versus C_4 differentiation. Pigs are omnivores with a flexible feeding strategy, which may comprise C_3 and C_4 vegetation as well as some animal foods from terrestrial (or even aquatic) ecosystems (e.g. Leister, 1939; Kurtén, 1968; Harris and Cerling, 2002). In our dataset, we see that where the herbivores tend to be selective, the opportunistic suids demonstrate the full isotopic spectrum of available resources in any given habitat. Thus, the omnivorous feeding strategy of suids makes their enamel stable isotope composition less suitable than that of the herbivores for use as a proxy for changes in the C_3 versus C_4 vegetation balance.

There is a strong positive correlation between $\delta^{13}C$ and $\delta^{18}O$ in the herbivore dataset, $r(100) = 0.65$, $p < 0.001$. This observation fits our expectation that drier climates correlate with a greater availability of C_4 plants, and may thus suggest good preservation of both $\delta^{13}C$ and $\delta^{18}O$ values, suitable for robust interpretation of environmental change.

5.1. Hoekgrot

Our dataset for the Holocene Hoekgrot site comprises two bovids (Bos javanicus, or banteng) and two suids. The carbon isotope values for these specimens indicate open canopy C_3 vegetation as a likely primary food source. It must be noted that these isotope values do not exclude the possibility that these animals utilized

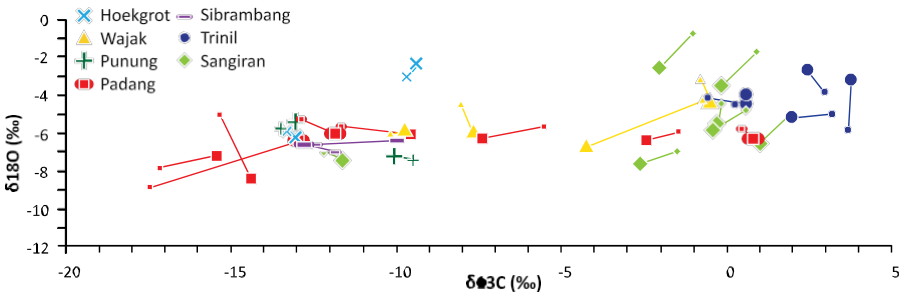

Fig. 2. Cross plot of $\delta^{13}C$ and $\delta^{18}O$ values of leached versus untreated specimens. Large symbols denote untreated samples; small symbols indicate corresponding samples treated with the pre-leaching method described in Bocherens et al. (1996).

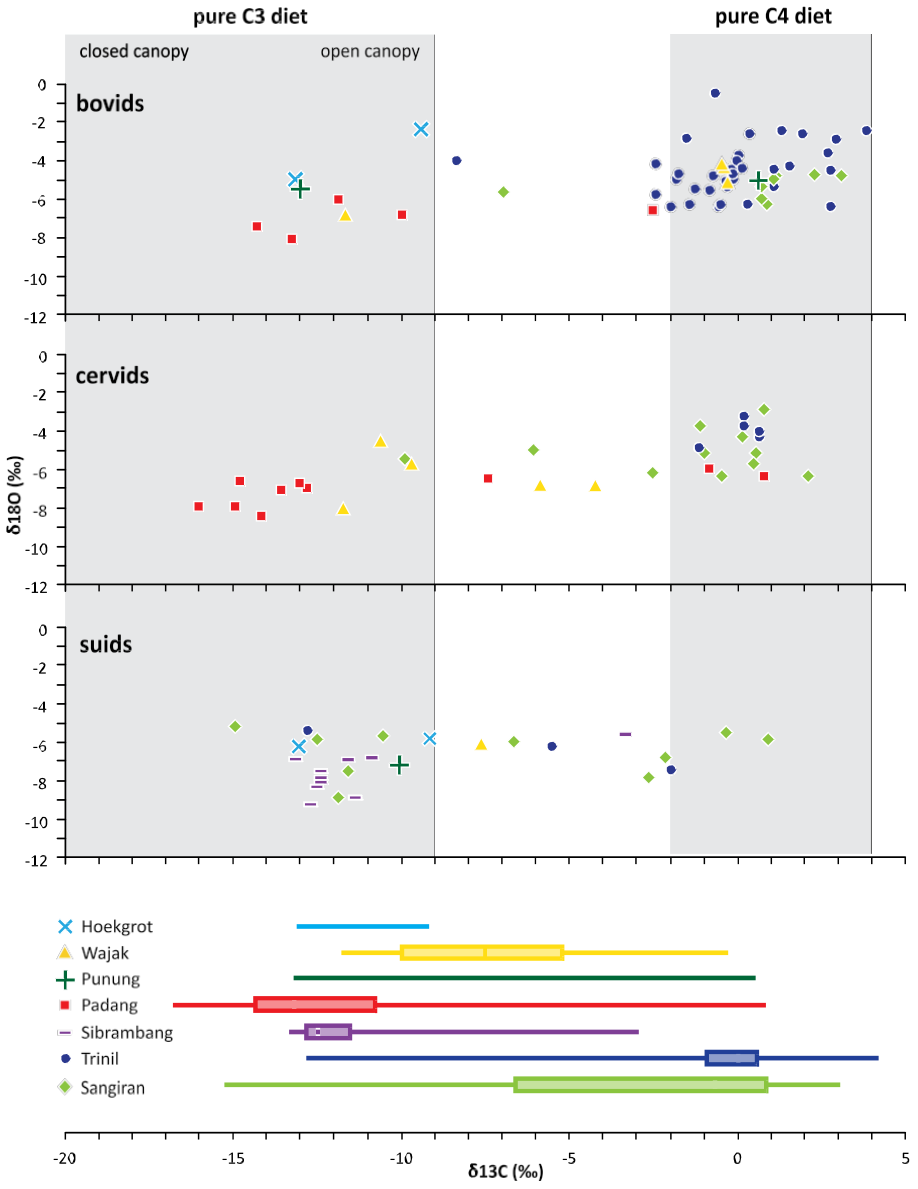

Fig. 3. Cross plot of $d^{13}C$ and $d^{18}O$ values of enamel from bovids, cervids and suids. All values are of untreated samples. Serial intra-tooth samples averaged per specimen (see Appendix A). Grey areas denote approximate $d^{13}C$ ranges of tooth enamel from ungulates with a pure C_3 or C_4 diet (Cerling et al., 1997; Cerling et al., 2004; Kohn, 2010). Boxplots show the distribution of the total data set in quartiles, with whiskers representing total range.

vegetation over a somewhat broader $d^{13}C$ range, the lowest values derived from closed forest understory plants and the highest values from C_4 vegetation or water-stressed C_3 vegetation.

Observations of extant fauna show that B. javanicus does browse in the forest under certain circumstances (consuming considerable amounts of leaves, woody tissue, fruit and bamboo, a C_3 grass), but generally prefers open terrain grazing (Hoogerwerf, 1970; Muntasib, 2000; Timmins et al., 2008). Although the dataset is limited, we take this to suggest that C_4 grasslands were too scarce to form a primary dietary component for the Hoekgrot Bos javanicus population.

5.2. Wajak

Dating results indicate an MIS 3 glacial (Storm et al., 2013) or a Holocene interglacial (Shutler et al., 2004) provenance for Wajak, suggesting the possibility of a mix of both glacial and interglacial Wajak specimens in the collection. The Wajak bovids (Bos javanicus) are either specialized C_3 browsers or C_4 grazers, an apparent intra-species niche segregation that may indeed be the result of their origin in two distinct habitats differing strongly in the availability of C_4 vegetation. The $d^{13}C$ values for some of the analyzed cervids (two Muntiacus muntjak specimens and three cervids not determined to a species level) are among the relatively few intermediate values. They indicate a mixed C_3–C_4 diet and possibly a pure C_3 open canopy diet for the lowest values, similar to the modern adaptable diet of both species (Kitchener, 1990; Oka, 2000). The suid specimen also reflects a diet based on a combination of C_3 and C_4 food sources.

5.3. Punung

Dating of the Punung fauna (between 128 ± 15 and 118 ± 3 kyr old; Westaway et al., 2007b) places it close to the MIS 6 e MIS 5

glacial-interglacial transition (Lisiecki and Raymo, 2005). Based on the presence of rainforest-dependent species, it is thought to originate from MIS 5 (De Vos, 1983). Three specimens were available to us from Punung, none of which have been identified to species level. Two bovid specimens have $\delta^{13}C$ values of −13.1‰ and 0.6‰ $\delta^{13}C$, revealing a strong C_3eC_4 contrast. The bovid with the high $\delta^{13}C$ value suggests the availability of enough C_4 grassland to provide for an exclusive reliance on this food source, which seems unlikely under full rainforest conditions. The suid $\delta^{13}C$ value (−10.1‰) reflects a mainly C_3-based diet, but is >5‰ higher than we would expect for a diet obtained purely in a closed-canopy rainforest setting. Although the few data do not allow firm conclusions to be drawn, these isotope data raise the hypothesis that the Punung fauna represents different climate states, and may potentially include specimens of glacial (MIS 6?) origin.

5.4. Padang and Sibrambang

Based on taxonomic correlation with the Punung Fauna, the Padang Highlands cave faunas of Sumatra are assumed to originate from the MIS 5 interglacial. However, none of the cave faunas are independently dated. The Padang bovids and cervids in this study (not determined to species level) have an average $\delta^{13}C$ value of −11.4 ± 4.9‰ $\delta^{13}C$ (n ¼ 15). The majority of these herbivores utilized a diet primarily composed of C_3 vegetation. Some of the Padang cervids exhibit the lowest $\delta^{13}C$ values in this study, which suggests the presence of closed-canopy conditions. This indeed fits well with Padang faunas as representing a rainforest environment. Of the total of 15 samples, three Padang herbivores testify of a C_4-dominated diet, suggesting grasslands may have been available at some point. The suid (Sus sp.) tooth samples from the Sibrambang assemblage (−11.6 ± 2.4‰ $\delta^{13}C$, n ¼ 11) are C_3-dominated with one outlier indicating considerable C_4-consumption. As records from the LGM show that glacial conditions do not necessarily promote open habitats in the Padang Highlands themselves (Niedermeyer et al., 2014) the influence of C_4 vegetation in faunas from this area may point towards presence of grasslands within migration distance.

5.5. Trinil

The specimens from the Pleistocene site Trinil originate from the Hauptknochenschicht (HK; main bone layer). Joordens et al. (2015) recently refined the age framework of this site by dating undisturbed sediments preserved in fossil bivalve shells from Trinil HK and determined a minimum age of 0.43 ± 0.05 Ma and a maximum age of 0.54 ± 0.1 Ma. The bovid specimens analyzed in this study include Bubalus palaeokerabau, Duboisia santeng, and specimens not determined to species level, and their $\delta^{13}C$ values form a tight cluster (average $\delta^{13}C$: 0.2 ± 1.5‰, n ¼ 24) in the range indicating a pure C_4 diet. The exception is one conspicuous outlying B. palaeokerabau specimen (S782, with a $\delta^{13}C$ value of −8.4‰) which represents a C_3eC_4 mixed diet. We note, however, that the tooth enamel of this specimen has a grey-white color atypical for Trinil HK specimens, which may suggest diagenetic alteration or indicate that this concerns a misplaced specimen. Based on macroscopic inspection of the outer surface we have no direct reason to suspect poor preservation, but the divergent appearance is reason to doubt the origin of this specimen. The cervids (Axis lydekkeri) fall in the same isotope range as the bovids, exclusively relying on C_4 grasses. The broader spread of Sus brachygnathus well into the C_3 range indicates that this vegetation type is available in the region, or that the pig exploited animal resources with low $\delta^{13}C$ values. The only carnivore analyzed in this study, the Trinil Panthera tigris has isotope values of −5.6‰ $\delta^{13}C$ and −6.6‰ $\delta^{18}O$, reflecting a food chain with a mixed C_3/C_4 base.

With an average $\delta^{13}C$ value of −0.2 ± 2.6‰ (n ¼ 43) this site is clearly C_4-dominated. The classification of the Trinil paleoenvironment as open with possibly some trees (De Vos et al., 1982; De Vos, 1995; Louys and Meijaard, 2010) is in good agreement with our isotope results. It is not surprising to find the large water buffalo B. palaeokerabau grazing C_4 plants in these circumstances, and although cervids like Axis lydekkeri are often adaptable mixed feeders (Kitchener, 1990; Oka, 2000), they here appear to be grazers by preference. It is interesting to note that the isotope characterization of the three Duboisia santeng specimens as pure C_4 grazers (−0.3e0.4‰ $\delta^{13}C$) is in direct contrast to mesowear analyses performed on Trinil HK D. santeng specimens by Rozzi et al. (2013), who conclude that this small bovid was a forest dwelling browser which only occasionally included abrasive vegetation in its diet.

The consistent C_4-dominated isotope signal supports the view that the Trinil specimens in the Dubois and Selenka collections were excavated from a relatively narrow stratigraphical interval - representing a dry, glacial climate state - without admixture of material from strata with a contrasting climatic background. This may suggest that the origin of the Trinil specimens lies in (glacial) MIS 12, 14 or 16 (Lisiecki and Raymo, 2005).

5.6. Sangiran

The Sangiran specimens originate from a stratigraphic sequence that may span over several hundred thousand years, rather than a narrow stratigraphic and temporal interval. It is uncertain if they derive from the Sangiran Formation, the younger Bapang Formation, or be of mixed origin. Larick et al. (2001) established a $^{40}Ar/^{39}Ar$ age of 1.51 ± 0.08 Ma for the Bapang/Sangiran Formation contact, and 1.02 ± 0.06 Ma at the Upper Tuff layer above the hominin-bearing sequence. Through magnetostratigraphic correlation of a section of the Upper Tuff, Hyodo et al. (2011) places the uppermost age limit for this sequence at 776 ± 2 ka.

The Sangiran herbivores carry a C_4-dominated signal (average $\delta^{13}C$: −2.9 ± 5.1‰, n ¼ 30). All bovids are B. palaeokerabau showing a strong C_4 grazing signal, with the exception of one specimen giving a C_3eC_4 mixed signal. The pattern is similar for the cervids (not determined to species level). Suid $\delta^{13}C$ values fall into two clusters, one being strongly C_3-dominated and one strongly C_4-dominated. Suid carbon isotope values as low as −14.2‰ may suggest that closed-canopy C_3 vegetation was present at some time in the Sangiran sequence.

6. Linking vegetation balance to climatic background

While the total range of $\delta^{13}C$ values in all examined sites spans the entire C_3eC_4 spectrum, most individual sites are strongly dominated by either C_3 or C_4 vegetation. For Java, palynological and leaf wax data show that temporal variation in C_3 versus C_4 vegetation balance is linked to glacial-interglacial climate change (van der Kaars and Dam, 1997; van der Kaars et al., 2000; Niedermeyer et al., 2014; Russell et al., 2014; Wicaksono et al., 2015). The combination of a dominant C_4 signal and relatively high $\delta^{18}O$ values in the herbivore tooth enamel from a given site on Java thus corresponds to cold, dry glacial conditions. In contrast, warmer, humid interglacials result in a C_3-dominated signal and relatively low $\delta^{18}O$ values. The vegetation balance in the Padang Highlands of Sumatra is different, because it may be C_3-dominated even during glacials (Maloney, 1980; Morley, 1982; Newsome and Flenley, 1988; Bird et al., 2005; Cannon et al., 2009; Niedermeyer et al., 2014). Our specimens from this area mainly testify to pure C_3 diets, but several outliers show that a significant amount of C_4 grassland was available at some time interval.

Species-specific feeding strategies do not explain the strong C_3eC_4 differentiation in the herbivore $\delta^{13}C$ values, as we also see this variability within species and more generally within the cervids, generally considered to be adaptive and often mixed-vegetation feeders (Kitchener, 1990; Oka, 2000). Carbon isotope values of modern and fossil herbivores from South and East Africa do not show such strong clustering; instead, mixed C_3eC_4 feeding is commonly observed there (e.g. Cerling et al., 2003; Sponheimer et al., 2003; Bedaso et al., 2013). We hypothesize that the observed $\delta^{13}C$ clustering is closely tied to the unique climatic threshold conditions in Sundaland. The rapid flooding and emergence of the Sunda Shelf immediately impacts the precipitation regime (Griffiths et al., 2013), acting as a threshold amplifier for the transitions between glacial and interglacial climate states. This is reflected in the abruptness of the corresponding changeover in the vegetation balance, and ultimately expressed in the relative absence of intermediate $\delta^{13}C$ values in herbivore enamel as we observe in this extensive dataset.

7. Stable isotope values in Homo erectus bone

Tooth material of Sundaland hominins was not available to us, but we did have access to bone samples of seven Homo erectus bones from Sangiran and Trinil (Table 2). Since bone is generally more susceptible to post depositional alteration, careful diagenetic screening is a necessity when attempting to produce meaningful bone stable isotope data.

The sampled bone fragment from Trinil Femur III has been previously subjected to SEM inspection by Day and Molleson (1973), along with Trinil Femur I and VI. They concluded that these bones are well mineralized and well preserved, with "mature osteons and bony lacunae comparable to those of normal mammalian bone" and preserved collagen bundles indicating rapid mineralization. Our own SEM observations on a fresh fracture of the fragment corroborate these finds (Appendix B, Fig. B2) although we found that the Haversian canals are sometimes infilled by secondary minerals (calcite). As an analog we examined a Trinil HK bovid bone (specimen DUB782, Appendix B, Fig. B), in which well-preserved individual osteons and even osteocytes are observed, with relatively few microfissures. Cracks and part of the Haversian canals in this bone have also been partially filled with calcite. When examined under a cathodoluminescence microscope, homogeneous orange luminescence was observed in both the Trinil Femur III fragment and the Trinil bovid bone, possibly indicating a certain extent of element substitution (Mariano, 1988; Mason and Mariano, 1990).

When we next compared Trinil bovid tooth enamel to bovid bone from that assemblage (the enamel and bone samples taken from different specimens), we found that the $\delta^{13}C$ and $\delta^{18}O$ values of the bone samples are systematically lower than the enamel samples by on average 6.9‰ and 2.3‰, respectively (Appendix A, Fig. 4). Little is known about the possible in vivo bone-enamel isotope offset in hominins, but studies on modern suids and archaeological humans (Warinner and Tuross, 2009; Webb et al., 2014) lead us to surmise that the large offset we observe in Trinil bovids is unlikely to be explained by in vivo fractionation alone. We infer that although bone material from Trinil is structurally well preserved, its carbon and oxygen isotope compositions are likely to be diagenetically overprinted. The isotope composition of calcite infill found in Trinil bovid bone DUB782 (−12.0‰ $\delta^{13}C$, −7.1‰ $\delta^{18}O$; see Fig. 4) supports the notion that diagenetic alteration would lead to a decrease of carbon isotope values in Trinil specimens. However, since pre-leached bone samples (diamonds in Fig. 5) do not show a systematic offset towards higher $\delta^{13}C$ values, such an inferred diagenetic overprint appears not to be removed by pre-treatment.

The carbon isotope values of the untreated and pre-leached splits Trinil Femur III specimen itself both fall within the cluster of Trinil bovid bone isotope values, which is significantly offset from the isotope data of well preserved Trinil bovid enamel. We take this to indicate a significant diagenetic offset to lower $\delta^{13}C$ values for bone material from the Trinil HK layer. Given the evidence for a diagenetic shift to lower $\delta^{13}C$ values in Trinil HK, we tentatively hypothesize that the measured $\delta^{13}C$ value for Femur III can be taken as a minimum for the original in vivo value.

The Sangiran Homo erectus specimens came to us in powdered form, and we were thus unable to perform extensive diagenetic tests on these samples. For the untreated splits of Sangiran 1b, Sangiran 4 and Sangiran 5 we did observe a high signal intensity to sample weight ratio during stable isotope analysis, possibly indicating the presence of a considerable amount of exogenous carbonate. The average isotope values for the untreated sample splits are -5.6 ± 3.6‰ $\delta^{13}C$ and -6.2 ± 0.6‰ $\delta^{18}O$, with Sangiran 5 being a low-$\delta^{13}C$ outlier. Pre-leaching experiments resulted in unsystematic isotopic shifts, on average 0.9‰ for $\delta^{13}C$ and 0.6‰ for $\delta^{18}O$, which we take to indicate that also for the Sangiran bone samples such pretreatment does not appear to remove a clear diagenetic overprint. In the absence of independent evidence for the direction of possible diagenetic isotopic overprints for Sangiran material we are not able to make any projections of the original isotope signal of the Sangiran specimens analyzed.

In conclusion, we surmise diagenetic processes to have altered the carbon and oxygen isotopic composition of the Homo erectus bone samples in our study, and are currently not able to remove such diagenetic overprints. As a result we cannot reliably reconstruct the in vivo isotope values for the analyzed Homo erectus bones other than suggesting that the original carbon isotope ratios of the Trinil Femur III specimen have likely been higher than the values measured here. Our results underline the need to apply the isotopic approach to Homo erectus enamel instead of bone, as successfully pioneered in African hominins (e.g. van der Merwe et al., 2008; Cerling et al., 2013).

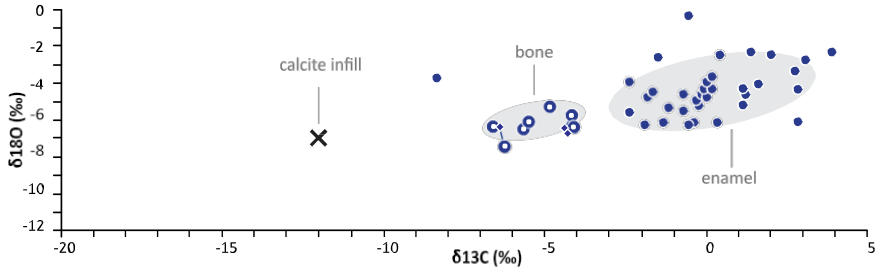

Fig. 4. Cross plot of $\delta^{13}C$ and $\delta^{18}O$ values of untreated Trinil bovid samples, with standard deviation ellipses for bone and enamel samples showing a marked offset. The bone and enamel samples have been taken from different specimens.

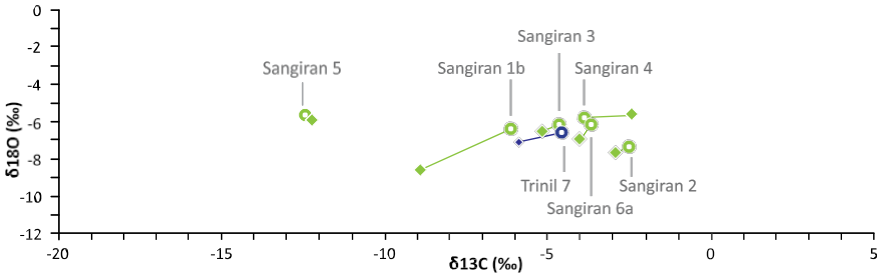

Fig. 5. Cross plot of Homo erectus bone $d^{13}C$ and $d^{18}O$ values. Diamonds denote samples treated with the pre-leaching method described in Bocherens et al. (1996).

8. Conclusions

Combining carbon stable isotope data from herbivore and omnivore taxa provides insight into habitat type and niche segregation, and ultimately contributes to our knowledge of the climatic backdrop for Sundaland fossil sites. For each site the bovids and cervids in our dataset tend to employ a feeding strategy focussing on either browsing or grazing. We believe that this duality reflects a relatively abrupt turnover in vegetation balance tied to the glacial-interglacial precipitation contrast, with the rapid flooding of the Sunda Shelf acting as a sharp threshold between the two states. The observed correlation between herbivore $d^{13}C$ and $d^{18}O$ values supports this interpretation, with enriched precipitation and vegetation $d^{18}O$ values coinciding with C_4-abundance during (inferred) glacial periods.

More extensive stable isotope research on these and other fossil assemblages, in existing as well as new collections, should be applied to further investigate the diet of individual taxa and the dynamic link between the climate and vegetation balance in the Sundaland region. In particular, this approach could be extended to include fossil tooth material from hominins in the Sundaland region. Our present data on herbivore and omnivore faunas provide the much-needed isotopic framework that will allow dietary interpretation of such hominin tooth isotopic data.

Our data further show that such extensive isotope analyses on material in existing fossil collections provides valuable insights in the inter-specimen isotopic variability of specific collections, which can potentially facilitate an independent assessment of the consistency of assemblage and curation of material in important historical collections.

Acknowledgments

We would like to thank Reinier van Zelst and Natasja den Ouden for facilitating access to the collections of the Naturalis Biodiversity Center. We are very grateful to Thomas Schossleitner for guiding us through the Selenka collection at the Museum für Naturkunde, and providing access to the original field book and maps of the Selenka expedition to Trinil. Faisal Bibi helped us in the species identification of Selenka specimens. Theya Molleson helped us identify a SEM stub sample from her original study as Trinil Femur III. Paul Albers digitalized the information contained in the Selenka field book and interpreted the sequence of numbered excavation layers in relation to the HK as excavated by Dubois. For their assistance in sample analysis, we thank Suzan Verdegaal, Remy van Baal, and Heather Blain. Gert van den Bergh provided us with valuable advice. The recommendations of two anonymous reviewers strongly improved this paper.

Appendix A. Supplementary data

Supplementary data related to this article can be found at http://dx.doi.org/10.1016/j.quascirev.2016.02.028.

References

Abram, N.J., McGregor, H.V., Gagan, M.K., Hantoro, W.S., Suwargadi, B.W., 2009. Oscillations in the southern extent of the Indo-Pacific warm pool during the mid-Holocene. Quat. Sci. Rev. 28, 2794e2803.
Antón, S.C., 2013. Homo erectus and related taxa. A Companion Paleoanthropology 497e516.
Bedaso, Z.K., Wynn, J.G., Alemseged, Z., Geraads, D., 2013. Dietary and paleoenvironmental reconstruction using stable isotopes of herbivore tooth enamel from middle Pliocene Dikika, Ethiopia: implication for Australopithecus afarensis habitat and food resources. J. Hum. Evol. 64, 21e38.
Bergman, R., Karsten, P., 1952. The Fluorine Content of Pithecanthropus and of Other Specimens from the Trinil Fauna, vol. 55, pp. 150e152 (series B).
Bernard, A., Daux, V., Lécuyer, C., Brugal, J.-P., Genty, D., Wainer, K., Gardien, V., Fourel, F., Jaubert, J., 2009. Pleistocene seasonal temperature variations recorded in the d 18 O of Bison priscus teeth. Earth Planet. Sci. Lett. 283, 133e143.
Bird, M.I., Taylor, D., Hunt, C., 2005. Palaeoenvironments of insular southeast Asia during the last glacial period: a savanna corridor in Sundaland? Quat. Sci. Rev. 24, 2228e2242.
Bocherens, H., Koch, P.L., Mariotti, A., Geraads, D., Jaeger, J.-J., 1996. Isotopic biogeochemistry (13C, 18O) of mammalian enamel from African Pleistocene hominid sites. Palaios 306e318.
Calvin, M., Bassham, J.A., 1962. The Photosynthesis of Carbon Compounds. WA Benjamin, New York.
Cannon, C.H., Morley, R.J., Bush, A.B., 2009. The current refugial rainforests of Sundaland are unrepresentative of their biogeographic past and highly vulnerable to disturbance. Proc. Natl. Acad. Sci. 106, 11188e11193.
Cerling, T.E., Andanje, S.A., Blumenthal, S.A., Brown, F.H., Chritz, K.L., Harris, J.M., Hart, J.A., Kirera, F.M., Kaleme, P., Leakey, L.N., 2015. Dietary changes of large herbivores in the Turkana Basin, Kenya 4 1 Ma. Proc. Natl. Acad. Sci. 112, 11467e11472.
Cerling, T.E., Harris, J.M., 1999. Carbon isotope fractionation between diet and bioapatite in ungulate mammals and implications for ecological and paleoecological studies. Oecologia 120, 347e363.
Cerling, T.E., Harris, J.M., MacFadden, B.J., Leakey, M.G., Quade, J., Eisenmann, V., Ehleringer, J.R., 1997. Global vegetation change through the Miocene/Pliocene boundary. Nature 389, 153e158.
Cerling, T.E., Harris, J.M., Passey, B.H., 2003. Diets of East African Bovidae based on stable isotope analysis. J. Mammal. 84, 456e470.
Cerling, T.E., Hart, J.A., Hart, T.B., 2004. Stable isotope ecology in the Ituri Forest. Oecologia 138, 5e12.
Cerling, T.E., Manthi, F.K., Mbua, E.N., Leakey, L.N., Leakey, M.G., Leakey, R.E., Brown, F.H., Grine, F.E., Hart, J.A., Kaleme, P., Roche, H., Uno, K.T., Wood, B.A., 2013. Stable isotope-based diet reconstructions of Turkana Basin hominins. Proc. Natl. Acad. Sci. U. S. A. 110, 10501e10506.
Craig, H., 1961. Isotopic variations in meteoric waters. Science 1702e1703.
Dansgaard, W., 1964. Stable isotopes in precipitation. Tellus 16, 436e468.
Day, M.H., 1986. Guide to Fossil Man. University of Chicago Press.
Day, M.H., Molleson, T., 1973. The Trinil Femora, Symposia of the Society for the Study of Human Biology, pp. 127e154.
De Vos, J., 1983. The Pongo faunas from Java and Sumatra and their significance for biostratigraphical and paleo-ecological interpretations. In: Proceedings of the Koninklijke Nederlandse Akademie Van Wetenschappen. Series B. Palaeontology, Geology, Physics and Chemistry, pp. 417e425. North-Holland.
De Vos, J., 1995. The migration of Homo erectus and Homo sapiens in South-East Asia and the Indonesian archipelago. Evolution and ecology of Homo erectus. Palaeo-Anthropology 1, 239e260.
De Vos, J., Sartono, S., Hardja-Sasmita, S., Sondaar, P., 1982. The Fauna From Trinil, Type Locality of Homo Erectus A, pp. 207e211.
den Tex, R.-J., Thorington, R., Maldonado, J.E., Leonard, J.A., 2010. Speciation dynamics in the SE Asian tropics: putting a time perspective on the phylogeny and biogeography of Sundaland tree squirrels. Sundasciurus. Mol. Phylogen. Evol. 55, 711e720.
DeNiro, M.J., Epstein, S., 1978. Influence of diet on the distribution of carbon isotopes in animals. Geochim. Cosmochim. Acta 42, 495e506.

Dubois, E., 1894. Pithecanthropus Erectus: Eine Menschenaehnliche Uebergangsform aus Java (Landesdruckerei).
Dubois, E., 1896. On Pithecanthropus erectus: a transitional form between man and the apes. J. Anthropol. Inst. G. B. Irel. 240e255.
Ehleringer, J.R., Cooper, T.A., 1988. Correlations between carbon isotope ratio and microhabitat in desert plants. Oecologia 76, 562e566.
Farquhar, G.D., Ehleringer, J.R., Hubick, K.T., 1989. Carbon isotope discrimination and photosynthesis. Annu. Rev. Plant Biol. 40, 503e537.
Fricke, H.C., Clyde, W.C., O'Neil, J.R., 1998. Intra-tooth variations in d18O (PO 4) of mammalian tooth enamel as a record of seasonal variations in continental climate variables. Geochim. Cosmochim. Acta 62, 1839e1850.
Gonfiantini, R., Gratziu, S., Tongiorgi, E., 1965. Oxygen isotopic composition of water in leaves. Isotopes Radiat. Soil-Plant Nutr. Stud. 405e410.
Griffiths, M.L., Drysdale, R.N., Gagan, M.K., Zhao, J.-x., Hellstrom, J.C., Ayliffe, L.K., Hantoro, W.S., 2013. Abrupt increase in east Indonesian rainfall from flooding of the Sunda Shelf ~9500 years ago. Quat. Sci. Rev. 74, 273e279.
Griffiths, M.L., Drysdale, R.N., Gagan, M.K., Zhao, J.x., Ayliffe, L.K., Hellstrom, J.C., Hantoro, W.S., Frisia, S., Feng, Y.x., Cartwright, I., Pierre, E.S., Fischer, M.J., Suwargadi, B.W., 2009. Increasing AustralianeIndonesian monsoon rainfall linked to early Holocene sea-level rise. Nat. Geosci. 2, 636e639.
Griffiths, M.L., Drysdale, R.N., Vonhof, H.B., Gagan, M.K., Zhao, J.-x., Ayliffe, L.K., Hantoro, W.S., Hellstrom, J.C., Cartwright, I., Frisia, S., Suwargadi, B.W., 2010. Younger DryaseHolocene temperature and rainfall history of southern Indonesia from d18O in speleothem calcite and fluid inclusions. Earth Planet. Sci. Lett. 295, 30e36.
Hanebuth, T.J., Voris, H.K., Yokoyama, Y., Saito, Y., Okuno, J.i, 2011. Formation and fate of sedimentary depocentres on Southeast Asia's Sunda Shelf over the past sea-level cycle and biogeographic implications. Earth-Sci. Rev. 104, 92e110.
Harris, J., Cerling, T., 2002. Dietary adaptations of extant and Neogene African suids. J. Zool. 256, 45e54.
Hatch, M.D., Slack, C.R., 1966. Photosynthesis by sugar-cane leaves. Biochem. J. 101, 103e111.
Helliker, B.R., Ehleringer, J.R., 2000. Establishing a grassland signature in veins: 18O in the leaf water of C3 and C4 grasses. Proc. Natl. Acad. Sci. 97, 7894e7898.
Hoogerwerf, A., 1970. Udjung Kulon: the Land of the Last Javan Rhinoceros (Brill Archive).
Huffman, O., Zaim, Y., Kappelman, J., Ruez, D., De Vos, J., Rizal, Y., Aziz, F., Hertler, C., 2006. Relocation of the 1936 Mojokerto skull discovery site near Perning, east Java. J. Hum. Evol. 50, 431e451.
Huffman, O.F., De Vos, J., Berkhout, A.W., Aziz, F., 2010. Provenience reassessment of the 1931e1933 Ngandong Homo erectus (Java), confirmation of the bone-bed origin reported by the discoverers. PaleoAnthropology 2010, 1e60.
Hutchison, C.S., 1989. The Palaeo-Tethyan Realm and Indosinian Orogenic System of Southeast Asia, Tectonic Evolution of the Tethyan Region. Springer, pp. 585e643.
Hyodo, M., Matsu'ura, S., Kamishima, Y., Kondo, M., Takeshita, Y., Kitaba, I., Danhara, T., Aziz, F., Kurniawan, I., Kumai, H., 2011. High-resolution record of the MatuyamaeBrunhes transition constrains the age of Javanese Homo erectus in the Sangiran dome, Indonesia. Proc. Natl. Acad. Sci. 108, 19563e19568.
Indriati, E., Antôn, S.C., 2008. Earliest Indonesian facial and dental remains from Sangiran, Java: a description of Sangiran 27. Anthropol. Sci. J. Anthropol. Soc. Nippon 116, 219e229.
Joordens, J.C., d'Errico, F., Wesselingh, F.P., Munro, S., de Vos, J., Wallinga, J., Ankjærgaard, C., Reimann, T., Wijbrans, J.R., Kuiper, K.F., 2015. Homo erectus at Trinil on Java used shells for tool production and engraving. Nature 518 (7538), 228e231.
Kaifu, Y., 2006. Advanced dental reduction in Javanese Homo erectus. Anthropol. Sci. 114, 35e43.
Kaifu, Y., Aziz, F., Baba, H., 2005a. Hominid mandibular remains from Sangiran: 1952e1986 collection. Am. J. Phys. Anthropol. 128, 497e519.
Kaifu, Y., Baba, H., Aziz, F., Indriati, E., Schrenk, F., Jacob, T., 2005b. Taxonomic affinities and evolutionary history of the Early Pleistocene hominids of Java: dentognathic evidence. Am. J. Phys. Anthropol. 128, 709e726.
Kitchener, D.J., 1990. Wild Mammals of Lombok Island. Western Australian Museum.
Koch, P.L., Fisher, D.C., Dettman, D., 1989. Oxygen isotope variation in the tusks of extinct proboscideans: a measure of season of death and seasonality. Geology 17, 515.
Koch, P.L., Tuross, N., Fogel, M.L., 1997. The effects of sample treatment and diagenesis on the isotopic integrity of carbonate in biogenic hydroxylapatite. J. Archaeol. Sci. 24, 417e429.
Kohn, M.J., 2010. Carbon isotope compositions of terrestrial C3 plants as indicators of (paleo) ecology and (paleo) climate. Proc. Natl. Acad. Sci. 107, 19691e19695.
Kolodny, Y., Raab, M., 1988. Oxygen isotopes in phosphatic fish remains from Israel: paleothermometry of tropical Cretaceous and Tertiary shelf waters. Palaeogeogr. Palaeoclimatol. Palaeoecol. 64, 59e67.
Kurtén, B., 1968. Pleistocene Mammals of Europe. Transaction Publishers.
Larick, R., Ciochon, R.L., Zaim, Y., Rizal, Y., Aziz, F., Reagan, M., Heizler, M., 2001. Early Pleistocene $^{40}Ar/^{39}Ar$ ages for Bapang formation hominins, central Jawa, Indonesia. Proc. Natl. Acad. Sci. 98, 4866e4871.
Lécuyer, C., Bogey, C., Garcia, J.P., Grandjean, P., Barrat, J.A., Floquet, M., Bardet, N., Pereda-Superbiola, X., 2003. Stable isotope composition and rare earth element content of vertebrate remains from the Late Cretaceous of northern Spain (Lano): did the environmental record survive? Palaeogeogr. Palaeoclimatol. Palaeoecol. 193, 457e471.
Lee-Thorp, J., Sponheimer, M., 2006. Contributions of biogeochemistry to understanding hominin dietary ecology. Am. J. Phys. Anthropol (Suppl. 43), 131e148.
Lee-Thorp, J.A., 2002. Preservation of Biogenic Carbon Isotopic Signals in Plio-pleistocene Bone and Tooth Mineral, Biogeochemical Approaches to Paleodietary Analysis. Springer, pp. 89e115.
Lee-Thorp, J.A., Sealy, J.C., Van Der Merwe, N.J., 1989. Stable carbon isotope ratio differences between bone collagen and bone apatite, and their relationship to diet. J. Archaeol. Sci. 16, 585e599.
Lee-Thorp, J.A., van der Merwe, N.J., Brain, C., 1994. Diet of Australopithecus robustus at Swartkrans from stable carbon isotopic analysis. J. Hum. Evol. 27, 361e372.
Leister, C., 1939. The wild pigs of the world. N. Y. Zool. Soc. 52, 131e139.
Leonard, J.A., Tex, R.J., Hawkins, M.T., Muñoz-Fuentes, V., Thorington, R., Maldonado, J.E., 2015. Phylogeography of vertebrates on the Sunda Shelf: a multi-species comparison. J. Biogeogr. 42 (5), 871e879.
Levin, N.E., Cerling, T.E., Passey, B.H., Harris, J.M., Ehleringer, J.R., 2006. A stable isotope aridity index for terrestrial environments. Proc. Natl. Acad. Sci. U. S. A. 103, 11201e11205.
Levin, N.E., Simpson, S.W., Quade, J., Cerling, T.E., Frost, S.R., 2008. Herbivore enamel carbon isotopic composition and the environmental context of Ardipithecus at Gona, Ethiopia. Geol. Soc. Am. Special Pap. 446, 215e234.
Lim, H.C., Zou, F., Taylor, S.S., Marks, B.D., Moyle, R.G., Voelker, G., Sheldon, F.H., 2010. Phylogeny of magpie-robins and shamas (Aves: Turdidae: Copsychus and Trichixos): implications for island biogeography in southeast Asia. J. Biogeogr. 37, 1894e1906.
Lisiecki, L.E., Raymo, M.E., 2005. A Pliocene-Pleistocene stack of 57 globally distributed benthic d18O records. Paleoceanography 20.
Longinelli, A., 1984. Oxygen isotopes in mammal bone phosphate: a new tool for paleohydrological and paleoclimatological research? Geochim. Cosmochim. Acta 48, 385e390.
Louys, J., Meijaard, E., 2010. Palaeoecology of Southeast Asian megafauna-bearing sites from the Pleistocene and a review of environmental changes in the region. J. Biogeogr. 1432e1449.
Luz, B., Kolodny, Y., 1989. Oxygen isotope variation in bone phosphate. Appl. Geochem 4, 317e323.
Maloney, B.K., 1980. Pollen analytical evidence for early forest clearance in North Sumatra. Nature 287, 324e326.
Mariano, A.N., 1988. Some further geological applications of cathodoluminescence. Cathodoluminescence Geol. Mater. 94e123.
Mason, R., Mariano, A., 1990. Cathodoluminescence activation in manganese-bearing and rare earth-bearing synthetic calcites. Chem. Geol. 88, 191e206.
Medina, E., Minchin, P., 1980. Stratification of d13C values of leaves in Amazonian rain forests. Oecologia 45, 377e378.
Morley, R., 1982. A palaeoecological interpretation of a 10,000 year pollen record from Danau Padang, central Sumatra, Indonesia. J. Biogeogr. 151e190.
Muntasib, E., 2000. The changes of feeding pattern of banteng (Bos javanicus) and its effect to Javan rhino (Rhinoceros sondaicus) in Ujung Kulon National Park, West Java. J. Media Konservasi 7, 71e74.
Myers, N., Mittermeier, R.A., Mittermeier, C.G., Da Fonseca, G.A., Kent, J., 2000. Biodiversity hotspots for conservation priorities. Nature 403, 853e858.
Newsome, J., Flenley, J., 1988. Late Quaternary vegetational history of the central highlands of Sumatra. II. Palaeopalynology Veg. Hist. J. Biogeogr. 555e578.
Niedermeyer, E.M., Sessions, A.L., Feakins, S.J., Mohtadi, M., 2014. Hydroclimate of the western Indo-Pacific warm pool during the past 24,000 years. Proc. Natl. Acad. Sci. 111, 9402e9406.
Oka, G.M., 2000. Factors Affecting the Management of Muntjac Deer (Muntiacus Muntjak) in Bali Barat National Park, Indonesia. Faculty of Environmental Management and Agriculture. University of Western Sydney, Hawkesbury.
Passey, B.H., Robinson, T.F., Ayliffe, L.K., Cerling, T.E., Sponheimer, M., Dearing, M.D., Roeder, B.L., Ehleringer, J.R., 2005. Carbon isotope fractionation between diet, breath CO_2, and bioapatite in different mammals. J. Archaeol. Sci. 32, 1459e1470.
Picard, S., Garcia, J.-P., Lécuyer, C., Sheppard, S.M., Cappetta, H., Emig, C.C., 1998. d18O values of coexisting brachiopods and fish: temperature differences and estimates of paleoewater depths. Geology 26, 975e978.
Pucéat, E., Lécuyer, C., Sheppard, S.M., Dromart, G., Reboulet, S., Grandjean, P., 2003. Thermal evolution of Cretaceous Tethyan marine waters inferred from oxygen isotope composition of fish tooth enamels. Paleoceanography 18.
Rozzi, R., Winkler, D.E., De Vos, J., Schulz, E., Palombo, M.R., 2013. The enigmatic bovid Duboisia santeng (Dubois, 1891) from the earlyemiddle Pleistocene of Java: a multiproxy approach to its paleoecology. Palaeogeogr. Palaeoclimatol. Palaeoecol. 377, 73e85.
Russell, J.M., Vogel, H., Konecky, B.L., Bijaksana, S., Huang, Y., Melles, M., Wattrus, N., Costa, K., King, J.W., 2014. Glacial forcing of central Indonesian hydroclimate since 60,000 y BP. Proc. Natl. Acad. Sci. 111, 5100e5105.
Sartono, S., 1968. Early man in Java e Pithecanthropus skull 7, a male specimen of Pithecanthropus erectus. I. In: Proceedings of the Koninklijke Nederlandse Akademie van Wetenschappen Series B-Physical Sciences, vol. 71, p. 396.
Sartono, S., 1971. Observations on a new skull of Pithecanthropus-erectuc (Pithecanthropus-VIII) from Sangiran, Central Java. In: Proceedings of the Koninklijke Nederlandse Akademie van Wetenschappen Series B-Physical Sciences, vol. 74, p. 185.
Sathiamurthy, E., Voris, H.K., 2006. Maps of Holocene sea level transgression and submerged lakes on the Sunda Shelf. Nat. Hist. J. Chulalongkorn Univ. (Suppl. 2), 1e43.

Selenka, L., Blanckenhorn, M., 1911. Die Pithecanthropus-Schichten auf Java. W. Engelmann.
Selenka, M.L., 1906e1907. Journal Java Expedition Trinil. Original Fieldbook Including Maps, Archived in the Selenka Collection. Museum für Naturkunde, Berlin, Germany.
Sharp, Z.D., Atudorei, V., Furrer, H., 2000. The effect of diagenesis on oxygen isotope ratios of biogenic phosphates. Am. J. Sci. 300, 222e237.
Shutler, R., Head, J., Donahue, D., Jull, A., Barbetti, M., Matsu'ura, S., De Vos, J., Storm, P., 2004. AMS radiocarbon dates on bone from cave sites in Southeast Java, Indonesia, including Wajak. Mod. Quat. Res. Southeast Asia 18, 89e94.
Slik, J.F., Aiba, S.-I., Bastian, M., Brearley, F.Q., Cannon, C.H., Eichhorn, K.A., Fredriksson, G., Kartawinata, K., Laumonier, Y., Mansor, A., 2011. Soils on exposed Sunda Shelf shaped biogeographic patterns in the equatorial forests of Southeast Asia. Proc. Natl. Acad. Sci. 108, 12343e12347.
Smith, B.N., Epstein, S., 1971. Two categories of 13C/12C ratios for higher plants. Plant Physiol. 47, 380e384.
Sponheimer, M., Lee-Thorp, J.A., 2006. Enamel diagenesis at South African Australopith sites: implications for paleoecological reconstruction with trace elements. Geochim. Cosmochim. Acta 70, 1644e1654.
Sponheimer, M., Lee-Thorp, J.A., DeRuiter, D.J., Smith, J.M., van der Merwe, N.J., Reed, K., Grant, C., Ayliffe, L.K., Robinson, T.F., Heidelberger, C., 2003. Diets of southern African bovidae: stable isotope evidence. J. Mammal. 84, 471e479.
Stanton Thomas, K.J., Carlson, S.J., 2004. Microscale d18O and d13C isotopic analysis of an ontogenetic series of the hadrosaurid dinosaur Edmontosaurus: implications for physiology and ecology. Palaeogeogr. Palaeoclimatol. Palaeoecol. 206, 257e287.
Sternberg, L.d.S.L., 1989. Oxygen and Hydrogen Isotope Ratios in Plant Cellulose: Mechanisms and Applications, Stable Isotopes in Ecological Research. Springer, pp. 124e141.
Stewart, G.R., Turnbull, M., Schmidt, S., Erskine, P., 1995. 13C natural abundance in plant communities along a rainfall gradient: a biological integrator of water availability. Funct. Plant Biol. 22, 51e55.
Storm, P., Wood, R., Stringer, C., Bartsiokas, A., de Vos, J., Aubert, M., Kinsley, L., Grün, R., 2013. U-series and radiocarbon analyses of human and faunal remains from Wajak, Indonesia. J. Hum. Evol. 64, 356e365.
Timmins, R., Duckworth, W., Hedges, S., Steinmetz, R., Pattavibool, A., 2008. Bos javanicus in IUCN 2010. IUCN Red List of Threatened Species. Version 2010.2.
Van den Bergh, G.D., de Vos, J., Sondaar, P.Y., 2001. The late Quaternary palaeogeography of mammal evolution in the Indonesian archipelago. Palaeogeogr. Palaeoclimatol. Palaeoecol. 171, 385e408.
van der Kaars, S., Dam, R., 1997. Vegetation and climate change in West-Java, Indonesia during the last 135,000 years. Quat. Int. 37, 67e71.
van der Kaars, S., Wang, X., Kershaw, P., Guichard, F., Setiabudi, D.A., 2000. A Late Quaternary palaeoecological record from the Banda Sea, Indonesia: patterns of vegetation, climate and biomass burning in Indonesia and northern Australia. Palaeogeogr. Palaeoclimatol. Palaeoecol. 155, 135e153.
van der Merwe, N.J., Masao, F.T., Bamford, M.K., 2008. Isotopic evidence for contrasting diets of early hominins Homo habilis and Australopithecus boisei of Tanzania. S. Afr. J. Sci. 104, 153e155.
van der Merwe, N.J., Medina, E., 1991. The canopy effect, carbon isotope ratios and foodwebs in Amazonia. J. Archaeol. Sci. 18, 249e259.
von Koenigswald, G.H.R., 1935. Die Fossilen Säugetierformen Javas. Koninklijke Akad. van Wetenschappen.
von Koenigswald, G.H.R., 1940. Neue Pithecanthropus-Funde, 1936-1938: ein Beitrag zur Kenntnis der Praehominiden (Landsdrukkerij).
Voris, H.K., 2000. Maps of Pleistocene sea levels in Southeast Asia: shorelines, river systems and time durations. J. Biogeogr. 27, 1153e1167.
Wang, Y., Cerling, T.E., 1994. A model of fossil tooth and bone diagenesis: implications for paleodiet reconstruction from stable isotopes. Palaeogeogr. Palaeoclimatol. Palaeoecol. 107, 281e289.
Warinner, C., Tuross, N., 2009. Alkaline cooking and stable isotope tissue-diet spacing in swine: archaeological implications. J. Archaeol. Sci. 36, 1690e1697.
Webb, E.C., White, C.D., Longstaffe, F.J., 2014. Investigating inherent differences in isotopic composition between human bone and enamel bioapatite: implications for reconstructing residential histories. J. Archaeol. Sci. 50, 97e107.
Westaway, K., Morwood, M.J., Roberts, R., Rokus, A., Zhao, J.-x., Storm, P., Aziz, F., Van Den Bergh, G., Hadi, P., de Vos, J., 2007b. Age and biostratigraphic significance of the Punung rainforest fauna, east Java, Indonesia, and implications for Pongo and Homo. J. Hum. Evol. 53, 709e717.
Westaway, K.E., Zhao, J.x., Roberts, R.G., Chivas, A.R., Morwood, M.J., Sutikna, T., 2007a. Initial speleothem results from western Flores and eastern Java, Indonesia: were climate changes from 47 to 5 ka responsible for the extinction of Homo floresiensis? J. Quat. Sci. 22, 429e438.
Wicaksono, S.A., Russell, J.M., Bijaksana, S., 2015. Compound-specific carbon isotope records of vegetation and hydrologic change in central Sulawesi, Indonesia, since 53,000 yr BP. Palaeogeogr. Palaeoclimatol. Palaeoecol. 430, 47e56.
Woodruff, D.S., 2010. Biogeography and conservation in Southeast Asia: how 2.7 million years of repeated environmental fluctuations affect today's patterns and the future of the remaining refugial-phase biodiversity. Biodivers. Conserv. 19, 919e941.
Zaim, Y., Ciochon, R.L., Polanski, J.M., Grine, F.E., Bettis, E.A., Rizal, Y., Franciscus, R.G., Larick, R.R., Heizler, M., Eaves, K.L., 2011. New 1.5 million-year-old Homo erectus maxilla from Sangiran (Central Java, Indonesia). J. Hum. Evol. 61, 363e376.